Oxidative Medicine and Cellular Longevity

Oxidants and Antioxidants in Metabolic Syndrome and Cancer

Guest Editors: Si Jin, Yongzhong Wu, Shiwei Deng, Jinxiang Zhang, and Xiao Qian Chen

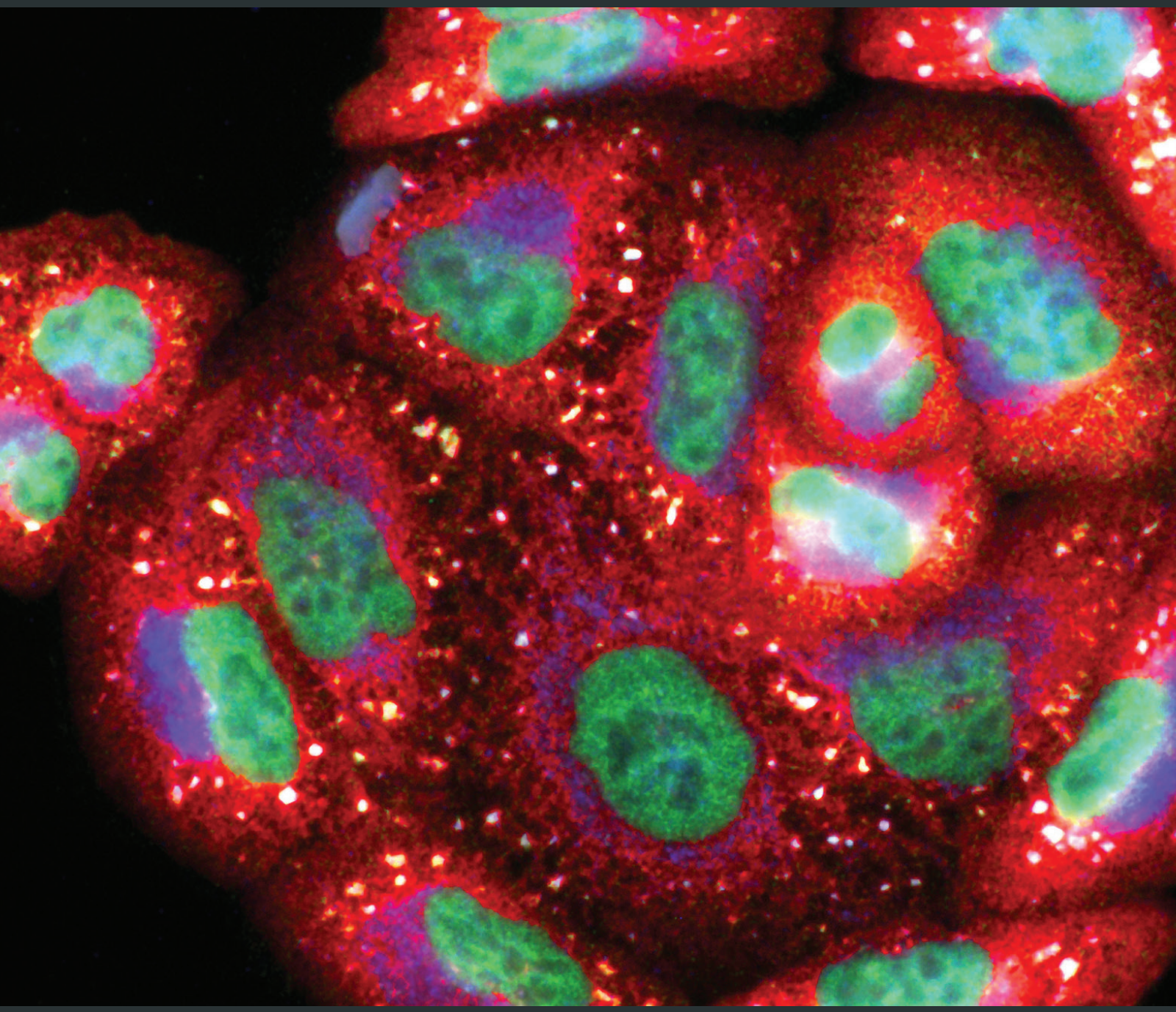

Oxidants and Antioxidants in Metabolic Syndrome and Cancer

Oxidative Medicine and Cellular Longevity

Oxidants and Antioxidants in Metabolic Syndrome and Cancer

Guest Editors: Si Jin, Yongzhong Wu, Shiwei Deng, Jinxiang Zhang, and Xiao Qian Chen

Editorial Board

Contents

Oxidants and Antioxidants in Metabolic Syndrome and Cancer, Si Jin, Yongzhong Wu, Shiwei Deng, Jinxiang Zhang, and Xiao Qian Chen
Volume 2014, Article ID 178962, 3 pages

Lithium Chloride Suppresses Colorectal Cancer Cell Survival and Proliferation through ROS/GSK-3β/NF-κB Signaling Pathway, Huili Li, Kun Huang, Xinghua Liu, Jinlin Liu, Xiaoming Lu, Kaixiong Tao, Guobin Wang, and Jiliang Wang
Volume 2014, Article ID 241864, 8 pages

Piperlongumine Inhibits Migration of Glioblastoma Cells via Activation of ROS-Dependent p38 and JNK Signaling Pathways, Qian Rong Liu, Ju Mei Liu, Yong Chen, Xiao Qiang Xie, Xin Xin Xiong, Xin Yao Qiu, Feng Pan, Di Liu, Shang Bin Yu, and Xiao Qian Chen
Volume 2014, Article ID 653732, 12 pages

PELP1 Suppression Inhibits Colorectal Cancer through c-Src Downregulation, Zhifeng Ning, Youzhi Zhang, Hanwei Chen, Jiliang Wu, Tieshan Song, Qian Wu, and Fuxing Liu
Volume 2014, Article ID 193523, 9 pages

***Caenorhabditis elegans*: A Useful Model for Studying Metabolic Disorders in Which Oxidative Stress Is a Contributing Factor**, Elizabeth Moreno-Arriola, Noemí Cárdenas-Rodríguez, Elvia Coballase-Urrutia, José Pedraza-Chaverri, Liliana Carmona-Aparicio, and Daniel Ortega-Cuellar
Volume 2014, Article ID 705253, 9 pages

Metabolic Syndrome: An Important Risk Factor for Parkinson's Disease, Pei Zhang and Bo Tian
Volume 2014, Article ID 729194, 7 pages

Piperlongumine Induces Apoptosis and Synergizes with Cisplatin or Paclitaxel in Human Ovarian Cancer Cells, Li-Hua Gong, Xiu-Xiu Chen, Huan Wang, Qi-Wei Jiang, Shi-Shi Pan, Jian-Ge Qiu, Xiao-Long Mei, You-Qiu Xue, Wu-Ming Qin, Fei-Yun Zheng, Zhi Shi, and Xiao-Jian Yan
Volume 2014, Article ID 906804, 10 pages

Insulin Regulates Glucose Consumption and Lactate Production through Reactive Oxygen Species and Pyruvate Kinase M2, Qi Li, Xue Liu, Yu Yin, Ji-Tai Zheng, Cheng-Fei Jiang, Jing Wang, Hua Shen, Chong-Yong Li, Min Wang, Ling-Zhi Liu, and Bing-Hua Jiang
Volume 2014, Article ID 504953, 10 pages

Leucocyte Telomere Shortening in relation to Newly Diagnosed Type 2 Diabetic Patients with Depression, Zhelong Liu, Jianhua Zhang, Jiangtao Yan, Yuping Wang, and Yongsheng Li
Volume 2014, Article ID 673959, 8 pages

Lentivirus-Mediated Nox4 shRNA Invasion and Angiogenesis and Enhances Radiosensitivity in Human Glioblastoma, Yongsheng Li, Na Han, Tiejun Yin, Lulu Huang, Shunfang Liu, Dongbo Liu, Cuihong Xie, and Mengxian Zhang
Volume 2014, Article ID 581732, 9 pages

Salidroside Stimulates Mitochondrial Biogenesis and Protects against H_2O_2-Induced Endothelial Dysfunction, Shasha Xing, Xiaoyan Yang, Wenjing Li, Fang Bian, Dan Wu, Jiangyang Chi, Gao Xu, Yonghui Zhang, and Si Jin
Volume 2014, Article ID 904834, 13 pages

Effect of *Centella asiatica* on Oxidative Stress and Lipid Metabolism in Hyperlipidemic Animal Models, Yun Zhao, Ping Shu, Youzhi Zhang, Limin Lin, Haihong Zhou, Zhentian Xu, Daqin Suo, Anzhi Xie, and Xin Jin
Volume 2014, Article ID 154295, 7 pages

Leptin Level and Oxidative Stress Contribute to Obesity-Induced Low Testosterone in Murine Testicular Tissue, Jian Zhao, Lingling Zhai, Zheng Liu, Shuang Wu, and Liping Xu
Volume 2014, Article ID 190945, 14 pages

Endogenous Ceramide Contributes to the Transcytosis of oxLDL across Endothelial Cells and Promotes Its Subendothelial Retention in Vascular Wall, Wenjing Li, Xiaoyan Yang, Shasha Xing, Fang Bian, Wanjing Yao, Xiangli Bai, Tao Zheng, Guangjie Wu, and Si Jin
Volume 2014, Article ID 823071, 11 pages

BL153 Partially Prevents High-Fat Diet Induced Liver Damage Probably via Inhibition of Lipid Accumulation, Inflammation, and Oxidative Stress, Jian Wang, Chi Zhang, Zhiguo Zhang, Qiang Chen, Xuemian Lu, Minglong Shao, Liangmiao Chen, Hong Yang, Fangfang Zhang, Peng Cheng, Yi Tan, Ki-Soo Kim, Ki Ho Kim, Bochu Wang, and Young Heui Kim
Volume 2014, Article ID 674690, 10 pages

Resveratrol Oligomers for the Prevention and Treatment of Cancers, You-Qiu Xue, Jin-Ming Di, Yun Luo, Ke-Jun Cheng, Xing Wei, and Zhi Shi
Volume 2014, Article ID 765832, 9 pages

Hindawi Publishing Corporation
Oxidative Medicine and Cellular Longevity
Volume 2014, Article ID 178962, 3 pages
http://dx.doi.org/10.1155/2014/178962

Editorial

Oxidants and Antioxidants in Metabolic Syndrome and Cancer

Si Jin,[1] Yongzhong Wu,[2] Shiwei Deng,[3] Jinxiang Zhang,[4] and Xiao Qian Chen[5]

[1] *Department of Pharmacology, Tongji Medical College, Huazhong University of Science and Technology, Wuhan 430030, China*
[2] *Laboratory of Molecular Pharmacology, Oxidative Signaling and Molecular Therapeutics Section, Center for Cancer Research, National Cancer Institute, Bethesda, MD 20892, USA*
[3] *Department of Pharmacology, University Medical Center of the Johannes Gutenberg University Mainz, Obere Zahlbacher Straße 67, 55131 Mainz, Germany*
[4] *Department of Surgery, Union Hospital, Tongji Medical College, Huazhong University of Science and Technology, Wuhan 430022, China*
[5] *Department of Pathophysiology, Tongji Medical College, Huazhong University of Science and Technology, Wuhan 430030, China*

Correspondence should be addressed to Si Jin; jinsi@mails.tjmu.edu.cn

Received 25 May 2014; Accepted 25 May 2014; Published 24 June 2014

Metabolic syndrome, which includes hypertension, hyperlipidemia, obesity, insulin resistance or glucose intolerance, and fatty liver diseases, significantly contributes to the increased risk of cardio- or cerebral-vascular diseases and diabetes [1]. Cancer represents a group of malignantly proliferative diseases. Recently, metabolic reprogramming changes were extremely highlighted in cancer cells, putting forward to a trend that cancer should also be treated as a type of metabolic disease [2]. As a matter of fact, statins, the most prescribed low density lipoprotein (LDL) lowering agents, and metformin, the most prescribed antidiabetic drug, have both been reported to associate with decreased cancer risk [3, 4].

Meanwhile, in the past decade, a growing body of evidence has implicated that increased oxidative stress is a common and key feature of metabolic diseases [5]. Whereas a recent hypothesis paper by Watson, the famous Nobel Prize winner, suggests that diabetes, dementias, cardiovascular disease, and some cancers may be linked to a failure to generate sufficient reactive oxygen species (ROS) [6], which maybe reflects the situations in end stages of these complex diseases. ROS play very important roles in carcinogenesis and the maintenance of cancer cells. The ROS levels are reported to be very high in cancer cells, which drive the high rate of proliferation in these malignant cells [7]. Whether prooxidants or antioxidants could be used to treat cancer or not remains elusive.

In this controversial context, we organized this special issue.

Although insulin is critically involved in metabolism regulation and closely associates with both diabetes and cancer, the precise molecular mechanism is not fully elucidated. In this special issue, Q. Li et al. conducted an interesting study, which demonstrates that insulin increases pyruvate kinase M2 (PKM2) expression through ROS for the regulation of glucose consumption and lactate production "*Insulin regulates glucose consumption and lactate production through reactive oxygen species and pyruvate kinase M2*". J. Zhao et al. demonstrated that pubertal obesity was associated with increased oxidative stress in testis tissue and high levels of leptin, which maybe the cause of male hypogonadism in obesity "*Leptin level and oxidative stress contribute to obesity-induced low testosterone in murine testicular tissue.*" Oxidized low density lipoprotein (oxLDL) is the major lipid found in atherosclerotic lesion and elevated plasma oxLDL is recognized to be a risk factor of atherosclerosis. W. Li et al. in this special issue emphasized the critical role of oxLDL transcytosis across endothelial cells in the initiation of atherosclerosis, providing novel insight into the pathogenesis of this complex metabolism disease "*Endogenous ceramide contributes to the transcytosis of oxLDL across endothelial cells and promotes its subendothelial retention in vascular wall.*" For the therapy of metabolic syndrome-related disorders, J. Wang et al. reported in this special issue that

amagnolia extract, named BL153, could prevent obesity-induced liver damage via inhibition of lipid accumulation, inflammation, oxidative stress "*BL153 partially prevents high fat diet induced liver damage probably via inhibition of lipid accumulation, inflammation, and oxidative stress.*" *Centella asiatica* is a traditional Chinese medicine which has been reported to have antioxidant effect in vitro. In this special issue, Y. Zhao et al. further reported that *Centella asiatica* decreased cholesterol and triglyceride in mice model "*Effect of Centella asiatica on oxidative stress and lipid metabolism in hyperlipidemic animal models.*" Salidroside (SAL) is an active component of *Rhodiola Rosea* with documented antioxidative properties. S. Xing et al. in this issue further demonstrated that SAL could protect endothelium against H_2O_2-induced injury via promoting mitochondrial biogenesis and function, thus preventing the over-activation of oxidative stress-related downstream signaling pathways "*Salidroside stimulates mitochondrial biogenesis and protects against H_2O_2-Induced endothelial dysfunction.*"

In cancer cells, the ROS is maintained at higher levels than normal cells and mainly exerts its proliferative actions. When ROS levels are further increased by prooxidants so as to exceed a border line level, the proapoptotic effects of ROS may exceed its proliferative effects and cytotoxic effects display in cancer cells, whereas the ROS levels in normal cells remain below the border line level which is nontoxic to normal cells. In consistent with this view, several studies in this special issue reported chemicals could kill cancer cells by inducing ROS accumulation as cancer killing agents. Piperlongumine (PL) is a natural alkaloid from *Piper longum* L., possessing highly selective and effective anticancer property. L.-H. Gong et al. reported in this special issue that PL notably induced cell apoptosis, G2/M phase arrest and intracellular ROS accumulation in a dose- and time-dependent manner. Pretreatment with antioxidant N–acety-L-cysteine could reverse the PL-induced ROS accumulation and cellular apoptosis. In addition, low-dose of PL/cisplatin or paclitaxel combination therapies had a synergistic anti-growth effect on human ovarian cancer cells "*Piperlongumine induces apoptosis and synergizes with cisplatin or paclitaxel in human ovarian cancer cells.*" Q. R. Liu et al. also reported that Piperlongumine effectively inhibited the migration of human glioma cells but not normal astrocytes in the scratch-wound culture model. PL increased ROS production, reduced glutathione, activated p38 and JNK pathway, increased IκB and suppressed NF-κB in LN229 cells after scratching "*Piperlongumine inhibits migration of glioblastoma cells via activation of ROS-dependent p38 and JNK signaling pathways*". Similarly, H. Li et al. also reported in this issue that Lithium chloride, the established glycogen synthase kinase-3β (GSK-3β) inhibitor, induced the apoptosis of colorectal cancer cells by induction of ROS signaling "*Lithium chloride suppresses colorectal cancer cell survival and proliferation through ROS/GSK-3β/NF-κB signaling pathway.*"

In contrast to above observations which demonstrate that induction of ROS may be used to treat cancers, Y-Q. Xue et al., in this special issue reviews the preventive or anticancer properties of resveratrol oligomers. Resveratrol is a naturally derived phytoalexin stilbene isolated from grapes and other plants with documented antioxidant activity "*Resveratrol oligomers for the prevention and treatment of cancers.*" In line with this review, Y. Li et al. reported that NADPH oxidase 4 (Nox4)-derived reactive oxygen species might play crucial roles in the invasion, angiogenesis and radioresistance in glioblastoma. Inhibition of Nox4 by lentivirus-mediated small hairpin interfering RNA (shRNA) could be a strategy to overcome radioresistance and in turn improve the therapeutic efficacy "*Lentivirus-mediated Nox4 shRNA invasion and angiogenesis and enhances radiosensitivity in human glioblastoma.*" These studies suggest that in addition to prooxidant therapy, antioxidants may also be the right option to treat cancers as cancer inhibiting agents.

In addition to above mentioned pathological or pharmacological studies, Elizabeth Moreno-Arriola et al. present an interesting review which suggests that *Caenorhabditis elegans,* which may be one of the most famous model organisms, is also a suitable disease model reflecting the oxidative status in metabolic disorders, providing new approaches for studying metabolic diseases "*Caenorhabditis elegans: a useful model for studying metabolic disorders in which oxidative stress is a contributing factor.*"

From these collected studies in this special issue, we appear to come to the consensus that upregulated oxidative stress indeed promotes the development of both metabolic syndrome and cancer. Antioxidants are suitable choices for the prevention or treatment of metabolic syndrome-based cardiovascular diseases or diabetic mellitus, which are also classified as chronic nonresolving inflammatory diseases [8]. However, for the treatment of cancers, both prooxidants and antioxidants might work via different mechanisms, provided that the drug selectivity on targeted tissue is guaranteed. We hope that the studies and discussions gathered in this issue reflect the current trend in this area and could, to some extent, stimulate more in-depth studies in this somehow controversial field.

Acknowledgments

We appreciate the great efforts of all authors and reviewers participating in this issue. Without their invaluable contribution, this special issue would not be a success.

Si Jin
Yongzhong Wu
Shiwei Deng
Jinxiang Zhang
Xiao Qian Chen

References

[1] I. Padmalayam and M. Suto, "Role of adiponectin in the metabolic syndrome: current perspectives on its modulation as a treatment strategy," *Current Pharmaceutical Design*, vol. 19, no. 32, pp. 5755–5763, 2013.

[2] C. V. Dang, "Links between metabolism and cancer," *Genes & Development*, vol. 26, no. 9, pp. 877–890, 2012.

[3] B. J. Quinn, H. Kitagawa, R. M. Memmott, J. J. Gills, and P. A. Dennis, "Repositioning metformin for cancer prevention and

treatment," *Trends in Endocrinology & Metabolism*, vol. 24, no. 9, pp. 469–480, 2013.

[4] S. F. Nielsen, B. G. Nordestgaard, and S. E. Bojesen, "Statin use and reduced cancer-related mortality," *The New England Journal of Medicine*, vol. 367, no. 19, pp. 1792–1802, 2012.

[5] C. K. Roberts and K. K. Sindhu, "Oxidative stress and metabolic syndrome," *Life Sciences*, vol. 84, no. 21-22, pp. 705–712, 2009.

[6] J. D. Watson, "Type 2 diabetes as a redox disease," *The Lancet*, vol. 383, no. 9919, pp. 841–843, 2014.

[7] C. Gorrini, I. S. Harris, and T. W. Mark, "Modulation of oxidative stress as an anticancer strategy," *Nature Reviews Drug Discovery*, vol. 12, no. 12, pp. 931–947, 2013.

[8] C. Nathan and A. Ding, "Nonresolving inflammation," *Cell*, vol. 140, no. 6, pp. 871–882, 2010.

Hindawi Publishing Corporation
Oxidative Medicine and Cellular Longevity
Volume 2014, Article ID 241864, 8 pages
http://dx.doi.org/10.1155/2014/241864

Research Article

Lithium Chloride Suppresses Colorectal Cancer Cell Survival and Proliferation through ROS/GSK-3β/NF-κB Signaling Pathway

Huili Li,[1] Kun Huang,[2] Xinghua Liu,[1] Jinlin Liu,[1] Xiaoming Lu,[1] Kaixiong Tao,[1] Guobin Wang,[1] and Jiliang Wang[1]

[1] *Department of Surgery, Union Hospital, Tongji Medical College, Huazhong University of Science and Technology, 430022 Wuhan, China*
[2] *Department of Cardiovascular Diseases, Union Hospital, Tongji Medical College, Huazhong University of Science and Technology, 430022 Wuhan, China*

Correspondence should be addressed to Guobin Wang; wangguobin68@126.com and Jiliang Wang; wang_jiliang@hotmail.com

Received 9 February 2014; Revised 30 April 2014; Accepted 4 May 2014; Published 5 June 2014

Academic Editor: Si Jin

Glycogen synthase kinase-3β (GSK-3β), a serine/threonine protein kinase, has been regarded as a potential therapeutic target for multiple human cancers. In addition, oxidative stress is closely related to all aspects of cancer. We sought to determine the biological function of lithium, one kind of GSK-3β inhibitors, in the process of reactive oxygen species (ROS) production in colorectal cancer. In this study, we analyzed the cell apoptosis and proliferation by cell viability, EdU, and flow cytometry assays through administration of LiCl. We used polymerase chain reaction and Western blotting to establish the effect of GSK-3β inhibition on the nuclear factor-κB (NF-κB) pathway. Results showed administration of LiCl increased apoptosis and the level of ROS in colorectal cancer cells. Furthermore, the underlying mechanisms could be mediated by the reduction of NF-κB expression and NF-κB-mediated transcription. Taken together, our results demonstrated that therapeutic targeting of ROS/GSK-3β/NF-κB pathways may be an effective way for colorectal cancer intervention, although further preclinical and clinical testing are desirable.

1. Introduction

Colorectal cancer accounts for approximately 9.7% of all cancers worldwide. It is the third most common cancer and the fourth leading cause of cancer death. The 5-year survival rate for patients with colorectal cancer and metastatic colorectal cancer is less than 60% and 20%, respectively, because of the tumor's resistance to chemotherapy and radiation therapy [1]. Recently, molecular targeting drugs have been suggested for colorectal cancer treatment, but the cost of these drugs is much higher than traditional antitumor drugs. Thus, the identification of novel therapeutic targets and drugs with lower price in colorectal cancer is urgently needed.

Lithium has been an FDA-approved and preferred drug for the treatment of mood disorders for many years, and cumulative evidence has pointed to its potential use as an anticancer agent. Lithium could alter the biochemical properties of a variety of transcription factors and thus exert important physiological or pathophysiological functions in cancer development. There are diverse factors that contribute to colorectal cancer progression and chemoresistance. The transcription factor NF-κB has been shown to be crucial for tumor progression and chemoresistance in colorectal cancer by increasing expression of some target genes such as antiapoptotic Bcl-2 protein and survivin [2]. And previous studies suggest a positive role for GSK-3β in the regulation of NF-κB activity [3–6]. It has been demonstrated that lithium is a specific and noncompetitive inhibitor of GSK-3β in vitro and in vivo, and consequently it may be an inhibitor of the NF-κB pathway. Although recent studies suggest this drug inhibits cell cycle progression and cell proliferation via upregulating the expression of GSK-3β in different cell types [7–10], the role of lithium in the proliferation and survival of colorectal cancer remains elusive.

In this study, for the first time, we present evidence that pharmacological inhibition of GSK-3β by lithium treatment can inhibit colon cancer cell line SW480 survival and proliferation in a dose and time-dependent pattern. Moreover, we observed that lithium treatment can induce the accumulation of reactive oxidative species and inhibit the activation of GSK-3β, as well as the expression of NF-κB and its target genes Bcl-2 and survivin. All the results demonstrated that lithium could increase the generation of reactive oxygen species (ROS) and lead to decreased cell survival and proliferation via the ROS/GSK-3β/NF-κB pathway. Our results suggested that GSK-3β could be a novel potential therapeutic target in the treatment of colorectal cancer and lithium should be a novel potential antitumor drug with lower price.

2. Materials and Method

2.1. Reagents and Cell Culture. Lithium chloride (LiCl, a conventional GSK-3β inhibitor) was purchased from Sigma. Human colon cancer cell line SW480 was purchased from the American Type Culture Collection (ATCC, Manassas, VA, USA). Cells were maintained in PRMI 1640 (Gibco, Grand Island, NY, USA) supplemented with 10% fetal bovine serum (Gibco), 100 U/mL penicillin, and 100 μg/mL streptomycin (Invitrogen) and kept in a humidified atmosphere at 37°C with 5% CO_2 in air.

2.2. Cell Viability Assay. To determine the cell viability, cells were plated onto 24-well plates (5×10^4 cells/well). After 24 h incubation with different concentrations (0 mM, 10 mM, 20 mM, 40 mM, and 60 mM) of LiCl and incubation with 40 mM LiCl for different times (6 h, 12 h, 24 h, and 48 h), 0.5 mg/mL 3-(4,5-dimethylthiazole-2-yl)-2,5-diphenyl tetrazolium bromide (MTT, Sigma) was added to the cell suspension for further 4 h, followed by addition of dimethyl sulfoxide (DMSO, Sigma) at 100 μL/well for cell lysis. Then, absorbance was measured at 562 nm. Each assay was carried out in triplicate.

2.3. Cell Proliferation Assay. Cell proliferation was determined by using Cell-Light 5-ethynyl-2-deoxyuridine (EdU) DNA Cell Proliferation Kit (RIBOBio. Co., Ltd) [11]. Briefly, cells (1×10^5) were cultured in 24-well plates. After stimulation with different concentrations (0 mM, 10 mM, 20 mM, 40 mM, and 60 mM) of LiCl for 24 h, cells were exposed to 50 μM EdU for 2 h at 37°C. The cells were then fixed in 4% formaldehyde for 30 min at room temperature and permeabilized in 0.5% Triton X-100 for 10 min. Cells were washed with PBS, and each well was incubated with 200 μM 1 × Apollo reaction cocktail for 30 min, followed by 1 × Hoechst 33342 (200 mL per well) for staining nuclei. The stained cells were imaged under a fluorescent microscope (IX71, Olympus).

2.4. Determination of Apoptosis. Apoptosis in the colon cancer cell line was measured using the Annexin V-FITC/7-AAD Apoptosis Detection kit (BD Bioscience, CA, USA). After 24 h incubation with different concentrations (0 mM, 10 mM, 20 mM, 40 mM, and 60 mM) of LiCl in 6-well plates at a density of 2×10^5 cells/well, fluorescent intensities were determined by flow cytometry (Becton-Dickinson, CA, USA). Alive cells grouped in the lower left part of the panel, early apoptotic cells grouped in the lower right part of the panel, and late apoptotic cells grouped in the higher right part of the panel. The experiment was repeated at least three times.

2.5. Measurements of ROS Generation. Colon cancer cells were cultured in 24-well plates, and after stimulation with different concentrations (0 mM, 10 mM, 20 mM, 40 mM, and 60 mM) of LiCl for 24 h, cells were loaded with the fluorescent dye H2DCF-DA (10 μM, Beyotime Institute of Biotechnology, Haimen, China) for 20 minutes at 37°C. H2DCF-DA fluorescence was detected at excitation and emission wavelengths of 488 nm and 520 nm, respectively. ROS formation was measured using a multiwell fluorescence scanner (EnSpire 2300, Perkin Elmer, USA).

2.6. Western Blotting Analysis. Protein extracted from cells stimulated with different concentrations (0 mM, 10 mM, 20 mM, 40 mM, and 60 mM) of LiCl for 24 h was separated on 10% SDS-polyacrylamide electrophoresis gels and transferred to nitrocellulose membranes. Membranes were then blocked with 5% nonfat milk in TBS for 3 hours. After incubation with primary antibodies against GSK-3β and its fractions phosphorylated at the serine 9 residue (phospho-GSK-3β^{Ser9}) (diluted 1 : 1000; Cell Signaling Technology, Beverly, MA, USA), the tyrosine 216 residue (phospho-GSK-3β^{Tyr216}) (diluted 1 : 1000; BD Biosciences), NF-κB p65 (diluted 1 : 1000, R&D), Bcl-2 (diluted 1 : 200, Santa Cruz), survivin (diluted 1 : 200, Santa Cruz), β-actin (diluted 1 : 500, Santa Cruz), respectively, in TBS at 4°C overnight, followed by incubation with HRP-conjugated secondary antibody (diluted 1 : 5000) for 3 h. Specific band was detected with chemiluminescence assay (ECL detection reagents, Pierce). The intensity of the β-actin band was used as a loading control for comparison between samples.

2.7. Real-Time RT-RCR. Total RNA from cultured and stimulated cells (with different concentration of LiCl for 24 h) was isolated using Trizol reagent (Takara Biotechnology) according to manufacturer's instruction. 1 μg of total RNA was reverse transcribed using the PrimeScript RT reagent kit (Takara Biotechnology, Dalian, China). The mRNA levels were determined by real-time RT-PCR with ABI PRISM 7900 sequence detector system (applied biosystem) according to the manufacturer's instructions. GAPDH was used as endogenous control. Relative gene expression level was calculated using the comparative Ct method formula $2^{-\Delta\Delta Ct}$. The sequences of primers for PCR were listed in Supplemental Table 1 (see Supplementary Material available online at http://dx.doi.org/10.1155/2014/241864).

2.8. Statistical Analysis. Data are shown as mean ± SEM of at least three independent experiments. The significance of differences was estimated by one-way ANOVA. All statistical analyses were performed with SPSS software (version 11.0, SPSS, Inc.), and statistical significance was set at $P < 0.05$.

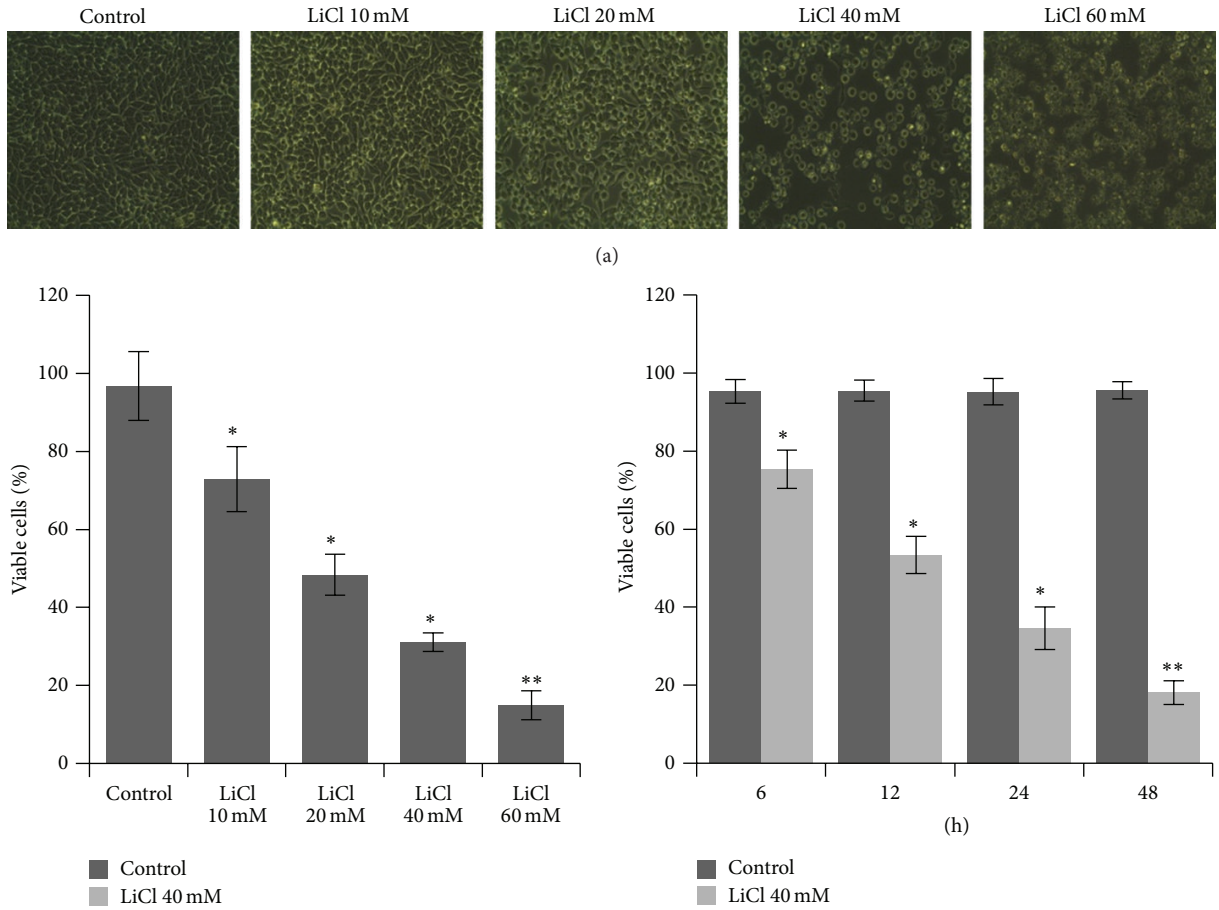

Figure 1: (a) Morphological changes of SW480 cells exposed to different concentrations of LiCl (10 mM, 20 mM, 40 mM, and 60 mM). (b) The percentage of viable SW480 cells. Cells were treated with different concentrations of LiCl (10 mM, 20 mM, 40 mM, and 60 mM) or treated with LiCl for 6, 12, 24, or 48 hours, respectively. Each point is mean ± SEM for at least three individual experiments. Original magnification, ×100. $^{*}P < 0.05$ and $^{**}P < 0.01$ versus Control group.

3. Result

3.1. LiCl Decreased Survival of SW480 Cells. To investigate the role of LiCl in the survival of colon cancer cells, the cell viability was analyzed firstly by light microscopic examination and MTT assay. Light microscopic examination revealed that, compared with the Control group, LiCl caused progressive loss of cell morphology of SW480 cells (Figure 1(a)). Then the cell survival was assessed by MTT method. The results showed that treatment with LiCl caused a gradual reduction in the percentage of viable cells in a dose dependent model. Thereafter the cells were treated with 40 mM LiCl for different times. We found that increase of the incubation time led to a decrease in the percentage of viable cells in time-dependent pattern (Figure 1(b)).

3.2. LiCl Suppressed Proliferation of SW480 Cells. In order to further characterize the effect of LiCl on the proliferation of colon cancer cells, EdU proliferation assay was also performed. After exposure to different concentration of LiCl for 24 h, the proliferation rate of SW480 significantly decreased from 51.35 ± 1.27% to 44.52 ± 2.59%, 37.09 ± 1.60%, 25.29 ± 2.98%, and 4.58 ± 2.61%, respectively, as shown in Figure 2. These results suggested that LiCl contributed to the reduced proliferation of SW480 cells.

3.3. LiCl Induced Apoptosis in SW480 Cells. Since NF-κB is a potential target of GSK-3β-dependent cell survival pathway, we detected early apoptotic cells (Annexin V+/7-AAD−) and late apoptotic cells (Annexin V+/7-AAD+) by flow cytometry. Either the early or the late apoptotic cell fractions in the LiCl treated cells were significantly higher than the untreated ones 8.81% (LiCl, 0 mM, 8.21% early, 0.60% late), and the number of apoptotic cells reached 9.00% (LiCl, 10 mM, 8.33% early, 0.67% late), 11.58% (LiCl, 20 mM, 10.46% early, 1.12% late), 19.01% (LiCl, 40 mM, 17.86% early, 1.15% late), and 36.71% (LiCl, 60 mM, 34.73% early, 1.98% late) after 24 h of exposure (Figure 3). It was demonstrated that the number of apoptotic cells dose dependently increased with LiCl treatment. These results confirmed that LiCl treatment led to SW480 cells apoptosis.

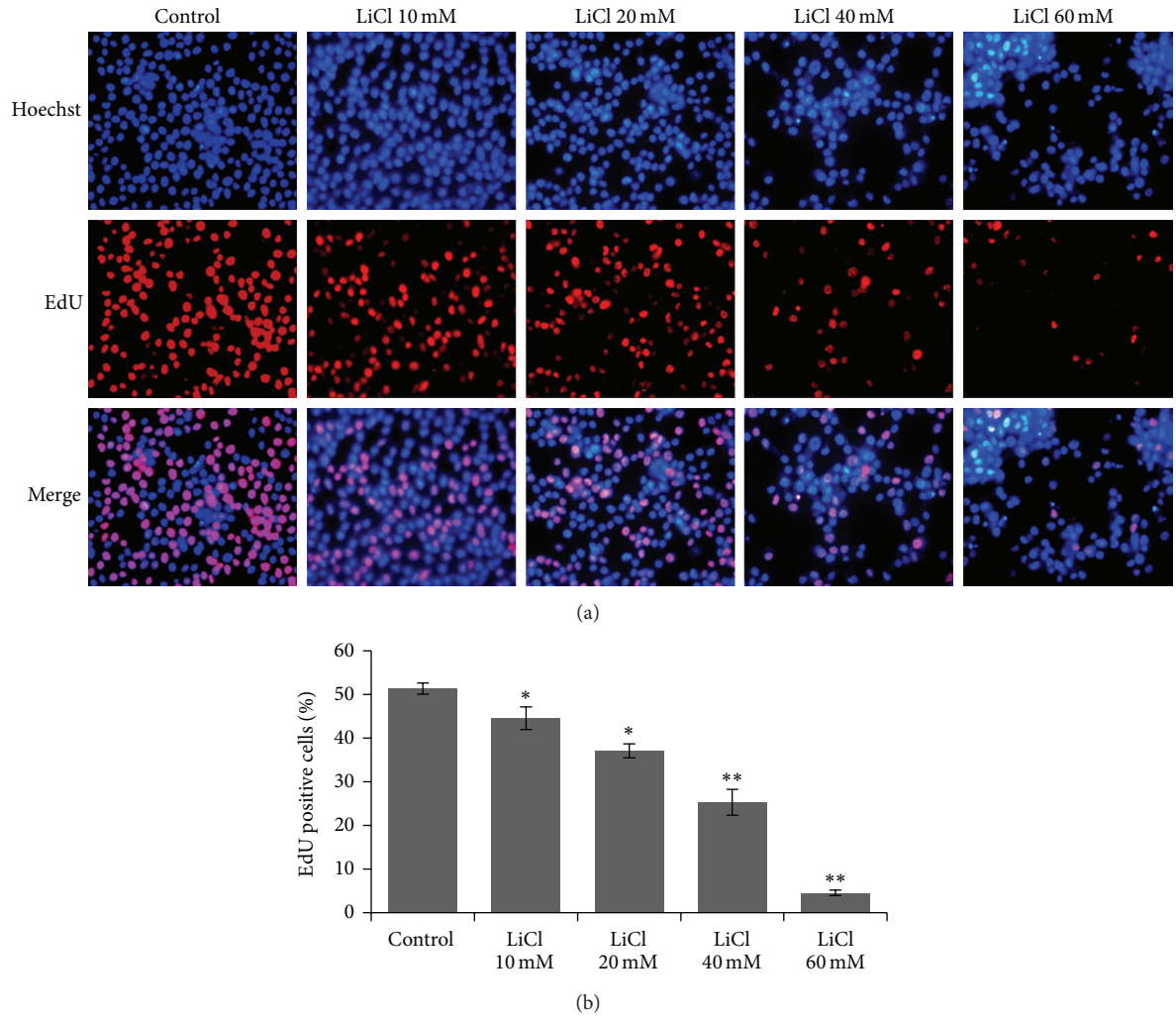

Figure 2: LiCl inhibited proliferation in SW480 cells. Cell proliferation assay was preformed, in which EdU-labeled proliferative cells (red) and Hoechst-stained nuclei (blue) were observed under a fluorescent microscope. Cells were treated with vehicles (PBS) and different concentrations of LiCl (10 mM, 20 mM, 40 mM, and 60 mM), respectively. Data are representative of at least three independent experiments and are expressed as the mean ± SEM. Original magnification, ×100. $^{*}P < 0.05$ and $^{**}P < 0.01$ versus Control group.

3.4. LiCl Stimulated ROS Generation. To explore the underlying mechanism, we measured the levels of intracellular reactive oxidative species (ROS). In H2DCF-DA loaded SW480 cells treated with different concentration of LiCl (10–60 mM), fluorescence intensity increased in a dose dependent manner, suggesting an increase in the generation of ROS (Figure 4). The results showed that LiCl acted as a prooxidant in colon cancer cells.

3.5. Role of GSK-3β in LiCl-Mediated ROS Production. To determine whether LiCl might inhibit GSK-3β activation under the oxidative damage, immunoblot experiments were performed using an antibody directed against GSK-3β and two fractions of phosphor-GSK-3β (Ser9 and Tyr216). This allowed us to detect levels of inactive (phosphorylated Ser9) and active (phosphorylated Tyr216) fractions of GSK-3β, respectively. When LiCl was added to SW480 cells, it was able to increase the levels of phosphorylation at Ser9, while reducing that at Tyr216 of GSK-3β (Figure 5). So it may be reasonable to speculate that GSK-3β inhibition was involved in the prooxidant effects of LiCl.

3.6. LiCl Inhibited GSK-3β Activity and NF-κB Pathway Expression. Multiple factors contribute to colon cancer progression, including activation of NF-κB, whose target genes have an important function in cancer cell survival. As the involvement of GSK-3β in the regulation of NF-κB activity is known to be significant for cancer cell growth, we investigated the levels of NF-κB pathway including Bcl-2 and survivin in LiCl treated SW480 cells. Treating with LiCl decreased NF-κB expression in a concentration dependent manner (Figure 6(a)). Then we determined the effect of LiCl treatment on apoptosis-related proteins in SW480 cells. The expression of the NF-κB-regulated genes Bcl-2 and survivin was decreased by treating with LiCl in a concentration dependent manner too. Real-time PCR and immunoblotting had got the same results (Figures 6(b)–6(d)).

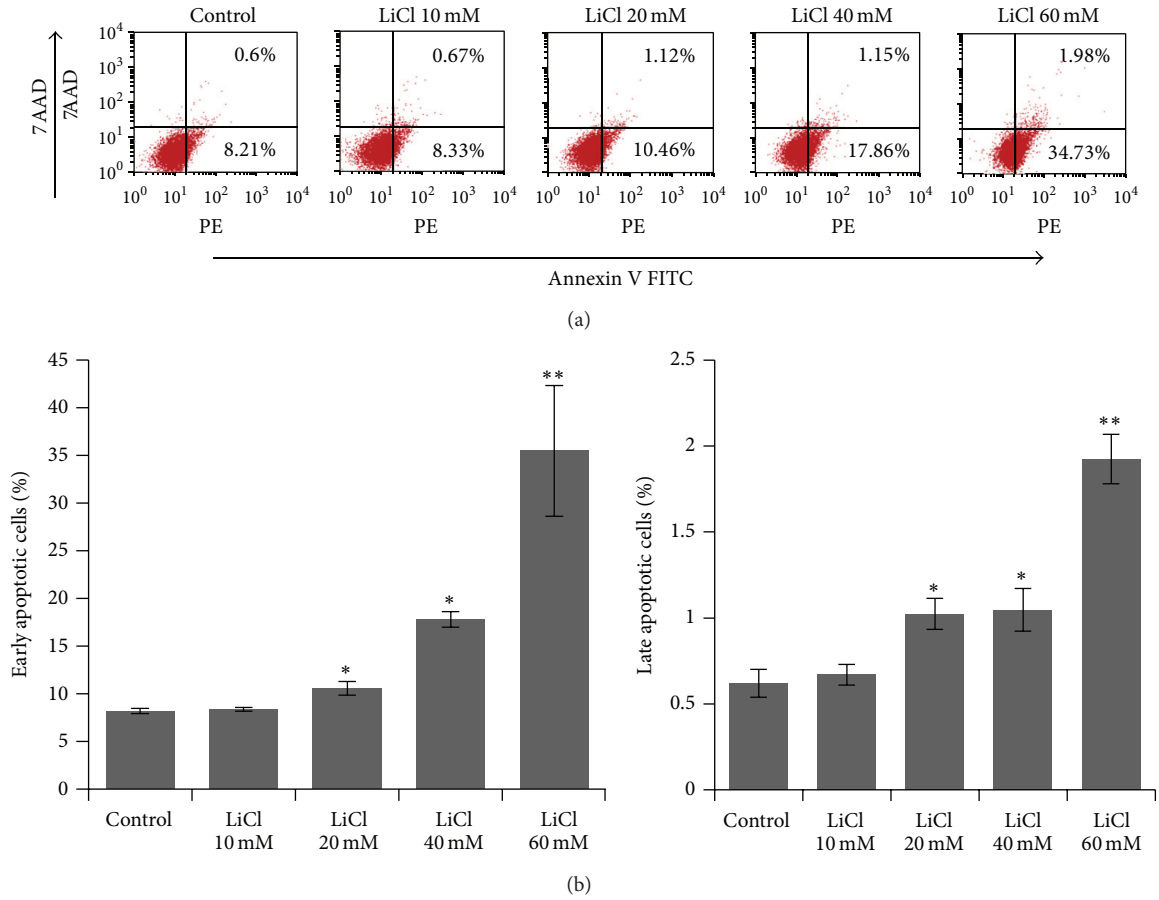

FIGURE 3: Quantification of early and late apoptosis in SW480 cells treated with different concentrations of LiCl for 24 h was determined by flow cytometry. Representative results were from three independent experiments. Data were shown as mean ± SEM. $^{*}P < 0.05$ and $^{**}P < 0.01$ versus Control group.

4. Discussion

The present study showed that LiCl played a critical role in the survival, proliferation, and apoptosis of colorectal cancer cell via the ROS/GSK-3β/NF-κB pathway. Our results suggest that targeting GSK-3β may be of benefit for the therapeutic activity of anticancer drugs against colorectal tumor.

Oxidative stress is an overproduction of reactive oxygen species that overwhelms the cellular antioxidant capacity. So it seems that increased ROS generation and oxidative stress have the central role in lithium cytotoxic mechanism. In our study, we showed for the first time that LiCl exerted the prooxidant effects in colon cancer cells. Previous studies have demonstrated that administration with lithium for 15 minutes significantly increased intracellular ROS levels in rat hepatocytes [12]. On the contrary, another group showed that, following chronic treatment of neuronal cells with lithium, this ion exhibited obvious antioxidant effects [13]. So the role of lithium as well as the implication of GSK-3β in the induction of ROS remains an area of intensive research.

GSK-3 is a pluripotent serine-threonine kinase with numerous intracellular target proteins. GSK-3 isoforms are encoded by distinct genes: GSK-3α and GSK-3β [14]. GSK-3β, known to be a survival factor for cancer, is constitutively activated in colorectal cancer cells. Deregulation of GSK-3β has been implicated in tumorigenesis and cancer progression including that of colorectal cancer [15]. LiCl has been shown to induce cell growth arrest, apoptosis, and terminal differentiation in various human malignant tumors by targeting GSK-3β [16]. So we used LiCl to inhibit the activity of GSK-3β pharmacologically and found the increased generation of ROS, which implied the involvement of ROS in inactivation of GSK-3β in the regulation of cancer development.

NF-κB is an important transcription factor involved in growth arrest and apoptosis by regulating the expression of numerous target genes such as Bcl-2 and survivin [17, 18]. Analysis of Bcl-2 and survivin expression levels had been proved to be a useful diagnostic marker and an important source of prognostic information in cancer. NF-κB activity could be boosted by chemotherapeutic stress, leading to tumor chemoresistance. Inactivation of NF-κB could make cancer cells more sensitive to chemotherapy. Here, we found that inhibition of GSK-3β suppresses NF-κB-mediated expression of Bcl-2 and survivin. So we provided evidence that GSK-3β may serve as a therapeutic target in colorectal cancer.

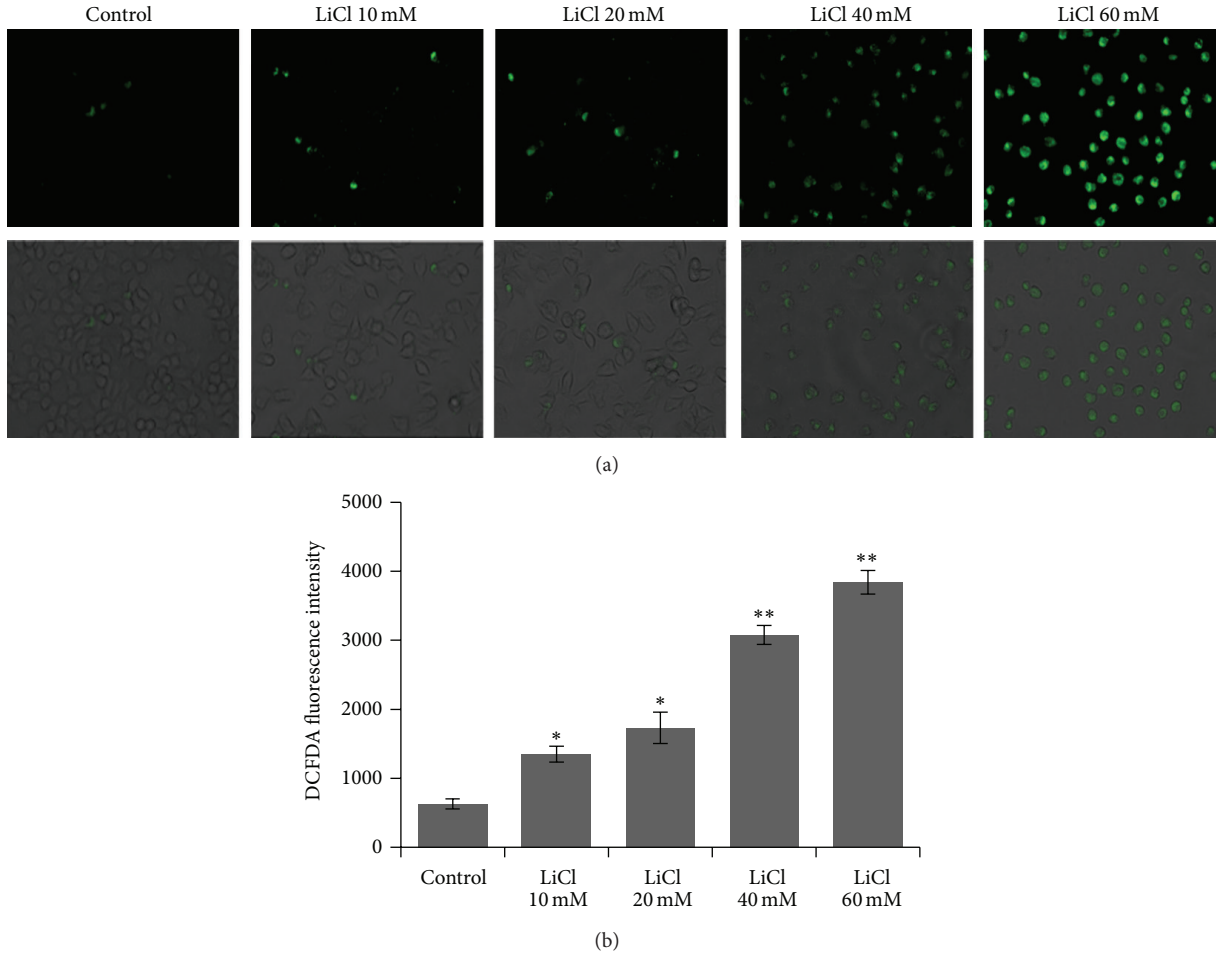

Figure 4: SW480 cells were loaded with a fluorescent probe H2DCF-DA (10 μM) for 20 minutes and observed under fluorescence microscopy. Representative photomicrographs showing ROS within the cytoplasm of cells and merged images showing cell morphology. Fluorescent signals were quantified using a fluorometer at excitation and emission wavelengths of 488 nm and 520 nm, respectively. $^{*}P < 0.05$ and $^{**}P < 0.01$ versus Control group. Original magnification, ×200.

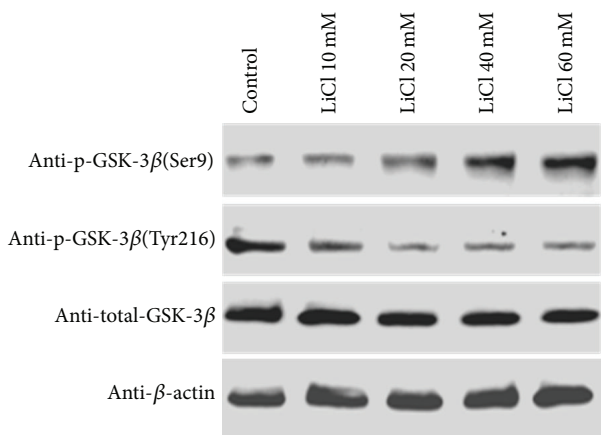

Figure 5: Expression of GSK-3β and presence of phosphor-GSK-3β(Ser9) (inactive form) and phosphor-GSK-3β(Tyr216) (active form) were detected in extracts of SW480 cells treated with LiCl. The amount of protein extract in each sample was monitored by expression of β-actin.

Colorectal cancer is the malignant tumour occurring in the colorectal lumen, and the colorectal lumen can be connected with the outside through the anus. This makes contact with lump body of colorectal cancer and locoregional therapy through colonoscopy or other possible means. This is the difference on the treatment between colorectal cancer and other kinds of tumors. In this study, we treated colorectal cancer cells with high concentration of lithium chloride, as we considered the convenience of local treatment for colorectal tumors. With the help of colonoscopy, implementation of high drug concentration in local areas of tumors in colorectal lumen is possible, which could make drugs contacting with cancer tumors directly, in order to achieve local targeted therapy and reduce side effects to a minimum. In clinical works, local treatment is one of the important approaches of treatments for colorectal cancer, including local chemotherapy. In patients with possible intestinal obstruction, if the symptoms of intestinal obstruction could be relieved before the surgical operation and supplemented by adjuvant chemotherapy, the success rate for surgical treatment and the prognosis of

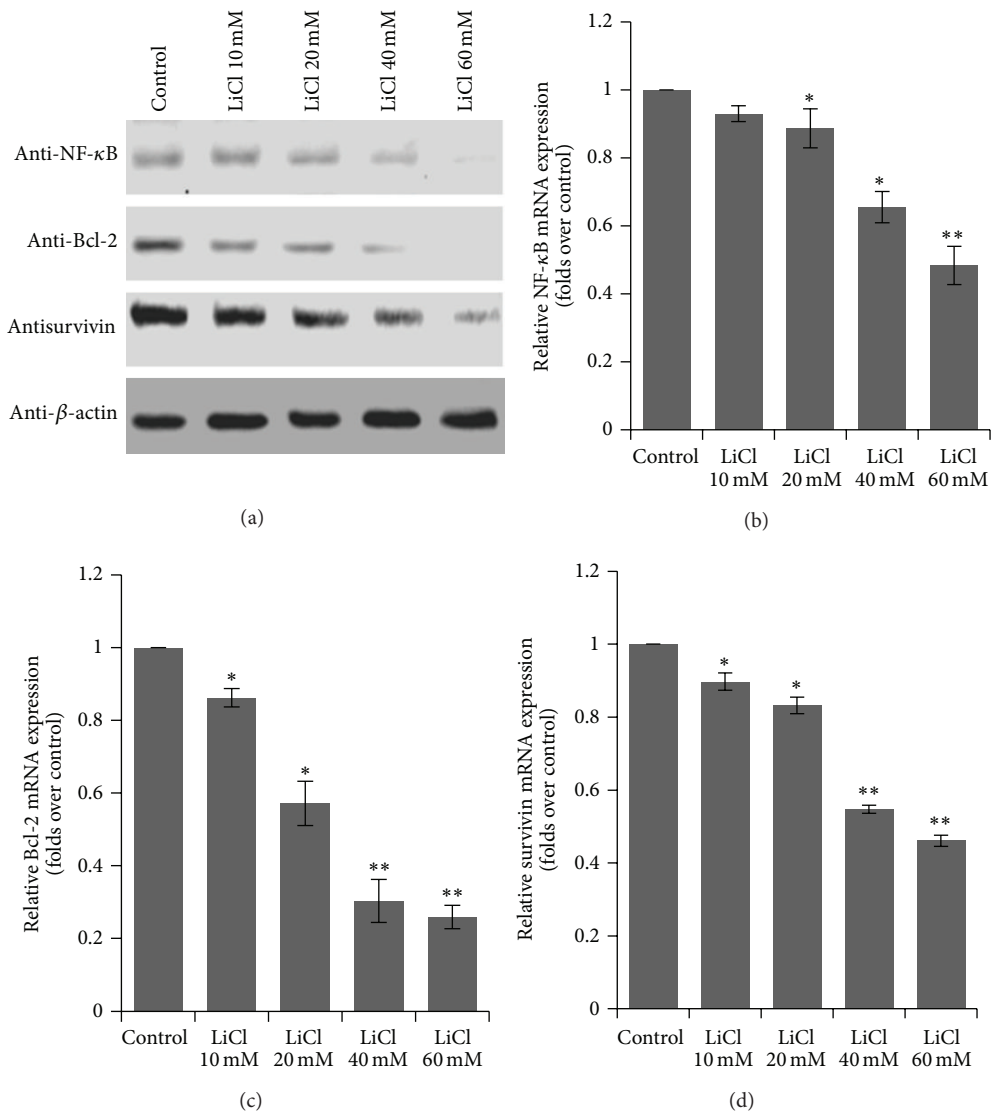

Figure 6: Effect of LiCl on the expression of NF-κB, Bal-2, and survivin protein and mRNA levels. (a) The protein expression of NF-κB, Bal-2, and survivin. (b-c) The mRNA levels of NF-κB, Bal-2, and survivin were analyzed by real-time PCR. The SW480 cells treated with vehicles (PBS) and different concentrations of LiCl (10 mM, 20 mM, 40 mM, and 60 mM), respectively. Data are expressed as mean ± SEM for at least three individual experiments. $^{*}P < 0.05$ and $^{**}P < 0.01$ versus Control group.

patients will be greatly improved. In some other investigators' studies, the use of high doses of lithium chloride had been discussed [19, 20]. For example, Suganthi et al. [20] used lithium chloride with the dose of almost 2 times more than ours to observe the effects on tumor cells. This study suggests that the local release of lithium agent around intestinal tumors could promote the apoptosis of the tumor cells and raise the sensitivity of tumors to chemotherapy drugs, which may achieve the goal of lifting intestinal obstruction and avoid side effects caused by systemic application [21–24].

There are several limitations in our work. Firstly, we did not examine the molecular mechanism of GSK-3β in the regulation of NF-κB signaling. Secondly, our results were obtained from cell lines, while the situation in the patients with colorectal carcinoma may need more investigation.

In summary, we have demonstrated that inhibition of GSK-3β by lithium could induce the production of ROS and suppress the proliferation of colorectal cells by the downregulation of activity of NF-κB and NF-κB-mediated target genes transcription, which may be of benefit for clinical outcome in patients suffering from colon cancer in future.

5. Conclusions

Our work has demonstrated a new mechanism of the GSK-3β inhibitor lithium; this drug could lead to decreased cell survival and proliferation by the ROS/GSK-3β/NF-κB pathway.

Conflict of Interests

The authors declare that they have no conflict of interests.

Authors' Contribution

Li Huili and Huang Kun contributed equally to this work.

Acknowledgment

This work was supported by Natural Science Foundation of Hubei Province (2011CDB378 to Wang Jiliang).

References

[1] F. Mehrkhani, S. Nasiri, K. Donboli, A. Meysamie, and A. Hedayat, "Prognostic factors in survival of colorectal cancer patients after surgery," *Colorectal Disease*, vol. 11, no. 2, pp. 157–161, 2009.

[2] L.-Q. Yang, D.-C. Fang, R.-Q. Wang, and S.-M. Yang, "Effect of NF-κB, survivin, Bcl-2 and Caspase 3 on apoptosis of gastric cancer cells induced by tumor necrosis factor related apoptosis inducing ligand," *World Journal of Gastroenterology*, vol. 10, no. 1, pp. 22–25, 2004.

[3] M. P. Coghlan, A. A. Culbert, D. A. Cross et al., "Selective small molecule inhibitors of glycogen synthase kinase-3 modulate glycogen metabolism and gene transcription," *Chemistry and Biology*, vol. 7, no. 10, pp. 793–803, 2000.

[4] K. P. Hoeflich, J. Luo, E. A. Rubie, M.-S. Tsao, O. Jin, and J. R. Woodgett, "Requirement for glycogen synthase kinase-3β in cell survival and NF-κB activation," *Nature*, vol. 406, no. 6791, pp. 86–90, 2000.

[5] A. V. Ougolkov, N. D. Bone, M. E. Fernandez-Zapico, N. E. Kay, and D. D. Billadeau, "Inhibition of glycogen synthase kinase-3 activity leads to epigenetic silencing of nuclear factor κB target genes and induction of apoptosis in chronic lymphocytic leukemia B cells," *Blood*, vol. 110, no. 2, pp. 735–742, 2007.

[6] A. V. Ougolkov, M. E. Fernandez-Zapico, D. N. Savoy, R. A. Urrutia, and D. D. Billadeau, "Glycogen synthase kinase-3β participates in nuclear factor κB-mediated gene transcription and cell survival in pancreatic cancer cells," *Cancer Research*, vol. 65, no. 6, pp. 2076–2081, 2005.

[7] R. Pardo, A. G. Andreolotti, B. Ramos, F. Picatoste, and E. Claro, "Opposed effects of lithium on the MEK-ERK pathway in neural cells: inhibition in astrocytes and stimulation in neurons by GSK3 independent mechanisms," *Journal of Neurochemistry*, vol. 87, no. 2, pp. 417–426, 2003.

[8] R. J. W. Stump, F. J. Lovicu, S. L. Ang, S. K. Pandey, and J. W. McAvoy, "Lithium stabilizes the polarized lens epithelial phenotype and inhibits proliferation, migration, and epithelial mesenchymal transition," *Journal of Pathology*, vol. 210, no. 2, pp. 249–257, 2006.

[9] A. Sun, I. Shanmugam, J. Song, P. F. Terranova, J. B. Thrasher, and B. Li, "Lithium suppresses cell proliferation by interrupting E2F-DNA interaction and subsequently reducing S-phase gene expression in prostate cancer," *Prostate*, vol. 67, no. 9, pp. 976–988, 2007.

[10] J.-S. Wang, C.-L. Wang, J.-F. Wen, Y.-J. Wang, Y.-B. Hu, and H.-Z. Ren, "Lithium inhibits proliferation of human esophageal cancer cell line Eca-109 by inducing a G2/M cell cycle arrest," *World Journal of Gastroenterology*, vol. 14, no. 25, pp. 3982–3989, 2008.

[11] A. Salic and T. J. Mitchison, "A chemical method for fast and sensitive detection of DNA synthesis in vivo," *Proceedings of the National Academy of Sciences of the United States of America*, vol. 105, no. 7, pp. 2415–2420, 2008.

[12] M. R. Eskandari, J. K. Fard, M.-J. Hosseini, and J. Pourahmad, "Glutathione mediated reductive activation and mitochondrial dysfunction play key roles in lithium induced oxidative stress and cytotoxicity in liver," *BioMetals*, vol. 25, no. 5, pp. 863–873, 2012.

[13] R. S. Jope and G. V. W. Johnson, "The glamour and gloom of glycogen synthase kinase-3," *Trends in Biochemical Sciences*, vol. 29, no. 2, pp. 95–102, 2004.

[14] B. W. Doble and J. R. Woodgett, "GSK-3: tricks of the trade for a multi-tasking kinase," *Journal of Cell Science*, vol. 116, part 14, pp. 1175–1186, 2003.

[15] W. M. de Araújo, F. C. B. Vidal, W. F. de Souza, J. C. M. de Freitas Junior, W. de Souza, and J. A. Morgado-Diaz, "PI3K/Akt and GSK-3β prevents in a differential fashion the malignant phenotype of colorectal cancer cells," *Journal of Cancer Research and Clinical Oncology*, vol. 136, no. 11, pp. 1773–1782, 2010.

[16] Z.-Q. Fu, Y. Yang, J. Song et al., "LiCl attenuates thapsigargin-induced tau hyperphosphorylation by inhibiting GSK-3β in vivo and in vitro," *Journal of Alzheimer's Disease*, vol. 21, no. 4, pp. 1107–1117, 2010.

[17] I. A. Arbab, C. Y. Looi, A. B. Abdul et al., "Dentatin induces apoptosis in prostate cancer cells via Bcl-2, Bcl-xL, Survivin downregulation, caspase-9, -3/7 activation, and NF-κB inhibition," *Evidence-Based Complementary and Alternative Medicine*, vol. 2012, Article ID 856029, 15 pages, 2012.

[18] J. P. Cao, H. Y. Niu, H. J. Wang, X. G. Huang, and D. S. Gao, "NF-kappaB p65/p52 plays a role in GDNF up-regulating Bcl-2 and Bcl-w expression in 6-OHDA-induced apoptosis of MN9D cell," *International Journal of Neuroscience*, vol. 123, no. 10, pp. 705–710, 2013.

[19] H.-R. Tang and Q. He, "Effects of lithium chloride on the proliferation and apoptosis of K562 leukemia cells," *Hunan Yi Ke Da Xue Xue Bao*, vol. 28, no. 4, pp. 357–360, 2003.

[20] M. Suganthi, G. Sangeetha, G. Gayathri, and B. Ravi Sankar, "Biphasic dose-dependent effect of lithium chloride on survival of human hormone-dependent breast cancer cells (MCF-7)," *Biological Trace Element Research*, vol. 150, no. 1–3, pp. 477–486, 2012.

[21] P. A. Sabancı, M. Ergüven, N. Yazıhan et al., "Sorafenib and lithium chloride combination treatment shows promising synergistic effects in human glioblastoma multiforme cells in vitro but midkine is not implicated," *Neurological Research*, vol. 36, no. 3, pp. 189–197, 2014.

[22] J. T. Adler, D. G. Hottinger, M. Kunnimalaiyaan, and H. Chen, "Combination therapy with histone deacetylase inhibitors and lithium chloride: a novel treatment for carcinoid tumors," *Annals of Surgical Oncology*, vol. 16, no. 2, pp. 481–486, 2009.

[23] A. Bilir, M. Erguven, N. Yazihan, E. Aktas, G. Oktem, and A. Sabanci, "Enhancement of vinorelbine-induced cytotoxicity and apoptosis by clomipramine and lithium chloride in human neuroblastoma cancer cell line SH-SY5Y," *Journal of Neuro-Oncology*, vol. 100, no. 3, pp. 385–395, 2010.

[24] M. O. Nowicki, N. Dmitrieva, A. M. Stein et al., "Lithium inhibits invasion of glioma cells; possible involvement of glycogen synthase kinase-3," *Neuro-Oncology*, vol. 10, no. 5, pp. 690–699, 2008.

Hindawi Publishing Corporation
Oxidative Medicine and Cellular Longevity
Volume 2014, Article ID 653732, 12 pages
http://dx.doi.org/10.1155/2014/653732

Research Article

Piperlongumine Inhibits Migration of Glioblastoma Cells via Activation of ROS-Dependent p38 and JNK Signaling Pathways

Qian Rong Liu,[1] Ju Mei Liu,[1] Yong Chen,[1] Xiao Qiang Xie,[1] Xin Xin Xiong,[1] Xin Yao Qiu,[1] Feng Pan,[1,2] Di Liu,[2] Shang Bin Yu,[1] and Xiao Qian Chen[1]

[1] *Department of Pathophysiology, School of Basic Medicine, Key Laboratory of Neurological Diseases, Ministry of Education and Hubei Provincial Key Laboratory of Neurological Diseases, Tongji Medical College, Huazhong University of Science and Technology, Wuhan 430030, China*
[2] *Department of Urology, Union Hospital, Huazhong University of Science and Technology, Wuhan 430022, China*

Correspondence should be addressed to Xiao Qian Chen; chenxiaoqian66@gmail.com

Received 14 February 2014; Revised 21 April 2014; Accepted 25 April 2014; Published 22 May 2014

Academic Editor: Si Jin

Piperlongumine (PL) is recently found to kill cancer cells selectively and effectively via targeting reactive oxygen species (ROS) responses. To further explore the therapeutic effects of PL in cancers, we investigated the role and mechanisms of PL in cancer cell migration. PL effectively inhibited the migration of human glioma (LN229 or U87 MG) cells but not normal astrocytes in the scratch-wound culture model. PL did not alter EdU^+-cells and cdc2, cdc25c, or cyclin D1 expression in our model. PL increased ROS (measured by DCFH-DA), reduced glutathione, activated p38 and JNK, increased IκBα, and suppressed NFκB in LN229 cells after scratching. All the biological effects of PL in scratched LN229 cells were completely abolished by the antioxidant N-acetyl-L-cysteine (NAC). Pharmacological administration of specific p38 (SB203580) or JNK (SP600125) inhibitors significantly reduced the inhibitory effects of PL on LN229 cell migration and NFκB activity in scratch-wound and/or transwell models. PL prevented the deformation of migrated LN229 cells while NAC, SB203580, or SP600125 reversed PL-induced morphological changes of migrated cells. These results suggest potential therapeutic effects of PL in the treatment and prevention of highly malignant tumors such as glioblastoma multiforme (GBM) in the brain by suppressing tumor invasion and metastasis.

1. Introduction

Reactive oxygen species (ROS) plays a crucial role in the processes of tumor genesis, progression, and metastasis. Cancer cells usually possess higher levels of ROS and higher antioxidant activities in an uncontrolled status as compared to normal cells [1]. As a result, cancer cells are unable to cope with additional oxidative stress and become vulnerable to ROS [2, 3]. Therefore, targeting ROS is an important therapeutic strategy for cancer as exemplified by cancer drugs such as daunorubicin [4], vincristine [5], paclitaxel, docetaxel, and 2-methoxyestradiol [6]. Exploring the mechanisms of ROS-based treatment is required for further improving the efficacy and specificity of cancer drugs [3].

Piperlongumine (piplartine, PL), a primary constituent of *Piper longum* (long pepper), exists in the fruits and roots of the plant [7]. It is reported that PL possesses analgesic [8], antidepressant [9], cardioprotective [10], antiplatelet [11, 12], anti-inflammatory [13], and antiatherosclerotic [14] effects. Recently, PL is identified as a highly selective cytotoxic compound for cancer cells but not normal cells [15]. PL directly binds to and inhibits the antioxidant enzyme glutathione S-transferase pi 1 (GSTP1), resulting in elevated levels of ROS and subsequent cancer-selective cell death [15]. Accumulating evidence has suggested that PL might be a potential chemotherapeutic in human cancer [15–18].

Metastasis is the main cause of mortality in cancer while the key process of metastasis is the migration of cancer cells to invade adjacent tissues [19, 20]. Glioblastoma multiforme (GBM), a grade IV astrocytoma, is the most common and most aggressive malignant primary brain tumor in humans with a median survival time of less than 14 months after

routine radiation therapy and chemotherapy following resection [21]. Due to the confined space of the brain and highly integrity of neuronal-astrocytic interactions, the invasion of glioma cells is particularly devastating. We have recently reported that PL can selectively kill GBM cells but not normal astrocytes [22]. To further explore the therapeutic or preventive effects of PL in GBM, we investigated the biological effects and mechanisms of PL in GBM cell migration.

In this study, we demonstrated that PL inhibited GBM cell migration effectively. The mechanisms of PL's action included ROS accumulation, p38 and JNK activation, and NFκB nuclear translocation.

2. Materials and Methods

2.1. Reagents. Piperlongumine (PL), N-acetyl-L-cysteine (NAC), 2,7-dichlorodihydrofluorescein diacetate (DCFH-DA), and Hoechst 33342 were purchased from Sigma-Aldrich (St. Louis, MO, USA). SB203580 and SP600125 were purchased from Cell Signaling Technology, Inc. (Danvers, MA, USA). DMEM and fetal bovine serum (FBS) were purchased from Life Technologies, Inc. (Grand Island, NY, USA). Antibodies against NFκB p65, IκBα, glyceraldehyde-3-phosphate dehydrogenase (GAPDH), and β-actin were purchased from Santa Cruz Biotechnology (Heidelberg, Germany), and the antibodies against p-p38, total p38, p-JNK, and total-JNK were from Cell Signaling Technology.

2.2. Cell Culture and Drug Treatments. Human GBM cell lines LN229 and U87 MG (U87) were kindly provided by Prof. Haian Fu (Emory University, GA, USA) and were cultured in DMEM containing 5% or 10% FBS, respectively. Primary cultures of rat cerebral cortical astrocytes were cultured as described previously [23]. All cells were maintained in a humidified atmosphere of 95% air and 5% CO_2 at 37°C.

PL was dissolved in dimethyl sulfoxide (DMSO) at a stock concentration of 50 mM. The final concentration of PL was 0–20 μM with a maximal DMSO concentration less than 0.05%. DMSO of the same concentration in PL solutions was used as the vehicle control. The antioxidant NAC (3 mM), SB203580 (p38 pathway specific inhibitor, 10 μM), and SP600125 (JNK pathway specific inhibitor, 10 μM) were added 2 h before PL treatment.

2.3. Scratch-Wound Culture Model and Cell Migration Assay. Cancer cells were planted in a 35 mm dish and incubated for 24 h to form a monolayer with confluence. For wound-healing study, monolayer cells were scratched with a 200 μL pipette tip and the wound edges were micrographed and were treated with PL immediately; then the wound edges were remicrographed 24 h after PL treatment. To investigate the earlier cell migration (3 or 6 h) after scratching, GBM cells were pretreated with PL for 6 h and then monolayer cells were scratched. After the wounded edges were micrographed immediately after scratching, the cultures were incubated for another 3 or 6 h in DMEM containing 20% FBS [24]. Cells were then fixed with 4% paraformaldehyde for 30 min, stained by Hoechst 33342, and micrographed. The width of wound (i.e., the gap between the two opposite wound edges) was measured using the Image-Pro Plus software. The relative migration rate was calculated by the reduction of the wound width between immediately after scratch and 6 h after scratch. This value reflects the distance migrated by the leading edge of the wound during the given time interval.

2.4. Measurement of ROS. Intracellular ROS production was determined by 2,7-dichlorodihydrofluorescein diacetate (DCFH-DA) staining followed by fluorescent microscope [22]. Briefly, cells were incubated with 10 μM DCFH-DA solution at 37°C for 0.5 h, washed with PBS twice, and photographed under a conventional fluorescent microscope (Olympus, Tokyo, Japan). For each culture, a minimum of 9 random fields were captured.

2.5. Measurement of Reduced Glutathione. Treated cells were washed twice with PBS, scraped off the plates, and then subjected to sonication. Protein concentration was assessed by using bicinchoninic acid assay kit (Beyotime, Nantong, China) and reduced glutathione (GSH) was measured by using a kit (Nanjing Jiangcheng Bioengineering Institute, Nanjing, China) according to the manufacturer's instructions. Results are expressed as μmol of GSH per gram of protein (μmol/g prot) [25].

2.6. Western Blot Analysis. Western blot analysis was performed as described previously [26, 27]. Briefly, cells were seeded in 35 mm dishes and incubated for 24 h. After PL treatment for 6 h, cells were scratched and incubated in DMEM supplemented with 20% FBS for another 3 h. For the whole cell lysates, the cells were gathered in RIPA lysis buffer (Beyotime, Nantong, China) and sonicated. The supernatants were removed as protein samples after centrifugation. Cytosolic and nuclear extract were isolated by using a kit from Sangon Biotech (Shanghai, China) according to the manufacturer's instructions. Equal amounts of total soluble proteins were subjected to western blot analysis. The blots were visualized with corresponding fluorescent secondary antibodies and the bands were quantified by using the Odyssey Infrared Imaging System (LI-COR Bioscience, USA).

2.7. Transwell Cell Migration Assay. LN229 cells were seeded at the concentration of 1×10^5 per well into the upper chamber of a transwell apparatus with an 8 μm pore size membrane (BD Bioscience, NJ, USA) in DMEM containing drugs of determined concentration. The medium of lower chamber was changed to DMEM containing 10% FBS 6 h after the initial cell seeding. After another 24 h incubation, cells remaining in the upper surface of the filter were scraped off with cotton swabs. Cells migrating to the lower surface of the filter were stained with Giemsa, examined by microscopy, and photographed. The migrated cell number was expressed as the average number of migrated cells per microscopic field (×50) over seven fields.

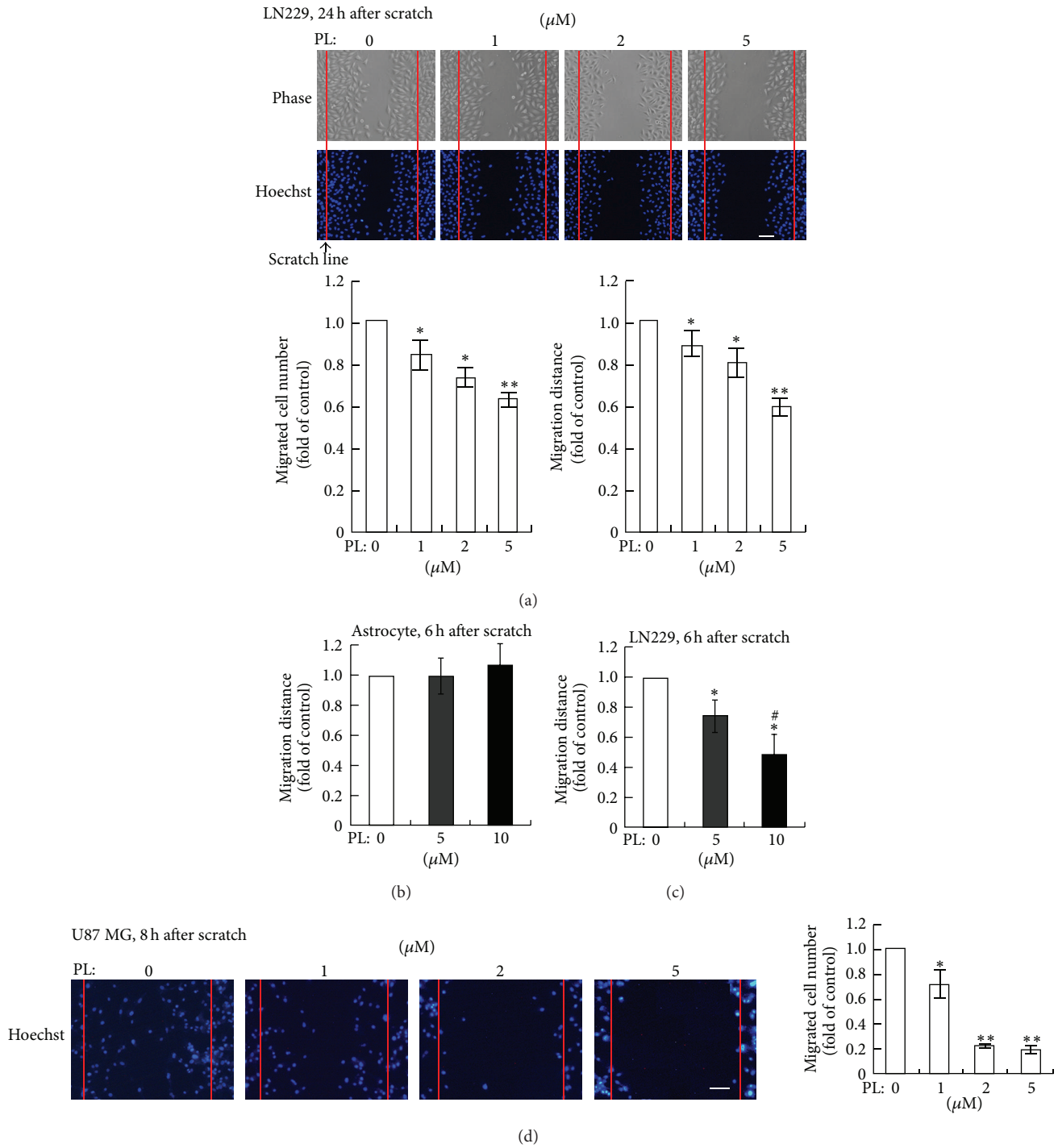

Figure 1: PL inhibits migration of GBM cells but not normal astrocytes in scratch-wound assay in vitro. (a) Effects of PL on wound-healing 24 h after scratch in LN229 cells. LN229 cells in confluence were scratched, washed twice with DMEM, and then treated with different concentration (0, 1, 2, or 5 μM) of PL for 24 h. The cultures were fixed and stained with Hoechst 33342. The red lines indicated the scratch lines. The number of migrated cells between the opposite scratch lines was counted and the distance migrated by the cells at the leading edge was measured. $^{*}P < 0.05$ and $^{**}P < 0.01$ compared to group of 0 μM of PL. (b) Effects of PL on cell migration in primary cultured astrocytes. Cultured astrocytes in confluence were treated with different concentration (0, 5, or 10 μM) of PL for 6 h before cell scratch. The migration distance was measured 6 h after scratching. (c) Effects of PL on cell migration in LN229 cells. Migration of LN229 cells was measured 6 h after scratching upon PL treatment. $^{*}P < 0.05$ compared to group of 0 μM of PL; $^{\#}P < 0.05$ compared to group of 5 μM of PL. (d) Effects of PL on cell migration in U87 MG cells at 8 h after scratching upon PL pretreatment. $^{*}P < 0.05$ and $^{**}P < 0.01$ compared to group of 0 μM of PL. Bar: 50 μm.

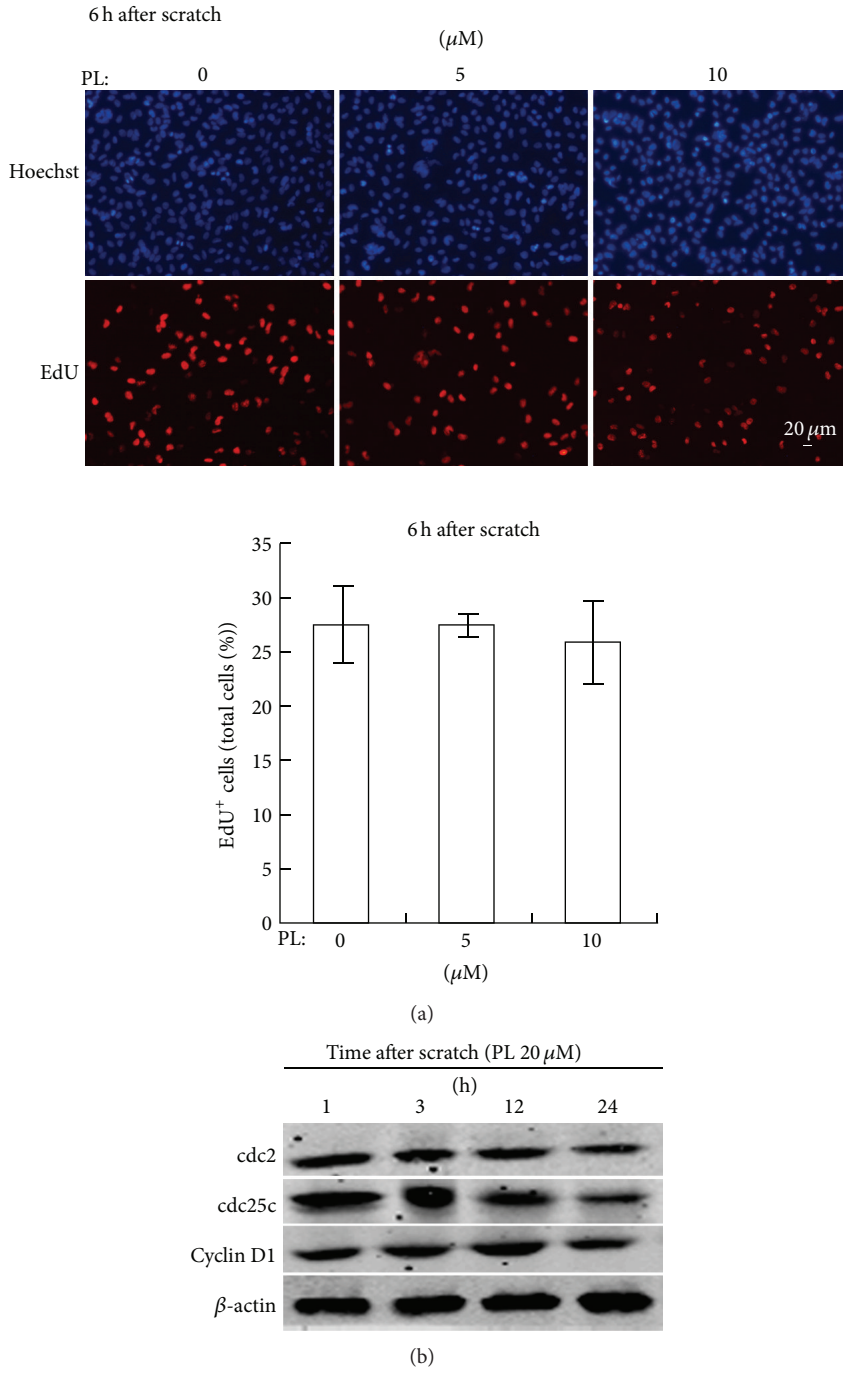

Figure 2: Effects of PL on cell proliferation in LN229 cells. (a) Effects of PL on EdU^+-stained cells at 6 h after scratching upon PL treatment. (b) Representative western blot results of cdc2, cdc25c, and cyclin D1 at various time points (1, 3, 12, and 24 h) after scratching upon 20 μM of PL treatment in LN229 cells. β-actin was used as a loading control.

2.8. EdU (5′-Ethynyl-2′-deoxyuridine) Labeling. LN229 cells (2×10^5) were plated in each well of 12-well plates. EdU (10 μM) from the EdU Kit (Ribobio, Guangzhou, China) was used for labeling according to the manufacturer's instructions as reported previously [27].

2.9. Statistical Analyses. All experiments were repeated independently at least three times. The values were expressed as mean ± SEM and statistics were performed with a 2-way ANOVA followed by the Student-Newman-Keuls test. P values of less than 0.05 were considered statistically significant.

3. Results

3.1. PL Inhibits Migration of GBM Cells but Not Normal Astrocytes in Cultures after Scratch. We tested the effects

of PL on cell migration in GBM cell lines by using the well-known scratch-wound model. After confluent LN229 cells were scratched (the scratch line was indicated by the red line in Figure 1(a), upper panels), PL was administrated immediately. Clearly, the cell numbers and the migration distances were decreased between the opposite scratch lines at 24 h after scratching at various concentrations (1, 2, or 5 μM) of PL (Figure 1(a)). To reduce the effect of cell proliferation after scratching, cell migration was measured at 6 h after scratching with PL pretreatment (6 h before scratching). In normal cultured astrocytes (3-4 weeks in cultures), PL at 5 and 10 μM did not affect the migration of astrocytes (Figure 1(b)). In LN229 cells, PL significantly reduced the migration distance of LN229 cells in a dose-dependent manner (0, 5, and 10 μM) (Figure 1(c)). Since PL at 5 and 10 μM does not cause cell death of GBM cells or astrocytes within 6 h [22], these data revealed a selective inhibitory effect of PL on the migration of GBM cells.

In addition to LN229 cells, we examined the effect of PL on cell migration in another GBM cell line, which are U87 MG cells. Results of Hoechst staining clearly showed that migrated cells were reduced evidently at 8 h after scratching upon various concentrations (1, 2, and 5 μM) of PL (Figure 1(d), upper panels). Statistical analysis demonstrated that PL significantly reduced the numbers of migrated U87 cells in a dosage-dependent manner (Figure 1(d), lower panel).

3.2. Effects of PL on LN229 Cell Proliferation. To exclude the possible effects of cell proliferation after scratching and PL treatment in our assay, we measured newly divided LN229 cells at 6 h after scratching with PL pretreatment. Results of EdU staining demonstrated that the percentage of EdU^+-stained cells (representing newly divided cells) was not altered at 6 h after scratching upon 5 or 10 μM of PL (Figure 2(a)). Further, results of western blot showed that expression of cell cycle-associated proteins such as cdc2, cdc25C, and cyclin D1 was not altered evidently at 1, 3, or 12 h after scratching upon 20 μM PL (Figure 2(b)). These evidences suggested that cell migration but not cell cycle or cell proliferation was the major factor contributing to the reduced migrated cells in the scratched area upon PL treatment within the time-scale in our model.

3.3. PL Inhibits GBM Cell Migration via ROS Accumulation. Since PL exhibited a selective inhibitory effect on GBM cell migration, we further investigated its underlying mechanisms. Previous studies have suggested that PL exerts its anticancer effects via increasing ROS [15, 22, 28, 29]; we speculated that PL might suppress GBM cell migration via inducing ROS. LN229 cells in confluence were treated with PL immediately after cell scratch and intracellular ROS was detected by specific ROS marker DCFH-DA. The fluorescent intensities of DCFH-DA (representing intracellular ROS levels) were evidently enhanced in LN229 cells along the scratch line (indicated by the red line) 3 h after PL treatment (10 and 20 μM) (Figure 3(a)). Pretreatment of antioxidant NAC (3 mM) reduced DCFH-DA fluorescence to the control level (PL 0 μM) (Figure 3(a)). Consistent to the increase of ROS, treatment with PL for 3 h significantly reduced cellular GSH levels in scratched LN229 cells in a dosage-dependent manner (Figure 3(b)). The reduction of GSH by PL was completely reversed in the presence of NAC (Figure 3(b)). These data demonstrated that PL induced ROS accumulation in scratched LN229 cells.

We then tested whether ROS accumulation contributed to the PL-inhibited cell migration in LN229 cells. Morphological micrographs (phase) and nuclear staining (Hoechst) clearly showed that LN229 cells were migrating toward the nude areas of wound from the scratch edges (indicated by red lines) and cell numbers were increased in the wound areas 6 h after scratch (Figure 3(c)). PL at 10 μM evidently reduced cell migration and the migrated cells (Figure 3(c)). NAC completely reversed the inhibitory effects of PL on LN229 cell migration (Figure 3(c)). Statistical analysis demonstrated that the migration distance of LN229 cells was significantly reduced by PL (10 μM) but this effect was completely abolished by NAC (Figure 3(c)). These data demonstrated that PL suppressed LN229 cell migration via ROS accumulation.

3.4. PL Suppresses LN229 Cell Migration via ROS-Dependent p38 and JNK Activation. To address how ROS accumulation causes PL-suppressed LN229 cell migration, we analyzed the effects of PL on p38 and JNK activation, two classical ROS-activated signaling pathways, in scratched LN229 cells. Western blot demonstrated that PL significantly increased the levels of p-p38 and p-JNK in a dosage-dependent manner in LN229 cells 3 h after scratch while the scratch injury itself did not alter p-p38 and p-JNK levels (Figures 4(a) and 4(b)). Pretreatment of NAC completely abolished the PL-induced p38 and JNK activation (Figures 4(a) and 4(b)). We then tested whether the activation of p38 and JNK contributed to the effects of PL on LN229 cell migration. Pretreatment of SB203580 and SP600125 increased LN229 cell migration 6 h after cell scratch (Figure 4(c)). Statistical analysis demonstrated that the inhibition of both p38 and JNK pathways significantly increased the migration distance of LN229 cells upon PL treatment (Figure 4(d)).

Further, we verified the effects of PL, NAC, p38, and JNK inhibitors on LN229 cell migration in another cell migration model, that is, the transwell migration assay. The results demonstrated that the numbers of LN229 cells migrating through the transwell were significantly reduced 24 h after PL treatment (5 and 10 μM) (Figures 5(a) and 5(b)). Pretreatment of NAC, SB203580, or SP600125 significantly increased the migrated LN229 cells in the presence of PL (10 μM) (Figures 5(a) and 5(b)). Concomitantly, the morphology of LN229 cells was changed from spindle shape with long processes to elliptical shape without evident process (enlarged micrographs in Figure 5(c)). Pretreatment of NAC, SB203580, or SP600125 resumed the spindle shape of migrated LN229 cells in the presence of PL (Figure 5(c)).

3.5. PL Inactivates NFκB via ROS, p38, and JNK-Mediated Signaling. Since NFκB is heavily involved in cancer metastasis and is considered to be a downstream target of ROS,

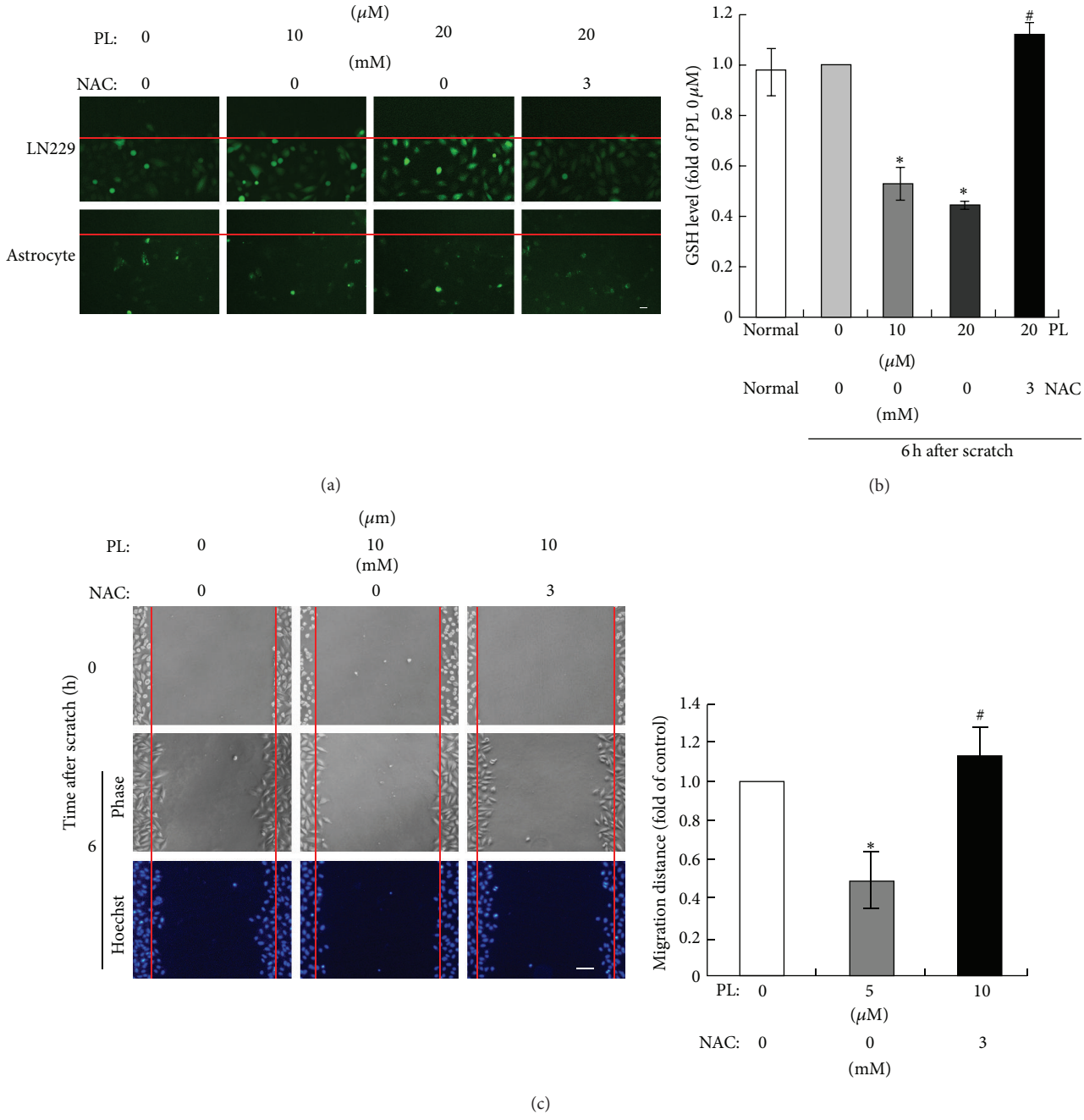

Figure 3: PL suppresses migration of LN229 cells via ROS accumulation. (a) PL increased ROS levels in LN229 cells but not in astrocytes after scratch. LN229 cells or cultured astrocytes were scratched and then treated with 0, 10, or 20 μM PL for 3 h and then stained with DCFH-DA. NAC (3 mM) was administrated 2 h before cell scratch. Representative micrographs showed that the fluorescent intensity of DCFH-DA was enhanced after PL treatment. The red lines indicated the initial edges of scratches. Bar: 20 μm. (b) PL reduced GSH in LN229 cells after scratch. LN229 cells were scratched and then treated with 0, 10, or 20 μM PL for 3 h and the cellular GSH level was measured. Normal, unscratched cultures without PL treatment. $^{*}P < 0.05$ compared to group of 0 μM of PL; $^{\#}P < 0.05$ compared to group of 20 μM of PL. (c) Effects of PL and NAC on LN229 cell migration after cell scratch. The red lines indicated the initial edges of scratches. Bar: 50 μm. $^{*}P < 0.05$ compared to group of DMSO; $^{\#}P < 0.05$ compared to group of 10 μM of PL.

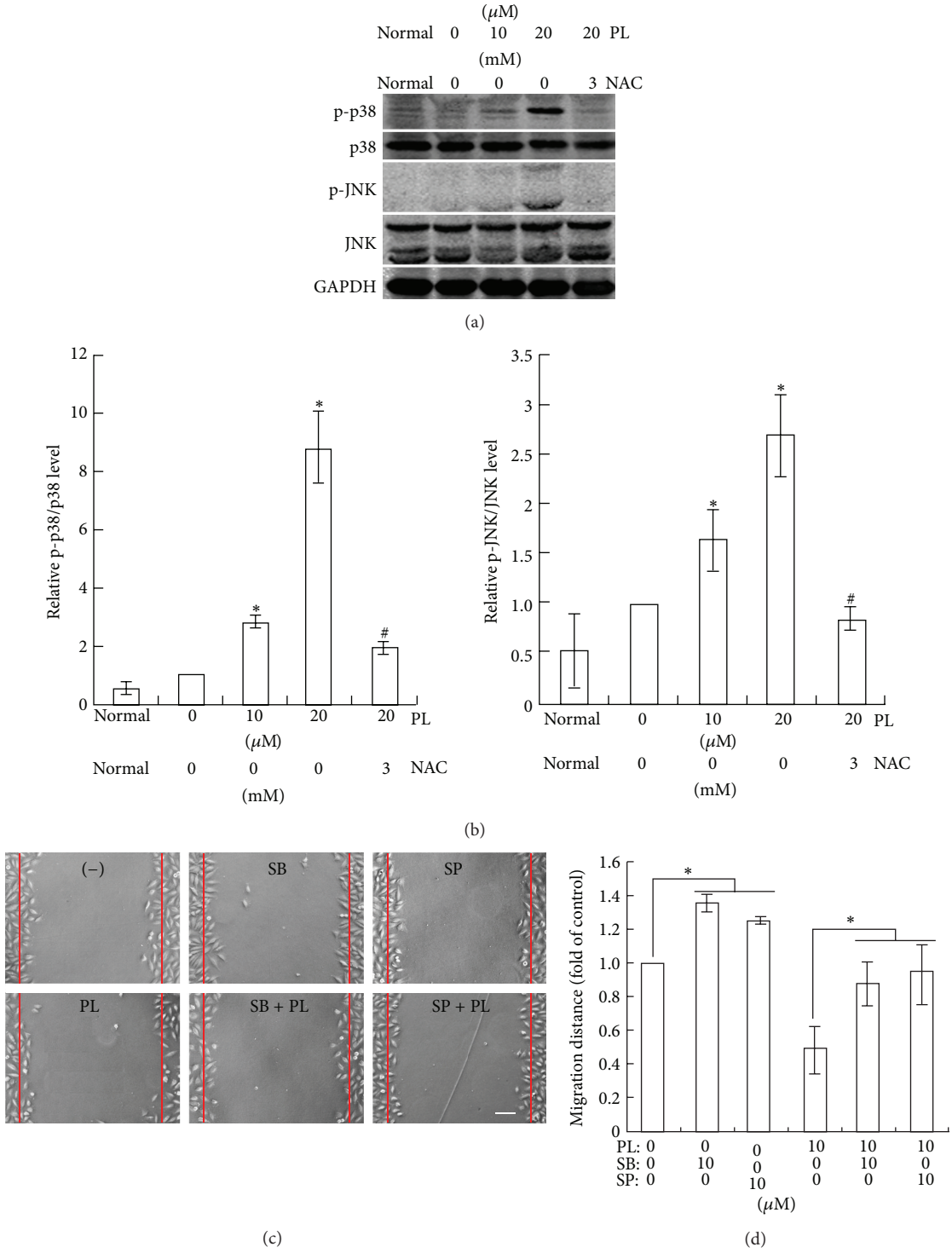

Figure 4: Activation of p38 and JNK by ROS accumulation contributes to PL's effect on LN229 cell migration. (a) Representative western blots of JNK and p38 phosphorylation at 3 h after scratch in PL-treated LN229 cells. GAPDH was used as a loading control. (b) Statistical analysis of p38 and JNK phosphorylation of western blot results. Normal, unscratched cultures without PL treatment. $^{*}P < 0.05$ compared to group of 0 μM of PL; $^{\#}P < 0.05$ compared to group of 20 μM of PL treatment alone. (c) Representative micrographs showing the effects of PL on LN229 cell migration at 6 h after scratch in the presence of PL, SB203580, or SP600125. SB203580 (10 μM) and SP600125 (10 μM) were administrated 2 h before PL treatment. Bar: 50 μm. (d) Statistical analysis of migrated distance of LN229 cells upon PL, SB203580, or SP600125. $^{*}P < 0.05$.

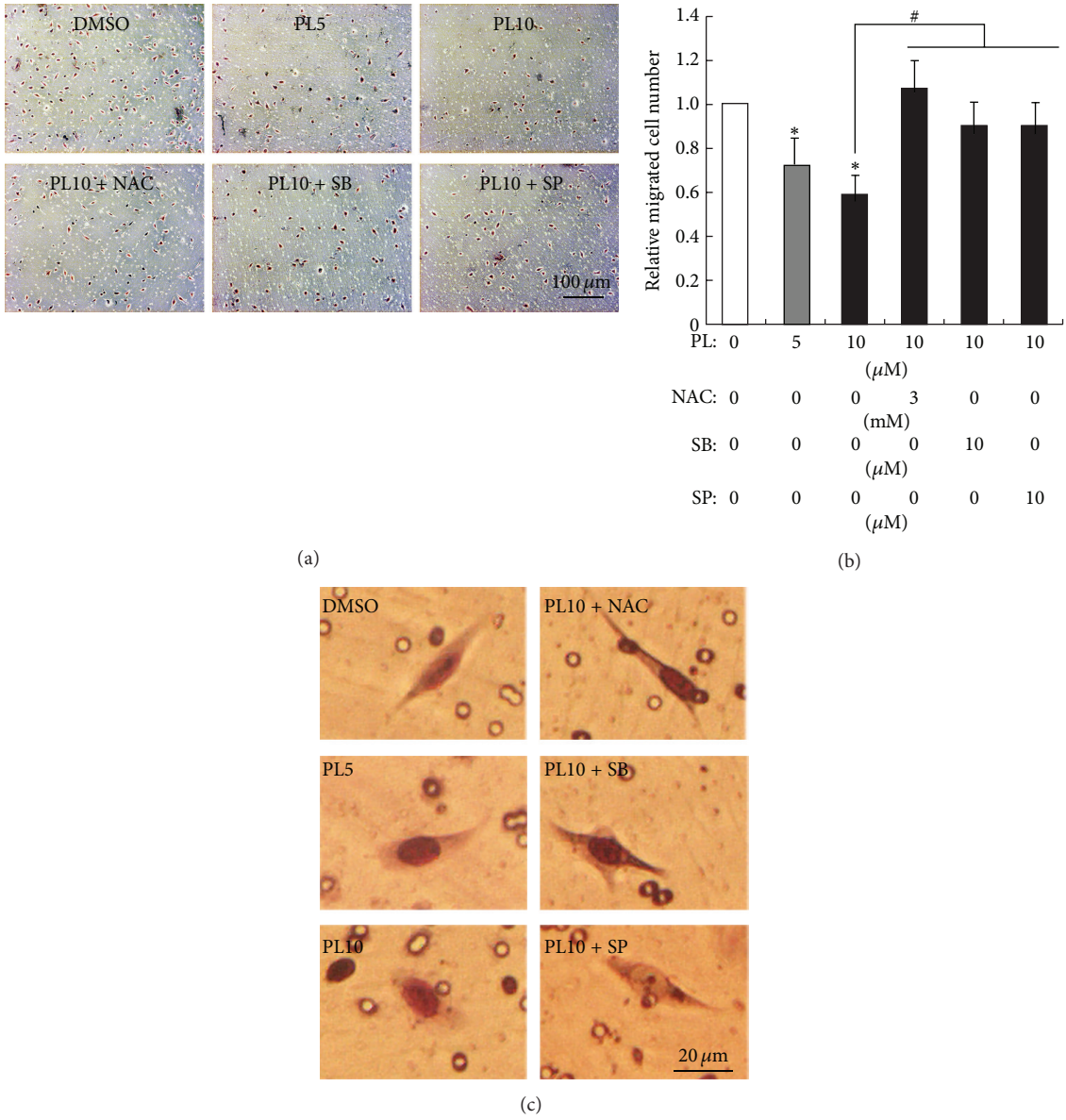

Figure 5: Effects of PL on LN229 cell migration in transwell cell migration assay. (a) Representative micrographs show the effects of PL on LN229 cell migration and the cell morphology of migrated LN229 cells. LN229 cells were seeded into the upper chamber of transwell apparatus in DMEM containing PL (0, 5, or 10 μM) together with or without NAC (3 mM), SB203580 (10 μM), or SP600125 (10 μM). The medium in the lower chamber was replaced with DMEM containing 10% FBS in order to induce cell migration 6 h after PL incubation. Migrated cells in the lower surface of the filter were stained and microphotographed 24 h after cell migration induction by serum. (b) Statistical analysis of migrated cell numbers in different groups. $^{*}P < 0.05$ compared to group of 0 μM of PL (DMSO); $^{\#}P < 0.05$ compared to group of 10 μM of PL treatment alone. (c) Morphology of migrated LN229 cells at higher magnification.

p38, and JNK, we analyzed the nuclear translocation of NFκB and the expression of IκBα, which binds to NFκB and retains it in the cytoplasm. Results of western blot clearly showed that IκBα and cytoplasmic NFκB (cyto NFκB) were evidently increased in LN229 cells at 3 h after scratching upon 10 or 20 μM PL while nuclear NFκB (nuc NFκB) was decreased as compared to vehicle control (0 μM PL) (Figure 6(a)). Administration of NAC completely reversed the effects of PL on the IκBα and cyto/nuc NFκB expression while inhibitors of p38 (SB203580) or JNK (SP600125) partially attenuated PL's effects (Figure 6(a)). Statistical analysis demonstrated that relative nuc/cyto NFκB ratio (representing NFκB activity) was significantly reduced by PL while NAC, SB203580, or SP600125 could reverse PL's effect on NFκB nuclear translocation (Figure 6(b)).

4. Discussion

In the present study, we have demonstrated that PL is effective in suppressing the migration of GBM cells. This anticancer

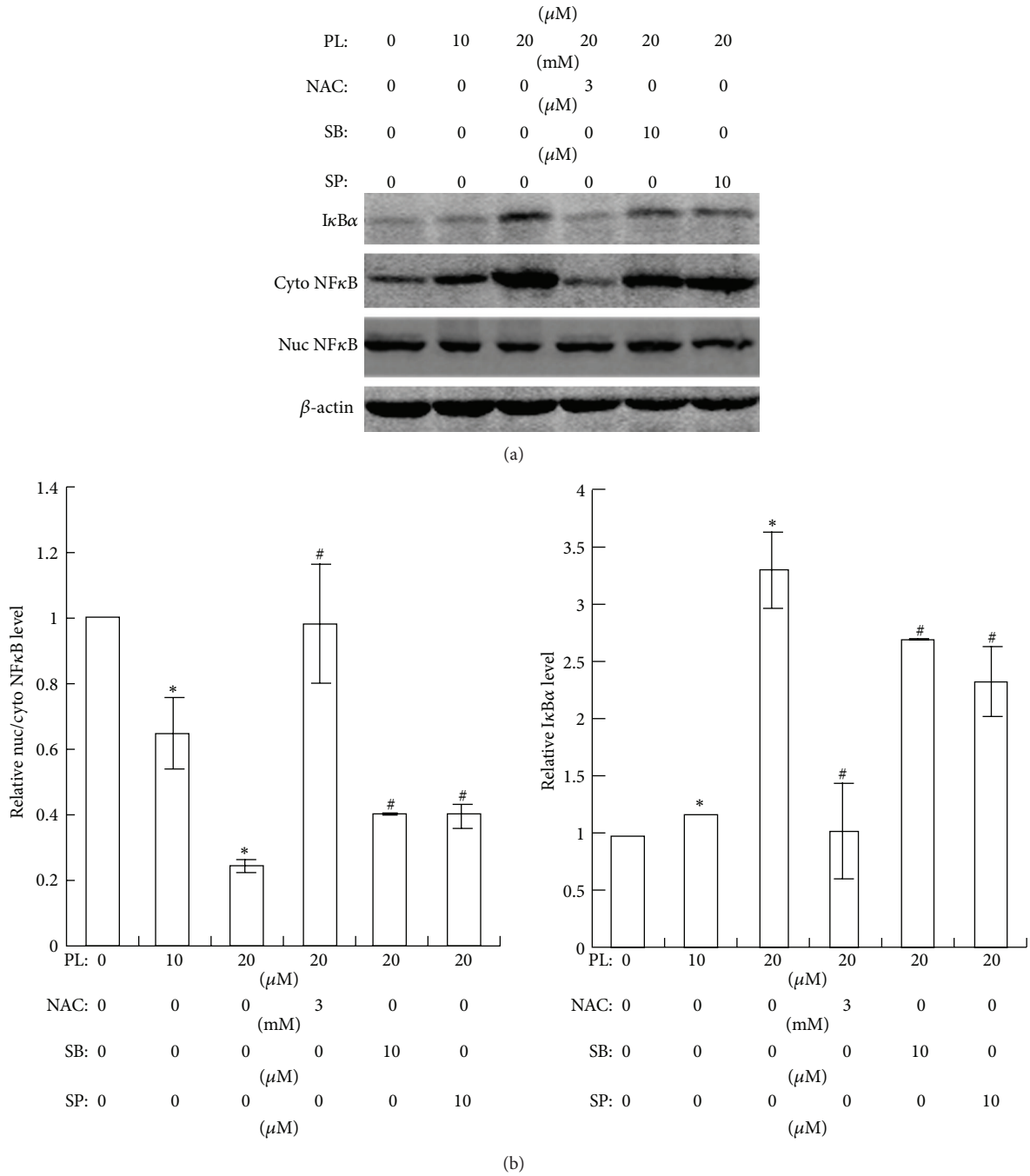

Figure 6: Effects of PL on NFκB nuclear translocation and IκBα expression in LN229 cells. (a) Representative western blots of NFκB and IκBα at 3 h after scratching in LN229 cells. Cells were pretreated with PL for 6 h; NAC, SB203580, or SP600125 was administrated 2 h before PL treatment. Cytosolic (cyto) and nuclear (nuc) protein were isolated and subjected to western blot analysis. β-actin was set as loading control. (b) Statistical analysis of nuc/cyto NFκB of western blot results. Statistical analysis of IκBα expression of western blot results. $^{*}P < 0.05$ compared to group of 0 μM of PL; $^{\#}P < 0.05$ compared to group of 20 μM of PL treatment alone.

effect of PL depends on enhanced ROS in LN229 cells. ROS-dependent p38/JNK activation and inhibition of NFκB nuclear translocation contribute to PL's inhibitory effects on LN229 cell migration.

The migration of cancer cells is pivotal for cancer invasion and metastasis [30–32]. Cancer malignancy is proportional to cancer cell's migration ability. GBM is one of the most invasive cancers refractory for present therapy [21]. We found that PL at lower concentration (1 μM) was effective in inhibiting LN229 and U87 cell migration while PL at higher concentration (10 μM) did not interfere with the mobility of normal astrocytes (Figure 1(b)), suggesting that

normal brain functions might not be disturbed during PL therapy. Since we measured cell migration within 6 h after the induction of migration at a lower PL dosage as compared to the half inhibitory concentration of PL in LN229 and U87 (10–20 μmol/L) [22] and PL at 5 or 10 μmol/L did not inhibit cell proliferation in scratch-wound model (Figure 2), therefore, the death and proliferation of LN229 was negligible in our assays. Moreover, we tested the ability of LN229 cell migration in two different systems. Thus, the effects of PL on cancer cell migration are reliable. Interestingly, migrated LN229 cells in transwell assay showed remarkable morphological changes (Figure 5(c)).It is well-known that cell migration requires cell deformation [31, 33]. The round shape of LN229 cells in the presence of PL might make them difficult to be transformed. It is reported that p38 activation could upregulate E-cadherin and downregulate N-cadherin and vimentin in malignant HaCaT cells [34], which are key molecules mediating cancer cell migration or invasion. It is likely that PL might alter the expression of cadherin or vimentin and thus induce the morphological changes in GBM cells. Further elucidating the mechanisms of cell deformation in the presence of PL is desirable.

ROS accumulation seems to be required for the anticancer effects of PL as verified in various studies since ROS is elevated and the use of antioxidant NAC completely abolishes all biological functions of PL in cancer cells [15, 17, 22, 28]. However, it is recently reported that NAC is not a specific antioxidant as it also suppresses the inhibitor of proteasome [35]. Thus, it is necessary to test further the effects of more antioxidants on PL's functions and elucidate the sources and mechanisms of ROS elevation in PL-treated cancer cells. In LN229 cells after scratch, cellular ROS was elevated while glutathione was reduced, suggesting that PL elevated ROS via impairing ROS clearance system. Until now, how PL increases cellular ROS remains unclear although it is suggested that the binding of PL to GSTP1 or CBR1 might contribute to PL-induced ROS [15].

The mechanisms underlying ROS's biological functions are extremely complicated [36]. Identifying key molecules downstream ROS-mediated signaling pathways in cancer cells is required for improving the therapeutic effects of drugs or developing novel anticancer reagents [37, 38]. In LN229 cells after the scratch injury, p38 and JNK were activated notably by PL. Since NAC completely abolished p38 and JNK activation, p38 and JNK were downstream targets of ROS elevation upon PL treatment [22]. Pharmacological assays demonstrated that the inhibition of p38 or JNK by specific inhibitors significantly reduced PL's effect on LN229 cell migration. Therefore, both p38 and JNK signaling pathways contributed to ROS-induced inhibition of LN229 cell migration in the presence of PL. Since p38 and JNK exert suppressive [39, 40] or promoting [41, 42] effects on cancer metastasis in different cellular contexts, further dissecting p38 and JNK signaling pathways in PL-treated GBM cells might be helpful for understanding the mechanisms of the anticancer effects of PL.

PL exerted prominent effects on reducing nuclear translocation of NFκB and NAC completely reversed the inhibitory effect of PL on NFκB activation. Considering the essential role of NF-κB in cell migration via activating snail and repressing E-cadherin [43, 44], it is conceivable that PL might exert its effects on cell migration via ROS-NFκB pathway. Since p38 and JNK activation depended on ROS accumulation and inhibitors of p38 or JNK could partially reverse the effects of PL on NFκB activity, we speculated that p38 and JNK were intermediate players between ROS and NFκB.

5. Conclusion

In summary, the natural compound piperlongumine can effectively and selectively suppress cancer cell migration. This action of PL depends on PL-induced ROS-p38/JNK-NFκB signaling pathway. Our data suggest that PL is a potential therapeutic for highly invasive cancers such as GBM.

Conflict of Interests

The authors declare that there is no conflict of interests regarding the publication of this paper.

Acknowledgments

This work was supported by grants from the National Nature Science Foundation of China (Grant no. 81070937, 81172397), the Fundamental Research Funds for the Central Universities, HUST (no. 2013ZHYX017) to Xiao Qian Chen, and the China Postdoctoral Science Foundation (no. 2013M542026) to Feng Pan.

References

[1] T. P. Szatrowski and C. F. Nathan, "Production of large amounts of hydrogen peroxide by human tumor cells," *Cancer Research*, vol. 51, no. 3, pp. 794–798, 1991.

[2] B. Benassi, M. Marani, M. Loda, and G. Blandino, "USP2a alters chemotherapeutic response by modulating redox," *Cell Death & Disease*, vol. 4, article e812, 2013.

[3] A. Acharya, I. Das, D. Chandhok, and T. Saha, "Redox regulation in cancer: a double-edged sword with therapeutic potential," *Oxidative Medicine and Cellular Longevity*, vol. 3, no. 1, pp. 23–34, 2010.

[4] V. Mansat-de Mas, C. Bezombes, A. Quillet-Mary et al., "Implication of radical oxygen species in ceramide generation, c-Jun N-terminal kinase activation and apoptosis induced by daunorubicin," *Molecular Pharmacology*, vol. 56, no. 5, pp. 867–874, 1999.

[5] E. Groninger, G. J. Meeuwsen-De Boer, S. S. De Graaf, W. A. Kamps, and E. S. De Bont, "Vincristine induced apoptosis in acute lymphoblastic leukaemia cells: a mitochondrial controlled pathway regulated by reactive oxygen species?" *International Journal of Oncology*, vol. 21, no. 6, pp. 1339–1345, 2002.

[6] H. L. Lin, T. Y. Liu, G. Y. Chau, W. Y. Lui, and C. W. Chi, "Comparison of 2-methoxyestradiol-induced, docetaxel-induced, and paclitaxel-induced apoptosis in hepatoma cells and its correlation with reactive oxygen species," *Cancer*, vol. 89, no. 5, pp. 983–994, 2000.

[7] B.-S. Park, D.-J. Son, Y.-H. Park, T. W. Kim, and S.-E. Lee, "Antiplatelet effects of acidamides isolated from the fruits of

Piper longum L," *Phytomedicine*, vol. 14, no. 12, pp. 853–855, 2007.

[8] G. Vedhanayaki, G. V. Shastri, and A. Kuruvilla, "Analgesic activity of *Piper longum* Linn. root," *Indian Journal of Experimental Biology*, vol. 41, no. 6, pp. 649–651, 2003.

[9] F. Cícero Bezerra Felipe, J. Trajano Sousa Filho, L. E. de Oliveira Souza et al., "Piplartine, an amide alkaloid from *Piper tuberculatum*, presents anxiolytic and antidepressant effects in mice," *Phytomedicine*, vol. 14, no. 9, pp. 605–612, 2007.

[10] A. S. Wakade, A. S. Shah, M. P. Kulkarni, and A. R. Juvekar, "Protective effect of *Piper longum* L. on oxidative stress induced injury and cellular abnormality in adriamycin induced cardiotoxicity in rats," *Indian Journal of Experimental Biology*, vol. 46, no. 7, pp. 528–533, 2008.

[11] I.-L. Tsai, F.-P. Lee, C.-C. Wu et al., "New cytotoxic cyclobutanoid amides, a new furanoid lignan and anti-platelet aggregation constituents from *Piper arborescens*," *Planta Medica*, vol. 71, no. 6, pp. 535–542, 2005.

[12] J. B. Fontenele, L. K. A. M. Leal, E. R. Silveira, F. H. Felix, C. F. Bezerra Felipe, and G. S. B. Viana, "Antiplatelet effects of piplartine, an alkamide isolated from *Piper tuberculatum*: possible involvement of cyclooxygenase blockade and antioxidant activity," *Journal of Pharmacy and Pharmacology*, vol. 61, no. 4, pp. 511–515, 2009.

[13] J. S. Bang, D. H. Oh, H. M. Choi et al., "Anti-inflammatory and antiarthritic effects of piperine in human interleukin 1β-stimulated fibroblast-like synoviocytes and in rat arthritis models," *Arthritis Research and Therapy*, vol. 11, no. 2, article R49, 2009.

[14] D. J. Son, S. Y. Kim, S. S. Han et al., "Piperlongumine inhibits atherosclerotic plaque formation and vascular smooth muscle cell proliferation by suppressing PDGF receptor signaling," *Biochemical and Biophysical Research Communications*, vol. 427, no. 2, pp. 349–354, 2012.

[15] L. Raj, T. Ide, A. U. Gurkar et al., "Selective killing of cancer cells by a small molecule targeting the stress response to ROS," *Nature*, vol. 475, no. 7355, pp. 231–234, 2011.

[16] H. Randhawa, K. Kibble, H. Zeng, M. P. Moyer, and K. M. Reindl, "Activation of ERK signaling and induction of colon cancer cell death by piperlongumine," *Toxicol In Vitro*, vol. 27, no. 6, pp. 1626–1633, 2013.

[17] Y. Wang, J. W. Wang, X. Xiao et al., "Piperlongumine induces autophagy by targeting p38 signaling," *Cell Death & Disease*, vol. 4, article e824, 2013.

[18] S. S. Han, V. S. Tompkins, D. J. Son et al., "Piperlongumine inhibits LMP1/MYC-dependent mouse B-lymphoma cells," *Biochemical and Biophysical Research Communications*, vol. 436, no. 4, pp. 660–665, 2013.

[19] H. Yamaguchi, J. Wyckoff, and J. Condeelis, "Cell migration in tumors," *Current Opinion in Cell Biology*, vol. 17, no. 5, pp. 559–564, 2005.

[20] M. Lohela and Z. Werb, "Intravital imaging of stromal cell dynamics in tumors," *Current Opinion in Genetics and Development*, vol. 20, no. 1, pp. 72–78, 2010.

[21] R. Stupp, W. P. Mason, M. J. Van Den Bent et al., "Radiotherapy plus concomitant and adjuvant temozolomide for glioblastoma," *The New England Journal of Medicine*, vol. 352, no. 10, pp. 987–996, 2005.

[22] J. M. Liu, F. Pan, L. Li et al., "Piperlongumine selectively kills glioblastoma multiforme cells via reactive oxygen species accumulation dependent JNK and p38 activation," *Biochemical and Biophysical Research Communications*, vol. 437, no. 1, pp. 87–93, 2013.

[23] X. Q. Chen, J. G. Chen, Y. Zhang, W. W. L. Hsiao, and A. C. H. Yu, "14-3-3γ is upregulated by in vitro ischemia and binds to protein kinase Raf in primary cultures of astrocytes," *Glia*, vol. 42, no. 4, pp. 315–324, 2003.

[24] C.-C. Liang, A. Y. Park, and J.-L. Guan, "In vitro scratch assay: a convenient and inexpensive method for analysis of cell migration in vitro," *Nature Protocols*, vol. 2, no. 2, pp. 329–333, 2007.

[25] D. Kesanakurti, C. Chetty, M. D. Rajasekhar, M. Gujrati, and J. S. Rao, "Functional cooperativity by direct interaction between PAK4 and MMP-2 in the regulation of anoikis resistance, migration and invasion in glioma," *Cell Death & Disease*, vol. 3, article e445, 2012.

[26] L. Li, Q. R. Liu, X. X. Xiong et al., "Neuroglobin promotes neurite outgrowth via differential binding to PTEN and Akt," *Molecular Neurobiology*, vol. 49, no. 1, pp. 149–162, 2014.

[27] J. Zhang, S. J. Lan, Q. R. Liu, J. M. Liu, and X. Q. Chen, "Neuroglobin, a novel intracellular hexa-coordinated globin, functions as a tumor suppressor in hepatocellular carcinoma via Raf/MAPK/Erk," *Molecular Pharmacology*, vol. 83, no. 5, pp. 1109–1119, 2013.

[28] K. V. Golovine, P. B. Makhov, E. Teper et al., "Piperlongumine induces rapid depletion of the androgen receptor in human prostate cancer cells," *Prostate*, vol. 73, no. 1, pp. 23–30, 2013.

[29] S. Pei, M. Minhajuddin, K. P. Callahan et al., "Targeting aberrant glutathione metabolism to eradicate human acute myelogenous leukemia cells," *The Journal of Biological Chemistry*, vol. 288, no. 47, pp. 33542–33558, 2013.

[30] J. J. Bravo-Cordero, L. Hodgson, and J. Condeelis, "Directed cell invasion and migration during metastasis," *Current Opinion in Cell Biology*, vol. 24, no. 2, pp. 277–283, 2012.

[31] S. R. Walker, M. Chaudhury, E. A. Nelson, and D. A. Frank, "Microtubule-targeted chemotherapeutic agents inhibit signal transducer and activator of transcription 3 (STAT3) signaling," *Molecular Pharmacology*, vol. 78, no. 5, pp. 903–908, 2010.

[32] M. L. Gardel, I. C. Schneider, Y. Aratyn-Schaus, and C. M. Waterman, "Mechanical integration of actin and adhesion dynamics in cell migration," *Annual Review of Cell and Developmental Biology*, vol. 26, pp. 315–333, 2010.

[33] F. Yin, Z. Xu, Z. Wang et al., "Elevated chemokine CC-motif receptor-like 2 (CCRL2) promotes cell migration and invasion in glioblastoma," *Biochemical and Biophysical Research Communications*, vol. 429, pp. 168–172, 2012.

[34] Y. Yang, Y. Li, K. Wang, Y. Wang, W. Yin, and L. Li, "P38/NF-κB/snail pathway is involved in caffeic acid-induced inhibition of cancer stem cells-like properties and migratory capacity in malignant human keratinocyte," *PLoS ONE*, vol. 8, no. 3, Article ID e58915, 2013.

[35] M. Halasi, M. Wang, T. S. Chavan, V. Gaponenko, N. Hay, and A. L. Gartel, "ROS inhibitor N-acetyl-L-cysteine antagonizes the activity of proteasome inhibitors," *Biochemical Journal*, vol. 454, no. 2, pp. 201–208, 2013.

[36] A. Colquhoun, "Lipids, mitochondria and cell death: implications in neuro-oncology," *Molecular Neurobiology*, vol. 42, no. 1, pp. 76–88, 2010.

[37] S. Saeidnia and M. Abdollahi, "Antioxidants: friends or foe in prevention or treatment of cancer: the debate of the century," *Toxicology and Applied Pharmacology*, vol. 271, no. 1, pp. 49–63, 2013.

[38] C. Lopez-Haber and M. G. Kazanietz, "Cucurbitacin I inhibits Rac1 activation in breast cancer cells by a reactive oxygen species-mediated mechanism and independently of Janus tyrosine kinase 2 and P-Rex1," *Molecular Pharmacology*, vol. 83, no. 5, pp. 1141–1154, 2013.

[39] J. A. Hickson, D. Huo, D. J. Vander Griend, A. Lin, C. W. Rinker-Schaeffer, and S. D. Yamada, "The p38 kinases MKK4 and MKK6 suppress metastatic colonization in human ovarian carcinoma," *Cancer Research*, vol. 66, no. 4, pp. 2264–2270, 2006.

[40] D. J. Vander Griend, M. Kocherginsky, J. A. Hickson, W. M. Stadler, A. Lin, and C. W. Rinker-Schaeffer, "Suppression of metastatic colonization by the context-dependent activation of the c-Jun NH2-terminal kinase kinases JNKK1/MKK4 and MKK7," *Cancer Research*, vol. 65, no. 23, pp. 10984–10991, 2005.

[41] Q. Huang, F. Lan, X. Wang et al., "IL-1beta-induced activation of p38 promotes metastasis in gastric adenocarcinoma via upregulation of AP-1/c-fos, MMP2 and MMP9," *Molecular Cancer*, vol. 13, no. 1, p. 18, 2014.

[42] X. Ma, W. Li, H. Yu et al., "Bendless modulates JNK-mediated cell death and migration in Drosophila," *Cell Death & Differentiation*, vol. 21, no. 3, pp. 407–415, 2014.

[43] R. Dong, Q. Wang, X. L. He, Y. K. Chu, J. G. Lu, and Q. J. Ma, "Role of nuclear factor kappa B and reactive oxygen species in the tumor necrosis factor-α-induced epithelial-mesenchymal transition of MCF-7 cells," *Brazilian Journal of Medical and Biological Research*, vol. 40, no. 8, pp. 1071–1078, 2007.

[44] K. Zhang, J. Zhao, X. Liu et al., "Activation of NF-B upregulates snail and consequent repression of E-cadherin in cholangiocarcinoma cell invasion," *Hepato-Gastroenterology*, vol. 58, no. 105, pp. 1–7, 2011.

Hindawi Publishing Corporation
Oxidative Medicine and Cellular Longevity
Volume 2014, Article ID 193523, 9 pages
http://dx.doi.org/10.1155/2014/193523

Research Article

PELP1 Suppression Inhibits Colorectal Cancer through c-Src Downregulation

Zhifeng Ning,[1,2] Youzhi Zhang,[3] Hanwei Chen,[4] Jiliang Wu,[1] Tieshan Song,[2] Qian Wu,[2] and Fuxing Liu[2]

[1] *Hubei Province Key Laboratory on Cardiovascular, Cerebrovascular, and Metabolic Disorders, Hubei University of Science and Technology, Xianning 437100, China*
[2] *The Basic Medical School, Hubei University of Science and Technology, Xianning 437100, China*
[3] *School of Pharmacy, Hubei University of Science and Technology, Xianning 437100, China*
[4] *Wuhan Blood Center, Wuhan 430030, China*

Correspondence should be addressed to Fuxing Liu; liufx6505@126.com

Received 13 February 2014; Accepted 20 April 2014; Published 22 May 2014

Academic Editor: Xiaoqian Chen

Proline-, glutamic acid-, and leucine-rich protein 1 (PELP1), a coregulator of estrogen receptors alpha and beta, is a potential protooncogene implicated in several human cancers, including sexual hormone-responsive or sexual hormone-nonresponsive cancers. However, the functions of PELP1 in colorectal cancer remain unclear. In this study, western blot and bioinformatics revealed that PELP1 expression was higher in several colorectal cancer cell lines than in immortalized normal colorectal epithelium. PELP1 silencing by short hairpin RNA promoted the senescence and inhibited the proliferation, colony formation, migration, invasion, and xenograft tumor formation of the CRC cell line HT-29. Moreover, PELP1 silencing was accompanied by c-Src downregulation. c-Src upregulation partly alleviated the damage in HT-29 malignant behavior induced by PELP1 RNA interference. In conclusion, PELP1 exhibits an oncogenic function in colorectal cancer through c-Src upregulation.

1. Introduction

Colorectal cancer (CRC) is the second leading cause of cancer-related death in the developed countries [1, 2]. In China, the morbidity and mortality rates of CRC have rapidly increased over the past two decades; these rates are affected by many factors, including age, population, westernization lifestyle, and industrial pollution. Early-stage CRC lacks specific symptoms; thus, this disease is usually diagnosed at a relatively late stage. The five-year survival rate of early-stage CRC is 85% after surgical resection, whereas that of stage III CRC with lymph node metastasis is <50% after surgery [3]. Cancer results from the activation of numerous protooncogenes and the inhibition of tumor suppressors. CRC is characterized by the mutation of tumor suppressor genes, protooncogenes, DNA repair genes, growth factors and their receptor genes, apoptosis-related genes, and cell cycle checkpoint genes [4]. These diverse genes constitute a complicated regulated network implicated in CRC oncogenesis. However, interference with a single gene is not enough to cure cancer. Therefore, the master regulators of downstream effector genes involved in carcinogenesis must be urgently identified [5].

The specific functions of estrogen signaling in CRC remain unclear. Many studies implicated the dysregulation of estrogen receptors (ERs) in CRC [6–9]. However, the specific functions of ERα and ERβ in the cancerogenesis of colorectal epithelium remain controversial. Some researches [6, 8] implied that ERβ is the predominant form expressed in the normal colorectal epithelium and reduced in CRC. Thus, ERβ exerts protective effects against CRC; this finding is contradictory to the report that the ERβ protein is significantly upregulated in colorectal epithelial cells of carcinomas [10]. ERα is reportedly rarely expressed in normal colorectal epithelium and lacks functions in CRC carcinogenesis. However, several studies reported that the ERα gene

Table 1: Interference sequence for shRNA.

shRNA number	Sequence (3′-5′)
Negative control	GCAAGCTGACCCTGAAGTTGAGAACTTTGAAGTCCCAGTCGAACG
1	GGAGAAACAAAGGUUAUUUGAGAACTUUUAUUGGAAACAAAGAGG
2	CACAGUCUCACAUCGUUUAGAGAACTAUUUGCUACACUCUGACAC
3	CCAGGAGCTTGTTGAAGAAGAGAACTAAGAAGTTGTTCGAGGACC

is frequently hypermethylated in CRC [11, 12], suggesting that ERα hypermethylation can predict CRC progression. ERα upregulation in ERα-negative CRC cell lines can suppress cell growth [13]. The reversal of a hypermethylated inactive ERα can inhibit CRC in vitro and in vivo [14]. The estrogen-ER signaling pathway is evidently involved in CRC development. Therefore, comprehensive research must be conducted to elucidate the functions of ER in CRC.

Proline-, glutamic acid-, and leucine-rich protein 1 (PELP1) is a modulator of nongenomic actions of estrogen receptors (NMAR) and a coregulator of ER; PELP1 has been implicated in many physiological [15–17] and pathological processes [18]. Research has demonstrated that PELP1 is a protooncogene in hormone-responsive cancers, such as breast [19, 20], ovarian [21], endometrial [22, 23], and prostate cancers [24]. Moreover, some researchers determined the functions of PELP1 in hormone-nonresponsive cancers, such as brain tumor [25], lung cancer [26], and colorectal cancer [27, 28].

PELP1 is upregulated in CRC tissues [27, 28]. However, the exact function of PELP1 in CRC remains unknown. In the present study, we investigated the functions of PELP1 in several CRC cell lines. Bioinformatics and western blot showed that PELP1 expression was higher in CRC cell lines than in normal colorectal epithelium. PELP1 silencing by short hairpin RNA (shRNA) promoted the senescence and inhibited the proliferation, colony formation, migration, invasion, and xenograft tumor formation of the CRC cell line HT-29. Moreover, PELP1 silencing was accompanied by c-Src downregulation. c-Src upregulation partly recovered the oncogenic function of PELP1. These results demonstrated that PELP1 suppression can inhibit CRC in vitro and in vivo through c-Src downregulation.

2. Materials and Methods

2.1. Cell Line. The CRC cell lines COLO205, HT-29, SW-620, HCC-2998, and HCT-15 and normal colon epithelium cell line FHC were purchased from American Type Culture Collection (Manassas, VA). The five CRC cell lines were cultured in RPMI1640 medium supplemented with 10% fetal bovine serum, 100 U/mL penicillin, and 100 μg/mL streptomycin. FHC was cultured in DMEM/F12 medium with the same supplement as the CRC cell lines. All cell lines were maintained at 37°C in a humidified atmosphere of 5% CO_2 in an open-air incubator.

2.2. Bioinformatics. We performed a bioinformatics analysis on Oncomine (https://www.oncomine.org/resource/login.html) to analyze PELP1 expression in the CRC cell lines. We used a personal account to enter the Oncomine website. We input PELP1 on the search box to begin the search. After entering the page for PELP1 expression survey in almost all human cancer cell lines or tissues, we focused on CRC and obtained PELP1 expression data from the Lee et al. [29], Shankavaram et al. [30], and Garnett [31] cell line datasets. After data standardization, we presented PELP1 expression data in the five CRC cell lines as mean ± standard deviation (SD).

2.3. shRNA Interference of PELP1. HT-29 cells were seeded in 24-well plates (Corning) until they reached 50% to 60% confluence prior to transfection. Then, stable transfection was performed. Three shRNA sequences targeting the PELP1 gene were designed and synthesized by Shanghai Jima Pharmaceutical Technology, China. The three shRNA sequences of PELP1 and the negative control sequence are listed in Table 1. Lipofectamine LTX and Plus Reagent (Invitrogen) were used to transfect shRNA into HT-29 cells according to the manufacturer's protocol. The medium containing transfection reagents was replaced with RPMI1640 medium supplemented with 10% FBS at 18 h after the transfection. The cells were collected at 48 h after the transfection, processed in the following experiments, and then prepared for protein extraction. The silence efficiency of PELP1 was tested by western blot.

2.4. Western Blot. Total protein was extracted from HT-29-shRNA or HT-29-control cells using RIPA lysate buffer as described in our previous research [32]. After quantification by a bicinchoninic acid protein assay kit (Beyotime Biotechnology, China), equal amounts of proteins (20 μg to 25 μg) were separated by 12% sodium dodecyl sulfate-polyacrylamide gel electrophoresis (PAGE) and processed for immunoblotting with a rabbit multiclonal antibody for PELP1 (diluted at 1 : 100, Santa Cruz) and c-Src (diluted at 1 : 500, Santa Cruz). A mouse polyclonal anti-β-actin antibody (diluted at 1 : 2000, Boster Biological Engineering, China) was used as an internal control. All protein bands were scanned using ChemiImager 5500 V2.03 software, and the integrated density values were calculated by a computerized image analysis system (Fluor Chen 2.0) and normalized with that of β-actin.

2.5. MTT. Cell viability and proliferation activity were determined with the MTT assay. HT-29-shRNA or HT-29-control

cells were seeded in 96-well plates (Costar) at a density of 5,000 cells per well in complete medium (RPMI1640 supplemented with 10% FBS, 1% p/s) and then incubated for 12 h under standard conditions (37°C and 5% CO_2). The total volume in each well was 200 μL. From the next day to the seventh day, 20 μL of MTT (5 mg/mL) was added into each well. After additional incubation for 4 h, the solution in each well was replaced with dimethyl sulfoxide (Sigma, USA) to solubilize formazan, the metabolic product of MTT. The plates were kept on a shaking mixer for 10 min to guarantee complete solubilization of formazan, and the optical density was recorded at 490 nm using a microplate luminometer. Results were expressed as means ± SD, and a growth curve was constructed. Data were analyzed by one-way ANOVA with the post hoc Tukey test applied for paired comparisons.

2.6. Plate Colony Forming Assay. Colony forming ability was examined by the plate colony formation assay. HT-29-shRNA or HT-29-control cells were seeded into six-centimeter plates (Costar) at a density of 3,000 cells per plate in complete medium and then incubated for approximately 2 weeks under standard conditions (37°C and 5% CO_2). The cells were washed twice with phosphate-buffered saline (PBS) and then fixed with methanol for 15 min. After staining with 0.1% crystal violet for 20 min, the number of positive colonies with diameters exceeding 50 μm was counted under a light microscope with 100× magnification. The colony forming rate was calculated by dividing the number of positive colonies by the total number of cells seeded.

2.7. Transwell Small Chamber Invasion and Migration Assay. For the invasion assay, Transwell small chambers with 8 μm pore filters were coated with 12 μL of ice-cold Matrigel (7.5 mg/mL protein). In total, 50,000 HT-29-shRNA or HT-29-control cells were added to the upper chamber of these Matrigel chambers in 200 μL of serum-free RPMI 1640 medium. Then, the cells were placed in 24-well plates in 500 μL of RPMI 1640 medium containing 10% FBS. After 22 h of incubation, the cells were fixed with methanol and then stained with 0.1% crystal violet. Cotton tips were used to remove the cells that remained in the Matrigel or attached to the upper side of the filter. The number of cells on the lower side of the filter was counted under a light microscope.

The methods used for the migration assay were almost the same as for the invasion assay described above, except that no Matrigel was used to coat the well and the incubation time was 16 h.

2.8. β-Galactosidase (β-Gal) Staining. The cells were washed in PBS, fixed for 3 min to 5 min (room temperature) in 2% formaldehyde/0.2% glutaraldehyde (or 3% formaldehyde), washed again, and then incubated at 37°C (no CO_2) with a fresh senescence-associated β-Gal stain solution containing 1 mg of 5-bromo-4-chloro-3-indolyl β-D-galactoside per mL (stock = 20 mg of dimethylformamide per mL)/40 mM citric acid/sodium phosphate, pH 6.0/5 mM potassium ferrocyanide/5 mM potassium ferricyanide/150 mM NaCl/2 mM $MgCl_2$. Staining was evident within 2 h to 4 h and peaked within 12 h to 16 h. To detect lysosomal, β-Gal, the citric acid/sodium phosphate was pH 4.0.

2.9. Nude Mice Subcutaneous Xenograft Assay. Male BALB/c (nu/nu) mice aged 6 to 8 weeks were obtained from the Experimental Animal Center of Guangdong Province. The mice were housed and maintained in laminar flow cabinets under specific pathogen-free conditions according to the regulations and standards approved by the Animal Care and Ethics Committee of Shantou University Medical College.

To establish s.c. tumors, 1.5×10^6 HT-29-shRNA or HT-29-control cells were resuspended in 200 μL of RPMI1640 serum-free medium and injected via an 18-gauge needle into the s.c. space of both flanks of the mice. Tumor progression was documented once weekly by measurements using calipers, and tumor volumes were calculated by the following formula: length × width × height × 0.52 (in mm). The mice were given ethane anesthesia and then euthanized by cervical dislocation.

2.10. Stable Transfection of c-Src. The human c-Src coding region gene with a 376 bp sequence was amplified from homogenized HT-29 by RT-PCR. The sequences of the PCR primers used for c-Src in this study were as follows: sense, 5′-TGTTCGGAGGCTTCAACTCC-3′ and antisense, 5′-CAGTAGGCACCTTTCGTGGT-3′. The PCR products were cloned into a TA expression vector (Invitrogen, Carlsbad, CA, USA), and the sequence of the c-Src coding region was confirmed by sequencing. The resulting plasmids (pc-Src) were propagated in *Escherichia coli* and then purified through cesium chloride gradient. For gene transfection, HT-29-shRNA or HT-29-control cells were seeded in six-well plates at a concentration of 5×10^5 cells per well. HT-29-shRNA or HT-29-control cells approaching 80% to 90% confluence were transfected with 4 mg pc-Src with 10 mL of Lipofectamine 2000 (Invitrogen) following the manufacturer's protocol. The cells transfected with empty plasmid pcDNA3.1 (mock) were used as negative controls.

2.11. Quantitative RT-PCR. The cells or tissues were harvested with Trizol Reagent (Invitrogen, Carlsbad, CA, USA), and total RNA was isolated according to the manufacturer's instructions. cDNA synthesis was performed using the Superscript III RT-PCR kit (Invitrogen). Real-time PCR was carried out using a Cepheid SmartCycler II (Sunnyvale, CA, USA) with gene-specific real-time PCR primers. Results were normalized to GAPDH transcript levels, and the difference in fold expression was calculated using the ΔΔ CT method. The primers used for c-Src were as follows: sense, 5′-CTCTTCAGAGCCCTTGCTCA-3′ and antisense, 5′-ATTCACCCTCCCCCAAGGAA-3′. The length of the PCR products was 193 bp.

2.12. Statistics Analysis. Data from all quantitative assays were expressed as mean ± SD andwere analyzed using one-way ANOVA and independent-samples t-test. All statistical

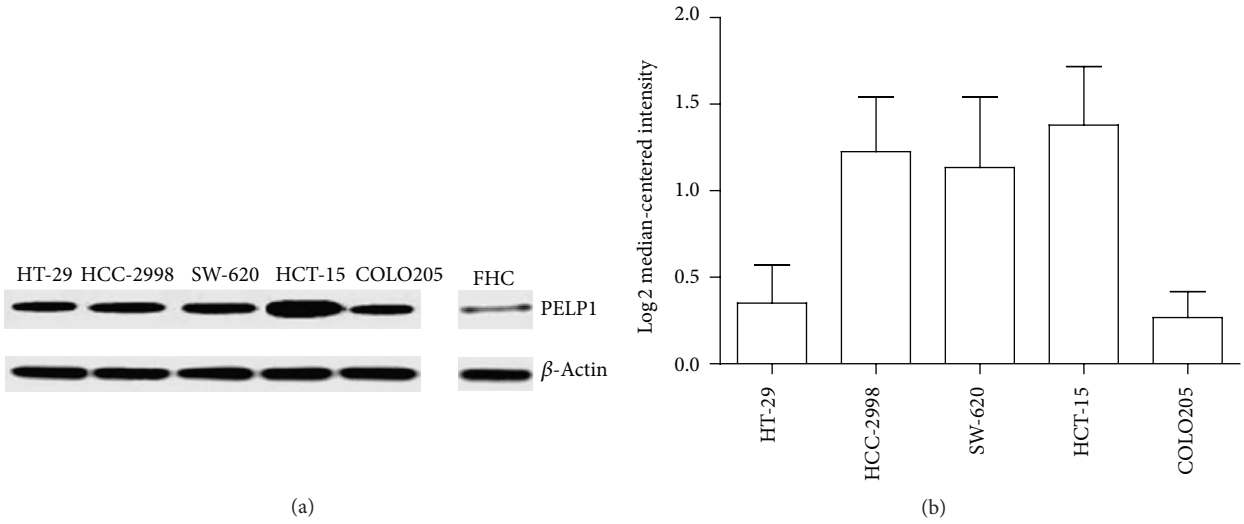

Figure 1: PELP1 expression was upregulated inCRC. (a) Western blot revealed that PELP1 protein expression was higher in the CRC cell lines HT-29, HCC-2998, SW-620, HCT-15, and COLO205 than in the normal colorectal epithelium FHC. (b) Informatics data suggested that PELP1 mRNA expression was increased in these five CRC cell lines.

analyses were performed and visualized by GraphPad Prism 5.0. $P < 0.05$ was considered statistically significant.

3. Results

3.1. PELP1 Was Upregulated in CRC Cell Lines as Revealed by Western Blot and Bioinformatics. We performed western blot to test the protein expression of PELP1 in the CRC lines COLO205, HT-29, SW-620, HCC-2998, and HCT-15 and in the normal cell line FHC. As shown in Figure 1(a), PELP1 protein expression was higher in the CRC cell lines than in the immortalized colorectal epithelium. The bioinformatics data (Figure 1(b)) obtained from the Oncomine database also showed that PELP1 was upregulated in the CRC cell lines. These results implied that PELP1 served oncogenic functions in CRC.

3.2. PELP1 Downregulation by shRNA Inhibited CRC In Vitro. To identify the oncogenic function of PELP1 in CRC, we utilized shRNA to silence PELP1 expression in HT-29. After transfection shRNA #3 of PELP1 into HT-29, PELP1 expression decreased by 90% (Figure 2(a)). PELP1 silencing reduced the proliferation, colony formation (by 57.5%), migration (by 69.3%), and invasion (by 58%) abilities of HT-29 (Figures 2(b)–2(e)). β-Gal senescence assay demonstrated that PELP1 silencing promoted the senescence of HT-29 (Figure 2(f)). These results suggested that PELP1 downregulation inhibited the malignant behavior of CRC in vitro.

3.3. PELP1 Downregulation by shRNA Inhibited Xenograft Formation Ability of CRC in Nude Mice. Xenograft formation ability reflects the malignant characteristic of cancer cells. We performed a subcutaneous xenograft formation experiment on nude mice to assess whether or not PELP1 can influence the xenograft formation ability of HT-29. After stable transfection with PELP1-shRNA in HT-29, HT-29-control and HT-29-shRNA cells were inoculated subcutaneously in both flanks of the nude mice. Results showed that PELP1-shRNA reduced the xenograft formation ability of HT-29 in nude mice (Figure 3).

3.4. Oncogenic Function of PELP1 in CRC Was Mediated by c-Src Upregulation. c-Src is a known protooncogene in colon cancer. Thus, we focused on the relationship between PELP1 and c-Src in CRC carcinogenesis. We tested c-Src expression by quantitative RT-PCR and western blot after PELP1 silencing by shRNA in HT-29 to explore the mechanism of PELP1 downregulation in suppressing CRC carcinogenesis. c-Src was reduced after PELP1 silencing at the mRNA (Figure 4(a)) and protein (Figure 4(b)) expression levels. To analyze whether or not c-Src participates in promoting the function of PELP1 in CRC, we upregulated the expression of c-Src after PELP1 silencing. As stated previously, PELP1 downregulation can inhibit the malignant behavior of CRC. Surprisingly, Src elevation can counteract the inhibition of CRC induced by PELP1 silencing (Figures 4(c)–4(g)). Therefore, the suppressing function of PELP1 downregulation in CRC carcinogenesis was mediated by c-Src inhibition.

4. Discussion

In the present study, the oncogenic function of the ER coregulator PELP1 or NMAR was identified in CRC, a common and highly invasive type of cancer. We primarily clarified the oncogenic mechanism of PELP1 in relation to c-Src, an important oncogene. Although CRC cannot be completely regarded as a hormone-responsive cancer, emerging evidence implied that steroid hormones such as estrogen and androgen participate in CRC pathogenesis. However, the functions of

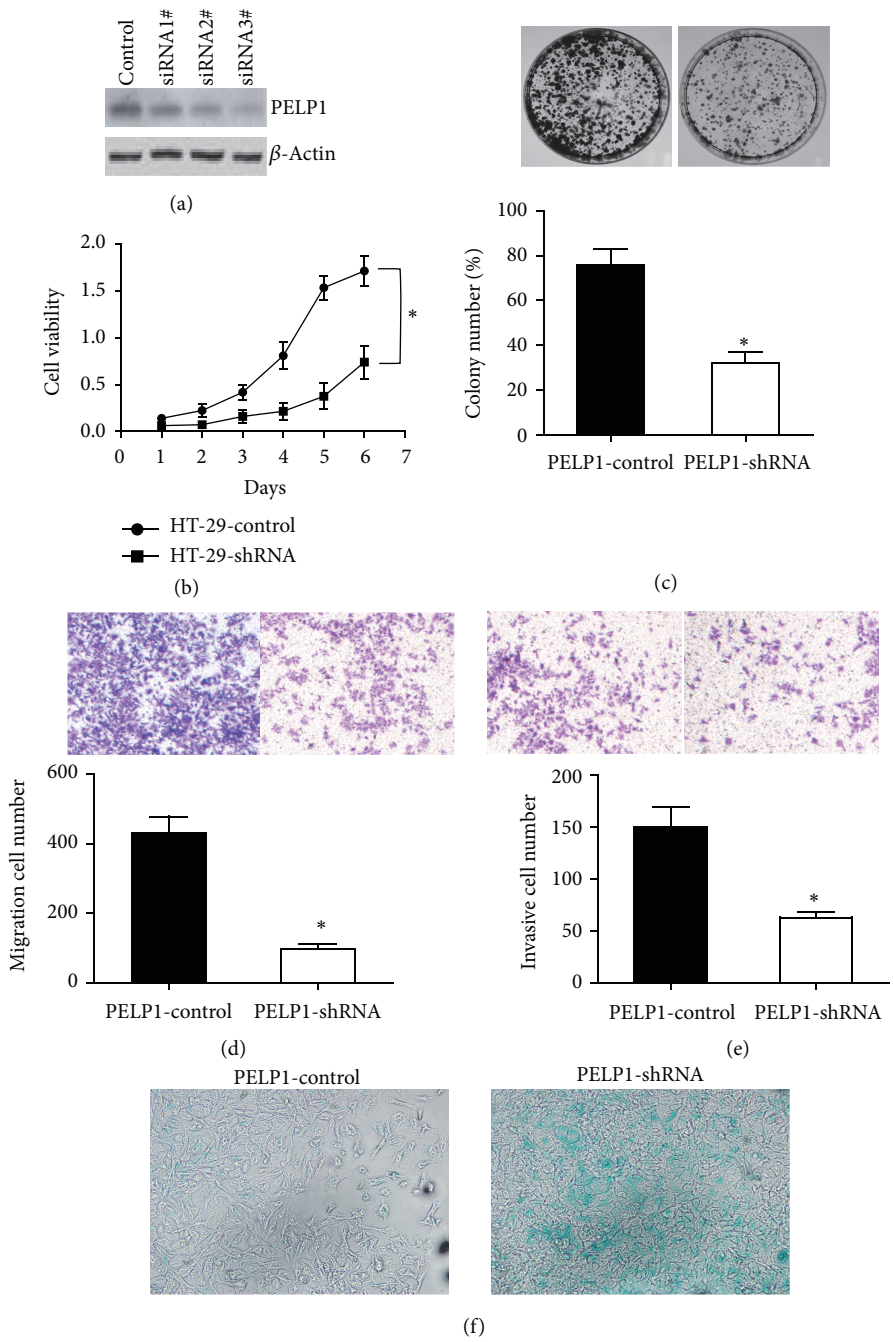

Figure 2: PELP1 downregulation inhibited the CRC cell line HT-29 in vitro. (a) After transfection with shRNA, PELP1 protein expression was decreased by 90%. shRNA #3 was selected for further investigations. (b) After PELP1 silencing, the cell viability of HT-29 was inhibited. (c) PELP1 silencing inhibited the colony formation ability of HT-29 by 57.5% (lower panel). A representative colony formation assay is shown (upper panel). (d) PELP1 silencing inhibited the migration ability of HT-29 by 69.3% (lower panel). A representative migration assay is shown (upper panel). (e) PELP1 silencing inhibited the invasion ability of HT-29 by 58% (lower panel). A representative invasive assay is shown (upper panel). (f) Senescence was induced by PELP1 silencing in HT-29. A representative β-Gal assay is shown.

ER and AR in CRC are complex and controversial because many complicated signaling pathways are involved in estrogen and androgen signaling. ERβ is usually regarded as a protective factor in CRC, and ERα is believed to have no participation in CRC [33]. Different from ERs, androgen receptors (ARs) serve no [34] suppressive [35] or promoting functions [36] in CRC. As a nuclear receptor coregulator, PELP1 can interact with ERs, ARs, glucocorticoid receptors, and progesterone receptors [37]. Therefore, we analyzed the functions of PELP1 in CRC to elucidate the complex signaling network involving ER and AR.

Two recent studies have evaluated the expression of PELP1 in CRC tissues by using immunohistochemistry [27, 28]. However, their findings were inconsistent. Tzelepi et al.

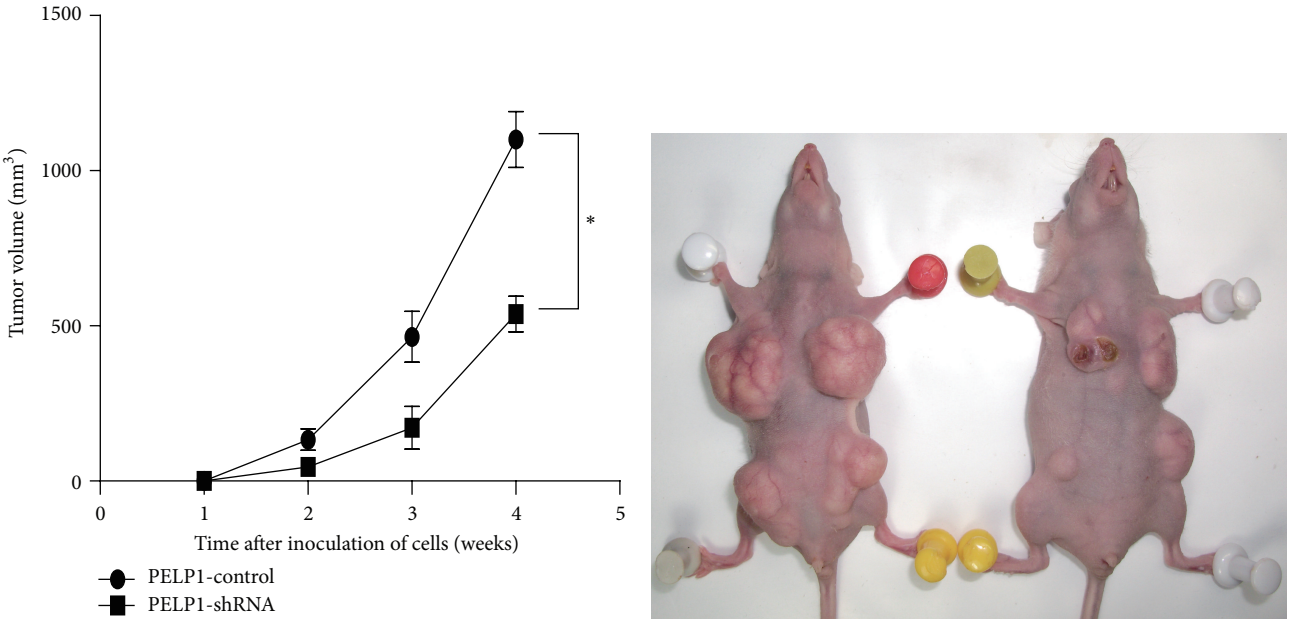

Figure 3: PELP1 downregulation inhibited the CRC cell line HT-29 in nude mice xenograft assay. PELP1 silencing inhibited CRC growth in nude mice (a). A representative nude mice xenograft assay is shown in (b).

[27] claimed that PELP1 expression decreases from normal colorectal epithelium to cancerous colorectal epithelium; by contrast, Grivas et al. [28] found that PELP1 protein expression in epithelial cells increases during colorectal tumorigenesis despite the fact that PELP1 overexpression in epithelial cells correlates with prolonged overall survival. Moreover, Grivas et al. [28] found that ERβ expression in epithelial cells is upregulated during colorectal tumorigenesis in male patients. They also found that ERβ expression correlates with increased risk of relapse, implying that ERβ serves an oncogenic function in male CRC patients. The present experimental results seemed to be partly consistent with those of Grivas et al. That is, bioinformatics and western blot assay demonstrated that the mRNA and protein expression levels of PELP1 increased in the CRC cell lines COLO205, HT-29, SW-620, HCC-2998, and HCT-15. Moreover, we found that the malignant behavior of CRC was inhibited in vitro and in vivo after PELP1 silencing by shRNA. These results suggested that PELP1 served an oncogenic function in CRC.

A decade ago, Peyton Rous described a filterable agent (i.e., virus) that can induce solid tumor formation in birds. After approximately 50 years, the Rous *sarcoma virus* was identified from Rous' filterable agent. Extensive research into the molecular biology and genetics of Rous *sarcoma virus* identified v-Src as a viral oncogene responsible for malignant transformation. Then, Bishop and Varmus [38] demonstrated that v-Src has a cellular counterpart, the first identified protooncogene c-Src. c-Src is a nonreceptor tyrosine kinase that is abnormally expressed in many human cancers and is linked with malignant biological behavior related to proliferation, adhesion, migration, invasion, and metastasis [39]. The oncogenic function of c-Src in CRC has been explored in different studies. The dysregulation of c-Src contributed to the initiation and development of CRC. In the present study, we linked PELP1 with c-Src in CRC. Several scholars have identified the fact that an interaction exists between PELP1 and c-Src. For example, Chakravarty et al. [40] found that estrogen-mediated extranuclear signaling promotes cytoskeleton reorganization through the ER-Src-PELP1-phosphoinositide 3-kinase-ILK1 pathway in breast cancer. PELP1 silencing can significantly inhibit c-Src activation. Dimple et al. [41] suggested that PELP1 downregulation reduces the proliferation and tumorigenic potential of ovarian cancer cells and affects the magnitude of c-Src and protein kinase B (AKT) signaling in a nude mouse model. Rajhans et al. [42] found that the PELP1-mediated induction of aromatase requires functional Src and phosphatidylinositol-3-kinase pathways. Conversely, c-Src phosphorylates PELP1 at the C terminal (tyrosine 920) domain [43]. However, PELP1 can function independent of c-Src. Kayahara et al. [44] found that PELP1 functionally interacts with both NH2- and COOH-terminal glucocorticoid receptor domains to modulate transactivation; they also found through inhibitor and c-Src knockdown studies that the function of PELP1 is independent of c-Src activity. In the present study, we found that the oncogenic function of PELP1 was partially mediated by c-Src in CRC. PELP1 silencing by shRNA downregulated c-Src expression. In addition, c-Src upregulation partly recovered the oncogenic function of PELP1. Our research suggested that the oncogenic effect of PELP1 in CRC was partly mediated by c-Src.

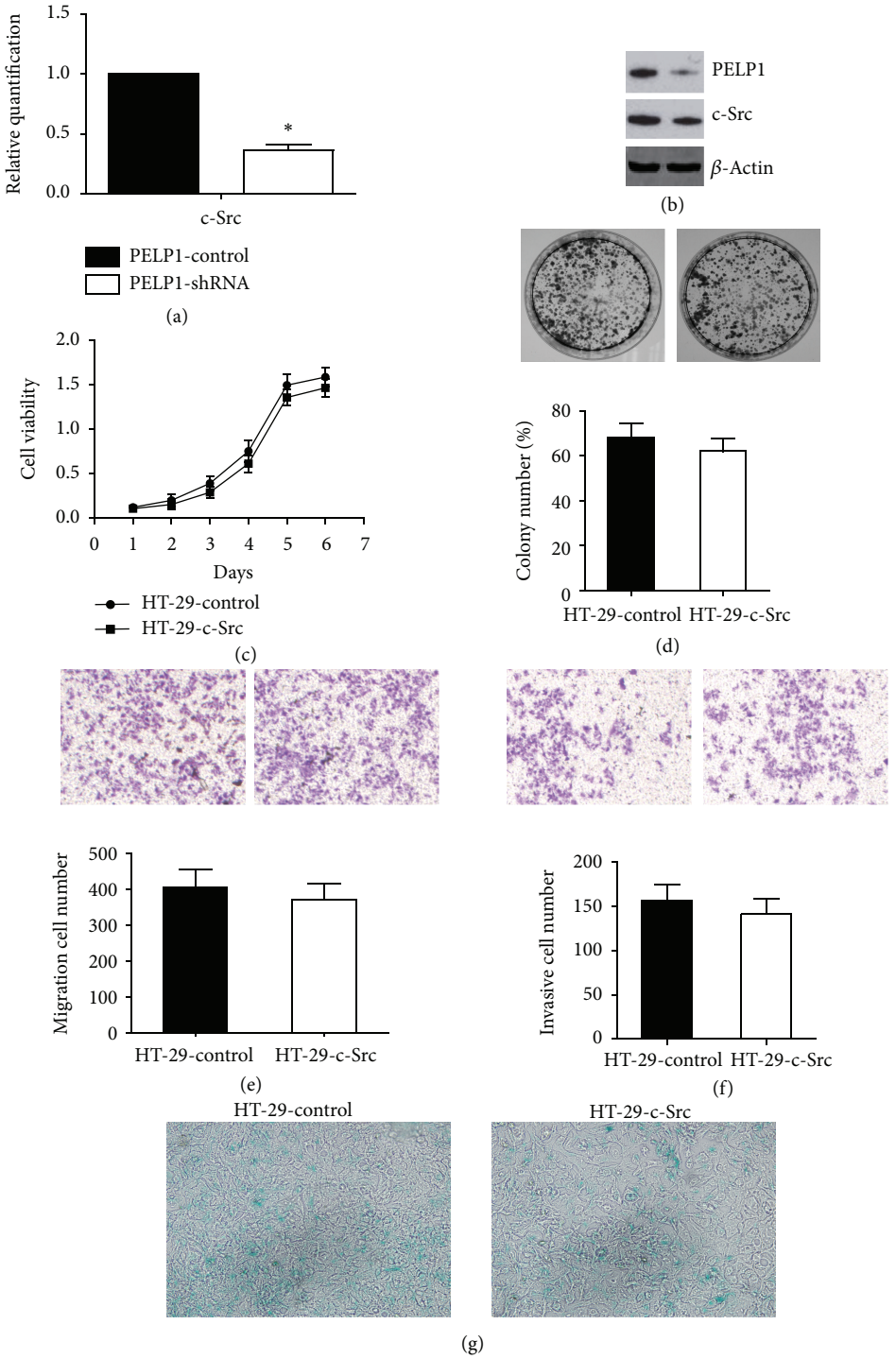

Figure 4: PELP1 silencing suppressed CRC through c-Src downregulation. (a) PELP1 silencing was accompanied by the downregulation of c-Src mRNA as determined by quantitative RT-PCR. (b) PELP1 silencing was accompanied by c-Src protein downregulation as determined by western blot. (c) Decreased cell viability induced by PELP1 silencing was recovered by c-Src upregulation in HT-29. (d) Decreased colony formation ability was recovered by c-Src upregulation in HT-29. (e) Decreased migration ability was recovered by c-Src upregulation in HT-29. (f) Decreased invasion ability was recovered by c-Src upregulation in HT-29. (g) Induced senescence by PELP1 silencing was inhibited after c-Src upregulation.

5. Conclusions

PELP1, a nuclear receptor coregulator, exerts oncogenic action in CRC. PELP1 silencing by shRNA promoted the senescence and inhibited the proliferation, colony formation, migration, invasion, and xenograft tumor formation of CRC. Moreover, PELP1 silencing was accompanied by c-Src downregulation. c-Src upregulation partly recovered the oncogenic function of PELP1. This study is the first to identify the oncogenic function of PELP1 in CRC, a hormone-nonresponsive cancer. Therefore, PELP1 can be regarded as a therapeutic target in hormone-nonresponsive cancers.

Abbreviations

PELP1: Proline-, glutamic acid-, and leucine-rich protein 1
c-Src: Cellular counterpart of Rous sarcoma virus
ER: Estrogen receptor
CRC: Colorectal cancer.

Conflict of Interests

The authors declare that there is no conflict of interests regarding the publication of this paper.

Authors' Contribution

Zhifeng Ning, Youzhi Zhang, and Hanwei Chen contributed equally to this work.

Acknowledgment

This work was supported by the Key Project of Hubei Province Education Department (D20122802).

References

[1] T. Gansler, P. A. Ganz, M. Grant et al., "Sixty years of ca: A cancer journal for clinicians," *CA Cancer Journal for Clinicians*, vol. 60, no. 6, pp. 345–350, 2010.

[2] A. Jemal, R. Siegel, J. Xu, and E. Ward, "Cancer statistics, 2010," *CA Cancer Journal for Clinicians*, vol. 60, no. 5, pp. 277–300, 2010.

[3] J. B. O'Connell, M. A. Maggard, and C. Y. Ko, "Colon cancer survival rates with the new American Joint Committee on Cancer sixth edition staging," *Journal of the National Cancer Institute*, vol. 96, no. 19, pp. 1420–1425, 2004.

[4] S. Narayan and D. Roy, "Role of APC and DNA mismatch repair genes in the development of colorectal cancers," *Molecular Cancer*, vol. 2, article 41, 2003.

[5] D. M. Lonard and B. W. O'Malley, "Nuclear receptor coregulators: judges, juries, and executioners of cellular regulation," *Molecular Cell*, vol. 27, no. 5, pp. 691–700, 2007.

[6] A. Rudolph, C. Toth, M. Hoffmeister et al., "Expression of oestrogen receptor beta and prognosis of colorectal cancer," *British Journal of Cancer*, vol. 107, pp. 831–839, 2012.

[7] Y. Q. He, J. Q. Sheng, X. L. Ling et al., "Estradiol regulates miR-135b and mismatch repair gene expressions via estrogen receptor-β in colorectal cells," *Experimental & Molecular Medicine*, vol. 44, pp. 723–732, 2012.

[8] D. Saleiro, G. Murillo, R. V. Benya, M. Bissonnette, J. Hart, and R. G. Mehta, "Estrogen receptor-beta protects against colitis-associated neoplasia in mice," *International Journal of Cancer*, vol. 131, pp. 2553–2561, 2012.

[9] R. M. Hasson, A. Briggs, A. M. Carothers et al., "Estrogen receptor α or β loss in the colon of Min/+ mice promotes crypt expansion and impairs TGFβ and HNF3β signaling," *Carcinogenesis*, vol. 35, no. 1, pp. 96–102, 2014.

[10] P. D. Grivas, V. Tzelepi, G. Sotiropoulou-Bonikou, Z. Kefalopoulou, A. G. Papavassiliou, and H. Kalofonos, "Estrogen receptor α/β, AIB1, and TIF2 in colorectal carcinogenesis: do coregulators have prognostic significance?" *International Journal of Colorectal Disease*, vol. 24, no. 6, pp. 613–622, 2009.

[11] A. Jubb, S. Bell, and P. Quirke, "Methylation and colorectal cancer," *The Journal of Pathology*, vol. 195, pp. 111–134, 2001.

[12] Y. Kondo and J. P. J. Issa, "Epigenetic changes in colorectal cancer," *Cancer and Metastasis Reviews*, vol. 23, no. 1-2, pp. 29–39, 2004.

[13] J.-P. J. Issa, Y. L. Ottaviano, P. Celano, S. R. Hamilton, N. E. Davidson, and S. B. Baylin, "Methylation of the oestrogen receptor CpG island links ageing and neoplasia in human colon," *Nature Genetics*, vol. 7, no. 4, pp. 536–540, 1994.

[14] F. Al-Azzawi and M. Wahab, "Estrogen and colon cancer: current issues," *Climacteric*, vol. 5, no. 1, pp. 3–14, 2002.

[15] J. Wang, S. Song, L. Shi et al., "Temporal expression of pelp1 during proliferation and osteogenic differentiation of rat bone marrow mesenchymal stem cells," *PLoS ONE*, vol. 8, Article ID 0075477, 2013.

[16] Y. Yan, W. Zeng, S. Song et al., "Vitamin C induces periodontal ligament progenitor cell differentiation via activation of ERK pathway mediated by PELP1," *Protein Cell*, vol. 4, pp. 620–627, 2013.

[17] J. Wang, Q. Zhu, S. Song et al., "Increased PELP1 expression in rat periodontal ligament tissue in response to estrogens treatment," *Journal of Molecular Histology*, vol. 44, pp. 347–356, 2013.

[18] B. J. Girard, A. R. Daniel, C. A. Lange, and J. H. Ostrander, "PELP1: a review of PELP1 interactions, signaling, and biology," *Molecular and Cellular Endocrinology*, vol. 8, pp. 00326–00322, 2013.

[19] I. M. Bennani-Baiti, "Integration of ERalpha-PELP1-HER2 signaling by LSD1 (KDM1A/AOF2) offers combinatorial therapeutic opportunities to circumventing hormone resistance in breast cancer," *Breast Cancer Research*, vol. 14, article 112, 2012.

[20] V. Cortez, M. Mann, S. Tekmal et al., "Targeting the PELP1-KDM1 axis as a potential therapeutic strategy for breast cancer," *Breast Cancer Research*, vol. 14, article R108, 2012.

[21] S. Aust, P. Horak, D. Pils et al., "The prognostic value of estrogen receptor beta and proline-, glutamic acid- and leucine-rich protein 1 (PELP1) expression in ovarian cancer," *BMC Cancer*, vol. 13, pp. 1471–2407, 2013.

[22] J. Wan and X. Li, "PELP1/MNAR suppression inhibits proliferation and metastasis of endometrial carcinoma cells," *Oncology Reports*, vol. 28, pp. 2035–2042, 2012.

[23] R. K. Vadlamudi, S. Balasenthil, R. R. Broaddus, J.-Å. Gustafsson, and R. Kumar, "Deregulation of estrogen receptor coactivator proline-, glutamic acid-, and leucine-rich protein-1/modulator of nongenomic activity of estrogen receptor in human endometrial tumors," *Journal of Clinical Endocrinology and Metabolism*, vol. 89, no. 12, pp. 6130–6138, 2004.

[24] P. Ravindranathan, T. K. Lee, L. Yang et al., "Peptidomimetic targeting of critical androgen receptor-coregulator interactions in prostate cancer," *Nature Communications*, vol. 4, article 1923, 2013.

[25] Z. Kefalopoulou, V. Tzelepi, V. Zolota et al., "Prognostic value of novel biomarkers in astrocytic brain tumors: nuclear receptor co-regulators AIB1, TIF2, and PELP1 are associated with high tumor grade and worse patient prognosis," *Journal of Neuro-Oncology*, vol. 106, no. 1, pp. 23–31, 2012.

[26] D. C. Márquez-Garbán, H. W. Chen, M. C. Fishbein, L. Goodglick, and R. J. Pietras, "Estrogen receptor signaling pathways in human non-small cell lung cancer," *Steroids*, vol. 72, no. 2, pp. 135–143, 2007.

[27] V. Tzelepi, P. Grivas, Z. Kefalopoulou, H. Kalofonos, J. N. Varakis, and G. Sotiropoulou-Bonikou, "Expression of estrogen receptor co-regulators NCoR and PELP1 in epithelial cells and myofibroblasts of colorectal carcinomas: cytoplasmic translocation of NCoR in epithelial cells correlates with worse prognosis," *Virchows Archiv*, vol. 454, no. 1, pp. 41–53, 2009.

[28] P. D. Grivas, V. Tzelepi, G. Sotiropoulou-Bonikou, Z. Kefalopoulou, A. G. Papavassiliou, and H. Kalofonos, "Expression of ERa,ERß and co-regulator PELP1/MNAR in colorectal cancer: prognostic significance and clinicopathologic correlations," *Cellular Oncology*, vol. 31, no. 3, pp. 235–247, 2009.

[29] J. K. Lee, D. M. Havaleshko, H. Cho et al., "A strategy for predicting the chemosensitivity of human cancers and its application to drug discovery," *Proceedings of the National Academy of Sciences of the United States of America*, vol. 104, no. 32, pp. 13086–13091, 2007.

[30] U. T. Shankavaram, W. C. Reinhold, S. Nishizuka et al., "Transcript and protein expression profiles of the NCI-60 cancer cell panel: an integromic microarray study," *Molecular Cancer Therapeutics*, vol. 6, no. 3, pp. 820–832, 2007.

[31] M. J. Garnett, E. J. Edelman, S. J. Heidorn et al., "Systematic identification of genomic markers of drug sensitivity in cancer cells," *Nature*, vol. 483, no. 7391, pp. 570–575, 2012.

[32] H. Dong, H. Guo, L. Xie et al., "The metastasis-associated gene MTA3, a component of the Mi-2/NuRD transcriptional repression complex, predicts prognosis of gastroesophageal junction adenocarcinoma," *PLoS ONE*, vol. 8, Article ID e62986, 2013.

[33] A. Barzi, A. M. Lenz, M. J. Labonte, and H. J. Lenz, "Molecular pathways: estrogen pathway in colorectal cancer," *Clinical Cancer Research*, vol. 19, pp. 5842–5848, 2013.

[34] M. N. Passarelli, A. I. Phipps, J. D. Potter et al., "Common single-nucleotide polymorphisms in the estrogen receptor beta promoter are associated with colorectal cancer survival in postmenopausal women," *Cancer Research*, vol. 73, pp. 767–775, 2013.

[35] M. L. Slattery, C. Sweeney, M. Murtaugh et al., "Associations between vitamin D, vitamin D receptor gene and the androgen receptor gene with colon and rectal cancer," *International Journal of Cancer*, vol. 118, no. 12, pp. 3140–3146, 2006.

[36] M. Mariani, G. F. Zannoni, S. Sioletic et al., "Gender influences the class III and V beta-tubulin ability to predict poor outcome in colorectal cancer," *Clinical Cancer Research*, vol. 18, pp. 2964–2975, 2012.

[37] R. K. Vadlamudi and R. Kumar, "Functional and biological properties of the nuclear receptor coregulator PELP1/MNAR," *Nuclear receptor signaling*, vol. 5, article e004, 2007.

[38] M. GS, "The hunting of the Src," *Nature Reviews Molecular Cell Biology*, vol. 2, pp. 467–475, 2001.

[39] S. Zhang and D. Yu, "Targeting Src family kinases in anti-cancer therapies: turning promise into triumph," *Trends in Pharmacological Sciences*, vol. 33, no. 3, pp. 122–128, 2012.

[40] D. Chakravarty, S. S. Nair, B. Santhamma et al., "Extranuclear functions of ER impact invasive migration and metastasis by breast cancer cells," *Cancer Research*, vol. 70, no. 10, pp. 4092–4101, 2010.

[41] C. Dimple, S. S. Nair, R. Rajhans et al., "Role of PELP1/MNAR signaling in ovarian tumorigenesis," *Cancer Research*, vol. 68, no. 12, pp. 4902–4909, 2008.

[42] R. Rajhans, H. B. Nair, S. S. Nair et al., "Modulation of in situ estrogen synthesis by proline-, glutamic acid-, and leucine-rich protein-1: potential estrogen receptor autocrine signaling loop in breast cancer cells," *Molecular Endocrinology*, vol. 22, no. 3, pp. 649–664, 2008.

[43] B. J. Cheskis, J. Greger, N. Cooch et al., "MNAR plays an important role in ERa activation of Src/MAPK and PI3K/Akt signaling pathways," *Steroids*, vol. 73, no. 9-10, pp. 901–905, 2008.

[44] M. Kayahara, J. Ohanian, V. Ohanian, A. Berry, R. Vadlamudi, and D. W. Ray, "MNAR functionally interacts with both NH2- and COOH-terminal GR domains to modulate transactivation," *The American Journal of Physiology—Endocrinology and Metabolism*, vol. 295, no. 5, pp. E1047–E1055, 2008.

Hindawi Publishing Corporation
Oxidative Medicine and Cellular Longevity
Volume 2014, Article ID 705253, 9 pages
http://dx.doi.org/10.1155/2014/705253

Review Article

Caenorhabditis elegans: A Useful Model for Studying Metabolic Disorders in Which Oxidative Stress Is a Contributing Factor

Elizabeth Moreno-Arriola,[1] Noemí Cárdenas-Rodríguez,[2] Elvia Coballase-Urrutia,[2] José Pedraza-Chaverri,[3] Liliana Carmona-Aparicio,[2] and Daniel Ortega-Cuellar[1]

[1] *Laboratory of Experimental Nutrition, National Institute of Pediatrics, 04530 Mexico City, DF, Mexico*
[2] *Laboratory of Neurochemistry, National Institute of Pediatrics, 04530 Mexico City, DF, Mexico*
[3] *Department of Biology, Faculty of Chemistry, University City, UNAM, 04150 Mexico City, DF, Mexico*

Correspondence should be addressed to Liliana Carmona-Aparicio; c_apariccio@yahoo.com.mx
and Daniel Ortega-Cuellar; dortega@unam.mx

Received 13 February 2014; Revised 25 April 2014; Accepted 29 April 2014; Published 18 May 2014

Academic Editor: Xiaoqian Chen

Caenorhabditis elegans is a powerful model organism that is invaluable for experimental research because it can be used to recapitulate most human diseases at either the metabolic or genomic level *in vivo*. This organism contains many key components related to metabolic and oxidative stress networks that could conceivably allow us to increase and integrate information to understand the causes and mechanisms of complex diseases. Oxidative stress is an etiological factor that influences numerous human diseases, including diabetes. *C. elegans* displays remarkably similar molecular bases and cellular pathways to those of mammals. Defects in the insulin/insulin-like growth factor-1 signaling pathway or increased ROS levels induce the conserved phase II detoxification response via the SKN-1 pathway to fight against oxidative stress. However, it is noteworthy that, aside from the detrimental effects of ROS, they have been proposed as second messengers that trigger the mitohormetic response to attenuate the adverse effects of oxidative stress. Herein, we briefly describe the importance of *C. elegans* as an experimental model system for studying metabolic disorders related to oxidative stress and the molecular mechanisms that underlie their pathophysiology.

1. Introduction

Diabetes mellitus is a metabolic disorder that affects millions of people worldwide and contributes considerably to global mortality [1]. Diabetes is characterized by poor control of glucose homeostasis. Although many advances have been made in understanding the pathophysiology of diabetes mellitus, its prevalence continues to increase, in part because of lifestyle changes and increased overall life expectancy. Diverse studies have demonstrated that oxidative stress participates in the progression of diabetes complications [2–4]. This progression occurs in part because high glucose concentrations in diabetes lead to glucose oxidation via the tricarboxylic acid cycle (TCA), which in turn generates electron donors (NADH, $FADH_2$) for the respiratory chain (RC) that consequently induce the overproduction of reactive oxygen species (ROS). This ROS overproduction triggers an adverse response by modulating several metabolic and signaling pathways, exacerbating diabetic complications [5]. Therefore, there is an urgent need for new approaches for the prevention and treatment of this disease. Most studies have been performed using rodent models of type 1 or type 2 diabetes in which hyperglycemia is induced via genetic, pharmacological, or dietary manipulation. However, there is a huge knowledge gap between the pathogenic mechanisms that cause diabetic complications and the treatments, which prevents the development of appropriate therapeutic interventions. Improving the understanding of the mechanisms that modulate the numerous metabolic pathways in humans requires studies using model organisms that recapitulate most aspects of human disease at either the phenotypic or genomic level *in vivo*. The worm *C. elegans* represents a relevant

model for elucidating the metabolic regulation mechanisms at the molecular level, matching or even improving upon the available mammalian model. Throughout this review, we will provide evidence for similarities between *C. elegans* and mammals that could contribute to the elucidation of the molecular pathways that are implicated in human diseases.

2. Oxidative Protection System in *C. elegans*

2.1. Overview of C. elegans. The number of studies that use *C. elegans* as a model system has grown significantly in recent decades. Interest in this nematode has suddenly soared for many reasons. First, *C. elegans* was the first animal for which the genome was completely sequenced [6]. Second, it is estimated that more than half of *C. elegans* genes are homologous to genes implicated in human diseases [7, 8]. Third, this model organism is maintained under simple experimental conditions in the laboratory and has an optically transparent body that is amenable to the use of fluorescent probes to visualize oxidative stress within the nematodes *in vivo* [9, 10]. *C. elegans* contains many cell types that represent the major tissues of complex metazoans, such as muscle, intestinal, nervous, and epithelial tissue [11]. However, caution is warranted because this organism exhibits important differences from mammals; for example, it does not possess a circulatory system, which could limit its utility as a model for some diseases. Despite this difference, *C. elegans* shares many similarities with mammals, including signaling pathways, such as the insulin/insulin-like growth factor-1 signaling (IIS) pathway [12]. In summary, *C. elegans* is a very useful system for studying the organismal integration of the oxidative stress response [13].

2.2. Aspects of the Mitochondrial System Shared between Mammals and C. elegans. In mammals, the principal metabolic machinery that produces energy from nutrients is the mitochondrion, which drives ATP formation throughout the entire body via oxidative phosphorylation (OXPHOS), a system that comprises several redox reactions in the RC that are coupled to ATP synthesis [14]. Typically, the mitochondrial RC, which is the final pathway of OXPHOS, consists of five macromolecular enzymatic complexes (I–V) that catalyze the transfer of electrons from reducing equivalents (NADH or succinate) from the Krebs cycle through the chain [15]. These proteins have been highly conserved throughout evolution [16] and include NADH-coenzyme Q (CoQ; also referred to as ubiquinone) reductase (complex I); succinate-CoQ reductase (complex II); CoQ-cytochrome c reductase (complex III); cytochrome c oxidase (complex IV); and ATP synthase (complex V). Ubiquinone and cytochrome c are two freely diffusible molecules that mediate the transfer of electrons between the complexes [17].

In lower eukaryotes, such as *C. elegans*, the function of the electron transport system, its size, and its genetic contents are similar to those of mammals [18, 19]. Recently, Li et al. described the use of a shotgun proteomic approach to identify mitochondrial proteins in *C. elegans*, finding that 405 *C. elegans* mitochondrial proteins possess human homologs, indicating a relatively high conservation of mitochondrial proteins between eukaryotic organisms [20]. Interestingly, mutations in several mitochondrial components (collectively referred to as Mit mutants) can disrupt the mitochondrial electron transport chain and exert various effects on the life expectancy of *C. elegans*. A mutation of *nuo-1*, which encodes for mitochondrial complex I, exhibits hallmark characteristics of complex I dysfunction in the mammalian system. These properties include lactic acidosis, decreased mitochondrial respiration, hypersensitivity to exogenous oxidative stressors (hyperoxia or paraquat), and decreased lifespan, conceivably due to elevated oxidative stress [21]. Conversely, mutations of the *isp-1* and *nuo-6* genes that encode subunits of complexes I and III, respectively, increase the lifespan without affecting the ATP levels [22]. In general, the information available to date indicates that the RC metabolism and bioenergetics of the nematode are very similar to those of mammals, and several pathways of intermediary energy metabolism are also conserved in *C. elegans* [18, 20, 23–25].

3. Machinery against Oxidative Stress in *C. elegans*

Aside from its bioenergetic activity, the OXPHOS system is understood to be the major endogenous source of cellular ROS [26, 27], thus contributing to mitochondrial damage and potentially triggering diverse pathologies related to redox signaling [28]. Therefore, a basic conception of how mitochondria produce ROS and how these molecules function is vital for understanding a range of currently important pathologies. The principal ROS include the superoxide anion ($O_2^{\bullet-}$), hydrogen peroxide (H_2O_2), and the hydroxyl radical ($HO^{\bullet}$). $O_2^{\bullet-}$ is typically the primary ROS species and is generated via the interaction between an oxygen molecule and NADPH oxidase or other components (flavines, quinones, and thioles) and contributes to cell damage via oxidative stress [29]. Cellular redox homeostasis is maintained by a set of delicate balances between ROS production and the antioxidant system. Numerous antioxidant enzymes, such as superoxide dismutase (SOD), catalase (CAT), glutathione peroxidase (GPx), and peroxiredoxins (Prxs), have been identified to defend against ROS overproduction [30–32] (Figure 1).

3.1. SOD. In mammals, SOD family enzymes represent the first line of antioxidant defense against ROS. SOD converts $O_2^{\bullet-}$ to H_2O_2, which can subsequently be converted to water by CAT, GPx, or Prxs [33]. SOD is the only enzyme that can detoxify superoxide [34] and is found in various cellular compartments. SOD1 (Cu/ZnSOD) is the predominant superoxide scavenger and is localized in the cytoplasm, the mitochondrial intermembrane space, the nucleus, and lysosomes. SOD2 (MnSOD) and SOD3 are localized in the mitochondria and the extracellular matrix, respectively [29].

Similar to mammals, *C. elegans* possesses six SOD isoforms; two are mitochondrial (known as MnSODs) and are

Table 1: A comparison of evolutionarily conserved antioxidant enzymes expressed in mammals and *C. elegans*.

Mammals			*C. elegans*		
Enzyme	Cellular localization	Ref.	Enzyme	Cellular localization	Ref.
SOD1 (Cu/ZnSOD)	Cytosol Mitochondria Nucleus Lysosomes	[29]	Cu/ZnSODs (*sod-1* and *sod-5*)	Cytosol	[35–37, 42]
SOD2 (MnSOD)	Mitochondria	[29]	MnSODs (*sod-2* and *sod-3*)	Mitochondria	
SOD3	Extracellular matrix	[29]	Predicted Cu/ZnSOD (*sod-4*)	Extracellular matrix	
Catalase	Cytosol Peroxisomes	[43]	*ctl-1* *ctl-2*, *ctl-3*	Cytosol Peroxisomes	[44, 45]
Peroxiredoxins (PrxI -VI)	Ubiquitous	[46]	prdx-3 prdx-2	Mitochondria Intestine	[47] [48]
Glutathione peroxidase (GPx1-8)	Ubiquitous	[49]	*gpx1-8*	Unknown	[50]
Glutathione S-transferases (GSTs)	Cytosol Mitochondria Endoplasmic reticulum Nucleus Plasma membrane	[51]	*Ce*-GST-p24 (gst-4/*K08F4.7*), *CeGSTP2-2* (*gst-10*) and *GSTO-1* (C29E4.7)	Intestine Muscle cells Neurons	[52]

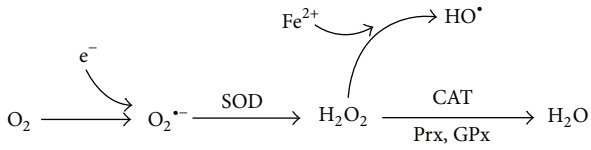

Figure 1: Machinery that protects against oxidative stress and intracellular ROS overproduction. The principal ROS include the superoxide anion ($O_2^{\bullet-}$), hydrogen peroxide (H_2O_2), and the hydroxyl radical ($HO^{\bullet}$). Cellular redox homeostasis is maintained by a set of antioxidant enzymes, such as superoxide dismutase (SOD), catalase (CAT), glutathione peroxidase (GPx), and peroxiredoxin (Prx).

encoded by the *sod-2* and *sod-3* genes; two are cytosolic (Cu/ZnSODs) and are encoded by *sod-1* and *sod-5*; and two are predicted to be extracellular Cu/ZnSOD isoforms, both of which are encoded by *sod-4* (Table 1). *sod-2* and *sod-1* are highly expressed during normal development. *sod-3* and *sod-5* are minor isoforms whose expression levels are increased during the dauer stage [35, 36]. Several research groups have eliminated the expression of individual *sod* genes and have found that deletion of each gene displays little or no detrimental effect on the *C. elegans* lifespan [37–40]. More recently, Van Raamsdonk and Hekimi demonstrated that *C. elegans* containing quintuple mutations of genes *sod-1, sod-2, sod-3, sod-4*, and *sod-5* (*sod-12345*) exhibited a normal lifespan, but SOD activity was also required to survive acute stressors. Additionally, their results indicate that superoxide not only is a toxic byproduct of metabolism but also is involved in a ROS-mediated signaling mechanism that can result in increased longevity. The same study also questions the notion that oxidative stress is the primary cause of aging [41].

3.2. CAT. CAT is a H_2O_2 oxidoreductase heme-containing enzyme that removes H_2O_2 to generate oxygen and water during oxidative stress. Increased CAT activity helps to overcome the damage to tissue metabolism by reducing the toxic levels of H_2O_2 [53].

The *C. elegans* genome possesses three catalase genes, encoding *ctl-1, ctl-2*, and *ctl-3* [54]. *ctl-1* is cytosolic, whereas *ctl-2* and *ctl-3* are peroxisomal (Table 1). *ctl-1* and *ctl-2* play roles in the organismal lifespan [44, 45], whereas *ctl-3* remains uncharacterized. Similar to SOD, the functions of catalases in the lifespan are ambiguous because the loss of *ctl-2* shortens the lifespan [44]; however, other findings indicate that oxidative stress induced by dietary restriction increases catalase activity [55].

3.3. GPx. GPx is the general term for a family of multiple isozymes (GPx1–8) that catalyze the reduction of H_2O_2 or oxidized lipids to water using glutathione (GSH) as an electron donor [49, 56].

As in humans, *C. elegans* contains several genes corresponding to GPx (*gpx-1* to *gpx-8*), but limited data are available regarding these proteins. *gpx-1* (F26E4.12) encodes a phospholipid hydroperoxide GPx that is a homolog of human GPx4. The *gpx-1* enzyme is predicted to catalyze the reduction of phospholipid hydroperoxides using glutathione because loss of *gpx-1* activity via RNAi results in increased

cellular levels of the unsaturated aldehyde 4-hydroxynonenal (4-HNE), a lipid peroxidation product [50].

3.4. GST. GSTs are another set of cellular detoxification enzymes that catalyze the conjugation of exogenous and endogenous compounds to GSH to prevent oxidative stress-induced injury [57].

The *C. elegans* genome contains over 50 putative GSTs [52]. Of these, three GSTs, referred to as *Ce*-GST-p24 *(K08F4.7), CeGSTP2-2 (gst-10)*, and *GSTO-1 (C29E4.7)*, modulate the oxidative stress response (Table 1) [52]. In fact, the separate overexpression of each of these three genes led to an increased resistance to some stress inducers, such as juglone, paraquat, and cumene hydroperoxide, and silencing of these GSTs via RNAi resulted in increased sensitivity to the aforementioned prooxidant compounds [58–60].

3.5. Prxs. Prxs are a large ubiquitous family of proteins that possess cysteine-containing redox active centers [61, 62] that use peroxidatic cysteine to reduce hydroperoxides and release water. These enzymes are classified according to their cysteine contents: there are one-cysteine (Prx VI) and two-cysteine peroxiredoxins (I–IV, V). Prxs function as a signal regulator at specific locations by modulating the local ROS levels in a redox-dependent manner [29].

The *C. elegans* genome includes three Prx genes: prdx-2, prdx-3, and prdx-6 (which should not be confused with the prx, or peroxisomal membrane protein, genes); however, only two of these genes have been studied. PRDX-2 is an enzyme that protects against the toxic effects of H_2O_2; however, it is also noteworthy that the loss of this protein triggers increased resistance to oxidative stress apparently via a signaling mechanism that increases the levels of other antioxidants and phase II detoxification enzymes [48] in a manner that is independent of the SKN-1 pathway, mentioned later. Nonetheless, despite their increased resistance to some forms of oxidative stress, *prdx-2* mutant animals are short-lived, suggesting that *prdx-2* may promote longevity and protect against environmental stress via distinct mechanisms [48]. However, no effect on oxidative stress has been detected for *prdx-3*, but it does display mitochondrial uncoupling activity, suggesting its importance in energy metabolism [47].

4. Oxidative Stress and Disease

Given the wide spectrum of oxidative species that are generated in the cell, it is clear that many biomolecules (DNA, proteins, lipids, and others) are vulnerable to ROS attack. This damage may lead to or exacerbate several metabolic diseases. Despite its evolutionary distance from mammals, *C. elegans* represents an adequate model to complement both *in vitro* and *in vivo* vertebrate models of oxidative stress. This model system has provided insight into the molecular mechanisms of signal transduction pathways, such as the oxidative stress and IIS pathways, that influence numerous human diseases, including diabetes [63, 64]. In diabetic patients, some metabolic abnormalities include mitochondrial $O_2^{\bullet-}$ overproduction and increased formation of advanced glycation end products (AGEs) and lipid peroxidation of low-density lipoprotein (LDL) via a superoxide-dependent pathway, resulting in several effects that are toxic to organisms [65, 66]. Similar to mammals, Schlotterer et al. recently proposed that *C. elegans* represents a suitable organism to study glucose toxicity because exposing nematodes to high glucose concentrations exerts detrimental effects on longevity, increasing ROS production and AGE modification of mitochondrial proteins in an insulin pathway-independent manner [67].

4.1. Nuclear Factor E2-Related Factor (NRF-2) Signaling Pathways Defend against Oxidative Stress and Metabolic Diseases. Eukaryotic cells possess Nrf-2 signaling pathways that defend against oxidative stress by inducing the expression of phase II detoxification genes [68, 69]. Nrf-2 is a basic leucine zipper-containing transcription factor that binds to antioxidant response element (ARE) sequences in the promoter regions of specific genes to modulate the antioxidant response system [70]. Under normal physiological conditions, Nrf-2 is inactivated by binding to Kelch-like ECH-associating protein 1 (Keap1) in the cytoplasm. However, under oxidative stress, Nrf-2 is released from Keap1 and is translocated to the nucleus, where it binds to ARE and transactivates genes corresponding to detoxifying and antioxidant enzymes, such as γ-glutamyl cysteine ligase (γ-GCL), the cystine/glutamate antiporter (xCT), μ-GST, heme oxygenase-1 (HO-1), and others [71–73]. Additionally, Nrf-2 has been suggested to be involved in energy-related pathologies, such as diabetes and obesity [74]. For instance, streptozotocin-induced diabetic mice lacking the Nrf-2 gene exhibit increases in both oxidative stress and blood glucose levels, most likely via the enhanced mRNA expression of gluconeogenic genes (glucose-6-phosphatase and phosphoenolpyruvate carboxykinase) and the diminished expression of glycolytic genes (pyruvate kinase) [74]. Similar to diet-induced obese mice, the activation of Nrf-2 using oltipraz, a synthetic dithiolethione, triggers the regulation of detoxifying enzymes via Nrf-2 [75], improving insulin resistance and obesity and reducing oxidative stress [76]. In addition, constitutive Nrf-2 activation inhibited lipid accumulation in white adipose tissue, suppressed adipogenesis, induced insulin resistance and glucose intolerance, and increased hepatic steatosis in Lep (ob/ob) mice [77]. Thus, it is hypothesized that the transcription factor Nrf2, in addition to its role in protecting organisms against oxidative stress, may be a critical target for preventing diabetes mellitus.

4.2. Oxidative Stress Resistance via the SKN-1 and IIS Pathways in C. elegans. In *C. elegans*, SKN-1 is the ortholog of mammalian Nrf-2 and is also activated in response to elevated levels or oxidative stress or to compounds such as H_2O_2, paraquat, and juglone via the induction of phase II detoxification gene transcription [78, 79]. In fact, it is suggested that the increased lifespan of *C. elegans* under caloric restriction occurs due to SKN-1 activation via increased stress tolerance resulting from reduced IIS pathway activity [80, 81].

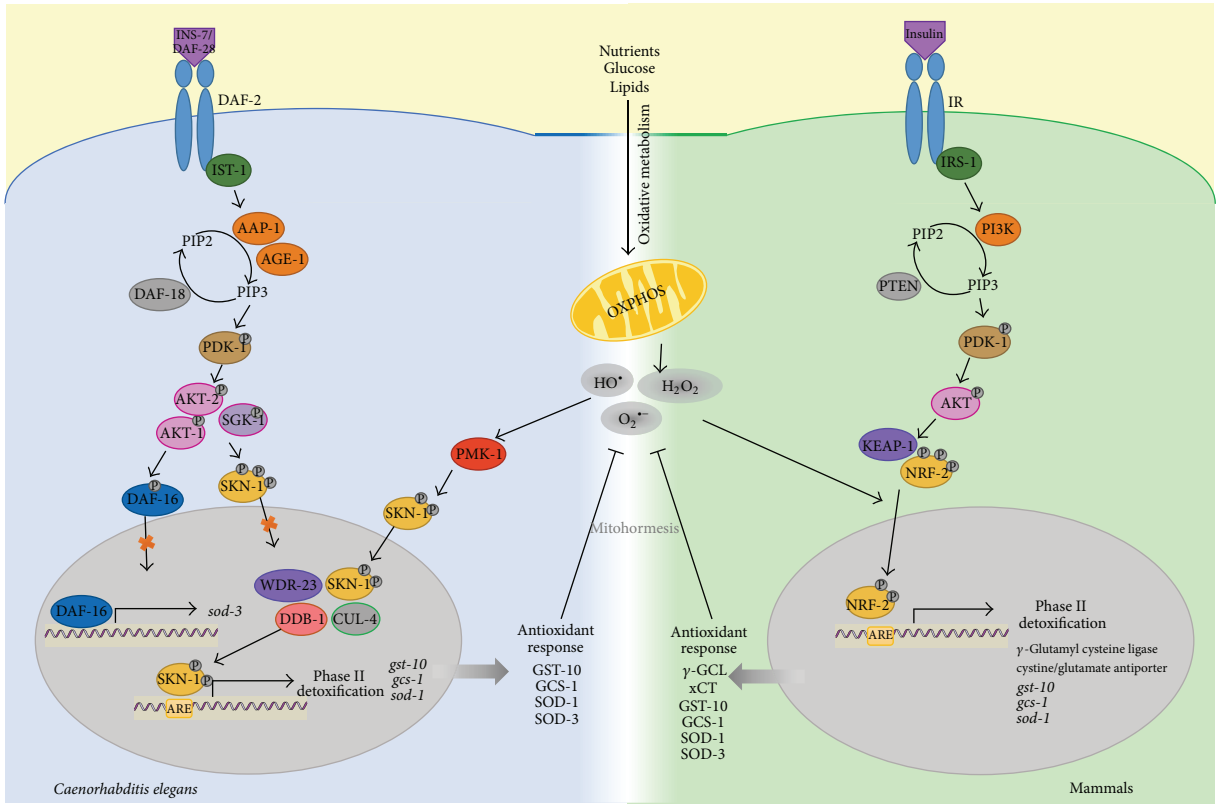

Figure 2: Cross-talk between mitochondrial metabolism and the IIS pathway is required to trigger the mitohormetic response in *C. elegans*. The *C. elegans* IIS pathway contains components that are nearly identical to those of mammals [87]; under conditions of nutrient supply, the IIS pathway is initiated by the binding of DAF-28 or INS-7 [88, 89] to DAF-2 [12, 90], subsequently triggering a cascade of phosphorylation events to activate specific kinases that inactivate the transcriptional factor DAF-16 and its target genes (e.g., *sod-3*) [86, 91]. A similar mechanism occurs for the transcriptional factor SKN-1 via the kinases AKT-1/2 and SGK-1. Conversely, the transcriptional activity of SKN-1 is augmented by some stressors, such as oxidative stress, as a consequence of OXPHOS activity via PMK-1 kinase, culminating in the nuclear translocation of SKN-1 and its interaction with the DNA-binding sites (AREs) of its target genes (*gst-10*, *gcs-1*, and *sod-1*). Finally, an antioxidant response is activated to prevent ROS-mediated cellular damage, which may support the mitohormetic theory. DAF-28 and INS-7, insulin-like peptides; DAF-2, insulin/IGF-1 receptor; IST-1, insulin receptor substrate 1 ortholog; AGE-1 and AAP-1, phosphatidylinositol 3-kinases; PIP2, phosphatidylinositol (4,5)-bisphosphate; PIP3, phosphatidylinositol-3,4,5-trisphosphate (PtdIns(3,4,5)P3); PDK-1, 3-phosphoinositide-dependent kinase 1; DAF-18, homologous to human PTEN; AKT1/2 and SGK-1, orthologs of the serine/threonine kinase Akt/PKB; DAF-16, FOXO transcription factor; SKN-1, skinhead family member 1, the ortholog of mammalian Nrf-2; PMK-1, the p38 MAPK ortholog; WDR-23, possible functional homolog of Keap1; DDB-1/CUL-4, ubiquitin ligase complex; ARE, antioxidant response element; OXPHOS, oxidative phosphorylation; GST-10/gst-10, glutathione S-transferase-10; GCS-1/*gcs*-1, γ-glutamyl cysteine synthetase-1; and SOD-1/sod-1 and SOD-3/*sod-3*, superoxide dismutase-1 and -3, respectively.

The regulation mechanisms of SKN-1 are divergent from those of mammals because *C. elegans* does not possess a recognizable Keap1 protein. Alternatively, *C. elegans* expresses WDR-23, a protein that acts as a homolog of Keap1, by promoting the nuclear translocation [82] and binding of SKN-1 to ARE sites [83]. SKN-1 activity is regulated by phosphorylation. Thus, under basal conditions inhibitory phosphorylation by AKT-1/2 and SGK-1 (key components of the IIS pathway) inactivates SKN-1 by maintaining it in the cytosol [79]. Conversely, under conditions of oxidative stress or reduced IIS pathway activity (induced by caloric restriction), the PMK-1 protein (ortholog of the mammalian p38 MAPK) phosphorylates SKN-1 to promote its nuclear translocation and subsequently induce the transcription of phase II detoxification genes, such as *gcs-1* (encoding γ-glutamyl cysteine synthetase), *gst-10* (encoding isoforms of glutathione S-transferase), and *sod-1* (encoding SOD) [79, 84, 85] to generate the ROS response (Figure 2). Another ROS protection mechanism is conferred by DAF-16 via the IIS pathway, which regulates MnSOD gene expression [86]. Evidence has demonstrated that defects in the IIS pathway change the level of cellular energy metabolism (e.g., glucose uptake) and activate DAF-16, increasing the gene expression of *sod-3*, which in turn triggers the activity of this mitochondrial antioxidant system [81] (Figure 2). Therefore, based on the above findings, *C. elegans* represents a useful model organism to study the roles of the SKN-1 and IIS pathways as master regulators of the cellular defense system against oxidative stress.

5. The Roles of ROS as Second Messengers (Mitohormesis) and in Disease

As mentioned above, ROS have been associated with cellular damage. However, diverse studies have challenged the concept of ROS as simply detrimental; instead, they have been proposed as second messengers that trigger a program of transcriptional and metabolic shifts that initiate an adaptive ROS signaling response to attenuate the adverse effects of oxidative stress [92, 93]. Positive effects of ROS have been detected in both humans and *C. elegans*. Healthy young men undergoing physical exercise efficiently increased ROS production and thus counteracted insulin resistance [94]. These findings are consistent with the concept of mitohormesis, in which exercise-induced oxidative stress causes an adaptive response to promote the endogenous antioxidant defense [94]. This adaptive response to ROS, often referred to as mitochondrial hormesis, the hormetic response, or mitohormesis [95], results in compensatory biological processes following an initial disruption of homeostasis [96]. Similar effects have been demonstrated in *C. elegans* (Figure 2); when this nematode is in an active growth and nutrient consumption state, elevated ROS levels activate its stress response and delay aging [97].

ROS have been suggested as second messengers under mild stress conditions, which in turn enhance vitality, in part, because mitochondrial ROS production alters various signaling pathways, functioning as an alarm system that alerts cells to some stressors and responds in a manner that corresponds to the intensity of the detected damage. In fact, ROS appear to function as a signaling intermediate to facilitate cellular adaptation to some types of stress, although it remains to be clarified whether ROS are important for maintaining homeostasis in the absence of oxidative stress [49]. Accordingly, it is plausible that, in circumstances in which both mitochondrial activity and, hence, ROS production are augmented (e.g., diabetes or exercise), the hormetic response may be activated to increase ROS production, upregulating the expression of ROS-neutralizing enzymes, such as SOD2 and GPx. This response involves, in part, the transcription factor SNK-1/Nrf-2, which promotes the transcription of the aforementioned enzymes (Figure 2) [98]. It is noteworthy that the hormetic response may explain why, because of environmental risk factors or lifestyle, not all individuals predisposed to develop diabetes ultimately progress to overt disease. In summary, transiently increased levels of oxidative stress may improve rather than worsen the stress response, reflecting a potentially health-promoting process to prevent metabolic diseases, such as insulin resistance and diabetes, which is consistent with the concept of mitohormesis.

Historically, the principal theory regarding oxidative stress is that the ROS-induced accumulation of molecular damage significantly contributes to numerous human diseases, including diabetes, cardiovascular diseases, atherosclerosis, cancer, and aging [99]. The aforementioned characteristics of *C. elegans* render it a robust model system to investigate oxidative stress, and this model might contribute greatly to our understanding of the role of mitochondria and their integration into the oxidative stress network to regulate the health of the cell and organism.

6. Concluding Remarks

Despite extensive research using various model organisms, there are many unanswered questions concerning the connection between oxidative stress and the pathogenesis of metabolic diseases. Therefore, the development of animal models that serve as models of human diseases has ushered in the study of metabolic diseases. The *C. elegans* model system offers several distinct advantages, including its easy manipulation and maintenance in the laboratory and its high genetic homology to humans, that facilitate multiple studies at both the metabolic and molecular levels. Despite the important differences between nematodes and humans that must be considered, studies using *C. elegans* could significantly contribute to the knowledge gained from classical model organisms by facilitating the generation of results that cannot be produced using whole organisms *in vivo* and the identification of novel and rational treatments. Essentially, the findings from *C. elegans* described in this review indicate similar strategies to fight against oxidative stress, and *C. elegans* can conceivably be used as a powerful model system to delineate the genetic and molecular mechanisms that could be involved in human metabolic diseases, such as diabetes.

Conflict of Interests

The authors declare that there is no conflict of interests regarding the publication of this paper.

References

[1] D. R. Whiting, L. Guariguata, C. Weil, and J. Shaw, "IDF Diabetes Atlas: global estimates of the prevalence of diabetes for 2011 and 2030," *Diabetes Research and Clinical Practice*, vol. 94, no. 3, pp. 311–321, 2011.

[2] D. Pitocco, F. Zaccardi, E. di Stasio et al., "Oxidative stress, nitric oxide, and diabetes," *The Review of Diabetic Studies*, vol. 7, no. 1, pp. 15–25, 2010.

[3] N. Bashan, J. Kovsan, I. Kachko, H. Ovadia, and A. Rudich, "Positive and negative regulation of insulin signaling by reactive oxygen and nitrogen species," *Physiological Reviews*, vol. 89, no. 1, pp. 27–71, 2009.

[4] M. Brownlee, "The pathobiology of diabetic complications: a unifying mechanism," *Diabetes*, vol. 54, no. 6, pp. 1615–1625, 2005.

[5] A. Naudi, M. Jove, V. Ayala et al., "Cellular dysfunction in diabetes as maladaptive response to mitochondrial oxidative stress," *Experimental Diabetes Research*, vol. 2012, Article ID 696215, 14 pages, 2012.

[6] C. elegans Sequencing Consortium, "Erratum: genome sequence of the nematode *C. elegans*: a platform for investigating biology (1998,282(5396):2012-8)," *Science*, vol. 283, no. 5410, p. 2103, 1999.

[7] L. W. Hillier, A. Coulson, J. I. Murray, Z. Bao, J. E. Sulston, and R. H. Waterston, "Genomics in *C. elegans*: so many genes, such a little worm," *Genome Research*, vol. 15, no. 12, pp. 1651–1660, 2005.

[8] T. W. Harris, N. Chen, F. Cunningham et al., "WormBase: a multi-species resource for nematode biology and genomics," *Nucleic Acids Research*, vol. 32, pp. D411–D417, 2004.

[9] S. Brenner, "The genetics of *Caenorhabditis elegans*," *Genetics*, vol. 77, no. 1, pp. 71–94, 1974.

[10] T. T. Le, H. M. Duren, M. N. Slipchenko, C.-D. Hu, and J.-X. Cheng, "Label-free quantitative analysis of lipid metabolism in living *Caenorhabditis elegans*," *Journal of Lipid Research*, vol. 51, no. 3, pp. 672–677, 2010.

[11] D. Hall and Z. Altun, *C. Elegans Atlas*, Cold Spring Harbor Laboratory Press, Cold Spring Harbor, NY, USA, 2008.

[12] K. D. Kimura, H. A. Tissenbaum, Y. Liu, and G. Ruvkun, "daf-2, an insulin receptor-like gene that regulates longevity and diapause in *Caenorhabditis elegans*," *Science*, vol. 277, no. 5328, pp. 942–946, 1997.

[13] C. Kenyon, "The first long-lived mutants: discovery of the insulin/IGF-1 pathway for ageing," *Philosophical Transactions of the Royal Society B: Biological Sciences*, vol. 366, no. 1561, pp. 9–16, 2011.

[14] G. C. Brown, "Control of respiration and ATP synthesis in mammalian mitochondria and cells," *The Biochemical Journal*, vol. 284, part 1, pp. 1–13, 1992.

[15] S. B. Vafai and V. K. Mootha, "Mitochondrial disorders as windows into an ancient organelle," *Nature*, vol. 491, no. 7424, pp. 374–383, 2012.

[16] D. C. Wallace, "Mitochondrial diseases in man and mouse," *Science*, vol. 283, no. 5407, pp. 1482–1488, 1999.

[17] L. Gao, K. Laude, and H. Cai, "Mitochondrial pathophysiology, reactive oxygen species, and cardiovascular diseases," *Veterinary Clinics of North America—Small Animal Practice*, vol. 38, no. 1, pp. 137–155, 2008.

[18] R. R. Murfitt, K. Vogel, and D. R. Sanadi, "Characterization of the mitochondria of the free living nematode, *Caenorhabditis elegans*," *Comparative Biochemistry and Physiology B: Comparative Biochemistry*, vol. 53, no. 4, pp. 423–430, 1976.

[19] R. Okimoto, J. L. Macfarlane, D. O. Clary, and D. R. Wolstenholme, "The mitochondrial genomes of two nematodes, *Caenorhabditis elegans* and *Ascaris suum*," *Genetics*, vol. 130, no. 3, pp. 471–498, 1992.

[20] J. Li, T. Cai, P. Wu et al., "Proteomic analysis of mitochondria from *Caenorhabditis elegans*," *Proteomics*, vol. 9, no. 19, pp. 4539–4553, 2009.

[21] L. I. Grad and B. D. Lemire, "Mitochondrial complex I mutations in *Caenorhabditis elegans* produce cytochrome c oxidase deficiency, oxidative stress and vitamin-responsive lactic acidosis," *Human Molecular Genetics*, vol. 13, no. 3, pp. 303–314, 2004.

[22] W. Yang and S. Hekimi, "Two modes of mitochondrial dysfunction lead independently to lifespan extension in *Caenorhabditis elegans*," *Aging Cell*, vol. 9, no. 3, pp. 433–447, 2010.

[23] W. G. Wadsworth and D. L. Riddle, "Developmental regulation of energy metabolism in *Caenorhabditis elegans*," *Developmental Biology*, vol. 132, no. 1, pp. 167–173, 1989.

[24] B. C. Mullaney and K. Ashrafi, "*C. elegans* fat storage and metabolic regulation," *Biochimica et Biophysica Acta—Molecular and Cell Biology of Lipids*, vol. 1791, no. 6, pp. 474–478, 2009.

[25] J. Kuang and P. R. Ebert, "The failure to extend lifespan via disruption of complex II is linked to preservation of dynamic control of energy metabolism," *Mitochondrion*, vol. 12, no. 2, pp. 280–287, 2012.

[26] W. Dröge, "Free radicals in the physiological control of cell function," *Physiological Reviews*, vol. 82, no. 1, pp. 47–95, 2002.

[27] M. P. Murphy, "How mitochondria produce reactive oxygen species," *The Biochemical Journal*, vol. 417, no. 1, pp. 1–13, 2009.

[28] R. S. Balaban, S. Nemoto, and T. Finkel, "Mitochondria, oxidants, and aging," *Cell*, vol. 120, no. 4, pp. 483–495, 2005.

[29] D. Trachootham, W. Lu, M. A. Ogasawara, N. R.-D. Valle, and P. Huang, "Redox regulation of cell survival," *Antioxidants & Redox Signaling*, vol. 10, no. 8, pp. 1343–1374, 2008.

[30] H. Kamata and H. Hirata, "Redox regulation of cellular signalling," *Cellular Signalling*, vol. 11, no. 1, pp. 1–14, 1999.

[31] K. J. A. Davies, "Oxidative stress, antioxidant defenses, and damage removal, repair, and replacement systems," *IUBMB Life*, vol. 50, no. 4-5, pp. 279–289, 2000.

[32] T. Finkel and N. J. Holbrook, "Oxidants, oxidative stress and the biology of ageing," *Nature*, vol. 408, no. 6809, pp. 239–247, 2000.

[33] I. Fridovich, "Superoxide radical and superoxide dismutases," *Annual Review of Biochemistry*, vol. 64, pp. 97–112, 1995.

[34] I. Fridovich, "The biology of oxygen radicals," *Science*, vol. 201, no. 4359, pp. 875–880, 1978.

[35] D. Gems and R. Doonan, "Antioxidant defense and aging in *C. elegans*: is the oxidative damage theory of aging wrong?" *Cell Cycle*, vol. 8, no. 11, pp. 1681–1687, 2009.

[36] D. Gems, "Ageing and oxidants in the nematode *Caenorhabditis elegans*," *SEB Experimental Biology Series*, vol. 62, pp. 31–56, 2009.

[37] R. Doonan, J. J. McElwee, F. Matthijssens et al., "Against the oxidative damage theory of aging: superoxide dismutases protect against oxidative stress but have little or no effect on life span in *Caenorhabditis elegans*," *Genes & Development*, vol. 22, no. 23, pp. 3236–3241, 2008.

[38] K. Yen, H. B. Patel, A. L. Lublin, and C. V. Mobbs, "SOD isoforms play no role in lifespan in ad lib or dietary restricted conditions, but mutational inactivation of SOD-1 reduces life extension by cold," *Mechanisms of Ageing and Development*, vol. 130, no. 3, pp. 173–178, 2009.

[39] S. Yanase, A. Onodera, P. Tedesco, T. E. Johnson, and N. Ishii, "SOD-1 deletions in *Caenorhabditis elegans* alter the localization of intracellular reactive oxygen species and show molecular compensation," *The Journals of Gerontology A: Biological Sciences and Medical Sciences*, vol. 64, no. 5, pp. 530–539, 2009.

[40] J. M. van Raamsdonk and S. Hekimi, "Deletion of the mitochondrial superoxide dismutase sod-2 extends lifespan in *Caenorhabditis elegans*," *PLoS Genetics*, vol. 5, no. 2, Article ID e1000361, 2009.

[41] J. M. van Raamsdonk and S. Hekimi, "Superoxide dismutase is dispensable for normal animal lifespan," *Proceedings of the National Academy of Sciences of the United States of America*, vol. 109, no. 15, pp. 5785–5790, 2012.

[42] J. A. White and J. G. Scandalios, "Deletion analysis of the maize mitochondrial superoxide dismutase transit peptide," *Proceedings of the National Academy of Sciences of the United States of America*, vol. 86, no. 10, pp. 3534–3538, 1989.

[43] K. Murakami, Y. Ichinohe, M. Koike et al., "VCP Is an integral component of a novel feedback mechanism that controls intracellular localization of catalase and H_2O_2 levels," *PloS ONE*, vol. 8, no. 2, Article ID e56012, 2013.

[44] O. I. Petriv and R. A. Rachubinski, "Lack of peroxisomal catalase causes a progeric phenotype in *Caenorhabditis elegans*," *The Journal of Biological Chemistry*, vol. 279, no. 19, pp. 19996–20001, 2004.

[45] J. Taub, J. F. Lau, C. Ma et al., "A cytosolic catalase is needed to extend adult lifespan in *C. elegans* daf-C and clk-1 mutants," *Nature*, vol. 399, no. 6732, pp. 162–166, 1999.

[46] E. Schröder, J. P. Brennan, and P. Eaton, "Cardiac peroxiredoxins undergo complex modifications during cardiac oxidant stress," *The American Journal of Physiology—Heart and Circulatory Physiology*, vol. 295, no. 1, pp. H425–H433, 2008.

[47] M. Ranjan, J. Gruber, L. F. Ng, and B. Halliwell, "Repression of the mitochondrial peroxiredoxin antioxidant system does not shorten life span but causes reduced fitness in *Caenorhabditis elegans*," *Free Radical Biology & Medicine*, vol. 63, pp. 381–389, 2013.

[48] M. Oláhová, S. R. Taylor, S. Khazaipoul et al., "A redox-sensitive peroxiredoxin that is important for longevity has tissue- and stress-specific roles in stress resistance," *Proceedings of the National Academy of Sciences of the United States of America*, vol. 105, no. 50, pp. 19839–19844, 2008.

[49] L. A. Sena and N. S. Chandel, "Physiological roles of mitochondrial reactive oxygen species," *Molecular Cell*, vol. 48, no. 2, pp. 158–167, 2012.

[50] J. Benner, H. Daniel, and B. Spanier, "A glutathione peroxidase, intracellular peptidases and the tor complexes regulate peptide transporter PEPT-1 in *C. elegans*," *PLoS ONE*, vol. 6, no. 9, Article ID e25624, 2011.

[51] H. Raza, "Dual localization of glutathione S-transferase in the cytosol and mitochondria: implications in oxidative stress, toxicity and disease," *The FEBS Journal*, vol. 278, no. 22, pp. 4243–4251, 2011.

[52] B. Leiers, A. Kampkötter, C. G. Grevelding, C. D. Link, T. E. Johnson, and K. Henkle-Dührsen, "A stress-responsive glutathione S-transferase confers resistance to oxidative stress in *Caenorhabditis elegans*," *Free Radical Biology & Medicine*, vol. 34, no. 11, pp. 1405–1415, 2003.

[53] M. Zamocky, P. G. Furtmüller, and C. Obinger, "Evolution of catalases from bacteria to humans," *Antioxidants & Redox Signaling*, vol. 10, no. 9, pp. 1527–1548, 2008.

[54] P. L. Larsen, "Aging and resistance to oxidative damage in *Caenorhabditis elegans*," *Proceedings of the National Academy of Sciences of the United States of America*, vol. 90, no. 19, pp. 8905–8909, 1993.

[55] T. J. Schulz, K. Zarse, A. Voigt, N. Urban, M. Birringer, and M. Ristow, "Glucose restriction extends *Caenorhabditis elegans* life span by inducing mitochondrial respiration and increasing oxidative stress," *Cell Metabolism*, vol. 6, no. 4, pp. 280–293, 2007.

[56] R. Margis, C. Dunand, F. K. Teixeira, and M. Margis-Pinheiro, "Glutathione peroxidase family—an evolutionary overview," *The FEBS Journal*, vol. 275, no. 15, pp. 3959–3970, 2008.

[57] A. E. Salinas and M. G. Wong, "Glutathione S-transferases—a review," *Current Medicinal Chemistry*, vol. 6, no. 4, pp. 279–309, 1999.

[58] C. Burmeister, K. Lüersen, A. Heinick et al., "Oxidative stress in *Caenorhabditis elegans*: protective effects of the Omega class glutathione transferase (GSTO-1)," *FASEB Journal*, vol. 22, no. 2, pp. 343–354, 2008.

[59] S. Ayyadevara, M. R. Engle, S. P. Singh et al., "Lifespan and stress resistance of *Caenorhabditis elegans* are increased by expression of glutathione transferases capable of metabolizing the lipid peroxidation product 4-hydroxynonenal," *Aging Cell*, vol. 4, no. 5, pp. 257–271, 2005.

[60] W. N. Tawe, M.-L. Eschbach, R. D. Walter, and K. Henkle-Dührsen, "Identification of stress-responsive genes in *Caenorhabditis elegans* using RT-PCR differential display," *Nucleic Acids Research*, vol. 26, no. 7, pp. 1621–1627, 1998.

[61] S. G. Rhee, K.-S. Yang, S. W. Kang, H. A. Woo, and T.-S. Chang, "Controlled elimination of intracellular H_2O_2: regulation of peroxiredoxin, catalase, and glutathione peroxidase via post-translational modification," *Antioxidants & Redox Signaling*, vol. 7, no. 5-6, pp. 619–626, 2005.

[62] K. Isermann, E. Liebau, T. Roeder, and I. Bruchhaus, "A peroxiredoxin specifically expressed in two types of pharyngeal neurons is required for normal growth and egg production in *Caenorhabditis elegans*," *Journal of Molecular Biology*, vol. 338, no. 4, pp. 745–755, 2004.

[63] M. S. Gami and C. A. Wolkow, "Studies of *Caenorhabditis elegans* DAF-2/insulin signaling reveal targets for pharmacological manipulation of lifespan," *Aging Cell*, vol. 5, no. 1, pp. 31–37, 2006.

[64] M. Brownlee, "Biochemistry and molecular cell biology of diabetic complications," *Nature*, vol. 414, no. 6865, pp. 813–820, 2001.

[65] D. Giugliano, A. Ceriello, and G. Paolisso, "Diabetes mellitus, hypertension, and cardiovascular disease: which role for oxidative stress?" *Metabolism: Clinical and Experimental*, vol. 44, no. 3, pp. 363–368, 1995.

[66] M. Kawamura, J. W. Heinecke, and A. Chait, "Pathophysiological concentrations of glucose promote oxidative modification of low density lipoprotein by a superoxide-dependent pathway," *The Journal of Clinical Investigation*, vol. 94, no. 2, pp. 771–778, 1994.

[67] A. Schlotterer, G. Kukudov, F. Bozorgmehr et al., "*C. elegans* as model for the study of high glucose-mediated life span reduction," *Diabetes*, vol. 58, no. 11, pp. 2450–2456, 2009.

[68] J. D. Hayes and M. McMahon, "Molecular basis for the contribution of the antioxidant responsive element to cancer chemoprevention," *Cancer Letters*, vol. 174, no. 2, pp. 103–113, 2001.

[69] A. Cuadrado, P. Moreno-Murciano, and J. Pedraza-Chaverri, "The transcription factor Nrf2 as a new therapeutic target in Parkinson's disease," *Expert Opinion on Therapeutic Targets*, vol. 13, no. 3, pp. 319–329, 2009.

[70] P. Moi, K. Chan, I. Asunis, A. Cao, and Y. W. Kan, "Isolation of NF-E2-related factor 2 (Nrf2), a NF-E2-like basic leucine zipper transcriptional activator that binds to the tandem NF-E2/AP1 repeat of the β-globin locus control region," *Proceedings of the National Academy of Sciences of the United States of America*, vol. 91, no. 21, pp. 9926–9930, 1994.

[71] M. McMahon, K. Itoh, M. Yamamoto, and J. D. Hayes, "Keap1-dependent proteasomal degradation of transcription factor Nrf2 contributes to the negative regulation of antioxidant response element-driven gene expression," *The Journal of Biological Chemistry*, vol. 278, no. 24, pp. 21592–21600, 2003.

[72] M.-K. Kwak, N. Wakabayashi, and T. W. Kensler, "Chemoprevention through the Keap1-Nrf2 signaling pathway by phase 2 enzyme inducers," *Mutation Research—Fundamental and Molecular Mechanisms of Mutagenesis*, vol. 555, no. 1-2, pp. 133–148, 2004.

[73] G. P. Sykiotis and D. Bohmann, "Stress-activated cap'n'collar transcription factors in aging and human disease," *Science Signaling*, vol. 3, no. 112, p. re3, 2010.

[74] L. M. Aleksunes, S. A. Reisman, R. L. Yeager, M. J. Goedken, and C. D. Klaassen, "Nuclear factor erythroid 2-related factor 2 deletion impairs glucose tolerance and exacerbates hyperglycemia in type 1 diabetic mice," *The Journal of Pharmacology and Experimental Therapeutics*, vol. 333, no. 1, pp. 140–151, 2010.

[75] T. W. Kensler, G.-S. Qian, J.-G. Chen, and J. D. Groopman, "Translational strategies for cancer prevention in liver," *Nature Reviews Cancer*, vol. 3, no. 5, pp. 321–329, 2003.

[76] Z. Yu, W. Shao, Y. Chiang et al., "Oltipraz upregulates the nuclear factor (erythroid-derived 2)-like 2 [corrected](NRF2) antioxidant system and prevents insulin resistance and obesity induced by a high-fat diet in C57BL/6J mice," *Diabetologia*, vol. 54, no. 4, pp. 922–934, 2011.

[77] J. Xu, S. R. Kulkarni, A. C. Donepudi, V. R. More, and A. L. Slitt, "Enhanced Nrf2 activity worsens insulin resistance, impairs lipid accumulation in adipose tissue, and increases hepatic steatosis in leptin-deficient mice," *Diabetes*, vol. 61, no. 12, pp. 3208–3218, 2012.

[78] J. H. An and T. K. Blackwell, "SKN-1 links *C. elegans* mesendodermal specification to a conserved oxidative stress response," *Genes & Development*, vol. 17, no. 15, pp. 1882–1893, 2003.

[79] J. M. A. Tullet, M. Hertweck, J. H. An et al., "Direct Inhibition of the Longevity-Promoting Factor SKN-1 by Insulin-like Signaling in *C. elegans*," *Cell*, vol. 132, no. 6, pp. 1025–1038, 2008.

[80] R. Kaletsky and C. T. Murphy, "The role of insulin/IGF-like signaling in *C. elegans* longevity and aging," *DMM Disease Models and Mechanisms*, vol. 3, no. 7-8, pp. 415–419, 2010.

[81] Y. Honda and S. Honda, "The daf-2 gene network for longevity regulates oxidative stress resistance and Mn-superoxide dismutase gene expression in *Caenorhabditis elegans*," *FASEB Journal*, vol. 13, no. 11, pp. 1385–1393, 1999.

[82] K. P. Choe, A. J. Przybysz, and K. Strange, "The WD40 repeat protein WDR-23 functions with the CUL4/DDB1 ubiquitin ligase to regulate nuclear abundance and activity of SKN-1 in *Caenorhabditis elegans*," *Molecular and Cellular Biology*, vol. 29, no. 10, pp. 2704–2715, 2009.

[83] T. K. Blackwell, B. Bowerman, J. R. Priess, and H. Weintraub, "Formation of a monomeric DNA binding domain by Skn-1 bZIP and homeodomain elements," *Science*, vol. 266, no. 5185, pp. 621–628, 1994.

[84] P. Back, F. Matthijssens, C. Vlaeminck, B. P. Braeckman, and J. R. Vanfleteren, "Effects of sod gene overexpression and deletion mutation on the expression profiles of reporter genes of major detoxification pathways in *Caenorhabditis elegans*," *Experimental Gerontology*, vol. 45, no. 7-8, pp. 603–610, 2010.

[85] S.-K. Park, P. M. Tedesco, and T. E. Johnson, "Oxidative stress and longevity in *Caenorhabditis elegans* as mediated by SKN-1," *Aging Cell*, vol. 8, no. 3, pp. 258–269, 2009.

[86] L. R. Lapierre and M. Hansen, "Lessons from *C. elegans*: signaling pathways for longevity," *Trends in Endocrinology and Metabolism*, vol. 23, no. 12, pp. 637–644, 2012.

[87] A. Taguchi and M. F. White, "Insulin-like signaling, nutrient homeostasis, and life span," *Annual Review of Physiology*, vol. 70, pp. 191–212, 2008.

[88] W. Li, S. G. Kennedy, and G. Ruvkun, "daf-28 encodes a *C. elegans* insulin superfamily member that is regulated by environmental cues and acts in the DAF-2 signaling pathway," *Genes & Development*, vol. 17, no. 7, pp. 844–858, 2003.

[89] E. A. Malone, T. Inoue, and J. H. Thomas, "Genetic analysis of the roles of daf-28 and age-1 in regulating *Caenorhabditis elegans* dauer formation," *Genetics*, vol. 143, no. 3, pp. 1193–1205, 1996.

[90] C. Kenyon, J. Chang, E. Gensch, A. Rudner, and R. Tabtiang, "A *C. elegans* mutant that lives twice as long as wild type," *Nature*, vol. 366, no. 6454, pp. 461–464, 1993.

[91] C. Kenyon, "The plasticity of aging: insights from long-lived mutants," *Cell*, vol. 120, no. 4, pp. 449–460, 2005.

[92] S. V. Kharade, N. Mittal, S. P. Das, P. Sinha, and N. Roy, "Mrg19 depletion increases S. cerevisiae lifespan by augmenting ROS defence," *FEBS Letters*, vol. 579, no. 30, pp. 6809–6813, 2005.

[93] E. A. Schroeder and G. S. Shadel, "Alternative mitochondrial fuel extends life span," *Cell Metabolism*, vol. 15, no. 4, pp. 417–418, 2012.

[94] M. Ristow, K. Zarse, A. Oberbach et al., "Antioxidants prevent health-promoting effects of physical exercise in humans," *Proceedings of the National Academy of Sciences of the United States of America*, vol. 106, no. 21, pp. 8665–8670, 2009.

[95] É. le Bourg, "Hormesis, aging and longevity," *Biochimica et Biophysica Acta*, vol. 1790, no. 10, pp. 1030–1039, 2009.

[96] E. J. Calabrese and L. A. Baldwin, "Defining hormesis," *Human & Experimental Toxicology*, vol. 21, no. 2, pp. 91–97, 2002.

[97] W. Yang and S. Hekimi, "A mitochondrial superoxide signal triggers increased longevity in *Caenorhabditis elegans*," *PLoS Biology*, vol. 8, no. 12, Article ID e1000556, 2010.

[98] H. Kolb and D. L. Eizirik, "Resistance to type 2 diabetes mellitus: a matter of hormesis?" *Nature Reviews: Endocrinology*, vol. 8, no. 3, pp. 183–192, 2012.

[99] K. B. Beckman and B. N. Ames, "The free radical theory of aging matures," *Physiological Reviews*, vol. 78, no. 2, pp. 547–581, 1998.

Hindawi Publishing Corporation
Oxidative Medicine and Cellular Longevity
Volume 2014, Article ID 729194, 7 pages
http://dx.doi.org/10.1155/2014/729194

Review Article

Metabolic Syndrome: An Important Risk Factor for Parkinson's Disease

Pei Zhang[1,2] and Bo Tian[1,2]

[1] *Department of Neurobiology, Tongji Medical School, Huazhong University of Science and Technology, 13 Hangkong Road, Wuhan, Hubei 430030, China*
[2] *Key Laboratory of Neurological Diseases, Ministry of Education, Wuhan, Hubei 430030, China*

Correspondence should be addressed to Bo Tian; tianbo@mails.tjmu.edu.cn

Received 14 February 2014; Accepted 21 April 2014; Published 14 May 2014

Academic Editor: Xiaoqian Chen

Metabolic syndrome is becoming commoner due to a rise in obesity rates among adults. Generally speaking, a person with metabolic syndrome is twice as likely to develop cardiovascular disease and five times as likely to develop diabetes as someone without metabolic syndrome. Increasing oxidative stress in metabolic syndrome and Parkinson's disease is mentioned in the comprehensive articles; however, the system review about clear relation between metabolic syndrome and Parkinson's disease is deficient. In this review, we will focus on the analysis that the metabolic syndrome may be a risk factor for Parkinson's disease and the preventions that reduce the incident of Parkinson's disease by regulating the oxidative stress.

1. Introduction

Metabolic syndrome is a prevalent and increasing public health problem worldwide related to many chronic diseases. Its components mainly include at least insulin resistance, central obesity, glucose intolerance, dyslipidemia with elevated triglycerides, low HDL cholesterol, microalbuminuria, predominance of small dense LDL-cholesterol particles, hypertension, endothelial dysfunction, high waist circumference, oxidative stress, inflammation, tumors, neurodegeneration, and atherosclerosis-based ischemic cardio- or cerebral-vascular disease. Meanwhile, recent studies have indicated that increased oxidative stress is the core and a general character of metabolism-related disease. Parkinson's disease, during the past decades, is one of the most frequent neurodegenerative disorders that cause dementia and it is one of the leading chronic diseases in all countries and it also displays the high level of reactive oxygen species (ROS). A growing body of evidence that has implicated the components of metabolic syndrome may contribute to the pathophysiology of Parkinson's disease. In the current brief review, we extend this work to search for findings from studies that provide evidence to clarify it and propose some prevention to delay the progression of Parkinson's disease via regulating the oxidative homeostasis.

2. The Components of Metabolic Syndrome Act as the Risk Factors for Parkinson's Disease

Risk factors for Parkinson's disease are either the result of genetic susceptibility (e.g., SNCA, PARK, PINK, and LRRK2 single nucleotide polymorphisms) or environmental exposure of a person's health to an event that can accelerate or further worsen dysfunction of the central nerve system. Metabolic syndrome is a crucial element of the environmental exposure of the global human health. Following up we will, respectively, introduce the components of metabolic syndrome that act as the risk factors for Parkinson's disease.

2.1. Fat and Obesity. Obesity continues to increase rapidly in the United States [1] and it is well established that obesity can increase the risk of Parkinson's disease and decrease life expectancy. A study has proved that high skinfold thickness in midlife was associated with Parkinson's disease [2]. And

another study found that obesity in middle age increases the risk of future dementia independently of comorbid conditions. Perhaps adiposity works together with other risk factors to increase neurodegenerative disease [3]. In addition, some evidence shows that body mass index is associated with a risk of Parkinson's disease and the effect is graded and independent of other risk factors [4].

In an animal model of Parkinson's disease, high fat diet may lower the threshold for developing Parkinson's disease through affecting glucose transport and decreasing phosphorylation of HSP27 and degradation of IκBα in the nigrostriatal system, at least following dopamine-specific toxin exposure [5, 6]. Moreover, increasing inflammatory signaling, adipokine levels, oxidative or nitrosative stress, mitochondrial dysfunction, and lipid metabolism have all been shown to occur with high fat feeding [7–9].

2.2. Glucose, Hyperglycemia, Insulin Resistance, and Diabetes. High glucose induced cell death is sustained by oxidative, nitrosative stress and mitochondrial superoxide generation through cleavage of the caspase 3 to regulate the apoptotic pathway [10–14]. In aging, hyperglycemia is also associated with Parkinson's disease through damage in central nervous system, a consequence of long-term exposure to glucose [15, 16]. Indeed, epidemiologic studies have implicated that prior type 2 diabetes is also the risk factor of developing Parkinson's disease [17]. Although, in different regions, the Parkinson's disease patients' brain exhibits similar cellular and functional changes with signs of increased oxidative stress, reduced mitochondrial function, reduced glucose uptake, and increased peroxidation of cellular membranes [18].

2.3. Hypertension. Many studies have been carried out on this topic: whether hypertension is the risk factor for Parkinson's disease. Much work, both theoretical and practical, has been reported recently in this field that hypertension is less frequent in Parkinson's disease patient than general population and others show that there is no difference between Parkinson's disease patients and healthy people [19, 20]. Nonetheless, a large prospective study suggested that Parkinson's disease risk is not significantly related to history of hypertension (RR = 0.96; 95% CI = 0.80 to 1.15) [21]. Although a lot of effort is being spent on proving the relation between Parkinson's disease and hypertension, the surely inerrable conclusion has yet to be reached.

2.4. Hyperhomocysteinemia and Endothelial Dysfunction. Hyperhomocysteinemia, a risk factor for endothelial dysfunction [22], has been involved in the pathophysiology of neurodegenerative disorders such as Alzheimer disease and Parkinson disease [23]. And homocysteine leads to endothelial dysfunction that hydrogen peroxide plays a critical role in mediating cell injury *in vitro* [24]. Large increases in cellular oxidative stress and inflammations occurred in response to high homocysteine that induced toxicity by decreased NAD+ [25–29]. In comparison, recent studies have also demonstrated that homocysteine is largely involved in antioxidant and reductive cellular biochemistry [30].

2.5. Inflammations. The involvement of inflammation in Parkinson's disease was initially proposed by McGeer et al. [31] who described the upregulation of HLA-DR-positive reactive microglia in the substantia nigra of Parkinson's disease patients in 1988. Additionally, they also reported that activated microglia was a contributor of proinflammatory and neurotoxic factors in Parkinson's disease patients [32]. Neuroinflammation which was induced by exposure to either toxicants or infectious agents with proinflammatory characteristics as a major factor in the pathogenesis of PD is wildly accepted at present. Plenty of cytokines such as tumor-necrosis factor-α (TNF-α) [32, 33], interleukin 1β (IL-1β) and IL-6 [32, 34–36], and the quantities of ROS [32] have been postulated to be involved in the etiology of Parkinson's disease. Furthermore, recent evidence indicates that endoplasmic reticulum (ER) stress [37–40] and inflammation coordinate the pathogenesis of Parkinson's diseases.

3. Targeting Oxidative Homeostasis as a Therapeutic Strategy against Parkinson's Disease

A growing number of studies have been completed to confirm that stimulation of oxidative stress that initiates apoptosis in many cells and animal models [11, 14, 41] is pivotal to the evolution of metabolic syndrome, diabetes, diabetic neuropathy, and several neurodegenerative disorders, such as Parkinson's disease and Alzheimer disease [42–46]. Though application of antioxidants and some measures in the field of preventing Parkinson's disease have proliferated in recent years, a phyletic classification is lacking. Here we introduce the potential mechanism under a variety of antioxidants or other therapeutic strategies to reduce the oxidation stress.

3.1. Plant Extract. Previous works, such as Bournival et al. [41, 47], Bureau et al. [48], and Gélinas and Martinoli [49], reported that several plant extracts are powerful in neuroprotective activity of dopaminergic neurons against the oxidative burden provoked by administration of the potent parkinsonian toxin MPP+ *in vitro* or 1-methyl-4-phenyl-1,2,3,6-tetrahydropyridine (MPTP) *in vivo*. The plant extract, which contains resveratrol and quercetin and sesamin [41, 47, 48], fermented papaya preparation [50], cinnamon polyphenols [51], and estradiol and phytoestrogens [49], was inhibited by oxidative stress that damages the normal physiological function of cellular organelle by regulating caspase 3, DNA fragment, estrogen receptors, cytokines, Akt, p38, MAPK, and ERK pathway.

An additional research which focuses on the extremely important antioxidant properties of cannabinoids, extract of hemp plant, may contribute to the neuroprotective effect in Parkinson's disease through banding the canonical cannabinoid CB1 and CB2 receptors [52–55].

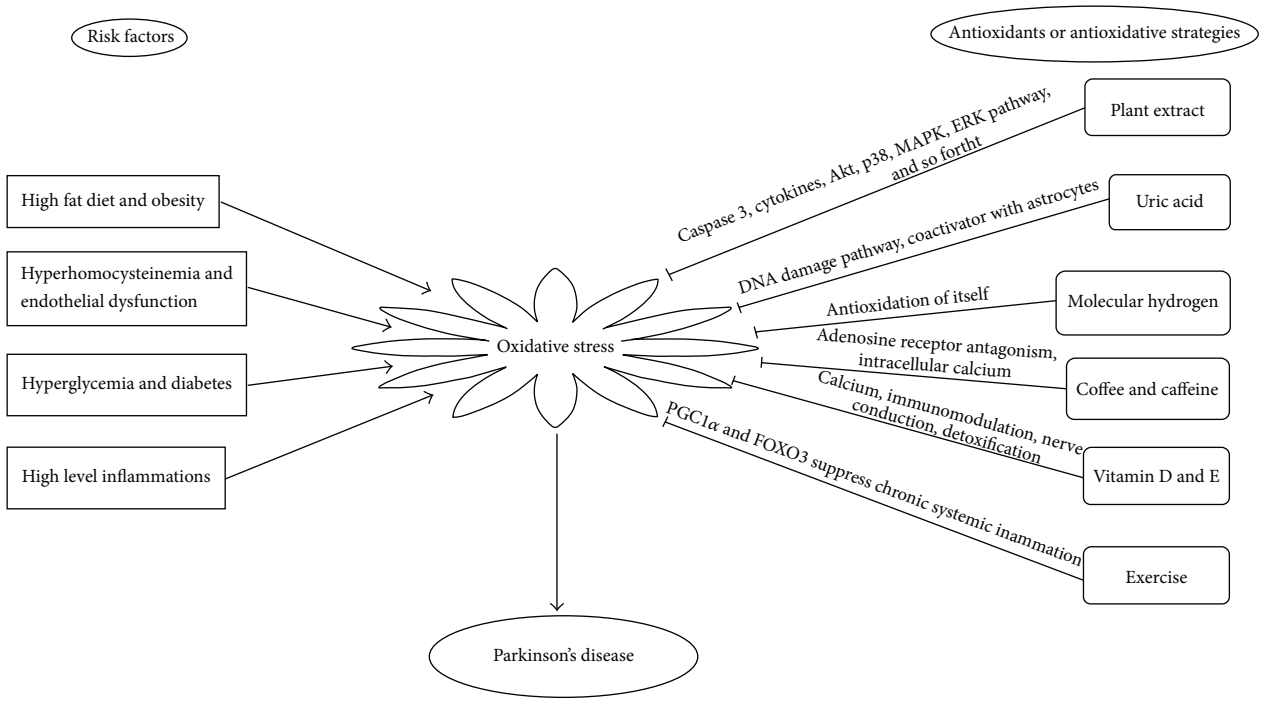

Figure 1: Summary of this review about oxidative stress and Parkinson's disease.

3.2. Uric Acid. A large community-based survey indicated that the associated higher serum uric acid was able to decrease the prevalence of Parkinson's disease [56]. Similarly, it has been observed that UA levels in the serum of patients with Parkinson's disease are lower than in controls and that increased levels of UA are associated with a lower risk of Parkinson's disease [56–59]. Evidence was also proved that physiological concentration of uric acid would exert antioxidant effects, attenuating neuronal lesions caused by oxygen radicals, generated during an acute ischemic stroke and in cases of Parkinson's disease [60]. It had been established that the protective mechanisms of uric acid may be through regulating the DNA damage pathway [60–62]. The recent study from Massachusetts General Hospital found that the urate's ability to protect neurons requires the presence of astrocytes in Parkinson's disease unexpectedly [63].

3.3. Molecular Hydrogen. Hydrogen has great potential for improving oxidative stress-related diseases by inhaling H_2 gas, injecting saline with dissolved H_2, or drinking water with dissolved H_2 [64]. Recent basic and clinical research has revealed that hydrogen is an important physiological regulatory factor with antioxidant, anti-inflammatory, and antiapoptotic protective effects on cells and organs [65]. Meanwhile, a large number of studies report that molecular hydrogen acts as a novel antioxidant and prevents or ameliorates diseases associated with oxidative stress in animal experiments [66–77] and clinical tests [78–81]. Molecular hydrogen improves obesity and diabetes by inducing hepatic FGF21 and stimulating fatty acid and glucose expenditure in mice [64]. Another research reported that molecular hydrogen is protective against 6-hydroxydopamine-induced nigrostriatal degeneration in a rat model of Parkinson's disease [75]. However, little is known about the mechanism that H_2 acts on to prevent oxidative stress in Parkinson's disease.

3.4. Coffee and Caffeine Intake. Higher coffee and caffeine intake is associated with a significantly lower incidence of Parkinson's disease as discussed by Ross et al. [82]. Caffeine, a well-known central nervous system stimulant, inhibits the dopamine neurotransmission through adenosine receptor antagonism and mobilizes of intracellular calcium [83–85]. In addition, caffeine was regarded as an antioxidant against all the three reactive oxygen species, hydroxyl radical, peroxyl radical, and singlet oxygen [86].

3.5. Vitamin D and Vitamin E. Individuals with higher serum vitamin D concentrations showed a reduced risk of Parkinson disease. The relative risk between the highest and lowest quartiles was 0.33 (95% confidence interval, 0.14–0.80) [87]. Even so, the exact mechanisms by which vitamin D may protect against Parkinson disease are not fully understood [87]. High vitamin D status, however, has been shown to exhibit neuroprotective effects through antioxidative mechanisms, neuronal calcium regulation, immunomodulation, enhanced nerve conduction, and detoxification mechanisms [88–90]. Furthermore, the central issue in all these studies is to declare that high intake of dietary vitamin E [91, 92] may protect against the occurrence of PD, but vitamin C or β carotene does not [92]. And the protective influence for Parkinson's disease was seen with both moderate intake (relative risk:

0.81; 95% CI: 0.67–0.98) and high intake (0.78, 0.57–1.06) of vitamin E [92, 93].

3.6. Exercise. Inadequate physical activity has also been shown unequivocally to increase the morbidity and mortality rates of associated chronic disorders [94–96]. Exercise reduces the level of systemic inflammation by increasing the release of adrenaline, cortisol, growth hormone, prolactin, and other factors that have immunomodulatory effects and decreasing expression of toll-like receptors at the surface of monocytes, which have been suggested to be involved in mediating systemic inflammation [97–99]. Many results of the present research synthesis support the fact that the patients with PD improve their physical performance, activities of daily living [100, 101], and the effect of pharmacologic therapy [102] through exercise. The transcriptional coactivator PGC1α controls muscle plasticity and suppresses chronic systemic inflammation via repressing FOXO3 activity, increasing vascularization, ROS detoxification, and mitochondrial and metabolic gene expression [95]. The more specific mechanisms of the fact that exercise mediates the beneficial and advantageous effects for Parkinson's disease remain enigmatic.

4. Summary

This review summarizes the data to support a link between oxidative stress and Parkinson's disease (Figure 1). Parkinson's disease (PD) is a progressive neurodegenerative disorder affecting the elder population mainly and its pathophysiology as well performs a metabolism-related dysfunction. It has been believed generally that oxidative stress was found during Parkinson's disease development when it occurs in early stage. Oxidative stress also is a crucial feather of metabolic syndrome. Undoubtedly, Parkinson's disease should be treated as a metabolic disease. Numbers of antioxidants are effective and efficient in the prevention and treatment of Parkinson's disease by modulating the oxidative stress, but Parkinson's disease whether or not is a metabolic syndrome still needs further epidemiological, basic science and clinical research. At present, considerable studies in a new direction are guiding future research on the relationship between Parkinson's disease and metabolic syndrome.

Conflict of Interests

The authors declare that they have no conflict of interests regarding the publication of this paper.

Acknowledgment

This study was supported by NSFC (nos. 31071208 and 31371384).

References

[1] A. H. Mokdad, M. K. Serdula, W. H. Dietz, B. A. Bowman, J. S. Marks, and J. P. Koplan, "The spread of the obesity epidemic in the United States, 1991–1998," *Journal of the American Medical Association*, vol. 282, no. 16, pp. 1519–1522, 1999.

[2] R. D. Abbott, G. W. Ross, L. R. White et al., "Midlife adiposity and the future risk of Parkinson's disease," *Neurology*, vol. 59, no. 7, pp. 1051–1057, 2002.

[3] R. A. Whitmer, E. P. Gunderson, E. Barrett-Connor, C. P. Quesenberry Jr., and K. Yaffe, "Obesity in middle age and future risk of dementia: a 27 year longitudinal population based study," *British Medical Journal*, vol. 330, no. 7504, pp. 1360–1362, 2005.

[4] G. Hu, P. Jousilahti, A. Nissinen, R. Antikainen, M. Kivipelto, and J. Tuomilehto, "Body mass index and the risk of Parkinson disease," *Neurology*, vol. 67, no. 11, pp. 1955–1959, 2006.

[5] J. K. Morris, G. L. Bomhoff, J. A. Stanford, and P. C. Geiger, "Neurodegeneration in an animal model of Parkinson's disease is exacerbated by a high-fat diet," *American Journal of Physiology-Regulatory Integrative and Comparative Physiology*, vol. 299, no. 4, pp. R1082–R1090, 2010.

[6] J. Y. Choi, E. H. Jang, C. S. Park, and J. H. Kang, "Enhanced susceptibility to 1-methyl-4-phenyl-1,2,3,6-tetrahydropyridine neurotoxicity in high-fat diet-induced obesity," *Free Radical Biology and Medicine*, vol. 38, no. 6, pp. 806–816, 2005.

[7] P. Cano, D. P. Cardinali, M. J. Ríos-Lugo, M. P. Fernández-Mateos, C. F. Reyes Toso, and A. I. Esquifino, "Effect of a high-fat diet on 24-hour pattern of circulating adipocytokines in rats," *Obesity*, vol. 17, no. 10, pp. 1866–1871, 2009.

[8] A. A. Gupte, G. L. Bomhoff, R. H. Swerdlow, and P. C. Geiger, "Heat treatment improves glucose tolerance and prevents skeletal muscle insulin resistance in rats fed a high-fat diet," *Diabetes*, vol. 58, no. 3, pp. 567–578, 2009.

[9] R. M. Uranga, A. J. Bruce-Keller, C. D. Morrison et al., "Intersection between metabolic dysfunction, high fat diet consumption, and brain aging," *Journal of Neurochemistry*, vol. 114, no. 2, pp. 344–361, 2010.

[10] R. Tsuruta, M. Fujita, T. Ono et al., "Hyperglycemia enhances excessive superoxide anion radical generation, oxidative stress, early inflammation, and endothelial injury in forebrain ischemia/reperfusion rats," *Brain Research*, vol. 1309, pp. 155–163, 2010.

[11] I. G. Obrosova, V. R. Drel, P. Pacher et al., "Oxidative-nitrosative stress and poly(ADP-ribose) polymerase (PARP) activation in experimental diabetic neuropathy: the relation is revisited," *Diabetes*, vol. 54, no. 12, pp. 3435–3441, 2005.

[12] C. Szabo, "Multiple pathways of peroxynitrite cytotoxicity," *Toxicology Letters*, vol. 140-141, pp. 105–112, 2003.

[13] A. M. Vincent, J. L. Edwards, M. Sadidi, and E. L. Feldman, "The antioxidant response as a drug target in diabetic neuropathy," *Current Drug Targets*, vol. 9, no. 1, pp. 94–109, 2008.

[14] D. A. Allen, M. M. Yaqoob, and S. M. Harwood, "Mechanisms of high glucose-induced apoptosis and its relationship to diabetic complications," *Journal of Nutritional Biochemistry*, vol. 16, no. 12, pp. 705–713, 2005.

[15] D. R. Tomlinson and N. J. Gardiner, "Glucose neurotoxicity," *Nature Reviews Neuroscience*, vol. 9, no. 1, pp. 36–45, 2008.

[16] G. Hu, P. Jousilahti, S. Bidel, R. Antikainen, and J. Tuomilehto, "Type 2 diabetes and the risk of Parkinson's disease," *Diabetes Care*, vol. 30, no. 4, pp. 842–847, 2007.

[17] L. D. Mercer, B. L. Kelly, M. K. Horne, and P. M. Beart, "Dietary polyphenols protect dopamine neurons from oxidative insults and apoptosis: investigations in primary rat mesencephalic cultures," *Biochemical Pharmacology*, vol. 69, no. 2, pp. 339–345, 2005.

[18] A. D. Pradhan, J. E. Manson, N. Rifai, J. E. Buring, and P. M. Ridker, "C-reactive protein, interleukin 6, and risk of developing type 2 diabetes mellitus," *Journal of the American Medical Association*, vol. 286, no. 3, pp. 327–334, 2001.

[19] G. Scigliano, M. Musicco, P. Soliveri, I. Piccolo, G. Ronchetti, and F. Girotti, "Reduced risk factors for vascular disorders in Parkinson disease patients: a case-control study," *Stroke*, vol. 37, no. 5, pp. 1184–1188, 2006.

[20] A. Morano, F. J. Jimenez-Jimenez, J. A. Molina, and M. A. Antolin, "Risk-factors for Parkinson's disease: case-control study in the province of Caceres, Spain," *Acta Neurologica Scandinavica*, vol. 89, no. 3, pp. 164–170, 1994.

[21] K. C. Simon, H. Chen, M. Schwarzschild, and A. Ascherio, "Hypertension, hypercholesterolemia, diabetes, and risk of Parkinson disease," *Neurology*, vol. 69, no. 17, pp. 1688–1695, 2007.

[22] K. S. Woo, P. Chook, Y. I. Lolin et al., "Hyperhomocyst(e)inemia is a risk factor for arterial endothelial dysfunction in humans," *Circulation*, vol. 96, pp. 2542–2544, 1997.

[23] I. I. Kruman, C. Culmsee, S. L. Chan et al., "Homocysteine elicits a DNA damage response in neurons that promotes apoptosis and hypersensitivity to excitotoxicity," *Journal of Neuroscience*, vol. 20, no. 18, pp. 6920–6926, 2000.

[24] R. T. Wall, J. M. Harlan, L. A. Harker, and G. E. Striker, "Homocysteine-induced endothelial cell injury in vitro: a model for the study of vascular injury," *Thrombosis Research*, vol. 18, no. 1-2, pp. 113–121, 1980.

[25] C. Gomes Trolin, B. Regland, and L. Oreland, "Decreased methionine adenosyltransferase activity in erythrocytes of patients with dementia disorders," *European Neuropsychopharmacology*, vol. 5, no. 2, pp. 107–114, 1995.

[26] F. Blandini, R. Fancellu, E. Martignoni et al., "Plasma homocysteine and L-DOPA metabolism in patients with Parkinson disease," *Clinical Chemistry*, vol. 47, no. 6, pp. 1102–1104, 2001.

[27] T. Bottiglieri and K. Hyland, "S-adenosylmethionine levels in psychiatric and neurological disorders: a review," *Acta Neurologica Scandinavica, Supplementum*, vol. 89, no. 154, pp. 19–26, 1994.

[28] J. Loscalzo, "The oxidant stress of hyperhomocyst(e)inemia," *The Journal of Clinical Investigation*, vol. 98, no. 1, pp. 5–7, 1996.

[29] K. Kurz, B. Frick, C. Fürhapter et al., "Homocysteine metabolism in different human cells," *Issues*, vol. 24, 2013.

[30] B. Zappacosta, A. Mordente, S. Persichilli et al., "Is homocysteine a pro-oxidant?" *Free Radical Research*, vol. 35, no. 5, pp. 499–505, 2001.

[31] P. L. McGeer, S. Itagaki, B. E. Boyes, and E. G. McGeer, "Reactive microglia are positive for HLA-DR in the substantia nigra of Parkinson's and Alzheimer's disease brains," *Neurology*, vol. 38, no. 8, pp. 1285–1291, 1988.

[32] P. S. Whitton, "Inflammation as a causative factor in the aetiology of Parkinson's disease," *British Journal of Pharmacology*, vol. 150, no. 8, pp. 963–976, 2007.

[33] M. G. Tansey, T. C. Frank-Cannon, M. K. McCoy et al., "Neuroinflammation in Parkinson's disease: is there sufficient evidence for mechanism-based interventional therapy?" *Frontiers in Bioscience*, vol. 13, no. 2, pp. 709–717, 2008.

[34] M. Mogi, M. Harada, T. Kondob et al., "Interleukin-1β, interleukin-6, epidermal growth factor and transforming growth factor-α are elevated in the brain from parkinsonian patients," *Neuroscience Letters*, vol. 180, no. 2, pp. 147–150, 1994.

[35] D. Blum-Degena, T. Müller, W. Kuhn, M. Gerlach, H. Przuntek, and P. Riederer, "Interleukin-1β and interleukin-6 are elevated in the cerebrospinal fluid of Alzheimer's and de novo Parkinson's disease patients," *Neuroscience Letters*, vol. 202, no. 1-2, pp. 17–20, 1995.

[36] T. Müller, D. Blum-Degen, H. Przuntek, and W. Kuhn, "Interleukin-6 levels in cerebrospinal fluid inversely correlate to severity of Parkinson's disease," *Acta Neurologica Scandinavica*, vol. 98, no. 2, pp. 142–144, 1998.

[37] Y. Imai, M. Soda, H. Inoue, N. Hattori, Y. Mizuno, and R. Takahashi, "An unfolded putative transmembrane polypeptide, which can lead to endoplasmic reticulum stress, is a substrate of Parkin," *Cell*, vol. 105, no. 7, pp. 891–902, 2001.

[38] Y. Imai, M. Soda, S. Hatakeyama et al., "CHIP is associated with Parkin, a gene responsible for familial Parkinson's Disease, and enhances its ubiquitin ligase activity," *Molecular Cell*, vol. 10, no. 1, pp. 55–67, 2002.

[39] R. J. Kaufman, "Orchestrating the unfolded protein response in health and disease," *Journal of Clinical Investigation*, vol. 110, no. 10, pp. 1389–1398, 2002.

[40] Y. Imai, M. Soda, and R. Takahashi, "Parkin suppresses unfolded protein stress-induced cell death through its E3 ubiquitin-protein ligase activity," *Journal of Biological Chemistry*, vol. 275, no. 46, pp. 35661–35664, 2000.

[41] J. Bournival, P. Quessy, and M. Martinoli, "Protective effects of resveratrol and quercetin against MPP+ -induced oxidative stress act by modulating markers of apoptotic death in dopaminergic neurons," *Cellular and Molecular Neurobiology*, vol. 29, no. 8, pp. 1169–1180, 2009.

[42] A. Whaley-Connell, P. A. McCullough, and J. R. Sowers, "The role of oxidative stress in the metabolic syndrome," *Reviews in Cardiovascular Medicine*, vol. 12, no. 1, pp. 21–29, 2011.

[43] C. Zhou, Y. Huang, and S. Przedborski, "Oxidative stress in Parkinson's disease: a mechanism of pathogenic and therapeutic significance," *Annals of the New York Academy of Sciences*, vol. 1147, pp. 93–104, 2008.

[44] A. M. Vincent, M. Brownlee, and J. W. Russell, "Oxidative stress and programmed cell death in diabetic neuropathy," *Annals of the New York Academy of Sciences*, vol. 959, pp. 368–383, 2002.

[45] A. P. Rolo and C. M. Palmeira, "Diabetes and mitochondrial function: role of hyperglycemia and oxidative stress," *Toxicology and Applied Pharmacology*, vol. 212, no. 2, pp. 167–178, 2006.

[46] P. I. Moreira, M. S. Santos, R. Seiça, and C. R. Oliveira, "Brain mitochondrial dysfunction as a link between Alzheimer's disease and diabetes," *Journal of the Neurological Sciences*, vol. 257, no. 1-2, pp. 206–214, 2007.

[47] J. Bournival, M. A. Francoeur, J. Renaud, and M. G. Martinoli, "Quercetin and sesamin protect neuronal PC12 cells from high-glucose-induced oxidation, nitrosative stress, and apoptosis," *Rejuvenation Research*, vol. 15, no. 3, pp. 322–333, 2012.

[48] G. Bureau, F. Longpré, and M. Martinoli, "Resveratrol and quercetin, two natural polyphenols, reduce apoptotic neuronal cell death induced by neuroinflammation," *Journal of Neuroscience Research*, vol. 86, no. 2, pp. 403–410, 2008.

[49] S. Gélinas and M. Martinoli, "Neuroprotective effect of estradiol and phytoestrogens on MPP+-induced cytotoxicity in neuronal PC12 cells," *Journal of Neuroscience Research*, vol. 70, no. 1, pp. 90–96, 2002.

[50] O. I. Aruoma, Y. Hayashi, F. Marotta, P. Mantello, E. Rachmilewitz, and L. Montagnier, "Applications and bioefficacy of the functional food supplement fermented papaya preparation," *Toxicology*, vol. 278, no. 1, pp. 6–16, 2010.

[51] H. Cao, B. Qin, K. S. Panickar, and R. A. Anderson, "Tea and cinnamon polyphenols improve the metabolic syndrome," *Agro Food Industry Hi-Tech*, vol. 19, no. 6, pp. 14–17, 2008.

[52] M. García-Arencibia, S. González, E. de Lago, J. A. Ramos, R. Mechoulam, and J. Fernández-Ruiz, "Evaluation of the neuroprotective effect of cannabinoids in a rat model of Parkinson's disease: importance of antioxidant and cannabinoid receptor-independent properties," *Brain Research*, vol. 1134, no. 1, pp. 162–170, 2007.

[53] A. W. Zuardi, J. A. S. Crippa, J. E. C. Hallak et al., "Cannabidiol for the treatment of psychosis in Parkinsons disease," *Journal of Psychopharmacology*, vol. 23, no. 8, pp. 979–983, 2009.

[54] G. W. Booz, "Cannabidiol as an emergent therapeutic strategy for lessening the impact of inflammation on oxidative stress," *Free Radical Biology and Medicine*, vol. 51, no. 5, pp. 1054–1061, 2011.

[55] P. Pacher, S. Bátkai, and G. Kunos, "The endocannabinoid system as an emerging target of pharmacotherapy," *Pharmacological Reviews*, vol. 58, no. 3, pp. 389–462, 2006.

[56] A. Winquist, K. Steenland, and A. Shankar, "Higher serum uric acid associated with decreased Parkinson's disease prevalence in a large community-based survey," *Movement Disorders*, vol. 25, no. 7, pp. 932–936, 2010.

[57] E. Andreadou, C. Nikolaou, F. Gournaras et al., "Serum uric acid levels in patients with Parkinson's disease: their relationship to treatment and disease duration," *Clinical Neurology and Neurosurgery*, vol. 111, no. 9, pp. 724–728, 2009.

[58] B. Álvarez-Lario and J. Macarrón-vicente, "Is there anything good in uric acid?" *QJM*, vol. 104, no. 12, Article ID hcr159, pp. 1015–1024, 2011.

[59] H. Chen, T. H. Mosley, A. Alonso, and X. Huang, "Plasma urate and Parkinson's disease in the atherosclerosis risk in communities (ARIC) study," *American Journal of Epidemiology*, vol. 169, no. 9, pp. 1064–1069, 2009.

[60] M. Cucuianu and I. Brudasca, "Gout, hyperuricemia and the metabolic syndrome," *Revista Româna de Medicina de Laborator*, vol. 20, no. 3-4, 2012.

[61] R. G. Cutler, "Antioxidants and aging," *American Journal of Clinical Nutrition*, vol. 53, supplement 1, pp. 373S–379S, 1991.

[62] B. N. Ames, R. Cathcart, E. Schwiers, and P. Hochstein, "Uric acid provides an antioxidant defense in humans against oxidant- and radical-caused aging and cancer: a hypothesis," *Proceedings of the National Academy of Sciences of the United States of America*, vol. 78, no. 11, pp. 6858–6862, 1981.

[63] S. Cipriani, C. A. Desjardins, T. C. Burdett et al., "Urate and its transgenic depletion modulate neuronal vulnerability in a cellular model of Parkinson's disease," *PLoS ONE*, vol. 7, no. 5, Article ID e37331, 2012.

[64] N. Kamimura, K. Nishimaki, I. Ohsawa, and S. Ohta, "Molecular hydrogen improves obesity and diabetes by inducing hepatic FGF21 and stimulating energy metabolism in db/db mice," *Obesity*, vol. 19, no. 7, pp. 1396–1403, 2011.

[65] C. S. Huang, T. Kawamura, Y. Toyoda, and A. Nakao, "Recent advances in hydrogen research as a therapeutic medical gas," *Free Radical Research*, vol. 44, no. 9, pp. 971–982, 2010.

[66] I. Ohsawa, K. Nishimaki, K. Yamagata, M. Ishikawa, and S. Ohta, "Consumption of hydrogen water prevents atherosclerosis in apolipoprotein E knockout mice," *Biochemical and Biophysical Research Communications*, vol. 377, no. 4, pp. 1195–1198, 2008.

[67] K. Fukuda, S. Asoh, M. Ishikawa, Y. Yamamoto, I. Ohsawa, and S. Ohta, "Inhalation of hydrogen gas suppresses hepatic injury caused by ischemia/reperfusion through reducing oxidative stress," *Biochemical and Biophysical Research Communications*, vol. 361, no. 3, pp. 670–674, 2007.

[68] A. Nakao, D. J. Kaczorowski, Y. Wang et al., "Amelioration of rat cardiac cold ischemia/reperfusion injury with inhaled hydrogen or carbon monoxide, or both," *Journal of Heart and Lung Transplantation*, vol. 29, no. 5, pp. 544–553, 2010.

[69] B. M. Buchholz, D. J. Kaczorowski, R. Sugimoto et al., "Hydrogen inhalation ameliorates oxidative stress in transplantation induced intestinal graft injury," *American Journal of Transplantation*, vol. 8, no. 10, pp. 2015–2024, 2008.

[70] K. Hayashida, M. Sano, I. Ohsawa et al., "Inhalation of hydrogen gas reduces infarct size in the rat model of myocardial ischemia-reperfusion injury," *Biochemical and Biophysical Research Communications*, vol. 373, no. 1, pp. 30–35, 2008.

[71] K. Nagata, N. Nakashima-Kamimura, T. Mikami, I. Ohsawa, and S. Ohta, "Consumption of molecular hydrogen prevents the stress-induced impairments in hippocampus-dependent learning tasks during chronic physical restraint in mice," *Neuropsychopharmacology*, vol. 34, no. 2, pp. 501–508, 2009.

[72] N. Nakashima-Kamimura, T. Mori, I. Ohsawa, S. Asoh, and S. Ohta, "Molecular hydrogen alleviates nephrotoxicity induced by an anti-cancer drug cisplatin without compromising anti-tumor activity in mice," *Cancer Chemotherapy and Pharmacology*, vol. 64, no. 4, pp. 753–761, 2009.

[73] J. S. Cardinal, J. Zhan, Y. Wang et al., "Oral hydrogen water prevents chronic allograft nephropathy in rats," *Kidney International*, vol. 77, no. 2, pp. 101–109, 2010.

[74] K. Fujita, T. Seike, N. Yutsudo et al., "Hydrogen in drinking water reduces dopaminergic neuronal loss in the 1-methyl-4-phenyl-1,2,3,6-tetrahydropyridine mouse model of Parkinson's disease," *PLoS ONE*, vol. 4, no. 9, Article ID e7247, 2009.

[75] Y. Fu, M. Ito, Y. Fujita et al., "Molecular hydrogen is protective against 6-hydroxydopamine-induced nigrostriatal degeneration in a rat model of Parkinson's disease," *Neuroscience Letters*, vol. 453, no. 2, pp. 81–85, 2009.

[76] I. Ohsawa, M. Ishikawa, K. Takahashi et al., "Hydrogen acts as a therapeutic antioxidant by selectively reducing cytotoxic oxygen radicals," *Nature Medicine*, vol. 13, no. 6, pp. 688–694, 2007.

[77] H. Oharazawa, T. Igarashi, T. Yokota et al., "Protection of the retina by rapid diffusion of hydrogen: administration of hydrogen-loaded eye drops in retinal ischemia-reperfusion injury," *Investigative Ophthalmology and Visual Science*, vol. 51, no. 1, pp. 487–492, 2010.

[78] S. Kajiyama, G. Hasegawa, M. Asano et al., "Supplementation of hydrogen-rich water improves lipid and glucose metabolism in patients with type 2 diabetes or impaired glucose tolerance," *Nutrition Research*, vol. 28, no. 3, pp. 137–143, 2008.

[79] A. Nakao, Y. Toyoda, P. Sharma, M. Evans, and N. Guthrie, "Effectiveness of hydrogen rich water on antioxidant status of subjects with potential metabolic syndrome-an open label pilot study," *Journal of Clinical Biochemistry and Nutrition*, vol. 46, no. 2, pp. 140–149, 2010.

[80] M. Nakayama, S. Kabayama, H. Nakano et al., "Biological effects of electrolyzed water in hemodialysis," *Nephron-Clinical Practice*, vol. 112, no. 1, pp. c9–c15, 2009.

[81] Y. Suzuki, M. Sano, K. Hayashida, I. Ohsawa, S. Ohta, and K. Fukuda, "Are the effects of α-glucosidase inhibitors on

cardiovascular events related to elevated levels of hydrogen gas in the gastrointestinal tract?" *FEBS Letters*, vol. 583, no. 13, pp. 2157–2159, 2009.

[82] G. W. Ross, R. D. Abbott, H. Petrovitch et al., "Association of coffee and caffeine intake with the risk of Parkinson disease," *Journal of the American Medical Association*, vol. 283, no. 20, pp. 2674–2679, 2000.

[83] A. Nehlig, J.-L. Daval, and G. Debry, "Caffeine and the central nervous system: mechanisms of action, biochemical, metabolic and psychostimulant effects," *Brain Research Reviews*, vol. 17, no. 2, pp. 139–169, 1992.

[84] P. Popoli, M. G. Caporali, and A. Scotti de Carolis, "Akinesia due to catecholamine depletion in mice is prevented by caffeine. Further evidence for an involvement of adenosinergic system in the control of motility," *Journal of Pharmacy and Pharmacology*, vol. 43, no. 4, pp. 280–281, 1991.

[85] J. W. Daly, "Caffeine analogs: biomedical impact," *Cellular and Molecular Life Sciences*, vol. 64, no. 16, pp. 2153–2169, 2007.

[86] T. P. Devasagayam, J. P. Kamat, H. Mohan, and P. C. Kesavan, "Caffeine as an antioxidant: inhibition of lipid peroxidation induced by reactive oxygen species," *Biochimica et Biophysica Acta*, vol. 1282, pp. 63–70, 1996.

[87] P. Knekt, A. Kilkkinen, H. Rissanen, J. Marniemi, K. Sääksjärvi, and M. Heliövaara, "Serum vitamin D and the risk of Parkinson disease," *Archives of Neurology*, vol. 67, no. 7, pp. 808–811, 2010.

[88] J. S. Buell and B. Dawson-Hughes, "Vitamin D and neurocognitive dysfunction: preventing "D"ecline?" *Molecular Aspects of Medicine*, vol. 29, no. 6, pp. 415–422, 2008.

[89] H. L. Newmark and J. Newmark, "Vitamin D and Parkinson's disease—a hypothesis," *Movement Disorders*, vol. 22, no. 4, pp. 461–468, 2007.

[90] D. W. Eyles, S. Smith, R. Kinobe, M. Hewison, and J. J. McGrath, "Distribution of the Vitamin D receptor and 1α-hydroxylase in human brain," *Journal of Chemical Neuroanatomy*, vol. 29, no. 1, pp. 21–30, 2005.

[91] M. C. de Rijk, M. M. Breteler, J. H. den Breeijen et al., "Dietary antioxidants and Parkinson disease. The Rotterdam study," *Archives of Neurology*, vol. 54, no. 6, pp. 762–765, 1997.

[92] M. Etminan, S. S. Gill, and A. Samii, "Intake of vitamin E, vitamin C, and carotenoids and the risk of Parkinson's disease: a meta-analysis," *Lancet Neurology*, vol. 4, no. 6, pp. 362–365, 2005.

[93] E. R. Miller III, R. Pastor-Barriuso, D. Dalal, R. A. Riemersma, L. J. Appel, and E. Guallar, "Meta-analysis: high-dosage vitamin E supplementation may increase all-cause mortality," *Annals of Internal Medicine*, vol. 142, no. 1, pp. 37–46, 2005.

[94] G. Erikssen, K. Liestøl, J. Bjømholt, E. Thaulow, L. Sandvik, and J. Mrikssen, "Changes in physical fitness and changes in mortality," *The Lancet*, vol. 352, no. 9130, pp. 759–762, 1998.

[95] C. Handschin and B. M. Spiegelman, "The role of exercise and PGC1α in inflammation and chronic disease," *Nature*, vol. 454, no. 7203, pp. 463–469, 2008.

[96] F. B. Hu, W. C. Willett, T. Li, M. J. Stampfer, G. A. Colditz, and J. E. Manson, "Adiposity as compared with physical activity in predicting mortality among women," *New England Journal of Medicine*, vol. 351, no. 26, pp. 2694–2703, 2004.

[97] D. C. Nieman, "Current perspective on exercise immunology," *Current Sports Medicine Reports*, vol. 2, no. 5, pp. 239–242, 2003.

[98] M. Gleeson, B. McFarlin, and M. Flynn, "Exercise and toll-like receptors," *Exercise Immunology Review*, vol. 12, pp. 34–53, 2006.

[99] M. Gleeson, "Immune function in sport and exercise," *Journal of Applied Physiology*, vol. 103, no. 2, pp. 693–699, 2007.

[100] A. M. Crizzle and I. J. Newhouse, "Is physical exercise beneficial for persons with Parkinson's disease?" *Clinical Journal of Sport Medicine*, vol. 16, no. 5, pp. 422–425, 2006.

[101] I. Reuter, M. Engelhardt, K. Stecker, and H. Baas, "Therapeutic value of exercise training in Parkinson's disease," *Medicine and Science in Sports and Exercise*, vol. 31, no. 11, pp. 1544–1549, 1999.

[102] S. S. Palmer, J. A. Mortimer, and D. D. Webster, "Exercise therapy for Parkinson's disease," *Archives of Physical Medicine and Rehabilitation*, vol. 67, no. 10, pp. 741–745, 1986.

Hindawi Publishing Corporation
Oxidative Medicine and Cellular Longevity
Volume 2014, Article ID 906804, 10 pages
http://dx.doi.org/10.1155/2014/906804

Research Article

Piperlongumine Induces Apoptosis and Synergizes with Cisplatin or Paclitaxel in Human Ovarian Cancer Cells

Li-Hua Gong,[1] Xiu-Xiu Chen,[1] Huan Wang,[2] Qi-Wei Jiang,[3] Shi-Shi Pan,[1] Jian-Ge Qiu,[3] Xiao-Long Mei,[3] You-Qiu Xue,[3] Wu-Ming Qin,[3] Fei-Yun Zheng,[1] Zhi Shi,[3] and Xiao-Jian Yan[1]

[1] *Department of Gynecology, The First Affiliated Hospital of Wenzhou Medical College, Shangcai Village South, Ouhai District, Wenzhou, Zhejiang 325000, China*
[2] *Department of Gynecology, The Third Affiliated Hospital of Sun-Yat Sen University, Guangzhou, Guangdong 510632, China*
[3] *Department of Cell Biology and Institute of Biomedicine, College of Life Science and Technology, Jinan University, Room 708, The 2nd Engineer and Scientific Building, 601 Huangpu RoadWest, Guangzhou, Guangdong 510632, China*

Correspondence should be addressed to Zhi Shi; tshizhi@jnu.edu.cn and Xiao-Jian Yan; yxjbetter@126.com

Received 14 February 2014; Revised 1 April 2014; Accepted 3 April 2014; Published 8 May 2014

Academic Editor: Si Jin

Piperlongumine (PL), a natural alkaloid from *Piper longum L.*, possesses the highly selective and effective anticancer property. However, the effect of PL on ovarian cancer cells is still unknown. In this study, we firstly demonstrate that PL selectively inhibited cell growth of human ovarian cancer cells. Furthermore, PL notably induced cell apoptosis, G2/M phase arrest, and accumulation of the intracellular reactive oxidative species (ROS) in a dose- and time-dependent manner. Pretreatment with antioxidant N-acety-L-cysteine could totally reverse the PL-induced ROS accumulation and cell apoptosis. In addition, low dose of PL/cisplatin or paclitaxel combination therapies had a synergistic antigrowth effect on human ovarian cancer cells. Collectively, our study provides new therapeutic potential of PL on human ovarian cancer.

1. Introduction

Ovarian cancer is the most lethal cancer of female reproductive tract, accounting for ~16,000 deaths annually [1]. The high mortality results partially from the nonspecific and commonly misinterpreted symptoms associated with the disease. As a result, more than 70% of patients are diagnosed only after the disease has progressed to a late stage [2]. Cytoreduction surgery combined with cisplatin (DDP) or paclitaxel (TX) chemotherapy in ovarian cancer results in a clinical remission but is infrequently a cure. Improving the current responses to chemotherapy is a key for achieving a better outcome and we have demonstrated that silence of survivin could effectively increase the sensitivity of ovarian cancer cells to chemotherapeutical drugs [3–6]. Etiology of ovarian cancer is still unknown; several theories such as gonadotropin theory and genetic alteration have been proposed as the mechanism of carcinogenesis [7]. A role for chronic oxidative stress has been proposed in the etiology of malignant transformation and elevation of reactive oxygen species (ROS) levels has been observed in many cancer cells relative to nontransformed cells [8, 9]. Therefore, the elevated ROS in cancer cells provide for a prospect of selective cancer treatment [10, 11].

Piperlongumine (PL) is a biologically active alkaloid isolated from the long pepper (*Piper longum* Linn) which is used to treat cough, respiratory infections, stomachache, and other diseases in Indian Ayurvedic medicine [12]. The chemical structure of PL has been well-characterized (Figure 1(a)). Recently, PL has shown potential cytotoxic and antitumor properties on several types of cancer cells, including hematological [13], gastrointestinal [14], central nervous system [15], and other solid tumors [16]. Its cytotoxicity was observed in the micromolar range in tumor cells, but not in normal cells

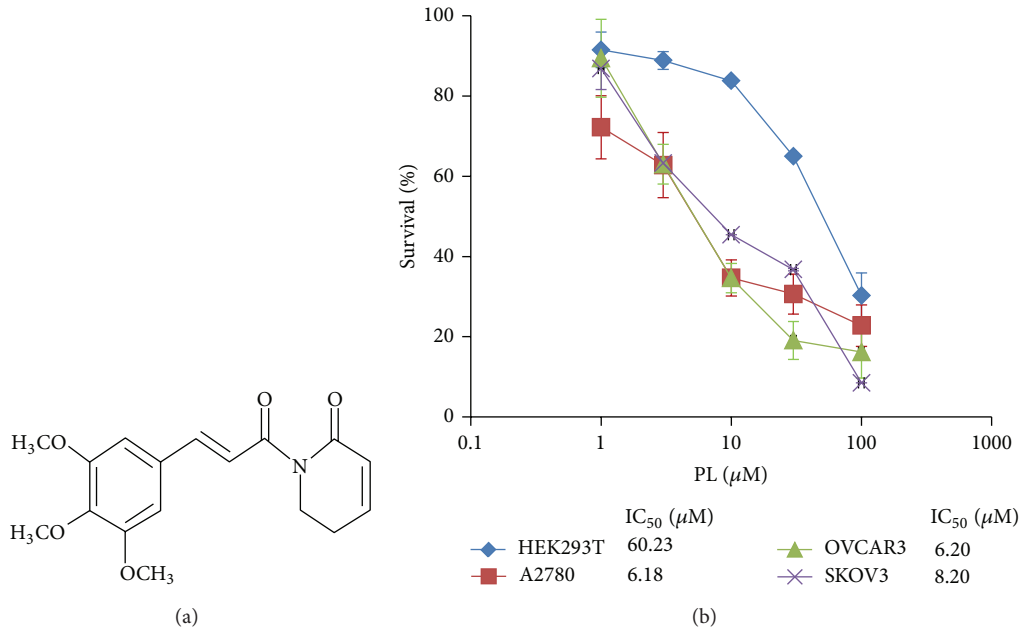

Figure 1: PL selectively inhibited the growth of human ovarian cancer cells. (a) Structure of PL. (b) The growth curves of PL-treated A2780, OVCAR3, SKOV3, and HEK293T cells. Cells were grown in 96-well plates for 24 hr and treated with PL (0, 1, 3, 10, 30, and 100 μM) for 72 hr. Cell survival was measured by MTT assay and the IC_{50} value of PL in each cell lines was calculated.

[14, 16–18]. Quantitative proteomics approaches identified two strong PL-binding proteins, S-transferase pi 1 (GSTP1) and carbonyl reductase 1, known to regulate oxidative stress by modulating redox and ROS homeostasis [18]. Consistent with this theory, when PL interacted directly with GSTP1, protein glutathionylation was identified as a process associated with cellular toxicity [19]. Furthermore, PL induced cell cycle arrest in G1 or G2/M phase followed by mitochondrial-dependent apoptosis [20]. More recently, PL also promoted autophagy and mediates cell death in several cancer cell lines [21, 22].

In the present study, we firstly demonstrate that PL selectively inhibited cell growth and induced ROS-dependent cell apoptosis and G2/M cell cycle arrest in human ovarian cancer. Furthermore, PL synergizes with DDP and TX to inhibit the growth of human ovarian cancer cells. Our results provide new drug therapeutic potential of PL on human ovarian cancer.

2. Materials and Methods

2.1. Cells Lines and Reagents. The human epithelia ovarian cancer (EOC) lines A2780, OVCAR3, and SKOV3 and human embryonic kidney cell line HEK293T were cultured in DMEM (Gibco, NY, USA) culture medium supplemented with 10% fetal bovine serum (Gibco, NY, USA) at 37°C and 5% CO_2. PL, N-acetyl-L-cysteine (NAC), dihydroethidium (DHE), anti-β-actin antibody, and other chemicals were purchased from Sigma Chemical Co. (St. Louis, MO, USA). Anti-cleaved-PARP (C-PARP) antibody was from Cell Signaling Technologies (Danvers, MA, USA).

2.2. MTT Assay. Cells were harvested with trypsin and resuspended in a final concentration of 5×10^4 cells/mL. Aliquot (100 μL) for each cell suspension was distributed evenly into 96-well multiplates. The different concentrations of PL (10 μL/well) were added to designated wells. After 72 hours (hr), 10 μL of 3-(4,5-dimethylthiazol-2yl)-2,5-diphenyl tetrazolium bromide (MTT) solution (5 mg/mL) was added to each well, and the plate was further incubated for 4 hr, allowing viable cells to change the yellow MTT into dark-blue formazan crystals. Subsequently, the medium was discarded and 100 μL of dimethylsulfoxide (DMSO) was added to each well to dissolve the formazan crystals. The absorbance in individual well was determined at 490 nm by multidetection microplate reader 680 (BioRad, PA, USA). The concentrations required to inhibit growth by 50% (IC_{50}) were calculated from survival curves using the Bliss method [23, 24]. For drug combination experiments, cells were cotreated with different concentrations of PL and DDP or TX for 72 hr. The data were analyzed by CompuSyn software with the results showed in combination index (CI) values, where CI <1, =1, and >1 indicate synergism, additive effect, and antagonism, respectively.

2.3. Apoptosis Analysis. Cell apoptosis was evaluated with flow cytometry (FCM) assay. Briefly, cells were harvested and washed twice with cold phosphate-buffered saline (PBS), stained with Annexin V-FITC and propidium iodide (PI) in the binding buffer, and detected by FACSCalibur FCM (BD, CA, USA) after 15 min incubation at room temperature in the dark. Fluorescence was measured at an excitation wave

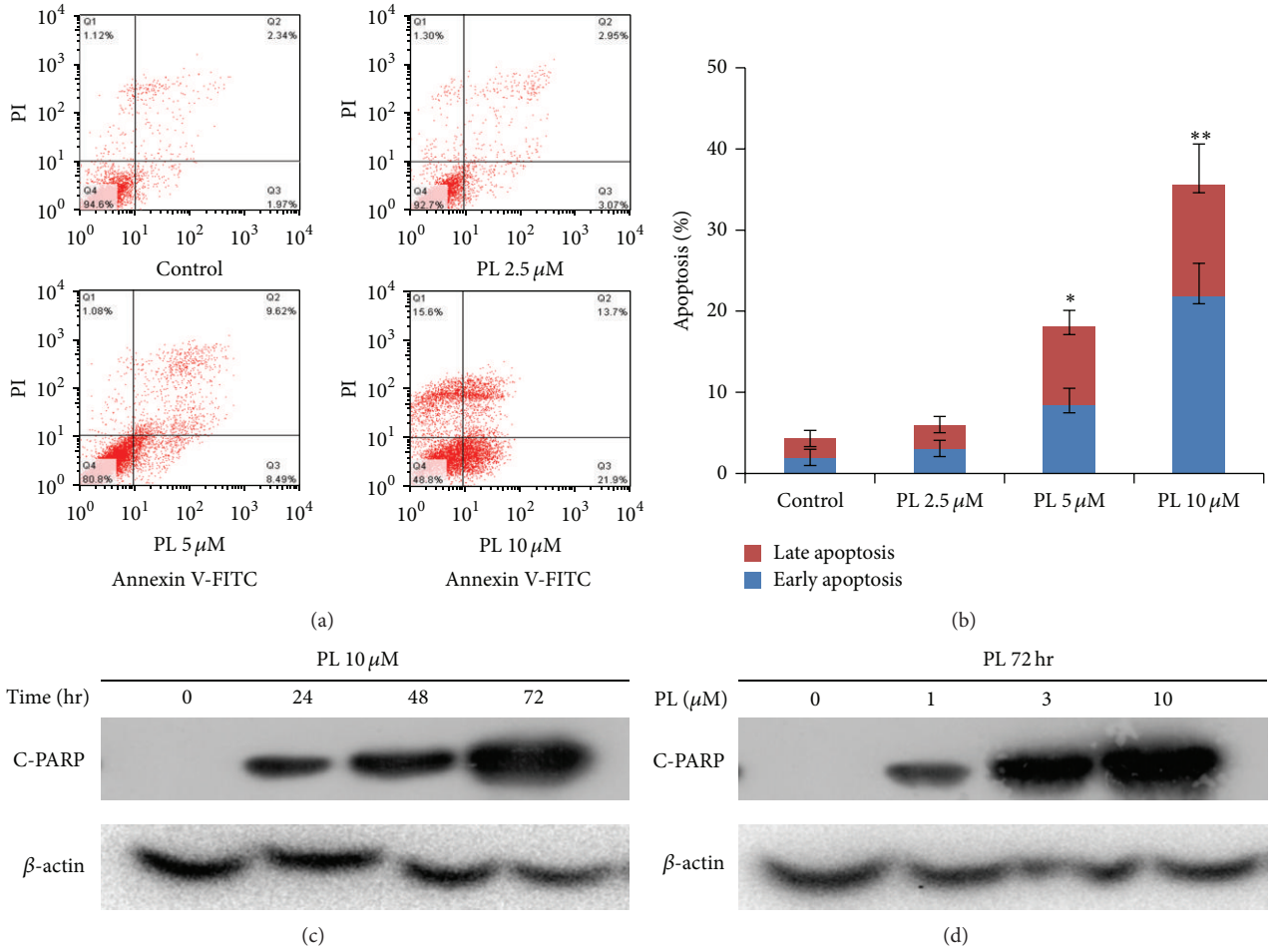

FIGURE 2: PL induced apoptosis in OVCAR3 ovarian cancer cells. (a) The results of cell apoptosis in PL-treated OVCAR3 cells. Cells were treated with the indicated concentration of PL for 48 hr, stained with Annexin V/PI, and examined by FCM. The proportions of Annexin V+/PI− and Annexin V+/PI+ cells indicated the early and late stages of apoptosis. (b) The quantified results of (a). (c) and (d) Representative Western blotting analysis of C-PARP in OVCAR3 cells treated with the indicated PL. β-actin was used as loading control. $^{*}P < 0.05$ and $^{**}P < 0.01$ versus corresponding control.

length of 480 nm through FL-1 (530 nm) and FL-2 (585 nm) filters. The early apoptotic cells (Annexin V positive only) and late apoptotic cells (Annexin V and PI positive) were quantified.

2.4. Measurement of ROS Production. Cells were incubated with 10 μM of DHE for 30 min at 37°C, washed twice with PBS, and immediately microphotographed under a conventional fluorescent microscope (Olympus, Japan). For each well, 5 fields were taken randomly.

2.5. Cell Cycle Analysis. Cells were harvested and washed twice with cold PBS and then fixed with ice-cold 70% (v/v) ethanol for 30 min at 4°C. After centrifugation at 200 ×g for 10 min, cells were washed twice with PBS, resuspended with 0.5 mL PBS containing PI (50 μg/mL), Triton X-100 (0.1%, v/v), 0.1% sodium citrate, and DNase-free RNase (100 μg/mL), and detected by FCM after 15 min incubation at room temperature in the dark. Fluorescence was measured at an excitation wave length of 480 nm through a FL-2filter (585 nm). Data were analyzed using ModFit LT 3.0 software (Becton Dickinson).

2.6. Western Blot Analysis. Cells were harvested and washed twice with cold PBS and then resuspended and lysed in RIPA buffer (1% NP-40, 0.5% sodium deoxycholate, 0.1% SDS, 10 ng/mL PMSF, 0.03% aprotinin, and 1 μM sodium orthovanadate) at 4°C for 30 min. Lysates were centrifuged for 10 min at 14,000 ×g and supernatants were stored at −80°C as whole cell extracts. Total protein concentrations were determined with Bradford assay. Proteins were separated on 12% SDS-PAGE gels and transferred to polyvinylidene

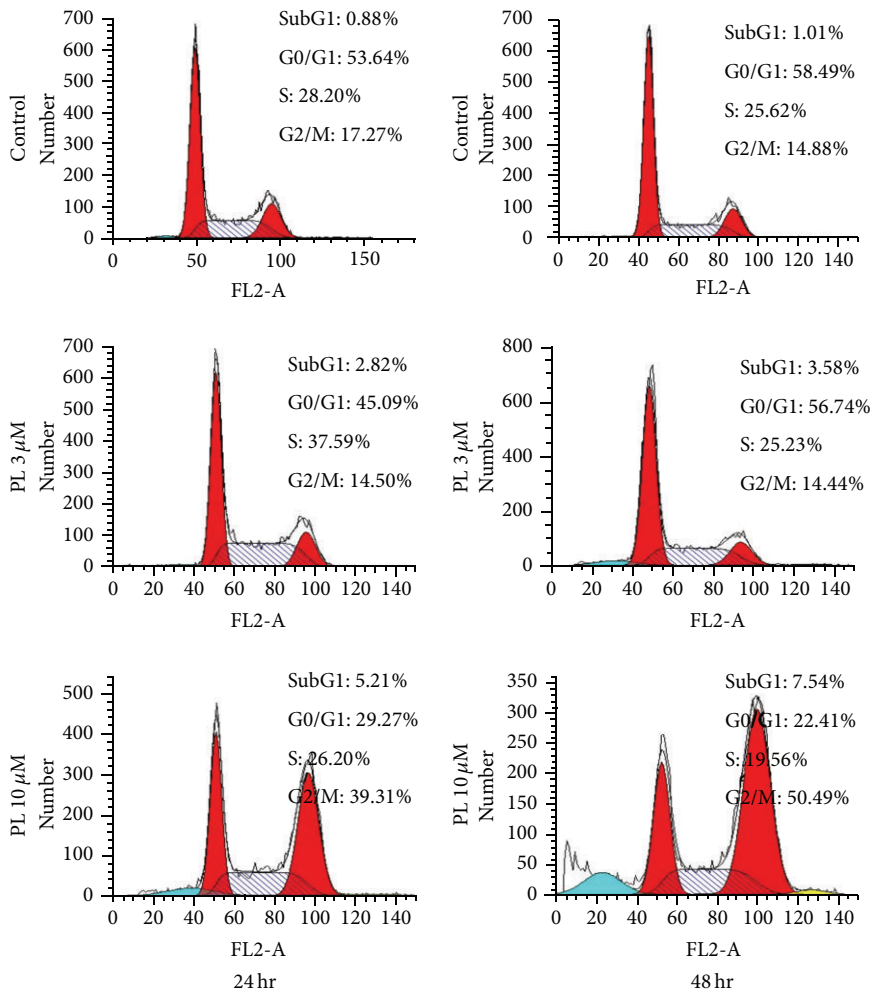

(a)

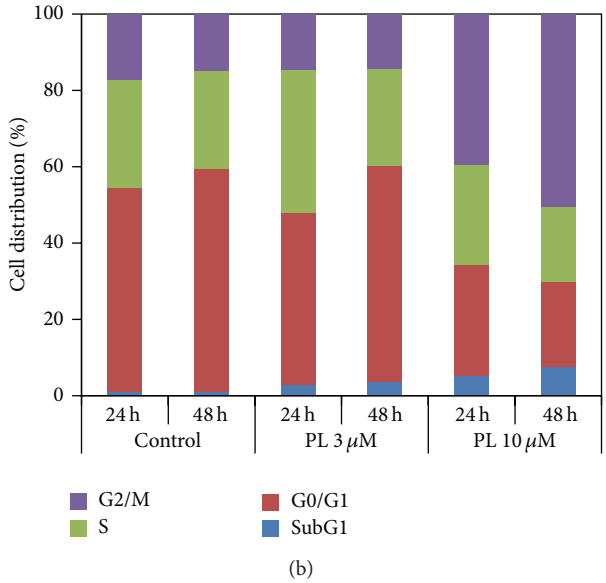

(b)

Figure 3: PL induced subG1 accumulation and G2/M arrest in OVCAR3 ovarian cancer cells. (a) The results of cell cycle distribution in PL-treated OVCAR3 cells. Cells were treated with the indicated PL, stained with PI, and examined by FCM. The percentages of subG1, G1/G0, S, and G2/M phase were calculated using ModFit LT 3.0 software. (b) The quantified results of (a).

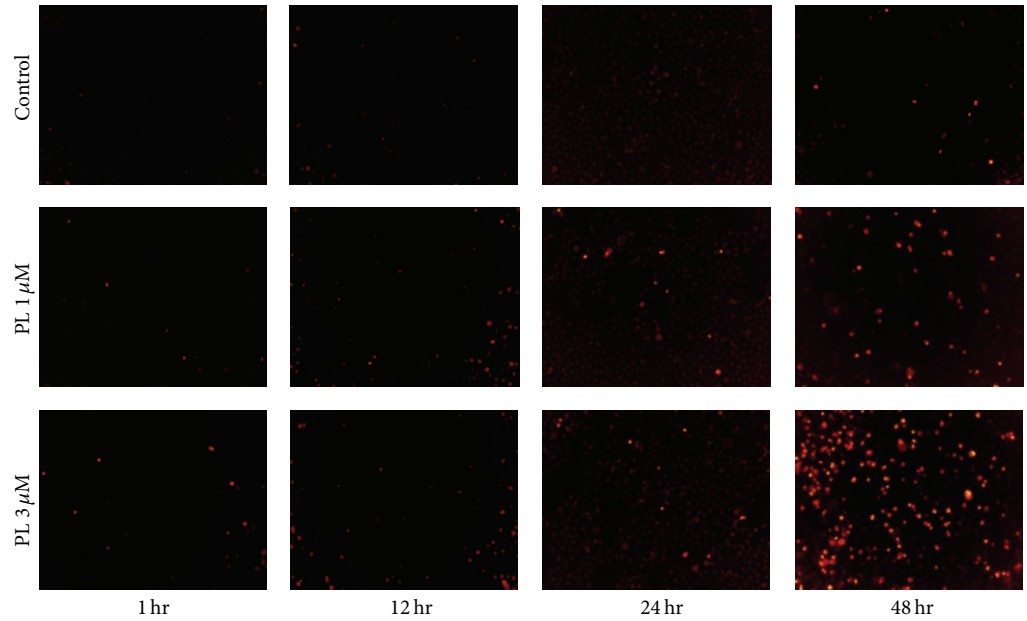

Figure 4: Piperlongumine induced ROS accumulation in OVCAR3 ovarian cancer cells. Cells were treated with PL as indicated, incubated with DHE, and microphotographed under a conventional fluorescent microscope.

difluoride membranes. Membranes were blocked with 5% BSA and incubated with the indicated primary antibodies. Corresponding horseradish peroxidase-conjugated secondary antibodies were used against each primary antibody. Proteins were detected using the chemiluminescent detection reagents and films.

2.7. Statistical Analysis. All experiments were repeated at least 3 times and the differences were determined by using Student's t-test. The significance was determined at $P < 0.05$.

3. Results

3.1. PL Selectively Inhibited the Growth of Ovarian Cancer Cells. To determine the effect of PL on ovarian cancer cells, three ovarian cancer cell lines A2780, OVCAR3, and SKOV3 and human embryonic kidney cell line HEK293T were treated with either the vehicle control (DMSO) or increasing concentrations of PL range from 1 μM to 100 μM for 72 hr. As shown in Figure 1(b), the results of MTT assay revealed that the growth of three ovarian cancer cell lines was similarly inhibited by PL in a concentration-dependent manner. The IC_{50} values of PL after 72 hr exposure were 6.18 μM, 6.20 μM, and 8.20 μM in A2780, OVCAR3, and SKOV3, respectively (Figure 1(b)). However, PL showed the much weaker inhibition effect on the human normal HEK293T cells than three ovarian cancer cell lines and the IC_{50} values of PL were 60.23 μM to HEK293T. These data suggested that PL selectively inhibits the growth of human ovarian cancer cells compared with normal cells.

3.2. PL Induced Apoptosis in OVCAR3 Ovarian Cancer Cells. To determine whether the growth inhibition of ovarian cancer cells by PL was due to the induction of apoptosis, cell apoptosis was assessed by FCM with Annexin V/PI staining. OVCAR3 cells were treated with the different concentrations of PL for 48 hr, stained with Annexin V/PI, and examined by FCM. As shown in Figures 2(a) and 2(b), PL treatment mostly induced apoptosis in OVCAR3 cells and both proportions of Annexin V+/PI− (early stage of apoptosis) and Annexin V+/PI+ (late stage of apoptosis) cells were increased with the elevated PL concentrations.

To further detect the apoptosis induced by PL, the expression of apoptosis marker cleaved-PARP (C-PARP) proteins was analyzed by Western blot in OVCAR3 cells with or without PL treatment. Compared with the loading control β-actin proteins, the levels of C-PARP proteins in OVCAR3 cells were increased in a dose- and time-dependent manner after being treated with PL (Figures 2(c) and 2(d)). Together, these results indicated that the growth inhibition of PL on ovarian cancer cells might be due to the induction of apoptosis.

3.3. PL Induced SubG1 Accumulation and G2/M Arrest in OVCAR3 Ovarian Cancer Cells. In addition to the evaluation of PL-induced growth inhibition and proapoptosis effect, the effect of PL on cell cycle distribution was analyzed by FCM with PI staining. OVCAR3 cells were treated with PL (3 μM and 10 μM) for 24 hr and 48 hr, stained with PI, and examined by FCM. The percentages of subG1, G1/G0, S, and G2/M phase were calculated using ModFit LT 3.0 software. Compared to the control groups, the subG1 and G2/M

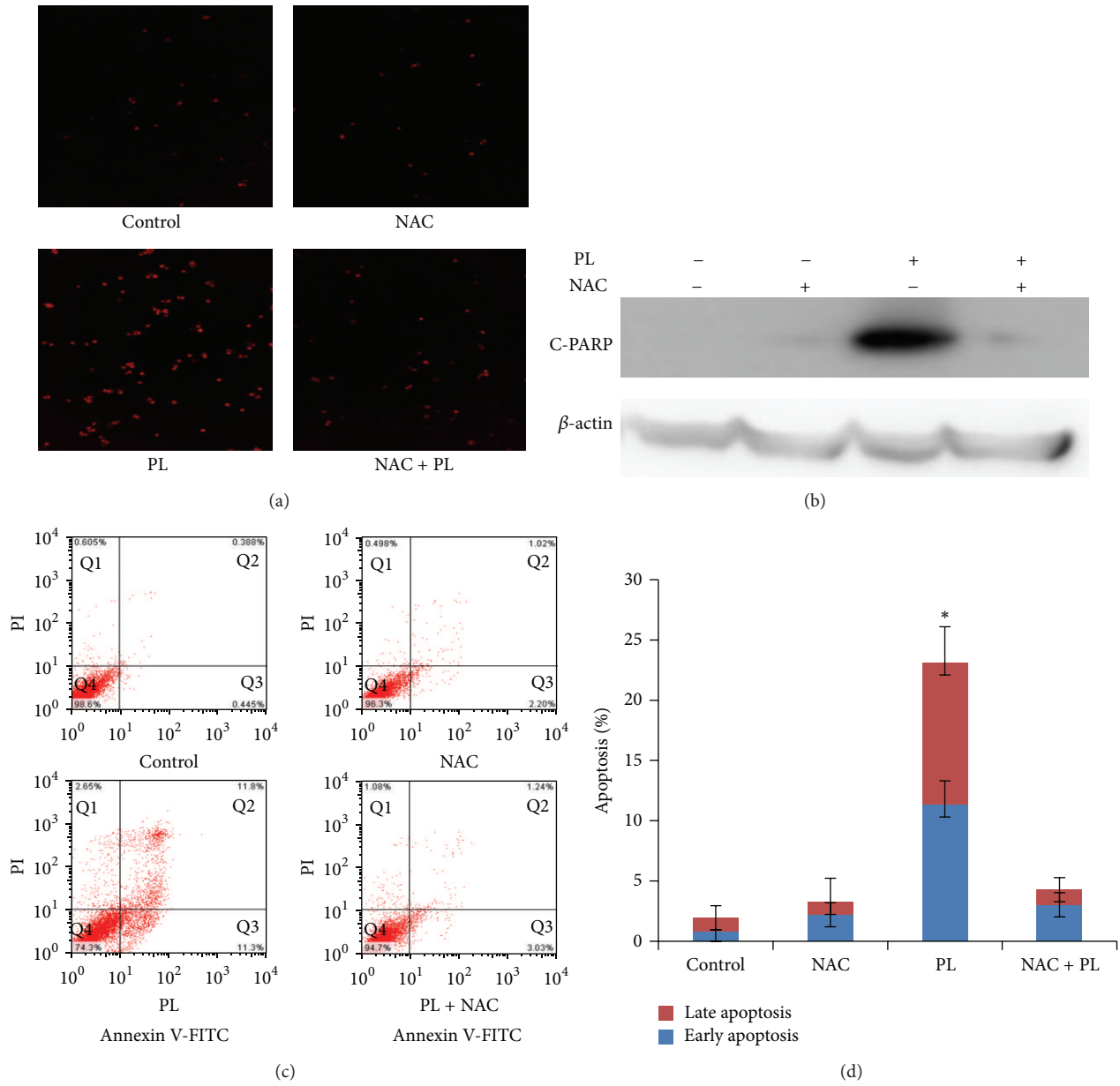

FIGURE 5: ROS generation was critical for PL-induced apoptosis in OVCAR3 ovarian cancer cells. (a) ROS accumulation and (c) cell apoptosis in PL-treated OVCAR3 cells were reversed by NAC. Cells were treated with PL (10 μM) for 24 hr in the presence or absence of 3 mM NAC pretreatment for 1 hr. The apoptosis was detected by FCM with Annexin V/PI staining and the expression of C-PARP proteins was analyzed by Western blot. (c) The quantified results of (d). (b) Representative Western blotting analysis of C-PARP in OVCAR3 cells treated as indicated. β-actin was used as loading control. $^{*}P < 0.05$ and $^{**}P < 0.01$ versus corresponding control.

groups of PL-treated OVCAR3 cells were dose- and time-dependently increased (Figures 3(a) and 3(b)). Therefore, the effect of PL on cell cycle distribution in OVCAR3 cells is the induction of subG1 accumulation which indicated apoptosis-associated chromatin degradation and arrest of cell cycle in G2/M phase.

3.4. ROS Generation Was Critical for PL-Induced Apoptosis in OVCAR3 Ovarian Cancer Cells. Numerous anticancer agents exhibit antitumor activity via ROS-dependent activation of apoptotic cell death [25] and it has previously been reported that the elevated intracellular ROS mediated PL-induced apoptosis in several human cancer cells (EJ, MDA-MB-231, U2OS, and MDA-MB-435) [18]. Dihydroethidium (DHE) is a classic ROS fluorescent probe, which can penetrate through living cell membrane freely and be oxidized by intracellular ROS to oxide ethidium that conjugated with DNA to emit the detectable red fluorescence. As shown in Figure 4, PL exposure resulted in a time- and concentration-dependent ROS accumulation in OVCAR3 cells. Significant intracellular ROS generation was observed when the cells were treated just

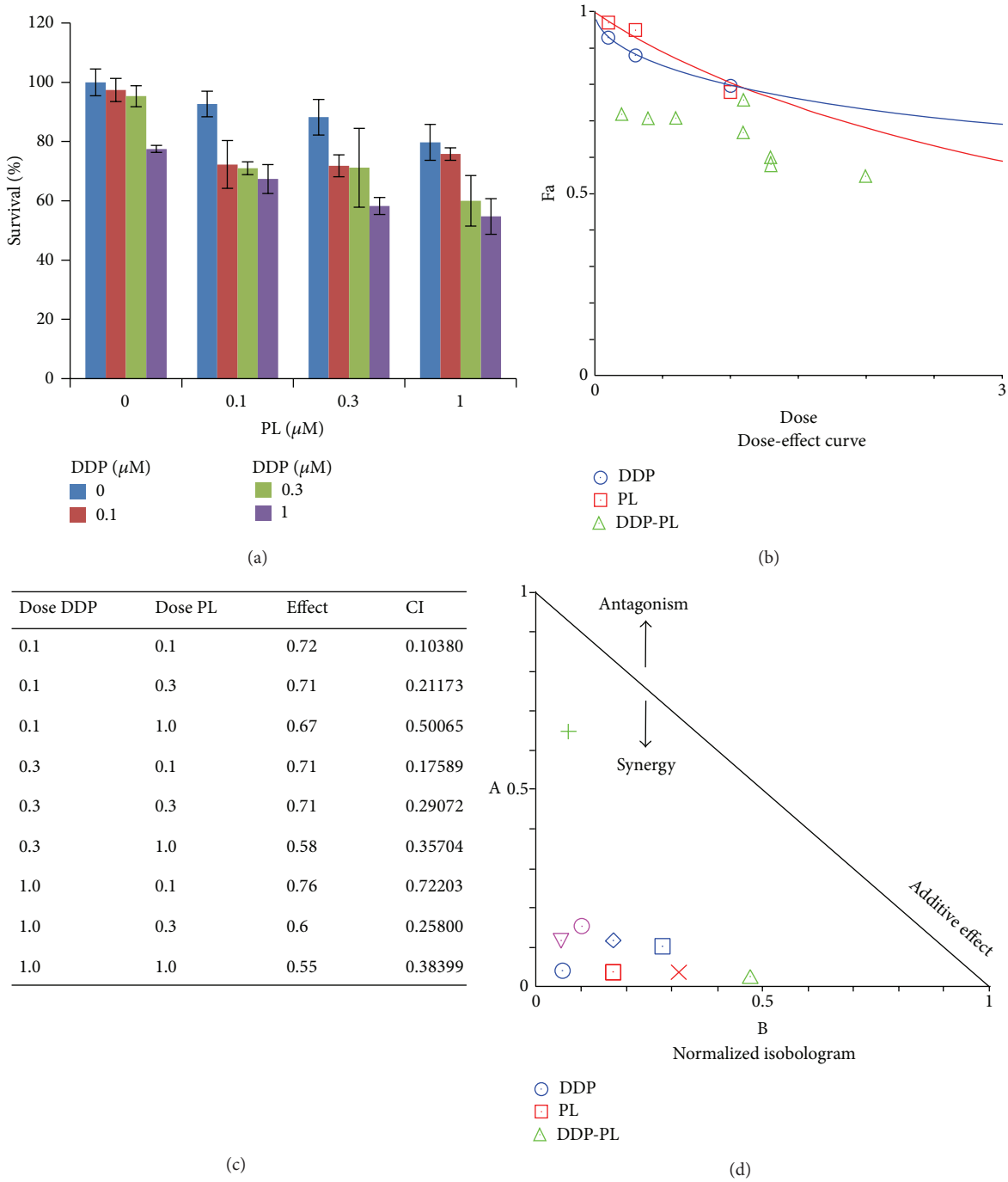

Dose DDP	Dose PL	Effect	CI
0.1	0.1	0.72	0.10380
0.1	0.3	0.71	0.21173
0.1	1.0	0.67	0.50065
0.3	0.1	0.71	0.17589
0.3	0.3	0.71	0.29072
0.3	1.0	0.58	0.35704
1.0	0.1	0.76	0.72203
1.0	0.3	0.6	0.25800
1.0	1.0	0.55	0.38399

FIGURE 6: PL synergized with DDP in OVCAR3 ovarian cancer cells. (a) The growth histogram of OVCAR3 treated with the indicated PL and DDP. Cells were treated with PL (range from 0.1 to 1 μM) combined with DDP (0.1 to 1 μM) and cell survival was detected by MTT assay. The data were analyzed by CompuSyn software with the results showing dose-effect curve (b), CI values (c), and normalized isobologram (d).

for as little as 1 hr; ROS production was increasing and being maintained even at 48 hr, indicating a rapid and sustained generation of ROS in the PL-treated cells. As predicted, the PL-induced ROS accumulation was greatly reduced by NAC due to its ability to elevate intracellular glutathione to prevent the production of ROS (Figures 5(a) and 5(b)).

To further investigate the relationship between the ROS generation and PL-induced apoptosis, OVCAR3 cells were treated with PL (10 μM) for 24 hr in the presence or absence of 3 mM NAC pretreatment for 1 hr. The apoptosis was detected by FCM with Annexin V/PI staining and the expression of C-PARP proteins was analyzed by Western blot. As shown

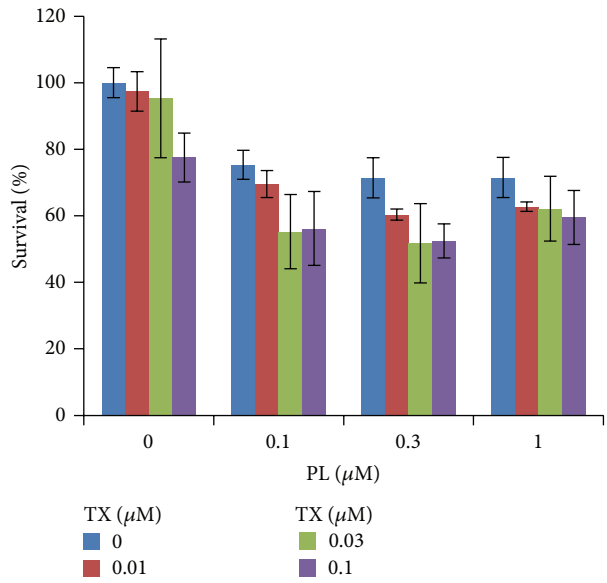

(a)

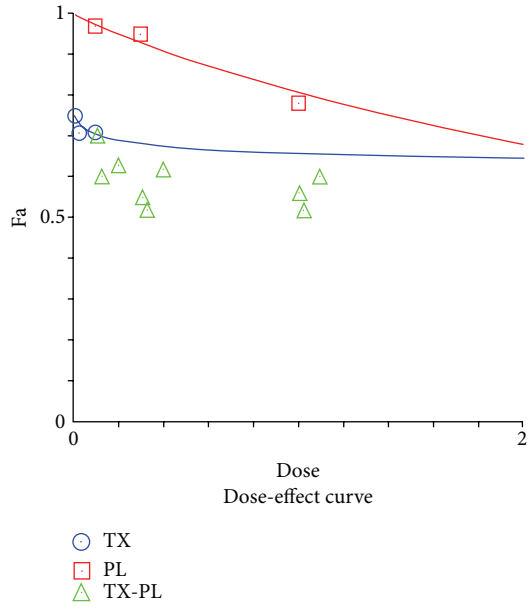

(b)

Dose TX	Dose PL	Effect	CI
0.01	0.1	0.7	0.13944
0.01	0.3	0.55	0.08402
0.01	1.0	0.56	0.29193
0.03	0.1	0.6	0.03616
0.03	0.3	0.52	0.07415
0.03	1.0	0.52	0.24709
0.1	0.1	0.63	0.06198
0.1	0.3	0.62	0.12699
0.1	1.0	0.6	0.35115

(c)

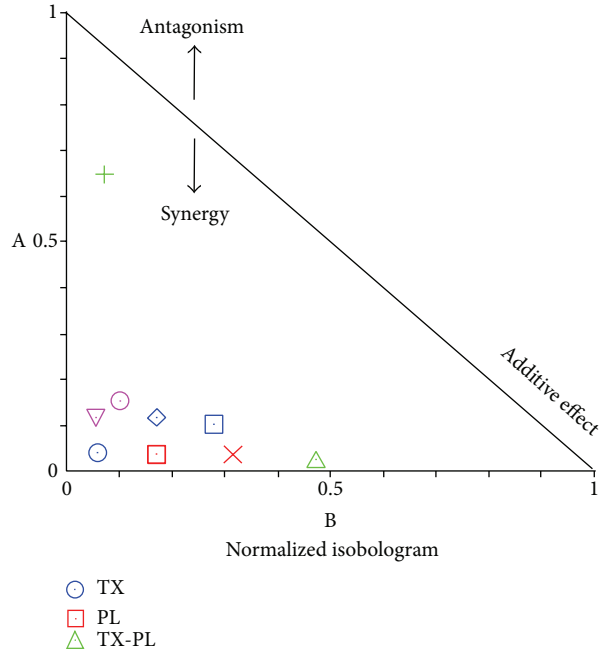

(d)

Figure 7: PL synergized with TX in OVCAR3 ovarian cancer cells. (a) The growth histogram of OVCAR3 treated with the indicated PL and TX. Cells were treated with PL (range from 0.1 to 1 μM) combined with TX (0.01 to 0.1 μM) and cell survival was detected by MTT assay. The data were analyzed by CompuSyn software with the results showing dose-effect curve (b), CI values (c), and normalized isobologram (d).

in Figures 5(c) and 5(d), PL-induced apoptosis and the increased expression of C-PARP proteins were completely blocked by NAC. These data suggested that ROS generation is critical for PL-induced apoptosis in OVCAR3 ovarian cancer cells.

3.5. PL Synergized with DDP or TX in OVCAR3 Ovarian Cancer Cells. Combinations of agents at low doses can reduce side effects of chemotherapy and improve the compliance of patients with chemotherapy; thus investigating novel agents for combination chemotherapy to overcome drug resistance

and achieve better therapeutic effects is of vital significance. For example, a new synthetic compound phenoxodiol exerted potent anticancer activity combined with DDP against ovarian cancer [26]. Currently, DDP and TX are the two of main chemotherapeutic drugs for ovarian cancer in clinic. The present study tested whether lower dose of two drugs in combination (PL + DDP or PL + TX) was able to exert a synergistic antitumor activity compared to PL, DDP, or TX treatment alone. OVCAR3 cells were treated with PL (range from 0.1 to 1 μM) combined with DDP (0.1 to 1 μM) or TX (0.01 to 0.1 μM) and cell survival was detected by MTT assay. As shown in Figures 6 and 7, the cell survival was decreased in the combination of lower dose PL with either DDP or TX. The CI values of both combination were <1, suggesting that the antigrowth effect of combination is synergistic rather than additive. These observations demonstrated that PL was able to sensitize OVCAR3 ovarian cancer cells to both DDP and TX.

4. Discussion

In this report, we firstly demonstrated that PL selectively mediated time- and concentration-dependent antigrowth effects on human ovarian cancer cells. The IC_{50} value after 72 hr treatment with PL ranges from 6 to 8 μM in three human ovarian cancer cell lines, was similar to the IC_{50} value of PL in other solid cancers [14]. The results of FCM analysis showed that PL treatment increased both early and later stage of apoptosis, subG1 accumulation and G2/M phase arrest. Inhibition of the intercellular ROS accumulation by NAC could totally block PL-induced apoptosis. Moreover, PL synergistically enhanced the antigrowth effect of DDP or TX, which suggested that PL might be a potential chemosensitizer for ovarian cancer chemotherapy.

The intracellular production of ROS greatly contributes to the regulation of cell survival and death [27]. Although cancer cells become well adapted to persistent intrinsic oxidative stress, a further increase in ROS above the toxic threshold level may result in cell death [28]. Chemotherapeutical agents including DDP, TX and etoposide induce apoptotic cell death by increasing the intracellular ROS levels. However, continuous DDP treatment may reduce cellular ROS levels and cancer cells may become drug resistant. The chemoresistance of ovarian cancer was also linked to increased cellular glutathione content [29]. Furthermore, an elevation of the cellular ROS level by exogenous ROS generation in combination with DDP resensitized drug-resistant cancer cells [30]. It has been postulated that PL kills carcinoma cells by targeting their "nononcogene codependency" on elevated antioxidative defense pathways acquired in response to cell transformation-induced oxidative stress [18]. Our findings on ovarian cancer cells have suggested that PL-mediated growth inhibition was related to G2/M phase arrest and apoptosis by the increasing intercellular ROS. Previously reported, a dose-dependent decrease of cdc-2 expression but not cyclinB1 changing was associated with PL-mediated cell cycle arrest in PC-3 cells [16]. The present study has attributed the generation of ROS to the proapoptotic effect of PL in ovarian cancer cells, which was in agreement with the previous findings in other cancer cell types [12, 18].

Altogether, the present study offers the first evidence that PL selectively inhibited cell growth and induced ROS-dependent cell apoptosis and G2/M cell cycle arrest in human ovarian cancer. Furthermore, PL synergizes with DDP and TX to inhibit the growth of human ovarian cancer cells. Further *in vivo* experiments may aid in the confirmation of the therapeutic efficacy of this agent for patients with ovarian cancer.

Conflict of Interests

The authors declare that they have no conflict of interests.

Authors' Contribution

Li-Hua Gong and Xiu-Xiu Chen contributed equally to the work.

Acknowledgments

This work was supported by funds from the Chinese National Natural Science Foundation no. 31271444 and no. 81201726 (Zhi Shi), the Foundation for Research Cultivation and Innovation of Jinan University no. 21612407 (Zhi Shi), the Specialized Research Fund for the Doctoral Program of Higher Education no. 20124401120007 (Zhi Shi), Science and Technology Program of Guangzhou no. 14200010 (Zhi Shi), the Scientific Research Foundation of the Education Department of Zhejiang Province, China, no. Y201016398 (Xiao-Jian Yan), and the Natural Science Foundation of Zhejiang Province, China, no. LQ12H16004 (Xiao-Jian Yan).

References

[1] J. Permuth-Wey and T. A. Sellers, "Epidemiology of ovarian cancer," *Methods in Molecular Biology*, vol. 472, pp. 413–437, 2009.

[2] S. A. Cannistra, "Cancer of the ovary," *The New England Journal of Medicine*, vol. 351, no. 24, pp. 2519–2529, 2004.

[3] L. Chen, L. Liang, X. Yan et al., "Survivin status affects prognosis and chemosensitivity in epithelial ovarian cancer," *International Journal of Gynecological Cancer*, vol. 23, no. 2, pp. 256–263, 2013.

[4] X.-J. Yan, L.-Z. Liang, Z.-Y. Zeng, Z. Shi, and L.-W. Fu, "Effect of survivin shRNA on chemosensitivity of human ovarian cancer cell line OVCAR3 to paclitaxel," *Ai Zheng*, vol. 25, no. 4, pp. 398–403, 2006.

[5] X.-J. Yan, L.-Z. Liang, Z.-Y. Zeng, L.-W. Fu, and Z. Shi, "Influence of short hairpin RNA on survivin mRNA expression and chemosensitivity to paclitaxel in ovarian cancer cells," *Zhonghua Fu Chan Ke Za Zhi*, vol. 40, no. 9, pp. 609–613, 2005.

[6] X. J. Yan, L. H. Gong, F. Y. Zheng, K. J. Cheng, Z. S. Chen, and Z. Shi, "Triterpenoids as reversal agents for anticancer drug resistance treatment," *Drug Discovery Today*, 2013.

[7] C. K. Bose, "Follicle stimulating hormone receptor in ovarian surface epithelium and epithelial ovarian cancer," *Oncology Research Featuring Preclinical and Clinical Cancer Therapeutics*, vol. 17, no. 5, pp. 231–238, 2008.

[8] T. P. Szatrowski and C. F. Nathan, "Production of large amounts of hydrogen peroxide by human tumor cells," *Cancer Research*, vol. 51, no. 3, pp. 794–798, 1991.

[9] P. T. Schumacker, "Reactive oxygen species in cancer cells: live by the sword, die by the sword," *Cancer Cell*, vol. 10, no. 3, pp. 175–176, 2006.

[10] J. Fang, T. Seki, and H. Maeda, "Therapeutic strategies by modulating oxygen stress in cancer and inflammation," *Advanced Drug Delivery Reviews*, vol. 61, no. 4, pp. 290–302, 2009.

[11] Y. Q. Xue, J. M. Di, Y. luo, K. J. Cheng, X. Wei, and Z. Shi, "Resveratrol oligomers for the prevention and treatment of cancers," *Oxidative Medicine and Cellular Longevity*, vol. 2014, Article ID 765832, 9 pages, 2014.

[12] D. P. Bezerra, C. Pessoa, M. O. de Moraes, N. Saker-Neto, E. R. Silveira, and L. V. Costa-Lotufo, "Overview of the therapeutic potential of piplartine (piperlongumine)," *European Journal of Pharmaceutical Sciences*, vol. 48, no. 3, pp. 453–463, 2013.

[13] D. P. Bezerra, G. C. G. Militão, F. O. de Castro et al., "Piplartine induces inhibition of leukemia cell proliferation triggering both apoptosis and necrosis pathways," *Toxicology in Vitro*, vol. 21, no. 1, pp. 1–8, 2007.

[14] D. P. Bezerra, C. Pessoa, M. O. de Moraes et al., "Antiproliferative effects of two amides, piperine and piplartine, from Piper species," *Zeitschrift fur Naturforschung C: Journal of Biosciences*, vol. 60, no. 7-8, pp. 539–543, 2005.

[15] J. M. Liu, F. Pan, L. Li et al., "Piperlongumine selectively kills glioblastoma multiforme cells via reactive oxygen species accumulation dependent JNK and p38 activation," *Biochemical and Biophysical Research Communications*, vol. 437, no. 1, pp. 87–93, 2013.

[16] E.-H. Kong, Y.-J. Kim, Y.-J. Kim et al., "Piplartine induces caspase-mediated apoptosis in PC-3 human prostate cancer cells," *Oncology Reports*, vol. 20, no. 4, pp. 785–792, 2008.

[17] D. P. Bezerra, F. O. De Castro, A. P. N. N. Alves et al., "In vitro and in vivo antitumor effect of 5-FU combined with piplartine and piperine," *Journal of Applied Toxicology*, vol. 28, no. 2, pp. 156–163, 2008.

[18] L. Raj, T. Ide, A. U. Gurkar et al., "Selective killing of cancer cells by a small molecule targeting the stress response to ROS," *Nature*, vol. 475, no. 7355, pp. 231–234, 2011.

[19] D. J. Adams, M. J. Dai, G. Pellegrino et al., "Synthesis, cellular evaluation, and mechanism of action of piperlongumine analogs," *Proceedings of the National Academy of Sciences of the United States of America*, vol. 109, no. 38, pp. 15115–15120, 2012.

[20] D. P. Bezerra, D. J. Moura, R. M. Rosa et al., "Evaluation of the genotoxicity of piplartine, an alkamide of Piper tuberculatum, in yeast and mammalian V79 cells," *Mutation Research—Genetic Toxicology and Environmental Mutagenesis*, vol. 652, no. 2, pp. 164–174, 2008.

[21] P. Makhov, K. Golovine, E. Teper et al., "Piperlongumine promotes autophagy via inhibition of Akt/mTOR signalling and mediates cancer cell death," *British Journal of Cancer*, vol. 110, pp. 899–907, 2014.

[22] Y. Wang, J. W. Wang, X. Xiao et al., "Piperlongumine induces autophagy by targeting p38 signaling," *Cell Death and Disease*, vol. 4, p. e824, 2013.

[23] Z. Shi, Y.-J. Liang, Z.-S. Chen et al., "Reversal of MDR1/P-glycoprotein-mediated multidrug resistance by vector-based RNA interference in vitro and in vivo," *Cancer Biology & Therapy*, vol. 5, no. 1, pp. 39–47, 2006.

[24] C. S. Weil, "Tables for convenient calculation of median-effective dose (LD50 or ED50) and instructions in their use," *Biometrics*, vol. 8, no. 1, pp. 249–263, 1952.

[25] J. Fang, H. Nakamura, and A. K. Iyer, "Tumor-targeted induction of oxystress for cancer therapy," *Journal of Drug Targeting*, vol. 15, no. 7-8, pp. 475–486, 2007.

[26] D.-A. Silasi, A. B. Alvero, T. J. Rutherford, D. Brown, and G. Mor, "Phenoxodiol: pharmacology and clinical experience in cancer monotherapy and in combination with chemotherapeutic drugs," *Expert Opinion on Pharmacotherapy*, vol. 10, no. 6, pp. 1059–1067, 2009.

[27] M. Ott, V. Gogvadze, S. Orrenius, and B. Zhivotovsky, "Mitochondria, oxidative stress and cell death," *Apoptosis*, vol. 12, no. 5, pp. 913–922, 2007.

[28] J. P. Fruehauf and F. L. Meyskens Jr., "Reactive oxygen species: a breath of life or death?" *Clinical Cancer Research*, vol. 13, no. 3, pp. 789–794, 2007.

[29] S. Okuno, H. Sato, K. Kuriyama-Matsumura et al., "Role of cystine transport in intracellular glutathione level and cisplatin resistance in human ovarian cancer cell lines," *British Journal of Cancer*, vol. 88, no. 6, pp. 951–956, 2003.

[30] A. K. Maiti, "Gene network analysis of oxidative stress-mediated drug sensitivity in resistant ovarian carcinoma cells," *The Pharmacogenomics Journal*, vol. 10, no. 2, pp. 94–104, 2010.

Hindawi Publishing Corporation
Oxidative Medicine and Cellular Longevity
Volume 2014, Article ID 504953, 10 pages
http://dx.doi.org/10.1155/2014/504953

Research Article

Insulin Regulates Glucose Consumption and Lactate Production through Reactive Oxygen Species and Pyruvate Kinase M2

Qi Li,[1] Xue Liu,[1] Yu Yin,[1,2] Ji-Tai Zheng,[1] Cheng-Fei Jiang,[1] Jing Wang,[1] Hua Shen,[3] Chong-Yong Li,[1] Min Wang,[1] Ling-Zhi Liu,[4] and Bing-Hua Jiang[1,4]

[1] *Department of Pathology, State Key Lab of Reproductive Medicine, Cancer Center, Nanjing Medical University, Nanjing 210029, China*
[2] *Department of Pathology, Anhui Medical University, Hefei 230032, China*
[3] *Department of Oncology, The First Affiliated Hospital of Nanjing Medical University, Nanjing 210029, China*
[4] *Department of Pathology, Anatomy and Cell Biology, Thomas Jefferson University, Philadelphia, PA 19107, USA*

Correspondence should be addressed to Bing-Hua Jiang; binghjiang@yahoo.com

Received 12 February 2014; Accepted 11 April 2014; Published 8 May 2014

Academic Editor: Jinxiang Zhang

Although insulin is known to regulate glucose metabolism and closely associate with liver cancer, the molecular mechanisms still remain to be elucidated. In this study, we attempt to understand the mechanism of insulin in promotion of liver cancer metabolism. We found that insulin increased pyruvate kinase M2 (PKM2) expression through reactive oxygen species (ROS) for regulating glucose consumption and lactate production, key process of glycolysis in hepatocellular carcinoma HepG2 and Bel7402 cells. Interestingly, insulin-induced ROS was found responsible for the suppression of miR-145 and miR-128, and forced expression of either miR-145 or miR-128 was sufficient to abolish insulin-induced PKM2 expression. Furthermore, the knockdown of PKM2 expression also inhibited cancer cell growth and insulin-induced glucose consumption and lactate production, suggesting that PKM2 is a functional downstream effecter of insulin. Taken together, this study would provide a new insight into the mechanism of insulin-induced glycolysis.

1. Introduction

Insulin is known to play an important role in human glucose metabolism [1]. Many human diseases cause glucose metabolism disorders such as diabetes and cancer [2, 3]. However, the molecular mechanisms of insulin in regulating glucose metabolism of cancer remain to be elucidated. Changes of rate-limiting glycolytic enzymes are observed during cancer metabolism. Among these enzymes, pyruvate kinase (PK) plays a crucial role in catalyzing the formation of pyruvate and ATP from phosphoenolpyruvate and ADP [4, 5]. There are four isoforms of PK in mammals, PKL, PKR, PKM1, and PKM2. PKL, PKR, and PKM1 are tissue-specific isoenzymes, whereas PKM2 is considered an embryonic and cancer cell-specific isoform [6]. Evidence supports that the loss of the tissue-specific isoenzymes and subsequent expression of PKM2 are involved in tumor initiation as well as malignant progression. Knockdown of PKM2 expression or the replacement of PKM2 with PKM1 has been demonstrated to inhibit cancer metabolism and tumor growth [5, 7]. Transcription factors such as HIF-1α and other genes relevant to tumorigenesis are potent PKM2 activators, while a number of genes associated with cell proliferation, metabolism, and tumor growth are downstream targets of PKM2 [8–10].

Lines of evidence in recent years have suggested a crucial role of reactive oxygen species (ROS) in cancer cellular functions [11]. High levels of endogenous ROS production are associated with cancer development [12, 13]. ROS, especially hydrogen peroxide (H_2O_2), are also induced by a variety of external stimulators including growth factors such as insulin [14]. However, the role of ROS production in cancer cells in response to insulin-induced glucose metabolism remains to be elucidated.

Recently, miRNAs are known to be involved in many human diseases, such as diabetes and cancer [15, 16]. miRNAs are small, noncoding RNAs that have been confirmed to be

a new kind of gene expression regulators through negatively regulating protein-coding genes. The causal roles of miRNAs in cancer have been well documented and miRNA-based anticancer therapies are in development [17, 18]. Several miRNAs with evident roles in cancer are reported to participate in insulin and ROS signaling pathways. For example, Let-7 family regulates multiple aspects glucose metabolism in multiple organs [19]; miR-143 regulates glucose metabolism of cancer cells by targeting hexokinase 2 isoform (HK2) [20]; miR-21 is an important target of ROS [21]. Despite these studies, whether or not miRNAs take part in insulin-induced PKM2 expression and the underlying mechanisms by which PKM2 exerts effects in this pathology remain unclear.

In the present study, we plan to study whether (1) ROS are involved in insulin-regulated glycolysis in hepatocellular carcinoma cells; (2) insulin regulates PKM2 expression via ROS production; (3) insulin upregulates PKM2 expression in ROS dependent manner through miRNAs expression; and (4) PKM2 is required for insulin-induced aerobic glycolysis. These studies will determine the role of ROS/miRNAs/PKM2 in mediating insulin effects and are helpful to understand the mechanism of insulin in regulating hepatocellular carcinoma cell glycolysis.

2. Materials and Methods

2.1. Reagents and Cell Culture. Human HepG2 hepatocellular carcinoma cells were obtained from American Type Culture Collection (Manassas, VA, USA). Human hepatocellular carcinoma cell lines BeL7402 were obtained from the Cell Bank of the Chinese Academy of Science (Shanghai, China). Cells were cultured in Dulbecco's modified Eagle's medium (DMEM) supplemented with 5% FBS, penicillin (100 U/mL), and streptomycin (100 μg/mL) at 37°C in 5% CO_2 incubator. Trypsin (0.25%)/EDTA solution was used to detach the cells for subculturing the cells. Insulin was purchased from Sigma (St. Louis, MO).

2.2. ROS Measurement. HepG2 cells were seeded in a 12-well plate at 8×10^4 cells/well and cultured at 37°C for 24 h. The cells were then incubated in serum-free medium for 24 h, followed by the pretreatment with catalase (1500 U/mL) for 1 h. CM-H2DCFDA (5 μM) (Invitrogen, USA) was added and incubated with the cells for 10 min. Cells were then stimulated with insulin (200 nM) for 10 min. The cells were washed twice with phosphate-buffered saline (PBS) and fixed with 10% buffered formalin. The images were captured with a fluorescence microscope.

2.3. Malondialdehyde (MDA) Analysis. MDA levels in the cells were determined by the thiobarbituric acid (TBA) method using an assay kit according to manufactory guidance (Beyotime Biotechnology, Shanghai, China). Briefly, protein samples were incubated with TBA at 100°C for 15 min, followed by a centrifugation at 1000 ×g for 10 min. Supernatants were transferred to a 96-well plate, and the absorbance was measured at 532 nm. The MDA levels were analyzed and normalized to each sample protein concentration.

2.4. Measurement of Glucose Consumption and Lactate Production. A total of 5×10^4 cells per well were seeded in 24-well plates and treated as above. Cells were trypsinized and counted, while the supernatants of cell culture medium were collected. The media were assayed immediately for glucose and lactate levels by using glucose assay kit and lactate assay kit (Biovision, Mountain View, CA) according to the manufacturer's instruction. The glucose consumption and lactate production were normalized to cell number. The experiments were performed with three replicates and repeated for three times.

2.5. Real-Time RT-PCR. Total RNAs from cells were isolated using TRIzol (Invitrogen, USA) according to the manufacturer's instruction. cDNA synthesis was performed with 1 μg total RNAs using PrimeScriptTM RT reagent kit (Takara, China). Aliquots of these cDNAs were used for quantitative real-time PCR using SYBR Premix DimerEraser (Takara, China). Expression levels of miR-145 and miR-128 were normalized to U6 levels, expression levels of PKM2 were normalized to GAPDH level for each sample, and fold changes were calculated by relative quantification ($2^{-\Delta\Delta Ct}$). Primers used were listed in Supplementary Table 1 in Supplementary Material available online at http://dx.doi.org/10.1155/2014/504953.

2.6. Western Blotting and Antibodies. Cells were harvested and lysed in radioimmunoprecipitation assay (RIPA) buffer supplemented with proteinase inhibitors cocktail. The protein extracts were separated by SDS-polyacrylamide gel electrophoresis (SDS-PAGE), transferred to nitrocellulose membranes, and incubated with antibodies against PKM2 (Signalway Biotechnology, Pearland, TX), HIF-1α (BD Biosciences, Sparks, MD), p70S6K1 (Cell Signaling Technology, Danvers, MA), and GAPDH (Sigma, St. Louis, MO). The protein bands were detected by incubating with horseradish peroxidase- (HRP-) conjugated antibodies and visualized using the Super Signal West Pico Chemiluminescent Substrate Kits (Thermo Scientific, Rockford, IL).

2.7. Transient Transfection. Double strands miR-145 and miR-128 and scrambled control precursors were synthesized by Gene-pharma (Shanghai, China). HepG2 and Bel7402 cells were transfected with miR-145, miR-128, or scramble control precursor by Lipofectamine 2000 (Invitrogen, USA) according to the manufacturer's instruction. The sequences of miRNA precursors were listed in Supplementary Table 2.

Small interfering RNA (siRNA) duplex oligonucleotides targeting human PKM2 (siPKM2) or scrambled control (siSCR) were purchased from GenePharma (Shanghai, China). HepG2 and Bel7402 cells were transfected with siPKM2 or siSCR using Lipofectamine RNAiMax (Invitrogen) in serum-free Opti-MEM according to the manufacturer's instruction. The sequences of small interfering RNA for PKM2 were listed in Supplementary Table 3.

2.8. Cell Proliferation Assay. HepG2 and Bel7402 cells were transfected with siPKM2 or the scrambled control and cultured at 37°C for 24 h. The cells were then trypsinized,

resuspended, and seeded in a 96-well plate at 3000 cells per well. The cell proliferation was measured at 12 h, 24 h, 48 h, 72 h, and 96 h using a Cell Counting Kit-8 (CCK-8) (Dojindo Laboratories, Kumamoto, Japan) according to the manufacturer's instruction. All experiments were performed in triplicate and were repeated for three times.

2.9. Statistical Analysis. Numerical results were presented as mean ± SD. Statistical analysis was performed based on a Student's t-test at the significance level of $P < 0.05$ using GraphPad Prisms Software.

3. Results

3.1. Evidence for the Involvement of ROS in Insulin-Regulated Glycolysis in Hepatocellular Carcinoma Cells. Although insulin has been associated with a variety of cancers and liver cell functions [22, 23], and ROS as secondary messengers mediate the cancers signals, it remains unknown whether ROS participate in transmitting insulin signaling. To this end, ROS levels in response to insulin treatment were analyzed in HepG2 cells. The cells were cultured in serum-free medium, followed by the treatment of insulin. As shown in Figures 1(a) and 1(b), treatment of cells with insulin led to higher ROS levels. Addition of ROS scavenger catalase blocked the effect of insulin treatment. Further experiments were performed in HepG2 and Bel7402 cells using MDA analysis, a stable indicator of oxidative stress. The results showed that MDA levels in the insulin treatment were increased approximately 2-fold when compared with that in the cells without insulin treatment. Catalase administration significantly decreased insulin-induced MDA level (Figure 1(c)). These data suggest that insulin is able to induce ROS production.

Next, we examined the effect of ROS on insulin-regulating glucose energy metabolism. Insulin dramatically increased glucose consumption and lactate production in HepG2 and Bel7402 cells. Administration of catalase attenuated the increase in glucose metabolism induced by insulin (Figures 1(d) and 1(e)). Thus, it appears that ROS participate in insulin-regulated glycolysis.

3.2. Insulin Induced PKM2 Expression through ROS Production. Pyruvate kinase M2 (PKM2), the key kinase, catalyzes the last reaction of glycolysis and converts phosphoenolpyruvate (PEP) to pyruvate producing ATP. The expression levels of PKM2 are used as one of the important metabolic signatures of tumor cells. To test whether insulin promotes glycolysis through regulating PKM2 expression, HepG2 cells and Bel7402 cells were cultured in serum-free medium for 24 h and exposed to 200 nM of insulin for 0 h, 3 h, 6 h, and 12 h. The immunoblotting results showed that insulin significantly induced PKM2 expression in a time-dependent manner (Figures 2(a) and 2(b)).

Since we showed that ROS were induced by insulin, we tested whether insulin induced PKM2 expression through ROS production. Pretreatment of HepG2 and Bel7402 cells with catalase greatly suppressed the PKM2 protein levels induced by insulin (Figures 2(c) and 2(d)). Further experiments were performed by using real-time PCR to analyze PKM2 mRNA expression levels. Similarly, PKM2 mRNA levels were enhanced in response to insulin treatment and decreased by catalase treatment (Figure 2(e)). This result suggests that insulin-induced PKM2 expression requires ROS production.

3.3. Insulin Upregulates PKM2 Expression in ROS Dependent Manner through miR-145 and miR-128 Expression. There is accumulating evidence for the miRNAs expression which may be altered in response to exogenous agents that, at least in part, induce intracellular insulin and oxidative stress [21, 24]. Hydrogen peroxide treatment suppressed miR-145 and miR-128 expression (Figure S1), suggesting that ROS inhibit miR-145 and miR-128 expression. To test whether insulin affect miR-145 and miR-128 expression through ROS, we showed that pretreatment of HepG2 and Bel7402 cells with catalase greatly induced the expression levels of miR-145 and miR-128 suppressed by insulin (Figure 3(a)). This result suggests that insulin-regulated expression of miR-145 and miR-128 requires ROS production.

Our previous studies demonstrated that p70S6K1 is a direct target of miR-145 and miR-128 in ovarian cancer cells and glioma cells [25, 26]. We detected p70S6 K1 and HIF-1α levels in response to insulin treatment. As shown in Figures 3(b), 3(c), and 3(d), p70S6K1 and HIF-1α protein levels were increased after insulin treatment, and addition of miR-128 or miR-145 precursors inhibited insulin-induced p70S6K1 and HIF-1α expression. This result indicates that miR-128 or miR-145 is required for insulin-induced expression of p70S6K1 and HIF-1α. Since we showed that miR-128 and miR-145 are required for insulin-induced p70S6K1 and HIF-1α expression, we tested whether insulin-suppressing miR-128 and miR-145 could play a role in PKM2 expression in HepG2 and Bel7402 cells. To test this, the cells were pretreated with miR-128 and miR-145 and then stimulated with insulin. miR-128 and miR-145 treatment inhibited insulin-induced expression of PKM2 (Figures 3(b) and 3(e)), indicated that miR-128 and miR-145 are required for insulin-induced PKM2 expression.

3.4. PKM2 Is Critical for Insulin-Induced Aerobic Glycolysis and Cell Growth. To test whether the inhibition of PKM2 expression attenuates insulin-induced glycolysis, HepG2 and Bel7402 cells were transfected with siRNA against PKM2 or scrambled control siRNA. After transfection with siPKM2, the expression levels of PKM2 were markedly inhibited by 70–80% when compared to scrambled control (Figures 4(a) and 4(b)). Insulin increased glucose consumption and lactate production by 2-fold when compared to control group without insulin treatment, while PKM2 knockdown inhibited insulin-induced glucose consumption and lactate production to 50% and 60%, respectively (Figures 4(c) and 4(d)). These results confirm that PKM2 is an important regulator in insulin-regulating glycolysis.

Given that the energy metabolism is critical to the survival and proliferation of cancer cells, we examined the

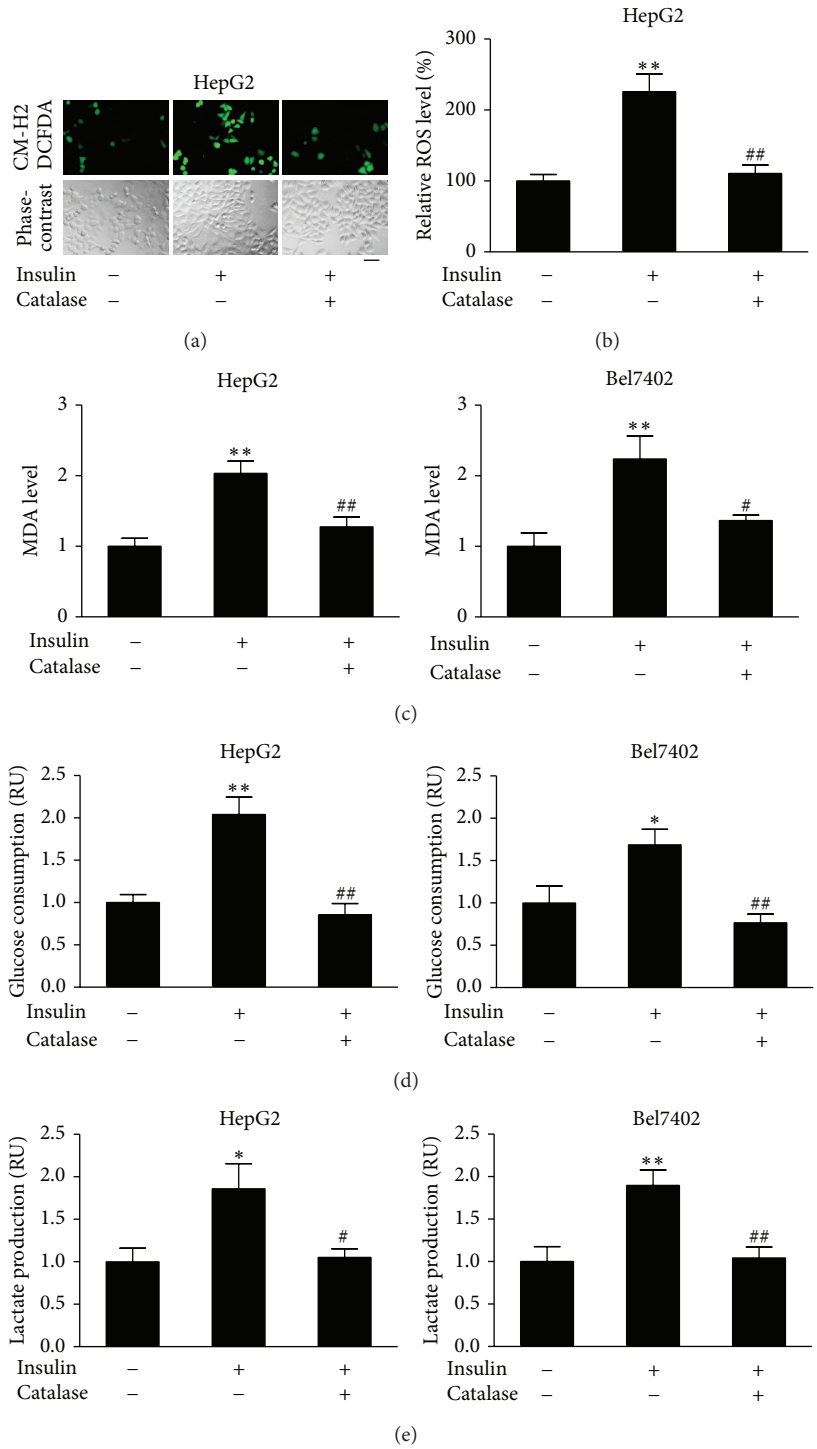

Figure 1: Insulin promoted MDA production, glucose consumption and lactate production through ROS production in hepatocellular carcinoma cells. (a) HepG2 cells were seeded in a 12-well plate at 8×10^4 cells/well and cultured at 37°C for 24 h. The cells were then incubated in serum-free medium for 24 h, followed by the pretreatment with catalase (1500 U/mL) for 1 h. CM-H2DCFDA (5 μM) was added and incubated with the cells for 10 min. Cells were then stimulated with insulin (200 nM) for 10 min. The cells were washed thrice with 1x PBS. The representative images were captured with a fluorescence microscope. Bar, 50 μm. (b) Levels of ROS fluorescence signals were quantified by ImageJ; $^{**}P < 0.01$ compared with that of the same cell line treated without insulin and catalase; $^{\#\#}P < 0.01$ compared to the cells treated with insulin alone. (c) HepG2 and Bel7402 cells were cultured in serum-free medium overnight. Then, the cells were treated with catalase (1500 U/mL) for 1 h, followed by insulin treatment (200 nM) for 12 h. The proteins were collected and subjected to MDA analysis. Data were presented by mean ± SD ($n = 3$). ** Significant difference compared with that of the same cell line treated or without insulin and catalase ($P < 0.01$); $^{\#}$ and $^{\#\#}$ significant difference compared to the cells treated with insulin alone ($P < 0.05$ and $P < 0.01$, resp.). (d) and (e) HepG2 cells and Bel7402 cells were seeded in 24-well plates and cultured in serum-free medium for 24 h, followed by the treatment with catalase (1500 U/mL) for 1 h. Cells were then stimulated with insulin (200 nM) for 12 h. The medium was collected, and the glucose consumption and lactate production levels were analyzed. Data were mean ± SD from three independent experiments. $^{**}P < 0.01$ and $^{*}P < 0.05$ compared with that of the same cell line treated without insulin and catalase; $^{\#}P < 0.05$ and $^{\#\#}P < 0.01$ compared to the cells treated with insulin alone.

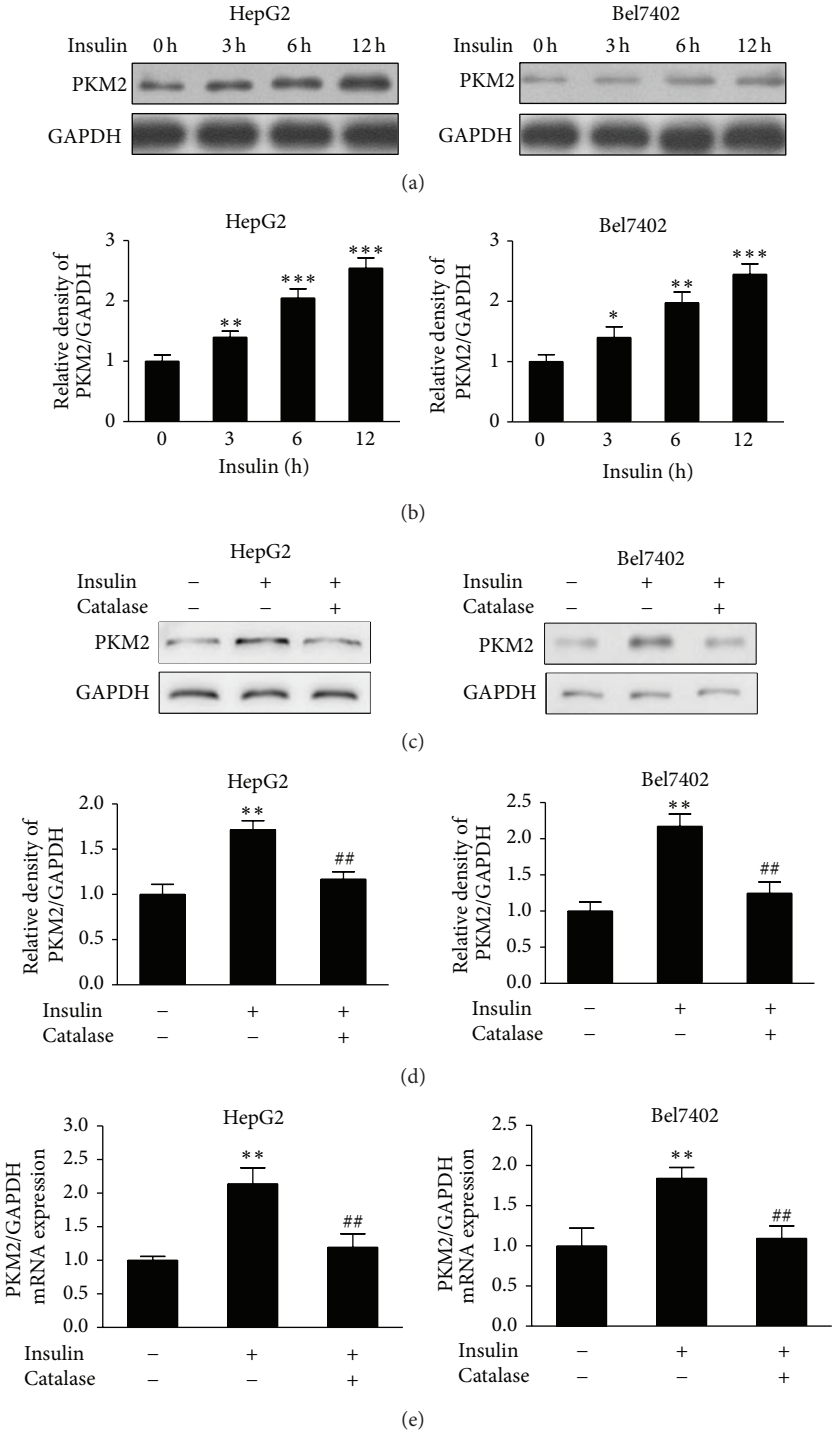

Figure 2: Insulin-induced PKM2 expression was inhibited by catalase. (a) HepG2 cells and Bel7402 cells were cultured to 70% confluence and then starved in serum-free medium for 24 h. The cells were exposed to 200 nM of insulin for 0 h, 3 h, 6 h, and 12 h. PKM2 levels were determined by immunoblotting. (b) Relative densities of PKM2/GAPDH from three independent experiments were normalized to those of control and presented as mean ± SD. * Significant difference compared to control without insulin treatment ($P < 0.05$). (c) The starved HepG2 cells and Bel7402 cells were pretreated with catalase (1500 U/mL) for 1 h, followed by stimulation with insulin (200 nM) for 6 h. Protein expression was determined by immunoblotting. (d) Results were expressed as a percentage of the control cultures and were the mean ± SD from three replications. (e) HepG2 cells and Bel7402 cells were treated as in (c). Total RNAs were extracted and used for real-time RT-PCR for detecting PKM2 and GAPDH mRNA levels. ** Significant difference compared to the control without insulin and catalase treatment treated without insulin and catalase treatment ($P < 0.01$); ## significant difference compared to the cells treated with insulin alone ($P < 0.01$).

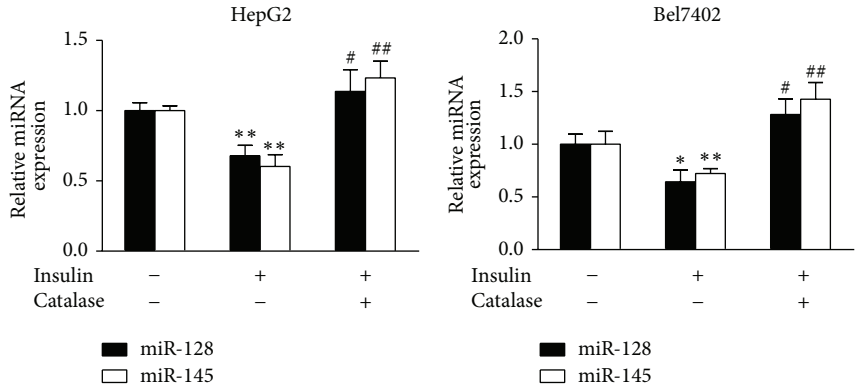

(a)

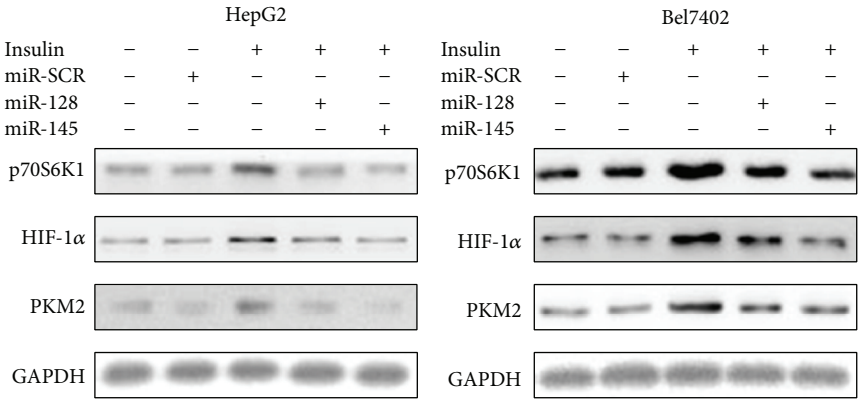

(b)

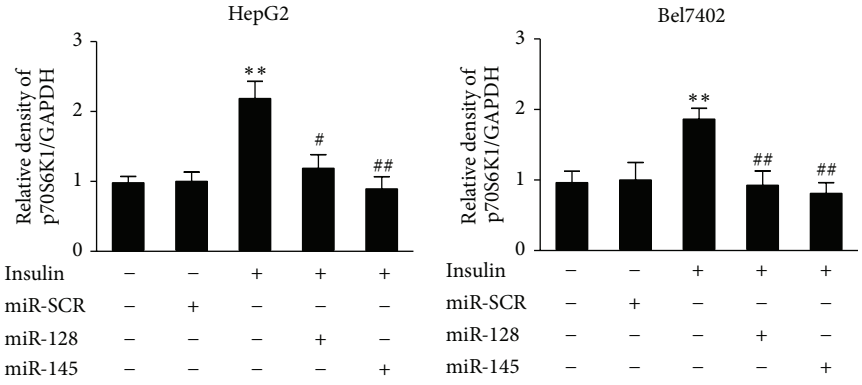

(c)

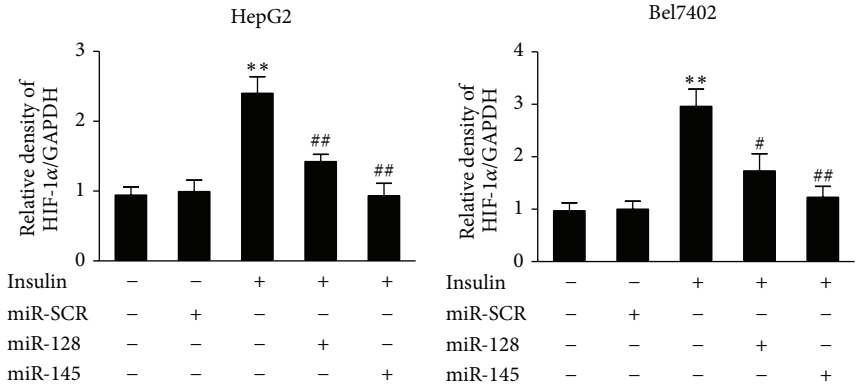

(d)

Figure 3: Continued.

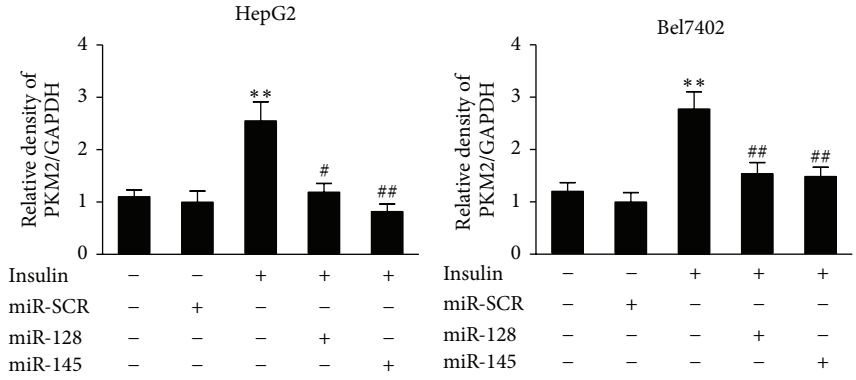

(e)

Figure 3: miR-145 and miR-128 are suppressed by insulin and involved in insulin-induced PKM2 expression. (a) HepG2 cells and Bel7402 cells were cultured overnight and switched to serum-free medium for 20 h. The starved cells were pretreated with catalase (1500 U/mL) for 1 h. Insulin (200 nM) was added and the cells were incubated for 6 h. Total RNAs were extracted and used for real-time RT-PCR for detecting the expression levels of miR-145, miR-128, and U6. * and ** Significant difference compared to control ($P < 0.05$ and $P < 0.01$); ## significant difference compared to treatment with insulin alone ($P < 0.01$). (b) HepG2 cells and Bel7402 cells were transfected with miR-145, miR-128, or miRNA scrambled control precursor. After transfection for 24 h, cells were cultured in serum-free medium for 20 h and treated without or with insulin (200 nM) for 6 h. Protein expression levels of p70S6K1, HIF-1α, PKM2, and GAPDH were determined by immunoblotting. (c), (d), and (e) Relative protein densities were quantified using ImageJ software. Results are presented as mean ± SD from three independent experiments. * and ** Significant difference compared to the value of the scramble control ($P < 0.05$ and $P < 0.01$); # and ## significant difference compared to that treated with insulin alone ($P < 0.05$ and $P < 0.01$).

effect of PKM2 on cell proliferation. When compared to siSCR treatment, inhibition of PKM2 in HepG2 and Bel7402 cells inhibited cell proliferation after the culture for 3-4 days, suggesting that PKM2 affects cell growth *in vitro* (Figure 4(e)). Taken together, these data indicate that PKM2 is critical for cell growth.

4. Discussion

Insulin has been shown to induce glucose metabolism and associated with a variety of cancer development in solid tumors [1, 27]. However, the mechanisms of insulin in glucose metabolism in cancer cells have not been directly examined. PKM2 is the last rate-limiting glycolytic enzymes of the glycolytic metabolism, which is preferentially expressed in embryonic tissue and cancer cells [4, 5]. Studies demonstrate that during tumor initiation as well as malignant progression PKM1 disappear and PKM2 reappears which leads to the switch from regular cell metabolism to aerobic glycolysis [28, 29]. Previous researches have shown that PKM2 may be induced by transcription factors, such as HIF-1α, while a number of genes associated with cell proliferation, metabolism, and tumor growth are downstream targets of PKM2.

Recent evidence has demonstrated the importance of ROS as secondary messengers in a variety of cellular functions [11–13]. Here, we present evidence that ROS promoted the effects of insulin-induced glycolysis and PKM2 expression in the cultured hepatocellular carcinoma cells. In general, insulin led to an increase in ROS levels and addition of catalase blocked the effect of insulin treatment. This result is consistent with our previous study of insulin-induced generation of H_2O_2 in PC-3 cells [14]. More importantly, ROS levels were positively correlated with insulin-induced glycolysis. PKM2 has been reported essential for glycolytic metabolism and insulin stimulates expression of the PKM2 [5, 28]. We further explored the role of ROS in the insulin-induced PKM2 expression. Results showed that insulin significantly induced PKM2 protein and mRNA expression levels and catalase greatly suppressed the effect induced by insulin. Expression levels of PKM2 protein and mRNA were affected, indicating the possible involvement of other factors in insulin-induced PKM2 expression.

Several miRNAs are reported to be altered in response to exogenous agents such as insulin and ROS [19–21]. In this study, we demonstrated that insulin suppressed expression levels of miR-145 and miR-128 through ROS production. Our previous studies showed that miR-145 and miR-128 inhibit HIF-1α expression by directly targeting p70S6K1 [25, 26]. Human *PKM2* gene sequence revealed a candidate HRE within the first intron containing the HIF-1 binding site 5′-ACGTG-3′ followed by a 5′-CACA-3′ sequence, which is found in many HREs [9, 30]. Correlation between miR-145 and miR-128 expression and insulin-regulated PKM2 expression further support our conclusion that insulin upregulates PKM2 expression through miR-145 and miR-128 expression. However, the mechanism by which insulin and ROS inhibit miR-145 and miR-128 is currently unknown. One possibility is that insulin and ROS may affect miR-145 and miR-128 expression through DNA hypermethylation. DNA hypermethylation has been shown to be associated with aberrant miRNA expression profiles in cancer [31–33]. Further studies are needed to address how insulin and ROS activate miR-145 and miR-128 in HepG2 and Bel7402 cells.

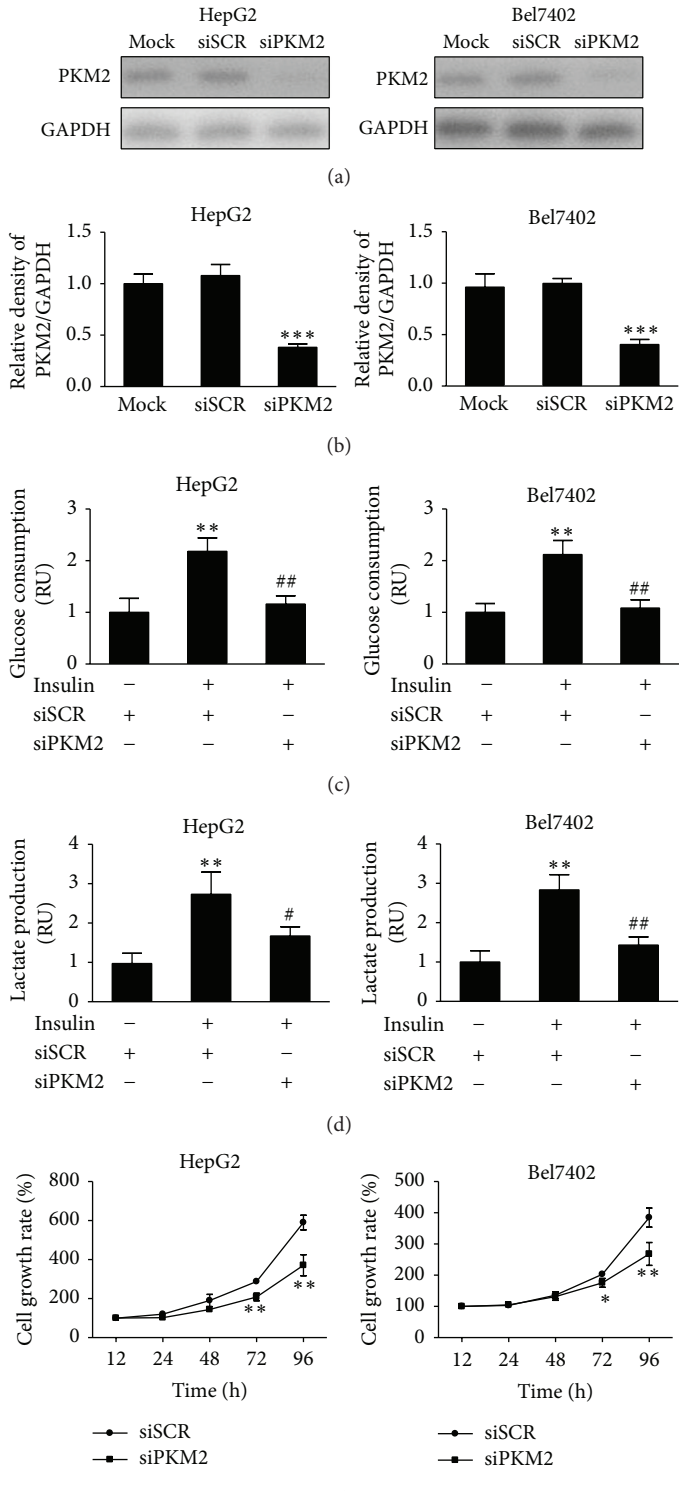

Figure 4: Knockdown of PKM2 is sufficient to inhibit insulin-induced glucose consumption, lactate production, and cell proliferation. (a) HepG2 and Bel7402 cells were transfected with siRNA against PKM2 (siPKM2) or scramble control (siSCR) for 48 h. The protein levels of PKM2 were analyzed by immunoblotting. (b) Relative densities of PKM2/GAPDH from three independent experiments were normalized to those of control and presented as mean ± SD. *** indicate significant difference when compared to scramble control at $P < 0.001$. (c) and (d) HepG2 and Bel7402 cells were transfected with siRNA against PKM2 (siPKM2) or scramble control (siSCR) for 24 h, followed by starving in serum-free medium for 24 h. Then, cells were stimulated with insulin (200 nM) for 12 h. Cells were trypsinized and counted, while the medium was collected. The glucose consumption and lactate production levels were analyzed. Data were mean ± SD from three independent experiments. $^{**}P < 0.01$ significant difference when compared to cell treated with siSCR; $^{\#}P < 0.05$ and $^{\#\#}P < 0.01$ significant difference compared to cell treated with siSCR and insulin. (e) HepG2 and Bel7402 cells were transfected with siRNA against PKM2 (siPKM2) or scramble control (siSCR) for 24 h. The cells were then trypsinized and resuspended. Cells at 3000 cells per well in a 96-well plate. The cell proliferation was measured at 12 h, 24 h, 48 h, 72 h, and 96 h. Values represent means ± SD. * and ** Compared to scramble control ($P < 0.05$ and $P < 0.01$).

In addition, we have shown that knockdown of PKM2 expression decreased insulin-induced aerobic glycolysis and cancer cell proliferation. This possibly explains the link between high insulin levels and elevated cancer risk. Moreover, this study may provide some useful information that PKM2 may act as a potential strategy for therapeutic purpose in liver cancer treatment in the future.

In conclusion, the results from the present study indicate that ROS promoted the effects of insulin-induced glycolysis and PKM2 expression in human hepatocellular carcinoma cells, that insulin upregulates PKM2 expression in ROS dependent manner through miR-145 and miR-128 suppression, and that PKM2 is important for insulin-induced aerobic glycolysis and cell proliferation. Our results contribute to understanding the role of insulin in cancer metabolism and also providing new insights into the role of PKM2 in pathogenesis of liver cancer.

Conflict of Interests

The authors declare that there is no conflict of interests regarding the publication of this paper.

Authors' Contribution

Qi Li, Xue Liu, and Yu Yin contributed equally to this work.

Acknowledgments

This study was supported in part by the National Key Basic Research Program of China (2011CB504003), the National Natural Science Foundation of China (81071642 and 30871296), and NIEHS, National Institutes of Health, Grant R01ES020868.

References

[1] D. R. Matthews, J. P. Hosker, A. S. Rudenski, B. A. Naylor, D. F. Treacher, and R. C. Turner, "Homeostasis model assessment: insulin resistance and β-cell function from fasting plasma glucose and insulin concentrations in man," *Diabetologia*, vol. 28, no. 7, pp. 412–419, 1985.

[2] H. Ying, A. C. Kimmelman, C. A. Lyssiotis et al., "Oncogenic Kras maintains pancreatic tumors through regulation of anabolic glucose metabolism," *Cell*, vol. 149, no. 3, pp. 656–670, 2012.

[3] O. Tavana and C. Zhu, "Too many breaks (brakes): pancreatic β-cell senescence leads to diabetes," *Cell Cycle*, vol. 10, no. 15, pp. 2471–2484, 2011.

[4] T. Nowak and C. Suelter, "Pyruvate kinase: activation by and catalytic role of the monovalent and divalent cations," *Molecular and Cellular Biochemistry*, vol. 35, no. 2, pp. 65–75, 1981.

[5] H. R. Christofk, M. G. V. Heiden, M. H. Harris et al., "The M2 splice isoform of pyruvate kinase is important for cancer metabolism and tumour growth," *Nature*, vol. 452, no. 7184, pp. 230–233, 2008.

[6] A. Dąębrowska, J. Pietkiewicz, K. Dąębrowska, E. Czapińska, and R. Danielewicz, "Interaction of M1 and M2 isozymes pyruvate kinase from human tissues with phospholipids," *Biochimica et Biophysica Acta*, vol. 1383, no. 1, pp. 123–129, 1998.

[7] H.-S. Shi, D. Li, J. Zhang et al., "Silencing of PKM2 increases the efficacy of docetaxel in human lung cancer xenografts in mice," *Cancer Science*, vol. 101, no. 6, pp. 1447–1453, 2010.

[8] Q. Sun, X. Chen, J. Ma et al., "Mammalian target of rapamycin up-regulation of pyruvate kinase isoenzyme type M2 is critical for aerobic glycolysis and tumor growth," *Proceedings of the National Academy of Sciences of the United States of America*, vol. 108, no. 10, pp. 4129–4134, 2011.

[9] W. Luo, H. Hu, R. Chang et al., "Pyruvate kinase M2 is a PHD3-stimulated coactivator for hypoxia-inducible factor 1," *Cell*, vol. 145, no. 5, pp. 732–744, 2011.

[10] W. Yang, Y. Xia, H. Ji et al., "Nuclear PKM2 regulates β-catenin transactivation upon EGFR activation," *Nature*, vol. 480, no. 7375, pp. 118–122, 2011.

[11] W. Dröge, "Free radicals in the physiological control of cell function," *Physiological Reviews*, vol. 82, no. 1, pp. 47–95, 2002.

[12] R. H. Burdon, "Superoxide and hydrogen peroxide in relation to mammalian cell proliferation," *Free Radical Biology and Medicine*, vol. 18, no. 4, pp. 775–794, 1995.

[13] T. P. Szatrowski and C. F. Nathan, "Production of large amounts of hydrogen peroxide by human tumor cells," *Cancer Research*, vol. 51, no. 3, pp. 794–798, 1991.

[14] Q. Zhou, L.-Z. Liu, B. Fu et al., "Reactive oxygen species regulate insulin-induced VEGF and HIF-1α expression through the activation of p70S6K1 in human prostate cancer cells," *Carcinogenesis*, vol. 28, no. 1, pp. 28–37, 2007.

[15] P. Kantharidis, B. Wang, R. M. Carew, and H. Y. Lan, "Diabetes complications: the microRNA perspective," *Diabetes*, vol. 60, no. 7, pp. 1832–1837, 2011.

[16] P. P. Medina and F. J. Slack, "MicroRNAs and cancer: an overview," *Cell Cycle*, vol. 7, no. 16, pp. 2485–2492, 2008.

[17] S. Srikantan, M. Gorospe, and K. Abdelmohsen, "Senescence-associated microRNAs linked to tumorigenesis," *Cell Cycle*, vol. 10, no. 19, pp. 3211–3212, 2011.

[18] R. Garzon, G. Marcucci, and C. M. Croce, "Targeting microRNAs in cancer: rationale, strategies and challenges," *Nature Reviews Drug Discovery*, vol. 9, no. 10, pp. 775–789, 2010.

[19] R. J. A. Frost and E. N. Olson, "Control of glucose homeostasis and insulin sensitivity by the Let-7 family of microRNAs," *Proceedings of the National Academy of Sciences of the United States of America*, vol. 108, no. 52, pp. 21075–21080, 2011.

[20] S. D. Jordan, M. Krüger, D. M. Willmes et al., "Obesity-induced overexpression of miRNA-143 inhibits insulin-stimulated AKT activation and impairs glucose metabolism," *Nature Cell Biology*, vol. 13, no. 4, pp. 434–448, 2011.

[21] S. Jajoo, D. Mukherjea, T. Kaur et al., "Essential role of NADPH oxidase-dependent reactive oxygen species generation in regulating microRNA-21 expression and function in prostate cancer," *Antioxidants & Redox Signaling*, vol. 19, no. 16, pp. 1863–1876, 2013.

[22] R. Huxley, A. Ansary-Moghaddam, A. B. de González, F. Barzi, and M. Woodward, "Type-II diabetes and pancreatic cancer: a meta-analysis of 36 studies," *British Journal of Cancer*, vol. 92, no. 11, pp. 2076–2083, 2005.

[23] H. B. el-Serag, H. Hampel, and F. Javadi, "The association between diabetes and hepatocellular carcinoma: a systematic review of epidemiologic evidence," *Clinical Gastroenterology and Hepatology*, vol. 4, no. 3, pp. 369–380, 2006.

[24] V. Rottiers and A. M. Naar, "MicroRNAs in metabolism and metabolic disorders," *Nature Reviews Molecular Cell Biology*, vol. 13, no. 4, pp. 239–250, 2012.

[25] Q. Xu, L.-Z. Liu, X. Qian et al., "MiR-145 directly targets p70S6K1 in cancer cells to inhibit tumor growth and angiogenesis," *Nucleic Acids Research*, vol. 40, no. 2, pp. 761–774, 2012.

[26] Z.-M. Shi, J. Wang, Z. Yan et al., "MiR-128 inhibits tumor growth and angiogenesis by targeting p70S6K1," *PLoS ONE*, vol. 7, no. 3, Article ID e32709, 2012.

[27] A. R. Saltiel and C. R. Kahn, "Insulin signalling and the regulation of glucose and lipid metabolism," *Nature*, vol. 414, no. 6865, pp. 799–806, 2001.

[28] T. Hitosugi, S. Kang, M. G. V. Heiden et al., "Tyrosine phosphorylation inhibits PKM2 to promote the warburg effect and tumor growth," *Science Signaling*, vol. 2, no. 97, Article ID ra73, 2009.

[29] K. Yamada and T. Noguchi, "Regulation of pyruvate kinase M gene expression," *Biochemical and Biophysical Research Communications*, vol. 256, no. 2, pp. 257–262, 1999.

[30] R. Fukuda, H. Zhang, J.-W. Kim, L. Shimoda, C. V. Dang, and G. Semenza, "HIF-1 regulates cytochrome oxidase subunits to optimize efficiency of respiration in hypoxic cells," *Cell*, vol. 129, no. 1, pp. 111–122, 2007.

[31] K.-W. Tsai, H.-W. Kao, H.-C. Chen, S.-J. Chen, and W.-C. Lin, "Epigenetic control of the expression of a primate-specific microRNA cluster in human cancer cells," *Epigenetics*, vol. 4, no. 8, pp. 587–592, 2009.

[32] H. M. O'Hagan, H. P. Mohammad, and S. B. Baylin, "Double strand breaks can initiate gene silencing and SIRT1-dependent onset of DNA methylation in an exogenous promoter CpG island," *PLoS Genetics*, vol. 4, no. 8, Article ID e1000155, 2008.

[33] H. O'Hagan, W. Wang, S. Sen et al., "Oxidative damage targets complexes containing DNA methyltransferases, SIRT1, and polycomb members to promoter CpG islands," *Cancer Cell*, vol. 20, no. 5, pp. 606–619, 2011.

Hindawi Publishing Corporation
Oxidative Medicine and Cellular Longevity
Volume 2014, Article ID 673959, 8 pages
http://dx.doi.org/10.1155/2014/673959

Research Article

Leucocyte Telomere Shortening in relation to Newly Diagnosed Type 2 Diabetic Patients with Depression

Zhelong Liu,[1] Jianhua Zhang,[1] Jiangtao Yan,[2] Yuping Wang,[1] and Yongsheng Li[3]

[1] *Division of Endocrinology, Tongji Hospital, Tongji Medical College, Huazhong University of Science and Technology, Jiefang Avenue 1095, Wuhan 430030, China*
[2] *Division of Cardiology, Tongji Hospital, Tongji Medical College, Huazhong University of Science and Technology, Jiefang Avenue 1095, Wuhan 430030, China*
[3] *Division of Emergency Internal Medicine, Tongji Hospital, Tongji Medical College, Huazhong University of Science and Technology, Wuhan 430030, China*

Correspondence should be addressed to Yongsheng Li; dr.ysli@hotmail.com

Received 14 February 2014; Accepted 9 April 2014; Published 29 April 2014

Academic Editor: Si Jin

The goal of this study is to investigate the association between oxidative stress and telomere length shortening in the comorbid depression and diabetes. Therefore, 71 patients with newly diagnosed type 2 diabetes (T2D) and 52 subjects with normal glycemic level (control, Ctrl) were enrolled. Depressive status was identified with the Depression Subscale of Hospital Anxiety and Depression Scale (HADS-D). Leukocyte telomere length ratio (T/S ratio) was determined with quantitative PCR. Oxidative stress status was evaluated with 8-hydroxy-desoxyguanosine (8-OHdG) assay kit. Some other biochemical blood testing was also performed. The data showed that T2D patients had higher proportion of depression evaluated by the HADS-D ($x^2 = 4.196$, $P = 0.041$). T/S ratio was significantly negatively correlated with 8-OHdG, HADS-D, age, HbA1c, FPG, and HOMA-IR. In addition, HADS-D was significantly positively correlated with HbA1c, FPG, HOMA-IR, and 8-OHdG. Both HADS-D and 8-OHdG were the major independent predictors for T/S ratio. This study indicates that oxidative stress contributes to both telomere length shortening and depression development in newly diagnosed type 2 diabetic patients, while in depression status, some other mechanisms besides oxidative stress may also affect the telomere length.

1. Introduction

Telomeres are tandem repeats of DNA sequence, TTAGGG at the end of eukaryotic chromosomes [1]. The important function of telomere is to protect the genomic DNA from being degenerating and maintain the genomic stability [2]. The telomere decreases with repeated cell division. When the shortened length gets to some exact extent, the cell develops to senescence. Oxidative stress is considered to be tightly related to the procedure of telomere decrease as it can induce the strand breaks of telomeric DNA [3, 4].

Recently increasing evidence showed the association between the shortening of leucocyte telomere length and several age-related diseases, including type 2 diabetes [5–7]. Type 2 diabetes (T2D), characterized with the clinical chronic hyperglycemia and insulin resistance, is nowadays one of the most threatening problems to the global public health. Although it has not been fully comprehended, more and more evidence shows that both oxidative stress and cell premature senescence may take an important part in the mechanism of T2D [5]. Some previous studies including our work suggested a probable relationship between oxidative stress and the leucocyte telomere length shortening in diabetic patients [8, 9].

The association of psychological stress and illness with telomere length change has also been reported lately [10, 11]. Depression, one of the most common forms of psychological disorders, often cooccurs with type 2 diabetes [12]. Diabetic patients with depression have higher HbA1c levels and poorer glycemic control [13]. They may have less physical exercises and be less compliant to take healthy diet and antidiabetic regimen [14]. What is more, it is verified that diabetic patients

with depression have higher mortality rates due to myocardial infarction [15] and a latest systematic review shows that depression is associated with almost 1.5-fold increase risk of mortality in people with diabetes [16]. However, the mechanism of the combination and linkage of depression and diabetes is still unknown.

Although the telomere length decrease is identified in diabetic or depressive patients, respectively, there is no research work reported in the population of cooccurring depression and diabetes till now. Therefore, the aim of our study was to investigate the association between oxidative stress and telomere length shortening in the comorbid depression and diabetes.

2. Research Design and Methods

2.1. Patients and Controls. A total of 71 patients with newly diagnosed type 2 diabetes (T2D) (male 40/female 31) were recruited from the Division of Endocrinology, Tongji Hospital, Tongji Medical College, Huazhong University of Science and Technology, Wuhan, Hubei, China, between January 2011 and June 2012. The subjects were questioned about their medical history and family history. The enrolled subjects were diagnosed with T2D no more than 1 month and had not received any antidiabetic agents yet. The diagnosis of diabetes was in accordance with World Health Organization criteria (fasting plasma glucose $\geqslant$ 7 mmol/L or 2-hour plasma glucose $\geqslant$ 11.1 mmol/L) [17]. 52 subjects with normal glycemic level were enrolled in control group (Ctrl group) (male 30/female 22). The individuals with pregnancy, acute inflammation, communicable diseases, cancer, stroke, severe cardiovascular disease, Alzheimer's disease, dementia, or severe cognitive disorders were excluded. In this study, the definition of drinkers was those who consumed liquor within the last 30 days and the average pure alcohol intake $\geqslant$10 g per week. This study was carried out in accordance with the principle of Helsinki Declaration and approved by the local ethical committee. All participants gave written informed consent to participate in this study.

2.2. Assessment of Anthropometric Data. All subjects took physical examination by a physician. Blood pressure was measured in the sitting position after resting for 10 min. Waist circumference was measured midway between the lowest rib and the iliac crest in the upright standing position. Hip circumference was measured at the greater trochanter.

2.3. Assessment of Depression. For screening of depression, we used the Depression Subscale of Hospital Anxiety and Depression Scale (HADS-D), which consists of 7 questions [18]. All the subjects completed the HADS-D separately, without any interaction with research staff. Depression was identified as the score $\geqslant$10.

2.4. Blood Samples Collection and Laboratory Measurement. Participants were fasted overnight for 10 hours and had blood samples drawn from an antecubital vein, then immediately aliquoted into cryotubes as plasma, buffy coat, and red blood cells. Fasting plasma glucose (FPG) was measured using glucose oxidase method (AVE 2852 half auto biochemical analyzer), fasting insulin (FIN) was measured using electrochemiluminescence assay (Elecsys 2010, Roche Instrument Center AG), and HbA1c was measured using high pressure liquid chromatography (variant II, Bio-Rad). Peripheral insulin resistance was estimated by homeostasis model assessment (HOMA-IR = FIN $\times$ FPG/22.5). Serum total cholesterol (TC), triacylglycerols (TG), high-density lipoprotein cholesterol (HDL-C), and low-density lipoprotein cholesterol (LDL-C) levels were measured using enzymatic method performed on clinical chemistry analyzer (Roche/Hitachi MODULAR analyzer).

2.4.1. Measurement of Relative Telomere Length. All buffy-coat cryotubes were stored in freezers at −80°C. Genomic DNA was extracted from peripheral white blood cells using the QG-Mini80 workflow with DB-S kit (Fujifilm Corporation, Tokyo, Japan) as instructed.

Telomere length ratio (T/S ration) was measured using a quantitative PCR-based technique [19]. In this method, the ratio of the telomere repeat copy number (T) and single-copy gene number (S) was compared for each sample. Reactions for DNA samples were run in 7 μL reaction volumes with ABI-7900 HT real-time thermal cycler (Applied Biosystems).

The primers are as follows.

Telomere-F 5′-CGGTTTGTTTGGGTTTGGGTT-TGGGTTTGGGTTTGGGTT-3′.

Telomere-R 5′-GGCTTGCCTTACCCTTACCCT-TACCCTTACCCTTACCCT-3′.

β-globin-F 5′-GCTTCTGACACAACTGTGTTC-ACTAGC-3′.

β-globin-R 5′-CACCAACTTCATCCACGTTCA-CC-3′.

β-globin-P FTGCATCTGACTCCTGAGGP.

Cycling conditions of telomere were as follows: 95°C incubation for 10 minutes followed by 35 cycles of 95°C for 15 seconds and 56°C for 1 min. As for the cycling conditions of β-globin, 95°C incubation for 10 minutes followed by 40 cycles of 95°C for 15 sec and 56°C for 1 min. The specificity of all of the amplification was determined by melting curve analysis.

2.4.2. Measurement of 8-OHdG. 8-OHdG in leucocyte DNA was quantified with OxiSelect oxidative DNA damage ELISA kit (Cell Biolab, Inc, San Diego, USA), which can be used to evaluate the degree of antioxidant stress [9].

2.5. Statistical Analysis. Analyses were performed with the SPSS 11.5 (SPSS) statistical package. Significance was defined as the P value was less than 0.05. All variables were tested for normal distribution of the data. Data are shown as means ± standard deviation (SD) in a normal distribution, while as median with interquartile range (IQR, 25th~75th percentile) in a nonnormal distribution. Continuous variables differences between two groups were analyzed with

Student's test and among multiple groups with ANOVA and for nonparametric data with the Mann-Whitney U test or Kruskal-Wallis H test, respectively. A chi-square test was utilized for categorical data. To evaluate the reliability of the questionnaire of HADS-D, the internal consistency was used, which was examined with the Cronbach's alpha, and the results >0.7 were judged as adequate. The Spearman correlation analysis was adopted to evaluate the correlation between telomere length and other factors including age, body mass index, waist circumference, waist-to-hip ratio, systolic and diastolic blood pressure, fasting plasma glucose, fasting insulin, HOMA-IR, HbA1c, lipids, 8-OHdG, and HADS-D. The correlation between HADS-D/8-OHdG and other factors was also examined in this way. Stepwise multiple linear regression was applied to determine independent predictors of T/S ratio in T2D group. Candidates for the stepwise multiple regressions were variables that yielded a P value of less than 0.15 in the univariate analysis. Then collinear variables were excluded when the Spearman's rank correlation coefficient was more than 0.7. The P value was no less than 0.10 for variables entered the regression.

3. Result

3.1. Main Clinical and Biological Parameters in Subjects. Subjects with and without T2D did not differ significantly in terms of the proportion of smokers, drinkers, and the use of aspirin, statin, and antihypertension drugs. The subjects in T2D group were significantly older than in the control group. The sex ratio was similar in the two groups.

The values of BMI, waist circumference, WHR, the values of systolic blood pressure, diastolic blood pressure, HbA1c, FPG, HOMA-IR, TC, TG, and 8-OHdG were higher in the patients with T2D, while the HDL level was lower in the T2D group. The T/S ratio in the T2D group was significantly shorter than in the control group (Table 1).

T2D group was further divided into two subgroups as with depression [T2D(D+)] and without depression (T2D(D−)); similarly, Ctrl groups also were subclassified as Ctrl(D+) and Ctrl(D−). Among the four subgroups, no significant difference was found in the indexes of age, proportion of male, smokers, drinkers, drugs used, SBP, FIN, HDL, and LDL. Comparing with the T2D(D−) patients, the T2D(D+) ones had higher HADS-D scores and T/S ratio with similar level of BMI, WHR, SBP, DBP, HbA1c, FPG, HOMA-IR, lipids, and 8-OHdG. Comparing with Ctrl(D+) patients, the T2D(D+) ones had higher proportion of hypotensive drugs and higher level of HbA1c, FPG, and TC. No remarkable difference was found in T/S, HOMA-IR, and 8-OHdG. Comparing with the Ctrl(D−) subjects, the Ctrl(D+) ones had higher BMI besides HADS-D scores. The Ctrl(D−) also showed lower level of telomere length (Table 2).

3.2. HADS-D Evaluation with Internal Consistency. The chi-square test showed that the T2D patients had higher proportion of depression than control subjects, evaluated by the HADS-D ($x^2 = 4.196$, $P = 0.041$) (Table 1). The internal consistency of the HADS-D, as calculated by Cronbach's α, was valued as 0.716 in T2D group and 0.730 in Ctrl group, respectively.

3.3. Correlation between T/S Ratio and Other Factors in Whole Population. The correlation between T/S ratio and other factors was analyzed in the whole population of the two groups ($N = 123$). It was shown that age ($r = -0.422$, $P = 0.000$), HADS-D ($r = -0.621$, $P = 0.000$), HbA1c ($r = -0.543$, $P = 0.000$), FPG ($r = -0.434$, $P = 0.000$), HOMA-IR ($r = -0.322$, $P = 0.000$), 8-OHdG ($r = -0.641$, $P = 0.000$), SBP ($r = -0.189$, $P = 0.036$), DBP ($r = -0.211$, $P = 0.019$), and TG ($r = -0.2$, $P = 0.026$) were significantly negatively correlated with T/S ratio, while FIN, age, BMI, wrist circumference, WHR, TC, TG, and LDL had no significant correlation with T/S ratio. This indicates that the decrease of telomere correlates with depression and oxidative stress besides aging, blood glucose level, and insulin resistance (Figure 1).

3.4. Correlation between HADS-D and Other Factors in Whole Population. It was shown that HbA1c ($r = 0.272$, $P = 0.002$), FPG ($r = 0.239$, $P = 0.008$), HOMA-IR ($r = 0.28$, $P = 0.002$), 8-OHdG ($r = 0.331$, $P = 0.000$), and age ($r = 0.202$, $P = 0.025$) were significantly positively correlated with HADS-D, while other indexes had no significant correlation with HADS-D. These results suggested that depression related to hyperglycemia and insulin resistance besides telomere length shortening (as shown in Section 3.3).

3.5. Correlation between 8-OHdG and Other Factors in Whole Population. It was shown that HbA1c ($r = 0.685$, $P = 0.000$), FPG ($r = 0.595$, $P = 0.000$), HOMA-IR ($r = 0.381$, $P = 0.000$), age ($r = 0.267$, $P = 0.003$), BMI ($r = 0.236$, $P = 0.009$), wrist circumference ($r = 0.308$, $P = 0.001$), WHR ($r = 0.247$, $P = 0.006$), DBP ($r = 0.211$, $P = 0.002$), TC ($r = 0.342$, $P = 0.000$), and TG ($r = 0.258$, $P = 0.004$) were significantly positively correlated with 8-OHdG, while other indexes had no significant correlation with 8-OHdG. Thereby, oxidative stress relates to telomere length shortening, depression (as shown in Sections 3.2 and 3.3), aging, and insulin resistance with obesity.

3.6. Multiple Linear Regression Analysis in T2D Group. Stepwise multiple linear regression in T2D subjects was applied to evaluate independent predictors of T/S ratio. The results showed that both HADS-D and 8-OHdG were the major independent predictors of T/S ratio ($P = 0.000$, 0.001, resp.), thereby indicating that the type 2 diabetic patients with higher scores of HADS-D and in more severe oxidative stress status may have much more shortened telomere length. Other independent predictors included HbA1c, FPG, age, and SBP (Table 3).

4. Discussion

The result showed that oxidative stress could play an important role in the mechanism of telomere length shortening.

Table 1: Demographic, clinical, and biochemical parameters of the study subjects of T2D and Ctrl

	T2D $n = 71$	Ctrl $n = 52$	P
Age (yrs)	54.55 ± 8.37	51.27 ± 7.66	0.028
Male [(n (%)]	40 (56.34)	30 (57.69)	0.881
Current smokers [(n (%)]	21 (29.58)	14 (26.92)	0.784
Current drinkers [(n (%)]	13 (18.31)	8 (15.38)	0.670
Use of aspirin [(n (%)]	8 (11.27)	4 (7.69)	0.509
Use of statin [(n (%)]	7 (9.86)	4 (7.69)	0.677
Use of antihypertensive drugs[(n (%)]	6 (8.45)	5 (9.62)	0.823
HADS-D score (point)*	8 (6, 9)	8 (6, 9)	0.200
HADS-D ≥ 10 [(n (%)]	17 (23.9)	5 (9.6)	0.041
BMI (kg/m^2)	25.21 ± 2.19	23.86 ± 1.47	0.000
Waist circumstance (cm)	87.5 (81.8, 94.0)	82.0 (78.0, 86.0)	0.000
WHR	0.84 (0.77, 0.89)	0.80 (0.74, 0.84)	0.000
Systolic blood pressure (mmHg)	132 (120, 141)	127 (123, 130)	0.040
Diastolic blood pressure (mmHg)	81 (75, 88)	74 (68, 80)	0.000
HbA1c (%)	8.29 (7.58, 8.90)	5.10 (4.80, 5.40)	0.000
FPG (mmol/L)	8.72 ± 1.39	5.44 ± 0.35	0.000
FIN (mIU/L)	11.44 (6.99, 13.29)	12.22 (7.8, 14.32)	0.520
HOMA-IR	4.51 (2.73, 5.54)	2.93 (2.00, 3.29)	0.000
Total cholesterol (mmol/L)	4.69 ± 0.90	4.05 ± 0.54	0.000
Triglyceride (mmol/L)	1.86 (1.12, 2.31)	1.20 (0.86, 1.32)	0.000
HDL-cholesterol (mmol/L)	1.15 ± 0.24	1.22 ± 0.27	0.020
LDL-cholesterol (mmol/L)	2.47 ± 0.78	2.21 ± 0.67	0.050
8-OHdG (ng/mL)	1.75 ± 0.51	1.16 ± 0.31	0.000
T/S ratio	2.01 ± 0.47	2.28 ± 0.25	0.000

Data are means ± SD, n (%), or median (interquartile range).
T2D: type 2 diabetic group, Ctrl: control group, HADS-D: Depression Subscale of Hospital Anxiety and Depression Scale, BMI: body mass index, WHR: waist-to-hip ratio, FPG: fasting plasma glucose, FIN: fasting insulin, HOMA-IR: homeostasis model assessment-insulin resistance [HOMA-IR = FIN (mIU/L) × FPG (mmol/L)/22.5], 8-OHdG: Human 8-hydroxy-desoxyguanosine.
*The total score of HADS-D is 21 and depression was identified as the score ≥10.

Reactive oxygen species may induce deoxyguanosine conversion to 8-OHdG in the cellular nucleus, which is then released into blood [20]. Therefore, 8-OHdG was utilized as an indicator related to oxidative stress and remarkable negative correlation between 8-OHdG and T/S ratio was observed in the whole population studied, which is consistent with the previous findings [9]. On another side, compared with the diabetic subjects without depression, the diabetic patients with depression had higher level of 8-OHdG in this study. To our knowledge, it is the first time to evaluate the correlation between oxidative stress and depression with the detecting of blood 8-OHdG level and examining of HADS-D score. Furthermore, in both the diabetic and control subjects, the depressive ones had remarkable shorter telomere length than those free of depression, also indicating the relevance between depression and telomere degeneration. Up to now, it is the first time to show the interrelationship of oxidative stress and depression and telomere shortening in type 2 diabetic patients.

Interestingly, in diabetic group, the depressive ones had shorter telomere than those without depression, while their glycemia and 8-OHdG were in similar levels. That may be explained with the bias due to the small sample size in our study. Otherwise, there is the possibility that the depressive status might be more prone to induce telomere shortening throughout another mechanism rather than oxidative stress. Therefore, more studies must be made to answer this confusing question.

Insulin resistance is reported to be in relation to telomere length as the HOMA-IR and BMI are the important indexes for insulin resistance [21–23]. In our study, the T/S ratio is shown to be correlated with HOMA-IR but not with BMI in the whole population studied. In multiple linear regression analysis in T2D group, we failed to identify HOMA-IR to be independent predictor of T/S ratio as the 95% confidence interval for unstandardized coefficient is −0.003, 0.035 and the P value is 0.097. This may also be attributed to the small sample size of this study.

Table 2: Demographic, clinical, and biochemical parameters of the study subjects of subgroups with/without depression in T2D[a] and Ctrl[b] groups.

	T2D		Ctrl		F	P
	D+	D−	D+	D−		
	n = 17	n = 54	n = 6	n = 46		
Age (yrs)	54.71 ± 8.10	54.83 ± 8.58	55.33 ± 6.56	51.22 ± 8.32	1.823	0.147
Male [(n(%)]	10 (58.82)	24 (44.44)	3 (50.00)	19 (41.30)	—	0.656
Current smokers [(n(%)]	5 (29.41)	16 (29.63)	2 (33.33)	12 (26.09)	—	0.971
Current drinkers [(n(%)]	2 (11.76)	11 (20.37)	1 (16.67)	7 (15.22)	—	0.834
Use of aspirin [(n(%)]	1 (5.88)	7 (12.96)	0 (0.00)	4 (8.70)	—	0.653
Use of statin [(n(%)]	3 (17.65)	4 (7.41)	1 (16.67)	3 (6.52)	—	0.474
Use of antihypertensive drugs [(n(%)]	3 (17.64)$^{\#}$	3 (5.56)$^{\#}$	0 (0.00)	5 (10.87)	—	0.00
HADS-D (point)	12 (10, 12)$^{*\odot}$	7 (6, 8)$^{\#}$	12 (10, 12)*	7 (6, 8)	—	0.000
BMI (kg/m^2)	24.96 ± 1.93*	25.29 ± 2.28*	24.00 ± 2.32*	23.84 ± 1.36	5.033	0.003
Waist circumstance (cm)	87 (80, 91)*	88 (82, 94)*	81 (77, 87)	82 (78, 86)	—	0.000
WHR	0.82 (0.74, 0.88)	0.85 (0.79, 0.90)*	0.82 (0.75, 0.86)	0.80 (0.74, 0.84)	—	0.006
Systolic blood pressure (mmHg)	134 (120, 141)	131 (120, 141)	128 (123, 130)	126 (123, 130)	—	0.171
Diastolic blood pressure (mmHg)	79 (70, 84)	82 (75, 89)*	78 (72, 85)	74 (68, 131)	—	0.004
HbA1c (%)	8.4 (8, 9.1)$^{*\#}$	8.2 (7.5, 8.7)$^{*\#}$	5.3 (5.2, 5.5)	5.1 (4.7, 5.4)	—	0.000
FPG (mmol/L)	9.42 ± 1.66$^{*\#}$	8.50 ± 1.23$^{*\#}$	5.42 ± 0.28	5.44 ± 0.36	101.427	0.000
FIN (mIU/L)	12.55 (6.69, 15.02)	11.09 (6.99, 13.19)	12.95 (9.57, 16.40)	12.00 (7.74, 13.23)	—	0.617
HOMA-IR	5.54 (3.24, 6.25)*	4.19 (2.58, 5.02)*	3.09 (2.26, 3.70)	2.91 (2.00, 3.23)	—	0.000
Total cholesterol (mmol/L)	4.57 ± 1.03$^{*\#}$	4.73 ± 0.87$^{*\#}$	4.03 ± 0.26	4.06 ± 0.57	6.821	0.000
Triglyceride (mmol/L)	1.89 (1.34, 1.88)*	1.91 (1.08, 2.36)*	1.74 (1.18, 2.13)	1.23 (0.85, 1.55)	—	0.001
HDL-cholesterol (mmol/L)	1.15 ± 0.26	1.14 ± 0.23	1.20 ± 0.40	1.26 ± 0.25	1.841	0.143
LDL-cholesterol (mmol/L)	2.39 ± 0.92	2.50 ± 0.74	2.10 ± 0.81	2.22 ± 0.66	1.458	0.229
8-OHdG (ng/mL)	1.80 ± 0.42*	1.48 ± 0.44*	1.53 ± 0.26	1.09 ± 0.34	15.722	0.000
T/S ratio	1.70 (1.36, 2.06)$^{*\odot}$	2.11 (1.82, 2.42)*	2.01 (1.91, 2.13)*	2.32 (2.14, 2.47)	—	0.000

Data are means ± SD, n (%), or median (interquartile range).
T2D: type 2 diabetic group, Ctrl: control group, HADS-D: Depression Subscale of Hospital Anxiety and Depression Scale, BMI: body mass index, WHR: waist-to-hip ratio, FPG: fasting plasma glucose, FIN: fasting insulin, HOMA-IR: homeostasis model assessment-insulin resistance [HOMA - IR = FIN (mIU/L) × FPG (mmol/L)/22.5], 8-OHdG: Human 8-Hydroxy-desoxyguanosine.
[a]subgroup with/without depression in T2D is shown as T2D(D+)/T2D(D−), respectively,
[b]subgroup with/without depression in Ctrl group is shown as Ctrl(D+)/Ctrl(D−), respectively.
$^{*}P < 0.05$ for T2D(D+)/T2D(D−)/Ctrl(D+) versus Ctrl(D−).
$^{\#}P < 0.05$ for T2D(D+)/T2D(D−) versus Ctrl(D+).
$^{\odot}P < 0.05$ for T2D(D+) versus T2D(D−).

The development of depression may be related to many factors. Aged females are reported with higher risk of depression [24, 25]. Life styles such as smoking and drinking and some drugs including aspirin, statins, and antihypertension agents are also indicated to affect the development of depression [26–30]. As for this study, the levels of the sex ratio, age, and the proportion of smokers, drinkers, and the drugs used mentioned above in the depression subgroups between T2D and Ctrl were shown to be similar. Additionally, the duration of diabetes, the insulin injection, and the level of hyperglycemic control may also correlate with depression [16, 31]. For this reason, only patients of newly diagnosed diabetes were included, who had never received any antihyperglycemic treatment.

In this study, the status of depression was evaluated with the HADS-D. This scale was initially designed to identify depression in clinical psychiatric hospitals, yet it has also been adopted to screen depression in nonhospitalized population and considered to be accurate and convenient [32, 33]. It is a 7-item self-report questionnaire and each item is scored 0

Table 3: Predictors of leukocyte telomere length in type 2 diabetic patients.

	Univariate analysis		Multiple linear regression	
	Unstandardized coefficient (b)	P	Unstandardized coefficient (b) (95% confidence interval for b)	P
Age	−0.027	0.000	−0.012 (−0.019, −0.005)	0.002
BMI	0.011	0.683		
Waist circumference	−0.006	0.390		
WHR	0.074	0.920		
SBP	−0.005	0.138	−0.006 (−0.010, −0.003)	0.001
DBP	−0.002	0.748		
FPG	−0.204	0.000	−0.062 (−0.115, −0.009)	0.023
HbA1c	−0.287	0.000	−0.157 (−0.224, −0.090)	0.000
FIN	−0.003	0.744		
HOMA-IR	−0.026	0.135	0.016 (−0.003, 0.035)	0.097
Total cholesterol	−0.014	0.823		
Triglyceride	−0.041	0.473		
HDL	0.28	0.242		
LDL	−0.071	0.326		
HADS-D	−0.115	0.000	−0.057 (−0.080, −0.033)	0.000
8-OHdG	−0.599	0.000	−0.238 (−0.369, −0.103)	0.001

to 3 and a total score of 8 or greater indicates the presence of depression. However it was reported that the best accuracy was achieved with cutoff of 10 points in total [32]. The internal consistency of HADS-D was assessed with Cronbach's alpha coefficient, which was 0.716 for T2D group and 0.730 for Ctrl group. It is regarded as satisfactory since the value of Cronbach's alpha is over 0.7 [18].

There are still some limitations in this study. Firstly, this is a cross-sectional study and the sample size was small. So we should draw the conclusion very carefully and prospective studies with large sample size are needed to verify the findings. Secondly, although only the newly diagnosed patients were enrolled in this study, the hyperglycemic status without obvious diabetic symptoms might exist earlier before the diabetes was diagnosed [34]; therefore the latent hyperglycemia and oxidative stress could take effect on telomere length for some time. There may be discrepancy of the duration in the diabetic subjects and it is hard to be evaluated. Thirdly, the chronic diabetic complications including diabetic nephropathy, retinopathy, and neuropathy have not been evaluated in this study yet, which might indicate the long duration of diabetes. Fourthly, there are still some other factors that can affect the development of depression which are not evaluated in this study, such as economic income and social status [35, 36].

5. Conclusion

In summary, this study indicated that oxidative stress contributes to both telomere length shortening and depression development in newly diagnosed type 2 diabetic patients. What is more, in depression status some other mechanisms besides oxidative stress may also affect the telomere length. To fully elucidate the complicated interactions of diabetes and depression with oxidative stress and cell senility, more research work is needed in the future.

Abbreviations

T2D: Type 2 diabetes
Ctrl: Control group
T/S ratio: Telomere length ratio
8-OHdG: Human 8-hydroxy-desoxyguanosine
HADS-D: The Depression Subscale of Hospital Anxiety and Depression Scale
HOMA-IR: Homeostasis model assessment-insulin resistance
ROS: Reactive oxygen species
FPG: Fasting plasma glucose
FIN: Fasting insulin
TC: Total cholesterol
TG: Triacylglycerols

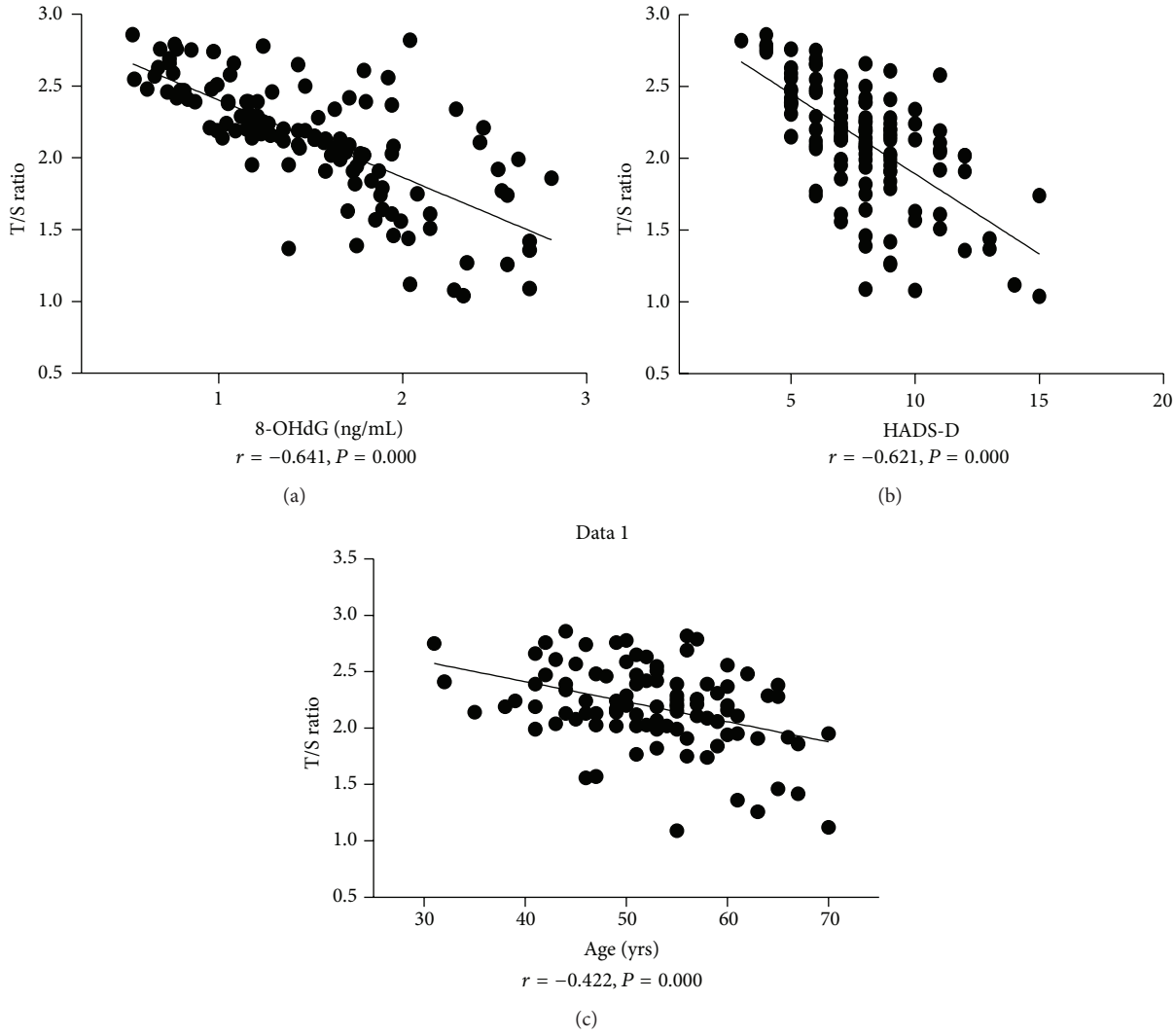

Figure 1: Correlation between T/S ratio and 8-OHdG(a), HADS-D (b), and age (c) in the whole population studied.

HDL-C: High-density lipoprotein cholesterol
LDL-C: Low-density lipoprotein cholesterol
BMI: Body mass index
WHR: Waist-to-hip ratio.

Conflict of Interests

The authors declare that they have no conflict of interests.

Acknowledgments

The authors thank all their colleagues working in the Department of Internal Medicine, Tongji Medical College, Huazhong University of Science and Technology. This work was supported in part by Grants from National Nature Science Foundation of China (no. 81070190), Nature Science Foundation of Hubei province (no. 2009CDB049 and no. 2011CDB207), and the Fundamental Research Funds for the Central Universities (HUST 2012QN190).

References

[1] D. Kejariwal, K. M. Stepien, T. Smith, H. Kennedy, D. A. Hughes, and M. J. Sampson, "Lack of association of colonic epithelium telomere length and oxidative DNA damage in Type 2 diabetes under good metabolic control," *BMC Endocrine Disorders*, vol. 8, article 12, 2008.

[2] E. H. Blackburn, "Switching and signaling at the telomere," *Cell*, vol. 106, no. 6, pp. 661–673, 2001.

[3] C. Autexier and N. F. Lue, "The structure and function of telomerase reverse transcriptase," *Annual Review of Biochemistry*, vol. 75, pp. 493–517, 2006.

[4] S. Makpol, A. Z. Abidin, K. Sairin, M. Mazlan, G. M. Top, and W. Z. W. Ngah, "γ-tocotrienol prevents oxidative stress-induced telomere shortening in human fibroblasts derived from different aged individuals," *Oxidative Medicine and Cellular Longevity*, vol. 3, no. 1, pp. 35–43, 2010.

[5] M. J. Sampson, M. S. Winterbone, J. C. Hughes, N. Dozio, and D. A. Hughes, "Monocyte telomere shortening and oxidative DNA damage in type 2 diabetes," *Diabetes Care*, vol. 29, no. 2, pp. 283–289, 2006.

[6] Q. Shen, X. Zhao, L. Yu et al., "Association of leukocyte telomere length with type 2 diabetes in mainland Chinese populations," *Journal of Clinical Endocrinology and Metabolism*, vol. 97, no. 4, pp. 1371–1374, 2012.

[7] O. Uziel, J. A. Singer, V. Danicek et al., "Telomere dynamics in arteries and mononuclear cells of diabetic patients, effect of diabetes and of glycemic control," *Experimental Gerontology*, vol. 42, no. 10, pp. 971–978, 2007.

[8] K. D. Salpea, P. J. Talmud, J. A. Cooper et al., "Association of telomere length with type 2 diabetes, oxidative stress and UCP2 gene variation," *Atherosclerosis*, vol. 209, no. 1, pp. 42–50, 2010.

[9] D. Ma, W. Zhu, S. Hu, X. Yu, and Y. Yang, "Association between oxidative stress and telomere length in Type 1 and Type 2 diabetic patients," *Journal of Endocrinological Investigation*, vol. 36, pp. 1032–1037, 2013.

[10] E. S. Epel, E. H. Blackburn, J. Lin et al., "Accelerated telomere shortening in response to life stress," *Proceedings of the National Academy of Sciences of the United States of America*, vol. 101, no. 49, pp. 17312–17315, 2004.

[11] J. H. Kim, H. K. Kim, J. H. Ko, H. Bang, and D. C. Lee, "The relationship between leukocyte mitochondrial DNA copy number and telomere length in community-dwelling elderly women," *PLoS ONE*, vol. 8, Article ID e67227, 2013.

[12] S. Ali, M. A. Stone, J. L. Peters, M. J. Davies, and K. Khunti, "The prevalence of co-morbid depression in adults with Type 2 diabetes: a systematic review and meta-analysis," *Diabetic Medicine*, vol. 23, no. 11, pp. 1165–1173, 2006.

[13] P. J. Lustman and R. E. Clouse, "Depression in diabetic patients: the relationship between mood and glycemic control," *Journal of Diabetes and its Complications*, vol. 19, no. 2, pp. 113–122, 2005.

[14] L. E. Egede, "Effect of depression on self-management behaviors and health outcomes in adults with type 2 diabetes," *Current Diabetes Reviews*, vol. 1, no. 3, pp. 235–243, 2005.

[15] J. F. Scherrer, L. D. Garfield, T. Chrusciel et al., "Increased risk of myocardial infarction in depressed patients with type 2 diabetes," *Diabetes Care*, vol. 34, no. 8, pp. 1729–1734, 2011.

[16] F. E. van Dooren, G. Nefs, M. T. Schram, F. R. Verhey, J. Denollet, and F. Pouwer, "Depression and risk of mortality in people with diabetes mellitus, a systematic review and meta-analysis," *PLoS ONE*, vol. 8, Article ID e57058, 2013.

[17] K. G. Albertiand and P. Z. Zimmet, "Definition, diagnosis and classification of diabetes mellitus and its complications. Part 1, diagnosis and classification of diabetes mellitus provisional report of a WHO consultation," *Diabetic Medicine*, vol. 15, pp. 539–553, 1998.

[18] M. M. Iversen, G. S. Tell, T. Riise et al., "History of foot ulcer increases mortality among individuals with diabetes: ten-year follow-up of the Nord-Trondelag health study, Norway," *Diabetes Care*, vol. 32, no. 12, pp. 2193–2199, 2009.

[19] Z. Yang, X. Huang, H. Jiang et al., "Short telomeres and prognosis of hypertension in a Chinese population," *Hypertension*, vol. 53, no. 4, pp. 639–645, 2009.

[20] N. Tentolouris, R. Nzietchueng, V. Cattan et al., "White blood cells telomere length is shorter in males with type 2 diabetes and microalbuminuria," *Diabetes Care*, vol. 30, no. 11, pp. 2909–2915, 2007.

[21] J. P. Gardner, S. Li, S. R. Srinivasan et al., "Rise in insulin resistance is associated with escalated telomere attrition," *Circulation*, vol. 111, no. 17, pp. 2171–2177, 2005.

[22] S. Demissie, D. Levy, E. J. Benjamin et al., "Insulin resistance, oxidative stress, hypertension, and leukocyte telomere length in men from the Framingham Heart Study," *Aging Cell*, vol. 5, no. 4, pp. 325–330, 2006.

[23] O. S. Al-Attas, N. M. Al-Daghri, M. S. Alokail et al., "Adiposity and insulin resistance correlate with telomere length in middle-aged Arabs: the influence of circulating adiponectin," *European Journal of Endocrinology*, vol. 163, no. 4, pp. 601–607, 2010.

[24] F. Cardin, F. Ambrosio, P. Amodio et al., "Quality of life and depression in a cohort of female patients with chronic disease," *BMC Surgery*, vol. 12, supplement 1, p. S10, 2012.

[25] V. K. Burt and K. Stein, "Epidemiology of depression throughout the female life cycle," *Journal of Clinical Psychiatry*, vol. 63, no. 7, pp. 9–15, 2002.

[26] P. Sun, J. B. Unger, Q. Guo et al., "Comorbidity between depression and smoking moderates the effect of a smoking prevention program among boys in China," *Nicotine and Tobacco Research*, vol. 9, supplement 4, pp. S599–S609, 2007.

[27] J. G. Rahola, "Somatic drugs for psychiatric diseases, aspirin or simvastatin for depression?" *Current Neuropharmacology*, vol. 10, pp. 139–158, 2012.

[28] F. P. Thorndike, R. Wernicke, M. Y. Pearlman, and D. A. F. Haaga, "Nicotine dependence, PTSD symptoms, and depression proneness among male and female smokers," *Addictive Behaviors*, vol. 31, no. 2, pp. 223–231, 2006.

[29] M. Workman and J. Beer, "Depression, suicide ideation, and aggression among high school students whose parents are divorced and use alcohol at home," *Psychological Reports*, vol. 70, no. 2, pp. 503–511, 1992.

[30] I. Lesser, H. Myers, K.-M. Lin, and E. M. Simonsick, "Letter to the editor," *Psychosomatic Medicine*, vol. 58, no. 5, pp. 515–516, 1996.

[31] G. Nefs, V. J. Pop, J. Denollet, and F. Pouwer, "The longitudinal association between depressive symptoms and initiation of insulin therapy in people with type 2 diabetes in primary care," *PLoS ONE*, vol. 8, Article ID e78865, 2013.

[32] A. Falavigna, O. Righesso, A. R. Teles et al., "Depression Subscale of the Hospital Anxiety and Depression Scale applied preoperatively in spinal surgery," *Arquivos de Neuro-Psiquiatria*, vol. 70, pp. 352–356, 2012.

[33] B. Andrews, J. Hejdenberg, and J. Wilding, "Student anxiety and depression: comparison of questionnaire and interview assessments," *Journal of Affective Disorders*, vol. 95, no. 1–3, pp. 29–34, 2006.

[34] "Screening for type 2 diabetes," *Diabetes Care*, vol. 23, supplement 1, pp. S20–S23, 2000.

[35] J. Hong, M. Knapp, and A. Mcguire, "Income-related inequalities in the prevalence of depression and suicidal behaviour: a 10-year trend following economic crisis," *World Psychiatry*, vol. 10, no. 1, pp. 40–44, 2011.

[36] T. Leone, E. Coast, S. Narayanan, and A. de Graft Aikins, "Diabetes and depression comorbidity and socio-economic status in low and middle income countries (LMICs): a mapping of the evidence," *Global Health*, vol. 8, p. 39, 2012.

Hindawi Publishing Corporation
Oxidative Medicine and Cellular Longevity
Volume 2014, Article ID 581732, 9 pages
http://dx.doi.org/10.1155/2014/581732

Research Article

Lentivirus-Mediated Nox4 shRNA Invasion and Angiogenesis and Enhances Radiosensitivity in Human Glioblastoma

Yongsheng Li,[1] Na Han,[2] Tiejun Yin,[2] Lulu Huang,[2] Shunfang Liu,[2] Dongbo Liu,[2] Cuihong Xie,[1] and Mengxian Zhang[2]

[1] *Department of Emergency Medicine, Tongji Hospital, Tongji Medical College, Huazhong University of Science & Technology, Wuhan 430030, China*
[2] *Department of Oncology, Tongji Hospital, Tongji Medical College, Huazhong University of Science & Technology, Jiefang Road 1095, Wuhan 430030, China*

Correspondence should be addressed to Mengxian Zhang; zhangmengxian@medmail.com.cn

Received 2 February 2014; Revised 30 March 2014; Accepted 4 April 2014; Published 27 April 2014

Academic Editor: Xiaoqian Chen

Radioresistance remains a significant therapeutic obstacle in glioblastoma. Reactive oxygen species (ROS) are associated with multiple cellular functions such as cell proliferation and apoptosis. Nox4 NADPH oxidase is abundantly expressed and has proven to be a major source of ROS production in glioblastoma. Here we investigated the effects of Nox4 on GBM tumor cell invasion, angiogenesis, and radiosensitivity. A lentiviral shRNA vector was utilized to stably knockdown Nox4 in U87MG and U251 glioblastoma cells. ROS production was measured by flow cytometry using the fluorescent probe DCFH-DA. Radiosensitivity was evaluated by clonogenic assay and survival curve was generated. Cell proliferation activity was assessed by a cell counting proliferation assay and invasion/migration potential by Matrigel invasion assay. Tube-like structure formation assay was used to evaluate angiogenesis ability *in vitro* and VEGF expression was assessed by MTT assay. Nox4 knockdown reduced ROS production significantly and suppressed glioblastoma cells proliferation and invasion and tumor associated angiogenesis and increased their radiosensitivity *in vitro*. Our results indicate that Nox4 may play a crucial role in tumor invasion, angiogenesis, and radioresistance in glioblastoma. Inhibition of Nox4 by lentivirus-mediated shRNA could be a strategy to overcome radioresistance and then improve its therapeutic efficacy for glioblastoma.

1. Introduction

Glioblastoma multiforme (GBM) is the most common and most malignant primary brain tumor in adults with a high degree of morbidity and mortality [1]. Recent advances in the treatment of glioblastoma multiforme published in the landmark study by Stupp et al. [2] changed the standard of care with the discovery that the addition of temozolomide (TMZ) to radiotherapy for newly diagnosed glioblastoma resulted in a clinically meaningful and statistically significant survival benefit with minimal additional toxicity. Despite this success, survival remains very low. Virtually all patients suffer tumor recurrence despite aggressive irradiation, emphasizing the radioresistant nature of GBMs and prompting investigators to seek alternate treatments through a better understanding of the cell biology and through some new molecular targets that may enhance current treatments.

Reactive oxygen species (ROS) are highly reactive O_2 metabolites that include superoxide anion (O_2^-), hydrogen peroxide (H_2O_2), and hydroxyl radical (OH^-). Although ROS are classically thought of as cytotoxic and mutagenic, recent evidence suggests that ROS serve as regulators of signal-transduction pathways for cell proliferation and survival [3]. Nox-family NADPH oxidases have proven to be a major source of ROS production in various cell types and have crucial roles in various physiological and pathological processes [4]. Several studies demonstrated that NADPH oxidase subunit 4 (Nox4) is expressed in several human tumors, such as glioblastoma [5], hepatocellular carcinoma [6], breast cancer [7], thyroid cancer [8], and melanoma [9],

and is involved in cellular senescence, resistance to apoptosis, tumorigenic transformation, cell proliferation, cell survival, and chemotherapy resistance. Strong evidence suggests that these processes are upregulated via Nox4 generation of ROS.

In glioblastoma, the expression levels of Nox4 mRNA were significantly higher than those in other astrocytomas (WHO grades II and III). Specific knockdown of Nox4 expression by RNA interference resulted in cell-growth inhibition and enhanced induction of apoptosis by chemotherapeutic agents [5], indicating that enhanced expression of Nox4 appears to be involved in cell proliferation and chemotherapy resistance in glioma cells. Most recent studies have shown that Nox4 played important roles in cycling hypoxia-mediated HIF-1 activation and further promoted tumor progression in glioblastoma [10, 11], suggesting that Nox4 might be a critical mediator of radioresistance in GBM, since hypoxia is known as a major reason for the resistance of tumor cells to radiation [12]. Lu et al. have shown that androgens increased ROS production by Nox4 and Nox2 in prostate cancer. Preradiation treatment of human prostate cancer cells with Nox inhibitors sensitized the cells to radiation similar to androgen deprivation therapy [13], further supporting the notion that enhanced Nox4 levels are protective against radiation-induced tumor cell death. Moreover, Nox4 has been shown to promote invasion and angiogenesis process in several solid organ tumors, such as renal cell carcinoma [14], ovarian cancer [15], and head and neck cancer [16]. Invasive tumor growth and active neovascularization are characteristic features of GBM, which contribute to its radioresistant phenotype. Based on these data, we hypothesized that Nox4 might be a critical mediator of invasion, angiogenesis, and radiation response in GBM and a potential target for developing better therapeutic methods.

To explore the potential impact of Nox4 on GBM radiosensitivity, invasion, and angiogenesis, a loss-of-function analysis was performed by applying a Nox4 short hairpin RNA- (shRNA-) expressing lentivirus to two GBM cell lines, U87MG and U251. Then the effect of Nox4 knockdown on the colonies formation, cell proliferation, and cell invasion ability of GBM was investigated. Moreover, capillary tube-like structure formation ability of human umbilical veins endothelial cells (HUVECs) that were cocultured with conditioned medium derived from GBM cells was measured. Our study demonstrates that Nox4 was involved in ROS generation and Nox4 knockdown inhibited cell invasion, angiogenesis, and promoted radiation response in human glioblastoma.

2. Methods and Materials

2.1. Cell Cultures and Treatment Conditions. Human glioblastoma (U87MG and U251) tumor cells were obtained from the American Type Culture Collection (ATCC; Manassas, VA) and were cultured in DMEM medium supplemented with 10% FCS, 50 mg/mL penicillin/streptomycin. Primary isolated human umbilical vein endothelial cells (HUVEC, Promocell) were cultured up to passage 8. Cells were maintained in culture at 37°C with 5% CO_2 and 95% humidity in serum reduced (5% FCS) modified Promocell medium (MPM) supplemented with 2 ng/mL VEGF, 4 ng/mL bFGF. For X-ray treatment, cells were cultured in 25 cm^2 flasks and then irradiated at 2.5 Gy/min, at room temperature, with an Elekta Precise Linear Accelerator operating at 6 MV.

2.2. Lentivirus-Mediated shRNA Knockdown of Gene Expression. pGIPZ-lentiviral shRNAmir vectors targeting human Nox4 gene and nonsilencing pGIPZ control vector were purchased from Open Biosystems (Thermo Fisher Scientific, Inc.). pGIPZ cloning vector contains Turbo GFP reporter and expresses a puromycin-resistant gene. Lentiviral shRNA was produced by cotransfection of the Trans-Lentiviral Packaging Mix with a shRNA transfer vector into HEK 293T packaging cells (Open Biosystems). Supernatants containing either the lentivirus expressing the Nox4 shRNA or the control shRNA were harvested 72 h after transfection. The lentiviruses were purified using ultracentrifugation, and the titer of the lentiviruses was determined. U87MG and U251 cells were transduced by the lentiviral particles at a multiplicity of infection (MOI) of 10 followed by puromycin selection for 10 days. The clones stably transfected with pGIPZ-lentiviral shRNAmir was referred to as Nox4 shRNA cells, whereas the cells stably transfected with pGIPZ nonsilencing control vector as scrambled cells. The knockdown of Nox4 was evaluated by real-time quantitative PCR and Western blot analysis.

2.3. Real-Time Quantitative RT-PCR (qRT-PCR). Total RNA extraction was performed using Trizol reagent (Invitrogen, Carlsbad, CA) according to the manufacturer's instruction and purity and integrity of the RNA was assessed with Agilent 2100 BioAnalyzer (Agilent Technologies, Palo Alto, CA, USA). Then qRT-PCR was performed using QuantiTect Primer Assay (QIAGEN) and QuantiTect SYBR Green RT-PCR Kit (QIAGEN) on a LightCycler 480 Instrument (Roche Diagnostics). The detection and quantification involved the following steps: reverse transcription at 50°C for 30 min, initial activation at 95°C for 15 min, followed by 40 cycles of denaturation at 94°C for 15 sec, annealing at 55°C for 30 sec, and extension at 72°C for 30 sec. Fluorescence data collection was performed at the extension step at 72°C. The relative expression of the target gene was calculated by normalizing the Cp (crossing point) values with those of housekeeping gene GAPDH. All assays were performed in triplicates.

2.4. Western Blot Analysis. Protein extracts were prepared by using RIPA lysis buffer and the protein concentrations were measured by the Bradford method using BCA Protein Assay Kit (Pierce Biotechnology, USA). Samples were immunoblotted with antibodies against Nox4 (Cell signalling). An anti-β-actin monoclonal antibody purchased from Sigma (St. Louis, MO) was used as an internal loading control. Blots were developed using ECL method and Western band densities were qualified using ImageJ software (National Institutes of Health).

2.5. Measurement of the Intracellular ROS Level. Intracellular ROS accumulation was measured by flow cytometry

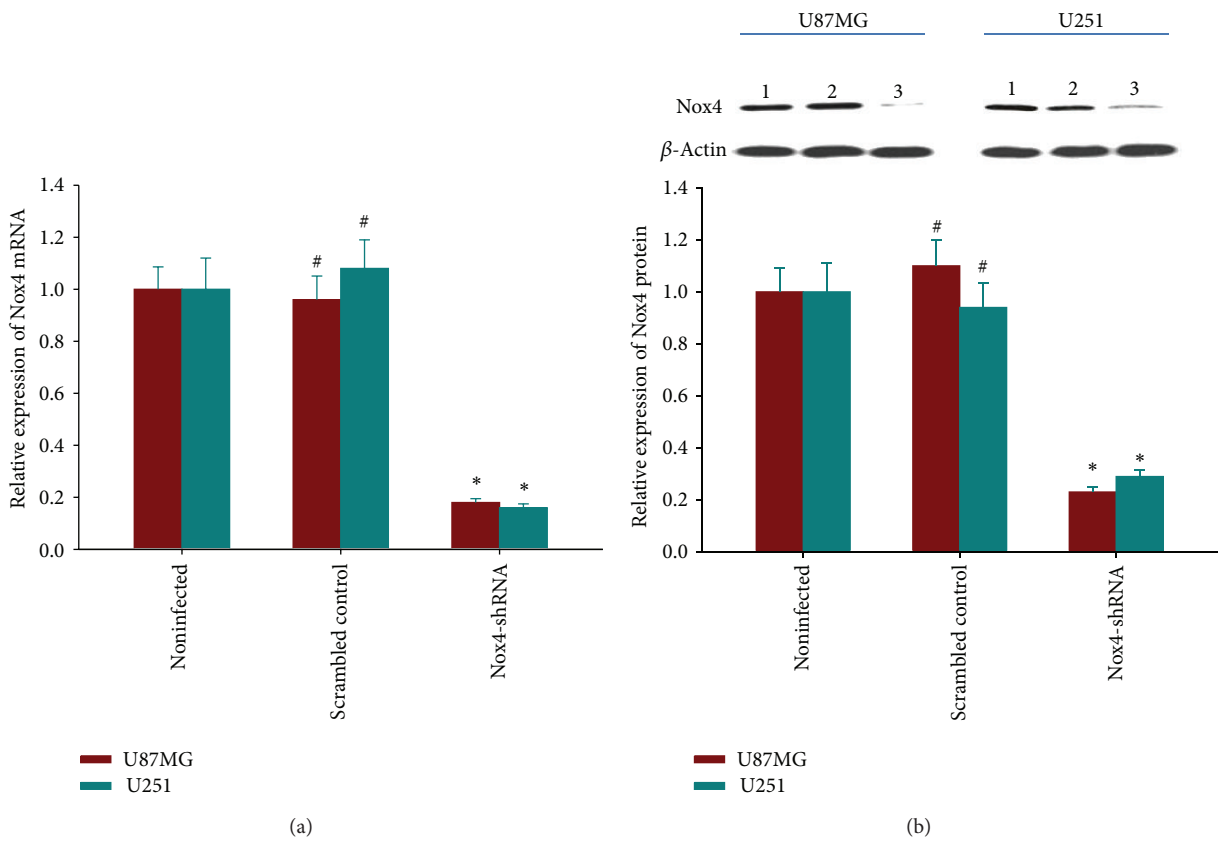

Figure 1: Verification of knockdown of Nox4 expression in U87MG and U251 cells by lentivirus-mediated RNA interference. (a) The expression levels of Nox4 mRNA were measured by qRT-PCR. There was a dramatic decrease of Nox4 mRNA in the Nox4 shRNA group ($P < 0.05$). No significant difference was observed between noninfected cells and scrambled control. (b) The expression levels of Nox4 protein were measured by Western blot (line 1, noninfected; line 2, scrambled control; line 3, Nox4-shRNA). The protein levels in the Nox4-shRNA group decreased significantly compared to scrambled and noninfected cells. The GAPDH gene and the β-actin protein are the internal controls for qRT-PCR and Western blot analysis, respectively. Columns, mean; bars, SD; $^{*}P < 0.05$, versus noninfected and scrambled control; $^{\#}P > 0.05$, versus noninfected.

using the fluorescent probe 2′,7′-dichlorodihydrofluorescein diacetate (DCFH-DA, Sigma-Aldrich). Cells were incubated with 10 μmol/L DCFH-DA for 30 min at 37°C in dark. After incubation, the cells were washed with phosphate buffered saline (PBS) and analyzed within 30 min using FACScan flow cytometer (Becton Dickinson, San Jose, CA, U.S.A) with the excitation source at 488 nm and emission wavelength of 525 nm. 10,000 cells were counted in each determination.

2.6. Clonogenic Assay. Increasing numbers of cells (10^2 to 5×10^4) were plated in 25 cm^2 flasks and irradiated with various doses (0~8 Gy) with 6 MV X-ray at a dose rate of 2.5 Gy/min. After 10 to 14 days' culture, colonies formed were stained with crystal violet (Sigma) and those with at least 50 cells were counted by microscopic inspection, and plating efficiency as well as clonogenic survival was calculated. The linear-quadratic (LQ) equation was fitted to data sets to generate survival curves and dose enhancement factor (DEF) for drugs was calculated at 10% surviving fraction. DEF values greater than 1.0 indicate enhancement of radiosensitivity.

2.7. Proliferation Assay. The effect of Nox4 knockdown on cell proliferation was assessed using a cell counting proliferation assay. In brief, 5×10^4 cells were seeded on 25 cm^2 flasks over night at standard conditions. The cells were exposed to a single 4 Gy irradiation with 6 MV X-ray and incubated for another 72 h, the cells were harvested and stained with trypan blue, and the total number of living cells was counted by microscopic inspection.

2.8. Matrigel Invasion Assays. The invasion of glioblastoma cells *in vitro* was measured on Matrigel-coated (0.78 mg/mL) transwell inserts with 8 μm pore size (BD, Biosciences). The Nox4 shRNA and scrambled cells were starved for 24 hours and then were harvested. 500 μL of cell suspension (1×10^5 cells/mL) per experiment was seeded into the upper well of the chamber containing serum free media. The lower chamber had been filled with DMEM with 10% BSA. After 12 hours of incubation, cells that had invaded the membrane were fixed with 70% ethanol and stained with 0.1% crystal violet and sealed on slides. Representative photos were taken and migrated cells were counted in 6 random high-power fields per chamber under a light microscope.

2.9. Tube Formation Assay. To evaluate *in vitro* angiogenesis activity, tube formation assays were performed with HUVEC. 24-well plates were coated with 300 μL Matrigel (BD, Biosciences). HUVECs were suspended in serum-free conditioned medium obtained from culture supernatant of Nox4 shRNA or scrambled cells treated with or without 4 Gy irradiation. HUVECs (5×10^4) were suspended in 500 μL of conditioned medium and then plated onto the polymerized Matrigel and incubated at 37°C for 6 h. The capillary tube-like structures formed by HUVECs were photographed and counted under a phase contrast inverted microscope.

2.10. ELISA for VEGF. U87MG and U251 cells transfected with Nox4-shRNA or scrambled shRNA were treated with or without 4 Gy radiation and then were plated in 6-well tissue culture plates at a density of 1×10^6 cells per well and incubated at 37°C. The supernatants were collected 12 h after radiation. VEGF concentration was determined using Quantikine ELISA kits (R&D Systems, MN, USA) according to the manufacturer's instructions.

2.11. Statistical Analysis. The results were expressed as the mean ± SD. Differences between the two groups were assessed using a two-tailed *t*-test. A P value less than 0.05 was considered statistically significant. Statistical analysis was performed with SPSS 13.0 statistical software (SPSS Inc., Chicago, Illinois).

3. Results

3.1. Lentivirus-Mediated shRNA Inhibited Nox4 mRNA and Protein Expression in GBM Cell Lines. To investigate the role of Nox4 in GBM, lentivirus vector encoding Nox4 shRNA was constructed and infected U87MG and U251 cell lines. Then, the lentivirus-transduced cells were selected by puromycin for 10 d and the clones stably transfected with pGIPZ-lentiviral shRNAmir (Nox4-shRNA) or pGIPZ non-silencing control vector (scrambled control) were successfully generated. The positive GFP expression in cells was still above 90% even in these clones cultured up to passage 15. To verify that the Nox4 gene was silenced by the lentivirus vector, the mRNA and protein levels in U87MG and U251 cells were assessed using real-time quantitative PCR and Western blot assays, respectively. Compared with the levels in uninfected and scrambled cells, the Nox4 mRNA and protein levels in U87MG and U251 cells infected with Nox4 shRNA decreased significantly (Figure 1), indicating the successful knockdown of Nox4 in the derived clones.

3.2. Nox4 Is Involved in ROS Generation in GBM Cell Lines. To test whether Nox4 mediates ROS production, intracellular superoxide production was evaluated by using flow cytometry in cells loaded with oxidation-sensitive DCFH-DA. Transfection of Nox4 shRNA resulted in a significant inhibition of ROS production as compared to scrambled controls (Figure 2), suggesting that Nox4 is one of the major sources of ROS generation in U87MG and U251 glioblastoma cells.

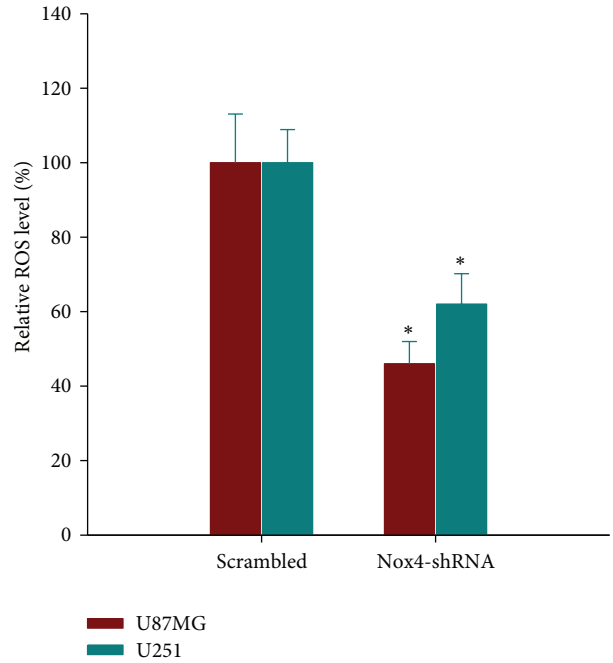

Figure 2: Inhibition of ROS production by Nox4-shRNAs. U87MG and U251 cells transfected with Nox4-shRNA or scrambled shRNA were labeled with DCFH-DA and alterations in the intracellular ROS level were measured by FACS analysis. DCF fluorescence shown in histogram was normalized to that in scrambled cells. The data are means ± SD. $^*P < 0.05$, versus scrambled.

3.3. Nox4 Silencing Enhanced Radiosensitivity of Glioblastoma Cells. To determine the effect of Nox4 silencing on GBM tumor cell radiosensitivity, clonogenic survival analysis was performed with U87MG and U251 stably transfected with Nox4 shRNA or scrambled control. As shown in Figure 3, Nox4 shRNA caused a significant reduction in clonogenic survival in cell cultures of both U87MGMG (left) and U251 (right) following radiation compared with that caused by scrambled shRNA combined with radiation, resulting in an increase in the radiosensitivity with a dose enhancement factor of 1.267 and 1.347 at a surviving fraction of 10%, respectively.

3.4. Nox4 Silencing Suppressed Glioblastoma Cell Proliferation. To investigate the effect of Nox4 silencing on the proliferation activity of GBM, a cell counting proliferation assay was performed. As shown in Figure 4, Nox4 shRNA transduced cells showed significantly reduced proliferation when compared with the scrambled control group ($P < 0.05$). Radiation treatment also inhibited the cell proliferation ($P < 0.05$). When radiation treatment was combined with Nox4 knockdown, a further reduction of the cell count was observed ($P < 0.05$).

3.5. Nox4 Silencing Inhibited Glioblastoma Cell Invasion. To evaluate the effect of Nox4 knockdown on invasion capacity of GBM cells, transwell system was utilized. As shown in Figure 5, Nox4 shRNA infected cells revealed

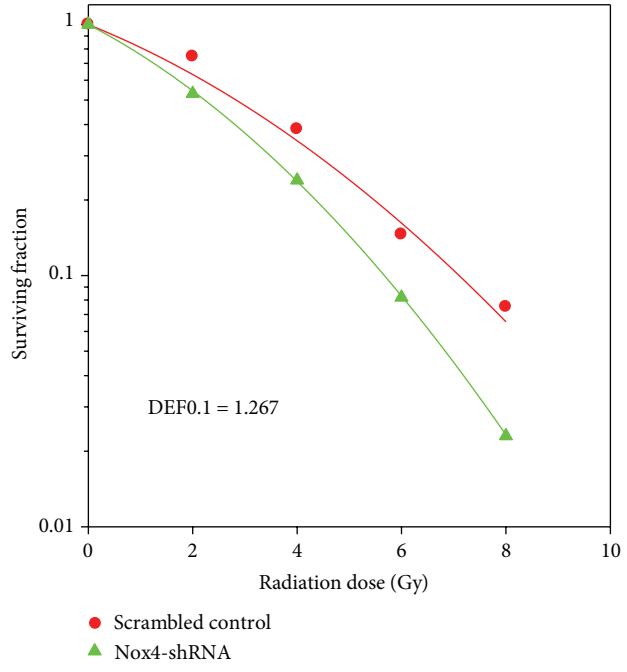

(a)

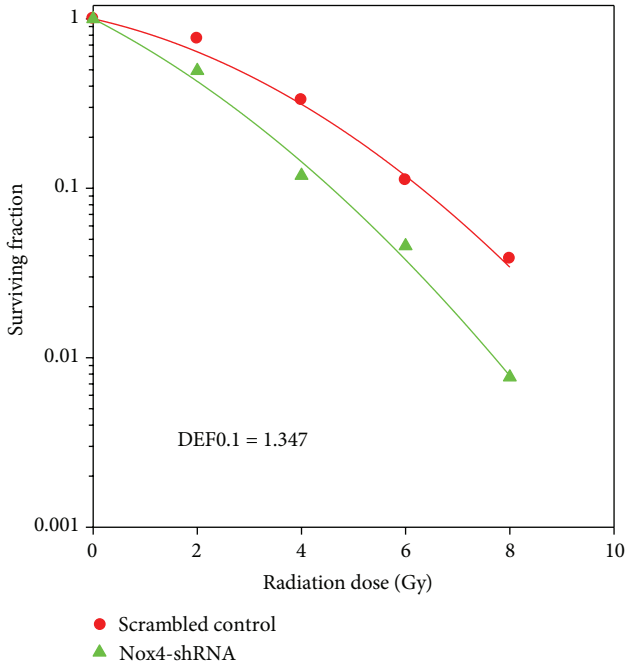

(b)

Figure 3: Effect of Nox4 silencing on radiosensitivity of glioblastoma cell lines was measured by clonogenic survival assay. Colony-forming efficiency was determined 10 to 14 d later and survival curves were generated and linear-quadratic (LQ) equation was fitted to data sets. (a) U87MG infected with Nox4-shRNA or scrambled control (DEF0.1 = 1.267 when shRNA versus scrambled control). (b) U251 infected with Nox4-shRNA or scrambled control (DEF0.1 = 1.347 when shRNA versus scrambled control). Points, mean; DEF, dose enhancement factor.

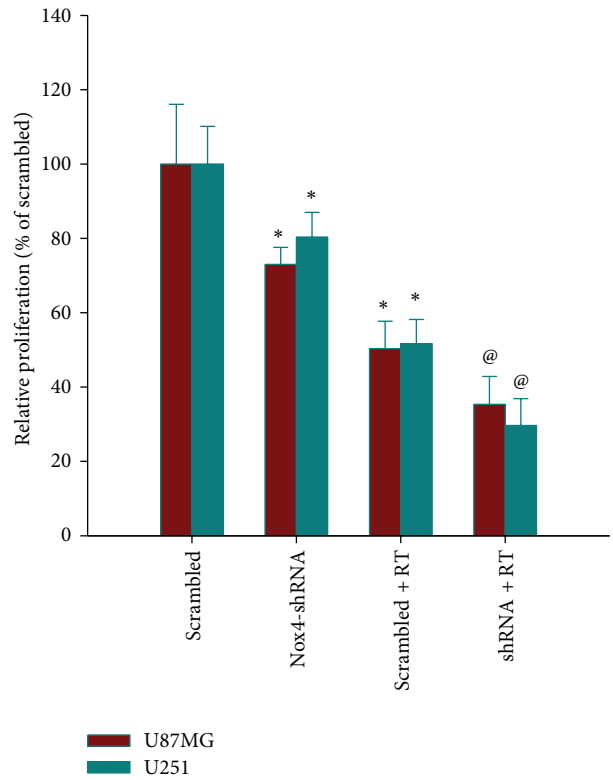

Figure 4: Effect of Nox4 silencing on the proliferation activity of GBM. Proliferation of U87MG and U251 cells transfected with Nox4-shRNA or scrambled shRNA was determined by cell count after 72 h exposure to 4 Gy irradiation. Relative numbers of cells are shown as histogram. Columns, mean; bars, SD; RT, radiation therapy; $^{*}P < 0.05$, versus scrambled; $^{@}P < 0.05$, versus scrambled and Nox4-shRNA and scrambled + RT.

a pronounced reduction in invasiveness when compared with the scrambled control group ($P < 0.05$). However, irradiation could markedly enhance invasion capability of both U87MG and U251 scrambled cells, which could be counteracted by knockdown of Nox4 ($P < 0.05$). These data suggested that Nox4 silencing could inhibit both constitutive and radiation-induced invasion of GBM cells.

3.6. Nox4 Silencing Inhibited Endothelial Cells Tube-Like Structure Formation In Vitro. The sprouting of endothelial cells and formation of tubes are crucial steps in the angiogenic process. To determine the effect of Nox4 knockdown on angiogenesis, we examined how Nox4 shRNA regulates tube-like structures formation of HUVECs *in vitro* using a coculture system. As shown in Figure 6(a), the tube-like structure formation was significantly suppressed by the conditioned medium (CM) from U87MG cells infected with Nox4 shRNA, compared with the CM from scrambled control cells. Moreover, CM from irradiated U87MG cells increased HUVECs tube-like structure formation compared to nonirradiated conditioned medium, and this kind of irradiation-induced tube formation was obvious inhibited by Nox4 knockdown.

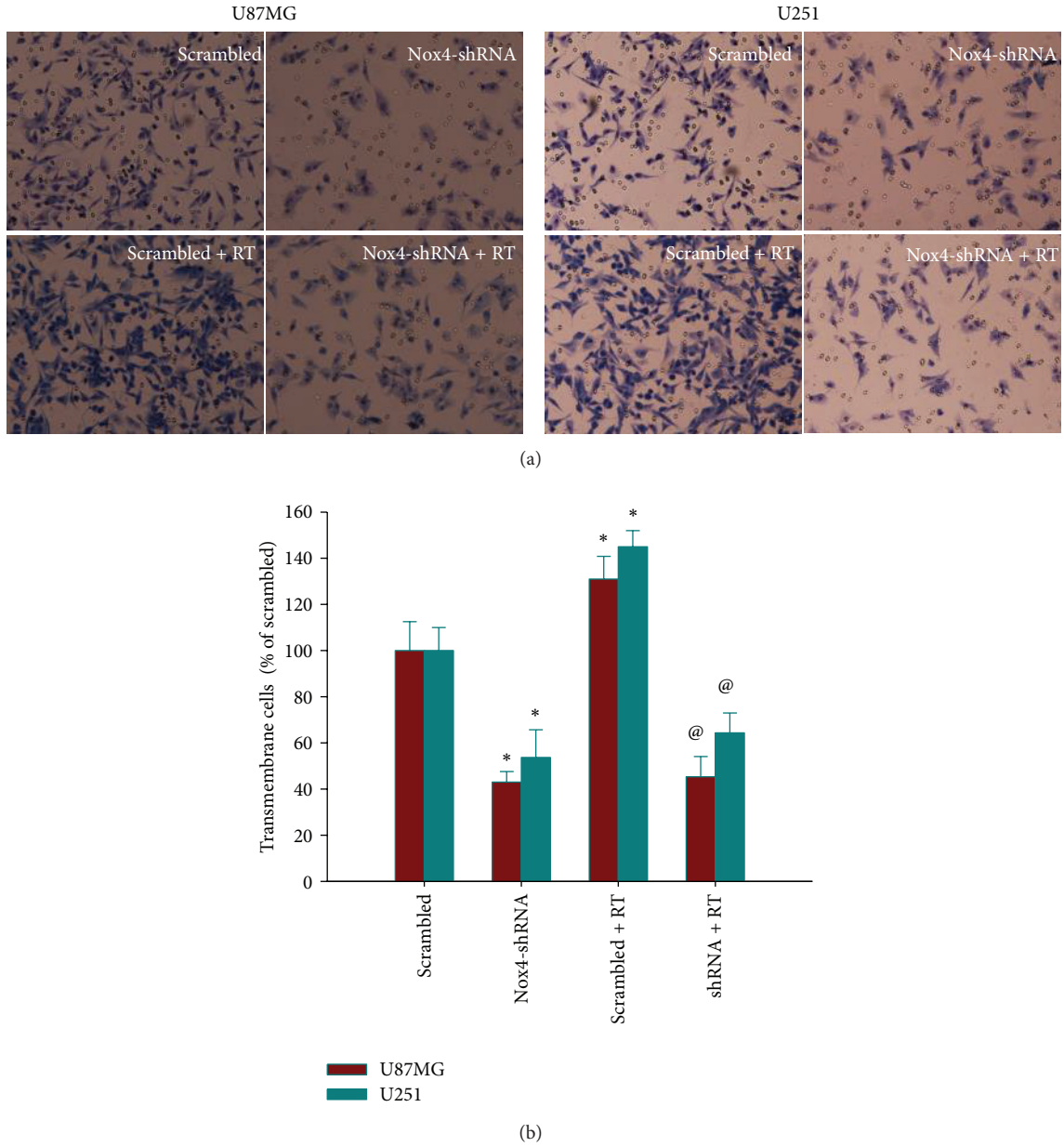

Figure 5: Effect of Nox4 knockdown on cell invasion in GBM. Matrigel invasion assays were performed. The numbers of invading cells were determined by counting the cells stained with 0.01% crystal violet solution in the lower side of the membrane. (a) Stained cells seen under a microscope (200x). (b) The number of transmembrane cells in each group. Columns, mean; bars, SD; RT, radiation therapy; $^{*}P < 0.05$, versus scrambled; $^{@}P < 0.05$ versus scrambled and scrambled + RT.

3.7. Nox4 Silencing Reduced VEGF Expression in Glioblastoma Cells. To determine if Nox4 knockdown could inhibit VEGF secretion, an ELISA assay was used to assess secreted VEGF levels in Nox4 shRNA or scrambled control treated with or without irradiation. These data are summarized in Figure 6(b); the secreted VEGF level of Nox4 shRNA infected cells was much lower than that of scrambled control group ($P < 0.05$). Moreover, irradiation could increase the VEGF level of GBM cells infected with scrambled control, and Nox4 shRNA attenuated the radiation-induced VEGF expression ($P < 0.05$).

4. Discussion

The clinical prognosis for glioblastoma patients is extremely dismal [17]. New strategies to treat this deadly disease are desperately needed. In the present study we showed that lentivirus-mediated shRNA silencing of Nox4 can decrease intracellular ROS production, leading to the inhibition of clonogenicity, proliferation and invasion of human GBM cells, and enhancement of their radiosensitivity. More importantly, Nox4 knockdown in GBM cells decreased the levels of VEGF expression and tumor induced angiogenesis.

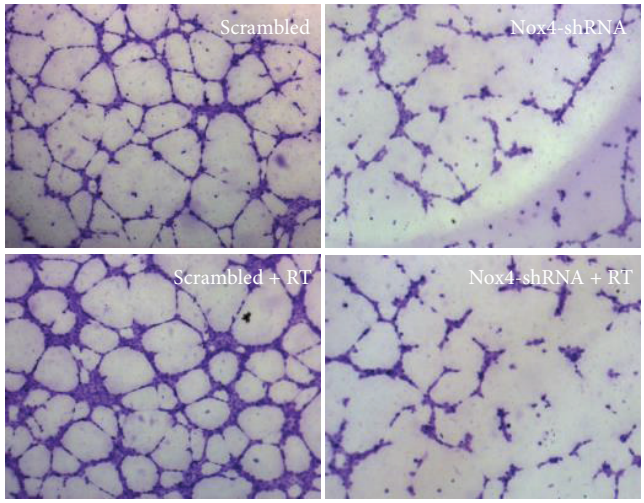

(a)

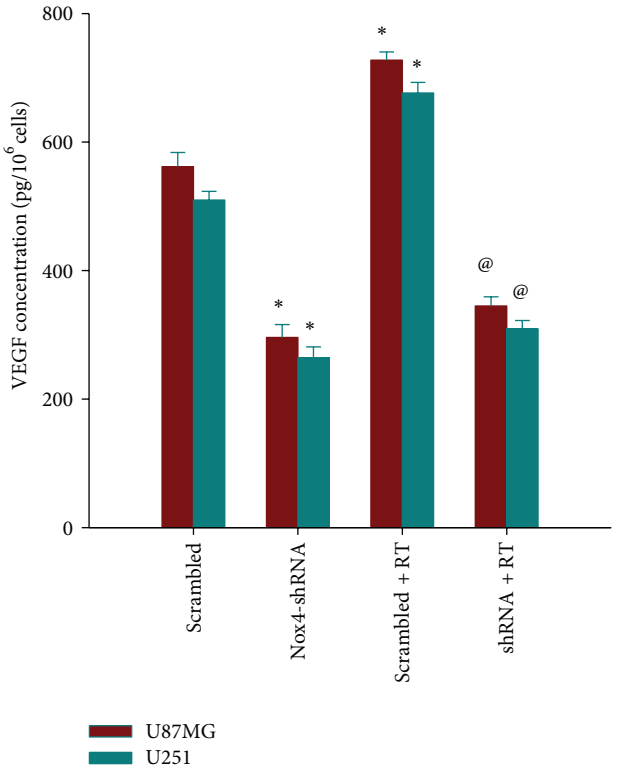

(b)

Figure 6: Nox4 silencing inhibited tube-like structure formation of endothelial cells and reduced VEGF expression in glioblastoma cells. (a) Tube-like structure formation ability of human umbilical veins endothelial cells (HUVECs) that were cocultured with conditioned medium derived from Nox4-shRNA or scrambled U87 cells, treated with or without 4 Gy irradiation, was measured. After incubation, endothelial cells were fixed, and tube-like structures were photographed (magnification, ×100). (b) Effects of Nox4-shRNA on expression of VEGF in U87MG and U251 cells. Cells were infected with Nox4-shRNA or scrambled control and treated with or without 4 Gy irradiation. Samples were collected at 24 h postradiation. VEGF protein levels in the culture supernatant were determined by ELISA. Columns, mean; bars, SD; RT, radiation therapy; $^{*}P < 0.05$, versus scrambled; $^{@}P < 0.05$, versus scrambled and scrambled + RT.

Although ROS have been conventionally thought to be a cause of stress-induced cell death, they may provide tumor cells with survival advantage over normal counterparts [18, 19]. The major therapeutic feature of radiation is the induction of toxic oxidative damage in targeted cancer cells. ROS are generated from cellular water by high-energy deposition during radiation, which oxidize DNA, proteins, and lipids and cause toxic oxidative damage in the cancer cells. However, ROS are formed constantly as byproducts of normal enzymatic metabolic reactions. Thus, to prevent overwhelming oxidative damage, cells maintain a basal redox balance between prooxidative and antioxidative reactions [20]. In some tumor models [13, 21], increased basal levels of ROS could stimulate the activation and the expression of stress molecules and antioxidative enzymes to better cope with the shift in redox balance. Thus, upon radiation these cells become less sensitive to toxic levels of ROS and resistant to radiation therapy. As shown in our study, one of the major sources of ROS generation in U87MG and U251 cells is the Nox4 (Figure 2). Accordingly, inhibition of Nox4 using lentivirus-mediated Nox4 shRNA suppressed glioblastoma cell proliferation and clonogenic survival following radiation (Figures 3 and 4). In this context, our findings provide further evidence for prosurvival activity of ROS and support the view that ROS are important intracellular signaling molecules regulating the balance between survival and cell death.

Local invasive growth is a key feature of glioblastoma, and the high invasion/migration character is considered to be a major therapeutic obstacle for glioblastoma treatment. A number of signaling pathways can be constitutively activated in migrating glioma cells, rendering these cells resistant to cytotoxic insults [22, 23]. Several studies have suggested a close relationship between ROS and tumor cell invasion and metastasis [24, 25]. ROS can serve as signaling molecules or can directly oxidize important cellular proteins. The signaling pathways that are associated with ROS include MAPK, PI3K, Rho-GTPase, and NF-κB. ROS can regulate cell adhesion pattern and activate GTPase that promotes cellular migration and invasion through upregulating matrix metalloproteinase (MMPS) or inhibiting tissue inhibitors of metalloproteinases (TIMPS) [26, 27]. In line with previous reports, our study demonstrated that Nox4 knockdown significantly attenuated glioblastoma tumor cell invasion. Although ionizing radiation is the mainstay of nonsurgical treatment in GBM, radiation may promote migration and invasiveness of glioblastoma cells [28, 29]. In agreement with these findings, our experiment indicated that radiation alone promoted glioblastoma cell invasion while Nox4 silencing using lentivirus-mediated shRNA strikingly suppressed radiation-provoked tumor cell invasion, supporting the critical role of Nox4-generated ROS in glioblastoma cell invasion. The data also rationalized the combination conventional radiotherapy with inhibition of Nox4 system with shRNA or a substance with similar properties to counteract the potential undesired proinvasive effect of radiotherapy.

In addition, activated tumor angiogenesis is another characteristic feature of GBM, contributing to tumor invasiveness and radioresistance. Accordingly, antiangiogenic therapy has

been successfully introduced into clinical glioblastoma treatment, for example, via VEGF/VEGFR signaling inhibition [30]. ROS derived from NADPH oxidase have been suggested to play an important role in physiological and pathological angiogenesis [31, 32]. They can function as signaling molecules to mediate various angiogenic-related responses such as cell proliferation, migration, and angiogenic gene expression in ECs and cancer cells. Xia et al. [15] reported that ROS regulated hypoxia-inducible factor 1 (HIF-1) and vascular endothelial growth factor (VEGF) expression in ovarian cancer cells. Elevated levels of endogenous ROS were required for inducing angiogenesis and tumor growth. Nox4 knockdown in ovarian cancer cells decreased the levels of VEGF and HIF-1A and tumor angiogenesis. This notion was corroborated in our study because Nox4 silencing significantly reduced the level of VEGF expression of nonirradiated glioblastoma cells and inhibit endothelial cells tube-like structure formation induced by conditioned medium from nonirradiated U87MG cells. Many studies have reported that radiotherapy can stimulate multiple signal transduction pathways simultaneously and alter the expression of proangiogenic molecules including VEGF in surviving cancer cells and host cells [33, 34]. In the present study, we further confirmed that irradiation induced a marked increase in VEGF protein expression in glioblastoma cells, and Nox4 shRNA could potentially block the radiation-induced enhancement of VEGF. Moreover, Nox4 shRNA was shown to inhibit tube-like structure formation of cocultured endothelial cells induced by X-ray irradiation. Therefore, knockdown of Nox4 suppressed both constitutive and radiation-induced angiogenesis *in vitro*, suggesting an important role of Nox4 derived ROS in angiogenesis process in glioblastoma.

In conclusion, our findings indicate that Nox4 is associated with tumor invasion, angiogenesis, and radioresistance in glioblastoma. Knockdown of Nox4 expression reduced ROS production significantly and suppressed glioblastoma cell proliferation and invasion and tumor induced angiogenesis as well as increased their radiosensitivity. Therefore, inhibition of Nox4 by lentivirus-mediated shRNA may be a strategy to overcome radioresistance and then improve its therapeutic efficacy for glioblastoma.

Conflict of Interests

The authors declare that there is no conflict of interests regarding the publication of this paper.

Acknowledgments

This work was supported in part by Grants from National Nature Science Foundation of China (nos. 81272780 and 81070190) and Huazhong University of Science and Technology's Frontier Exploration Fund (2013TS151).

References

[1] L. M. DeAngelis, "Brain tumors," *The New England Journal of Medicine*, vol. 344, no. 2, pp. 114–123, 2001.

[2] R. Stupp, W. P. Mason, M. J. Van Den Bent et al., "Radiotherapy plus concomitant and adjuvant temozolomide for glioblastoma," *The New England Journal of Medicine*, vol. 352, no. 10, pp. 987–996, 2005.

[3] P. D. Ray, B.-W. Huang, and Y. Tsuji, "Reactive oxygen species (ROS) homeostasis and redox regulation in cellular signaling," *Cellular Signalling*, vol. 24, no. 5, pp. 981–990, 2012.

[4] K. Block and Y. Gorin, "Aiding and abetting roles of NOX oxidases in cellular transformation," *Nature Reviews Cancer*, vol. 12, no. 9, pp. 627–637, 2012.

[5] T. Shono, N. Yokoyama, T. Uesaka et al., "Enhanced expression of NADPH oxidase Nox4 in human gliomas and its roles in cell proliferation and survival," *International Journal of Cancer*, vol. 123, no. 4, pp. 787–792, 2008.

[6] S. Senturk, M. Mumcuoglu, O. Gursoy-Yuzugullu, B. Cingoz, K. C. Akcali, and M. Ozturk, "Transforming growth factor-beta induces senescence in hepatocellular carcinoma cells and inhibits tumor growth," *Hepatology*, vol. 52, no. 3, pp. 966–974, 2010.

[7] K. A. Graham, M. Kulawiec, K. M. Owens et al., "NADPH oxidase 4 is an oncoprotein localized to mitochondria," *Cancer Biology and Therapy*, vol. 10, no. 3, pp. 223–231, 2010.

[8] U. Weyemi, B. Caillou, M. Talbot et al., "Intracellular expression of reactive oxygen species-generating NADPH oxidase NOX4 in normal and cancer thyroid tissues," *Endocrine-Related Cancer*, vol. 17, no. 1, pp. 27–37, 2010.

[9] M. Yamaura, J. Mitsushita, S. Furuta et al., "NADPH oxidase 4 contributes to transformation phenotype of melanoma cells by regulating G2-M cell cycle progression," *Cancer Research*, vol. 69, no. 6, pp. 2647–2654, 2009.

[10] C.-H. Hsieh, W.-C. Shyu, C.-Y. Chiang, J.-W. Kuo, W.-C. Shen, and R.-S. Liu, "NADPH oxidase subunit 4-mediated reactive oxygen species contribute to cycling hypoxia-promoted tumor progression in glioblastoma multiforme," *PLoS ONE*, vol. 6, no. 9, Article ID e23945, 2011.

[11] C. H. Hsieh, C. P. Wu, H. T. Lee, J. A. Liang, C. Y. Yu, and Y. J. Lin, "NADPH oxidase subunit 4 mediates cycling hypoxia-promoted radiation resistance in glioblastoma multiforme," *Free Radical Biology and Medicine*, vol. 53, no. 4, pp. 649–658, 2012.

[12] T. W. Meijer, J. H. Kaanders, P. N. Span, and J. Bussink, "Targeting hypoxia, HIF-1, and tumor glucose metabolism to improve radiotherapy efficacy," *Clinical Cancer Research*, vol. 18, no. 20, pp. 5585–5594, 2012.

[13] J. P. Lu, L. Monardo, I. Bryskin et al., "Androgens induce oxidative stress and radiation resistance in prostate cancer cells though NADPH oxidase," *Prostate Cancer and Prostatic Diseases*, vol. 13, no. 1, pp. 39–46, 2010.

[14] J. P. Fitzgerald, B. Nayak, K. Shanmugasundaram et al., "Nox4 mediates renal cell carcinoma cell invasion through hypoxia-induced interleukin 6- and 8- production," *PLoS ONE*, vol. 7, no. 1, Article ID e30712, 2012.

[15] C. Xia, Q. Meng, L.-Z. Liu, Y. Rojanasakul, X.-R. Wang, and B.-H. Jiang, "Reactive oxygen species regulate angiogenesis and tumor growth through vascular endothelial growth factor," *Cancer Research*, vol. 67, no. 22, pp. 10823–10830, 2007.

[16] E. V. Fletcher, L. Love-Homan, A. Sobhakumari, C. R. Feddersen, A. T. Koch, A. Goel et al., "EGFR inhibition induces proinflammatory cytokines via NOX4 in HNSCC," *Molecular Cancer Research*, vol. 11, no. 12, pp. 1574–1584, 2013.

[17] P. O. Zinn, R. R. Colen, E. M. Kasper, and J. K. Burkhardt, "Extent of resection and radiotherapy in GBM: a 1973 to 2007

surveillance, epidemiology and end results analysis of 21,783 patients," *International Journal of Oncology*, vol. 42, no. 3, pp. 929–934, 2013.

[18] L. Formentini, M. Sánchez-Aragó, L. Sánchez-Cenizo, and J. M. C. Cuezva, "The mitochondrial ATPase inhibitory factor 1 triggers a ROS-mediated retrograde prosurvival and proliferative response," *Molecular Cell*, vol. 45, no. 6, pp. 731–742, 2012.

[19] P. A. Cerutti, "Prooxidant states and tumor promotion," *Science*, vol. 227, no. 4685, pp. 375–381, 1985.

[20] M. Landriscina, F. Maddalena, G. Laudiero, and F. Esposito, "Adaptation to oxidative stress, chemoresistance, and cell survival," *Antioxidants and Redox Signaling*, vol. 11, no. 11, pp. 2701–2716, 2009.

[21] J. H. Pinthus, I. Bryskin, J. Trachtenberg et al., "Androgen induces adaptation to oxidative stress in prostate cancer: Implications for treatment with radiation therapy," *Neoplasia*, vol. 9, no. 1, pp. 68–80, 2007.

[22] L. Mariani, C. Beaudry, W. S. McDonough et al., "Death-associated protein 3 (Dap-3) is overexpressed in invasive glioblastoma cells *in vivo* and in glioma cell lines with induced motility phenotype in vitro," *Clinical Cancer Research*, vol. 7, no. 8, pp. 2480–2489, 2001.

[23] S. Y. Cho and R. L. Klemke, "Extracellular-regulated kinase activation and CAS/Crk coupling regulate cell migration and suppress apoptosis during invasion of the extracellular matrix," *Journal of Cell Biology*, vol. 149, no. 1, pp. 223–236, 2000.

[24] R. Hiraga, M. Kato, S. Miyagawa, and T. Kamata, "Nox4-derived ROS signaling contributes to TGF-beta-induced epithelial-mesenchymal transition in pancreatic cancer cells," *Anticancer Research*, vol. 33, no. 10, pp. 4431–4438, 2013.

[25] A. Kim, M. Im, N. H. Yim, Y. P. Jung, and J. Y. Ma, "Aqueous extract of bambusae caulis in taeniam inhibits PMA-induced tumor cell invasion and pulmonary metastasis: suppression of NF-κB activation through ROS signaling," *PLoS ONE*, vol. 8, no. 10, Article ID e78061, 2013.

[26] B. Zhang, Z. Liu, and X. Hu, "Inhibiting cancer metastasis via targeting NAPDH oxidase 4," *Biochem Pharmacol*, vol. 86, no. 2, pp. 253–266, 2013.

[27] W.-S. Wu, "The signaling mechanism of ROS in tumor progression," *Cancer and Metastasis Reviews*, vol. 25, no. 4, pp. 695–705, 2006.

[28] C. Wild-Bode, M. Weller, A. Rimner, J. Dichgans, and W. Wick, "Sublethal irradiation promotes migration and invasiveness of glioma cells: implications for radiotherapy of human glioblastoma," *Cancer Research*, vol. 61, no. 6, pp. 2744–2750, 2001.

[29] M. Zhang, S. Kleber, M. Röhrich et al., "Blockade of TGF-β signaling by the TGFβR-I kinase inhibitor LY2109761 enhances radiation response and prolongs survival in glioblastoma," *Cancer Research*, vol. 71, no. 23, pp. 7155–7167, 2011.

[30] I. Arrillaga-Romany, D. A. Reardon, and P. Y. Wen, "Current status of antiangiogenic therapies for glioblastomas," *Expert Opinion on Investigational Drugs*, vol. 23, no. 2, pp. 199–210, 2014.

[31] S. Coso, I. Harrison, C. B. Harrison et al., "NADPH oxidases as regulators of tumor angiogenesis: current and emerging concepts," *Antioxidants and Redox Signaling*, vol. 16, no. 11, pp. 1229–1247, 2012.

[32] M. Ushio-Fukai and Y. Nakamura, "Reactive oxygen species and angiogenesis: NADPH oxidase as target for cancer therapy," *Cancer Letters*, vol. 266, no. 1, pp. 37–52, 2008.

[33] I. Sofia Vala, L. R. Martins, N. Imaizumi et al., "Low doses of ionizing radiation promote tumor growth and metastasis by enhancing angiogenesis," *PloS ONE*, vol. 5, no. 6, 2010.

[34] B. J. Moeller, Y. Cao, C. Y. Li, and M. W. Dewhirst, "Radiation activates HIF-1 to regulate vascular radiosensitivity in tumors: role of reoxygenation, free radicals, and stress granules," *Cancer Cell*, vol. 5, no. 5, pp. 429–441, 2004.

Hindawi Publishing Corporation
Oxidative Medicine and Cellular Longevity
Volume 2014, Article ID 904834, 13 pages
http://dx.doi.org/10.1155/2014/904834

Research Article

Salidroside Stimulates Mitochondrial Biogenesis and Protects against H_2O_2-Induced Endothelial Dysfunction

Shasha Xing,[1,2] Xiaoyan Yang,[1,2] Wenjing Li,[1,2] Fang Bian,[1,2] Dan Wu,[1,2] Jiangyang Chi,[1,2] Gao Xu,[1,2] Yonghui Zhang,[1,2] and Si Jin[1,2]

[1] *Department of Pharmacology, Tongji Medical College, Huazhong University of Science and Technology, Wuhan 430030, China*
[2] *The Key Laboratory of Drug Target Research and Pharmacodynamic Evaluation of Hubei Province, Wuhan 430030, China*

Correspondence should be addressed to Si Jin; jinsi@mail.hust.edu.cn

Received 13 February 2014; Accepted 19 March 2014; Published 24 April 2014

Academic Editor: Shiwei Deng

Salidroside (SAL) is an active component of *Rhodiola rosea* with documented antioxidative properties. The purpose of this study is to explore the mechanism of the protective effect of SAL on hydrogen peroxide- (H_2O_2-) induced endothelial dysfunction. Pretreatment of the human umbilical vein endothelial cells (HUVECs) with SAL significantly reduced the cytotoxicity brought by H_2O_2. Functional studies on the rat aortas found that SAL rescued the endothelium-dependent relaxation and reduced superoxide anion ($O_2^{\bullet-}$) production induced by H_2O_2. Meanwhile, SAL pretreatment inhibited H_2O_2-induced nitric oxide (NO) production. The underlying mechanisms involve the inhibition of H_2O_2-induced activation of endothelial nitric oxide synthase (eNOS), adenosine monophosphate-activated protein kinase (AMPK), and Akt, as well as the redox sensitive transcription factor, NF-kappa B (NF-κB). SAL also increased mitochondrial mass and upregulated the mitochondrial biogenesis factors, peroxisome proliferator-activated receptor gamma-coactivator-1alpha (PGC-1α), and mitochondrial transcription factor A (TFAM) in the endothelial cells. H_2O_2-induced mitochondrial dysfunction, as demonstrated by reduced mitochondrial membrane potential ($\Delta\psi$m) and ATP production, was rescued by SAL pretreatment. Taken together, these findings implicate that SAL could protect endothelium against H_2O_2-induced injury via promoting mitochondrial biogenesis and function, thus preventing the overactivation of oxidative stress-related downstream signaling pathways.

1. Introduction

The role of oxidative stress in the development of the endothelial dysfunction has been studied extensively [1–4]. Excessive reactive oxygen species (ROS) not only reduces bioavailable nitric oxide (NO) through direct reaction to form peroxynitrite, but also leads to eNOS uncoupling and further induces more ROS production [5].

As a major cellular source of ROS, the contributions of mitochondria to the detrimental effects of cardiovascular risk factors have recently received increased attention [6–8]. Excessive mitochondrial ROS (mtROS) act to inspire pathologic cell-signaling cascades under conditions of comprehensive excessive oxidative stress [9–11]. NF-kappa B (NF-κB) activation occurs secondary to excessive mitochondrial ROS production in the endothelium, participating in a range of proinflammatory and prothrombotic alterations in the endothelial cells [12, 13].

Endothelial mitochondria have been found to have crucial roles in vascular path-physiology [14–16], and increasing evidences have indicated the importance of mitochondrial dysfunction in various vascular diseases, such as atherosclerosis, heart failure, and cardiac ischemia/reperfusion injury [17–19]. Previous studies have shown that dysregulation of mitochondrial biogenesis represents an early manifestation of endothelial dysfunction, shifting cell metabolism toward metabolic hypoxia in animals with impaired NO bioavailability [14]. Impairment of mitochondrial biogenesis is frequently observed in atherosclerosis and is thus likely to contribute to cellular energetic imbalance, oxidative stress, and endothelial dysfunction in these pathological conditions [20]. Since increased mitochondrial production of ROS due to impaired

mitochondrial biogenesis also appears to be a key event in the development of aging-related vascular pathologies [13, 21, 22], identification of mechanisms that promote mitochondrial biogenesis in the endothelial cells may provide new clues on the pathogenesis of vascular disease.

The health of mitochondria is in part regulated by their biogenesis and peroxisome proliferator-activated receptor gamma-coactivator-alpha (PGC-1α) is regarded as the key regulator [23]. In endothelial cells, PGC-1α also orchestrates cellular defenses against oxidative stress [24]. Mitochondrial transcription factor A (TFAM) is responsible for the transcriptional control of mtDNA and its translocation to the mitochondria is important to initiate mtDNA transcription and replication [25].

As described above, mitochondria are highly dynamic organelles, and their biogenesis is likely to be involved in the regulation of endothelial cell metabolism, redox regulation, and signal transduction [6, 16, 26]. Pathways that regulate mitochondrial biogenesis are potential therapeutic targets for the amelioration of endothelial dysfunction and vascular diseases [27].

Salidroside (SAL) is an active ingredient of the root of *Rhodiola rosea*, a well-known herb used to relieve high altitude sickness [28]. SAL has also been used to enhance both the physical and mental performance. SAL upregulates the levels of antioxidative enzymes glutathione peroxidase-1 and thioredoxin-1 to counteract oxidative stress [29]. Previous studies have shown that SAL promotes DNA repair enzyme Parp-1 to counteract oxidative stress [30]. Meanwhile, a recent study reported that SAL attenuated homocysteine-induced endothelial dysfunction by reducing oxidative stress [31]. As noted above, there is tightly relationship between reduction of mitochondrial biogenesis and endothelial dysfunction; the present study was conducted to determine whether SAL recovers the endothelial dysfunction induced by H_2O_2 through stimulating mitochondrial biogenesis and counteracting the oxidative stress-related eNOS and NF-κB signaling pathways.

2. Materials and Methods

2.1. Animals. Animals were treated in accordance with the guide for the Care and Use of Laboratory Animals published by the US National Institutes of Health and approved by the Local Animal Care Committee. Healthy Wistar rats (200–250 g) were purchased from the Center of Experimental Animals (Tongji Medical College, Huazhong University of Science and Technology, China) and maintained in a controlled environment with a light/dark cycle of 12 h, a temperature of 20 ± 2°C, and humidity of 50 ± 2%.

2.2. Cell Culture. The collection of human umbilical cords was approved by the Ethics Committee of Tongji Medical College, Huazhong University of Science and Technology (Wuhan, China) and conducted in accordance with the Declaration of [32]. Primary cultured human umbilical vein endothelial cells (HUVECs) were prepared as described in [33]. In brief, the umbilical cord was washed with cold PBS and then infused with 0.25% trypsin. After digestion stopped, the cells were collected by centrifuging for 10 min at 1 000 rpm. The cells were resuspended and then cultured in endothelial cell medium (ECM, Sciencell, Carlsbad, CA) at 37°C in an incubator with a humidified atmosphere of 5% CO_2. In all experiments, cells were used at passages 2–7.

2.3. Cell Viability Assays. To study the effect of SAL on H_2O_2-induced cytotoxicity, HUVECs were inoculated at a density of 2×10^4 per well in 96-well plates and cultured overnight; the cell viability was evaluated using the Cell Counting Kit-8 (Dojindo Laboratories, Kumamoto) [34]. Briefly, the HUVECs treated with H_2O_2 (Sigma, 4 h) or SAL (National Institute for Food and Drug Control, purity > 98%, 24 h) at the indicated concentration in OPTI-MEM (Gibco) before cell viability was measured. Moreover, to study the effect of SAL on H_2O_2-induced inhibition of cell viability, the cells were cultured as described above; after treatment with SAL for 20 h, the H_2O_2 (100 μM) was added to the medium for another 4 hours. At the end of the time period, the culture medium was removed. The cells were washed twice with PBS and incubated with CCK-8 solution at 37°C for 30 min. The absorbance was measured using a microplate reader with a test wavelength of 450 nm.

2.4. Free Radical Measurement in Cell Free System. The effects of SAL on scavenging hydroxyl radical ($OH^\bullet$), superoxide radical (O_2^-), and H_2O_2 were measured with commercially available kits (Nanjing Jiancheng Bioengineering Institute, China) according to the manufacturer's instructions. In brief, the $OH^\bullet$ was generated by the Fenton reaction and then treated with a chromogenic substrate nitrotetrazolium blue chloride (NBT) to yield a stable colored substance, which was measured using a microplate reader with a test wavelength of 450 nm. O_2^- was generated by the xanthine/xanthine oxidase system, O_2^- was detected by nitrite method, and the absorbance at 550 nm was measured. The reaction product of H_2O_2 and molybdic acid can be detected at 405 nm. Deionized water and ascorbic acid (Vc) were used as the blank and positive controls, respectively. The inhibition rate = (optical density of blank control groups—optical density of treatment groups)/optical density of blank control groups.

2.5. Vascular Function Measurement. The thoracic segments of the rat aorta were dissected and the surrounding connective tissues were cleaned off. Each aorta was cut into ring segments of 2~3 mm in length. The aortic rings were mounted in organ chambers filled with Krebs-Henseleit (KH) solution at 37°C with constant bubbling of 95% oxygen/5% carbon dioxide. KH solution contained (mM) 133 NaCl, 4.75 KCl, 1.5 $CaCl_2$, 1.25 $MgCl_2$, 25 $NaHCO_3$, and 11 D-glucose. Isometric tension was recorded with a force transducer (RM6240C, Chengdu Instrument Factory). A basal tension of 20 mN was applied to each vascular ring. After being placed in organ baths for 90 min, 0.5 μM phenylephrine (PE, Sigma) was first administered to the rings to test their contractility and then 1 μM acetylcholine (ACh, Sigma) was administered to assess the integrity of the endothelial layer.

Rings with less than 80% relaxation response to ACh were discarded. The aortic rings were pretreated with or without 10 μM SAL for 30 min before H_2O_2 100 μM was added to the bath. After precontracting with PE (0.1 μM), ACh (1×10^{-8} ~1×10^{-4} M) was added cumulatively to the bath to evoke the endothelium-dependent relaxation. The relaxation rate is the ratio between the tension relaxed by ACh and the tension contracted by PE.

2.6. Measurement of NO and Superoxide Anion ($O_2^{\bullet-}$). To measure intracellular NO and $O_2^{\bullet-}$ levels, the NO and $O_2^{\bullet-}$-specific fluorescent dye 4,5-diaminofluorescein diacetate (DAF-FM-DA, Beyotime Institute of Biotechnology) [35] and dihydroethidium (DHE, Beyotime Institute of Biotechnology) [36] were used to measure intracellular NO and $O_2^{\bullet-}$ levels, respectively. Briefly, confluent HUVECs in 96-well plates, after SAL (10 μM) or PBS treatment for 24 h, were washed twice with PBS followed by staining with 2.5 μM DAF-FM-DA or 5 μM DHE for 30 min at 37°C. After washing twice with PBS, the fluorescence intensities were measured as basal, and then 100 μM H_2O_2 was added. Using a fluorescence spectrophotometer (TECAN, INFINITE F200PRO), the fluorescence intensities of DAF-FM-DA were measured at an excitation wavelength of 485 nm and an emission wavelength of 535 nm, respectively, and DHE were measured at an excitation wavelength of 535 nm and an emission wavelength of 610 nm, respectively.

2.7. NF-κB Activity Assay. An ELISA-based assay was used to measure the NF-κB activity, as described previously [37–39]. In brief, after stimulation, cells were rinsed twice with cold PBS, and then RIPA containing a protease inhibitor cocktail (Roche, Basel, Switzerland) was added. After incubation on ice for 30 min, the lysate was centrifuged for 15 min at 14 000 rpm and the supernatant was collected. After being quantified with BCA reagent (Pierce, Rockford, IL), the cell extracts were incubated in a 96-well plate coated with the oligonucleotide containing the NF-κB consensus-binding site (5′-GGGACTTTCC-3′). Activated transcription factors from extracts specifically bound to the respective immobilized oligonucleotide. NF-κB activity was then detected with the primary antibody to NF-κB p65 (1 : 1000, Proteintech, China) and secondary antibody conjugated to horseradish peroxidase (1 : 10 1000, Abbkine, CA). Tetramethylbenzidine (100 μL, Sigma) was added in each microwell at 37°C before adding 100 μL of stopping solution (2M H_2SO_4). NF-κB activity was finally determined as absorbance values measured with a microplate reader at a wavelength of 450 nm.

2.8. Measurement of Mitochondrial Mass. Mitochondria mass was determined by using MitoTracker green, a mitochondrial-selective membrane potential-independent dye [40]. The cells grown on cover slips coated with 2% gelatin were incubated with SAL (1, 10 μM) for 24 h. At the end of the incubation, suspensions were removed and the cells were incubated with 200 nM MitoTracker green (Beyotime Institute of Biotechnology, China) in 37°C for 30 min. The images were captured with a fluorescence microscope (Olympus FV500) using 40× magnification objective [41]. The integrated fluorescence intensities were measured using the Image-Pro Plus software and normalized to the number of cells.

2.9. Measurement of Intracellular ATP Levels. After treatment, the HUVECs from each well of a 6-well dish (5×10^5/well) were washed twice with cold PBS and lysed with 0.5 M perchloric acid and briefly sonicated (5 to 10 times of a 1 sec burst) until cells were clearly disrupted. Samples were then neutralized with 2 M KOH and then centrifuged to remove the precipitate. ATP content was analyzed by HPLC (Agilent, Palo Alto, CA) with an LC-18T reverse-phase column (Agilent, Palo Alto, CA) at a flow rate of 0.3 mL/min, and the absorbance at 254 nm was recorded. The elution peak was compared with ATP standards (National Institute for Food and Drug Control, Beijing) to confirm its identity.

2.10. Assessment of Mitochondrial Membrane Potential ($\Delta\psi m$). JC-1 is a positively charged fluorescent compound which is taken up by mitochondria proportionally to the inner mitochondrial membrane potential [42]. The ratio of red (J-aggregate)/green (monomeric JC-1) emission is directly proportional to the $\Delta\psi$m. HUVECs were grown on 96-well plates treated with SAL (10 μM) for 20 h, and then H_2O_2 (100 μM) was added for another 4 h. Cells were rinsed with PBS and incubated in 100 μL JC-1 staining solution at 37°C for 20 min. Cells were then rinsed twice with JC-1 washing solution and analyzed with a fluorescence spectrophotometer. J-aggregates were recorded with an excitation wavelength of 535 nm and an emission wavelength of 610 nm, respectively, and monomeric JC-1 was recorded with an excitation wavelength of 485 nm and an emission wavelength of 535 nm, respectively.

2.11. Western Blot Analysis. Cells were homogenized in ice-cold RIPA lysis buffer containing protease inhibitor cocktail and phosSTOP (Roche, Basel, Switzerland). Equal amounts of protein (60 μg) were mixed with the loading buffer (Beyotime Institute of Biotechnology), boiled for 10 min, and separated by SDS-PAGE. After electrophoresis, proteins were transferred to polyvinylidene difluoride membranes (PVDF, Millipore, Temecula, CA). The membranes were blocked for 1 h in 5% milk. The membranes were then incubated overnight at 4°C with one of the following specific primary antibodies: rabbit anti-eNOS ser1177, anti-eNOS, anti-AMPKα thr172, anti-AMPKα, anti-β-actin (1 : 1 000, Cell Signaling Technology, Beverly, MA), anti-Akt ser473 (1 : 1 000, EPITOMICS, CA), anti-Akt (1 : 600, Proteintech), anti-TFAM (1 : 300, Proteintech), and anti-PGC-1α (1 : 200, Santa Cruz, CA). After washing, the membranes were incubated for 2 h at room temperature with secondary antibodies (Goat anti-rabbit IgG, goat anti-mouse IgG, 1 : 10 000, Abbkine, CA) and then washed. Finally, the blots were developed with enhanced chemiluminescence detection reagents (Thermo Scientific, Waltham, MA). Membranes were scanned using the Micro-Chemi bioimage analyzer (NDR, Israel) and quantified using Image J program and normalized against β-actin.

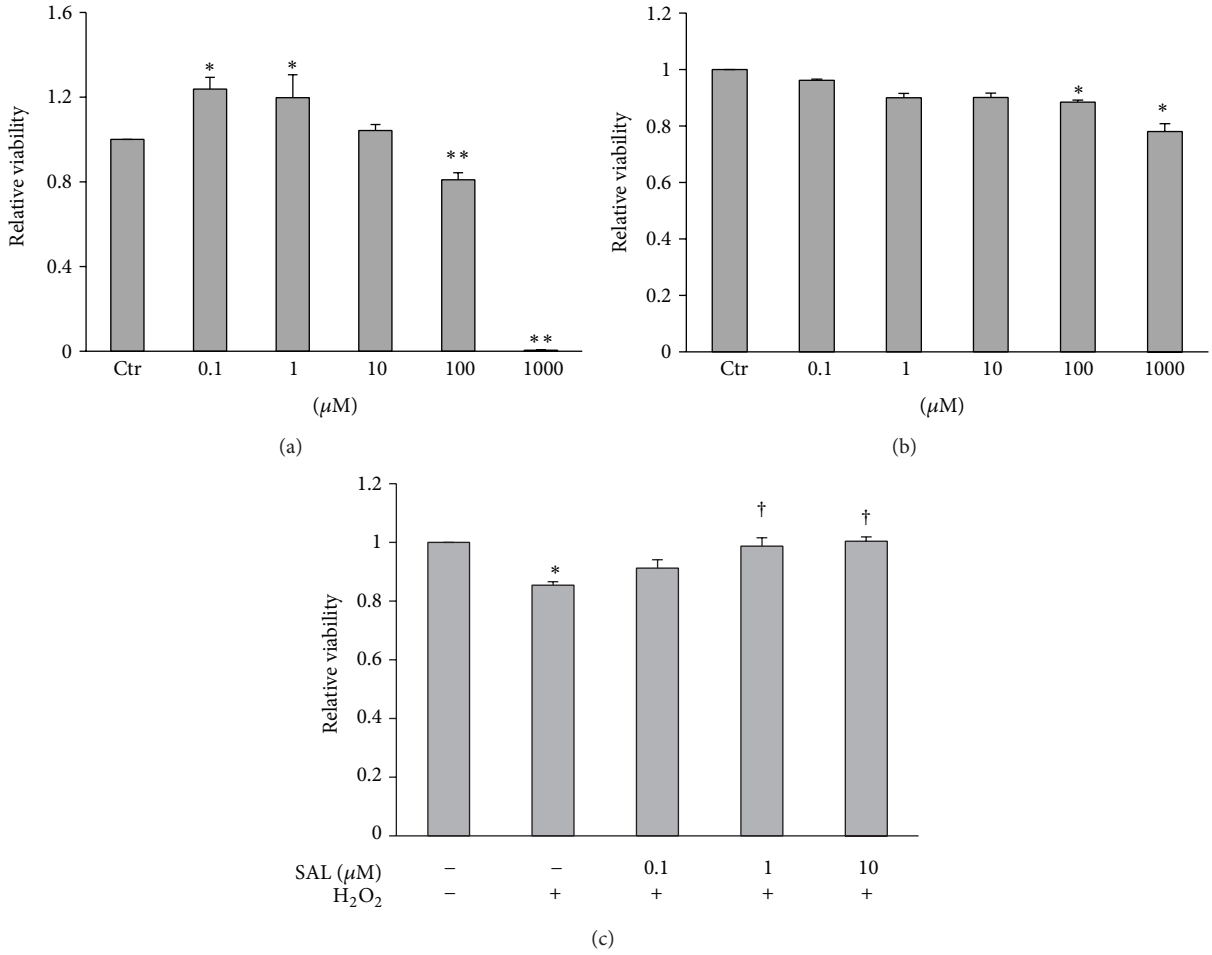

FIGURE 1: Protective effects of SAL on H_2O_2-induced cytotoxicity in HUVECs. (a) HUVECs were exposed to various concentrations of H_2O_2 for 4 h. (b) Cells were exposed to various concentrations of SAL for 24 h. (c) HUVECs were pretreated with SAL or vehicle for 20 h and then exposed to H_2O_2(100 μM) for 4 h. Cell viability was detected by CCK-8. Cell viability in untreated cells was assigned the value of 1. $^{*}P < 0.05$, $^{**}P < 0.01$ versus control; $^{\dagger}P < 0.05$ versus H_2O_2, $n = 3$–5.

2.12. Statistical Analysis. All data in this study are expressed as the mean ± SEM from at least three separate experiments. SPSS 13.0 was used for statistical analysis. Individual group statistical comparisons were analysed by unpaired Student's *t*-test with Bonferroni correction, and multiple groups comparisons were evaluated by one-way ANOVA with post hoc testing. A probability value of $P < 0.05$ was considered statistically significant.

3. Results

3.1. SAL Alleviates the Cytotoxicity Induced by H_2O_2 in HUVECs. In this study, H_2O_2 was used to induce oxidative stress in HUVECs. After exposure to H_2O_2 (100–1000 μM) for 4 h, HUVECs viability was reduced (Figure 1(a)). SAL at the concentration below 10 μM had no obvious effect on cell viability compared to control (Figure 1(b)). Pretreatment with SAL could reduce cell death induced by H_2O_2 in a concentration-dependent manner (Figure 1(c)).

3.2. Effect of SAL on ROS in Cell Free System. SAL has the effect of scavenging $OH^{\bullet}$ but not O_2^{-} or H_2O_2 at indicated concentration (Figures 2(a), 2(b), and 2(c)).

3.3. SAL Recovers H_2O_2-Induced Impairment of Endothelium-Dependent Relaxation in Rat Aortas. Treatment with H_2O_2 (100 μM) for 30 min markedly attenuated ACh-induced endothelium-dependent relaxation (EDR) in rat aortas. Exposure to SAL (10 μM, 30 min) prior to the addition of H_2O_2 partially rescued the impaired EDR (Figure 3(a)). Meanwhile, pretreatment with SAL (10 μM, 24 h) inhibited NO and $O_2^{\bullet-}$ production induced by H_2O_2 (100 μM) (Figures 3(b) and 3(c)).

3.4. SAL Decreased eNOS Activation Induced by H_2O_2 in HUVECs. Compared with control, H_2O_2 (100 μM, 4 h) or SAL (10 μM, 24 h) treatment significantly increased eNOS phosphorylation at ser1177 and Akt phosphorylation at Ser473 in HUVECs. Pretreatment with SAL (10 μM) for 24 h

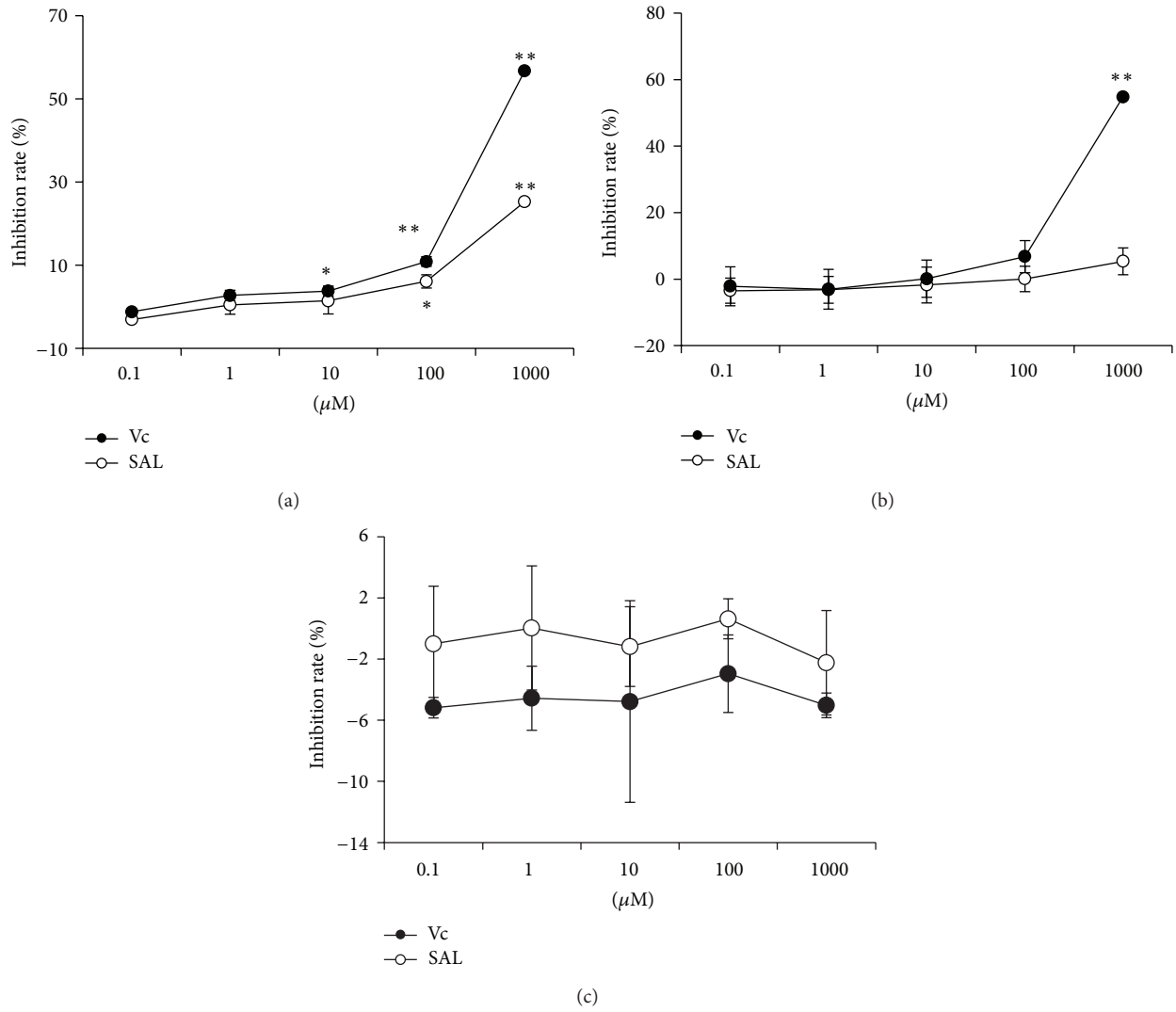

Figure 2: Effect of SAL on cell free ROS detection using different assay systems. (a) $OH^{\bullet}$ was generated by Fenton reaction, (b) O_2^- was generated by xanthine/xanthine oxidase, and (c) H_2O_2 was exogenously added. $^*P < 0.05$, $^{**}P < 0.01$ versus blank control, $n = 3$.

attenuated the activation of eNOS, AMPKα, and Akt induced by 100 μM H_2O_2 (Figures 4(a), 4(b), 4(c), and 4(d)).

3.5. SAL Inhibited the Activation of Transcription Factor NF-κB Induced by H_2O_2 in HUVECs. Activation of the transcription factor NF-κB has been associated with endothelial cells dysfunction and vascular inflammation in atherogenesis [43]. In line with previous studies, exposure to H_2O_2 could result in transient activation of NF-κB (Figure 5(a)), while exposure to SAL (10 μM) for indicated time significantly decreased the activity of transcription factor NF-κB in a time-dependent manner (Figure 5(b)). Pretreatment with SAL inhibited the activation of the NF-κB induced by 0.1 μM H_2O_2 (Figure 5(c)). To our surprise, we found that exposure to H_2O_2 (0.1 μM) for 30 min could result in transient activation of NF-κB, whereas H_2O_2 at the concentration of 100 μM slightly reduced rather than increased the NF-κB activity. SAL pretreatment can further reduce the activity of NF-κB (Figure 5(c)). To explain this result, we used TNF-α, a classical NF-κB inducer to treat HUVECs to detect the direct effect of H_2O_2 on DNA binding activity. The result indicated that H_2O_2 inhibited the DNA binding activity of activated NF-κB in a dose-dependent manner (Figure 5(d)).

3.6. SAL Induced Mitochondrial Biogenesis in Endothelial Cells. Our results showed that SAL (10 μM) increased the fluorescent intensity of MitoTracker green, suggesting that SAL increased the mitochondrial mass in HUVECs (Figure 6(a)). Consistent with this, the expression of PCG-1α and TFAM, the key regulators of mitochondrial biogenesis were significantly increased in HUVECs incubated with SAL (Figures 6(b) and 6(c)).

3.7. SAL Restores H_2O_2-Induced Mitochondrial Dysfunction. We used independent parameters to evaluate mitochondrial function ATP production and $\Delta\Psi$m. As shown in Figure 7,

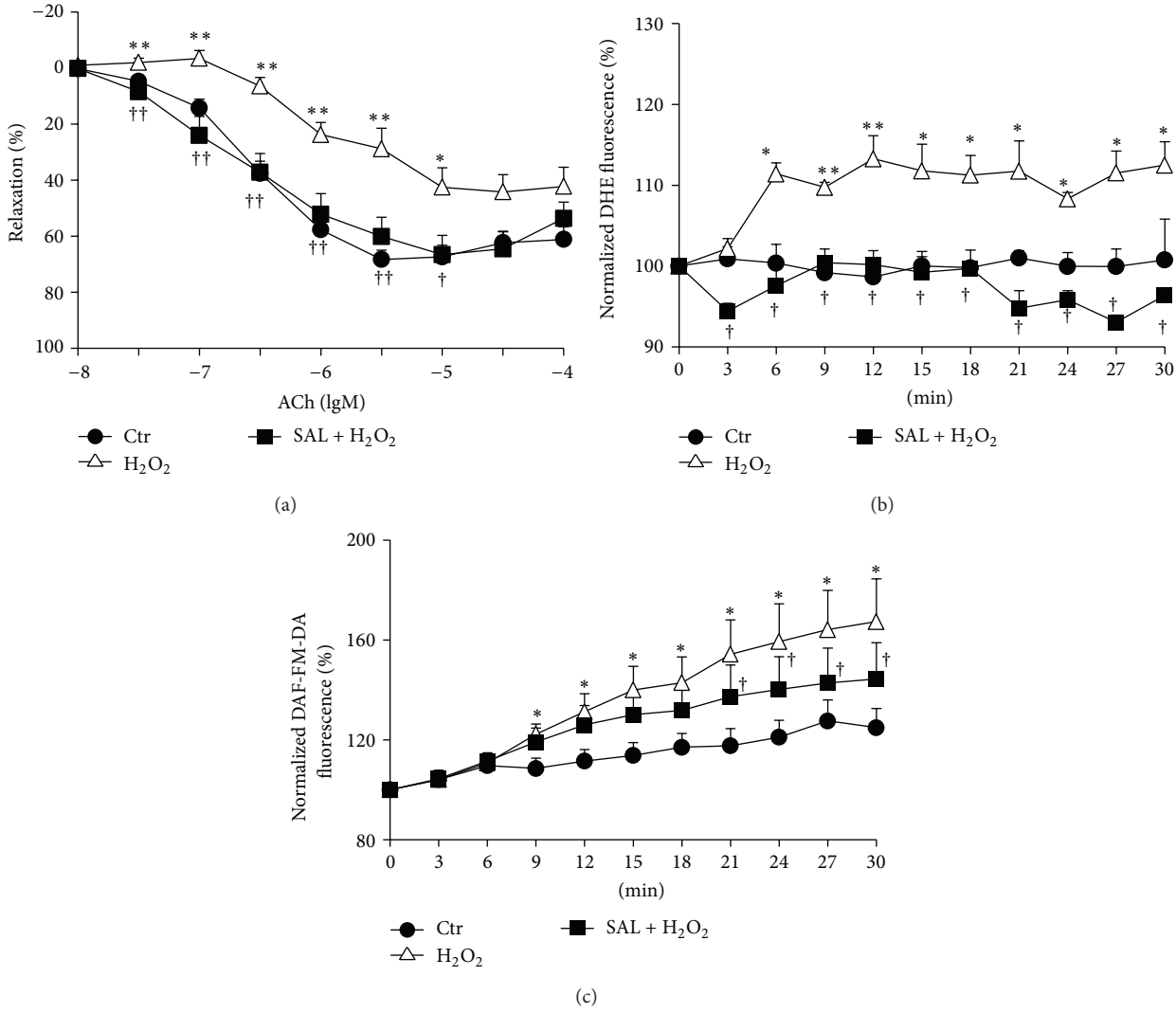

Figure 3: Protective effects of SAL on H_2O_2-induced impairment of endothelium-dependent relaxation. (a) Rat thoracic aorta was pretreated with or without SAL for 30 min, and then H_2O_2 (100 μM) was added to incubate for another 30 min. After precontracting with 1 μM PE, ACh was added accumulatively. Complete relaxation of aorta induced by ACh was considered as 100%. $^{*}P < 0.05$, $^{**}P < 0.01$ versus control; $^{\dagger}P < 0.05$, $^{\dagger\dagger}P < 0.01$ versus H_2O_2, $n = 8$–16. (b) HUVECs were pretreated with or without 10 μM SAL for 20 h and then loaded with DHE dye. After acquisition of basal data, H_2O_2 (100 μM) was added and the fluorescence was measured every 5 min within 30 min. The fluorescence of basal data was assigned the value of 100%. $^{*}P < 0.05$, $^{**}P < 0.01$ versus control; $^{\dagger}P < 0.05$ versus H_2O_2, $n = 4$. (c) HUVECs were pretreated with or without SAL for 20 h and then loaded with DAF-FM-DA dye. After acquisition of basal data, H_2O_2 (100 μM) was added and the fluorescence was measured every 5 min within 30 min. The fluorescence of basal data was assigned the value of 100%. $^{*}P < 0.05$ versus control; $^{\dagger}P < 0.05$ versus H_2O_2, $n = 4$.

H_2O_2 (100 μM) induced $\Delta\Psi$m collapse (a) and decreased ATP production (b) after 4 h of treatment in cultured HUVECs. Pretreatment with SAL (10 μM) for 24 h rescued mitochondrial function.

4. Discussion

There is increasing attention on the relationship between oxidative stress and endothelial cell injury [44–46]. The present study employed H_2O_2-induced oxidative stress in HUVECs as a cellular model to study the protective effect of SAL. In our experiments, pretreatment of SAL significantly prevents the impaired viability of HUVECs caused by H_2O_2 exposure. These results are in accordance with previous studies [47] and further confirmed the protective effects of SAL against injury induced by H_2O_2. Moreover, the antioxidative mechanism of SAL is not due to the direct reaction between SAL and H_2O_2 (Figure 2).

Overproduced ROS are known to harm the normal vascular function by limiting the beneficial effects of endothelium derived NO [48]. The enhanced production and release of ROS and/or the diminished bioavailability of NO within vascular wall lead to endothelial dysfunction that is widely

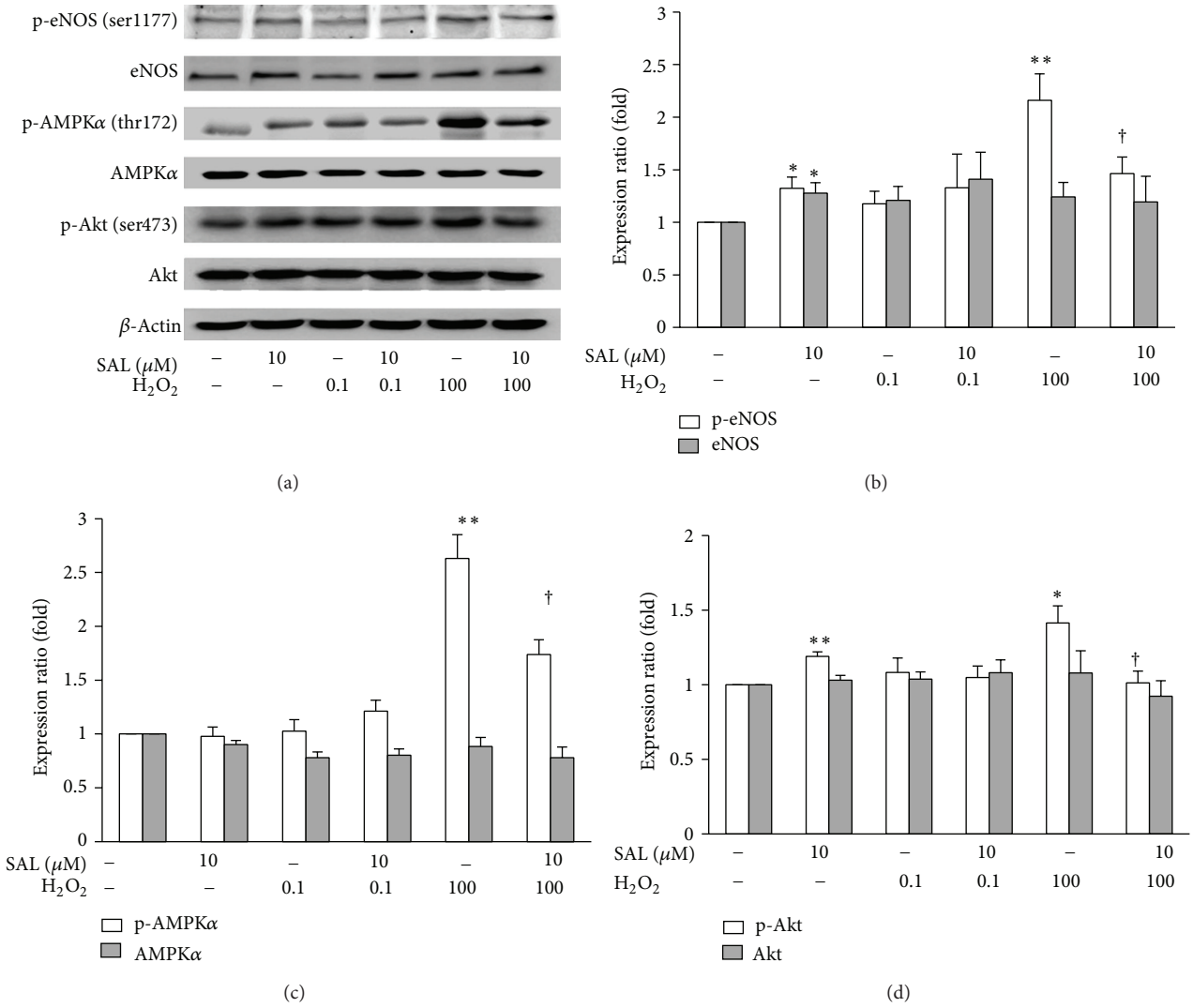

FIGURE 4: Effects of SAL on H_2O_2-induced activation of eNOS, AMPK, and Akt. After pretreatment with SAL (10 μM) for 20 h, H_2O_2 (0.1 μM or 100 μM) was added for another 4 h, and the lysates were analyzed by western blot. (a) Representative immunoblots. (b, c, d) The histogram shows quantitation of eNOS-ser1177, eNOS, AMPKa-thr172, AMPK, Akt-ser473, and Akt expression. The expressions were normalized to that obtained in untreated cells. $^{*}P < 0.05$, $^{**}P < 0.01$ versus control; $^{\dagger}P < 0.05$ versus H_2O_2, $n = 4$–6.

believed to be the early key event in the pathogenesis of various vascular complications [4, 49]. Although H_2O_2 elicits relaxation in rat, mouse, and rabbit aortas [50–53] and stimulates eNOS, resulting in higher NO levels [54], the effect of prolonged elevation of H_2O_2 is to impair endothelium-dependent relaxation [55]. Previous study showed that SAL prevented homocysteine-induced endothelial dysfunction through curtailing oxidative stress [31]. In our study, pretreatment with H_2O_2 induced significant impairment of endothelial dependent relaxation, while SAL had the capacity to rescue this impairment. As expected, incubation of HUVECs with H_2O_2 strikingly increased intracellular $O_2^{\bullet-}$, and this can be suppressed by pretreatment with SAL. These results strongly suggest that SAL inhibits H_2O_2-induced ROS production, contributing to the restoration of the endothelium-dependent vasorelaxation.

NO, derived from the action of eNOS in endothelial cells, is one of the most important mediators in the regulation of endothelial functions [56]. Phosphorylation of eNOS at ser1177 activates eNOS, while increased oxidative flux directly scavenges NO to lower NO bioavailability [57] and subsequently impairs endothelium-dependent vasodilatation [58]. Interestingly, as shown in many previous studies, H_2O_2 directly upregulated the levels of NO in endothelial cells, suggesting that overproduction of NO by endothelial cells in response to H_2O_2 stimulation was intended to protect the cells, rather than damage cells [59, 60]. An intriguing question that arises from this study is why SAL tends to inhibit H_2O_2-induced eNOS activation and NO production, while it *per se* appears to upregulate eNOS expression and activation (Figures 4 and 3(c)). We speculated here that the upregulation of eNOS activity and NO production by

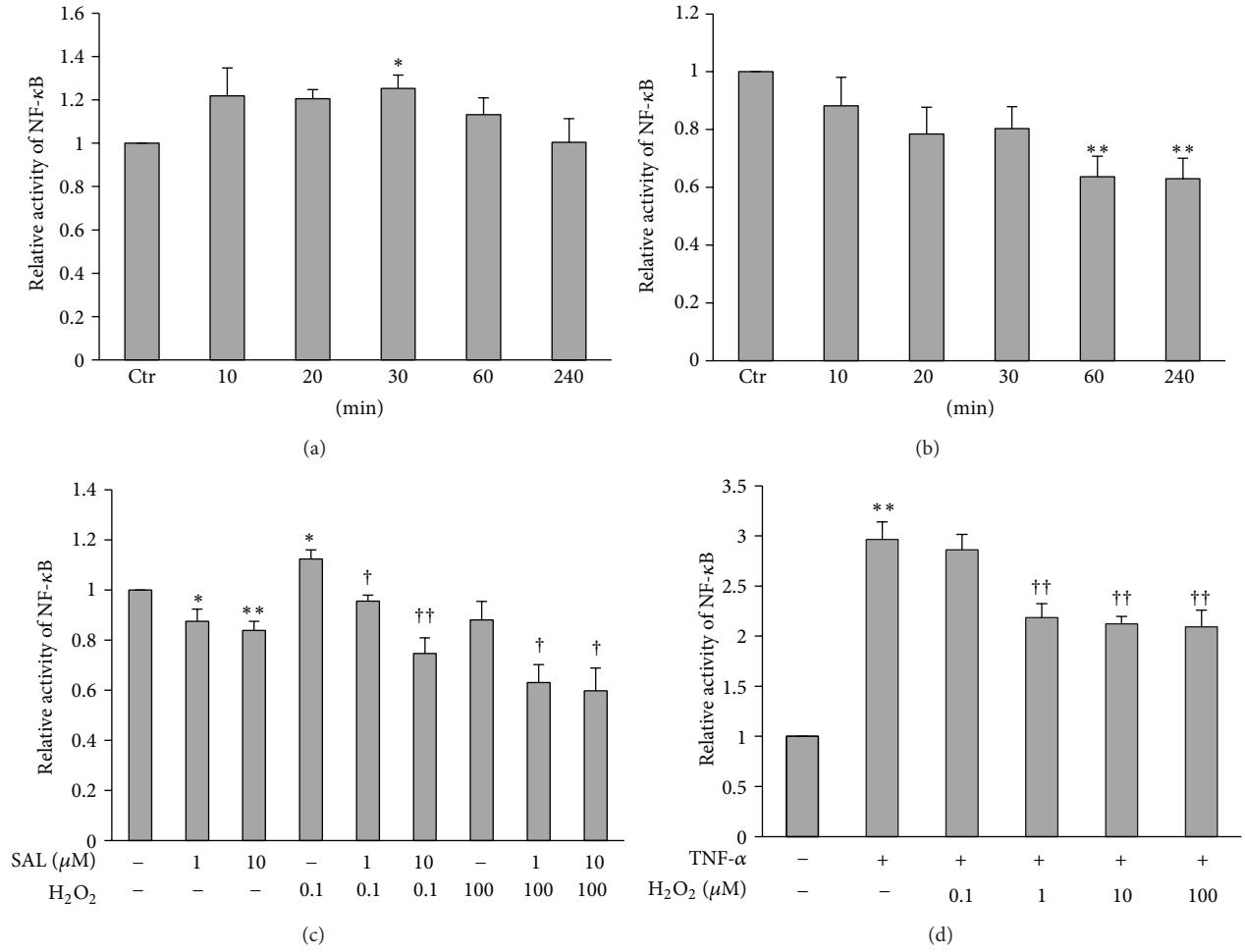

Figure 5: Effects of SAL on H_2O_2-induced activation of transcription factor NF-κB. Effects of H_2O_2 (0.1 μM) (a) and SAL (10 μM) (b) on transcription factor NF-κB activity. H_2O_2 (0.1 μM) or SAL (10 μM) was added for the indicated periods of time (0–4 h). The transcription activity in untreated cells was assigned the value of 1. $^{*}P < 0.05$, $^{**}P < 0.01$ versus control, $n = 4$. (c) Effects of SAL on H_2O_2-induced NF-κB activity. HUVECs were pretreated with SAL (1, 10 μM) for 10 min and then incubated with H_2O_2(0.1, 100 μM) for 30 min. $^{*}P < 0.05$, $^{**}P < 0.01$ versus control; $^{\dagger}P < 0.05$, $^{\dagger\dagger}P < 0.01$ versus H_2O_2, $n = 4$–6. (d) HUVECs were treated with TNF-α (30 ng/mL) for 30 min, and then total protein was extracted. The proteins were incubated with increasing concentrations of H_2O_2(0.1, 1, 10, and 100 μM) for 30 min, and then the activities of NF-κB were detected as described in Section 2. The transcription activity was normalized to that obtained in untreated cells. $^{**}P < 0.01$ versus control, $^{\dagger\dagger}P < 0.01$ versus TNF-α, $n = 3$.

long-term SAL treatment may be initiated by a transient mild mitochondrial depolarization and reduced oxygen demand, which in turn increase the tolerance of affected cells to subsequent oxidative insult that is greater in severity. But this needs to be further proved.

There are evidences that NO can repress the activation of NF-κB through degradation of IκBα [61] or inhibition of NF-κB DNA binding [62]. We also analyzed the effect of SAL on the activation of NF-κB induced by H_2O_2. Our date showed that SAL decreased the basal activity of NF-κB, meanwhile blocking the activation of NF-κB induced by H_2O_2 (Figure 5). H_2O_2 at the concentration of 100 μM slightly reduced rather than increased the NF-κB activity; meanwhile, pretreatment with SAL further reduced the activity. The possible explanation is that H_2O_2 *per se* induces the formation of active dimmers of P65 and P50 subunits and leads to their translocation to the nucleus. However, within the nucleus, the Cys 62 residue on the P50 subunit is oxidized to sulfenic acid and is further followed by S-glutathionylation, which inhibits the binding of NF-κB to the DNA [63–65]. To strengthen this hypothesis, we detected the direct effect of H_2O_2 on DNA binding activity. We used TNF-α, a classical NF-κB inducer to treat HUVECs. After cell lysis and total protein extraction, we incubated the proteins with increasing concentrations of H_2O_2 (0.1, 1, 10, and 100 μM) for 30 min, and then the activities of NF-κB were detected as described in Section 2. The results indicated that H_2O_2 dose dependently inhibited the DNA binding activity of activated NF-κB. Since NF-κB is a redox sensitive transcription factor, its activation participates in inflammation and mitochondrial biogenesis impairment [66]. We speculated that the protective effect of SAL on HUVECs

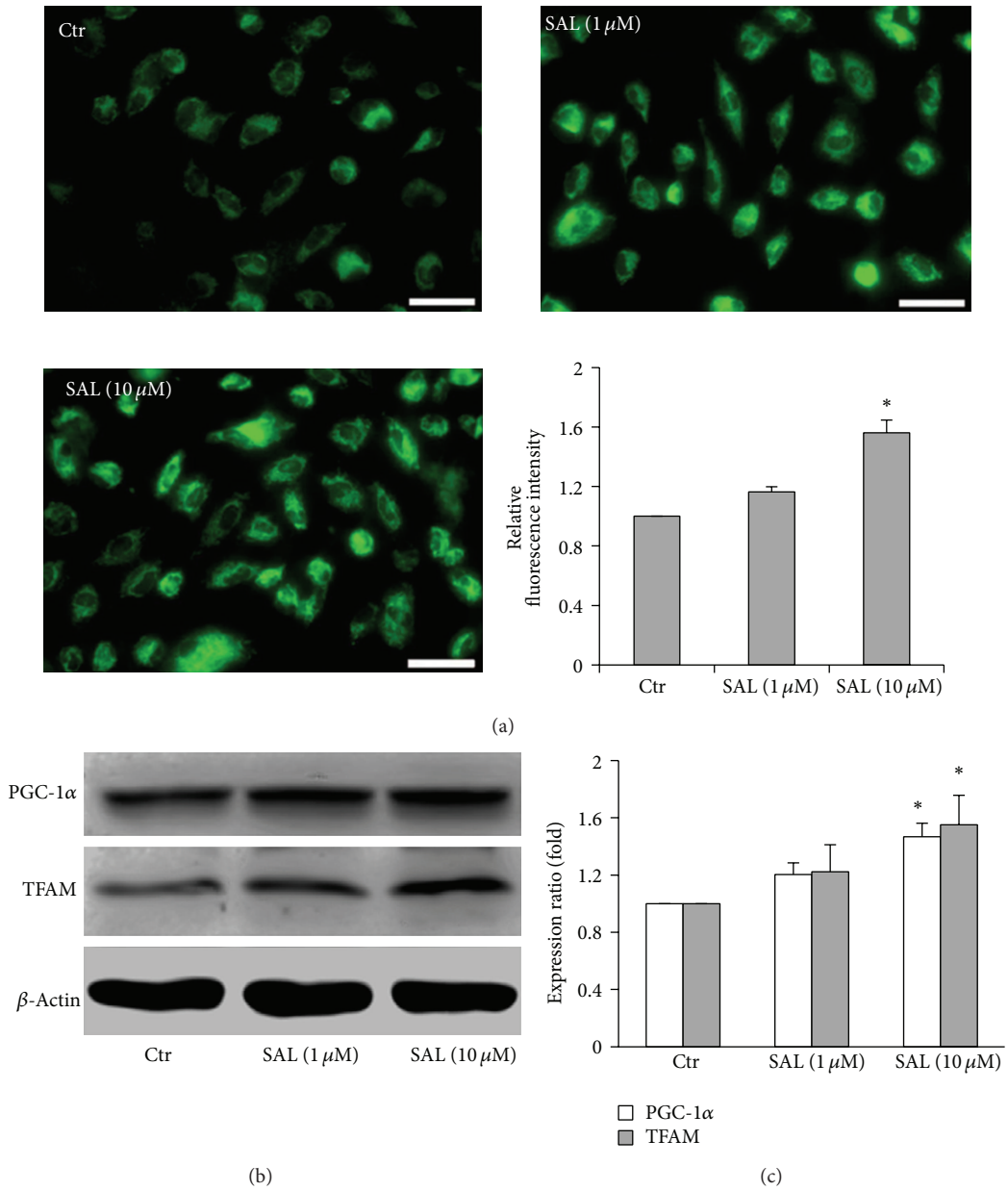

Figure 6: Effects of SAL on mitochondrial biogenesis. (a) Mitochondria mass was quantified using Mito Tracker Green. Scale bars = 50 μm. The fluorescence in untreated cells was assigned the value of 1. $^{*}P < 0.05$ versus control, $n = 4$. HUVECs were treated with SAL (1, 10 μM) for 24 h, and the total protein was extracted; the lysates were analyzed by western blot. (b) Representative immunoblots. (c) Summary histograms of the relative density of PGC-1α and TFAM normalized to β-actin. The expression in untreated cells was assigned the value of 1. $^{*}P < 0.05$ versus control, $n = 5$.

might be related to an interference with the NF-κB signaling pathway.

Moderate increases in NO stimulate mitochondrial biogenesis, mainly through cGMP-dependent gene expression and activation of regulatory factors including PGC-1α and TFAM [67, 68]. In cardiomyocytes, coimmunoprecipitation experiments demonstrated that the p65 subunit of NF-κB is constitutively bound to PGC-1α coactivator and blocks its activation of gene transcription and that NF-κB activation increases this binding [69]. Moreover, PGC-1α overexpression inhibits NF-κB activation in human aortic smooth muscular and endothelial cells [70]. So it is reasonable that the agents stimulating PGC-1α expression and mitochondrial biogenesis in the endothelial cells are beneficial to prevent the development of cardiovascular disease. Here we reported for the first time that SAL increased mitochondrial mass in HUVECs (Figure 6(a)). Inducible mitochondrial biogenesis is very important in vascular health [27, 71]. Moreover, mitochondrial proliferation reduces the flow of electron per unit mitochondria; SAL-induced mitochondrial biogenesis may contribute to the reduction of mitochondrial ROS production in HUVECs.

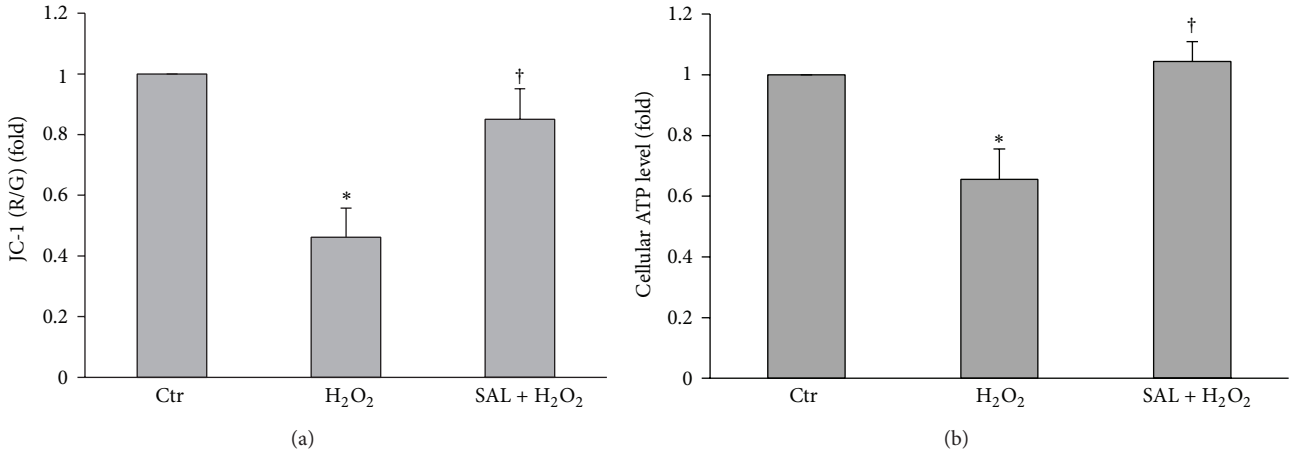

FIGURE 7: Effects of SAL on H_2O_2-induced mitochondrial dysfunction. HUVECs were pretreated with SAL (10 μM) for 20 h, and then H_2O_2(100 μM) was added to incubate for another 4 h. (a) Mitochondrial membrane potential and (b) ATP content were detected as described in Section 2. $\Delta\Psi$m and ATP content in untreated cells were assigned the value of 1. $^*P < 0.05$ versus control; $^\dagger P < 0.05$ versus H_2O_2, $n = 4$.

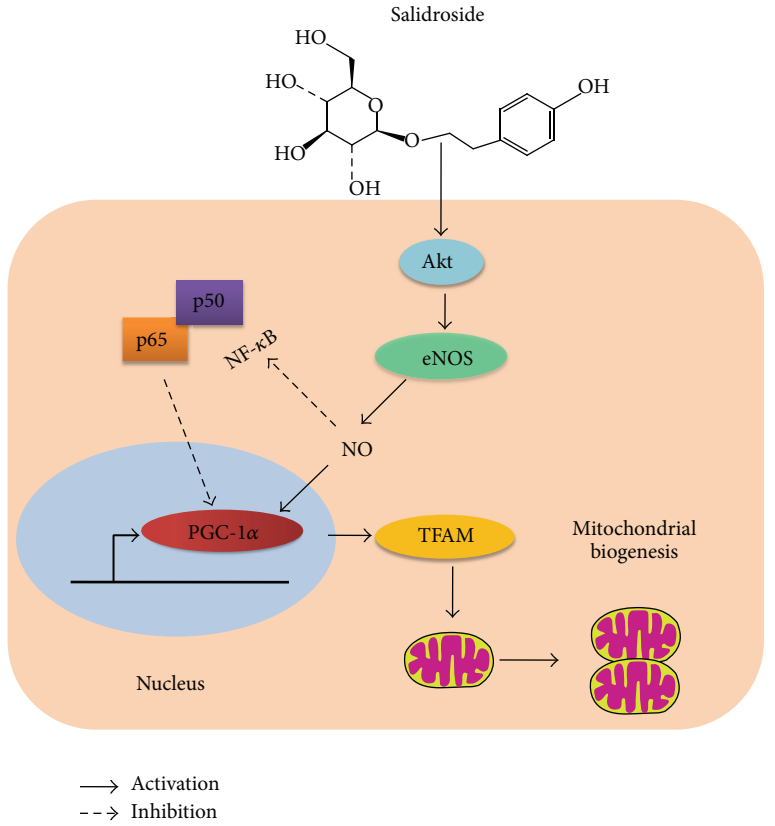

FIGURE 8: Schematic diagram of the potential mechanisms of SAL to induce mitochondrial biogenesis. SAL inhibited transcription factors NF-κB activity, enhanced eNOS activity, and NO production, which induced mitochondrial biogenesis subsequently.

To determine whether the effect of SAL on mitochondrial biogenesis is a consequence of the activation of mitochondrial biogenesis regulatory factors, we examined the expression of PGC-1α and TFAM. We found that SAL increased the expression of PGC-1α and TFAM (Figures 6(b) and 6(c)).

In addition to stimulating mitochondrial biogenesis, PGC-1α also contributes to the induction of ROS detoxifying enzymes, including catalase, superoxide dismutase, and heme oxygenase [72–75]. These findings imply that PGC-1α-mediated mitochondrial biogenesis in oxidative injured cells seems to offer a good source of "healthy mitochondria" which

detoxify mtROS by a large antioxidant defense system containing numerous redox enzymes of the electron-transport chain, ultimately decreasing net ROS production. These effects of SAL on mitochondrial biogenesis may partially explain its antioxidant properties.

Many evidences have revealed that H_2O_2 caused endothelial cell injury by inducing mitochondrial dysfunction [76, 77]. Due to localization to the inner mitochondrial membrane, lack of histone-like coverage and a less efficient DNA repair system compared with nuclear DNA, mtDNA is prone to oxidative stress [78]. Furthermore, the mutation is more likely to affect gene integrity because of the absence of intron in the mitochondrial genome [79]. Damaged mitochondria produce less ATP but more greater amounts of ROS, potentiating the signal and entering a vicious circle, which aggravate cardiovascular diseases [80]. As shown in Figure 7, SAL pretreatment abrogated the H_2O_2-induced collapse of $\Delta\Psi m$ and rescued the mitochondrial function, proved by increased ATP production. These effects of SAL decrease the potential for mtDNA damaged by H_2O_2; moreover, SAL enhanced mitochondrial biogenesis, which provides healthy mitochondria to replace the mitochondrial components damaged by ROS and maintain normal mitochondrial function. The protective effect of SAL on mitochondria is of paramount importance to maintain the endothelial homeostasis.

In summary, the present study demonstrated a novel mechanism of SAL to protect the endothelial cells from oxidative damage. By stimulating mitochondrial biogenesis (Figure 8) and counteracting the reactive oxygen species burst within mitochondria, SAL administration prevented the overactivation of several signaling pathways evoked by damaging oxidative stimuli and preserved the viability of endothelial cells, as well as the endothelial dependent vessel functions. Novel compounds with mitochondria biogenesis stimulating activities may become potential drug candidates for the prevention or treatment of such disorders associated with oxidative stress as metabolic syndrome or cancer and so forth.

Conflict of Interests

The authors declare that there is no conflict of interests regarding the publication of this paper.

Authors' Contribution

Shasha Xing and Xiaoyan Yang contributed equally to this work.

Acknowledgments

This work was supported by Grants from the National Natural Science Foundation of China (81373413, 81072634, and 81000080), the Ministry of Education of China (NCET-10-0409 and 2013YGYL008), and the National Science and Technology Major Projects (2013zx09103-001-020 and 2011zx09102-004-001).

References

[1] V. V. Makarenko, P. V. Usatyuk, G. Yuan et al., "Intermittent hypoxia-induced Endothelial barrier Dysfunction requires ROS-dependent MAP kinase activation," *American Journal of Physiology Cell Physiology*, 2014.

[2] N. Hermida and J. L. Balligand, "Low-density lipoprotein-cholesterol-induced endothelial dysfunction and oxidative stress: the role of statins," *Antioxidants & Redox Signaling*, vol. 20, no. 8, pp. 1216–1237, 2013.

[3] S. Wang, M. Zhang, B. Liang et al., "AMPKα2 deletion causes aberrant expression and activation of NAD(P)H oxidase and consequent endothelial dysfunction in vivo: role of 26S proteasomes," *Circulation Research*, vol. 106, no. 6, pp. 1117–1128, 2010.

[4] C. M. Sena, A. M. Pereira, and R. Seica, "Endothelial dysfunction—a major mediator of diabetic vascular disease," *Biochimica et Biophysica Acta*, vol. 1832, no. 12, pp. 2216–2231, 2013.

[5] A. L. Moens, R. Kietadisorn, J. Y. Lin, and D. Kass, "Targeting endothelial and myocardial dysfunction with tetrahydrobiopterin," *Journal of Molecular and Cellular Cardiology*, vol. 51, no. 4, pp. 559–563, 2011.

[6] P. Dromparis and E. D. Michelakis, "Mitochondria in vascular health and disease," *Annual Review of Physiology*, vol. 75, pp. 95–126, 2013.

[7] E. Marzetti, A. Csiszar, D. Dutta, G. Balagopal, R. Calvani, and C. Leeuwenburgh, "Role of mitochondrial dysfunction and altered autophagy in cardiovascular aging and disease: from mechanisms to therapeutics," *American Journal of Physiology—Heart and Circulatory Physiology*, vol. 305, no. 4, pp. H459–H476, 2013.

[8] J. R. Mercer, "Mitochondrial bioenergetics and therapeutic intervention in cardiovascular disease," *Pharmacology & Therapeutics*, vol. 141, no. 1, pp. 13–20, 2014.

[9] R. O. Poyton, K. A. Ball, and P. R. Castello, "Mitochondrial generation of free radicals and hypoxic signaling," *Trends in Endocrinology and Metabolism*, vol. 20, no. 7, pp. 332–340, 2009.

[10] S. R. Thomas, P. K. Witting, and G. R. Drummond, "Redox control of endothelial function and dysfunction: molecular mechanisms and therapeutic opportunities," *Antioxidants & Redox Signaling*, vol. 10, no. 10, pp. 1713–1765, 2008.

[11] M. T. Sorbara and S. E. Girardin, "Mitochondrial ROS fuel the inflammasome," *Cell Research*, vol. 21, no. 4, pp. 558–560, 2011.

[12] C. Banfi, M. Brioschi, S. S. Barbieri et al., "Mitochondrial reactive oxygen species: a common pathway for PAR1- and PAR2-mediated tissue factor induction in human endothelial cells," *Journal of Thrombosis and Haemostasis*, vol. 7, no. 1, pp. 206–216, 2009.

[13] Z. Ungvari, Z. Orosz, N. Labinskyy et al., "Increased mitochondrial H_2O_2 production promotes endothelial NF-κB activation in aged rat arteries," *American Journal of Physiology—Heart and Circulatory Physiology*, vol. 293, no. 1, pp. H37–H47, 2007.

[14] F. Addabbo, B. Ratliff, H.-C. Park et al., "The krebs cycle and mitochondrial mass are early victims of endothelial dysfunction: proteomic approach," *American Journal of Pathology*, vol. 174, no. 1, pp. 34–43, 2009.

[15] S. M. Davidson and M. R. Duchen, "Endothelial mitochondria: contributing to vascular function and disease," *Circulation Research*, vol. 100, no. 8, pp. 1128–1141, 2007.

[16] M. A. Kluge, J. L. Fetterman, and J. A. Vita, "Mitochondria and endothelial function," *Circulation Research*, vol. 112, no. 8, pp. 1171–1188, 2013.

[17] K. J. Krishnan, A. K. Reeve, D. C. Samuels et al., "What causes mitochondrial DNA deletions in human cells?" *Nature Genetics*, vol. 40, no. 3, pp. 275–279, 2008.

[18] M. G. Rosca and C. L. Hoppel, "Mitochondria in heart failure," *Cardiovascular Research*, vol. 88, no. 1, pp. 40–50, 2010.

[19] A. P. Halestrap, "Calcium, mitochondria and reperfusion injury: a pore way to die," *Biochemical Society Transactions*, vol. 34, part 2, pp. 232–237, 2006.

[20] J. Gutierrez, S. W. Ballinger, V. M. Darley-Usmar, and A. Landar, "Free radicals, mitochondria, and oxidized lipids: the emerging role in signal transduction in vascular cells," *Circulation Research*, vol. 99, no. 9, pp. 924–932, 2006.

[21] Z. Ungvari, N. Labinskyy, S. Gupte, P. N. Chander, J. G. Edwards, and A. Csiszar, "Dysregulation of mitochondrial biogenesis in vascular endothelial and smooth muscle cells of aged rats," *American Journal of Physiology—Heart and Circulatory Physiology*, vol. 294, no. 5, pp. H2121–H2128, 2008.

[22] R. Blake and I. A. Trounce, "Mitochondrial dysfunction and complications associated with diabetes," *Biochimica et Biophysica Acta*, vol. 1840, no. 4, pp. 1404–1412, 2014.

[23] R. C. Scarpulla, "Metabolic control of mitochondrial biogenesis through the PGC-1 family regulatory network," *Biochimica et Biophysica Acta*, vol. 1813, no. 7, pp. 1269–1278, 2011.

[24] I. S. Patten and Z. Arany, "PGC-1 coactivators in the cardiovascular system," *Trends in Endocrinology and Metabolism*, vol. 23, no. 2, pp. 90–97, 2012.

[25] R. C. Scarpulla, "Nuclear control of respiratory chain expression by nuclear respiratory factors and PGC-1-related coactivator," *Annals of the New York Academy of Sciences*, vol. 1147, pp. 321–334, 2008.

[26] J. M. Santos, S. Tewari, A. F. X. Goldberg, and R. A. Kowluru, "Mitochondrial biogenesis and the development of diabetic retinopathy," *Free Radical Biology and Medicine*, vol. 51, no. 10, pp. 1849–1860, 2011.

[27] Q. Xu, P. Xia, X. Li, W. Wang, Z. Liu, and X. Gao, "Tetramethylpyrazine ameliorates high glucose-induced endothelial dysfunction by increasing mitochondrial biogenesis," *PLoS ONE*, vol. 9, no. 2, Article ID e88243, 2014.

[28] A. Panossian and H. Wagner, "Stimulating effect of adaptogens: an overview with particular reference to their efficacy following single dose administration," *Phytotherapy Research*, vol. 19, no. 10, pp. 819–838, 2005.

[29] E. W. Qian, D. T. Ge, and S.-K. Kong, "Salidroside promotes erythropoiesis and protects erythroblasts against oxidative stress by up-regulating glutathione peroxidase and thioredoxin," *Journal of Ethnopharmacology*, vol. 133, no. 2, pp. 308–314, 2011.

[30] X. Li, J. Sipple, Q. Pang, and W. Du, "Salidroside stimulates DNA repair enzyme Parp-1 activity in mouse HSC maintenance," *Blood*, vol. 119, no. 18, pp. 4162–4173, 2012.

[31] S. B. Leung, H. Zhang, C. W. Lau, Y. Huang, and Z. Lin, "Salidroside improves homocysteine-induced endothelial dysfunction by reducing oxidative stress," *Evidence-Based Complementary and Alternative Medicine*, vol. 2013, Article ID 679635, 8 pages, 2013.

[32] J. R. Williams, "The declaration of Helsinki and public health," *Bulletin of the World Health Organization*, vol. 86, pp. 650–652, 2008.

[33] E. A. Jaffe, R. L. Nachman, C. G. Becker, and C. R. Minick, "Culture of human endothelial cells derived from umbilical veins. Identification by morphologic and immunologic criteria," *The Journal of Clinical Investigation*, vol. 52, no. 11, pp. 2745–2756, 1973.

[34] Y. Bai, A. K. Suzuki, and M. Sagai, "The cytotoxic effects of diesel exhaust particles on human pulmonary artery endothelial cells in vitro: role of active oxygen species," *Free Radical Biology and Medicine*, vol. 30, no. 5, pp. 555–562, 2001.

[35] S. Song, F. Zhou, W. R. Chen, and D. Xing, "PDT-induced HSP70 externalization up-regulates NO production via TLR2 signal pathway in macrophages," *FEBS Letters*, vol. 587, no. 2, pp. 128–135, 2013.

[36] K. Dasuri, P. Ebenezer, S. O. Fernandez-Kim et al., "Role of physiological levels of 4-hydroxynonenal on adipocyte biology: implications for obesity and metabolic syndrome," *Free Radical Research*, vol. 47, no. 1, pp. 8–19, 2013.

[37] S. Jin, D. Lu, S. Ye et al., "A simplified probe preparation for ELISA-based NF-κB activity assay," *Journal of Biochemical and Biophysical Methods*, vol. 65, no. 1, pp. 20–29, 2005.

[38] Y. Zhang, X. Yang, F. Bian et al., "TNF-α promotes early atherosclerosis by increasing transcytosis of LDL across endothelial cells: crosstalk between NF-κB and PPAR-γ," *Journal of Molecular and Cellular Cardiology*, vol. 72, pp. 85–94, 2014.

[39] L. Wang, H. Zhen, W. Yao et al., "Lipid raft-dependent activation of dual oxidase 1/H_2O_2/NF-κB pathway in bronchial epithelial cells," *American Journal of Physiology—Cell Physiology*, vol. 301, no. 1, pp. C171–C180, 2011.

[40] R. Zhou, A. S. Yazdi, P. Menu, and J. Tschopp, "A role for mitochondria in NLRP3 inflammasome activation," *Nature*, vol. 469, no. 7329, pp. 221–226, 2011.

[41] V. Parra, V. Eisner, M. Chiong et al., "Changes in mitochondrial dynamics during ceramide-induced cardiomyocyte early apoptosis," *Cardiovascular Research*, vol. 77, no. 2, pp. 387–397, 2008.

[42] M. Reers, T. W. Smith, and L. B. Chen, "J-aggregate formation of a carbocyanine as a quantitative fluorescent indicator of membrane potential," *Biochemistry*, vol. 30, no. 18, pp. 4480–4486, 1991.

[43] T. Collins, "Biology of disease: endothelial nuclear factor-κB and the initiation of the atherosclerotic lesion," *Laboratory Investigation*, vol. 68, no. 5, pp. 499–508, 1993.

[44] E. Schulz, T. Gori, and T. Münzel, "Oxidative stress and endothelial dysfunction in hypertension," *Hypertension Research*, vol. 34, no. 6, pp. 665–673, 2011.

[45] F. Giacco and M. Brownlee, "Oxidative stress and diabetic complications," *Circulation Research*, vol. 107, no. 9, pp. 1058–1070, 2010.

[46] A. Briasoulis, D. Tousoulis, E. S. Androulakis, N. Papageorgiou, G. Latsios, and C. Stefanadis, "Endothelial dysfunction and atherosclerosis: focus on novel therapeutic approaches," *Recent Patents on Cardiovascular Drug Discovery*, vol. 7, no. 1, pp. 21–32, 2012.

[47] M. C. Xu, H. M. Shi, H. Wang, and X. F. Gao, "Salidroside protects against hydrogen peroxide-induced injury in HUVECs via the regulation of REDD1 and mTOR activation," *Molecular Medicine Reports*, vol. 8, no. 1, pp. 147–153, 2013.

[48] L. M. Yung, F. P. Leung, X. Yao, Z.-Y. Chen, and Y. Huang, "Reactive oxygen species in vascular wall," *Cardiovascular and Hematological Disorders—Drug Targets*, vol. 6, no. 1, pp. 1–19, 2006.

[49] M. Félétou and P. M. Vanhoutte, "Endothelial dysfunction: a multifaceted disorder," *American Journal of Physiology—Heart and Circulatory Physiology*, vol. 291, no. 3, pp. H985–H1002, 2006.

[50] S. Fujimoto, T. Asano, M. Sakai et al., "Mechanisms of hydrogen peroxide-induced relaxation in rabbit mesenteric small artery," *European Journal of Pharmacology*, vol. 412, no. 3, pp. 291–300, 2001.

[51] Z.-W. Yang, A. Zhang, B. T. Altura, and B. M. Altura, "Hydrogen peroxide-induced endothelium-dependent relaxation of rat aorta: involvement of Ca^{2+} and other cellular metabolites," *General Pharmacology*, vol. 33, no. 4, pp. 325–336, 1999.

[52] A. Ellis, M. Pannirselvam, T. J. Anderson, and C. R. Triggle, "Catalase has negligible inhibitory effects on endothelium-dependent relaxations in mouse isolated aorta and small mesenteric artery," *British Journal of Pharmacology*, vol. 140, no. 7, pp. 1193–1200, 2003.

[53] A. Zembowicz, R. J. Hatchett, A. M. Jakubowski, and R. J. Gryglewski, "Involvement of nitric oxide in the endothelium-dependent relaxation induced by hydrogen peroxide in the rabbit aorta," *British Journal of Pharmacology*, vol. 110, no. 1, pp. 151–158, 1993.

[54] H. Cai, Z. Li, S. Dikalov et al., "NAD(P)H oxidase-derived hydrogen peroxide mediates endothelial nitric oxide production in response to angiotensin II," *The Journal of Biological Chemistry*, vol. 277, no. 50, pp. 48311–48317, 2002.

[55] C. M. Wong, L. M. Yung, F. P. Leung et al., "Raloxifene protects endothelial cell function against oxidative stress," *British Journal of Pharmacology*, vol. 155, no. 3, pp. 326–334, 2008.

[56] S. Dimmeler and A. M. Zeiher, "Nitric oxide—an endothelial cell survival factor," *Cell Death and Differentiation*, vol. 6, no. 10, pp. 964–968, 1999.

[57] W. T. Wong, S. L. Wong, X. Y. Tian, and Y. Huang, "Endothelial dysfunction: the common consequence in diabetes and hypertension," *Journal of Cardiovascular Pharmacology*, vol. 55, no. 4, pp. 300–307, 2010.

[58] X.-F. Niu, C. W. Smith, and P. Kubes, "Intracellular oxidative stress induced by nitric oxide synthesis inhibition increases endothelial cell adhesion to neutrophils," *Circulation Research*, vol. 74, no. 6, pp. 1133–1140, 1994.

[59] H. Cai, Z. Li, M. E. Davis, W. Kanner, D. G. Harrison, and S. C. Dudley Jr., "Akt-dependent phosphorylation of serine 1179 and mitogen-activated protein kinase kinase/extracellular signal-regulated kinase 1/2 cooperatively mediate activation of the endothelial nitric-oxide synthase by hydrogen peroxide," *Molecular Pharmacology*, vol. 63, no. 2, pp. 325–331, 2003.

[60] Z. Xia, M. Liu, Y. Wu et al., "N-acetylcysteine attenuates TNF-α-induced human vascular endothelial cell apoptosis and restores eNOS expression," *European Journal of Pharmacology*, vol. 550, no. 1–3, pp. 134–142, 2006.

[61] S. Mohan, M. Hamuro, G. P. Sorescu et al., "IκBα-dependent regulation of low-shear flow-induced NF-κB activity: role of nitric oxide," *American Journal of Physiology—Cell Physiology*, vol. 284, no. 4, pp. C1039–C1047, 2003.

[62] J. R. Matthews, C. H. Botting, M. Panico, H. R. Morris, and R. T. Hay, "Inhibition of NF-κB DNA binding by nitric oxide," *Nucleic Acids Research*, vol. 24, no. 12, pp. 2236–2242, 1996.

[63] E. Pineda-Molina, P. Klatt, J. Vázquez et al., "Glutathionylation of the p50 subunit of NF-κB: a mechanism for redox-induced inhibition of DNA binding," *Biochemistry*, vol. 40, no. 47, pp. 14134–14142, 2001.

[64] L. Jornot, H. Petersen, and A. F. Junod, "Modulation of the DNA binding activity of transcription factors CREP, NFκB and HSF by H_2O_2 and TNFα. Differences between in vivo and in vitro effects," *FEBS Letters*, vol. 416, no. 3, pp. 381–386, 1997.

[65] V. Oliveira-Marques, H. S. Marinho, L. Cyrne, and F. Antunes, "Role of hydrogen peroxide in NF-κB activation: from inducer to modulator," *Antioxidants & Redox Signaling*, vol. 11, no. 9, pp. 2223–2243, 2009.

[66] Y. Hasegawa, T. Saito, T. Ogihara et al., "Blockade of the nuclear factor-κB pathway in the endothelium prevents insulin resistance and prolongs life spans," *Circulation*, vol. 125, no. 9, pp. 1122–1133, 2012.

[67] E. Nisoli and M. O. Carruba, "Nitric oxide and mitochondrial biogenesis," *Journal of Cell Science*, vol. 119, part 14, pp. 2855–2862, 2006.

[68] E. Nisoli, E. Clementi, C. Paolucci et al., "Mitochondrial biogenesis in mammals: the role of endogenous nitric oxide," *Science*, vol. 299, no. 5608, pp. 896–899, 2003.

[69] D. Álvarez-Guardia, X. Palomer, T. Coll et al., "The p65 subunit of NF-B binds to PGC-1, linking inflammation and metabolic disturbances in cardiac cells," *Cardiovascular Research*, vol. 87, no. 3, pp. 449–458, 2010.

[70] H.-J. Kim, K.-G. Park, E.-K. Yoo et al., "Effects of PGC-1α on TNF-α-induced MCP-1 and VCAM-1 expression and NF-κB activation in human aortic smooth muscle and endothelial cells," *Antioxidants & Redox Signaling*, vol. 9, no. 3, pp. 301–307, 2007.

[71] A. Csiszar, N. Labinskyy, J. T. Pinto et al., "Resveratrol induces mitochondrial biogenesis in endothelial cells," *American Journal of Physiology—Heart and Circulatory Physiology*, vol. 297, no. 1, pp. H13–H20, 2009.

[72] J. Schilling, L. Lai, N. Sambandam, C. E. Dey, T. C. Leone, and D. P. Kelly, "Toll-like receptor-mediated inflammatory signaling reprograms cardiac energy metabolism by repressing peroxisome proliferator-activated receptor γ coactivator-1 signaling," *Circulation: Heart Failure*, vol. 4, no. 4, pp. 474–482, 2011.

[73] J. C. Won, J.-Y. Park, Y. M. Kim et al., "Peroxisome proliferator-activated receptor-γ coactivator 1-α overexpression prevents endothelial apoptosis by increasing ATP/ADP translocase activity," *Arteriosclerosis, Thrombosis, and Vascular Biology*, vol. 30, no. 2, pp. 290–297, 2010.

[74] I. Valle, A. Álvarez-Barrientos, E. Arza, S. Lamas, and M. Monsalve, "PGC-1α regulates the mitochondrial antioxidant defense system in vascular endothelial cells," *Cardiovascular Research*, vol. 66, no. 3, pp. 562–573, 2005.

[75] F. Ali, N. S. Ali, A. Bauer et al., "PPARσ and PGC1α act cooperatively to induce haem oxygenase-1 and enhance vascular endothelial cell resistance to stress," *Cardiovascular Research*, vol. 85, no. 4, pp. 701–710, 2010.

[76] H. Cai, "Hydrogen peroxide regulation of endothelial function: origins, mechanisms, and consequences," *Cardiovascular Research*, vol. 68, no. 1, pp. 26–36, 2005.

[77] Y.-M. Liu, B. Jiang, Y.-M. Bao, and L.-J. An, "Protocatechuic acid inhibits apoptosis by mitochondrial dysfunction in rotenone-induced PC12 cells," *Toxicology in Vitro*, vol. 22, no. 2, pp. 430–437, 2008.

[78] H. Huang and K. G. Manton, "The role of oxidative damage in mitochondria during aging: a review," *Frontiers in Bioscience*, vol. 9, pp. 1100–1117, 2004.

[79] F. M. Yakes and B. van Houten, "Mitochondrial DNA damage is more extensive and persists longer than nuclear DNA damage in human cells following oxidative stress," *Proceedings of the National Academy of Sciences of the United States of America*, vol. 94, no. 2, pp. 514–519, 1997.

[80] B. G. Hill, G. A. Benavides, J. R. Lancaster Jr. et al., "Integration of cellular bioenergetics with mitochondrial quality control and autophagy," *Biological Chemistry*, vol. 393, no. 12, pp. 1485–1512, 2012.

Hindawi Publishing Corporation
Oxidative Medicine and Cellular Longevity
Volume 2014, Article ID 154295, 7 pages
http://dx.doi.org/10.1155/2014/154295

Research Article

Effect of *Centella asiatica* on Oxidative Stress and Lipid Metabolism in Hyperlipidemic Animal Models

Yun Zhao,[1,2] Ping Shu,[1] Youzhi Zhang,[3] Limin Lin,[1] Haihong Zhou,[1] Zhentian Xu,[1] Daqin Suo,[1] Anzhi Xie,[1] and Xin Jin[1,2]

[1] *Medical College, Xiamen University, Xiang'an District, Xiamen 361000, China*
[2] *Xiamen Key Laboratory of Chiral Drugs, Xiamen 361000, China*
[3] *College of Pharmacy, Hubei University of Science and Technology, Xianning 437000, China*

Correspondence should be addressed to Xin Jin; xinjin@xmu.edu.cn

Received 14 February 2014; Revised 29 March 2014; Accepted 1 April 2014; Published 16 April 2014

Academic Editor: Si Jin

Hyperlipidemia and many other metabolic diseases are related to oxidative stress. *Centella asiatica* is a traditional Chinese medicine whose antioxidant effect in vitro has been reported. We are interested in whether it possesses this effect in vivo and hence modulates lipid metabolism. Therefore, experiments were carried out on mice and golden hamsters regarding its antioxidant and hypolipidemic effect. We observed that a fraction (CAF3) of the ethanol extract (CAE) of *Centella asiatica* had a cholesterol decrease of 79% and a triglyceride decrease of 95% in acute mice model, so CAF3 was further investigated in high-fat-fed hamster model. It was shown that CAF3 increased SOD and GSH-Px activities and decreased MDA level, and it also improved TC, TG, LDL-C, HDL-C, AST, and ALT levels. L-CAT and SR-BI gene expression in hamsters were increased. Taken together, our data suggest that the CAF3 fraction of *Centella asiatica* has antioxidant and hypolipidemic properties.

1. Introduction

Oxidative stress has been shown to damage the structural and functional integrity of the cell either by directly modifying cellular DNA, proteins, and membrane lipids or by initiating chain reactions that cause extensive oxidative damage to DNA, proteins, and membrane lipids [1]. As for hepatocytes, once its functions are bad, the lipid metabolism is affected.

Abnormal lipid metabolism or hyperlipidemia, the high risk for atherosclerosis, is the condition that can result in many kinds of cardiovascular diseases [2]. Nowadays, medicinal plants play the key role in promoting human health and treating diseases. Traditional Chinese medicine has been reported to treat hyperlipidaemia and prevent atherosclerosis in many developing countries [3, 4]. As they are normally considered to be less toxic than synthetic agents, natural agents are increasingly purported to exert potent beneficial actions to regulate serum TC and TG levels and may thus play the role in reducing synthetic drug use for the treatment of hyperlipidemia [5]. Therefore, increasing interests have been drawn towards plant products [6].

Centella asiatica (L.) Urb. is a perennial herbaceous creeper of the Apiaceae family. It contains triterpenes, namely, asiatic acid (AA), madecassic acids (MA), asiaticoside (AD), madecassoside (MD) [7], essential oils, amino acids, and other compounds. In addition, it can cure some diseases by traditional treatment in China and other Asian countries, and its many pharmacological effects have been validated by modern technology, such as anti-inflammatory [8], memory improvement [9], anticancer [10], antihepatoma [11], antioxidation [12], and antigenotoxic [13]. The antioxidant capacity of *Centella asiatica* in vitro is also reported [14, 15]; however, there are few reports about antioxidant and hypolipidemic activities in vivo. Thus, the aim of the present study was to evaluate the effects of the *Centella asiatica* on oxidative stress and hyperlipidemia in hyperlipidemic mice and hamster models and to further explore the mechanism.

2. Materials and Methods

2.1. Chemicals and Reagents. Fenofibrate (Sigma-Aldrich, St. Louis, MO, USA) was dissolved in distilled water and administered by gavage to the mice at 100 mg/kg body wt (BW). Xuezhikang (Beijing Wbl Peking University Biotech Co., Ltd, China) was dissolved in distilled water and administered by gavage to the hamsters at 250 mg/kg body wt (BW). Triton WR-1339 (Tyloxapol, Sigma-Aldrich, USA) was dissolved in saline and administered by intraperitoneal injection to the mice at 400 mg/kg body wt (BW).

2.2. Plant Material and Extraction. Centella asiatica dry plant was obtained from LuYan Pharma Co., Ltd., Fujian Province of China and authenticated by Dr. Qiu, an expert in Medical College of Xiamen University, Xiamen, China. The concentrated solution (CAE) was prepared according to the following procedure: the powdered plant material (1 kg) was soaked in 8000 mL 95% ethanol and stand for 1 day, then extracted twice more in 95% ethanol at 80°C for 3 h. The filtered extract was concentrated by a rotary evaporator with a water bath at 60°C.

CAE was filtered again before being added to a HPD-450 macroporous resin (Cang Zhou Bon Adsorber Technology Co., Ltd., China) column, which was then washed sequentially with two column volumes of 50%, 70%, and 95% aqueous ethanol, designated CAF1 to CAF3, respectively. Each eluate was concentrated by vacuum rotary evaporation. The concentrated solution was dried in a lyophilizer and stored at 4°C until used. The yields of CAF1, CAF2, and CAF3 in terms of starting dried plant material were of 0.638, 0.676, and 0.824% (w/w).

2.3. Animals. Adult male KM mice (23–27 g) and male Golden Syrian hamsters (80–90 g) were used for the experiments. Mice and hamsters were obtained from SLAC Laboratory Animal Co., Ltd and Songlian farm of Songjiang District in Shanghai, respectively. The animals were housed under standard conditions of light and dark cycles with free access to food and water. All the animal studies were approved by the local ethics committee for animal experimentation (approval number XMULAC20120075) and were conducted under the National Institutes of Health Guidelines for the Care and Use of Laboratory Animals. All efforts were made to minimize the number of animals used and their suffering.

2.4. Experimental Design

2.4.1. Triton WR-1339 Induced Hyperlipidaemia. Acute hyperlipidaemia, induced by intraperitoneal injection of Triton WR-1339, was used for the screening essay.

The mice were randomly divided into seven groups of 8 mice each. One group served as the normal control group (NCG) and another as the hyperlipidemia control groups (HCG) while the remaining 5 groups served as the medicated groups. NCG received intraperitoneal administration of normal saline and other groups of animals were treated with Triton WR-1339. NCG and HCG were treated with distilled water by intragastric administration. The medicated groups were treated with fenofibrate (HCG + Fen), CAE at 1500 mg/kg BW (HCG + CAE), CAF1 at 1000 mg/kg BW (HCG + CAF1), CAF2 at 1000 mg/kg BW (HCG + CAF2), and CAF3 at 1000 mg/kg BW (HCG + CAF3) by intragastric administration, respectively. After 12 hours, the animals were anaesthetized with 10% chloral hydrate (400 mg/kg). Blood samples were collected from their eyes and immediately centrifuged (3000 rpm/10 min). Serum was stored at −20°C for biochemical analysis.

2.4.2. High-Fat-Fed Hyperlipidaemia. After 7-day accommodation, hamsters were randomly divided into 6 groups of eight animals each. The first group received distilled water and normal chow diet (NCD) and the second group was administered distilled water and high-fat diet (HFD) while animals in group III received standard drugs, Xuezhikang (250 mg/kg per day), and HFD (HFD + XZK). The group V-VII was treated with CAF3 (100, 250, and 500 mg/kg per day) and HFD (HFD + C100, HFD + C250, and HFD + C500, resp.). The high-fat diet consisted of 88% standard pellet diet, 10% lard, and 2% cholesterol. The blood samples were collected from the hearts of hamsters after 5 weeks of treatment. Livers were removed, cut into small portions, and stored at −20°C before use.

2.5. Biochemical Assays. Serum TC, TG, high density lipoprotein cholesterol (HDL-C), low density lipoprotein cholesterol (LDL-C), aspartate amino transferase (AST), and alanine amino transferase (ALT) levels were determined. The livers were analyzed regarding their superoxide dismutase (SOD), glutathione peroxidase (GSH-Px), and malondialdehyde (MDA). TC, TG, LDL-C, and HDL-C were estimated by using the enzymatic kits (Beijing BHKT Clinical Reagent Co., Ltd, China). AST, ALT, SOD, and MDA were assayed by commercially available kits (Nanjing jiancheng Bioengineering Institute, China). The liver index referred to the ratio of liver weight to animal weight and TC/HDL-C ratio calculated as the ratio of serum TC to HDL-C levels.

2.6. Histological Analysis. Liver tissues from hamsters experiment were fixed in 10% phosphate-buffered formalin for 1 day. Then liver slides (5 μm thick) were cut with a cryostat microtome (Leica CM1950, Germany) and stained with hematoxylin and eosin (H&E) for microscopic examination.

2.7. Hepatic mRNA Expression of L-CAT and SR-BI. Total RNA was isolated from homogenized hamster livers by using TRIzol reagent (Invitrogen, Life Technologies, USA). Reverse transcriptions were performed in 20 μL mixture with 1 μg of total RNA according to the RT kit (MBI Fermentas, Canada). Primer sequences of hamster genes used in real-time PCR are listed as follows: L-CAT: 5′-TGGATGTGCTACCGTAAGACA-3′ (sense), 5′-TGTGGTTGTAGACAATCCTGGT-3′

(antisense) [16]; SR-BI: 5′-TTTGGAGTGGTAGTAAAA-AGGGC-3′ (sense), 5′-TGACATCAGGGACTCAGAGTA-G-3′ (antisense) [16], glyceraldehyde 3-phosphate dehydrogenase (GAPDH): 5′-GACCCCTTCATTGACCTCAAC-3′ (sen-se), 5′-GGAGATGATGACCCTTTTGGC-3′ (antisense) [17].

Real-time PCR was performed with the 7300 Real-Time PCR System (Applied Biosystems) and SYBR Green (Applied Biosystems) to measure gene expression. The cycling program was set as follows: thermal activation for 30 s at 95°C and 40 cycles of PCR (melting for 5 s at 95°C, followed by annealing/extension for 30 s at 60°C). LCAT and SR-BI gene expression data for individual samples were normalized to the corresponding GAPDH gene expression.

2.8. Analysis of AA, MA, AD, and MD in CAF3. AA, MA, AD, and MD in CAF3 were analyzed by high performance liquid chromatography (HPLC). The HPLC system was an Agilent, equipped with a UV detector at 205 nm. The standards, AA, MA, AD, and MD (Shanghai Yuanye Biotechnology Co., Ltd., China), and CAE, CAF1, CAF2, and CAF3 were dissolved in HPLC-grade methanol. The chromatographic analysis was performed at room temperature with a Cosmosil 5 C_{18}-MS-II (250 mm × 4.6 mm) column using gradient elution of methanol (A) and water (B) according to the following profile for AA and MA: 60%–98% A of 0–25 min, 98% A of 25–35 min; the following profile for AD and MD: 20%–70% A of 0–30 min, 70%–98% A of 30–35 min. The flow rate was 1 mL/min.

2.9. Statistical Analysis. Results were presented as means ± SEM. Data were analyzed by one-way ANOVA test, followed by the Student-Newman-Keuls method. Differences were considered significant at $P < 0.05$. The Prism 5 software package (GraphPad Software Inc., USA) was employed for statistical tests and graphical presentation of the data.

3. Results

3.1. Effect of Centella asiatica Extracts on Triton WR-1339 Induced Hyperlipidemia. It was shown that Triton induced the elevation of TC and TG in serum compared to NCG. As shown in Table 1, it was demonstrated that the levels of TC and TG decreased significantly in the Fen, CAE, and CAF3 treatment groups, compared with the HCG. Among the three groups, the CAF3-treated group had the most significant effects on lowering TC and TG ($P < 0.001$).

3.2. Effect of CAF3 on High-Fat-Diet- (HFD-) Induced Hyperlipidemia. We next investigated the hypolipidemic effects of CAF3 in high-fat-diet- (HFD-) induced hyperlipidemic golden hamster model. After 35 days of high-fat intake, the hamsters gained body weight, liver weight, and liver index (Table 2), but treatment with XZK or CAF3 (100, 250, and 500 mg/kg) appreciably decreased the gain.

The serum lipid profiles of the hamsters in all groups are given in Table 3. In HFD group, serum TC and TG levels were increased by 307% and 181%, respectively. In comparison to the HFD, treatment with XZK and CAF3 (100, 250 and 500 mg/kg) significantly reduced serum TC by 42.5%, 51.8%, 61.3%, and 48.2% and TG by 31.6%, 46.7%, 57.9%, and 23.0%, while LDL-C by 45.0%, 38.4%, 62.0%, and 68.6%. There was no significant difference among HFD and treatment groups for serum HDL-C. For the ratio of TC to HDL-C, HFD hamsters produced a significant increase in this marker while the XZK and CAF3 (100, 250, and 500 mg/kg) reduced it in different degrees.

Table 1: Effect of CA extracts on serum TC and TG levels in mice.

Groups	Dose (mg/kg d^{-1})	TC (mmol/L)	TG (mmol/L)
NCG	—	2.39 ± 0.09	0.26 ± 0.03
HCG	—	6.61 ± 0.62$^{\#\#}$	14.00 ± 1.67$^{\#\#\#}$
HCG + Fen	100	4.07 ± 0.70*	2.84 ± 0.68***
HCG + CAE	1500	2.55 ± 0.27**	4.69 ± 2.11***
HCG + CAF1	1000	4.95 ± 1.23	4.18 ± 1.56***
HCG + CAF2	1000	6.83 ± 1.13	6.99 ± 0.90***
HCG + CAF3	1000	1.39 ± 0.03***	0.65 ± 0.18***

Values are expressed as means ± SEM (standard error of mean) from eight animals in each group; NCG: normal control group; HCG: hyperlipidemia control groups; HCG + Fen: hyperlipidemic + fenofibrate group; HCG + CAE: crude extract group; HCG + CAF1–HCG + CAF3: hyperlipidemic + fractions group.
$^{\#\#}P < 0.01$, $^{\#\#\#}P < 0.001$ compared to NCG.
$^{*}P < 0.05$, $^{**}P < 0.01$, $^{***}P < 0.001$ compared to HCG.

As shown in Table 4, serum ALT and AST levels were significantly lowered in hamsters fed different doses of CAF3 and XZK as compared with HFD ($P < 0.001$).

We also measured the antioxidant activity of CAF3. It was demonstrated in Table 4 that activities of SOD and GSH-Px, two key antioxidant enzymes, were increased, while those of MDA, an indicator of lipid peroxidation, were significantly decreased with treatment of XZK and CAF3 for 35 days (100, 250 and 500 mg/kg).

3.3. Pathologic Changes. In order to examine the pathologic changes, we conducted the H&E staining of livers. It was revealed that the hepatocytes of animals in the NCD group had no hepatic steatosis, with normal hepatic sinusoids for mass transter (Figure 1(a)). But lipid deposits as macrovesicular and microvesicular steatosis were abundant in hamsters in HFD group, with damaged hepatic sinusoids (Figure 1(b)), compared to NCD group. It was also shown that treatment with XZK and different doses of CAF3 for 5 weeks substantially repressed these changes in HFD hamsters (Figures 1(c), 1(d), 1(e), and 1(f)). No necrotic cells or histologic evidence of hepatotoxicity was observed in standard or high-fat-diet-fed hamsters or any drug-treated hamsters.

3.4. Effect of CAF3 on LCAT and SR-BI mRNA Expression Levels. To better understand the mechanism of antihyperlipidemic activity of CAF3, we performed real-time PCR assay to investigate the mRNA expression of LCAT and SR-BI which play the key role in reversing cholesterol transport (RCT). It was revealed that the mRNA expression of LCAT and SR-BI was decreased in the hyperlipidemia model group,

Table 2: Effect of CAF3 on body weight, liver weight, and liver index in hyperlipidemic golden hamsters.

Groups	Dose (mg/kg d^{-1})	Initial body weight (g)	Final body weight (g)	Liver weight (g)	Liver index (g/100 g)
NCD	—	87.00 ± 3.83	96.75 ± 8.97	3.27 ± 0.41	3.33 ± 0.13
HFD	—	87.14 ± 4.74	124.50 ± 4.635$^{\#}$	7.12 ± 0.32$^{\#\#\#}$	5.73 ± 0.22$^{\#\#\#}$
HFD + XZK	250	87.13 ± 2.70	101.50 ± 4.48*	5.76 ± 0.32*	5.38 ± 0.10
HFD + C100	100	86.25 ± 2.34	104.00 ± 4.04*	5.35 ± 0.27**	5.06 ± 0.21
HFD + C250	250	85.20 ± 2.19	85.00 ± 5.58***	4.24 ± 0.32***	4.47 ± 0.18***
HFD + C500	500	84.60 ± 2.90	93.75 ± 8.12*	5.25 ± 0.53**	5.59 ± 0.24

Values are expressed as means ± SEM from 8 animals each group; NCD: normal chow diet group; HFD: high-fat diet group; HFD + XZK: high-fat diet + Xuezhikang group; HFD + C100, HFD + C250, HFD + C500: high-fat diet + CAF3 (100, 250, 500 mg/kg) group, respectively.
$^{\#}P < 0.05$, $^{\#\#\#}P < 0.001$ compared to NCD.
$^{*}P < 0.05$, $^{**}P < 0.01$, $^{***}P < 0.001$ compared to HFD.

Table 3: Effect of CAF3 on serum lipid profile in hyperlipidemic golden hamsters.

Groups	Dose (mg/kg d^{-1})	TC (mmol/L)	TG (mmol/L)	HDL-C (mmol/L)	LDL-C (mmol/L)	TC/HDL-C
NCD	—	1.75 ± 0.15	0.54 ± 0.10	1.16 ± 0.19	2.55 ± 0.25	1.71 ± 0.26
HFD	—	7.13 ± 1.15$^{\#\#\#}$	1.52 ± 0.16$^{\#\#\#}$	3.22 ± 0.28$^{\#\#\#}$	9.68 ± 1.33$^{\#\#\#}$	2.46 ± 0.22$^{\#}$
HFD + XZK	250	4.10 ± 0.32***	1.04 ± 0.07*	2.70 ± 0.17	5.32 ± 0.26***	1.66 ± 0.19*
HFD + C100	100	3.44 ± 0.16***	0.81 ± 0.08***	2.75 ± 0.28	5.96 ± 0.51***	1.40 ± 0.20**
HFD + C250	250	2.76 ± 0.18***	0.64 ± 0.05***	2.93 ± 0.15	3.68 ± 0.33***	0.91 ± 0.08***
HFD + C500	500	3.69 ± 0.61***	1.17 ± 0.21*	2.60 ± 0.13	3.04 ± 0.12***	1.35 ± 0.21**

Values are expressed as means ± SEM from 8 animals each group; NCD: normal chow diet group; HFD: high-fat diet group; HFD + XZK: high-Fat diet + Xuezhikang group; HFD + C100, HFD + C250, HFD + C500: high-fat diet + CAF3 (100, 250, 500 mg/kg) group, respectively.
$^{\#}P < 0.05$, $^{\#\#\#}P < 0.001$ compared to NCD.
$^{*}P < 0.05$, $^{**}P < 0.01$, $^{***}P < 0.001$ compared to HFD.

Table 4: Effect of EPF3 on liver in hyperlipidemic golden hamsters.

Groups	Dose (mg/kg d^{-1})	ALT (U/L)	AST (U/L)	SOD (U/mgprot)	GSH-Px (U/mgprot)	MDA (nmol/mgprot)
NCD	—	24.61 ± 8.81	17.01 ± 2.87	38.45 ± 5.54	3819 ± 305	0.46 ± 0.01
HFD	—	117.8 ± 29.09$^{\#\#\#}$	71.36 ± 12.15$^{\#\#\#}$	20.42 ± 1.41$^{\#\#}$	2160 ± 113$^{\#\#\#}$	0.62 ± 0.04$^{\#\#\#}$
HFD + XZK	250	31.58 ± 5.87***	23.41 ± 1.78***	32.08 ± 1.35*	3044 ± 122*	0.35 ± 0.02***
HFD + C100	100	21.55 ± 5.50***	20.09 ± 2.56***	27.62 ± 1.78	3272 ± 125*	0.35 ± 0.01***
HFD + C250	250	20.20 ± 3.15***	16.29 ± 1.73***	31.57 ± 3.26*	3693 ± 103**	0.40 ± 0.01***
HFD + C500	500	39.64 ± 13.05***	27.44 ± 4.06***	38.15 ± 2.72**	2610 ± 100	0.40 ± 0.01***

Values are expressed as means ± SEM from 8 animals each group; NCD: normal chow diet group; HFD: high-fat diet group; HFD + XZK: high-fat diet + Xuezhikang group; HFD + C100, HFD + C250, HFD + C500: high-fat diet + CAF3 (100, 250, 500 mg/kg) group, respectively.
$^{\#\#}P < 0.01$, $^{\#\#\#}P < 0.001$ compared to NCD.
$^{*}P < 0.05$, $^{**}P < 0.01$, $^{***}P < 0.001$ compared to HFD.

compared with NCD group (Figure 2). Both XZK and CAF3 at three different doses, with C250 having the best effect ($P < 0.01$), significantly elevated the LCAT and SR-BI mRNA levels compared with the HFD group, suggesting that LCAT and SR-BI were involved in the mechanism of lipid-lowering effect of CAF3.

3.5. Quantitative Determination of AA, MA, AD, and MD. Finally we conducted HPLC analysis to determine AA, MA, AD, and MD in CAF3, because they are the characteristic constituents in *Centella asiatica*. But the peaks of AD and MD were hardly separated from the peaks around them, so their data was not shown here. The result of AA and MA showed that the retention time of AA was 19.091 min and that of MA was 16.792 min. CAE, CAF1, CAF2, and CAF3, separately, showed a peak with the same wavelength and retention time of the AA and MA standard. The external standard method was used for quantification, and the result was shown in Table 5.

Table 5: Content of AA and MA in CAE and different fractions.

Content (w/w)	CAE	CAF1	CAF2	CAF3
AA	4.28%	1.35%	1.69%	7.64%
MA	3.36%	1.20%	1.35%	7.68%

4. Discussion and Conclusions

Hyperlipidemia is characterized by excessive amounts of fatty substances such as cholesterol, triglycerides, and lipoproteins

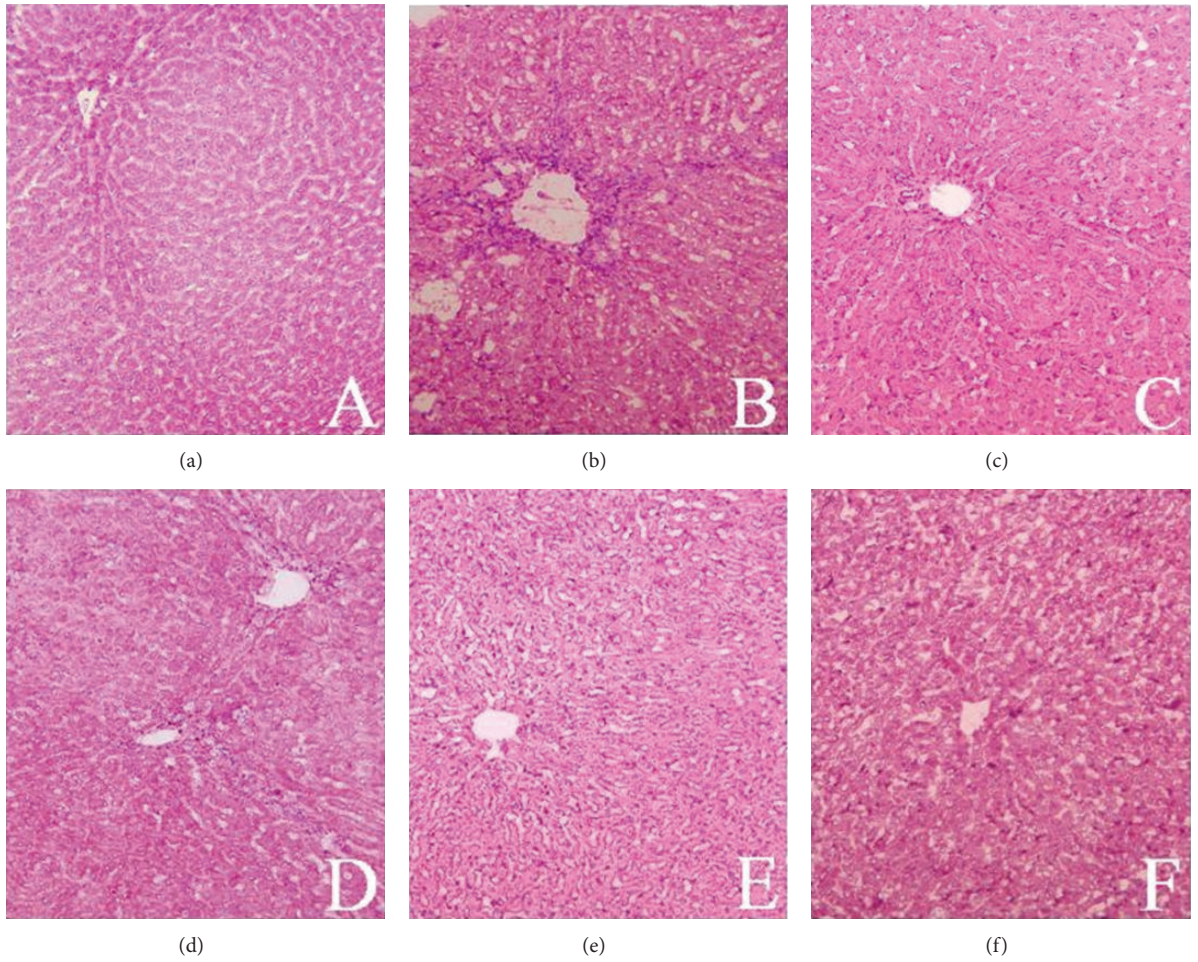

Figure 1: Histological examination detected by HE staining of golden hamsters liver frozen slices (magnification, ×100). (a) NCD; (b) HFD; (c) HFD + XZK (250 mg/kg) group; (d) HFD + C100 (100 mg/kg) group; (e) HFD + C250 (250 mg/kg) group; (f) HFD + C500 (500 mg/kg) group.

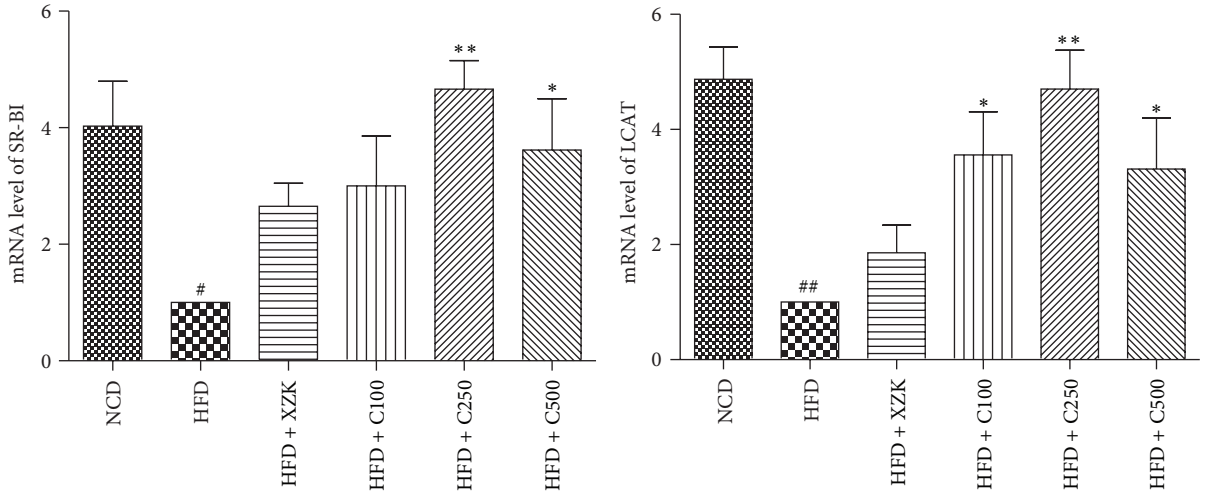

Figure 2: Effect of CAF3 on LCAT and SR-BI mRNA expression levels. A comparative threshold cycle (CT) method was used for relative quantification of gene expression using GAPDH for normalization. Measurements were carried out in triplicate for each sample. Data represents the mean of at least three independent experiments. $^{\#}P < 0.05$, $^{\#\#}P < 0.01$ compared to NCD. $^{*}P < 0.05$, $^{**}P < 0.01$ compared to HFD.

in the blood. The increase in the levels of the proteins and lipids can slow down metabolic processes because of blocked veins and arteries, which can result in cardiovascular disease [2]. The development of hyperlipidemia is related with high-fat diet and oxidative stress [18, 19]. There has been increasing interest in plants and natural products from them with respect to their antioxidant and lipid-lowering activity [6]. We use both acute and high-fat-fed hyperlipidemic models to illustrate the lipid-lowering effect of *Centella asiatica* and its antioxidant capacity in vivo.

The acute hyperlipidemic model was established by intraperitoneal injection of Triton WR-1339. Triton WR-1339 is a well-known nonionic detergent that has been used to induce acute hyperlipidemia in several animal models because of its ability to block TG-rich lipoprotein clearance and to increase hepatic cholesterol biosynthesis [20]. In our experiments, lipid concentrations (TC, TG, and LDL-C) in mice plasma were increased with Triton WR-1339 administration (Tables 2 and 3), similar to what was observed in other studies [21, 22]. Our result also demonstrated that CAF3 had the best effect on decreasing TG and TC level among all the *Centella asiatica* extracts and fractions. It suggests that the most effective compounds mainly were enriched in CAF3 by HPD-450 macroporous resin column chromatography.

The hypolipidemic effect of *Centella asiatica* was also estimated in high-fat-diet-induced hyperlipidemic hamster model. Hamsters have similar lipoprotein and bile acid metabolism patterns as humans [23]. We studied the effect of CAF3 on blood lipids of hamsters and it was shown that it lowered TC, TG, LDL-C, and TC/HDL-C (an indication of occurrence of coronary heart disease [24]) levels (Table 3). These results were consistent with those in the acute hyperlipidemia experiment in mice.

To explore the possible mechanism of hypolipidemic activity of *Centella asiatica*, we detected the gene expression of LCAT and SR-BI. LCAT is responsible for the synthesis of cholesteryl esters (CE) in human plasma [25]. It converts cholesterol into cholesteryl esters and may play the role in reversing cholesterol transport (RCT) [26]. LCAT activity was decreased in high-fat diet [27], and similar result has been reported in our study. SR-BI is a well-established HDL receptor and plays a key role in regulating plasma cholesterol levels [28]. Hepatic SR-BI expression is also an important positive regulator of RCT [29]. To conclude, LCAT and SR-BI jointly promote the process of RCT, which thus may play a role in reducing blood lipid and preventing hyperlipidemia. In the hamster study, we demonstrated that CAF3 enhanced the mRNA expression of LCAT and SR-BI in HFD-treated hamster livers. It indicates that the hypolipidaemic effect of CAF3 could be associated with upregulated RCT process.

Reactive oxygen species (ROS), commonly generated with a high-fat diet, have been observed in organs and tissues [30], as well as in the liver of the hyperlipidemic hamsters in our experiment. In our study, decreased SOD and GSH-Px and elevated MDA, which correlates with ROS, were detected when the hamsters were fed a high-fat diet (Table 4). As a result, hepatocytes of HFD hamsters were damaged, which was evident from elevated AST and ALT (Table 4) and H&E staining results of livers (Figure 1).

After treatment with CAF3 for 35 days, the hepatic levels of SOD and GSH-PX increased, and MDA decreased. This suggests that EPF3 has antioxidant capacity in vivo and hence protects the hepatocytes, which can tell from the reduced levels of AST and ALT (Table 4) and improved hepatic sinusoids (Figure 1). As the liver is in a better condition, it is able to regulate the metabolism of lipids more efficiently. This is confirmed by the reduction of the increased plasma lipid profile (Table 3).

It was reported that *Centella asiatica* is characteristic of some triterpenes, such as asiaticoside (AD), madecassoside (MD), asiatic acid (AA), and madecassic acid (MA) [31]. Therefore, we determined the contents of the four compounds in CAF3 to determine the active constituents against hyperlipaemia. The results showed that CAF3 contained the highest concentration of AA and MA, which happened to be reported to possess very good antioxidant capacity [14, 31]. AD and MD might also contribute to the hypolipidemic effect of *Centella asiatica*, but we cannot quantify them properly.

In conclusion, *Centella asiatica*, whose effective fraction is CAF3 and effective compounds are likely to be asiatic acid and madecassic acid, has antioxidant capacity both in vitro and in vivo, and it regulates lipid metabolism by antioxidant effect and LCAT and SR-BI enhancement. Taken together, *Centella asiatica* has the potential to be used for lipid regulation.

Conflict of Interests

The authors declare that there is no conflict of interests regarding the publication of this paper.

Authors' Contribution

Yun Zhao, Ping Shu, and Youzhi Zhang contributed equally to this work.

Acknowledgments

The authors would like to thank Professor Qiu Yan from the Medical College of Xiamen University for his valuable help. This study was supported by the Research Fund of Strait (Xiamen) Technology Platform in Traditional Chinese Medicine (3502Z20100006).

References

[1] S. H. H. Chan, M.-H. Tai, C.-Y. Li, and J. Y. H. Chan, "Reduction in molecular synthesis or enzyme activity of superoxide dismutases and catalase contributes to oxidative stress and neurogenic hypertension in spontaneously hypertensive rats," *Free Radical Biology and Medicine*, vol. 40, no. 11, pp. 2028–2039, 2006.

[2] W. P. Castelli, R. J. Garrison, P. W. F. Wilson, R. D. Abbott, S. Kalousdian, and W. B. Kannel, "Incidence of coronary heart disease and lipoprotein cholesterol levels. The Framingham study," *The Journal of the American Medical Association*, vol. 256, no. 20, pp. 2835–2838, 1986.

[3] D. Kuo, C. Yeh, P. Shieh, K. Cheng, F. Chen, and J. Cheng, "Effect of ShanZha, a Chinese herbal product, on obesity and dyslipidemia in hamsters receiving high-fat diet," *Journal of Ethnopharmacology*, vol. 124, no. 3, pp. 544–550, 2009.

[4] Y. Hou, W. Shao, R. Xiao et al., "Pu-erh tea aqueous extracts lower atherosclerotic risk factors in a rat hyperlipidemia model," *Experimental Gerontology*, vol. 44, no. 6-7, pp. 434–439, 2009.

[5] M. A. F. Jahromi, A. B. Ray, and J. P. N. Chansouria, "Antihyperlipidemic effect of flavonoids from *Pterocarpus marsupium*," *Journal of Natural Products*, vol. 56, no. 7, pp. 989–994, 1993.

[6] S. H. Thilakarathna and H. P. V. Rupasinghe, "Anti-atherosclerotic effects of fruit bioactive compounds: a review of current scientific evidence," *Canadian Journal of Plant Science*, vol. 92, no. 3, pp. 407–419, 2012.

[7] B. Singh and R. P. Rastogi, "A reinvestigation of the triterpenes of *Centella asiatica*," *Phytochemistry*, vol. 8, no. 5, pp. 917–921, 1969.

[8] J. S. Guo, C. L. Cheng, and M. W. Koo, "Inhibitory effects of *Centella asiatica* water extract and asiaticoside on inducible nitric oxide synthase during gastric ulcer healing in rats," *Planta Medica*, vol. 70, no. 12, pp. 1150–1154, 2004.

[9] M. H. V. Kumar and Y. K. Gupta, "Effect of different extracts of *Centella asiatica* on cognition and markers of oxidative stress in rats," *Journal of Ethnopharmacology*, vol. 79, no. 2, pp. 253–260, 2002.

[10] T. D. Babu, G. Kuttan, and J. Padikkala, "Cytotoxic and antitumour properties of certain taxa of Umbelliferae with special reference to *Centella asiatica* (L.) urban," *Journal of Ethnopharmacology*, vol. 48, no. 1, pp. 53–57, 1995.

[11] L. Lin, L. Liu, L. Chiang, and C. Lin, "*In vitro* anti-hepatoma activity of fifteen natural medicines from Canada," *Phytotherapy Research*, vol. 16, no. 5, pp. 440–444, 2002.

[12] R. Gupta and S. J. S. Flora, "Effect of *Centella asiatica* on arsenic induced oxidative stress and metal distribution in rats," *Journal of Applied Toxicology*, vol. 26, no. 3, pp. 213–222, 2006.

[13] Y. H. Siddique, G. Ara, T. Beg, M. Faisal, M. Ahmad, and M. Afzal, "Protective role of *Centella asiatica* L. extract against methyl methanesulphonate and cyclophosphamide induced genotoxic damage in cultured human lymphocytes," *Recent Progress in Medicinal Plants*, vol. 19, no. 1, pp. 369–381, 2007.

[14] P. Pakdeechote, S. Bunbupha, U. Kukongviriyapan, P. Prachaney, W. Khrisanapant, and V. Kukongviriyapan, "Asiatic acid alleviates hemodynamic and metabolic alterations via restoring eNOS/iNOS expression, oxidative stress, and inflammation in diet-induced metabolic syndrome rats," *Nutrients*, vol. 6, no. 1, pp. 355–370, 2014.

[15] K. H. Lin, Y. Y. Yang, C. M. Yang et al., "Antioxidant activity of herbaceous plant extracts protect against hydrogen peroxide-induced DNA damage in human lymphocytes," *BMC Research Notes*, vol. 6, article 490, 2013.

[16] Q. Liu, S. Liu, L. Li et al., "A dyslipidemia animal model induced by poloxamer 407 in golden hamsters and pilot study on the mechanism," *Acta Pharmaceutica Sinica*, vol. 46, no. 4, pp. 406–411, 2011.

[17] D. Yang, Y. Chang, C. Hsu, C. Liu, Y. Wang, and Y. Chen, "Protective effect of a litchi (*Litchi chinensis* Sonn.)-flower-water-extract on cardiovascular health in a high-fat/cholesterol-dietary hamsters," *Food Chemistry*, vol. 119, no. 4, pp. 1457–1464, 2010.

[18] Q. L. Huang, Y. Jin, L. N. Zhang, P. C. K. Cheung, and J. F. Kennedy, "Structure, molecular size and antitumor activities of polysaccharides from Poria cocos mycelia produced in fermenter," *Carbohydrate Polymers*, vol. 70, no. 3, pp. 324–333, 2007.

[19] W. Ibrahim, U.-S. Lee, C.-C. Yeh, J. Szabo, G. Bruckner, and C. K. Chow, "Oxidative stress and antioxidant status in mouse liver: effects of dietary lipid, vitamin E and iron," *Journal of Nutrition*, vol. 127, no. 7, pp. 1401–1406, 1997.

[20] S. Goldfarb, "Rapid increase in hepatic HMG CoA reductase activity and *in vivo* cholesterol synthesis after Triton WR-1339 injection," *Journal of Lipid Research*, vol. 19, no. 4, pp. 489–494, 1978.

[21] A. K. Khanna, F. Rizvi, and R. Chander, "Lipid lowering activity of *Phyllanthus niruri* in hyperlipemic rats," *Journal of Ethnopharmacology*, vol. 82, no. 1, pp. 19–22, 2002.

[22] H. Harnafi, N. E. H. Bouanani, M. Aziz, H. S. Caid, N. Ghalim, and S. Amrani, "The hypolipidaemic activity of aqueous *Erica multiflora* flowers extract in Triton WR-1339 induced hyperlipidaemic rats: a comparison with fenofibrate," *Journal of Ethnopharmacology*, vol. 109, no. 1, pp. 156–160, 2007.

[23] D. K. Spady, E. F. Stange, L. E. Bilhartz, and J. M. Dietschy, "Bile acids regulate hepatic low density lipoprotein receptor activity in the hamster by altering cholesterol flux across the liver," *Proceedings of the National Academy of Sciences of the United States of America*, vol. 83, no. 6, pp. 1916–1920, 1986.

[24] J. Y. Cherng and M. F. Shih, "Preventing dyslipidemia by *Chlorella pyrenoidosa* in rats and hamsters after chronic high fat diet treatment," *Life Sciences*, vol. 76, no. 26, pp. 3001–3013, 2005.

[25] L. Calabresi, S. Simonelli, M. Gomaraschi, and G. Franceschini, "Genetic lecithin:cholesterol acyltransferase deficiency and cardiovascular disease," *Atherosclerosis*, vol. 222, no. 2, pp. 299–306, 2012.

[26] D. J. Rader, E. T. Alexander, G. L. Weibel, J. Billheimer, and G. H. Rothblat, "The role of reverse cholesterol transport in animals and humans and relationship to atherosclerosis," *Journal of Lipid Research*, vol. 50, supplement, pp. S189–S194, 2009.

[27] M. Nakhjavani, A. Morteza, R. Karimi, Z. Banihashmi, and A. Esteghamati, "Diabetes induces gender gap on LCAT levels and activity," *Life Sciences*, vol. 92, no. 1, pp. 51–54, 2013.

[28] K. F. Kozarsky, M. H. Donahee, A. Rigotti, S. N. Iqbal, E. R. Edelman, and M. Krieger, "Overexpression of the HDL receptor SR-BI alters plasma HDL and bile cholesterol levels," *Nature*, vol. 387, no. 6631, pp. 414–417, 1997.

[29] Y. Zhang, J. R. da Silva, M. Reiliy, J. T. Billheimer, G. H. Rothblat, and D. J. Rader, "Hepatic expression of scavenger receptor class B type I (SR-BI) is a positive regulator of macrophage reverse cholesterol transport *in vivo*," *Journal of Clinical Investigation*, vol. 115, no. 10, pp. 2870–2874, 2005.

[30] M. Ming, L. Guanhua, Y. Zhanhai, C. Guang, and Z. Xuan, "Effect of the *Lycium barbarum* polysaccharides administration on blood lipid metabolism and oxidative stress of mice fed high-fat diet *in vivo*," *Food Chemistry*, vol. 113, no. 4, pp. 872–877, 2009.

[31] D. Bian, M. Liu, Y. Li, Y. Xia, Z. Gong, and Y. Dai, "Madecassoside, a triterpenoid saponin isolated from *Centella asiatica* herbs, protects endothelial cells against oxidative stress," *Journal of Biochemical and Molecular Toxicology*, vol. 26, no. 10, pp. 399–406, 2012.

Hindawi Publishing Corporation
Oxidative Medicine and Cellular Longevity
Volume 2014, Article ID 190945, 14 pages
http://dx.doi.org/10.1155/2014/190945

Research Article

Leptin Level and Oxidative Stress Contribute to Obesity-Induced Low Testosterone in Murine Testicular Tissue

Jian Zhao,[1] Lingling Zhai,[2] Zheng Liu,[1] Shuang Wu,[1] and Liping Xu[1]

[1] *Department of Pharmacology, Shenyang Pharmaceutical University, No. 103 Wenhua Road, Shenhe District, Shenyang, Liaoning 110016, China*
[2] *Department of Child and Adolescent Health, School of Public Health, China Medical University, Shenyang, Liaoning 110001, China*

Correspondence should be addressed to Jian Zhao; zll0625@sohu.com and Zheng Liu; zll0625@foxmail.com

Received 7 January 2014; Accepted 3 March 2014; Published 14 April 2014

Academic Editor: Shiwei Deng

Objective. This study evaluated the effects of obesity on the function of reproductive organs in male mice and the possible mechanism of male secondary hypogonadism (SH) in obesity. *Methods*. Ninety-six mice were randomly assigned to three groups: the control group, diet-induced obesity group, and diet-induced obesity resistant group for 8 weeks and 19 weeks. The effects of short- and long-term high-fat diet on the reproductive organs were determined by measuring sperm count and motility, relative testis weight, testosterone level, pathological changes and apoptosis of Leydig cells. Oxidative stress was evaluated by determining malondialdehyde, H_2O_2, NO levels, and GSH in testis tissues. CAT, SOD, GSH-Px and Nrf_2 mRNA were measured by real-time PCR. *Results*. Short- and long-term high-fat diet decreased sperm count and motility, relative testis weight, testosterone level; decreased CAT, SOD, GSH-Px and Nrf_2 mRNA expression; increased MDA, H_2O_2, NO and leptin levels; inhibited the activity of CAT and GSH-Px enzymes. Pathological injury and apoptosis of Leydig cells were found in testis tissue. *Conclusions*. Pathological damage of Leydig cells, oxidative stress in testis tissue, and high level of leptin may provide some evidence to clarify the mechanisms of male SH in obesity.

1. Introduction

There has been an increase in the prevalence of childhood obesity in both developed and developing countries [1]. In the United States, the incidence of childhood obesity is estimated to be 17%, or 12 million children aged between 2 and 19 years [1]. In addition, the prevalence of overweight and obesity is rising in China [2, 3]. Obesity is a multifactorial condition with syndromic and nonsyndromic variants [4–6] and has both immediate and long-term health consequences. Tracking of adiposity from childhood into adulthood is much stronger in obese children [5]. Unfortunately, there are few effective treatments for overweight and obese children [7–9].

It has been demonstrated that obesity has an impact on male reproduction [10]. Male obesity is associated with an increased incidence of low sperm concentration and a progressively low motile sperm count [11, 12]. Even in the absence of organic disease of the hypothalamo-pituitary unit, the prevalence of secondary (hypogonadotropic) hypogonadism (SH) in obese men has been demonstrated in several studies [10, 13, 14]. The pathogenesis and clinicopathological correlates of obesity-associated SH are incompletely understood on the basis of the current literature [15]. The mechanisms involved in the association between male SH and obesity are complex. However, male obesity per se is associated with lower plasma testosterone levels [14]. The development of reproductive organs and male secondary sexual characteristics is promoted by androgens. Spermatogenesis is closely related to androgen secretion. Reduced testosterone may contribute to male SH in obesity [16].

We hypothesize that the reasons for the decrease in testosterone are as follows. (1) Testosterone is mainly secreted in testicular Leydig cells and damage to testicular Leydig cells may contribute to decreased testosterone. (2) An increased number of adipose cells are found in obesity. Adipose cytokines such as leptin are secreted in adipose cells. The

level of adipose cytokines is high and may suppress secretion of testosterone. (3) Oxidative stress is closely related to SH. Approximately 15% of couples attempting to conceive are clinically infertile and male factor infertility is involved in 50% of these cases [17]. Testicular oxidative stress appears to be a common feature in male infertility and is likely to play a significant role in male infertility [18]. However, there is no evidence of an association between oxidative stress and male SH in obese patients.

In this study, weanling mice were fed a high-fat diet for 8 weeks and 19 weeks. The effects of short- and long-term high-fat diet on the function and development of reproductive organs in male mice were determined, as our aim was to assess whether pubertal obesity influenced the function and development of reproductive organs in adults. In addition, the possible mechanism of male SH in obesity was evaluated.

2. Materials and Methods

2.1. Animals, Diet, and Experimental Procedures. 96 4/5-week-old C57BL/6J male mice were obtained from the Experimental Animal Center, China Medical University, Shenyang, China. Mice were fed standard laboratory chow for the 1st week to allow them to adjust to their new environment. Then the mice were randomly assigned to a standard lab diet (10% of calories from fat, 20% of calories from protein, and 70% of calories from carbohydrates, 3.85 kcal/g) or a prepared high-fat diet, which contained 45% kcal from fat (the high-fat diet group) [19], for 8 or 19 weeks. The high-fat diet was made up of 73% standard chow diet plus 20% lard, 7% casein (Ao-boxing Biotech Company Ltd., Beijing, China), and trace amounts of multiple vitamins.

The animals were housed in a temperature- and humidity-controlled room (25 ± 2°C and 55 ± 10%, resp.) on a 12-hour light/dark cycle with free access to food and water. All experimental procedures conformed to the Institutional Guidelines for the Care and Use of Laboratory Animals of China Medical University, Shenyang, China, and to the National Institutes of Health Guide for Care and Use of Laboratory Animals (publication number 85-23, revised in 1985). All efforts were made to minimize the number of animals used and their suffering.

After 8 or 19 weeks on their respective diets, mice fed the high-fat diet were divided by body weight gain into DIO-R (diet-induced obesity resistant) and DIO (diet-induced obesity) mice, according to the method used by Levin and Keesey [20] shown in Figure 1. Twelve mice in the upper tertile of body weight gain (11.54 ± 0.42 g, 16.58 ± 1.39 g) were designated as DIO at 8 weeks and 19 weeks, respectively, and 12 mice in the lower tertile of body weight gain (BWG) (8.75±1.24 g, 12.00±1.23 g) as DIO-R at 8 weeks and 19 weeks, respectively. Mice with intermediate tertile body weight gain ($n = 24$) were excluded from this study. All mice in each group were sacrificed after 8 and 19 weeks of feeding.

2.2. Processing of Tissues and Assays. Body weight and food consumption were recorded. At 24 hours after receiving the last feed, animals were anesthetized with ether and blood samples were obtained from the vena cava. Serum was separated for measurement of the sex hormone, testosterone. Immediately after blood samples were collected, the epididymis was rapidly excised, and sperm count and motility were determined. Retroperitoneal fat, epididymal fat, epididymal tissue, and testis and seminal vesicles were obtained and weighed.

Six testicles from each group were prepared as a 5% or 10% homogenate in order to determine MDA, T-AOC, H_2O_2, SOD, GSH, GSH-Px, CAT, and NO levels. Six testicles from each group were immediately frozen at −80°C for gene expression studies.

Six testicles from each group were prepared for transmission electron microscopy. The testis was cut into fragments (1 mm × 1 mm × 1 mm), fixed in 2.5% glutaraldehyde with 0.1 M phosphate buffer (pH 7.2), postfixed in 1.0% osmium tetroxide (OsO_4), dehydrated in a progressive ethanol and acetone solution, embedded in Epon 812, sectioned using an LKB ultramicrotome, and stained with uranyl acetate followed by lead citrate, then observed by H-600 microscopy, and photographed.

The remaining six testicles from each group were prepared for pathological analysis.

All the contents and enzyme activities were normalized to the protein which was measured by the method of Lowry [21], using bovine serum albumin (BSA) as standard. Each sample was tested in triplicate.

2.3. Cauda Epididymal Sperm Count and Motility Measurements. Male C57BL/6J mice were weighed and anesthetized at 8 and 19 weeks. The left epididymis was immediately removed. The epididymis and vas deferens were dissected away from the fat. In a 6-well plate, the epididymis and vas deferens from each animal were placed in a well containing 1.0 mL of M2 buffer. The epididymis was then cut at the junction between the corpus and cauda epididymis, and the cauda was placed into a well with 1.0 mL of M2 buffer. Several cuts were made in the cauda epididymis with scissors, and sperm was gently pressed. Sperm was also obtained from the vas deferens in a separate well and then removed from the plate. The pressed sperm from the cauda epididymis was then collected in an Eppendorf tube. Using a hemocytometer (15 mL per side), sperm counts were determined as the number of sperm per microliter.

Sperm count and motility were assessed in accordance with WHO guidelines [22] (≥200 sperm counted for each sample). Sperm count was determined using a hemocytometer. Sperm motility was assessed blindly under a light microscope by classifying 200 sperms per animal as either progressive motile, nonprogressive motile, or immotile. Motility was then expressed as percent of total motile (progressive motile and nonprogressive motile sperm).

2.4. Pathological Analysis. Testicular tissue was removed and the tissue was fixed with 4% paraformaldehyde. Part of the testicular tissue from each mouse was cut into 4 μm thick pieces. Hematoxylin and eosin (HE) staining was performed

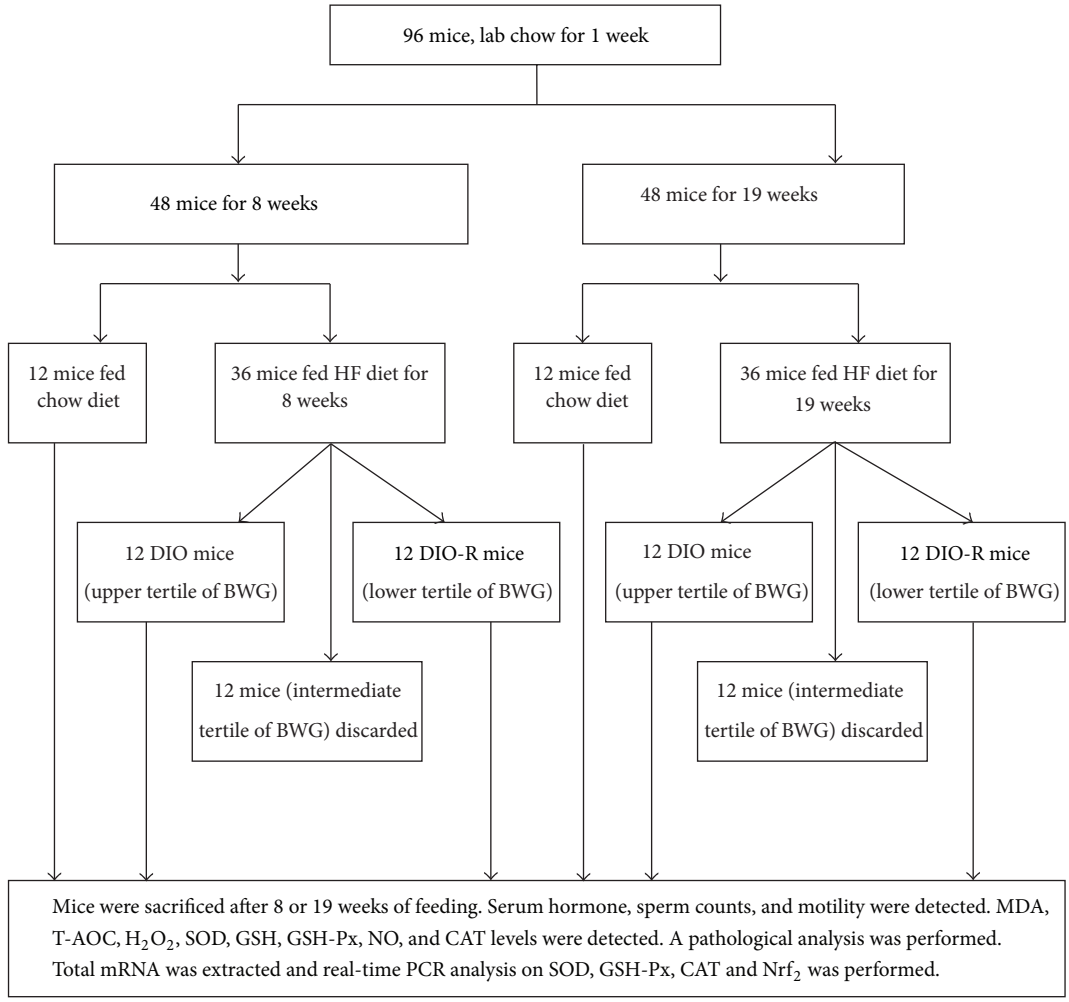

Figure 1: The flowchart of the animal experiment.

for morphological observation using an AX-70 microscope (Olympus, Japan).

The testicular tissue samples were dehydrated in a graded series of ethanol solution, embedded in paraffin, and coronal sectioned using a section cutter (Leica, USA) at a thickness of 4 μm. The testicular sections were processed for apoptosis TUNEL staining and were prepared for subsequent microscopic mounting (each group, $n = 6$, 3 sections per animal) as follows. (1) Paraffin sections were dewaxed. (2) 1% triton-100 was added for 15 min, and all slides were rinsed with PBS 3 times. (3) The enzyme was inactivated with 3% H_2O_2-methanol for 15 min; all slides were rinsed with PBS 3 times. (4) 100 μL TUNEL reaction mixture (or 100 μL control solution for negative control) was added to each slide and the slides were incubated in a humid chamber for 60 min at 37°C and then washed with PBS 3 times. (5) The slides were wiped around the tissue and 100 μL streptavidin-HRP was added to each sample. The slides were incubated in a humid chamber for 30 min at 37°C. The slides were washed once with PBS and then washed 3 times with 100 mM tris buffer and pH 8.2 for 5 min at room temperature. (6) DAB chromogenic was added. (7) dH_2O was added to stop the color reaction. Apoptotic cells were stained brown and normal cells were blue-violet. The apoptotic rate = (apoptotic cells/total number of cell) × 100%. A pathological analysis was performed in testis tissue. Total mRNA was extracted from testis tissue and real-time PCR analysis on SOD, GSH-Px, CAT and Nrf_2 was performed.

2.5. MDA Assay. The testis homogenate was added to the reaction mixture containing 0.1 mol/L phosphate buffer and 0.1 mol/L $FeCl_3$ in a total volume of 1.0 mL (pH = 7.4). The reaction was stopped by the addition of 1.0 mL 10% trichloroacetic acid (TCA), followed by 1.0 mL 0.67% TBA, and the tubes were placed in a boiling water bath for 20 min. The tubes were then moved to an ice bath and the contents were centrifuged at 2500 g for 10 min. The amount of MDA formed in each of the samples was assessed by measuring the optical density of the supernatant at 535 nm using tetraethoxypropane (TEP) as a standard. MDA content was expressed as nmol·mg^{-1} protein.

2.6. Glutathione Assay. GSH in testicular homogenate was determined by the reaction with 5,5′-dithiobis-(2-

Nitrobenzoic Acid) (DTNB). Briefly, 0.9 mL of 10% testicular homogenate was added to 0.1 mL of 50% TCA, and the samples were centrifuged at 3000 rpm for 15 min. Then 0.1 mL of supernatant was added in 4.4 mL of 0.1 M PBS and 0.5 mL of 0.04% DTNB to a total volume of 5.0 mL (pH 7.4). The absorbance of the solution was measured spectrophotometrically at 412 nm. The content of GSH was expressed as mg GSH g^{-1} protein.

2.7. GSH-Px, CAT, SOD, H_2O_2, NO, and T-AOC Assays. Assay kits for GSH-Px, CAT, SOD, H_2O_2, NO, and T-AOC were provided by Jiancheng Bioengineering Institute (Nanjing, China). The GSH-Px, CAT, SOD, H_2O_2, NO, and T-AOC contents were measured using these kits following the manufacturer's instructions. The GSH-Px, CAT, SOD, and T-AOC contents were expressed as U·mg^{-1} protein. H_2O_2 content was expressed as mmol g^{-1} protein. NO content was expressed as μmol g^{-1} protein.

2.8. Isolation of RNA and Real-Time PCR Analysis. Total mRNA was extracted from mouse testicular tissue in each group. Real-time PCR was performed with a SYBR green PCR kit (TaKaRa Biotechnology Co., Ltd., Dalian, China) using a real-time PCR system (Applied Biosystems 7500 Real-Time PCR system). Total RNA was extracted from testis using Trizol (TaKaRa Biotechnology Co., Ltd. Dalian, China). The quantity and integrity were characterized using a UV spectrophotometer. OD260/OD280 of total RNA was between 1.6 and 1.8.

Semiquantitative reverse transcription was performed using the PrimeScript RT reagent kit with DNA eraser. Reverse transcription was performed using an Applied Biosystems 2720 Thermal Cycler (Applied Biosystems, Singapore). Remove DNA reaction of 1 μg of total RNA was performed in a final volume of 10 μL, using 2.0 μL 5x gDNA Eraser Buffer, 1.0 μL gDNA Eraser and RNase-Free dH_2O. The reaction was incubated at 42°C for 2 min. Reverse transcription was performed in a final volume of 20 μL, using 10 μL outcome of remove DNA reaction, 1.0 μL Primescript RT Enzyme Mix I, 4.0 μL 5x Primescript buffer 2 and 1.0 μL RT prime Mix and RNase-Free ddH_2O. The reaction was incubated at 37°C for 15 min, then at 85°C for 5 s.

The gene-specific primers were designed by TaKaRa Co. All primers are listed in Table 1. The 50 μL PCR reaction mixture contained 25 μL of 2x PCR buffer, 2 μL of PCR forward primer (10 μM), 2 μL of PCR reverse primer (10 μM), 1 μL of ROX Reference Dye II (50x), 4 μL of template DNA, and 16 μL dH_2O. The initial denaturation was carried out at 95°C for 30 s, followed by amplification in 40 cycles, 95°C for 3 s, and 60°C for 34 s using the 7500 Real-Time PCR system (BD Co., USA). The relative expression analysis was carried out using the $2-\Delta\Delta CT$ method. For which ΔCT (test) = CT (target, test) − CT (reference, test), ΔCT (calibrator) = CT (target, calibrator) − CT (reference, calibrator), and $\Delta\Delta CT$ = ΔCT (Test) − ΔCT (calibrator). The relative expression was calculated by $2-\Delta\Delta CT$. The raw data were normalized to those of the housekeeping gene, β-actin. All reactions were performed in triplicate. Following amplification, a melting curve analysis was performed to verify the correct product according to its specific melting temperature (Tm) [23].

2.9. Statistical Analysis. Significant differences between obtained values (mean ± SD) were determined by one-way analysis of variance (ANOVA) followed by the least significant difference (LSD) multiple comparison test. A P value of <0.05 was considered significant.

3. Results

3.1. Body Weight and Body Fat. A significant difference in body weight was observed in male C57BL/6J mice fed the high-fat diet in comparison to age-matched littermates fed a normal diet at 8 weeks and 19 weeks ($P < 0.01$).

Mice fed the high-fat diet showed increased body weight averaging 28 g at 8 weeks in the DIO group, whereas mice in the DIO-R group averaged 24 g, and littermates fed the normal diet averaged 24 g at the same age (Figure 2(a)). Mice fed the high-fat diet showed increased body weight averaging 33 g at 19 weeks in the DIO group, whereas mice in the DIO-R group averaged 28 g, and littermates fed the normal diet averaged 27 g at the same age (Figure 2(b)).

Absolute and relative retroperitoneal (Ret) and epididymal (Epi) fat pads were significantly higher in the DIO group and DIO-R group versus the control group mice at 8 weeks and 19 weeks (Table 2) ($P < 0.01$).

3.2. Effect of Diet on Reproductive Organs. As shown in Table 2, DIO, DIO-R, and control mice did not exhibit significant differences in the absolute average weight of testes or epididymis at 8 weeks and 19 weeks. However, there was a significant decrease in the relative testis weight in the DIO group compared to the control group at 8 weeks ($P < 0.05$). There was a significant decrease in the relative testis weight and epididymal weight in the DIO group compared with the control group at 19 weeks ($P < 0.05$). The relative testis weight in the DIO group was lower than that in the DIO-R group at 8 weeks and 19 weeks. However, the absolute weight of seminal vesicles in the DIO and DIO-R groups was significantly higher than the normal group at 8 weeks ($P < 0.05$). The relative weight of seminal vesicles in the DIO and normal groups was lower than that in the DIO-R group at 8 weeks ($P < 0.01$).

3.3. Effect of Diet on Sperm Count and Motility. DIO, DIO-R, and control male mice exhibited no disparities in morphology or total sperm count collected from the cauda epididymis at 8 weeks. However, the DIO and DIO-R group exhibited a notable 28% decrease in sperm motility at 8 weeks ($P < 0.05$) (Figure 2(c)). At 19 weeks, there was a significant increase in total sperm count in the DIO-R group compared with the control group ($P < 0.05$). In addition, the DIO group exhibited a notable 37% decrease in sperm motility ($P < 0.05$) (Figure 2(d)).

3.4. Effect of Diet on Serum Testosterone and Leptin. As shown in Table 3, DIO and DIO-R mice exhibited decreased fasting

Table 1: Primer sequences for real-time RT-PCR analysis.

Gene	GenBank	Forward	Reverse
CAT	NM_009804	ACATGGTCTGGGACTTCTGG	CAAGTTTTTGATGCCCTGGT
GSH-Px	NM_008160	GTCCACCGTGTATGCCTTCT	TCTGCAGATCGTTCATCTCG
SOD	NM_0136713	TCAAGCGTGATTTGGGTCT	AGCGGAATAAGGCCTGTTGT
Nrf_2	NM_172086	CTCGCTGGAAAAAGAAGTGG	CCGTCCAGGAGTTCAGAGAG

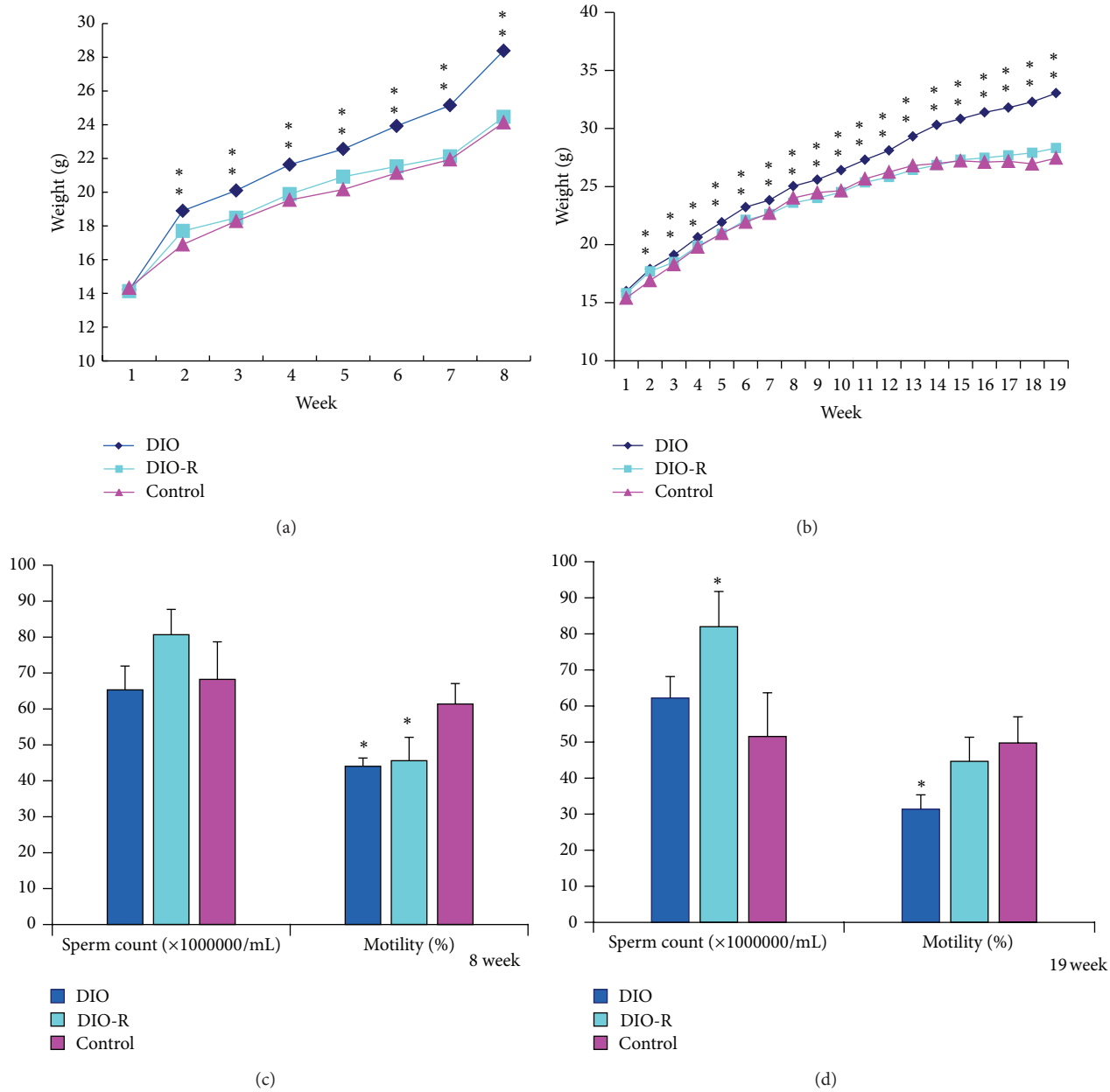

Figure 2: Effect of high-fat feeding on body weight and sperm count, motility in 8 weeks and 19 weeks. All data are expressed as means ± SD; $^{*}P < 0.05$, $^{**}P < 0.01$, versus control group. (a) Bodyweights at the end of 8 weeks of control mice ($n = 12$) fed a 10% fat diet and diet-induced obesity (DIO) mice ($n = 12$) and diet-induced obesity resistant (DIO-R) mice ($n = 12$) fed a 45% fat diet for the times indicated, (b) bodyweights at the end of 19 weeks of control mice ($n = 12$) fed a 10% fat diet and diet-induced obesity (DIO) mice ($n = 12$) and diet-induced obesity resistant (DIO-R) mice ($n = 12$) fed a 45% fat diet for the times indicated, (c) sperm count and motility in control ($n = 6$), DIO-R ($n = 6$), and DIO mice ($n = 6$) at the end of 8 weeks, and (d) sperm count and motility in control ($n = 6$), DIO-R ($n = 6$), and DIO mice ($n = 6$) at the end of 19 weeks.

Table 2: The retroperitoneal, epididymal fat weight and reproductive organs weight in 8 weeks and 19 weeks ($\overline{x} \pm$ SD).

	Group	n	Ret. fat (g)	Relative Ret. fat (g/100 g)	Epi. fat (g)	Relative Epi. fat (g/100 g)	Tes. weight (g)	Relative Tes. weight (g/100 g)	Epididymis weight (g)	Relative epididymis weight (g/100 g)	Sem. weight (g)	Relative Sem. weight (g/100 g)
8 weeks	DIO	12	$0.09 \pm 0.03^{**}$	$0.34 \pm 0.13^{**}$	$0.32 \pm 0.09^{**}$	$1.23 \pm 0.29^{**}$	0.19 ± 0.02	$0.77 \pm 0.06^{*\#}$	0.07 ± 0.01	0.29 ± 0.06	$0.22 \pm 0.02^{*}$	$0.87 \pm 0.11^{\#\#}$
	DIO-R	12	$0.08 \pm 0.03^{**}$	$0.37 \pm 0.13^{**}$	$0.32 \pm 0.07^{**}$	$1.49 \pm 0.25^{**}$	0.18 ± 0.01	0.86 ± 00.07	0.07 ± 0.01	0.31 ± 0.02	$0.24 \pm 0.03^{**}$	1.12 ± 0.15
	Control	12	0.03 ± 0.01	0.12 ± 0.04	0.19 ± 0.04	0.91 ± 0.18	0.18 ± 0.03	0.85 ± 0.10	0.06 ± 0.01	0.31 ± 0.05	0.19 ± 0.03	$0.91 \pm 0.16^{\#\#}$
19 weeks	DIO	12	$0.49 \pm 0.19^{**}$	$1.49 \pm 0.55^{**}$	$1.15 \pm 0.34^{**}$	$3.52 \pm 0.99^{**}$	0.20 ± 0.02	$0.62 \pm 0.08^{**\#\#}$	0.08 ± 0.01	$0.25 \pm 0.05^{**}$	0.31 ± 0.07	0.96 ± 0.21
	DIO-R	12	$0.20 \pm 0.06^{**}$	$0.73 \pm 0.22^{**}$	$0.62 \pm 0.19^{**}$	$2.27 \pm 0.67^{**}$	0.20 ± 0.01	0.72 ± 0.05	0.07 ± 0.01	0.27 ± 0.05	0.28 ± 0.060	1.02 ± 0.23
	Control	12	0.077 ± 0.037	0.28 ± 0.12	0.33 ± 0.06	1.19 ± 0.19	0.20 ± 0.02	0.75 ± 0.07	0.08 ± 0.01	0.30 ± 0.02	0.27 ± 0.06	1.01 ± 0.21

Note. Data are mean ± SD; $^{*}P < 0.05$ and $^{**}P < 0.01$ denote statistical significance compared with control group; $^{\#}P < 0.05$ and $^{\#\#}P < 0.01$ denote statistical significance compared with DIO-R group. Ret: retroperitoneal; Epi: epididymal; Tes: testis; Sem: seminal vesicles.

Relative ret. weight = retroperitoneal fat weight/body weight × 100. Relative Epi. fat weight = epididymal fat weight/body weight × 100. Relative Tes. weight = testis weight/body weight × 100. Relative epididymis weight = epididymis weight/body weight × 100. Relative Sem. weight = seminal vesicles weight/body weight × 100.

Table 3: Testosterone and leptin level in DIO, DIO-R, and control group ($\overline{x}$ ± SE).

Group	n	Testosterone (ng/mL)/8 W	Leptin (ng/mL)/8 W	Testosterone (ng/mL)/19 W	Leptin (ng/mL)/19 W
DIO	12	7.52 ± 0.25*	34.87 ± 4.37**	6.33 ± 0.56**	13.92 ± 1.96**
DIO-R	12	6.80 ± 0.23**	15.35 ± 2.69**	8.68 ± 1.68*	10.07 ± 1.37*
Control	12	10.81 ± 1.69	1.92 ± 0.34	12.68 ± 0.99	1.86 ± 0.24

Note. Data are mean ± SE. *$P < 0.05$ and **$P < 0.01$ denote statistical significance compared with control group.

levels of testosterone at 8 weeks. Significantly higher serum testosterone levels were observed in the control group when compared to the DIO and DIO-R group at 8 weeks and 19 weeks ($P < 0.05$). And significantly lower serum leptin levels were observed in the control group when compared to the DIO and DIO-R group at 8 weeks and 19 weeks ($P < 0.05$, $P < 0.01$).

3.5. Effect of Diet on Pathological Changes. To confirm the effects of exposure to the high-fat diet on morphological changes in testicular tissue, HE staining and electron microscopy were performed. Light microphotographs showed morphological changes in testicular cells after 8 and 19 weeks of the high-fat diet (Figure 3). No significant difference was observed between the groups. Electron microscopy of mouse testes was performed following the high-fat diet for 8 weeks and 19 weeks. Sperm formation was normal in the control group, and normal morphology of spermatids and normal stromal cells and blood vessels were found in all groups. However, a large number of lipid droplets, irregular karyotype, and heterochromatin side set were found in the DIO and DIO-R groups at 8 weeks and 19 weeks (Figure 4).

To determine testicular tissue apoptosis caused by high-fat diet, the TUNEL apoptosis assay was used to quantify the rate of cell apoptosis. This assay showed that few cells were viable (brown staining) in controls (Figures 5(a) and 5(d)). Many apoptotic cells (brown staining) were found in the DIO-8w, DIO-R-8w, DIO-19w, and DIO-R-19w groups (Figures 5(b), 5(c), 5(e), and 5(f)). The high-fat diet increased apoptosis rates by 1.24-, 1.36-, 1.48-, and 1.29-fold as compared to the normal control, respectively (Figure 5).

3.6. Effect of Diet on Oxidative Stress in Testis Tissue. The effect of diet on oxidative stress biomarkers is shown in Table 4. At 8 weeks, diet increased the levels of MDA in testis tissue to 81% and 14% of control in the DIO group and DIO-R group, respectively. When compared with the control group, H_2O_2 levels were increased to 1.53-fold and 1.55-fold in the DIO group and DIO-R group, respectively. NO levels were increased to 1.68-fold in the DIO group and DIO-R group, respectively. A significant decrease in the activity of CAT was observed in the DIO group and DIO-R group compared to the control group ($P < 0.05$) (Table 4). However, there was no difference in T-AOC, GSH, SOD, and GSH-Px levels in testis tissues compared to the control group.

At 19 weeks, it was found that diet increased the levels of MDA in testis tissue to 89% and 138% of the control in the DIO and DIO-R group, respectively. When compared with the control group, H_2O_2 levels were increased to 1.32-fold and 1.23-fold in the DIO group and DIO-R group, respectively. The NO levels in the DIO and DIO-R groups were significantly higher than those in the control group ($P < 0.05$). Although T-AOC levels decreased in both DIO and DIO-R groups, only T-AOC level in the DIO group was significantly lower than that in the control group ($P < 0.05$). The GSH level in the DIO group was significantly higher than that in the control group ($P < 0.05$). A significant decrease in the activity of CAT and GSH-Px was found in the DIO and DIO-R groups compared to the control group ($P < 0.05$) (Table 4). However, there was no difference in SOD levels in testis tissues compared with the control group.

3.7. The Effect of Diet on Antioxidant Gene Expression. The effect of diet on the gene expression level of SOD, GSH-Px, catalase, and Nrf_2 in testis tissue was confirmed by real-time PCR. Figure 6 shows the effect of diet on mRNA expression of the antioxidant genes SOD, GSH-Px, catalase, and Nrf_2 in testis tissue by quantitative detection of gene expression. At 8 weeks, the DIO and DIO-R groups showed significant upregulation of the catalase gene. Other gene expressions were similar between the 3 groups. However, at 19 weeks, the DIO group showed significant downregulation of all the studied genes.

4. Discussion

Testosterone is the most important sex hormone in males and plays a critical role in testis development, spermatogenesis, and maintenance of normal masculinization.

During puberty, testosterone is involved in many of the processes in the transition from a boy to manhood, including healthy development of male sex organs. Throughout adulthood, this hormone also plays an important role in maintaining libido and sperm production.

Disorders of the testes are caused by too little testosterone production. Obesity causes hormonal modification and hypogonadism [24]. Saboor Aftab et al. found that male obesity per se is associated with a lower plasma testosterone level [15]. In the present study, when mice were fed the high-fat diet for 8 or 19 weeks, we found the following: (1) lower plasma testosterone level; (2) decline in sperm motility; (3) Leydig cells damaged with increased apoptosis; (4) decreased testis and epididymis relative coefficient. Pubertal obesity may influence the function and development of reproductive organs in adults. Male obesity may cause hypogonadism which is a testicular disorder associated with low testosterone.

Table 4: MDA, H_2O_2, T-AOC, GSH, SOD, GSH-Px, and CAT level of testis tissue in 8 weeks and 19 weeks ($\overline{x} \pm$ SD).

	Group	n	MDA (nmol/mgprot)	T-AOC (U/mgprot)	SOD (U/mgprot)	GSH (mgGSH/gprot)	H_2O_2 (mmol/gprot)	CAT (U/mgprot)	GSH-Px (U/mgprot)	NO (umol/gprot)
8 weeks	DIO	12	$0.38 \pm 0.20^{**}$	1.03 ± 0.15	50.98 ± 10.26	12.78 ± 1.80	$16.55 \pm 3.73^{*}$	$1.07 \pm 0.31^{*}$	15.98 ± 3.10	$0.32 \pm 0.15^{**}$
	DIO-R	12	$0.24 \pm 0.12^{*}$	1.04 ± 0.20	49.71 ± 10.13	12.88 ± 1.66	$16.75 \pm 4.65^{*}$	$0.98 \pm 0.41^{*}$	13.71 ± 3.69	$0.32 \pm 0.10^{**}$
	Control	12	0.21 ± 0.07	0.94 ± 0.13	53.45 ± 14.64	13.09 ± 1.98	10.82 ± 1.16	1.52 ± 0.25	15.93 ± 3.36	0.19 ± 0.03
19 weeks	DIO	12	$0.89 \pm 0.24^{*}$	$0.73 \pm 0.23^{*}$	71.46 ± 10.63	$13.38 \pm 1.20^{*}$	$16.68 \pm 4.35^{*}$	$0.28 \pm 0.08^{*}$	$26.26 \pm 6.34^{*}$	$0.32 \pm 0.13^{**}$
	DIO-R	12	$1.12 \pm 0.51^{**}$	0.77 ± 0.24	76.97 ± 16.74	12.84 ± 2.81	15.58 ± 2.98	$0.15 \pm 0.07^{**}$	$26.03 \pm 6.34^{*}$	$0.27 \pm 0.06^{*}$
	Control	12	0.47 ± 0.12	0.94 ± 0.16	71.94 ± 7.56	10.92 ± 2.48	12.62 ± 2.69	0.53 ± 0.24	33.52 ± 5.42	0.18 ± 0.05

Note. Data are mean ± SD. $^{*}P < 0.05$ and $^{**}P < 0.01$ denote statistical significance compared with control group.

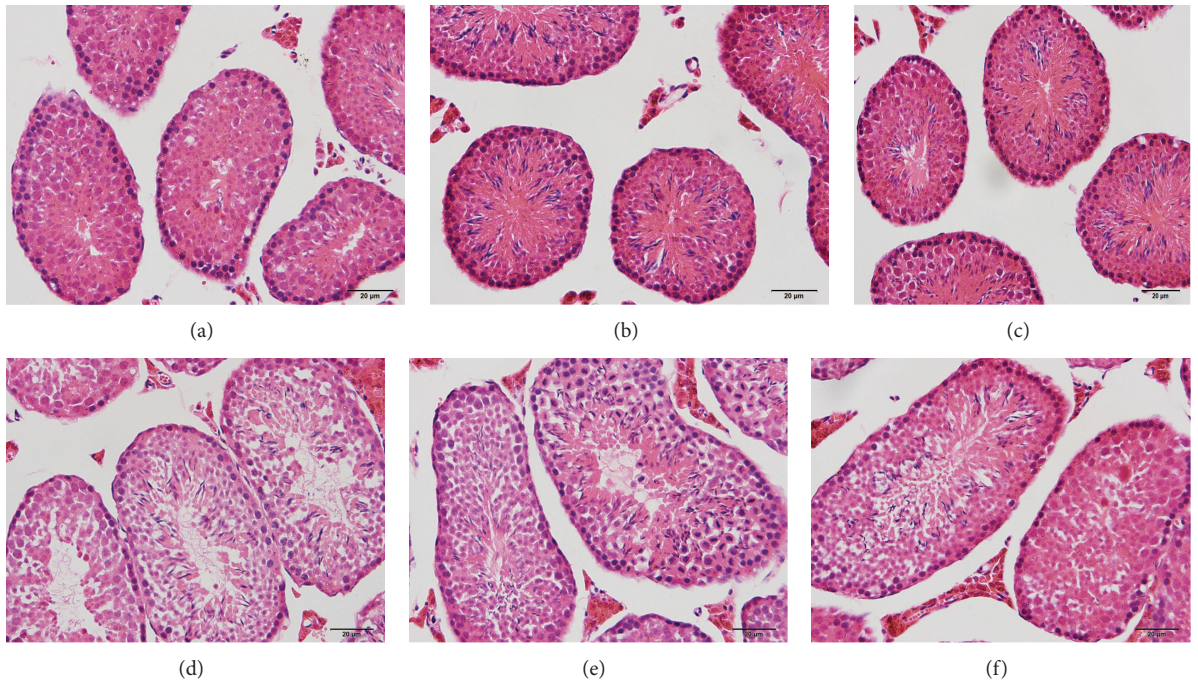

Figure 3: Light microphotographs showed the morphological changes of testicular cells after 8 and 19 weeks of high-fat diet. Photographs of control at 8 weeks (a), DIO group at 8 weeks (b), DIO-R group at 8 weeks (c), control group at 19 weeks (d), DIO group at 19 weeks (e), and DIO-R group (f) at 19 weeks were in this figure. The sections were stained with HE staining. Magnification ×40.

Lower plasma testosterone level plays an important role in male hypogonadism caused by obesity.

In this study, we will discuss the mechanism of low testosterone levels caused by fat intake.

(1) Pathologic Changes in Leydig Cells and Low Testosterone Level Induced by Fat. Leydig cells, also known as interstitial cells of Leydig, produce testosterone in the presence of luteinizing hormone (LH). A large amount of smooth endoplasmic reticulum (SER) is present in Leydig cells, and there is an abundance of the cholesterol synthesis enzyme in the SER. The SER has a strong ability to synthesize cholesterol and is involved in androgen synthesis. When synthesis is active, few lipid droplets are observed and the volume is small. When synthesis is inactive, there are more lipid droplets and the volume is large. The number and volume of lipid droplets can be used to assess the function of Leydig cells. In the present, a large number of lipid droplets and a larger volume in Leydig cells were found in the DIO group compared with the control group. This change in lipid droplets in Leydig cells may reflect the decreased function of testosterone secreted by Leydig cells in the DIO group.

Increased apoptosis of Leydig cells was also found in this study. Apoptosis results from the activation of an intracellular program that leads to cell death without the induction of an inflammatory response. The increase in apoptosis of Leydig cells can reflect degenerative changes in Leydig cells, and the secretion of testosterone in Leydig cells is also decreased. There are numerous molecular pathways related to apoptosis. The primary effect of oxidative stress is on the mitochondrial membrane, where associations between pro- and antiapoptotic members of the Bcl-2 family (e.g., Bax and Bcl-X L or Bcl-2 and Bcl W, resp.) are altered [25, 26] allowing the release of cytochrome c and the eventual activation of a caspase cascade, which ultimately results in the fragmentation of cell DNA [27, 28]. Consistent with this pathway, Bax may be the predominant proapoptotic molecule in mouse testis where it may exhibit increased expression after obesity-induced oxidative stress. We will prove it in another experience.

(2) High Leptin Level and Low Testosterone Level Induced by Fat. Leptin plays an important role in rodent and human reproduction [29, 30]. Recent research demonstrated that leptin directly inhibits human chorionic gonadotropin-(hCG-) stimulated testosterone secretion from rat Leydig cells in culture via a functional leptin receptor isoform and at concentrations within the range of obese men [31, 32]. Others have also shown that leptin inhibits basal and hCG-stimulated testosterone secretion in incubated rat testicular samples [33]. In addition, several studies have demonstrated that leptin levels are inversely correlated with testosterone [34–36]. This correlation is related to the suppressive effect of testosterone and its biologically active metabolite on leptin production [37]. In addition, it was recently proposed that testosterone may regulate ob gene expression [27]. The study by Isidori demonstrated that hyperleptinemia may have a role in the pathogenesis of reduced androgens in male obesity [38]. In this study, the serum concentration of leptin was inversely correlated with testosterone when mice were fed the high-fat diet for 8 or 19 weeks. Caprio et al. found that ob-R expression was present in embryonic, prepubertal, and

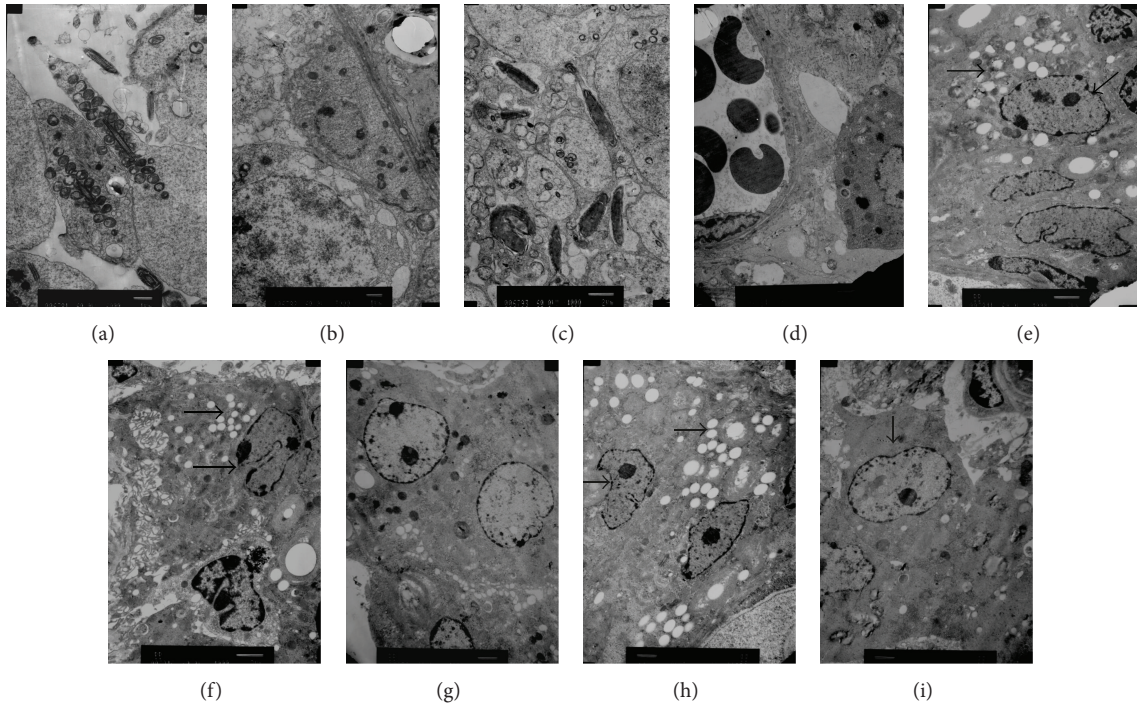

Figure 4: Electron microscopy of mice testes following the diet-induced fat for 8 weeks and 19 weeks shows a large number of lipid droplets, irregular karyotype, and heterochromatin side set (arrow) of Leydig cells ((e), (f), (h), and (i)) compared to control ((d) and (g)). (a) Normal sperm formation in the control group, (b) normal morphology of basement membrane, spermatogonia, and primary spermatocytes in the DIO group, (c) normal morphology of spermatids, (d) normal stromal cells and blood vessels, (e) in Leydig cells: a large number of lipid droplets, irregular karyotype, and heterochromatin side set found in DIO group at 8 weeks, (f) in Leydig cells: a large number of lipid droplets, irregular karyotype, and heterochromatin side set found in DIO-R group at 8 weeks, (g) normal Leydig cells, a small amount of fat vacuolar found in control group at 19 weeks, (h) in Leydig cells: a large number of lipid droplets, irregular karyotype, and heterochromatin side set found in DIO group at 19 weeks, and (i) in Leydig cells: irregular karyotype and heterochromatin side set found in DIO-R group at 19 weeks.

adult rat testes. It is conceivable that high leptin concentration in males may have a direct inhibitory effect on Leydig cell function [32]. Leptin levels in obese human subjects are the best hormonal predictor of obesity-related reduction in androgen response to hCG tests in vivo [38]. The ob → ob-R system in the testis may negatively regulate testosterone production by Leydig cells [32]. Therefore, an excess of circulating leptin may be an important contributor to the development of reduced androgens in male obesity [38].

(3) Oxidative Stress in Testicular Tissue and Low Level of Testosterone Induced by Fat Intake. Many conditions or events associated with male infertility are inducers of oxidative stress and increasing testicular oxidative stress leads to an increase in germ cell apoptosis and subsequent hypospermatogenesis [18]. Several conditions related to male infertility whether therapeutic or pathological generate more reactive oxygen species (ROS) which are associated with reduced intracellular antioxidant activity unable to counter the ROS-mediated detrimental effect. Turner and Lysiak found that very large increases in NO were associated with oxidative stress, which may override the effects of hypoxia-inducible factor 1 (HIF-1) and inhibit testosterone production [18]. Testicular oxidative stress may be associated with decreased testosterone level. In this study, MDA, NO, and H_2O_2 increased and T-AOC (8w and 19w), CAT (8w and 19w), and GSH-Px (19w only) decreased in obese mice. The gene expression of these antioxidant enzymes was found to be reduced at 19 weeks (Figures 2(a)–2(d)). Increased NO levels are recognized as an indication of oxidative stress leading to inhibition of testosterone production [39]. There is evidence that H_2O_2 and NO besides acting as independent signaling molecules may interrelate to form an oxidative death cycle. H_2O_2 acts as an upstream signal leading to NO production [18, 40]. These results suggest that obesity-induced excessive oxidative stress production affected normal histological structures and function of testicular tissue.

Puberty is a complex process by which the androgen secreted by Leydig cells in testis tissue was response to hCG critically. And children develop secondary sexual characteristics and reproductive competence. The reproduction of a pubertal boy may be influenced by unhealthy environments. Taneli et al. demonstrated that obesity affects testicular Leydig cell function in obese adolescents according to pubertal stages [41]. In addition, increased oxidative stress in prepubertal severely obese children and obese adolescents has been reported [42, 43]. Vendramini et al. also found a reduction in sperm production in the pubertal phase in obese Zucker rats [12]. Increased oxidative stress and lipid peroxidation in testis tissue in pubertal obesity (due

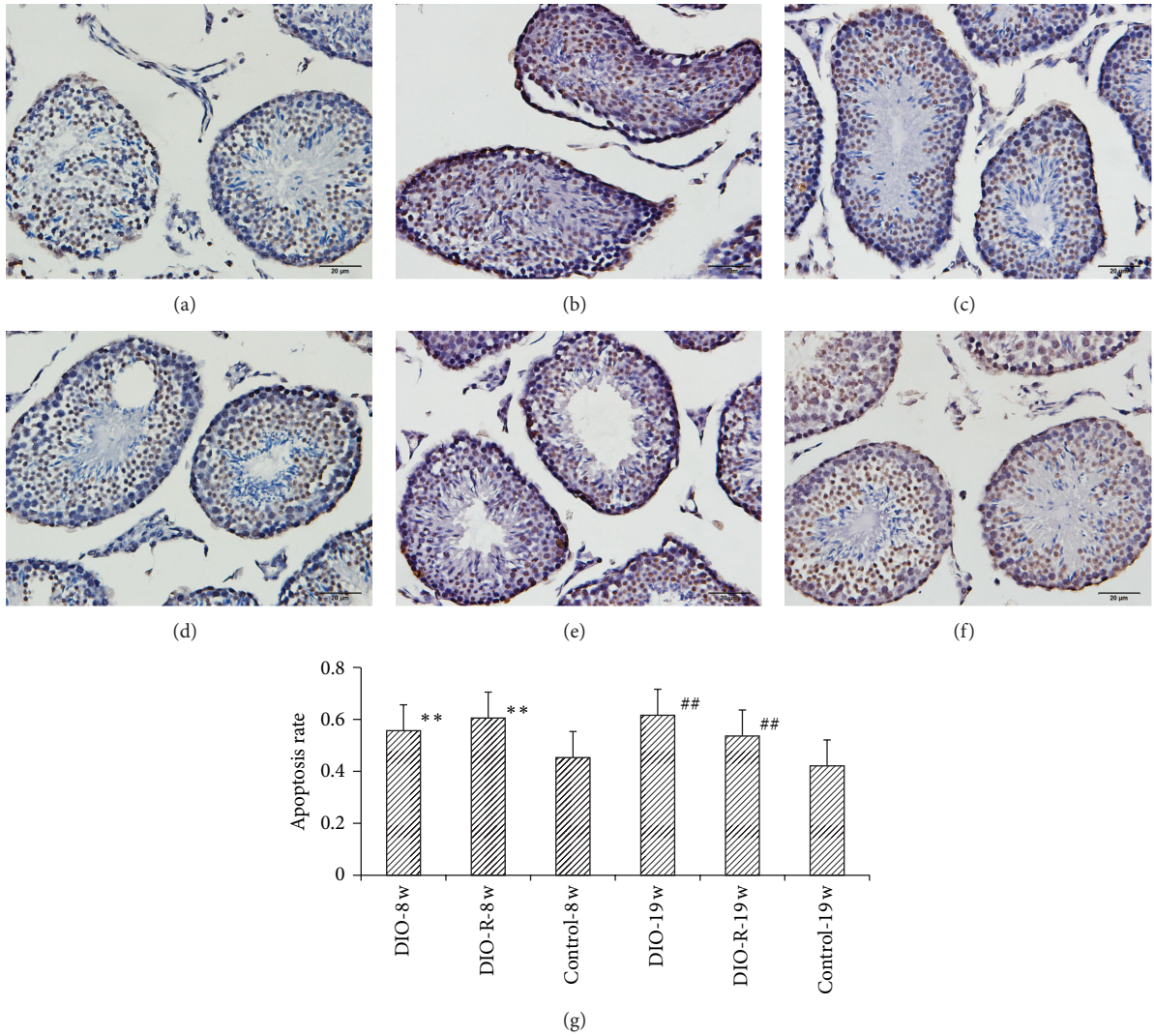

Figure 5: The figure showed the TUNEL apoptosis assay in Leydig cells after 8-week and 19-week high-fat diet. Photographs of control at 8 weeks (a), DIO group at 8 weeks (b), DIO-R group at 8 weeks (c), control group at 19 weeks (d), DIO group at 19 weeks (e), and DIO-R group (f) at 19 weeks were in this figure. The sections were stained with DAB, and the magnification was set at ×40. Data are mean ± SD for six animals in each group. The effects of 8-week and 19-week high-fat diet on Leydig cells apoptotic rate (g) were also shown in this figure. $^{**}P < 0.01$ denotes statistical significance compared with control-8w group; $^{\#\#}P < 0.01$ denotes statistical significance compared with control-19w group.

to fat accumulation) are extremely toxic to spermatozoa [44], Leydig cells in testis tissues may also be influenced, and androgen secretion may decrease. Secondary sexual characteristics and sexual maturity of males will be delayed by lower plasma testosterone. The reproduction of adult males will also be influenced. However, further investigation is needed to confirm these issues. These oxidants can cause tissue damage by a variety of mechanisms including DNA damage, lipid peroxidation, protein oxidation, depletion of cellular thiols, and activation of proinflammatory cytokine release [40]. The transcription factor, nuclear factor erythroid 2-related factor 2 (Nrf_2), is a central regulator of antioxidant and detoxification gene expression in response to electrophilic or oxidative stress [45]. Nrf_2, a member of the Cap "n" Collar family of basic region leucine zipper transcription factors, plays an important role in preventing the development of oxidative stress through upregulation of Nrf_2-related antioxidants [46, 47]. Moreover, Nrf_2-knockout mice showed an oxidative disruption in spermatogenesis [48]. In this study, the mRNA expression of Nrf_2 decreased, as well as the activities and mRNA expression of enzymatic antioxidants. Thus, oxidative stress caused by high-fat diet in testes may be improved by reducing the Nrf_2-antioxidant pathway.

It is interesting that reproductive hormone imbalance in obesity may affect the antioxidant status in testes. The immediate endocrine environment of the testes has a major impact on the antioxidant status of testes. Reproductive hormone imbalance, either hyper- or hypogonadotrophism, may contribute to the decline in antioxidant status in testes. Overstimulation of Leydig cells by chronic exposure to hCG (100 IU/day for 30 days in rats) also stimulates high

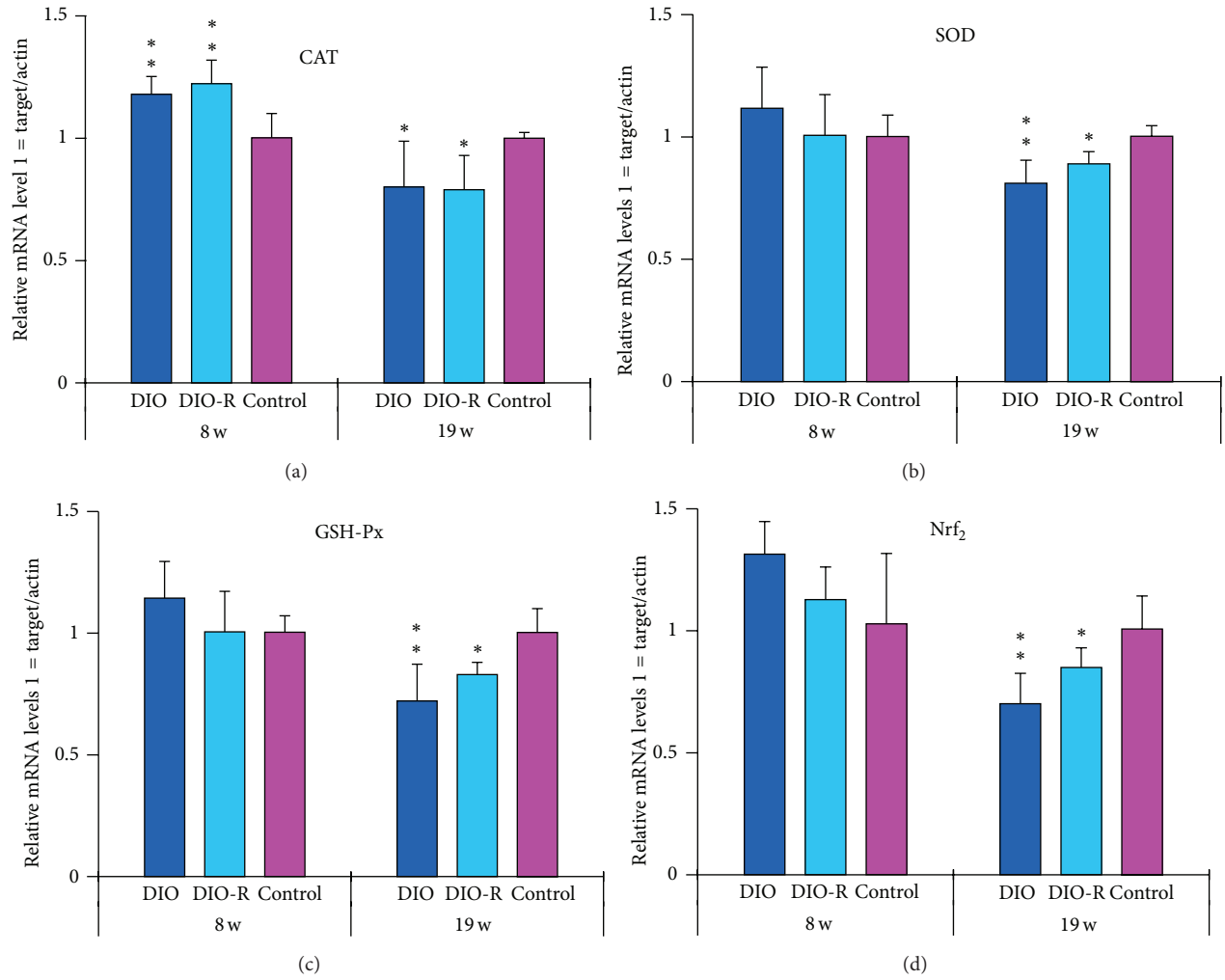

Figure 6: The alteration of CAT mRNA (a), SOD mRNA (b), GSH-Px mRNA (c), and Nrf_2 mRNA (d) in testicular tissue after high-fat diet at 8 and 19 weeks was shown in this figure. Data are mean ± SD for 6 animals in every group and each RNA preparation was run three times by real-time PCR; $^{*}P < 0.05$ and $^{**}P < 0.01$ denote statistical significance compared with control group.

levels of ROS production from these cells, which in turn stimulates lipid peroxidation, a reduction in antioxidant enzyme activities, germ cell apoptosis, and consequently disruption of spermatogenesis [49]. In contrast, research has shown that treatments including exposure to endocrine disruptors which diminish the intratesticular concentration of testosterone inhibit the testicular expression of antioxidant enzymes such as GPx, SOD, and catalase [50, 51]. When exogenous gonadotropin is administered to artificially elevate intratesticular testosterone levels, these suppressive effects on antioxidant expression, as well as the disruption of spermatogenesis, can be reversed [51, 52]. In this study, a low level of testosterone and high oxidative stress were observed in testis tissue. These findings further proved that hormone imbalance can aggravate oxidative stress in testis tissue in the obese state. However, further research on this topic is required.

In conclusion, short- (8 weeks) and long-term (19 weeks) high-fat diet increased Leydig cell pathological damage, apoptosis rates, lipid peroxidation, and serum leptin level; decreased sperm count, sperm motility, relative testis weight, and testosterone level; inhibited the activity of CAT and GSH-Px enzymes; decreased CAT, SOD, GSH-Px, and Nrf_2 mRNA expression. Pubertal obesity may influence the function and development of reproductive organs in adults. Pathological damage of Leydig cells, oxidative stress in testis tissue, and high leptin level may provide some evidence to clarify the mechanisms of male SH in obesity and possibly prevent it.

Conflict of Interests

The authors declare that there is no conflict of interests regarding the publication of this paper.

Acknowledgment

This work was supported by the National Natural Science Foundation of China (Grant nos. 81202227 and 30800920).

References

[1] R. Mendez and M. Grissom, "Disorders of childhood growth and development: childhood obesity," *FP Essentials*, vol. 410, pp. 20–24, 2013.

[2] J. Ma, C. H. Cai, H. J. Wang, B. Dong, Y. Song, and P. J. Hu, "The trend analysis of overweight and obesity in Chinese students during 1985 to 2010," *Chinese Journal of Preventive Medicine*, vol. 42, no. 9, pp. 776–780, 2012.

[3] J. C. Han, D. A. Lawlor, and S. Y. Kimm, "Childhood obesity," *The Lancet*, vol. 375, no. 9727, pp. 1737–1748, 2010.

[4] K. M. Flegal, R. Wei, C. L. Ogden, D. S. Freedman, C. L. Johnson, and L. R. Curtin, "Characterizing extreme values of body mass index-for-age by using the 2000 Centers for Disease Control and Prevention growth charts," *The American Journal of Clinical Nutrition*, vol. 90, no. 5, pp. 1314–1320, 2009.

[5] D. S. Freedman, Z. Mei, S. R. Srinivasan, G. S. Berenson, and W. H. Dietz, "Cardiovascular risk factors and excess adiposity among overweight children and adolescents: the Bogalusa Heart study," *Journal of Pediatrics*, vol. 150, no. 1, pp. 12–17, 2007.

[6] C. Koebnick, N. Smith, K. J. Coleman et al., "Prevalence of extreme obesity in a multiethnic cohort of children and adolescents," *Journal of Pediatrics*, vol. 157, no. 1, pp. 26–31, 2010.

[7] C. A. Johnston, C. Tyler, J. L. Palcic, S. A. Stansberry, M. R. Gallagher, and J. P. Foreyt, "Smaller weight changes in standardized body mass index in response to treatment as weight classification increases," *Journal of Pediatrics*, vol. 158, no. 4, pp. 624–627, 2011.

[8] M. Savoye, P. Nowicka, M. Shaw et al., "Long-term results of an obesity program in an ethnically diverse pediatric population," *Pediatrics*, vol. 127, no. 3, pp. 402–410, 2011.

[9] P. Danielsson, J. Kowalski, Ö. Ekblom, and C. Marcus, "Response of severely obese children and adolescents to behavioral treatment," *Archives of Pediatrics and Adolescent Medicine*, vol. 166, no. 12, pp. 1103–1108, 2012.

[10] P. Dandona and S. Dhindsa, "Update: hypogonadotropic hypogonadism in type 2 diabetes and obesity," *Journal of Clinical Endocrinology and Metabolism*, vol. 96, no. 9, pp. 2643–2651, 2011.

[11] A. O. Hammoud, N. Wilde, M. Gibson, A. Parks, D. T. Carrell, and A. W. Meikle, "Male obesity and alteration in sperm parameters," *Fertility and Sterility*, vol. 90, no. 6, pp. 2222–2225, 2008.

[12] V. Vendramini, A. P. Cedenho, S. M. Miraglia, and D. M. Spaine, "Reproductive function of the male obese Zucker rats: alteration in sperm production and sperm DNA damage," *Reproductive Science*, vol. 21, no. 2, pp. 221–229, 2014.

[13] C. Mammi, M. Calanchini, A. Antelmi et al., "Androgens and adipose tissue in males: a complex and reciprocal interplay," *International Journal of Endocrinology*, vol. 2012, Article ID 789653, 8 pages, 2012.

[14] J. Hofstra, S. Loves, B. van Wageningen, J. Ruinemans-Koerts, I. Janssen, and H. de Boer, "High prevalence of hypogonadotropic hypogonadism in men referred for obesity treatment," *Netherlands Journal of Medicine*, vol. 66, no. 3, pp. 103–109, 2008.

[15] S. A. Saboor Aftab, S. Kumar, and T. M. Barber, "The role of obesity and type 2 diabetes mellitus in the development of male obesity-associated secondary hypogonadism," *Clinical Endocrinology*, vol. 78, no. 3, pp. 330–337, 2013.

[16] K. Esposito and D. Giugliano, "Obesity, the metabolic syndrome, and sexual dysfunction in men," *Clinical Pharmacology and Therapeutics*, vol. 90, no. 1, pp. 169–173, 2011.

[17] G. S. Gerber and C. B. Brendler, "Evaluation of the urologic patient: history, physical examination, and the urinalysis," in *Campbell-Walsh Urology*, A. J. Wein, Ed., chapter 3, Saunders Elsevier, Philadelphia, Pa, USA, 9th edition, 2007.

[18] T. T. Turner and J. J. Lysiak, "Oxidative stress: a common factor in testicular dysfunction," *Journal of Andrology*, vol. 29, no. 5, pp. 488–498, 2008.

[19] H. Gu, L. Liu, S. Ma et al., "Inhibition of SOCS-3 in adipocytes of rats with diet-induced obesity increases leptin-mediated fatty acid oxidation," *Endocrinology*, vol. 36, no. 3, pp. 548–554, 2009.

[20] B. E. Levin and R. E. Keesey, "Defense of differfing body weight set points in diet-induced obese and resistant rats," *The American Journal of Physiology: Regulatory Integrative and Comparative Physiology*, vol. 274, no. 2, pp. R412–R419, 1998.

[21] Y. Deng, Z. F. Xu, W. Liu, B. Xu, H. B. Yang, and Y. G. Wei, "Riluzole-triggered GSH synthesis via activation of glutamate transporters to antagonize methylmercury-induced oxidative stress in rat cerebral cortex," *Oxidative Medicine and Cellular Longevity*, vol. 2012, Article ID 534705, 2012.

[22] WHO, *WHO Laboratory Manual for the Examination of Human Semen and Sperm-Cervical Mucus Interaction*, Cambridge University Press, Cambridge, UK, 1999.

[23] O. A. Alshabanah, M. M. Hafez, M. M. Al-Harbi et al., "Doxorubicin toxicity can be ameliorated during antioxidant L-carnitine supplementation," *Oxidative Medicine and Cellular Longevity*, vol. 3, no. 6, pp. 428–433, 2010.

[24] C. de Maddalena, S. Vodo, A. Petroni, and A. M. Aloisi, "Impact of testosterone on body fat composition," *Journal of Cellular Physiology*, vol. 227, no. 12, pp. 3744–3748, 2012.

[25] J. M. Adams and S. Cory, "The Bcl-2 protein family: arbiters of cell survival," *Science*, vol. 281, no. 5381, pp. 1322–1326, 1998.

[26] M. O. Hengartner, "The biochemistry of apoptosis," *Nature*, vol. 407, no. 6805, pp. 770–776, 2000.

[27] D. R. Green, "Apoptic pathways: the roads to ruin," *Cell*, vol. 94, no. 6, pp. 695–698, 1998.

[28] A. H. Wyllie, "Glucocorticoid-induced thymocyte apoptosis is associated with endogenous endonuclease activation," *Nature*, vol. 284, no. 5756, pp. 555–556, 1980.

[29] R. M. Cravo, R. Frazao, M. Perello et al., "Leptin signaling in Kiss1 neurons arises after pubertal development," *PLoS ONE*, vol. 8, no. 3, Article ID e58698, 2013.

[30] W. A. Zuure, A. L. Roberts, J. H. Quennell, and G. M. Anderson, "Leptin signaling in GABA neurons, but not glutamate neurons, is required for reproductive function," *The Journal of Neuroscience*, vol. 33, no. 45, pp. 17874–17883, 2013.

[31] M. Caprio, A. M. Isidori, A. R. Carta, C. Moretti, M. L. Dufau, and A. Fabbri, "Expression of functional leptin receptors in rodent Leydig cells," *Endocrinology*, vol. 140, no. 11, pp. 4939–4947, 1999.

[32] M. Caprio, E. Fabbrini, G. Ricci et al., "Ontogenesis of leptin receptor in rat Leydig cells," *Biology of Reproduction*, vol. 68, no. 4, pp. 1199–1207, 2003.

[33] M. Tena-Sempere, L. Pinilla, L. C. González, C. Diéguez, F. F. Casanueva, and E. Aguilar, "Leptin inhibits testosterone secretion from adult rat testis in vitro," *Journal of Endocrinology*, vol. 161, no. 2, pp. 211–218, 1999.

[34] R. Vettor, G. De Pergola, C. Pagano et al., "Gender differences in serum leptin in obese people: relationships with testosterone, body fat distribution and insulin sensitivity," *European Journal of Clinical Investigation*, vol. 27, no. 12, pp. 1016–1024, 1997.

[35] V. Luukkaa, U. Pesonen, I. Huhtaniemi et al., "Inverse correlation between serum testosterone and leptin in men," *Journal of Clinical Endocrinology and Metabolism*, vol. 83, no. 9, pp. 3243–3246, 1998.

[36] M. Wabitsch, W. F. Blum, R. Muche et al., "Contribution of androgens to the gender difference in leptin production in obese children and adolescents," *Journal of Clinical Investigation*, vol. 100, no. 4, pp. 808–813, 1997.

[37] H. Xi, L. Zhang, Z. Guo, and L. Zhao, "Serum leptin concentration and its effect on puberty in Naqu Tibetan adolescents," *Journal of Physiological Anthropology*, vol. 30, no. 3, pp. 111–117, 2011.

[38] A. M. Isidori, M. Caprio, F. Strollo et al., "Leptin and androgens in male obesity: evidence for leptin contribution to reduced androgen levels," *Journal of Clinical Endocrinology and Metabolism*, vol. 84, no. 10, pp. 3673–3680, 1999.

[39] A. Mehta, C. P. S. Sekhon, S. Giri, J. K. Orak, and A. K. Singh, "Attenuation of ischemia/reperfusion induced MAP kinases by N-acetyl cysteine, sodium nitroprusside and phosphoramidon," *Molecular and Cellular Biochemistry*, vol. 240, no. 1-2, pp. 19–29, 2002.

[40] H. Anand, M. M. Misro, S. B. Sharma, and S. Prakash, "Cytoprotective effects of fruit pulp of Eugenia jambolana on H_2O_2-induced oxidative stress and apoptosis in rat Leydig cells in vitro," *Andrologia*, vol. 45, no. 3, pp. 145–157, 2013.

[41] F. Taneli, B. Ersoy, B. Özhan et al., "The effect of obesity on testicular function by insulin-like factor 3, inhibin B, and leptin concentrations in obese adolescents according to pubertal stages," *Clinical Biochemistry*, vol. 43, no. 15, pp. 1236–1240, 2010.

[42] D. Montero, G. Walther, A. Perez-Martin, E. Roche, and A. Vinet, "Endothelial dysfunction, inflammation, and oxidative stress in obese children and adolescents: markers and effect of lifestyle intervention," *Obesity Reviews*, vol. 13, no. 5, pp. 441–455, 2012.

[43] A. Mohn, M. Catino, R. Capanna, C. Giannini, M. Marcovecchio, and F. Chiarelli, "Increased oxidative stress in prepubertal severely obese children: effect of a dietary restriction-weight loss program," *Journal of Clinical Endocrinology and Metabolism*, vol. 90, no. 5, pp. 2653–2658, 2005.

[44] K. J. Teerds, D. G. de Rooij, and J. Keijer, "Functional relationship between obesity and male reproduction: from humans to animal models," *Human Reproduction Update*, vol. 17, no. 5, pp. 667–683, 2011.

[45] D. V. Chartoumpekis, P. G. Ziros, A. Zaravinos et al., "Hepatic gene expression profiling in Nrf2 knockout mice after long-term high-fat diet-induced obesity," *Oxidative Medicine and Cellular Longevit*, vol. 2013, Article ID 340731, 17 pages, 2013.

[46] W. Cui, B. Li, Y. Bai et al., "Potential role for Nrf2 activation in the therapeutic effect of MG132on diabetic nephropathy in OVE26 diabetic mice," *The American Journal of Physiology: Endocrinology and Metabolism*, vol. 304, no. 1, pp. E87–E99, 2013.

[47] M. B. Sporn and K. T. Liby, "NRF2 and cancer: the good, the bad and the importance of context," *Nature Reviews*, vol. 12, no. 8, pp. 564–571, 2012.

[48] B. N. Nakamura, G. Lawson, J. Y. Chan et al., "Knockout of the transcription factor NRF2 disrupts spermatogenesis in an age-dependent manner," *Free Radical Biology and Medicine*, vol. 49, no. 9, pp. 1368–1379, 2010.

[49] D. K. Gautam, M. M. Misro, S. P. Chaki, M. Chandra, and N. Sehgal, "hCG treatment raises H_2O_2 levels and induces germ cell apoptosis in rat testis," *Apoptosis*, vol. 12, no. 7, pp. 1173–1182, 2007.

[50] A. Zini and P. N. Schlegel, "Effect of hormonal manipulation on mRNA expression of antioxidant enzymes in the rat testis," *Journal of Urology*, vol. 169, no. 2, pp. 767–771, 2003.

[51] D. Ghosh, U. B. Das, S. Ghosh, M. Mallick, and J. Debnath, "Testicular gametogenic and steroidogenic activities in cyclophosphamide treated rat: a correlative study with testicular oxidative stress," *Drug and Chemical Toxicology*, vol. 25, no. 3, pp. 281–292, 2002.

[52] V. Peltola, I. Huhtaniemi, T. Metsa-Ketela, and M. Ahotupa, "Induction of lipid peroxidation during steroidogenesis in the rat testis," *Endocrinology*, vol. 137, no. 1, pp. 105–112, 1996.

Hindawi Publishing Corporation
Oxidative Medicine and Cellular Longevity
Volume 2014, Article ID 823071, 11 pages
http://dx.doi.org/10.1155/2014/823071

Research Article

Endogenous Ceramide Contributes to the Transcytosis of oxLDL across Endothelial Cells and Promotes Its Subendothelial Retention in Vascular Wall

Wenjing Li,[1,2] Xiaoyan Yang,[1,2] Shasha Xing,[1,2] Fang Bian,[1,2] Wanjing Yao,[1,2] Xiangli Bai,[1,2] Tao Zheng,[1,2] Guangjie Wu,[1,2] and Si Jin[1,2]

[1] *Department of Pharmacology, Tongji Medical College, Huazhong University of Science and Technology, Wuhan 430030, China*
[2] *The Key Laboratory of Drug Target Research and Pharmacodynamic Evaluation of Hubei Province, Wuhan 430030, China*

Correspondence should be addressed to Si Jin; jinsi@mail.hust.edu.cn

Received 13 February 2014; Revised 17 March 2014; Accepted 21 March 2014; Published 10 April 2014

Academic Editor: Shiwei Deng

Oxidized low density of lipoprotein (oxLDL) is the major lipid found in atherosclerotic lesion and elevated plasma oxLDL is recognized to be a risk factor of atherosclerosis. Whether plasma oxLDL could be transported across endothelial cells and initiate atherosclerotic changes remains unknown. In an established *in vitro* cellular transcytosis model, the present study found that oxLDL could traffic across vascular endothelial cells and further that the regulation of endogenous ceramide production by ceramide metabolizing enzyme inhibitors significantly altered the transcytosis of oxLDL across endothelial cells. It was found that acid sphingomyelinase inhibitor, desipramine (DES), and *de novo* ceramide synthesis inhibitor, myriocin (MYR), both decreasing the endogenous ceramide production, significantly inhibited the transcytosis of oxLDL. Ceramidase inhibitor, N-oleoylethanolamine (NOE), and sphingomyelin synthase inhibitor, O-Tricyclo[5.2.1.02,6]dec-9-yl dithiocarbonate potassium salt (D609), both increasing the endogenous ceramide production, significantly upregulated the transcytosis of oxLDL. *In vivo*, injection of fluorescence labeled oxLDL into mice body also predisposed to the subendothelial retention of these oxidized lipids. The observations provided in the present study demonstrate that endogenous ceramide contributes to the transcytosis of oxLDL across endothelial cells and promotes the initiating step of atherosclerosis—the subendothelial retention of lipids in vascular wall.

1. Introduction

Atherosclerosis (AS) is the pathological basis of cerebro- and cardiovascular diseases, which are the leading causes of death in the elderly people [1]. The pathogenesis of AS is far from fully understood. In recent years, more and more evidences show that the initiating step of AS is likely to be the subendothelial retention of lipoprotein in intima, so called "response to retention" hypothesis [2–5], which highlights the role of accumulation of apoB-containing lipoproteins (mainly low density lipoprotein, LDL) in the subendothelial space, as well as extracellular matrix adhesion molecules, and so forth in the pathogenesis of AS.

To be deposited in the vascular intima, lipoproteins must pass through the barrier provided by vascular endothelium. The gap between the vascular endothelial cells is known to be about 3–6 nm in diameter, only allowing water, inorganic salts, and a handful of small proteins to pass through. Such macromolecule molecules as LDL in a diameter of about 20–30 nm are not generally able to pass through the endothelial barrier [6–8].

Recent studies have found LDL traffic across endothelial barrier mainly through transcytosis [9], which refers to a process of protein-rich particles passing through polar cells (such as endothelial cells, epithelial cells, etc.) by receptor or nonreceptor mediated mechanisms. LDL can be endocytosed by vascular endothelial cells in the lumen side and then exocytosed to the basolateral side [9]. A large number of studies have documented that the major LDL accumulated in AS plaques is in the oxidative modified form, namely, oxidized low density lipoprotein, oxLDL. Currently, oxLDL is recognized as the major causative factor of AS [10, 11]. Plasma

oxLDL levels were significantly increased in AS patients and have been considered as indicators of the early screening and diagnosis of coronary heart disease [12, 13]. Whether plasma oxLDL can pass through endothelial cells by transcytosis and further stick to intima to initiate the incidence of AS remains unknown.

In recent years, the role of lipid rafts (LRs) in the transmembrane transport of macromolecules has attracted much more attention [14–17]. Lipid rafts are membrane domains rich in sphingolipids and cholesterol [18, 19]. Endothelial caveolae used for LDL transcytosis is a specialized membrane raft domain [15]. Membrane fusion between vesicle membranes and sarcoplasmic membranes due to the formation of macromolecular complexes, such as t-SNARE and v-SNARE, is also dependent on the platform formed by fusion of membrane rafts [9]. Ceramide, the backbone of sphingolipids, is thought to participate in the development of atherosclerosis [20, 21]. Ceramide can be generated from sphingomyelin through activation of sphingomyelinase (SMases) or from the *de novo* pathway. Also, ceramide can be synthesized to sphingomyelin through activation of sphingomyelin synthase (SMS) or degraded into sphingosine by ceramidase, respectively. Inhibitors involved in ceramide metabolism commonly including acid sphingomyelinase (ASM) inhibitor, desipramine [22–24], *de novo* ceramide synthesis inhibitor, myriocin [25], ceramidase inhibitor (NOE) [26, 27], and sphingomyelin synthase inhibitor (D609) [28, 29].

Upon the stimulation of endogenous and exogenous factors, the sphingolipid (sphingomyelin) in endothelial cell membrane rafts undergoes hydrolysis by acid sphingomyelinase, releasing the hydrophilic phosphocholine group and generating hydrophobic product, ceramide [15]. The existence of intermolecular hydrogen bonds provides strong driving force for ceramide to fuse simultaneously. Through the integration of ceramide, many small membrane rafts can cluster together into larger microdomains, which provide signaling platforms for the interaction of transmembrane signal transduction [30–32]. Recent studies have also found that the ceramide produced by membrane rafts plays key roles in pathogen invasion into host cells, such as *Pseudomonas aeruginosa* [33–35]. In addition, ceramide can trigger and promote the exocytosis of Weibel-Palade bodies in endothelial cells [23].

Given the multiple origins of cellular ceramide, the current study aims to determine the roles of ceramide from different origins in mediating the transcytosis of oxLDL across the vascular endothelial cells and how these transcytosed oxLDL particles further promote AS changes in vascular walls.

2. Methods

2.1. Isolation and Culture of Human Umbilical Vein Endothelial Cells (HUVECs). The collection of human umbilical cords was approved by the Ethics Committee of Tongji Medical College, Huazhong University of Science and Technology (Wuhan, China), and conducted in accordance with the Declaration of Helsinki (2008). Primary HUVECs isolated from 0.01% EDTA-0.25% trypsin digested newborn umbilical cord were cultured in ECM (ScienCell) supplemented with 5% fetal bovine serum (FBS), 100 U/mL penicillin, 100 U/mL streptomycin, and 30 μg/mL endothelial cell growth supplement (ECGS) at 37°C under 5% CO_2 in a humidified atmosphere. For subculture, cells were harvested with 0.25% trypsin without EDTA when 80%~90% confluent. Before experiments, ECM was replaced with OPTI-MEM (Gibco) without FBS. All studies were performed using HUVECs of 2 to 8 passages [36–38].

2.2. Immunocytochemistry. After incubated with inhibitors (MYR, DES, D609, and NOE), respectively, for 12 h, HUVECs grown on gelatin-coated coverslips were fixed in 4% formaldehyde for 10 min and then washed in PBS for three times. Cells were stained with an anti-ceramide IgM antibody (Alexis, 1 : 100) for 1 h at 37°C and followed by CY3-conjugated goat anti-mouse secondary antibody (Bioss, 1 : 100) for another 2 h at room temperature [39–41]. Images were acquired using a custom-configured fluorescence microscope (Olympus FV500) [42]. The integrated fluorescence intensities were measured using the Image-Pro Plus software and normalized to the number of cells.

2.3. Intracellular Ceramide Extraction and Quantitation. Ceramide was extracted and quantified by HPLC-MS/MS (Thermo, LCQ DECA XP^{plus}) according to the principles described previously [43–46]. For extraction of cellular lipids, cells were lysed with distilled water and homogenized by sonication after incubation with inhibitors for 12 h. Protein concentrations were measured and the equal amounts of protein (500 μg) were adjusted to the volume of 800 μL in 1 M NaCl. C_{12}-ceramide (10 ng) was added to lysates as an internal standard and the resulting samples were extracted with chloroform/methanol (1 : 2) 3 mL for 3 h. Samples were then centrifuged at 3000 g, 5 min. Supernatants were transferred to the other tubes within CCL_4 and 1 M NaCl 1 mL, respectively. After centrifugation, the lower organic phase was obtained and evaporated to near dryness under a gentle stream of dry N_2. Meantime, samples were reconstituted by 100 μL methanol to measure ceramides C_{14}, C_{16}, $C_{24:1}$, and C_{24} by HPLC-MS/MS. The levels of each ceramide species were determined by their relative abundance normalized to C_{12}-ceramide and the gross of ceramides was quantified based on the standard curve which was constructed on ceramide standards (Avanti). The gross of these ceramides was used for statistics.

2.4. Cellular Uptake of oxLDL. oxLDL was labeled with fluorescein isothiocyanate (FITC; Biosharp) by a minor modification of a previously described method [47, 48]. In brief, oxLDL and FITC were mixed and incubated at 37°C for 2 h and then unbound FITC was removed by dialysis against PBS for 72 h at 4°C. Finally, FITC-oxLDL was stored at 4°C in the dark for further use. All procedures were performed in the dark. Cells were seeded on gelatin-coated glass coverslips

in 24-well culture dishes and incubated at 37°C and 5% CO_2. After being treated with the above inhibitors, respectively, for 9 h, cells were then incubated with 50 μg/mL FITC-oxLDL for 3 h. Images were obtained with a fluorescence microscope using a 40x objective. The integrated fluorescence intensities were measured using the Image-Pro Plus software and normalized to the number of cells.

2.5. oxLDL Retention in Isolated Umbilical Venous Wall. In a mixture of oxygen (95% O_2 and 5% CO_2) condition, the human umbilical venous rings were incubated with 50 μg/mL FITC-oxLDL and various inhibitors at 37°C for 3 h [47]. Then the tissues were frozen and sliced into thin sections of 8 μm with a freezing microtome (Leica CM1900) and further stained with DAPI. For each optical section, the space above the basilar membrane was defined as the region of interest (ROI). The fluorescence intensity was quantitated using Image-Pro Plus software. A weighted analysis was performed by first determining the area of fluorescence within the ROI of each optical section for three fluorescence intensity value ranges as follows: 160 to 190, 190 to 210, and 210 to 230. These three area measurements were then multiplied by 1, 3, or 5, respectively, to give greater weight to areas of highest intensity [49]. These weighted values were then summed for each optical section and divided by the area of ROI.

2.6. oxLDL Transcytosis. As described previously, the amount of oxLDL transcytosis was measured by a nonradioactive method *in vitro* [47, 48]. HUVECs were seeded on polyester membrane of costar transwell (6.5 mm diameter and 0.4 μm pore size) to form integrated cell monolayer. The integrity of cell monolayer was tested by a method described previously [50]. Two inserts of cell monolayers with equal integrity were divided into the same group: the noncompetitive insert and the competitive insert, respectively. Inhibitors were added to each group for 9 h. And then, the noncompetitive insert was incubated with 50 μg/mL FITC-oxLDL to determine the total amount of transendothelial oxLDL; paracellular transport was determined by incubation with 50 μg/mL FITC-oxLDL and 6-fold excess of unlabeled oxLDL (300 μg/mL) in competitive insert. After 3 h, samples were then collected from the outer chambers and further dialyzed against PBS to remove the free FITC. The relative fluorescence was measured via a fluorescence spectrophotometer (Tecan, Infinite F200PRO) with excitation and emission wavelengths of 490 nm and 520 nm, respectively. Meanwhile, background fluorescence determined by serum-free Opti-MEM was subtracted from the value of each sample. The amount of oxLDL transcytosis is the difference between the fluorescent intensity of the noncompetitive insert and the competitive insert.

2.7. Subendothelial oxLDL Retention In Vivo. Animals were treated in accordance with the guide for the Care and Use of Laboratory Animals published by the US National Institutes of Health and approved by the local animal care committee. Healthy C57BL/6J mice (18–20 g) were purchased from the Center of Experimental Animals (Tongji Medical College, Huazhong University of Science and Technology, China) and maintained in a controlled environment with a light/dark cycle of 12 h, a temperature of 20 ± 2°C, and a humidity of 50 ± 2%. Male C57BL/6J mice were randomly assigned to 6 treatment groups: groups 1-2 received 0.9% saline, groups 3–6 were intraperitoneally (i.p.) injected with myriocin 0.3 mg/kg three times over 5 days (days 1, 3, and 5) [51], desipramine 20 mg/kg/day for 5 days, D609 10 mg/kg for 12 h before sacrifice, and NOE 10 mg/kg/day for 5 days, respectively. C57 mice of groups 2–6 were injected via tail vein with FITC-oxLDL (50 μg/mouse) for 3 h before sacrifice, while mice of group 1 were injected with unlabeled oxLDL (50 μg/mouse). Mice were euthanized, and the hearts, spleens, and livers were quickly frozen in liquid nitrogen. Frozen sections of hearts, spleens, and livers were prepared as described previously [49, 52]. The sections were stained with DAPI. Due to the existence of spontaneous fluorescence in aortas, we use the difference in fluorescent intensity between the subendothelial layer and the whole vessel to stand for FITC-oxLDL fluorescent intensity. For each group, 20 sections were analyzed, which represent 5 interval sections per aorta from 4 mice.

2.8. Isolation of Cavolin-1-Enriched Membrane Raft Fractions. Caveolae-enriched membrane fractions were prepared by a detergent-free purification, as described previously [41, 53]. To isolate membrane raft fractions from the cell membrane, HUVECs were lysed in 2 mL 500 mmol/L Na_2CO_3 containing protease inhibitor cocktail. Cell extracts were homogenized with 15 strokes through a 25-gauge needle followed by sonication for 15 s three times on ice. Detecting the concentration of protein in the homogenate made sure that each group has equal amounts of protein. The final volume was adjusted to 2 mL with MBS containing 25 mmol/L 2-(N-morpholino)ethanesulfonic acid and 0.15 mol/L NaCl, pH 6.5. Homogenates were adjusted with 2 mL 90% sucrose density gradient medium prepared in MBS to 45% and overlaid with discontinuous 4 mL 30% and 4 mL 5% sucrose in the MBS buffer containing 250 mmol/L Na_2CO_3. Samples were then centrifuged at 39,000 rpm for 18 h at 4°C in a SW 41 rotor (Beckman Instruments). A total of 12 fractions per 1 mL were collected carefully from top to bottom. For immunoblot analysis of membrane raft-associated proteins, these fractions were precipitated by 10% cold trichloroacetic acid and washed with cold acetone, air-dried. The protein pellets were then dissolved in an SDS-PAGE lysis buffer for western blot analysis.

2.9. Western Blotting. After cells were incubated with the inhibitors, respectively, for 12 h, caveolin-1 enriched membrane fractions were isolated as described above and the final samples were detected by western blotting. The protein samples were separated by SDS-PAGE gel and then electrotransferred to PVDF membranes. Subsequently, blots were subjected to immunostaining with antibodies against Caveolin-1 (Cell Signaling Technology, 1 : 800), Cavin-1 (ANBO, 1 : 500), and lectin-like oxLDL receptor

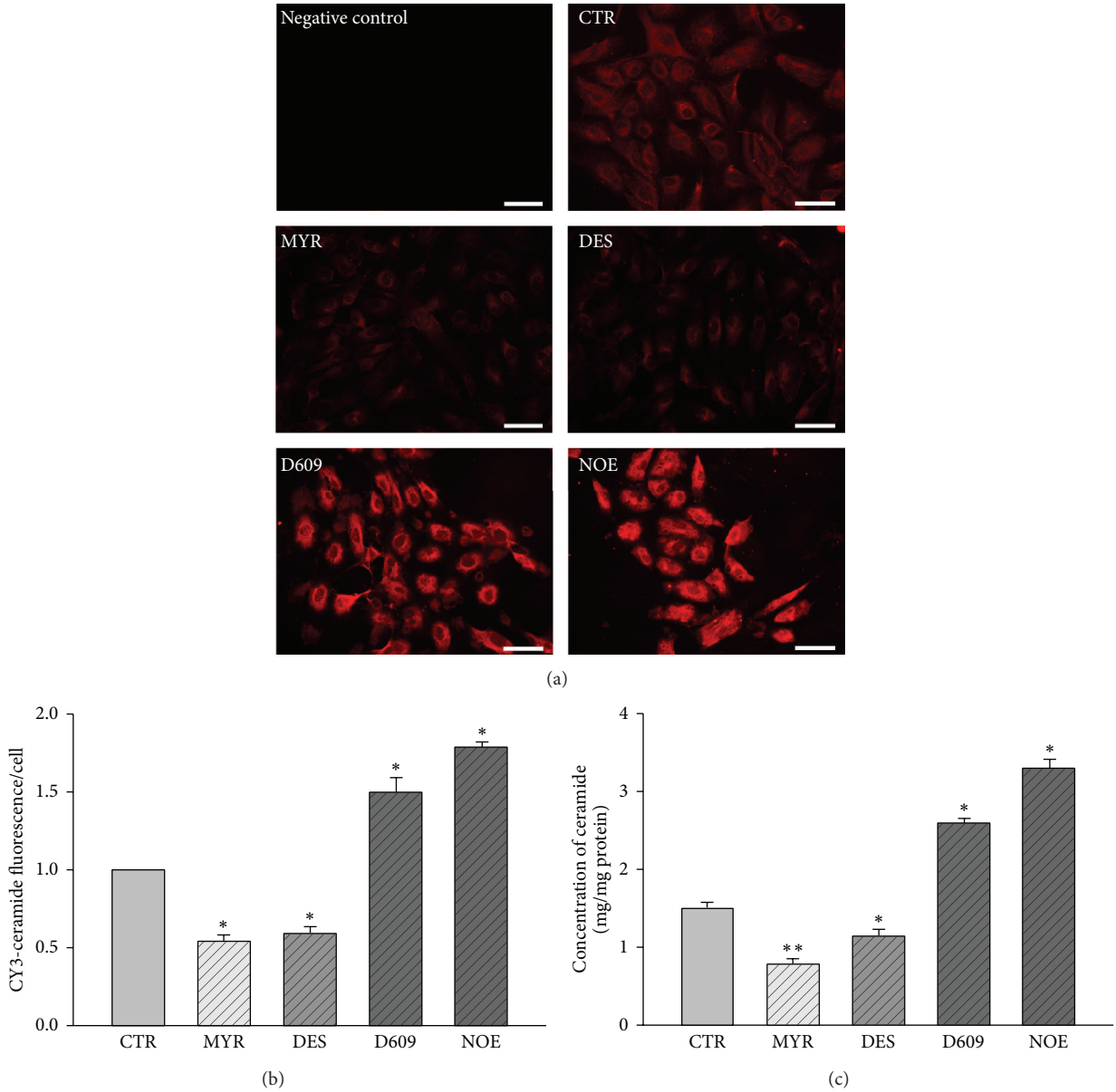

Figure 1: The effects of various inhibitors on ceramide concentration in HUVECs. HUVECs were incubated with 30 μM MYR, 10 μM DES, 30 μM D609, or 10 μM NOE for 12 h. Representative fluorescence microscopic images of ceramide (a) and quantification analysis (b) of immunofluorescent staining in HUVECs. Scale bars are equal to 50 μm. "Negative control" group was processed in the absence of primary antibody. (c) Concentration of ceramides in HUVECs quantified by HPLC-MS analysis. $^*P < 0.05$ versus control, $n = 3$.

(Lox-1, WuXi AppTec, 1 : 1000). After incubation for 1 h with a peroxidase-conjugated secondary antibody (Abbkine, 1 : 10000), bands were visualized by an ECL western blotting detection system (NDR, Israel). The band intensities were quantified using ImageJ software.

2.10. Statistical Analysis. All data are expressed as the mean ± SEM from at least three separate experiments. Significant differences between multiple groups were examined using ANOVA with Duncan's multiple-range testing. A value of $P < 0.05$ was considered significant.

3. Results

3.1. Endogenous Cellular Ceramide Production Is Regulated by Ceramide Metabolizing Enzyme Inhibitors. To determine the effects of various inhibitors on ceramide metabolism, ceramide concentration was detected by two methods. The representative fluorescence microscopic images and semi-quantitative results were shown in Figures 1(a) and 1(b). To further confirm the effects, we detected ceramides by HPLC/MS (Figure 1(c)). Results demonstrated that MYR and DES reduced ceramide concentration, while D609 and NOE increased ceramide concentration remarkably.

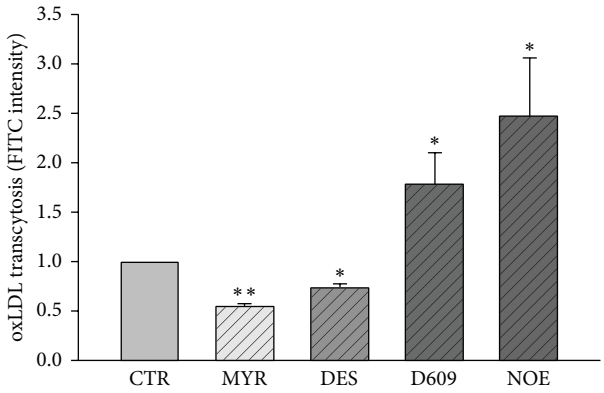

Figure 2: oxLDL transcytosis in the absence or presence of various inhibitors. HUVECs were incubated with 30 μM MYR, 10 μM DES, 30 μM D609, or 10 μM NOE for 12 h and FITC-oxLDL (50 μg/mL) or oxLDL (300 μg/mL) for 3 h. $^{*}P < 0.05$, $^{**}P < 0.01$ versus control, $n = 4$.

3.2. FITC-oxLDL Transcytosis across Endothelial Cell Monolayers. To determine whether the inhibitors alter the amount of oxLDL transport across HUVECs, we assayed the amount of oxLDL transcytosis across HUVECs. As shown in Figure 2, pretreatment with MYR or DES significantly decreased oxLDL transcytosis, while exposure to D609 or NOE significantly increased oxLDL transcytosis. These results were further confirmed by the observations of oxLDL uptake in cultured HUVECs. Since the oxLDL uptake by HUVECs is an intermediate phase of oxLDL transcytosis across HUVECs, it may also represent the amount of oxLDL transcytosis in a degree. As shown in Figures 3(a) and 3(b), fluorescence intensities in each individual cell were measured to reflect the amount of oxLDL uptake. It was found that the levels of oxLDL uptake were suppressed by MYR or DES, while elevated by D609 or NOE.

3.3. The Subendothelial Retention of oxLDL In Vitro. An experiment was conducted to test whether subendothelial retention of oxLDL would alter in the presence of various inhibitors. As summarized in Figures 4(a) and 4(b), more FITC-oxLDL accumulated in the region above the basilar membrane after D609 or NOE stimulation. However, the accumulation of FITC-oxLDL was significantly decreased in the presence of MYR or DES.

3.4. The Subendothelial Retention of oxLDL In Vivo. To validate the oxLDL transcytosis and subendothelial retention, the endothelial fluorescence intensities in aortic roots from C57 mouse were detected. Compared to mice injected with unlabeled oxLDL, aortas from mice injected with FITC-oxLDL showed stronger fluorescence intensities located under endothelium (Figure 5(a)). Similar to that shown in Figure 4, the space under endothelium in aortic root of mice treated with inhibitors accumulated more or less fluorescence. It was noted that, aortas from MYR-/DES-treated mice accumulated very little fluorescence under endothelium, while aortas from D609-/NOE-treated mice showed much stronger fluorescence signal. Supplemental Figure 1 (see Supplementary Material online at: http://dx.doi.org/10.1155/2014/823071) showed no difference in fluorescence accumulation in spleens or livers of mice in separate groups.

3.5. The Expression of LRs Components Related to oxLDL Transcytosis. Lipid rafts fractions were isolated as described before. Caveolin-1 enriched fractions (1 mL for each) were detected to determine LRs location (fractions 6 and 7) as shown in Figure 6(a). As shown in Figures 6(b) and 6(c), the expression of proteins involved in caveolae formation (caveolin-1 and cavin-1) as well as oxLDL receptor (Lox-1) could be regulated by inhibitors of ceramide related enzymes. Compared with control, MYR and DES significantly decreased the expressions of all proteins involved in oxLDL transport, while D609 and NOE increased the expressions.

4. Discussion

Ceramides are increasingly recognized to play essential roles in the pathogenesis of atherosclerosis [21, 54–58]. In the present study, for the first time, we demonstrated that endogenously produced ceramides in endothelial cells significantly contributed to the transcytosis of oxLDL across the endothelial cell barrier and facilitated the subendothelial retention of these oxidized lipids, further promoting the progression of atherosclerosis.

LDL *per se* is a spherical nanoparticle composed of lipid molecules surrounded by apoB100, which mediates the molecular recognition of LDL with its receptors. As compared to other types of lipoproteins, LDL contains more sphingolipids and cholesterol and has a property of resistance to detergent at low temperatures [7]. Previous reports have indicated elevated plasma sphingolipid levels in AS [59], pointing to the importance of ceramide in AS. But how ceramides affect atherogenesis remains to be further elucidated.

By immunostaining and HPLC-MS analysis, we first confirmed the inhibiting effects of the inhibitors of multiple enzymes involved in ceramide metabolism. We found that both *de novo* ceramide synthesis inhibitor, myriocin, and acid sphingomyelinase inhibitor, desipramine, could reduce the production of ceramide. However, ceramidase inhibitor, NOE, and sphingomyelin synthase inhibitor, D609, significantly upregulated the production of ceramide.

In an established *in vitro* model of oxLDL transcytosis across endothelial cell monolayer, we documented that myriocin and desipramine reduced the transcytosis of oxLDL; however, NOE and D609 significantly accelerated the transcytosis of oxLDL across endothelial cells. In this model, we used the difference of fluorescence between control and competitive inserts, which represent the total and paracellular transport of oxLDL, respectively, to reflect the transcytosis of oxLDL across endothelial cells. This method of detecting transcytosis had been validated by previous studies [47, 48]. The alterations of the transcytosis induced by various inhibitors in the present study are in consistence with the

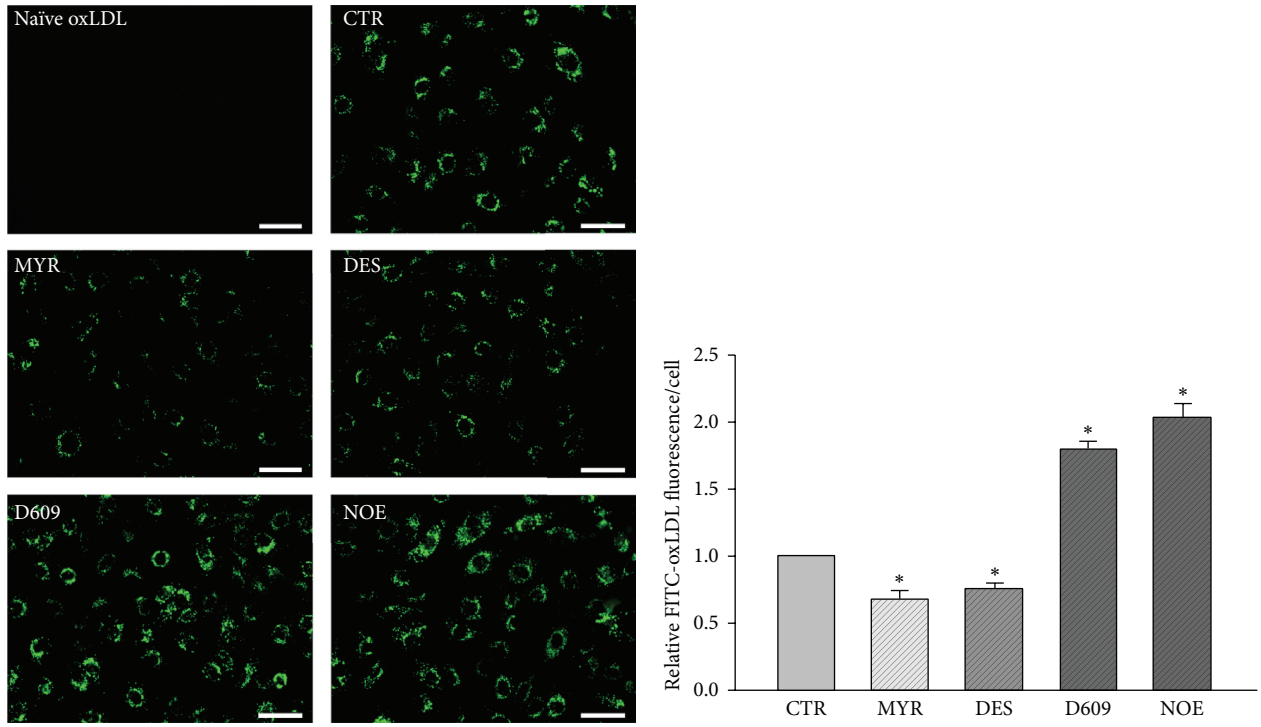

Figure 3: Fluorescence microscopic analysis of FITC-oxLDL uptake in HUVECs. HUVECs cultured on coverslips were pretreated with 30 μM MYR, 10 μM DES, 30 μM D609, or 10 μM NOE for 12 h, and oxLDL (50 μg/mL) was added to incubate for 3 h. (a) Representative fluorescence microscopic images of FITC-oxLDL uptake of HUVECs. Scale bars are equal to 50 μm. "Naïve oxLDL" group was incubated with unlabeled oxLDL. (b) Quantification analysis of FITC-oxLDL uptake in HUVECs. $^*P < 0.05$ versus control, $n = 3$.

alterations of intracellular ceramide production, strongly indicating that the endogenously produced ceramides facilitate the transcytosis of oxLDL across endothelial cells. For oxLDL to be transcytosed across endothelial cells, the oxLDL particles must be endocytosed in the lumen side of the endothelial cells and then be transferred to the basolateral side and further be exocytosed to the subendothelial space. During this process, an intermediate state of transcytosis is that these particles had already been endocytosed into the cytosol but had not been released yet. Therefore, the intracellular concentration of oxLDL particles also reflects the activity of transcytosis. The decrease of oxLDL particles in myriocin and desipramine treated cells, whereas the increase of oxLDL particles in NOE and D609 treated endothelial cells, further supports the promoting roles of ceramide in regulating oxLDL transcytosis. In isolated vascular preparations, when the umbilical vascular segments were incubated with fluorescence-labeled oxLDL particles, these particles can be transported to the subendothelial space in the vessel walls. Myriocin and desipramine, which inhibited the production of intracellular ceramide, also reduced the subendothelial retention of oxLDL. Vice versa, NOE and D609, which upregulated the ceramide level, increased the subendothelial retention of oxLDL in vessel walls.

To further confirm these effects in *in vivo* level, we also conducted animal experiments. Similar to those observations in cultured endothelial cells and isolated vascular segments, the two inhibitors, myriocin and desipramine, which suppressed the production of ceramide, attenuated the accumulation of oxLDL in the mouse aorta walls. However, NOE and D609, which stimulated the ceramide production, enhanced the subendothelial retention of oxLDL in vessel walls.

After the oxidative modification of LDL, oxLDL is generated, in which the sphingomyelin hydrolysis rate is 5-6 times of the naive LDL [60]; ceramide levels in oxLDL particles in AS lesions are 10–50 times the ceramide levels in plasma natural LDL [61]. Our results are in consistence with several observations in previous reports. Devlin CM reported that ASM plays a very important role in the pathogenesis of AS. AS lesions in double gene-deficient mice from hybridization of ASM knockout $Asm^{-/-}$ mice and apolipoprotein E knockout $Apoe^{-/-}$ mice were significantly smaller than those in $Apoe^{-/-}$ mice [49]. Loidl et al. reported that oxidation of phospholipids of modified LDL activates intracellular ASM [62]. These observations also strongly support the essential role of ceramide in the formation of atherosclerosis. However, McGovern et al. reported that patients of Niemann-Pick disease types A and B with a deficiency in ASM activity had low HDL and elevated LDL in plasma and had high incidences of coronary atherosclerosis [63]. This controversy may be due to the different roles of ASM in the metabolism of lipid profiles in liver and in the lipoprotein retention in vascular wall. On one side, ASM appears to be essential to

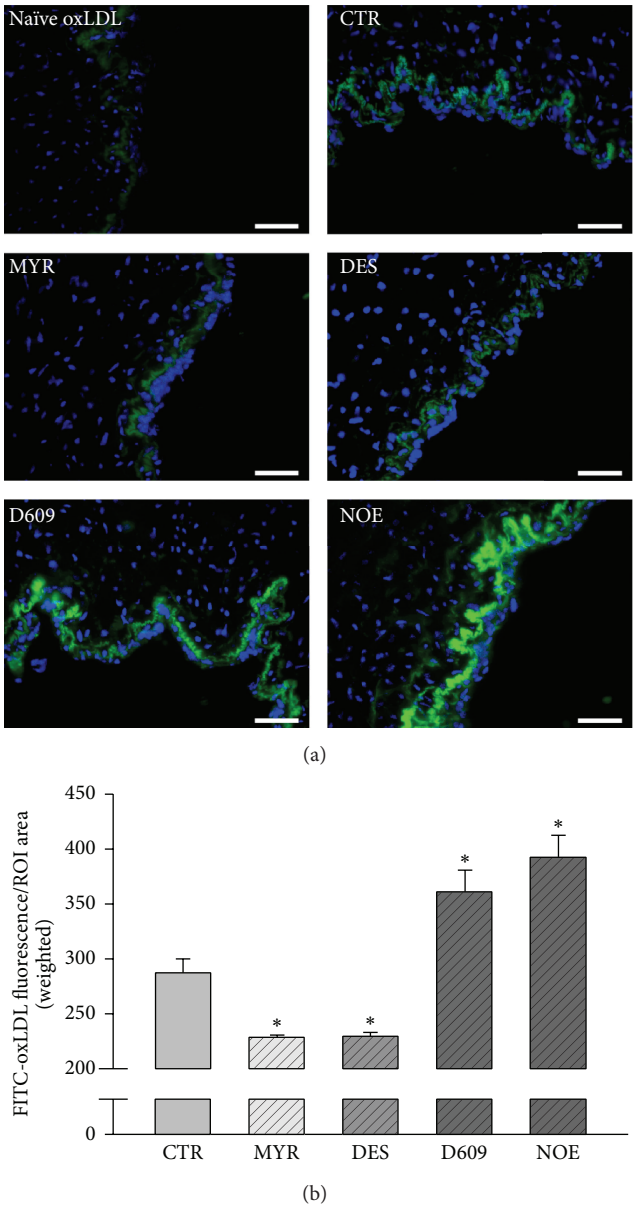

Figure 4: Fluorescence microscopic analysis of FITC-oxLDL (50 μg/mL) retention in human umbilical venous walls. (a) Representative fluorescence microscopic images of FITC-oxLDL retention in human umbilical venous walls stimulated by PBS or various inhibitors. Scale bars are equal to 300 μm. "Naïve oxLDL" group was incubated with unlabeled oxLDL. (b) Quantification analysis of FITC-oxLDL retention. $^{*}P < 0.05$ versus control, $n = 3$.

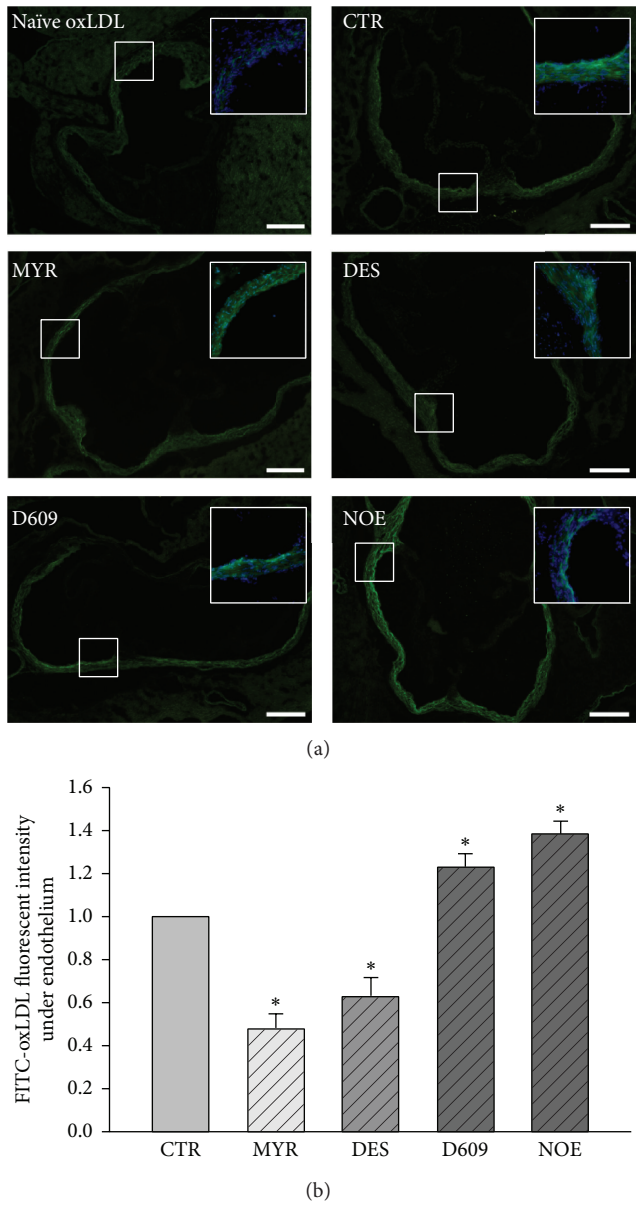

Figure 5: Fluorescence microscopic analysis of FITC-oxLDL retention in mouse aortic root. (a) Representative fluorescence microscopic images of aortic root sections of C57 mice after injection with FITC-oxLDL (50 μg/mouse). Scale bars are equal to 500 μm. Top-right panels, pictures with colocalization with DAPI. "Naïve oxLDL" group mice were injected with unlabeled oxLDL. (b) Quantification of FITC fluorescence intensity. $^{*}P < 0.05$ versus control, $n = 4$.

maintain the normal LDL and VLDL metabolism pathway. ASM deficiency in Niemann-Pick disease results in the elevation of plasma LDL and reduction of HDL, which are established risk factors of atherosclerosis. On the other side, ASM may directly promote the retention of lipoprotein particles into the subendothelial space of vascular wall and facilitate the progression of atherosclerosis. Our study focuses on the second aspect of ASM in vascular wall. This is very similar to the roles the LDL receptor (LDLR) plays in atherosclerosis. On one side, LDLR mediates the retention of LDL into the vascular wall and promotes the incidence of AS [64, 65]. On the other side, $Ldlr^{-/-}$ mice exhibit typical hypercholesterol and are more vulnerable to atherosclerosis [66, 67]. A recent paper by Li et al. suggested that the control of lysosome trafficking and fusion by ASM is essential to a normal autophagic flux in coronary arterial smooth muscle cells [68]. Basically, there is no doubt that ASM is beneficial under physiological conditions, but, in chronic pathological

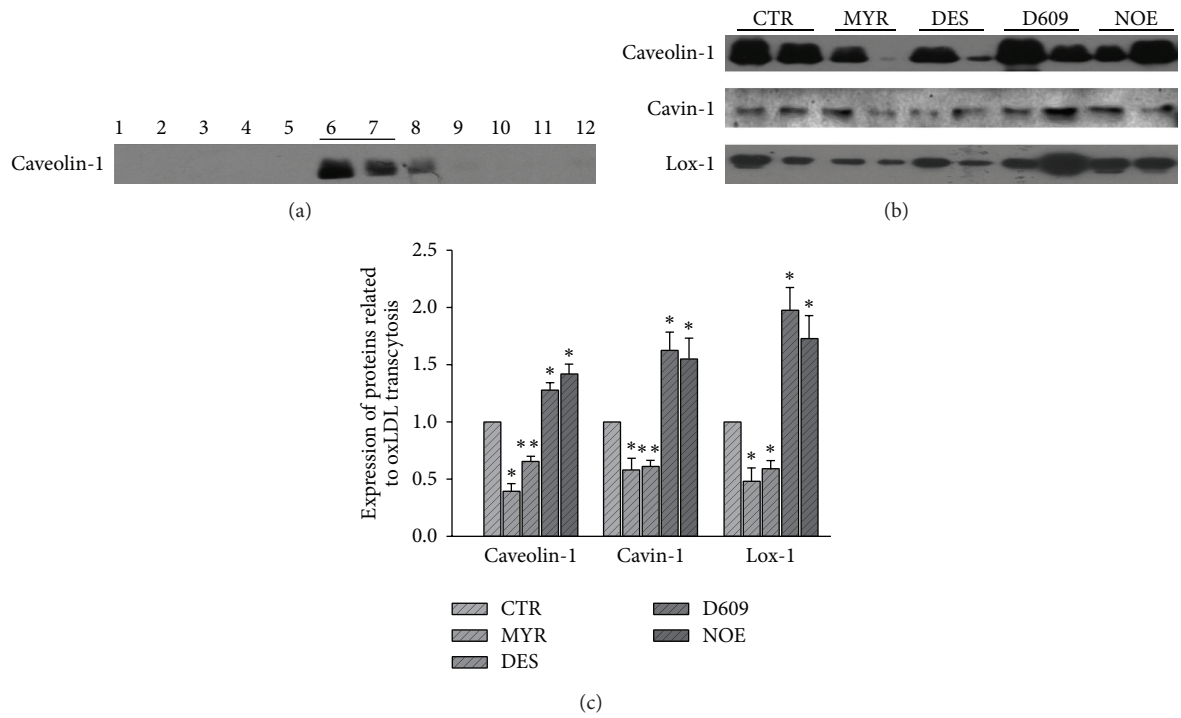

Figure 6: Expression of proteins related to oxLDL transcytosis in LRs in HUVECs. HUVECs were incubated with 30 μM MYR, 10 μM DES, 30 μM D609, or 10 μM NOE for 12 h and then LRs were isolated and detected with western blot. (a) Representative western blot showing the subcellular localization of the protein marker for LRs, caveolin-1. (b) Representative western blot showing the expression of proteins involved in oxLDL transcytosis in LRs, cavin-1 and Lox-1. (c) Quantitative analysis of the protein expression. $^{*}P < 0.05$, $^{**}P < 0.01$ versus control, $n = 4$.

conditions such as atherosclerosis, the ASM activities are persistently upregulated and would in turn drive the progression of diseases [49, 69]. In this situation, inhibition of ASM activity may be the right strategy for therapy.

We also preliminarily studied the mechanism why ceramide contributed to the transcytosis of oxLDL. Basically, oxLDL transcytosis in endothelial cells is mediated by its receptor, Lox-1 [70, 71], as well as many other essential proteins involved in endocytosis or exocytosis, including the caveolae structure protein, caveolin-1 [71, 72], and caveolae associated protein, cavin-1 [72, 73]. Lox-1 and caveolin-1 are both residing in membrane raft domains of endothelial cells. Cavin-1 also binds to caveolin-1 to help maintain the integrity of caveolae. Since ceramides are much less polar than sphingomyelin, these hydrophobic lipids are more ready to fuse simultaneously and contribute to the integrity of membrane raft structures [30], which will facilitate the lipid raft-dependent transcytosis. We studied whether ceramide could alter the expressions of these oxLDL transcytosis-related proteins in membrane rafts. We found that the expressions of Lox-1, caveolin-1, and cavin-1 in membrane raft domains were also significantly regulated by ceramide metabolizing enzyme inhibitors. DES and MYR decreased the expression of Lox-1, caveolin-1, and cavin-1 in membrane rafts. Whereas NOE and D609 upregulated the expressions of these proteins in membrane rafts. Our observations partially explain the critical role of ceramide in the transcytosis of oxLDL across endothelial cells. Some previous studies have also shown that oxLDL induced lipid rafts clustering in human coronary arterial endothelial cells [74] and Lox-1 increased in lipid rafts after oxLDL treatment [53]. oxLDL may also affect ceramide production in lipid rafts [74, 75]. These observations imply that oxLDL *per se* may also elicit a signaling to facilitate its own transcytosis, which would form a feedback forward mechanism and amplify the transcytosis process.

Collectively, both the *in vitro* and *in vivo* evidences provided in the present study strongly point to a conclusion that oxidized LDL, oxLDL, is able to traffic across the endothelial barrier through transcytosis and these processes are highly regulated by intracellular ceramide. Endogenous ceramide significantly promotes the transcytosis of oxLDL across endothelial cells. Therefore, novel compounds designed to manipulate the metabolism of ceramide production through targeting related enzymes may provide novel strategies for the prevention or treatment of atherosclerosis-related disorders.

Conflict of Interests

The authors declare that there is no conflict of interests regarding the publication of this paper.

Authors' Contribution

Wenjing Li and Xiaoyan Yang contributed equally to this work.

Acknowledgments

This study was supported by Grants from the National Natural Science Foundation of China (81072634, 81373413, 81000080, and 30870997) and Grants from the Ministry of Education of China (NCET-10-0409, 2013YGYL008, and 2011TS069).

References

[1] A. C. Lindsay and R. P. Choudhury, "Form to function: current and future roles for atherosclerosis imaging in drug development," *Nature Reviews Drug Discovery*, vol. 7, no. 6, pp. 517–529, 2008.

[2] K. Skålén, M. Gustafsson, E. K. Rydberg et al., "Subendothelial retention of atherogenic lipoproteins in early atherosclerosis," *Nature*, vol. 417, no. 6890, pp. 750–754, 2002.

[3] B. Staels, "Cardiovascular biology: a cholesterol tether," *Nature*, vol. 417, no. 6890, pp. 699–701, 2002.

[4] I. Tabas, K. J. Williams, and J. Borén, "Subendothelial lipoprotein retention as the initiating process in atherosclerosis: update and therapeutic implications," *Circulation*, vol. 116, no. 16, pp. 1832–1844, 2007.

[5] I. Tabas, "Macrophage death and defective inflammation resolution in atherosclerosis," *Nature Reviews Immunology*, vol. 10, no. 1, pp. 36–46, 2010.

[6] P. G. Frank, S. Pavlides, and M. P. Lisanti, "Caveolae and transcytosis in endothelial cells: role in atherosclerosis," *Cell and Tissue Research*, vol. 335, no. 1, pp. 41–47, 2009.

[7] R. M. Krauss and D. J. Burke, "Identification of multiple subclasses of plasma low density lipoproteins in normal humans," *Journal of Lipid Research*, vol. 23, no. 1, pp. 97–104, 1982.

[8] N. Simionescu, M. Simionescu, and G. E. Palade, "Open junctions in the endothelium of the postcapillary venules of the diaphragm," *Journal of Cell Biology*, vol. 79, no. 1, pp. 27–44, 1978.

[9] P. L. Tuma and A. L. Hubbard, "Transcytosis: crossing cellular barriers," *Physiological Reviews*, vol. 83, no. 3, pp. 871–932, 2003.

[10] S. Ehara, M. Ueda, T. Naruko et al., "Elevated levels of oxidized low density lipoprotein show a positive relationship with the severity of acute coronary syndromes," *Circulation*, vol. 103, no. 15, pp. 1955–1960, 2001.

[11] S. Xu, S. Ogura, J. Chen, P. J. Little, J. Moss, and P. Liu, "LOX-1 in atherosclerosis: biological functions and pharmacological modifiers," *Cellular and Molecular Life Sciences*, vol. 70, no. 16, pp. 2859–2872, 2013.

[12] S. Tsimikas and J. L. Witztum, "Measuring circulating oxidized low-density lipoprotein to evaluate coronary risk," *Circulation*, vol. 103, no. 15, pp. 1930–1932, 2001.

[13] E. Verhoye and M. R. Langlois, "Circulating oxidized low-density lipoprotein: a biomarker of atherosclerosis and cardiovascular risk?" *Clinical Chemistry and Laboratory Medicine*, vol. 47, no. 2, pp. 128–137, 2009.

[14] S. Staubach and F.-G. Hanisch, "Lipid rafts: signaling and sorting platforms of cells and their roles in cancer," *Expert Review of Proteomics*, vol. 8, no. 2, pp. 263–277, 2011.

[15] S. Jin, F. Zhou, F. Katirai, and P.-L. Li, "Lipid raft redox signaling: molecular mechanisms in health and disease," *Antioxidants & Redox Signaling*, vol. 15, no. 4, pp. 1043–1083, 2011.

[16] S. Jin and F. Zhou, "Lipid raft redox signaling platforms in vascular dysfunction: features and mechanisms," *Current Atherosclerosis Reports*, vol. 11, no. 3, pp. 220–226, 2009.

[17] P. Lajoie and I. R. Nabi, "Lipid rafts, caveolae, and their endocytosis," *International Review of Cell and Molecular Biology*, vol. 282, pp. 135–163, 2010.

[18] D. Lingwood, H.-J. Kaiser, I. Levental, and K. Simons, "Lipid rafts as functional heterogeneity in cell membranes," *Biochemical Society Transactions*, vol. 37, no. 5, pp. 955–960, 2009.

[19] K. Simons and E. Ikonen, "Functional rafts in cell membranes," *Nature*, vol. 387, no. 6633, pp. 569–572, 1997.

[20] J. D. Symons and E. D. Abel, "Lipotoxicity contributes to endothelial dysfunction: a focus on the contribution from ceramide," *Reviews in Endocrine and Metabolic Disorders*, vol. 14, no. 1, pp. 59–68, 2013.

[21] J. Bismuth, P. Lin, Q. Yao, and C. Chen, "Ceramide: a common pathway for atherosclerosis?" *Atherosclerosis*, vol. 196, no. 2, pp. 497–504, 2008.

[22] S. Elojeimy, D. H. Holman, X. Liu et al., "New insights on the use of desipramine as an inhibitor for acid ceramidase," *FEBS Letters*, vol. 580, no. 19, pp. 4751–4756, 2006.

[23] R. Bhatia, K. Matsushita, M. Yamakuchi, C. N. Morrell, W. Cao, and C. J. Lowenstein, "Ceramide triggers Weibel-Palade body exocytosis," *Circulation Research*, vol. 95, no. 3, pp. 319–324, 2004.

[24] M. Kölzer, N. Werth, and K. Sandhoff, "Interactions of acid sphingomyelinase and lipid bilayers in the presence of the tricyclic antidepressant desipramine," *FEBS Letters*, vol. 559, no. 1–3, pp. 96–98, 2004.

[25] T.-S. Park, R. L. Panek, M. D. Rekhter et al., "Modulation of lipoprotein metabolism by inhibition of sphingomyelin synthesis in ApoE knockout mice," *Atherosclerosis*, vol. 189, no. 2, pp. 264–272, 2006.

[26] P. Keul, K. Sattler, and B. Levkau, "HDL and its sphingosine-1-phosphate content in cardioprotection," *Heart Failure Reviews*, vol. 12, no. 3-4, pp. 301–306, 2007.

[27] E. Houben, J. P. Hachem, K. de Paepe, and V. Rogiers, "Epidermal ceramidase activity regulates epidermal desquamation via stratum corneum acidification," *Skin Pharmacology and Physiology*, vol. 21, no. 2, pp. 111–118, 2008.

[28] A. Meng, C. Luberto, P. Meier et al., "Sphingomyelin synthase as a potential target for D609-induced apoptosis in U937 human monocytic leukemia cells," *Experimental Cell Research*, vol. 292, no. 2, pp. 385–392, 2004.

[29] Z. Li, T. K. Hailemariam, H. Zhou et al., "Inhibition of sphingomyelin synthase (SMS) affects intracellular sphingomyelin accumulation and plasma membrane lipid organization," *Biochimica et Biophysica Acta*, vol. 1771, no. 9, pp. 1186–1194, 2007.

[30] S. Jin, F. Yi, and P.-L. Li, "Contribution of lysosomal vesicles to the formation of lipid raft redox signaling platforms in endothelial cells," *Antioxidants & Redox Signaling*, vol. 9, no. 9, pp. 1417–1426, 2007.

[31] S. Jin, F. Yi, F. Zhang, J. L. Poklis, and P.-L. Li, "Lysosomal targeting and trafficking of acid sphingomyelinase to lipid raft platforms in coronary endothelial cells," *Arteriosclerosis, Thrombosis, and Vascular Biology*, vol. 28, no. 11, pp. 2056–2062, 2008.

[32] A. Y. Zhang, F. Yi, S. Jin et al., "Acid sphingomyelinase and its redox amplification in formation of lipid raft redox signaling platforms in endothelial cells," *Antioxidants & Redox Signaling*, vol. 9, no. 7, pp. 817–828, 2007.

[33] J. M. Harouse, R. G. Collman, and F. Gonzalez-Scarano, "Human immunodeficiency virus type 1 infection of SK-N-MC cells: domains of gp120 involved in entry into a CD4-negative, galactosyl ceramide/3' sulfo-galactosyl ceramide-positive cell line," *Journal of Virology*, vol. 69, no. 12, pp. 7383–7390, 1995.

[34] J.-T. Jan, S. Chatterjee, and D. E. Griffin, "Sindbis virus entry into cells triggers apoptosis by activating sphingomyelinase, leading to the release of ceramide," *Journal of Virology*, vol. 74, no. 14, pp. 6425–6432, 2000.

[35] V. Teichgräber, M. Ulrich, N. Endlich et al., "Ceramide accumulation mediates inflammation, cell death and infection susceptibility in cystic fibrosis," *Nature Medicine*, vol. 14, no. 4, pp. 382–391, 2008.

[36] A. L. Cheung, "Isolation and culture of human umbilical vein endothelial cells (HUVEC)," *Current Protocols in Microbiology*, 2007.

[37] B. Baudin, A. Bruneel, N. Bosselut, and M. Vaubourdolle, "A protocol for isolation and culture of human umbilical vein endothelial cells," *Nature Protocols*, vol. 2, no. 3, pp. 481–485, 2007.

[38] E. A. Jaffe, R. L. Nachman, C. G. Becker, and C. R. Minick, "Culture of human endothelial cells derived from umbilical veins. Identification by morphologic and immunologic criteria," *The Journal of Clinical Investigation*, vol. 52, no. 11, pp. 2745–2756, 1973.

[39] S.-J. Jia, S. Jin, F. Zhang, F. Yi, W. L. Dewey, and P.-L. Li, "Formation and function of ceramide-enriched membrane platforms with CD38 during M1-receptor stimulation in bovine coronary arterial myocytes," *American Journal of Physiology: Heart and Circulatory Physiology*, vol. 295, no. 4, pp. H1743–H1752, 2008.

[40] G. Vielhaber, L. Brade, B. Lindner et al., "Mouse anti-ceramide antiserum: a specific tool for the detection of endogenous ceramide," *Glycobiology*, vol. 11, no. 6, pp. 451–457, 2001.

[41] L. Wang, H. Zhen, W. Yao et al., "Lipid raft-dependent activation of dual oxidase 1/H2o2/NF-κB pathway in bronchial epithelial cells," *American Journal of Physiology: Cell Physiology*, vol. 301, no. 1, pp. C171–C180, 2011.

[42] V. Zinchuk and O. Grossenbacher-Zinchuk, "Recent advances in quantitative colocalization analysis: focus on neuroscience," *Progress in Histochemistry and Cytochemistry*, vol. 44, no. 3, pp. 125–172, 2009.

[43] S. L. Schissel, X.-C. Jiang, J. Tweedie-Hardman et al., "Secretory sphingomyelinase, a product of the acid sphingomyelinase gene, can hydrolyze atherogenic lipoproteins at neutral pH. Implications for athereosclerotic lesion development," *The Journal of Biological Chemistry*, vol. 273, no. 5, pp. 2738–2746, 1998.

[44] A. Strelow, K. Bernardo, S. Adam-Klages et al., "Overexpression of acid ceramidase protects from tumor necrosis factor-induced cell death," *The Journal of Experimental Medicine*, vol. 192, no. 5, pp. 601–612, 2000.

[45] P. J. Honeycutt and J. E. Niedel, "Cytochalasin B enhancement of the diacylglycerol response in formyl peptide-stimulated neutrophils," *The Journal of Biological Chemistry*, vol. 261, no. 34, pp. 15900–15905, 1986.

[46] G. Seumois, M. Fillet, L. Gillet et al., "De novo C16- and C24-ceramide generation contributes to spontaneous neutrophil apoptosis," *Journal of Leukocyte Biology*, vol. 81, no. 6, pp. 1477–1486, 2007.

[47] F. Bian, X. Yang, F. Zhou et al., "CRP promotes atherosclerosis by increasing LDL transcytosis across endothelial cells," *British Journal of Pharmacology*, 2014.

[48] Y. Zhang, X. Yang, F. Bian et al., "TNF- α promotes early atheros clerosis by increasing transcytosis of LDL across endothelial cells: crosstalk between NF-κB and PPAR-γ," *Journal of Molecular and Cellular Cardiology*, vol. 72, pp. 85–94, 2014.

[49] C. M. Devlin, A. R. Leventhal, G. Kuriakose, E. H. Schuchman, K. J. Williams, and I. Tabas, "Acid sphingomyelinase promotes lipoprotein retention within early atheromata and accelerates lesion progression," *Arteriosclerosis, Thrombosis, and Vascular Biology*, vol. 28, no. 10, pp. 1723–1730, 2008.

[50] Z. Cankova, J.-D. Huang, H. S. Kruth, and M. Johnson, "Passage of low-density lipoproteins through Bruch's membrane and choroid," *Experimental Eye Research*, vol. 93, no. 6, pp. 947–955, 2011.

[51] E. N. Glaros, W. S. Kim, and B. Garner, "Myriocin-mediated up-regulation of hepatocyte apoA-I synthesis is associated with ERK inhibition," *Clinical Science*, vol. 118, no. 12, pp. 727–736, 2010.

[52] J. C. Frias, K. J. Williams, E. A. Fisher, and Z. A. Fayad, "Recombinant HDL-like nanoparticles: a specific contrast agent for MRI of atherosclerotic plaques," *Journal of the American Chemical Society*, vol. 126, no. 50, pp. 16316–16317, 2004.

[53] S. Matarazzo, M. C. Quitadamo, R. Mango, S. Ciccone, G. Novelli, and S. Biocca, "Cholesterol-lowering drugs inhibit lectin-like oxidized low-density lipoprotein-1 receptor function by membrane raft disruption," *Molecular Pharmacology*, vol. 82, no. 2, pp. 246–254, 2012.

[54] L. Chun, Z. Junlin, W. Aimin, L. Niansheng, C. Benmei, and L. Minxiang, "Inhibition of ceramide synthesis reverses endothelial dysfunction and atherosclerosis in streptozotocin-induced diabetic rats," *Diabetes Research and Clinical Practice*, vol. 93, no. 1, pp. 77–85, 2011.

[55] K. Kobayashi, E. Nagata, K. Sasaki, M. Harada-Shiba, S. Kojo, and H. Kikuzaki, "Increase in secretory sphingomyelinase activity and specific ceramides in the aorta of apolipoprotein E knockout mice during aging," *Biological and Pharmaceutical Bulletin*, vol. 36, no. 7, pp. 1192–1196, 2013.

[56] D. Gao, C. Pararasa, C. R. Dunston, C. J. Bailey, and H. R. Griffiths, "Palmitate promotes monocyte atherogenicity via de novo ceramide synthesis," *Free Radical Biology and Medicine*, vol. 53, no. 4, pp. 796–806, 2012.

[57] X.-C. Jiang, I. J. Goldberg, and T.-S. Park, "Sphingolipids and cardiovascular diseases: lipoprotein metabolism, atherosclerosis and cardiomyopathy," *Advances in Experimental Medicine and Biology*, vol. 721, pp. 19–39, 2011.

[58] Y. Fan, F. Shi, J. Liu et al., "Selective reduction in the sphingomyelin content of atherogenic lipoproteins inhibits their retention in murine aortas and the subsequent development of atherosclerosis," *Arteriosclerosis, Thrombosis, and Vascular Biology*, vol. 30, no. 11, pp. 2114–2120, 2010.

[59] X.-C. Jiang, F. Paultre, T. A. Pearson et al., "Plasma sphingomyelin level as a risk factor for coronary artery disease," *Arteriosclerosis, Thrombosis, and Vascular Biology*, vol. 20, no. 12, pp. 2614–2618, 2000.

[60] M. Grandl, S. M. Bared, G. Liebisch, T. Werner, S. Barlage, and G. Schmitz, "E-LDL and Ox-LDL differentially regulate ceramide and cholesterol raft microdomains in human macrophages," *Cytometry A*, vol. 69, no. 3, pp. 189–191, 2006.

[61] S. L. Schissel, J. Tweedie-Hardman, J. H. Rapp, G. Graham, K. J. Williams, and I. Tabas, "Rabbit aorta and human atherosclerotic lesions hydrolyze the sphingomyelin of retained low-density lipoprotein: proposed role for arterial-wall sphingomyelinase

in subendothelial retention and aggregation of atherogenic lipoproteins," *The Journal of Clinical Investigation*, vol. 98, no. 6, pp. 1455–1464, 1996.

[62] A. Loidl, E. Sevcsik, G. Riesenhuber, H.-P. Deigner, and A. Hermetter, "Oxidized phospholipids in minimally modified low density lipoprotein induce apoptotic signaling via activation of acid sphingomyelinase in arterial smooth muscle cells," *The Journal of Biological Chemistry*, vol. 278, no. 35, pp. 32921–32928, 2003.

[63] M. M. McGovern, T. Pohl-Worgall, R. J. Deckelbaum et al., "Lipid abnormalities in children with types A and B Niemann Pick disease," *The Journal of Pediatrics*, vol. 145, no. 1, pp. 77–81, 2004.

[64] G. Cichon, T. Willnow, S. Herwig et al., "Non-physiological overexpression of the low density lipoprotein receptor (LDLr) gene in the liver induces pathological intracellular lipid and cholesterol storage," *The Journal of Gene Medicine*, vol. 6, no. 2, pp. 166–175, 2004.

[65] O. C. Hibbitt, E. McNeil, M. M. P. Lufino, L. Seymour, K. Channon, and R. Wade-Martins, "Long-term physiologically regulated expression of the low-density lipoprotein receptor in vivo using genomic DNA mini-gene constructs," *Molecular Therapy*, vol. 18, no. 2, pp. 317–326, 2010.

[66] S. Zadelaar, R. Kleemann, L. Verschuren et al., "Mouse models for atherosclerosis and pharmaceutical modifiers," *Arteriosclerosis, Thrombosis, and Vascular Biology*, vol. 27, no. 8, pp. 1706–1721, 2007.

[67] L. Powell-Braxton, M. Véniant, R. D. Latvala et al., "A mouse model of human familial hypercholesterolemia: markedly elevated low density lipoprotein cholesterol levels and severe atherosclerosis on a low-fat chow diet," *Nature Medicine*, vol. 4, no. 8, pp. 934–938, 1998.

[68] X. Li, M. Xu, A. L. Pitzer et al., "Control of autophagy maturation by acid sphingomyelinase in mouse coronary arterial smooth muscle cells: protective role in atherosclerosis," *Journal of Molecular Medicine*, 2014.

[69] S. Marathe, G. Kuriakose, K. J. Williams, and I. Tabas, "Sphingomyelinase, an enzyme implicated in atherogenesis, is present in atherosclerotic lesions and binds to specific components of the subendothelial extracellular matrix," *Arteriosclerosis, Thrombosis, and Vascular Biology*, vol. 19, no. 11, pp. 2648–2658, 1999.

[70] M. Kumano-Kuramochi, Q. Xie, S. Kajiwara, S. Komba, T. Minowa, and S. Machida, "Lectin-like oxidized LDL receptor-1 is palmitoylated and internalizes ligands via caveolae/raft-dependent endocytosis," *Biochemical and Biophysical Research Communications*, vol. 434, no. 3, pp. 594–599, 2013.

[71] S.-W. Sun, X.-Y. Zu, Q.-H. Tuo et al., "Caveolae and caveolin-1 mediate endocytosis and transcytosis of oxidized low density lipoprotein in endothelial cells," *Acta Pharmacologica Sinica*, vol. 31, no. 10, pp. 1336–1342, 2010.

[72] A. Dávalos, C. Fernández-Hernando, G. Sowa et al., "Quantitative proteomics of caveolin-1-regulated proteins: characterization of polymerase I and transcript release factor/cavin-1 in endothelial cells," *Molecular & Cellular Proteomics*, vol. 9, no. 10, pp. 2109–2124, 2010.

[73] M. M. Hill, M. Bastiani, R. Luetterforst et al., "PTRF-cavin, a conserved cytoplasmic protein required for caveola formation and function," *Cell*, vol. 132, no. 1, pp. 113–124, 2008.

[74] Y. M. Wei, X. Li, J. Xiong et al., "Attenuation by statins of membrane raft-redox signaling in coronary arterial endothelium," *The Journal of Pharmacology and Experimental Therapeutics*, vol. 345, no. 2, pp. 170–179, 2013.

[75] Y.-X. Liu, G.-Z. Han, T. Wu et al., "Protective effect of α-lipoic acid on oxidized low density lipoprotein-induced human umbilical vein endothelial cell injury," *Pharmacological Reports*, vol. 63, no. 5, pp. 1180–1188, 2011.

Hindawi Publishing Corporation
Oxidative Medicine and Cellular Longevity
Volume 2014, Article ID 674690, 10 pages
http://dx.doi.org/10.1155/2014/674690

Research Article

BL153 Partially Prevents High-Fat Diet Induced Liver Damage Probably via Inhibition of Lipid Accumulation, Inflammation, and Oxidative Stress

Jian Wang,[1,2,3] Chi Zhang,[2,4] Zhiguo Zhang,[3,5] Qiang Chen,[3,5] Xuemian Lu,[2,4] Minglong Shao,[2,4] Liangmiao Chen,[2,4] Hong Yang,[2,4] Fangfang Zhang,[2,4] Peng Cheng,[2,4] Yi Tan,[2,3] Ki-Soo Kim,[6] Ki Ho Kim,[7] Bochu Wang,[1] and Young Heui Kim[7]

[1] *College of Bioengineering, Chongqing University, Chongqing 400044, China*
[2] *The Chinese-American Research Institute for Diabetic Complications, School of Pharmaceutical Sciences & Key Laboratory of Biotechnology Pharmaceutical Engineering, Wenzhou Medical University, Wenzhou 325035, China*
[3] *Department of Pediatrics of the University of Louisville, The Kosair Children's Hospital Research Institute, Louisville, KY 20202, USA*
[4] *Rui'an Center of the Chinese-American Research Institute for Diabetic Complications, The Third Affiliated Hospital of the Wenzhou Medical University, Wenzhou 325200, China*
[5] *Department of Cardiology at the First Hospital & School of Public Health, Jilin University, Changchun 130021, China*
[6] *Bioland Biotec Co., Ltd., Zhangjiang Modern Medical Device Park, Pudong, Shanghai 201201, China*
[7] *Bioland R&D Center, 59 Songjeongni 2-gil, Byeongcheon, Dongnam, Cheonan, Chungnam 330-863, Republic of Korea*

Correspondence should be addressed to Bochu Wang; wangbc2000@126.com and Young Heui Kim; yhkim1st@biolandkorea.com

Received 9 December 2013; Accepted 20 February 2014; Published 3 April 2014

Academic Editor: Si Jin

The present study was to investigate whether a *magnolia* extract, named BL153, can prevent obesity-induced liver damage and identify the possible protective mechanism. To this end, obese mice were induced by feeding with high fat diet (HFD, 60% kcal as fat) and the age-matched control mice were fed with control diet (10% kcal as fat) for 6 months. Simultaneously these mice were treated with or without BL153 daily at 3 dose levels (2.5, 5, and 10 mg/kg) by gavage. HFD feeding significantly increased the body weight and the liver weight. Administration of BL153 significantly reduced the liver weight but without effects on body weight. As a critical step of the development of NAFLD, hepatic fibrosis was induced in the mice fed with HFD, shown by upregulating the expression of connective tissue growth factor and transforming growth factor beta 1, which were significantly attenuated by BL153 in a dose-dependent manner. Mechanism study revealed that BL153 significantly suppressed HFD induced hepatic lipid accumulation and oxidative stress and slightly prevented liver inflammation. These results suggest that HFD induced fibrosis in the liver can be prevented partially by BL153, probably due to reduction of hepatic lipid accumulation, inflammation and oxidative stress.

1. Introduction

Obesity is becoming a health issue all over the world. It grows rapidly and always leads to severe complications such as cardiovascular disorder, diabetes, and cancer [1–3]. Liver is one of the most affected organs by obesity in the body, which leads to nonalcoholic fatty liver disease (NAFLD) [4]. NAFLD is a pathologic entity, including a spectrum of liver damage ranging from simple steatosis to nonalcoholic steatohepatitis (NASH), advanced fibrosis, and progression to cirrhosis [5]. The pathogenesis of NAFLD appears to involve a 2-hit process [6–8]. The first hit is the steatosis which is believed to be triggered by insulin resistance and the second hit which involves oxidative stress results in disease progression. The proinflammatory cytokines have been implicated in the pathogenesis of NAFLD and contribute to the increased risk for hepatocellular carcinoma. Therefore, attenuation of lipid accumulation, oxidative damage, and

inflammation associated with obesity is expected to exert beneficial effects and thus be a potential novel therapeutic strategy for NAFLD.

Magnolia officinalis is regarded as Chinese traditional medicine and used in the clinical practice for a long time to treat various disorders [9, 10]. Several constituents of the *Magnolia* such as honokiol, obovatol, and magnolol have been reported to have antioxidative [11, 12] and anti-inflammatory effects [13–15]. Honokiol has been shown to have the effect of anti-inflammation by inhibiting NF-κB activation, activin phosphorylation, and subsequent IκBα degradation [16, 17]. Consistent with the suppression effect of honokiol on NF-κB is that honokiol decreases levels of NF-κB target genes including tumor necrosis factor (TNF-) α, intercellular adhesion molecule (ICAM-) 1, and plasminogen activator inhibitor (PAI-) 1. Honokiol also plays critical role in scavenging reactive oxygen species via inhibition of TNF-α mediated NADPH oxidase (NOX) pathway in hepatocytes [18]. In addition to honokiol, other two main constituents of *Magnolia*, magnolol, and obovatol also showed the antioxidative effect by attenuation of ROS generation and the subsequent reduction of NF-κB activation [19, 20]. Both oxidative stress and inflammation cause fibrosis, which can be prevented by attenuation of transforming growth factor beta 1 (TGF-β1) and its downstream profibrotic factors such as connective tissue growth factor (CTGF) through inhibition of Smad-2/3 signaling pathway [21]. Furthermore, it was reported that magnolol regulated lipid metabolism by increase of fatty acid β-oxidation and lipolysis, finally reducing lipid accumulation in the tissue [22, 23].

The present study was to clarify whether BL153 has protective effects on HFD-induced liver damage and if so what is the possible mechanism. We found administration of BL153 significantly prevented chronic obesity-induced liver damage with the mechanism of reducing lipid accumulation and inhibiting inflammation and the associated oxidative stress.

2. Material and Methods

2.1. Experimental Protocols and Animals. *Magnolia* extract (BL153) was prepared as our previous report [24]. The major constituents and their structure of *magnolia* extract have been defined in previous studies [24–26]. All experiments involving mice conformed to the National Institutes of Health Guide for the Care and Use of Laboratory Animals and were approved by the University of Louisville Institutional Animal Care and Use Committee. Male C57BL/6J mice at 8 weeks of age were purchased from the Jackson Laboratory and housed in the University of Louisville Research Resources Center at 22°C with a 12-hour light/dark cycle. Mice were randomly divided into five groups ($n = 5$) and fed either a control diet (Ctrl, 10% kcal as fat; D12450B, Research Diets Inc. NJ) or a high fat diet (HFD, 60% kcal as fat; D12492B, Research Diets Inc. NJ) with or without BL153 for six months: (1) Ctrl group: mice were fed a control diet and supplemented with 0.5% ethanol; (2) HFD group: mice were fed a HFD and supplemented with 0.5% ethanol; (3) HFD+2.5 mg/kg group: mice were fed a HFD and supplemented with BL153 at the dose of 2.5 mg/kg; (4) HFD+5 mg/kg group: mice were fed a HFD and supplemented with BL153 at the dose of 5 mg/kg; and (5) HFD+10 mg/kg group: mice were fed a HFD and supplemented with BL153 at the dose of 10 mg/kg. Selection of 5 mg/kg and 10 mg/kg for the present study was based on a previous study [25], where treatment with BL153 at these two dose levels for a week showed a significantly protective effect. Since the treatment in the present study is longer than that, we also included one lower dose of BL153 at 2.5 mg/kg.

For preparing BL153 gavage solution, different doses of BL153 were dissolved into 100% ethanol and then diluted with ddH_2O into final concentration of 1.0 mg/mL (high dose group), 0.5 mg/mL (middle dose group), and 0.25 mg/mL (low dose group) with final concentration of ethanol at 0.5%, respectively. Therefore, the gavage volume was 1% (mL/g) of mouse body weight (e.g., 25 g mouse should be given 250 μL). Control groups were given same volume of ddH_2O with 0.5% ethanol. During the six-month feeding, body weight was measured every month, and the gavage volume was justified based on the body weight change. At the end of experiment, all mice were sacrificed and livers were collected for further analysis.

2.2. Histological Examination and Immunohistochemical Staining. The fixed liver tissue was cut into 3 mm thickness blocks. The tissue blocks were embedded in paraffin and cut into 4 μm slices. After being deparaffinized using xylene and ethanol dilutions and rehydration, the sections were stained with hematoxylin and eosin (H & E, DAKO, Carpinteria, CA) to examine the tissue structure, inflammatory cell infiltration, necrosis, and lipid accumulation as described previously [27, 28]. For immunohistochemical staining, sections were blocked with Superblock buffer (Pierce, Rockford, IL) for 30 min. Sections were then incubated with proper primary antibodies in 1 : 200 dilutions overnight at 4°C. After three washes with phosphate-buffered saline (PBS), these sections were incubated with horseradish peroxidase-labeled secondary antibody (Santa Cruz Biotechnology, Santa Cruz, CA) at room temperature for 1 h, followed by color development with diaminobenzidine for 2 min.

2.3. Oil Red O Staining and Triglyceride Assay for Lipid Accumulation. Cryosections from OCT-embedded tissue samples of the liver (10 mm thickness) were fixed in 10% buffered formalin for 5 min at room temperature, stained with Oil Red O for 1 h, washed with 10% isopropanol, and then counterstained with hematoxylin for 30 s. A Nikon microscope (Nikon, Melville, NY) was used to capture the Oil Red O-stained tissue sections at 40x magnification. For hepatic triglyceride levels assay, 200 mg of hepatic tissues was homogenized at 4°C in 2.0 mL diluted Standard Diluent using a Polytron tissue homogenizer. After centrifugation at 10000 ×g for 10 min at 4°C, samples were diluted by the ratio of 1 : 5 using the diluted Standard Diluent. Then, the triglyceride levels in liver tissue were measured according to the manufacturers' instructions provided in the triglyceride colorimetric assay kit (Cayman Chemical, CA).

2.4. Western Blot. Western blot assays were performed as described before [29]. Briefly, liver tissues were homogenized in RIPA lysis buffer (Santa Cruz Biotechnology, Santa Cruz, CA). Proteins were collected by centrifuging at 12,000 g at 4°C. The sample of total protein was separated on 10% SDS-PAGE gels and transferred to nitrocellulose membranes (Bio-Rad, Hercules, CA). These membranes were rinsed briefly in tris-buffered saline containing 0.05% Tween 20 (TBST), blocked in blocking buffer (5% milk and 0.5% BSA) for 1 h, and then incubated with different primary antibodies overnight at 4°C, followed by three washes with TBST and incubation with secondary horseradish peroxidase-conjugated antibody for 1 h at room temperature. Antigen-antibody complexes were then visualized using ECL kit (Amersham, Piscataway, NJ). The primary antibodies used here include those against 3-nitrotyrosine (3-NT, 1 : 2000, Millipore, Billerica, MA), 4-hydroxynonenal (4-HNE, 1 : 2000, Alpha Diagnostic International, San Antonio, TX), ICAM-1 (1 : 500), CTGF and β-actin (1 : 1000, Santa Cruz Biotechnology, Santa Cruz, CA), PAI-1 (1 : 2000, BD Biosciences, Sparks, MD), TNF-a (1 : 500), and TGF-β1 (1 : 1000; Cell Signaling, Danvers, MA).

2.5. Statistical Analysis. Data were collected from five animals for each group and presented as mean ± SD. One-way ANOVA was used to determine general difference, followed by a post hoc Tukey's test for the difference between groups using Origin 7.5 laboratory data analysis and graphing software. Statistical significance was considered as $P < 0.05$.

3. Results

3.1. HFD-Induced Obesity and the Effects of BL153. In order to identify whether BL153 can prevent obesity and the subsequent hepatic injury, HFD treatment was applied in this study to induce obesity mouse model. After 6 months of HFD feeding, the body weight was significantly increased, which indicated the establishment of the obesity mouse model (Figure 1(a)) but treatment with BL153 had no significant effects on HFD-induced body weight gain (Figure 1(a)). Additionally, HFD also significantly increased liver weight (Figure 1(b)) and the ratio of liver weight to tibia length (Figure 1(c)); treatment with BL153 slightly prevented HFD-induced liver weight increase (Figure 1(b)) but significantly prevented the ratio of liver weight to tibia length (Figure 1(c)), a more reasonable indicator of liver hypotrophy.

3.2. BL153 Attenuated HFD-Induced Hepatic Fibrosis. Liver weight increase is a feature of hepatic hypertrophy which is closely associated with liver fibrosis [30–32]. Moreover, fibrosis is a key step of the development of NAFLD [33, 34]. We next identified whether administration of BL153 prevents hepatic fibrosis under obese conditions. Western blot assay and immunohistochemical staining revealed that HFD treatment significantly upregulated hepatic CTGF expression which was significantly attenuated by administration of BL153 in a dose-dependent manner (Figures 2(a) and 2(b)). In order to further confirm our findings about the antifibrotic effect of BL153 in HFD fed mice, we also examined the expression of another classical fibrotic marker TGF-β1. Similar protective effects were observed that HFD significantly increased hepatic TGF-β1 expression, which was remarkably reduced by treatment of BL153 in a dose-dependent manner (Figure 2(c)).

3.3. Effects of BL153 on HFD-Induced Hepatic Steatosis. The above study revealed that BL153 significantly prevented HFD-induced hepatic hypertrophy and fibrosis. And lipid accumulation is the first step of NAFLD development [35, 36]. Thus, we tried to determine whether BL153 can prevent HFD-induced hepatic steatosis. Liver pathological examination with H&E staining is presented in Figure 3(a). The hepatic cell structure in Ctrl group was normal. However, HFD feeding increased hepatic damage with obviously hepatic necrosis (Figure 3(a)). Further examination of hepatic lipid accumulation status with Oil red O staining and triglyceride level assay revealed that HFD feeding significantly induced hepatic lipid accumulation compared to Ctrl group (Figures 3(b) and 3(c)). Administration of BL153 significantly, but not completely, prevented HFD-induced hepatic lipid accumulation (Figures 3(b) and 3(c)).

3.4. BL153 Attenuated HFD-Induced Hepatic Inflammation. Inflammation is the main pathological consequence of HFD-induced obesity characterized by release of inflammatory factors which contributes to insulin resistance [37–39]. Thus, we determined whether BL153 can prevent HFD-induced hepatic inflammation. The protein expression of classic inflammatory factors including ICAM-1, TNF-α, and PAI-1 was detected. Western blot assay revealed that HFD significantly upregulated the expression of TNF-α (Figure 4(a)), ICAM-1 (Figure 4(b)), and PAI-1 (Figure 4(c)) in the liver. However, all three doses of BL153 treatment significantly attenuated HFD-induced upregulation of TNF-α (Figure 4(a)), ICAM-1 (Figure 4(b)), and PAI-1 (Figure 4(c)), while no significant differences among the three doses of BL153 treatment were observed.

3.5. BL153 Attenuated HFD-Induced Hepatic Oxidative Stress. HFD-induced obesity generally leads to oxidative stress via release of multiple adipokines which in turn generates excessive reactive oxygen species [40]. Furthermore, obesity-associated inflammation is an oxidative stress enhancer, which interacts with each other and causes a vicious circle, promoting the development of insulin resistance [41, 42]. Thus, we next determined whether BL153 can prevent HFD-induced oxidative stress measured by 3-NT as an index of nitrosative damage (Figure 5(a)) and 4-HNE (lipid peroxide) as an index of oxidative damage (Figure 5(b)). The result showed that HFD feeding significantly upregulated the expression of 3-NT and 4-HNE in the liver, which were significantly attenuated by BL153 treatment in a dose-dependent manner (Figures 5(a) and 5(b)).

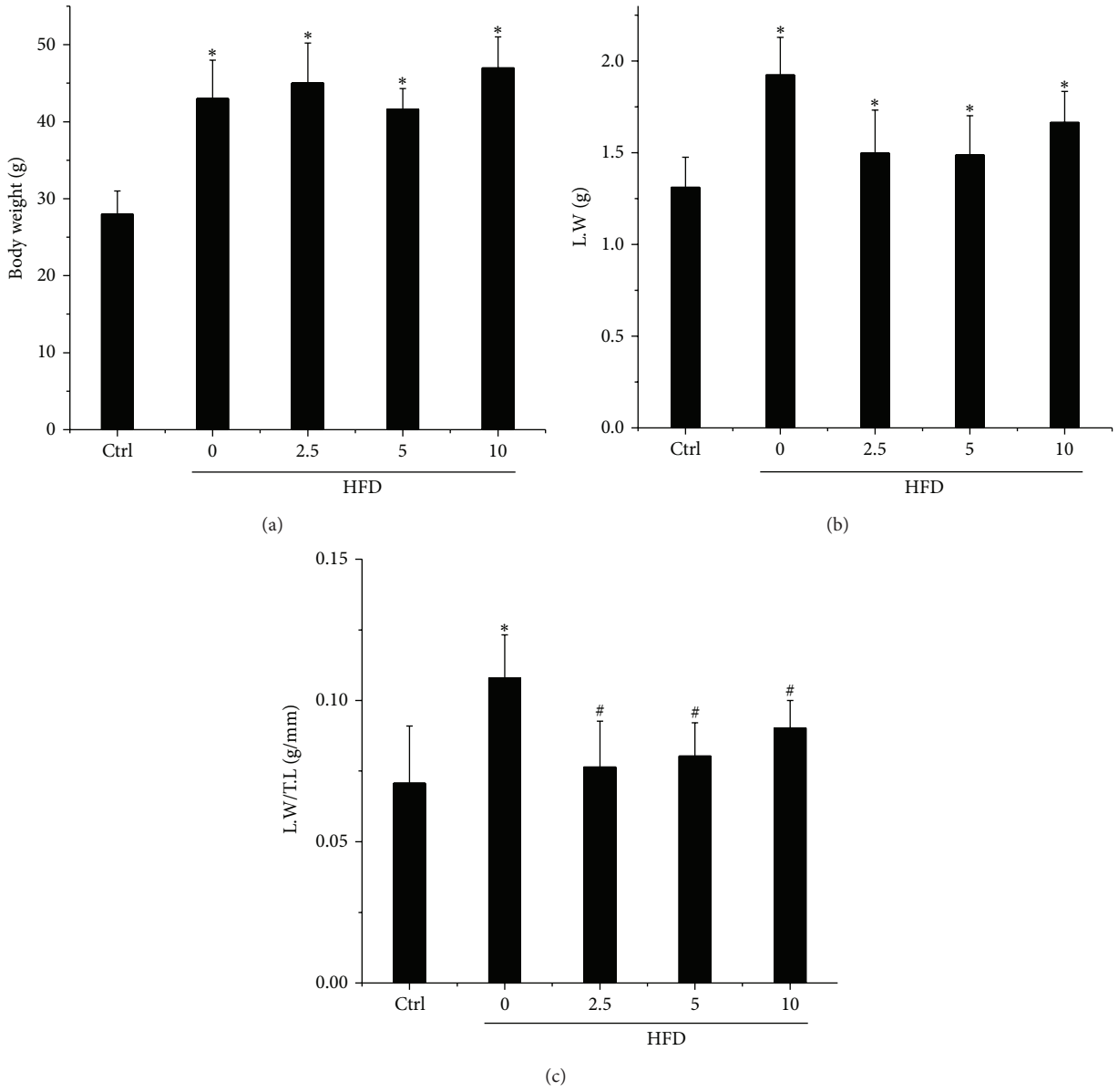

Figure 1: Effects of BL153 on body weight, liver weight, and the ratio of liver weight to tibia length. Mice were fed HFD to induce obesity; mouse models were simultaneously treated with or without BL153 at three dose levels (2.5, 5 or 10 mg/kg body weight) by gavage. The body weight (a) was monitored at 6 months after HFD feeding. Then, the mice were sacrificed and the liver weight (b) and the ratio of liver weight to tibia length (c) were examined. Data were presented as means ± SD ($n = 5$ at least in each group). $^{*}P < 0.05$ versus Ctrl group. $^{\#}P < 0.05$ versus HFD group. L.W = liver weight; T.L = tibia length; Ctrl: control; HFD: high fat diet.

4. Discussion

Obesity is currently a worldwide epidemic and among the most challenging health conditions. A major metabolic consequence of obesity is insulin resistance which underlies the pathogenesis of the metabolic syndrome such as NAFLD, the hepatic manifestation of obesity and metabolic syndrome [6, 43]. NAFLD is considered to be the most common liver disorder in western countries, estimated to affect at least one-quarter of the general population and rising up to 90% in morbidly obese individuals [44, 45]. It comprises a disease spectrum ranging from steatosis (fatty liver), through NASH, to fibrosis and ultimately liver cirrhosis. Previous studies mentioned that the pathogenesis of NAFLD commonly can be divided into two hits. The first hit, hepatic triglyceride accumulation (steatosis), increases susceptibility of the liver to injury mediated by second hit, such as inflammation and oxidative stress, which in turn lead to fibrosis [8, 46]. Therefore, finding a proper way which can simultaneously target both of the first and second hits, that is, lipid accumulation, oxidative stress, inflammation, and fibrosis, might be a potential approach to prevent the development of NAFLD in clinics.

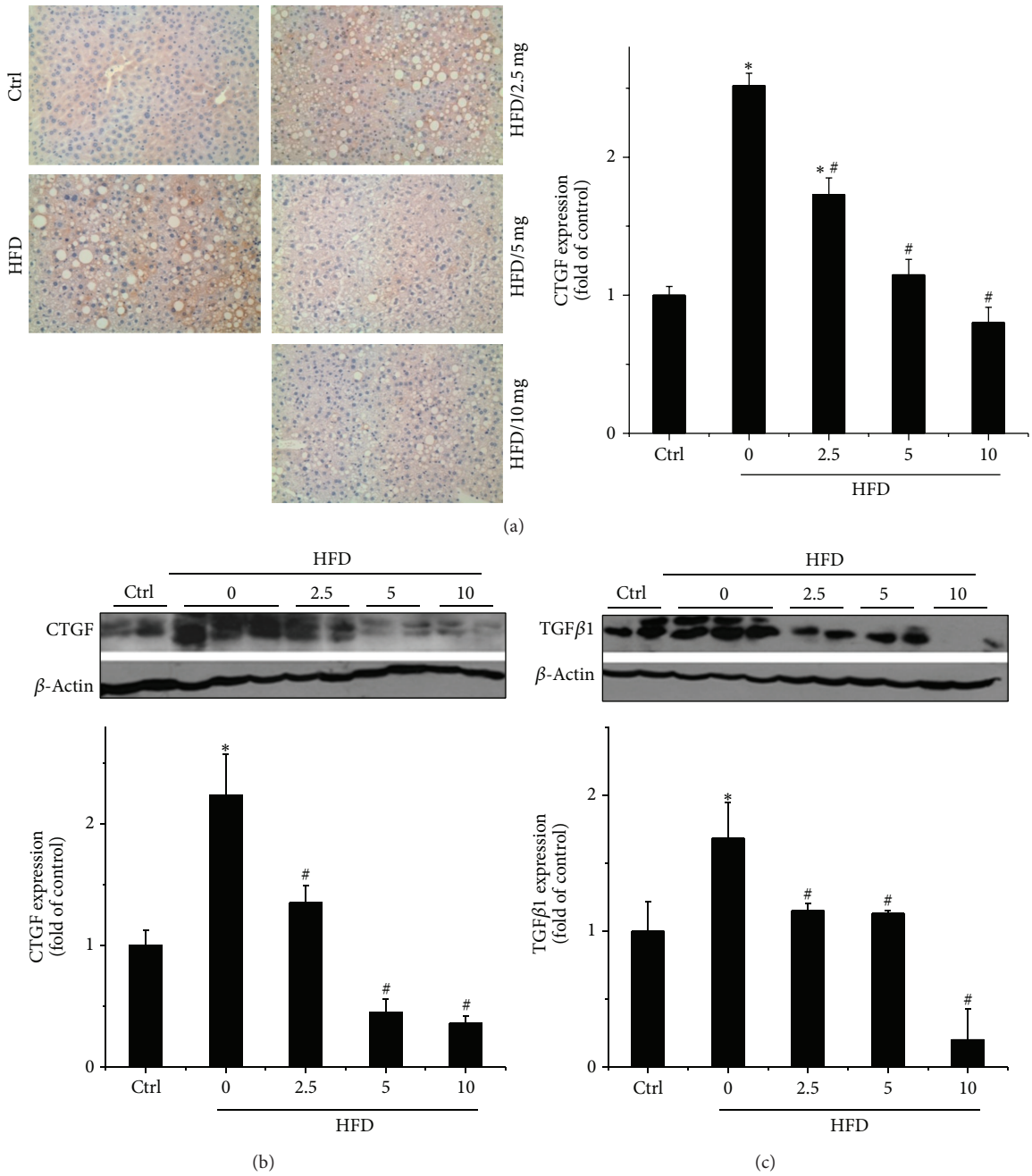

Figure 2: Effects of BL153 on HFD-induced fibrosis in the liver. The expression of fibrotic molecular maker CTGF was detected by immunohistochemical staining (a), and both CTGF (b) and TGF-β1 (c) were also detected by Western blot. Data were presented as means ± SD ($n = 5$ at least in each group). $^{*}P < 0.05$ versus Ctrl group. $^{\#}P < 0.05$ versus HFD group. CTGF: connective tissue growth factor; TGF-β1: transforming growth factor β1; Ctrl: control; HFD: high fat diet.

In the present study, we provide the first evidence that *magnolia* extract, BL153, attenuated obesity-associated liver damage in a HFD-induced obesity mouse model. Most importantly, BL153 treatment significantly attenuated obesity caused liver pathological changes, including hepatic hypertrophy, lipid accumulation, fibrosis, inflammation, and oxidative stress.

Magnolia has been used as Chinese traditional medicine to treat various disorders [9, 10]. It is reported that magnolol, a main compound isolated from *Magnolia* bark, reduces the number of intracellular stored lipid droplets by enhancing lipolysis and thus inhibits the formation of intracellular cholesterol esters [47]. It is unclear whether the liver weight lowering and anti-inflammation effects of BL153 are attributed to scavenging of lipid accumulation in liver. In our study, we examined the hepatic lipid accumulation in both HFD-fed and standard diet-fed mice by Oil Red O staining and triglyceride assay (Figure 3). The result showed that the

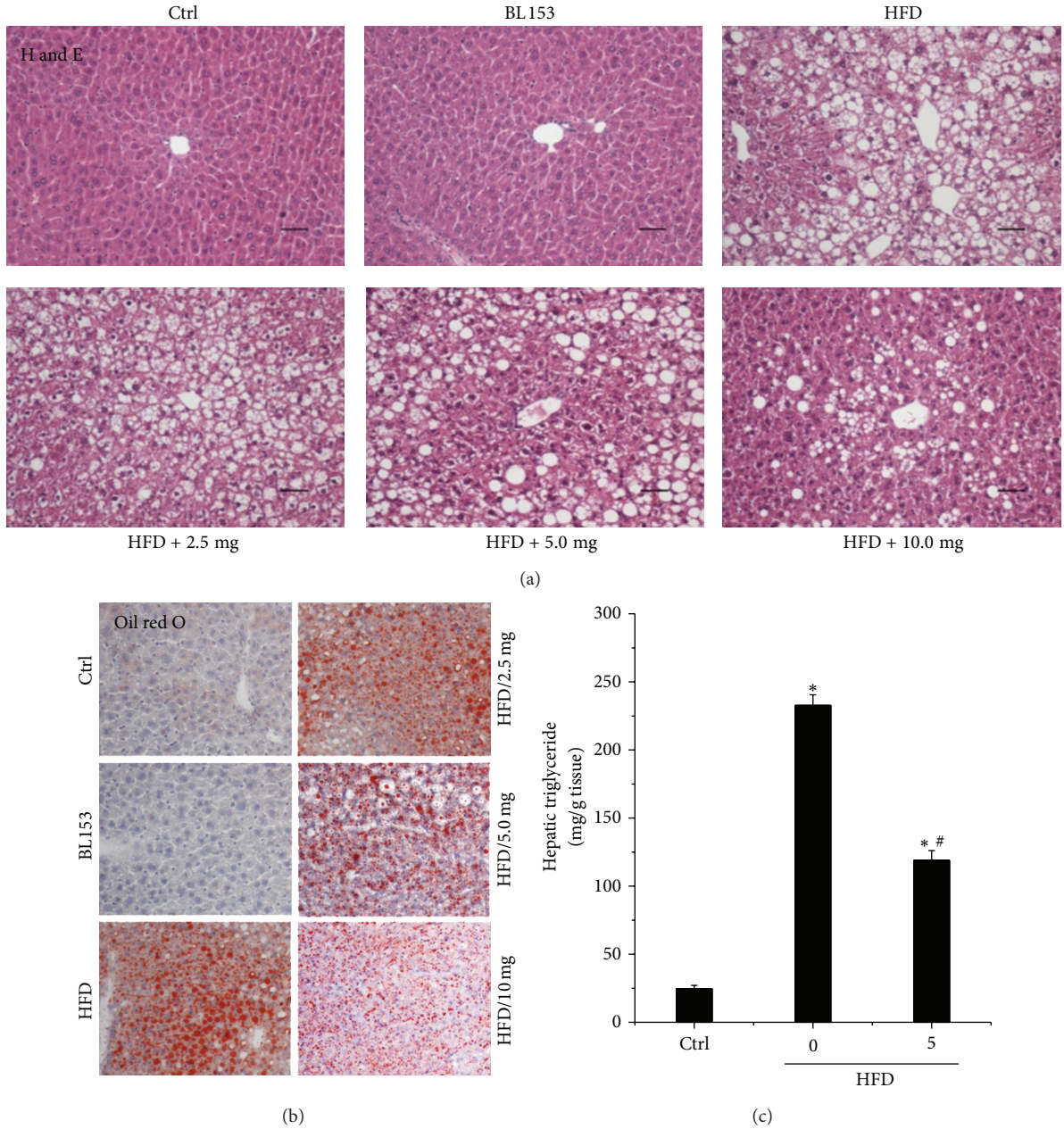

Figure 3: Effects of BL153 on HFD-induced hepatic lipid accumulation. Hepatic morphological changes were examined microscopically with H&E staining ((a) original magnification = 40). Hepatic lipid accumulation was examined by Oil Red O staining ((b) original magnification = 40) and triglyceride level assay (c). Data were presented as means ± SD ($n = 5$ at least in each group). $^{*}P < 0.05$ versus Ctrl group; $^{\#}P < 0.05$ versus HFD group. Ctrl: control; HFD: high fat diet.

fat droplets were obviously observed in the liver of HFD-fed mice associated with hepatic necrosis, which were significantly inhibited by BL153 treatment (Figure 3). The current study revealed that lowering hepatic lipid accumulation was the key mechanism of BL153 to fight against the first hit of NAFLD.

Liver weight increase is a main feature of hepatic hypertrophy associated with hepatic fibrosis, which is a key step during the development of NAFLD [48, 49]. Growing evidence demonstrated that *Magnolia* also showed great beneficial effect on antifibrosis. Administration of *Magnolia* cannot only prevent the cardiac fibrosis induced by ischemia/reperfusion but also the renal fibrosis induced by TGF-β1 [21, 50]. In the present study, we further confirmed that HFD significantly upregulated hepatic CTGF and TGF-β1 expression, which were remarkably attenuated by BL153 treatment in a dose-dependent manner (Figure 2).

As we know, inflammation and the associated oxidative stress also participate in the development of NAFLD. Moreover, other studies also mentioned that another constituent

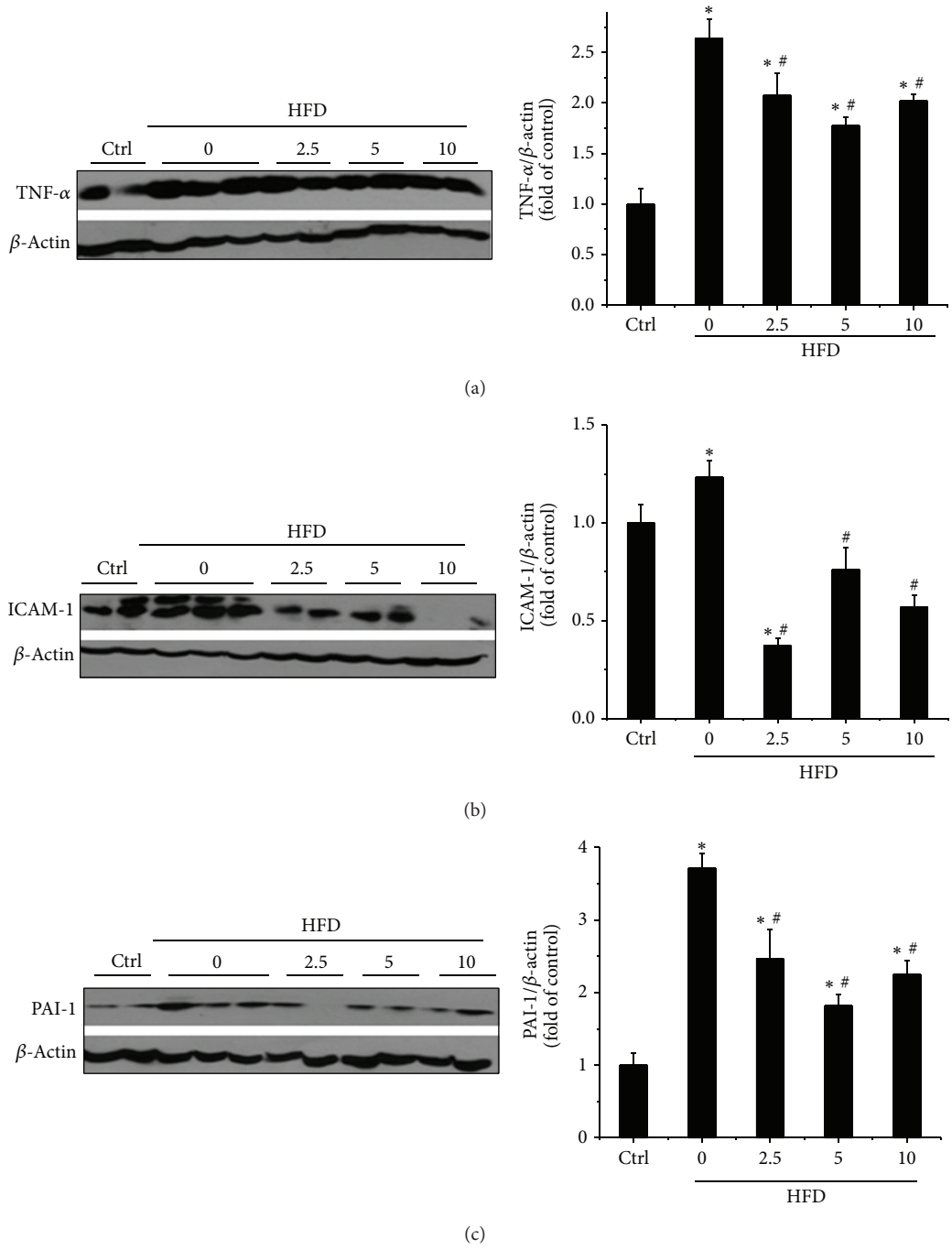

Figure 4: Effects of BL153 on HFD-induced hepatic inflammation. The expression of inflammatory factors, including TNF-a (a), ICAM-1 (b), and PAI-1 (c) was examined by Western blot. Data were presented as mean ± SD ($n = 5$ at least in each group). $^{*}P < 0.05$ versus Ctrl group; $^{\#}P < 0.05$ versus HFD group. TNF-a: tumor necrosis factor a; ICAM-1: intercellular adhesion molecule-1; PAI-1: plasminogen activator inhibitor-1; Ctrl: control; HFD: high fat diet.

of *Magnolia*, honokiol, plays inhibiting role on lipid accumulation-induced inflammation and oxidative stress [13–15, 51]. Therefore, we tried to determine whether anti-inflammation and antioxidation are the missing mechanisms of BL153 on preventing pathological process of HFD-induced liver damage. Our results indicated that HFD significantly upregulated the expression of hepatic inflammatory factors including TNF-α, ICAM-1, and PAI-1 (Figure 4) as well as the marker of oxidative stress including 3-NT and 4-HNE (Figure 5). Administration of BL153 significantly attenuated oxidative stress shown by decrease of 3-NT and 4-HNE expressions in the liver with a dose-dependent manner (Figure 5). BL153 also remarkably inhibited hepatic inflammatory factor expressions without significant differences

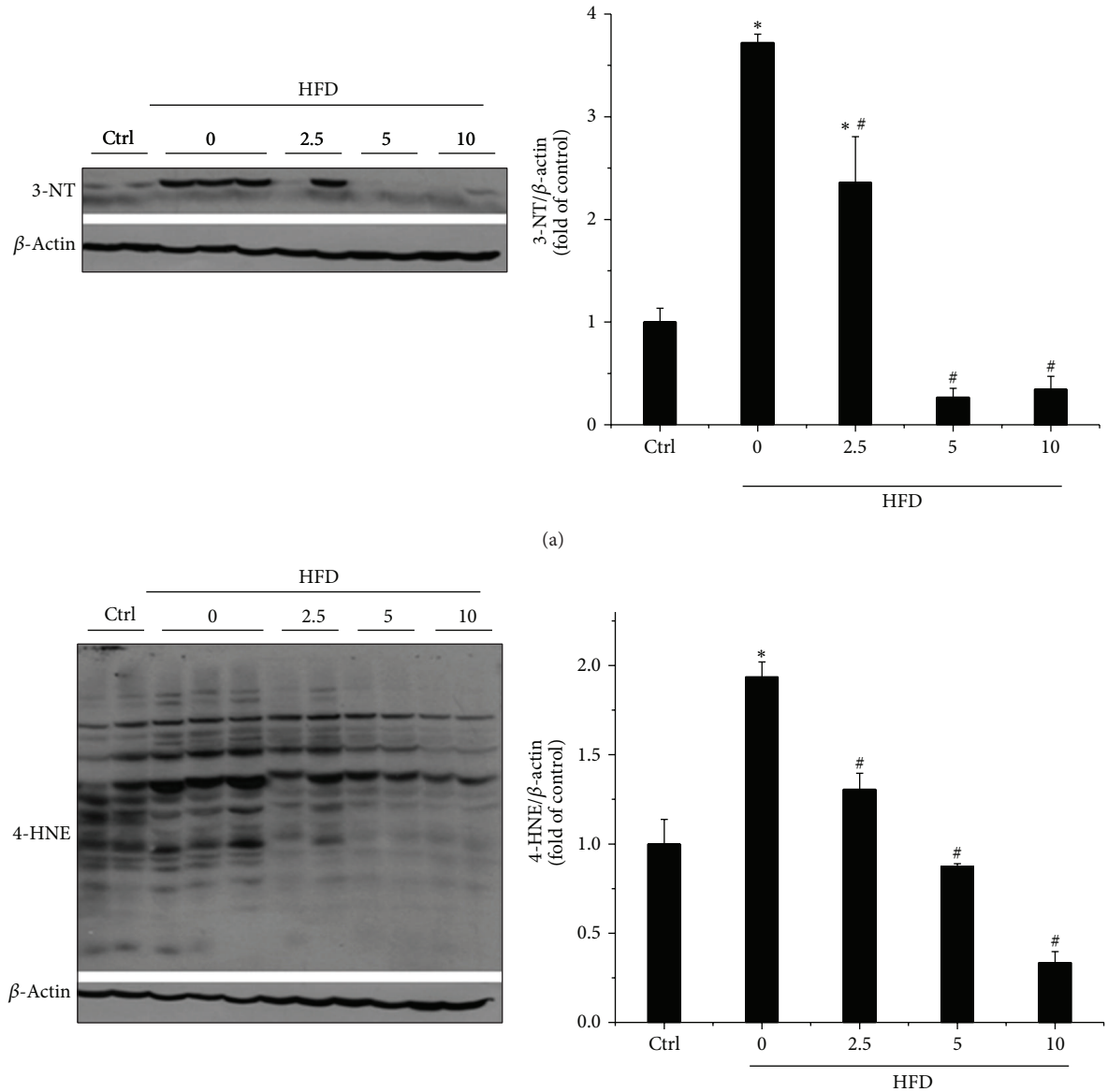

Figure 5: Effects of BL153 on HFD-induced hepatic oxidative stress. Hepatic expression of oxidative stress marker 3-NT (a) and 4-HNE (b) was examined by Western blot. Data were presented as mean ± SD ($n = 5$ at least in each group). $^{*}P < 0.05$ versus Ctrl group; $^{\#}P < 0.05$ versus 3-NT: 3-nitrotyrosine; 4-HNE: 4-hydroxynonenal HFD group. Ctrl: control; HFD: high fat diet.

among three dose level treatments (Figure 4), which implied that BL153 had different sensitivity to HFD-induced inflammation and oxidative stress.

In summary, the fat liver damage is a main consequence of the development of obesity induced by HFD. The *magnolia* extract BL153 can simultaneously induce beneficial effects on HFD-induced liver damage by inhibiting hepatic lipid accumulation, inflammation, oxidative stress, hypertrophy, and fibrosis.

Conflict of Interests

The authors have no conflict of interests to be declared.

Authors' Contribution

Jian Wang and Chi Zhang equally contributed to this paper.

Acknowledgments

This study was supported, in part, by Chungbuk Technopark Grant Biointernational Collaborating Research, funded by Chungbuk Province, Republic of Korea, and a collaborative project between University of Louisville and BioLand Co. Ltd. for "Screening Antidiabetes and/or Obesity Naturally Extracted Compounds," funded by BioLand Co., Ltd. (10-0826 Bioland). This study was also supported by the National

Science Foundation of China (81000294 & 81370917 to CZ) and the Research Development Fund of Wenzhou Medical University (QTJ13005 to CZ and QTJ 13007 to YT). The authors thank Dr. Lu Cai, who is from the Kosair Children's Hospital Research Institute of the University of Louisville, for his proof reading of this revised paper.

References

[1] P. Poirier, "Targeting abdominal obesity in cardiology: can we be effective?" *The Canadian Journal of Cardiology*, vol. 24, supplement D, pp. 13D–17D, 2008.

[2] C. L. Ogden, S. Z. Yanovski, M. D. Carroll, and K. M. Flegal, "The epidemiology of obesity," *Gastroenterology*, vol. 132, no. 6, pp. 2087–2102, 2007.

[3] Z. Lin, Z. Zhou, Y. Liu et al., "Circulating FGF21 levels are progressively increased from the early to end stages of chronic kidney diseases and are associated with renal function in Chinese," *PLoS ONE*, vol. 6, no. 4, Article ID e18398, 2011.

[4] G. C. Farrell and C. Z. Larter, "Nonalcoholic fatty liver disease: from steatosis to cirrhosis," *Hepatology*, vol. 43, supplement 1, no. 2, pp. S99–S112, 2006.

[5] L. A. Adams, J. F. Lymp, J. St. Sauver et al., "The natural history of nonalcoholic fatty liver disease: a population-based cohort study," *Gastroenterology*, vol. 129, no. 1, pp. 113–121, 2005.

[6] J. K. Dowman, J. W. Tomlinson, and P. N. Newsome, "Pathogenesis of non-alcoholic fatty liver disease," *QJM*, vol. 103, no. 2, pp. 71–83, 2010.

[7] K. F. Tacer and D. Rozman, "Nonalcoholic fatty liver disease: focus on lipoprotein and lipid deregulation," *Journal of Lipids*, vol. 2011, Article ID 783976, 14 pages, 2011.

[8] C. P. Day and O. F. W. James, "Steatohepatitis: a tale of two "hits"?" *Gastroenterology*, vol. 114, no. 4, pp. 842–845, 1998.

[9] H. Kuribara, E. Kishi, N. Hattori, M. Okada, and Y. Maruyama, "The anxiolytic effect of two oriental herbal drugs in Japan attributed to honokiol from *magnolia* bark," *Journal of Pharmacy and Pharmacology*, vol. 52, no. 11, pp. 1425–1429, 2000.

[10] Y. Li, C. Xu, Q. Zhang, J. Y. Liu, and R. X. Tan, "In vitro anti-*Helicobacter pylori* action of 30 Chinese herbal medicines used to treat ulcer diseases," *Journal of Ethnopharmacology*, vol. 98, no. 3, pp. 329–333, 2005.

[11] V. K. Bajpai, J. I. Yoon, and S. C. Kang, "Antioxidant and antidermatophytic activities of essential oil and extracts of *Magnolia liliflora* Desr," *Food and Chemical Toxicology*, vol. 47, no. 10, pp. 2606–2612, 2009.

[12] S. Dikalov, T. Losik, and J. L. Arbiser, "Honokiol is a potent scavenger of superoxide and peroxyl radicals," *Biochemical Pharmacology*, vol. 76, no. 5, pp. 589–596, 2008.

[13] J. Ock, H. S. Han, S. H. Hong et al., "Obovatol attenuates microglia-mediated neuroinflammation by modulating redox regulation," *British Journal of Pharmacology*, vol. 159, no. 8, pp. 1646–1662, 2010.

[14] Y.-R. Lin, H.-H. Chen, C.-H. Ko, and M.-H. Chan, "Effects of honokiol and magnolol on acute and inflammatory pain models in mice," *Life Sciences*, vol. 81, no. 13, pp. 1071–1078, 2007.

[15] M. E. Munroe, J. L. Arbiser, and G. A. Bishop, "Honokiol, a natural plant product, inhibits inflammatory signals and alleviates inflammatory arthritis," *The Journal of Immunology*, vol. 179, no. 2, pp. 753–763, 2007.

[16] S. I. Grivennikov and M. Karin, "Dangerous liaisons: STAT3 and NF-κB collaboration and crosstalk in cancer," *Cytokine and Growth Factor Reviews*, vol. 21, no. 1, pp. 11–19, 2010.

[17] M. Karin, "NF-κB and cancer: mechanisms and targets," *Molecular Carcinogenesis*, vol. 45, no. 6, pp. 355–361, 2006.

[18] E.-J. Park, S.-Y. Kim, Y.-Z. Zhao, and D. H. Sohn, "Honokiol reduces oxidative stress, c-jun-NH2-terminal kinase phosphorylation and protects against glycochenodeoxycholic acid-induced apoptosis in primary cultured rat hepatocytes," *Planta Medica*, vol. 72, no. 7, pp. 661–664, 2006.

[19] M. S. Choi, S. H. Lee, H. S. Cho et al., "Inhibitory effect of obovatol on nitric oxide production and activation of NF-κB/MAP kinases in lipopolysaccharide-treated RAW 264.7cells," *European Journal of Pharmacology*, vol. 556, no. 1–3, pp. 181–189, 2007.

[20] H.-C. Ou, F.-P. Chou, W. H.-H. Sheu, S.-L. Hsu, and W.-J. Lee, "Protective effects of magnolol against oxidized LDL-induced apoptosis in endothelial cells," *Archives of Toxicology*, vol. 81, no. 6, pp. 421–432, 2007.

[21] C.-K. Chiang, M.-L. Sheu, Y.-W. Lin et al., "Honokiol ameliorates renal fibrosis by inhibiting extracellular matrix and pro-inflammatory factors in vivo and in vitro," *British Journal of Pharmacology*, vol. 163, no. 3, pp. 586–597, 2011.

[22] J.-H. Chiu, J.-C. Wang, W.-Y. Lui, C.-W. Wu, and C.-Y. Hong, "Effect of magnolol on in vitro mitochondrial lipid peroxidation and isolated cold-preserved warm-reperfused rat livers," *Journal of Surgical Research*, vol. 82, no. 1, pp. 11–16, 1999.

[23] M. H. Lin, H. T. Chao, and C. Y. Hong, "Magnolol protects human sperm motility against lipid peroxidation: a sperm head fixation method," *Archives of Andrology*, vol. 34, no. 3, pp. 151–156, 1995.

[24] W. Cui, Y. Wang, Q. Chen et al., "*Magnolia* extract (BL153) ameliorates kidney damage in a high fat diet-induced obesity mouse model," *Oxidative Medicine and Cellular Longevity*, vol. 2013, Article ID 367040, 9 pages, 2013.

[25] Y. K. Lee, D. Y. Yuk, T. I. Kim et al., "Protective effect of the ethanol extract of *Magnolia officinalis* and 4-O-methylhonokiol on scopolamine-induced memory impairment and the inhibition of acetylcholinesterase activity," *Journal of Natural Medicines*, vol. 63, no. 3, pp. 274–282, 2009.

[26] Y.-J. Lee, Y. M. Lee, C.-K. Lee, J. K. Jung, S. B. Han, and J. T. Hong, "Therapeutic applications of compounds in the *Magnolia* family," *Pharmacology and Therapeutics*, vol. 130, no. 2, pp. 157–176, 2011.

[27] Y. Song, C. Li, and L. Cai, "Fluvastatin prevents nephropathy likely through suppression of connective tissue growth factor-mediated extracellular matrix accumulation," *Experimental and Molecular Pathology*, vol. 76, no. 1, pp. 66–75, 2004.

[28] G. Zhou, C. Li, and L. Cai, "Advanced glycation end-products induce connective tissue growth factor-mediated renal fibrosis predominantly through transforming growth factor β-independent pathway," *The American Journal of Pathology*, vol. 165, no. 6, pp. 2033–2043, 2004.

[29] C. Zhang, Y. Tan, W. Guo et al., "Attenuation of diabetes-induced renal dysfunction by multiple exposures to low-dose radiation is associated with the suppression of systemic and renal inflammation," *The American Journal of Physiology—Endocrinology and Metabolism*, vol. 297, no. 6, pp. E1366–E1377, 2009.

[30] S. C. Faria, K. Ganesan, I. Mwangi et al., "MR imaging of liver fibrosis: current state of the art," *Radiographics*, vol. 29, no. 6, pp. 1615–1635, 2009.

[31] D. C. Rockey, "Noninvasive assessment of liver fibrosis and portal hypertension with transient elastography," *Gastroenterology*, vol. 134, no. 1, pp. 8–14, 2008.

[32] C. C. Choong, S. K. Venkatesh, and E. P. Siew, "Accuracy of routine clinical ultrasound for staging of liver fibrosis," *Journal of Clinical Imaging Science*, vol. 2, article 58, 2012.

[33] V. Nobili, A. Alisi, A. Vania, C. Tiribelli, A. Pietrobattista, and G. Bedogni, "The pediatric NAFLD fibrosis index: a predictor of liver fibrosis in children with non-alcoholic fatty liver disease," *BMC Medicine*, vol. 7, article 21, 2009.

[34] D. A. Sass, P. Chang, and K. B. Chopra, "Nonalcoholic fatty liver disease: a clinical review," *Digestive Diseases and Sciences*, vol. 50, no. 1, pp. 171–180, 2005.

[35] Y. Kawano and D. E. Cohen, "Mechanisms of hepatic triglyceride accumulation in non-alcoholic fatty liver disease," *Journal of Gastroenterology*, vol. 48, no. 4, pp. 434–441, 2013.

[36] H.-R. Yao, J. Liu, D. Plumeri et al., "Lipotoxicity in HepG2 cells triggered by free fatty acids," *The American Journal of Translational Research*, vol. 3, no. 3, pp. 284–291, 2011.

[37] A. B. Goldfine, R. Silver, W. Aldhahi et al., "Use of salsalate to target inflammation in the treatment of insulin resistance and type 2 diabetes," *Clinical and Translational Science*, vol. 1, no. 1, pp. 36–43, 2008.

[38] S. E. Shoelson, L. Herrero, and A. Naaz, "Obesity, inflammation, and insulin resistance," *Gastroenterology*, vol. 132, no. 6, pp. 2169–2180, 2007.

[39] S. E. Shoelson, J. Lee, and A. B. Goldfine, "Inflammation and insulin resistance," *Journal of Clinical Investigation*, vol. 116, no. 7, pp. 1793–1801, 2006.

[40] A. Fernandez-Sanchez, E. Madrigal-Santillan, M. Bautista et al., "Inflammation, oxidative stress, and obesity," *International Journal of Molecular Sciences*, vol. 12, no. 5, pp. 3117–3132, 2011.

[41] H. Xu, G. T. Barnes, Q. Yang et al., "Chronic inflammation in fat plays a crucial role in the development of obesity-related insulin resistance," *Journal of Clinical Investigation*, vol. 112, no. 12, pp. 1821–1830, 2003.

[42] S. Furukawa, T. Fujita, M. Shimabukuro et al., "Increased oxidative stress in obesity and its impact on metabolic syndrome," *Journal of Clinical Investigation*, vol. 114, no. 12, pp. 1752–1761, 2004.

[43] M. Machado, P. Marques-Vidal, and H. Cortez-Pinto, "Hepatic histology in obese patients undergoing bariatric surgery," *Journal of Hepatology*, vol. 45, no. 4, pp. 600–606, 2006.

[44] R. S. Rector, J. P. Thyfault, Y. Wei, and J. A. Ibdah, "Non-alcoholic fatty liver disease and the metabolic syndrome: an update," *World Journal of Gastroenterology*, vol. 14, no. 2, pp. 185–192, 2008.

[45] M. Lazo and J. M. Clark, "The epidemiology of nonalcoholic fatty liver disease: a global perspective," *Seminars in Liver Disease*, vol. 28, no. 4, pp. 339–350, 2008.

[46] C. P. Day, "From fat to inflammation," *Gastroenterology*, vol. 130, no. 1, pp. 207–210, 2006.

[47] S.-M. Wang, L.-J. Lee, Y.-T. Huang, J.-J. Chen, and Y.-L. Chen, "Magnolol stimulates steroidogenesis in rat adrenal cells," *British Journal of Pharmacology*, vol. 131, no. 6, pp. 1172–1178, 2000.

[48] N. Crum-Cianflone, A. Dilay, G. Collins et al., "Nonalcoholic fatty liver disease among HIV-infected persons," *Journal of Acquired Immune Deficiency Syndromes*, vol. 50, no. 5, pp. 464–473, 2009.

[49] M. C. Lewis, M. L. Phillips, J. P. Slavotinek, L. Kow, C. H. Thompson, and J. Toouli, "Change in liver size and fat content after treatment with Optifast very low calorie diet," *Obesity Surgery*, vol. 16, no. 6, pp. 697–701, 2006.

[50] J. H. Ho and C. Y. Hong, "Cardiovascular protection of magnolol: cell-type specificity and dose-related effects," *Journal of Biomedical Science*, vol. 19, article 70, 2012.

[51] J. Li, X. Shao, L. Wu et al., "Honokiol: an effective inhibitor of tumor necrosis factor-α-induced up-regulation of inflammatory cytokine and chemokine production in human synovial fibroblasts," *Acta Biochimica et Biophysica Sinica*, vol. 43, no. 5, pp. 380–386, 2011.

Hindawi Publishing Corporation
Oxidative Medicine and Cellular Longevity
Volume 2014, Article ID 765832, 9 pages
http://dx.doi.org/10.1155/2014/765832

Review Article

Resveratrol Oligomers for the Prevention and Treatment of Cancers

You-Qiu Xue,[1] Jin-Ming Di,[2] Yun Luo,[2] Ke-Jun Cheng,[3] Xing Wei,[1] and Zhi Shi[1]

[1] *Department of Cell Biology & Institute of Biomedicine, College of Life Science and Technology, Jinan University, Guangzhou, Guangdong 510630, China*
[2] *Department of Urology, Third Affiliated Hospital of Sun Yat-sen University, Guangzhou, Guangdong 510630, China*
[3] *Chemical Biology Center, Lishui Institute of Agricultural Sciences, Lishui, Zhejiang 32300, China*

Correspondence should be addressed to Xing Wei; wei70@hotmail.com and Zhi Shi; tshizhi@jnu.edu.cn

Received 15 January 2014; Accepted 12 February 2014; Published 23 March 2014

Academic Editor: Xiaoqian Chen

Resveratrol (3,4′,5-trihydroxystilbene) is a naturally derived phytoalexin stilbene isolated from grapes and other plants, playing an important role in human health and is well known for its extensive bioactivities, such as antioxidation, anti-inflammatory, anticancer. In addition to resveratrol, scientists also pay attention to resveratrol oligomers, derivatives of resveratrol, which are characterized by the polymerization of two to eight, or even more resveratrol units, and are the largest group of oligomeric stilbenes. Resveratrol oligomers have multiple beneficial properties, of which some are superior in activity, stability, and selectivity compared with resveratrol. The complicated structures and diverse biological activities are of significant interest for drug research and development and may provide promising prospects as cancer preventive and therapeutical agents. This review presents an overview on preventive or anticancer properties of resveratrol oligomers.

1. Introduction

There are growing interests in using natural compounds as potential cancer therapeutics or cancer preventive agents for human diseases. Lots of epidemiological data illustrate that there is a significant correlation between dietary intake and incidence of many kinds of cancers, and the incidence of cancer trends to raise year by year in the world due to changes in modern lifestyles and diet custom [1–3]. Due to the unsatisfied effectiveness of current cancer chemotherapy, there is an urgent need of new anticancer drugs with high efficiency and low toxicity. Fighting cancers with novel natural products, especially those extracted from plants-derived diet, seems to be a fascinating strategy. Furthermore, *in vivo* and *in vitro* studies show that many dietary substances have anticancer properties [4, 5]. Resveratrol and its oligomers belong to such kind of dietary substances.

Resveratrol (3,4′,5-trihydroxystilbene) was first isolated from the roots of white hellebore, *Veratrum grandiflorum O. Loes* [6], found in at least 72 plant species including 12 families and 31 genera [7], and widely exist in edible foods and beverages such as mulberries, peanuts, grapes, and red wine [8]. Resveratrol can be classified either as a polyphenol or stilbene and is produced by plants to protect themselves against damage or infection in response to stresses such as heat, insects, bacteria, and fungus [9]. During the last decade, resveratrol attracted increasing attention due to its preventive potential towards the most severe contemporary human diseases, such as cancer, neurodegenerative disease, vascular disease, cardiovascular disease, and aging [10–13]. Resveratrol was reported to make a great influence on the process of carcinogenesis by affecting cancer initiation and progression [8, 14]. Resveratrol was shown to exert a different inhibition to various human tumors cells by *in vitro* experiments through multiple mechanisms as well as different *in vivo* animal models [15, 16]. In addition, there was no significant toxicity to mice after the daily oral administration of high doses of resveratrol for 28 days [17].

Chemical structure analysis showed that resveratrol was a polyphenol biphenyl, and multiple hydroxyl groups affected its biological activities as well as *cis*- or *trans*-structures [18, 19]. In addition to resveratrol, scientists also focus on its

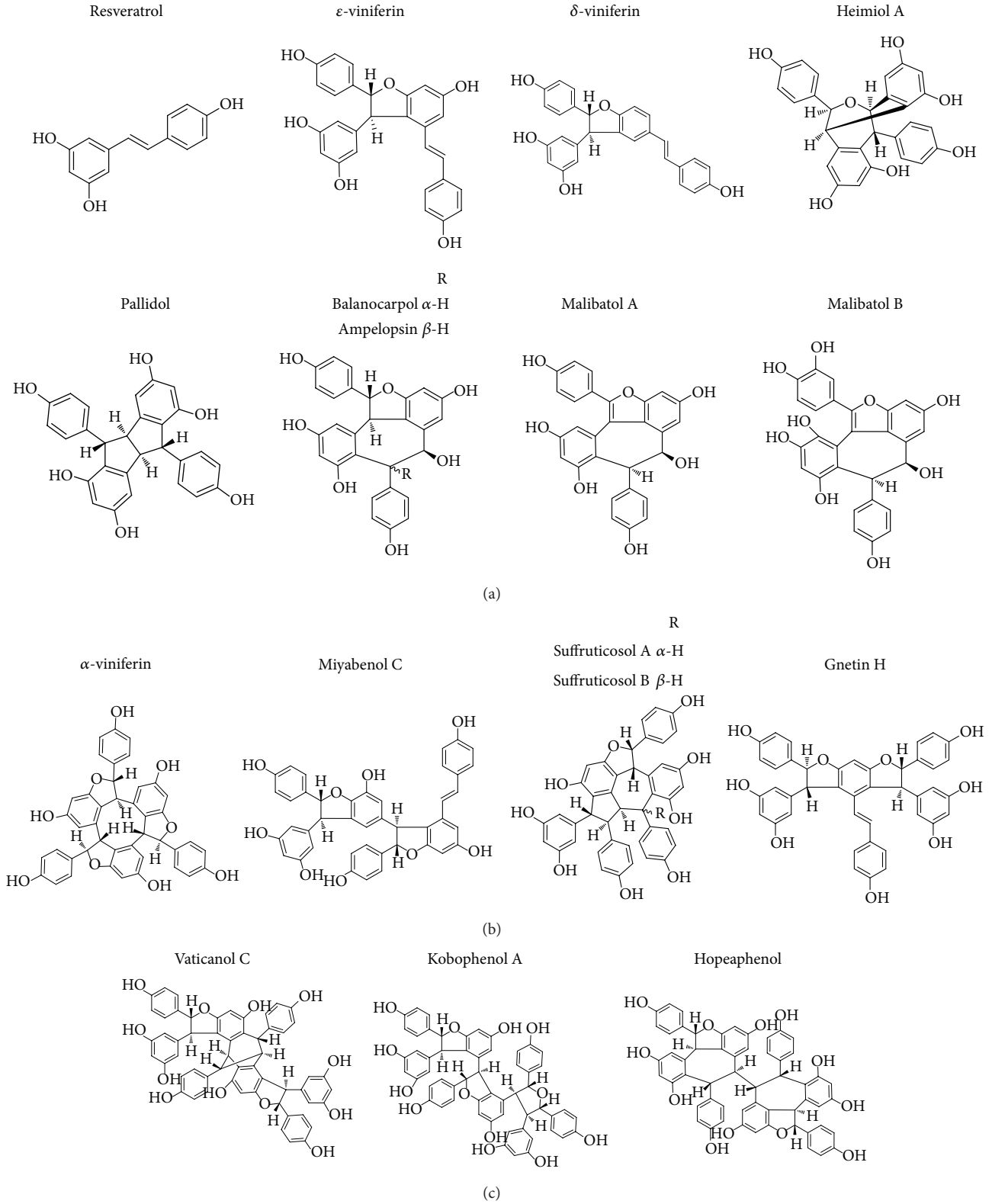

Figure 1: Structure of selected resveratrol oligomers. (a) Resveratrol and resveratrol dimers. (b) Resveratrol trimers. (c) Resveratrol tetramers.

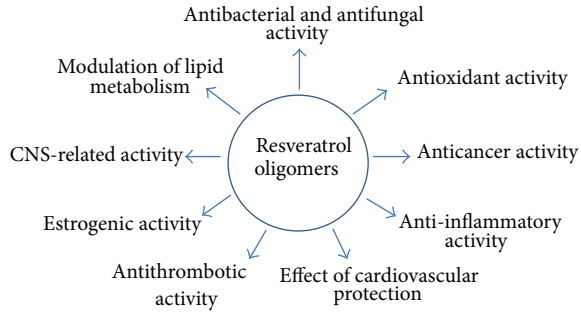

Figure 2: Bioactivities of resveratrol oligomers.

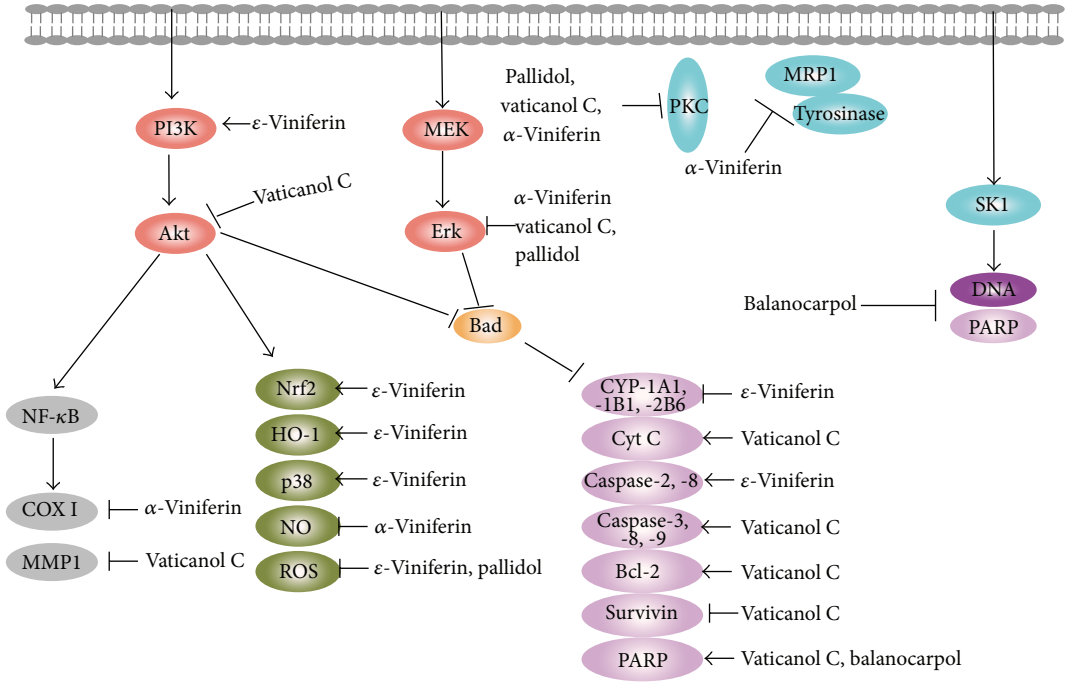

Figure 3: The potential molecular mechanism of resveratrol oligomers for the prevention and treatment of cancer.

derivatives, such as resveratrol oligomers. Resveratrol oligomers are characterized by the polymerization of two to eight resveratrol units and even more and are the largest group of oligomeric stilbenes (Figure 1) [20]. Resveratrol oligomers polyphenols were mainly isolated from five plant families, namely, Vitaceae, Leguminosae, Gnetaceae, Dipterocarpaceae, and Cyperaceae [20–23]. In addition, resveratrol oligomers were recognized as fungal detoxification products of resveratrol metabolism. These oligomers were found to exhibit widely biological activities, such as antibacterial, antifungal, anticancer, anti-HIV, and antioxidant activities (Figure 2) [24, 25]. Their intricate structures and diverse biological activities are of significant interests for drug research and development and may provide promising prospects as cancer preventive and therapeutical agents [26]. Although lots of studies showed various biochemical and pharmacological properties of resveratrol oligomers, so far there is no systematic review about these compounds. In this review, we summarize the recent progresses of the preventive and anticancer activities as well as related mechanisms of resveratrol oligomers (Tables 1 and 2 and Figure 3) and contemplate their prospects as preventive and anticancer agents.

2. Resveratrol Dimers

Resveratrol dimers are formed from two resveratrol monomers by oxidation reaction. Series of combination of monomers form different dimers which possess various activities.

2.1. ε-Viniferin. ε-Viniferin, first isolated from *Vitis vinifera* (Vitaceae), is classified as a model for its biosynthesis from resveratrol [21]. Similar to resveratrol, ε-viniferin also attracted attention as a phytoalexin and was reported to have antifungal, antibacterial, and antiviral activities [59]. To date, many studies of ε-viniferin are about the antioxidant and

Table 1: The anticancer activities of resveratrol oligomers.

Resveratrol oligomers	Cell lines and inhibition	References
ε-Viniferin	$C6^{+++}$, Hep $G2^{+}$, $HeLa^{++}$, $MCF\text{-}7^{+}$, $HT\text{-}29^{+}$ $U266^{++}$, RPMI 8226^{++}, $Jurkat^{+}$, $K562^{++}$, $U937^{++}$	[27–29]
Pallidol	$A549^{+++}$	[30]
Balanocarpol	$P\text{-}388^{++}$	[31, 32]
α-Viniferin	$HL\text{-}60^{+++}$, $MCF\text{-}7^{+}$, Hep $G2^{+}$, $A549^{+}$, $P\text{-}388^{+}$, $HCT\text{-}116^{++}$, $HT\text{-}29^{++}$, $Caco\text{-}2^{++}$	[22, 33]
Miyabenol C	$A54^{+++}$, NCI-H 446^{+++}, $U266^{+++}$, RPMI 8226^{+++} $Jurkat^{++}$, $K562^{+++}$, $U937^{+++}$	[22, 30, 34]
Vaticanol C	$SW\text{-}480^{+++}$, $DLD\text{-}1^{+}$, CoLo 201^{+}, $PC\text{-}3^{+}$, $LNCaP^{++}$ $SH\text{-}SY5Y^{++}$, $HL\text{-}60^{+++}$, $K562^{+}$, $U937^{++}$	[10, 35–37]
Kobophenol A	$A549^{+}$	[30]
Hopeaphenol	$SW\text{-}480^{+}$, $HL\text{-}60^{+}$, $P\text{-}388^{+++}$	[10, 28]

The plus signs indicated the ability to against human cancer cell lines: $^{+++}IC_{50}$ values less of 20 μM; $^{++}IC_{50}$ values range 20 μM to 50 μM; $^{+}IC_{50}$ values of 50 μM to 100 μM.

Table 2: The potential targets of resveratrol oligomers involved in apoptosis, cell proliferation, and inflammation.

Resveratrol oligomers	Cell cycle arrest	Induction of apoptosis	Inhibition of proliferation and inflammation	References
ε-Viniferin	G2/M	ROS↓, Caspase-2, 8↑, CYP1A1↓, CYP1B1↓, CYP2B6↓	Nrf2↑, HO-1↑, PI3K↑, p38↑	[38–44]
Pallidol	—	ROS↓	PKC↓, ERK↓	[45–48]
Balanocarpol	—	Cleaved PARP↑	DNA↓, SK1↓	[49, 50]
α-viniferin	S	—	PKC↓, Tyrosinase↓, MRP1↓, COX I↓, NO↓, STAT1↓, ERK↓, IFN-γ ↓	[45, 51–55]
Miyabenol C	G0/G1	—	PKC↓	[20, 22, 34, 56]
Vaticanol C	—	Caspase-3, 8, 9↑, Bad↑, Cytochrome C↑, Bcl-2↑, Survivin↓, Cleaved PARP↑	MEK↓, Akt↓	[10, 26, 32, 35–37, 57, 58]

The arrows indicate an increase (↑) or decrease (↓) in the levels, activity of the different signals, or phosphorylation status.

anticancer activities. The antioxidant activity of ε-viniferin is essential in the prevention of oxidative damage or chemical-induced cancer by inhibiting cancer initiation and progression [8, 60]. It was reported that ε-viniferin showed the better antioxidant properties to O_2^- radicals (IC_{50} value of 0.12 to 0.16 mM) than resveratrol (IC_{50} value of 0.92 to 0.98 mM) and could inhibit reactive oxygen species production [38, 61]. Cytochromes P450 (CYP) are important oxidative enzymes which metabolize xenobiotics including chemical carcinogens. Therefore, one method of cancer prevention is to inhibit carcinogens activation with inhibitors of these phase I enzymes. Modulation of those enzymes has a great influence on toxicity and carcinogenesis. ε-Viniferin displayed a more potent inhibitory effect than resveratrol for CYP enzymes including CYP1A1, CYP1A2, CYP1B1, CYP2A6, CYP2B6, CYP2E1, CYP3A4, and CYP4A (Ki 0.5 to 20 μM versus 10 to 100 μM, resp.), and this effect was not due to an inhibition of the nicotinamide adenine dinucleotide phosphate reductase [39]. ε-Viniferin could also regulate the phase II enzymes to induce carcinogen detoxification. There was a report that ε-viniferin had an inhibitory effect on noradrenaline and 5-hydroxytryotamine uptake by synaptosomes from rat brain and on the monoamine oxidase activity [40].

ε-Viniferin also showed the direct cytotoxicity to various cancer cells [41, 42]. It was reported that ε-viniferin could kill C6, Hep G2, HeLa, and MCF-7 cancer cell lines in a dose-dependent manner with IC_{50} values of 18.4, 74.3, 20.4, and 44.8 μg/mL, respectively [43]. In contrast, resveratrol showed stronger cytotoxicity against C6 and Hep G2 with IC_{50} values of 8.2 and 11.8 μg/mL and weaker cytotoxicity against HeLa and MCF-7 with IC_{50} values of 20.4 and 44.8 μg/mL, respectively [44]. In addition, ε-viniferin showed a potent anticancer activity against allografted sarcoma S-180 cells in mice and exerted antiproliferative as well as

proapoptotic effects on leukemic cells [27, 28, 44]. As for a panel of lymphoid and myeloid cell lines, including U266, RPMI8226, Jurkat, K562 and U937, ε-viniferin, and resveratrol both exert the antiproliferative and proapoptotic effect [28]. Further studies on the multiple myeloma cell line U266 showed that ε-viniferin and resveratrol could regulate cell cycle by affecting different targets [28]. In this model, ε-viniferin induced apoptosis by arresting cell cycle in G2/M, whereas cells treated with resveratrol were accumulated in S phase, and both of them induced apoptosis in a caspase-dependent manner by disrupting normal mitochondrial membrance potential [27, 28]. ε-Viniferin was also able to inhibit Hep G2 cell proliferation by blocking cell cycle at G2/M phase [60]. In human colon cancer cell lines, ε-viniferin was reported to slightly inhibit cells proliferation; however, resveratrol could inhibit cells proliferation and arrest cell cycle at S phase [62, 63]. Interestingly, the acetylated forms of ε-viniferin and resveratrol possessed more powerful anticancer effects than ε-viniferin and resveratrol [62], and this may pave a new avenue to search new cancer-preventive agents from resveratrol derivative or resveratrol oligomers analogs.

δ-Viniferin, a isomer of ε-viniferin, only exists in plants with a quite low content. There were only few reports about its chemical synthesis, which limited researches on its biological activities. However, δ-viniferin was shown to inhibit the cyclooxygenase-1 and -2 activities with IC_{50} values 5 μM [29, 64].

2.2. Pallidol. Pallidol, first isolated from *Cissus pallida*, is a natural ingredient of grape present in red wine at a level equal to that in resveratrol [65]. Pallidol was reported to show stronger antioxidant activity than resveratrol [66] and is a potent and selective singlet oxygen quencher in aqueous system. Reactive oxygen species (ROS), including singlet oxygen $^1O_2$, superoxide anion $O_2^{\bullet-}$, and hydroxyl radical $^{\bullet}OH$, were reported as being important agents causing aging and various human diseases, such as cancer, autoimmune disease, and Parkinson's disease [67]. Pallidol is a selective $^1O_2$ quencher but does not inhibit $O_2^{\bullet-}$ or $^{\bullet}OH$. $^1O_2$ [68] is an excited form of molecular oxygen and usually emerges in photo-sensitized oxidations in biological systems with the ability to react with various targets such as DNA and RNA [69]. Pallidol has a potent $^1O_2$quenching effect at low concentration. Therefore, it may be as a pharmacological agent in singlet oxygen-mediated diseases [68]. Additionally, it was reported that pallidol showed the inhibition of cell growth in a time-dependent manner similar to resveratrol in human colon cancer cells, including HCT-116, HT-29, and Caco-2 cell lines [26]. The peracetylated pallidol possessed strong cytotoxicity against KB, Caki-1, 1A9, MCF-7, and HCT-8 cell lines with IC_{50} values ranging from 1.6 to 8.0 μM [45]. Analysis of structure-activity relationship revealed that peracetylated derivatives could increase the anticancer activities of resveratrol oligomers. In addition, pallidol was shown to inhibit protein kinase C activity [30], suppressed the growth of lung cancer cells A549 [46], and exerted effects on 5-hydroxytryptamine 6 receptor-mediated Ca^{2+} responses and extracellular-signal-regulated kinases (ERK)1/2 phosphorylation as 5-hydroxytryptamine 6 receptor antagonists [70].

2.3. Balanocarpol. Balanocarpol was isolated from two endemic dipterocarp species *Balanocarpus zeylanicus* (Trimen) and *Hopea jucunda* (Thw.), and the latter is one of the main genuses of *Dipterocarpaceae* to produce varieties of resveratrol oligomers such as balanocarpol, heimiol A, and ampelopsin A, H [47, 48, 71]. Balanocarpol and resveratrol were reported as novel sphingosine kinase 1 (SK1) inhibitors by affecting SK1 expression and cancer cells growth and survival [72]. Balanocarpol was a mixed inhibitor (with sphingosine) of SK1 with K_{ic} = 90 ± 10 μM and K_{iu} of ~500 μM, while resveratrol was a competitive inhibitor (with sphingosine) of SK1 with a K_{ic} = 160 ± 40 μM, and both of them could reduce SK1 expression and DNA synthesis and induce poly ADP ribose polymerase (PARP) cleavage in MCF-7 cells [72].

3. Resveratrol Trimers

Resveratrol trimers are formed by three resveratrol monomers through head-to-ligation or circular structure, which may lead to their various biological activities. The representative trimers are discussed below.

3.1. α-Viniferin. α-Viniferin is a stilbene trimer isolated from *Caragana sinica*, *Caragana chamlagu,* and the stem bark of *Dryobalanops aromatica* [31]. It was reported that α-viniferin could inhibit the activity of some enzymes, such as protein kinase C (PKC) [30, 73], tyrosinase [49], prostaglandin H-2 synthase [50], and acetylcholinesterase [51]. α-Viniferin was shown to have inhibitory effect on PKC with IC_{50} values of 62.5 μM *in vitro* [30, 73]. In addition, α-viniferin could inhibit 2′,7′-bis-(carboxypropyl)-5(6)-carboxyfluorescein transport mediated by multidrug resistance protein 1 (MRP1) on the human erythrocyte membrane at low concentration [52]. Compared to resveratrol, α-viniferin showed 3- to 4-fold higher inhibition on cyclooxygenase activity [50]. α-Viniferin also showed significant anti-inflammatory activity on carrageenan-induced paw edema in mice through inhibiting cyclooxygenase-2 effects and nitric oxide synthase [74]. Furthermore, α-viniferin powerfully inhibited the signal transducer and activators of transcription 1 (STAT1) inducible inflammatory genes via suppressing ERK-mediated STAT1 activation in interferon-γ-stimulated macrophages [75].

α-Viniferin displayed a striking growth inhibitory effect on various cancer cell lines. It showed marked cytotoxic activity against HL-60 with IC_{50} values of 2.7 ± 0.5 μM and moderately cytotoxic activity against MCF-7, Hep G2, A549, and murine leukemia P-388 cells [53]. α-Viniferin also exerted selective antiproliferative activity against submandibular gland carcinoma but no effects on normal human oral cells such as pulp cells, periodontal ligament fibroblast, and gingival fibroblast [54]. In addition, α-viniferin inhibited the proliferation in a concentration- and time-dependent manner by arresting cell cycle at the S phase but not inducing apoptosis of human colon cancer cells *in vitro*, including HCT-116, HT-29, and Caco-2 cell lines, and was more efficient

with IC_{50} values ranging from 6 to 40 μM than resveratrol with IC_{50} values ranging from 120 to 170 μM [26]. Together, these studies emphasized the potential of α-viniferin for the prevention and treatment of cancer.

3.2. Miyabenol C. Miyabenol C, a stilbenoid and natural resveratrol trimer, was reported to possess lots of biological functions. It revealed that miyabenol C could inhibit the activity of rat PKC with IC_{50} values of 27.5 μM, which is similar to ε-viniferin [19]. In human lung carcinoma cell lines A549 and NCI-H446, miyabenol C showed cytotoxicity with IC_{50} values of 20 μM and induced apoptosis by inhibiting the effects of PKC isoenzymes [46, 55]. Miyabenol C possessed more potent antiproliferative and proapoptotic effects on different lymphoid and myeloid cell lines with IC_{50} values of 10 to 30 μM than resveratrol with IC_{50} values of 30 to 50 μM, and cells treated with resveratrol and miyabenol C were accumulated in S and G0/G1 phase, respectively [28].

4. Resveratrol Tetramers

Resveratrol tetramers are formed from four monomers or two different dimers or a monomer and a trimer, and their complex structures lead to different biological activities.

4.1. Vaticanol C. Vaticanol C, isolated from the stem bark of *Vatica rassak* in Dipterocarpaceae, was reported to exert various pharmacological properties, including antiproliferative, antioxidant, anti-inflammatory, and anticancer properties [33, 34, 56, 76]. In a panel of human cancer cell lines, including SW-480, LNCaP, SH-SY5Y, HL-60, and U937, vaticanol C was able to decrease cell viability and showed 4- to 7-fold more potent to induce the death of two cell lines (SW-480 and HL-60) than resveratrol [56]. In another study, the growth of the colon cancer cell lines SW-480, DLD-1, and COLO 201 was significantly inhibited after treated by vaticanol C. The vaticanol C-induced growth inhibition was concentration dependent [33, 56]. Further studies showed that vaticanol C-induced apoptosis was associated with the decrease of mitochondrial membrane potential, release of cytochrome c from mitochondria, and activation of caspases-3 and -9 and could be prevented by overexpression of Bcl-2 [56]. In addition, molecular studies demonstrated that the mechanism of vaticanol C-induced apoptosis was related to the decrease of pErk, pAkt, and pBad [76]. In a mouse model of metastatic mammary carcinoma cells BJMC-3879, the tumor growth was slightly inhibited by vaticanol C, but the multiplicity of metastasis to the lymph nodes and lungs was significantly suppressed due to induced apoptosis with the activation of caspases-3, -8, and -9 by ligand- and death-inducing signaling complex-independent pathway [35, 77]. Recently, there was a report that vaticanol C could activate peroxisome proliferators-activated receptor $\alpha/\beta/\delta$, and it suggested that vaticanol C could be a novel agent to afford beneficial effects against lifestyle-related diseases [36]. Vaticanol C also showed significant inhibition of matrix metalloproteinase-1 (MMP-1) production [23].

4.2. Kobophenol A. Kobophenol A, a natural tetramer of resveratrol, could be isolated from Chinese traditional medicine *Jin Quegen*, the roots of *Caragana sinica Rehd,* and *Caragana chamlagu*. It was reported that kobophenol A possessed the ability to inhibit the activity of PKC [30, 73] and the growth of lung cancer cell line A549 [46] and showed moderate activity against human colon cancer cell lines [26]. Kobophenol A could inhibit acetylcholinesterase activity and display antimicrobial activity on *Staphylococcus aureus* [51]. Additionally, kobophenol A showed the characteristics of selective estrogen receptor modulators and it may be as an agent for the prevention of osteoporosis [78].

4.3. Hopeaphenol. Hopeaphenol is a resveratrol tetramer isolated from *Dipterocarpaceae* like *Shorea ovalis* and wines from North Africa [57]. Hopeaphenol inhibited the growth of human cancer cells SW-480 and HL-60 [56] and murine leukemia cells P-388 [32]. It possessed potent cytotoxicity against the human epidermoid carcinoma of the nasopharynx [45], hepatoma [42], and also expounded anti-inflammatory [37], antimicrobial [58], and HIV-inhibitory activities [43].

5. Concluding Remarks

Resveratrol widely exists in nature and was extensively studied in clinical trials. However resveratrol oligomers were barely studied due to their rare resource and lacking of studying *in vivo* and in clinical trials. For drug research and design, resveratrol derivatives open a new perspective to selectively develop the health beneficial properties of those natural compounds for the prevention and treatment of human diseases such as cancers. A series of analogs were extracted from different kinds of plants in recent years, which showed more potency for the treatment of human diseases than the parental compound resveratrol. Furthermore, such analogs displayed improved pharmacological properties and various bioactivities, although those results were largely based on experiments with cell cultures or animal studies. There are more and more scientific data to support the use of resveratrol oligomers for human disease prevention or lifespan extension. Resveratrol oligomers target a wide range of molecules that influence cell proliferation, apoptosis, and metastasis. Although the preventive and anticancer mechanism of resveratrol oligomers cannot be limited to a specific pathway, protein, or gene, their use as preventive and anticancer agents has limitless possibilities in its natural and analog forms and should continue to be pursued in future studies.

Conflict of Interests

The authors declare that there is no conflict of interests regarding the publication of this paper.

Authors' Contribution

You-Qiu Xue, Jin-Ming Di, and Yun Luo contributed equally to this work.

Acknowledgments

This work was supported by funds from the National Natural Science Foundation of China no. 31271444 and no. 81201726 (Z. Shi), no. 30870650 and no. 31171304 (X. Wei), no. 81201694 (Y. Luo), and no. 81303305 (K. Cheng), the Fundamental Research Funds for the Central Universities of Jinan University no. 21612407 (Z. Shi) and no. 21612107 (X. Wei); Research Foundation for Doctoral Discipline of Higher Education no. 20124401120007 (Z. Shi), no. 20114401110007 (X. Wei), and no. 20120171120059 (Y. Luo); and Lishui Science and Technology Bureau Research Fund no. 20140212037 (K. Cheng).

References

[1] D. W. West, M. L. Slattery, L. M. Robison et al., "Dietary intake and colon cancer: sex- and anatomic site-specific associations," *American Journal of Epidemiology*, vol. 130, no. 5, pp. 883–894, 1989.

[2] D. W. West, M. L. Slattery, L. M. Robison, T. K. French, and A. W. Mahoney, "Adult dietary intake and prostate cancer risk in Utah: a case-control study with special emphasis on aggressive tumors," *Cancer Causes and Control*, vol. 2, no. 2, pp. 85–94, 1991.

[3] G. R. Howe, E. Benito, R. Castelleto et al., "Dietary intake of fiber and decreased risk of cancers of the colon and rectum: evidence from the combined analysis of 13 case-control studies," *Journal of the National Cancer Institute*, vol. 84, no. 24, pp. 1887–1896, 1992.

[4] M. S. Donaldson, "Nutrition and cancer: a review of the evidence for an anti-cancer diet," *Nutrition Journal*, vol. 3, article 19, 2004.

[5] P. Fresco, F. Borges, C. Diniz, and M. P. M. Marques, "New insights on the anticancer properties of dietary polyphenols," *Medicinal Research Reviews*, vol. 26, no. 6, pp. 747–766, 2006.

[6] M. Takaoka, "The phenolic substances of white hellebore (Veratrum Grandiflorum Loes fil.) II," *Nippon Kagaku Kaishi*, vol. 60, no. 12, pp. 1261–1264, 1939.

[7] K. P. L. Bhat and J. M. Pezzuto, "Cancer chemopreventive activity of resveratrol," *Annals of the New York Academy of Sciences*, vol. 957, pp. 210–229, 2002.

[8] M. Jang, L. Cai, G. O. Udeani et al., "Cancer chemopreventive activity of resveratrol, a natural product derived from grapes," *Science*, vol. 275, no. 5297, pp. 218–220, 1997.

[9] J. Burns, T. Yokota, H. Ashihara, M. E. J. Lean, and A. Crozier, "Plant foods and herbal sources of resveratrol," *Journal of Agricultural and Food Chemistry*, vol. 50, no. 11, pp. 3337–3340, 2002.

[10] K. B. Harikumar and B. B. Aggarwal, "Resveratrol: a multitargeted agent for age-associated chronic diseases," *Cell Cycle*, vol. 7, no. 8, pp. 1020–1037, 2008.

[11] P. Kovacic and R. Somanathan, "Multifaceted approach to resveratrol bioactivity: focus on antioxidant action, cell signaling and safety," *Oxidative Medicine and Cellular Longevity*, vol. 3, no. 2, pp. 86–100, 2010.

[12] S. D. Rege, S. Kumar, D. N. Wilson et al., "Resveratrol protects the brain of obese mice from oxidative damage," *Oxidative Medicine and Cellular Longevity*, vol. 2013, Article ID 419092, 7 pages, 2013.

[13] C. D. Venturini, S. Merlo, A. A. Souto, M. D. C. Fernandes, R. Gomez, and C. R. Rhoden, "Resveratrol and red wine function as antioxidants in the nervous system without cellular proliferative effects during experimental diabetes," *Oxidative Medicine and Cellular Longevity*, vol. 3, no. 6, pp. 434–441, 2010.

[14] Z. Dong, "Molecular mechanism of the chemopreventive effect of resveratrol," *Mutation Research*, vol. 523-524, pp. 145–150, 2003.

[15] M. Athar, J. H. Back, X. Tang et al., "Resveratrol: a review of preclinical studies for human cancer prevention," *Toxicology and Applied Pharmacology*, vol. 224, no. 3, pp. 274–283, 2007.

[16] J. A. Baur and D. A. Sinclair, "Therapeutic potential of resveratrol: the in vivo evidence," *Nature Reviews Drug Discovery*, vol. 5, no. 6, pp. 493–506, 2006.

[17] M. E. Juan, M. Pilar Vinardell, and J. M. Planas, "The daily oral administration of high doses of trans-resveratrol to rats for 28 days is not harmful," *Journal of Nutrition*, vol. 132, no. 2, pp. 257–260, 2002.

[18] D. Mikulski and M. Molski, "Quantitative structure-antioxidant activity relationship of trans-resveratrol oligomers, trans-4,4′-dihydroxystilbene dimer, trans-resveratrol-3-O-glucuronide, glucosides: Trans-piceid, cis-piceid, trans-astringin and trans-resveratrol-4′-O-β-D-glucopyranoside," *European Journal of Medicinal Chemistry*, vol. 45, no. 6, pp. 2366–2380, 2010.

[19] R. H. Cichewicz and S. A. Kouzi, "Resveratrol oligomers: structure, chemistry, and biological activity," *Studies in Natural Products Chemistry*, vol. 26, pp. 507–579, 2002.

[20] A. P. Lins, M. N. D. S. Ribeiro, O. R. Gottlieb, and H. E. Gottlieb, "Gnetins: resveratrol oligomers from Gnetum species," *Journal of Natural Products*, vol. 45, no. 6, pp. 754–761, 1982.

[21] S. Sotheeswaran and V. Pasupathy, "Distribution of resveratrol oligomers in plants," *Phytochemistry*, vol. 32, no. 5, pp. 1083–1092, 1993.

[22] T. Ito, T. Tanaka, M. Iinuma et al., "New resveratrol oligomers in the stem bark of Vatica pauciflora," *Tetrahedron*, vol. 59, no. 28, pp. 5347–5363, 2003.

[23] N. Abe, T. Ito, K. Ohguchi et al., "Resveratrol oligomers from Vatica albiramis," *Journal of Natural Products*, vol. 73, no. 9, pp. 1499–1506, 2010.

[24] L. Li, G. E. Henry, and N. P. Seeram, "Identification and bioactivities of resveratrol oligomers and flavonoids from carex folliculata Seeds," *Journal of Agricultural and Food Chemistry*, vol. 57, no. 16, pp. 7282–7287, 2009.

[25] W. Z. W. M. Zain, N. Ahmat, N. H. Norizan, and N. A. A. M. Nazri, "The evaluation of antioxidant, antibacterial and structural identification activity of trimer resveratrol from Malaysia's dipterocarpaceae," *Australian Journal of Basic and Applied Sciences*, vol. 5, no. 5, pp. 926–929, 2011.

[26] A. González-Sarrías, S. Gromek, D. Niesen, N. P. Seeram, and G. E. Henry, "Resveratrol oligomers isolated from carex species inhibit growth of human colon tumorigenic cells mediated by cell cycle arrest," *Journal of Agricultural and Food Chemistry*, vol. 59, no. 16, pp. 8632–8638, 2011.

[27] C. Quiney, C. Billard, A. M. Faussat et al., "Pro-apoptotic properties of hyperforin in leukemic cells from patients with B-cell chronic lymphocytic leukemia," *Leukemia*, vol. 20, no. 3, pp. 491–497, 2006.

[28] C. Barjot, M. Tournaire, C. Castagnino, C. Vigor, J. Vercauteren, and J.-F. Rossi, "Evaluation of antitumor effects of two vine stalk oligomers of resveratrol on a panel of lymphoid and myeloid cell lines: comparison with resveratrol," *Life Sciences*, vol. 81, no. 23-24, pp. 1565–1574, 2007.

[29] X. Vitrac, A. Bornet, R. Vanderlinde et al., "Determination of stilbenes (δ-viniferin, trans-astringin, trans-piceid, cis- and trans-resveratrol, ε-viniferin) in Brazilian wines," *Journal of Agricultural and Food Chemistry*, vol. 53, no. 14, pp. 5664–5669, 2005.

[30] G. Xu, L. P. Zhang, L. F. Chen, and C. Q. Hu, "Inhibition of protein kinase C by stilbenoids," *Acta Pharmaceutica Sinica*, vol. 29, no. 11, pp. 818–822, 1994.

[31] T. Shen, X.-N. Wang, and H.-X. Lou, "Natural stilbenes: an overview," *Natural Product Reports*, vol. 26, no. 7, pp. 916–935, 2009.

[32] M. Muhtadi, E. H. Hakim, L. D. Juliawaty et al., "Cytotoxic resveratrol oligomers from the tree bark of Dipterocarpus hasseltii," *Fitoterapia*, vol. 77, no. 7-8, pp. 550–555, 2006.

[33] T. Ito, Y. Akao, T. Tanaka, M. Iinuma, and Y. Nozawa, "Vaticanol C, a novel resveratrol tetramer, inhibits cell growth through induction of apoptosis in colon cancer cell lines," *Biological & pharmaceutical bulletin*, vol. 25, no. 1, pp. 147–148, 2002.

[34] T. A. Zykova, F. Zhu, X. Zhai et al., "Resveratrol directly targets COX-2 to inhibit carcinogenesis," *Molecular Carcinogenesis*, vol. 47, no. 10, pp. 797–805, 2008.

[35] M.-A. Shibata, Y. Akao, E. Shibata et al., "Vaticanol C, a novel resveratrol tetramer, reduces lymph node and lung metastases of mouse mammary carcinoma carrying p53 mutation," *Cancer Chemotherapy and Pharmacology*, vol. 60, no. 5, pp. 681–691, 2007.

[36] T. Tsukamoto, R. Nakata, E. Tamura et al., "Vaticanol C, a resveratrol tetramer, activates PPAR and PPARβ/δ in vitro and in vivo," *Nutrition and Metabolism*, vol. 7, article 46, 2010.

[37] K.-S. Huang, M. Lin, and G.-F. Cheng, "Anti-inflammatory tetramers of resveratrol from the roots of Vitis amurensis and the conformations of the seven-membered ring in some oligostilbenes," *Phytochemistry*, vol. 58, no. 2, pp. 357–362, 2001.

[38] C. Privat, J. P. Telo, V. Bernardes-Genisson, A. Vieira, J.-P. Souchard, and F. Nepveu, "Antioxidant properties of trans-ε-Viniferin as compared to stilbene derivatives in aqueous and nonaqueous media," *Journal of Agricultural and Food Chemistry*, vol. 50, no. 5, pp. 1213–1217, 2002.

[39] B. Piver, F. Berthou, Y. Dreano, and D. Lucas, "Differential inhibition of human cytochrome P450 enzymes by ε-viniferin, the dimer of resveratrol: comparison with resveratrol and polyphenols from alcoholized beverages," *Life Sciences*, vol. 73, no. 9, pp. 1199–1213, 2003.

[40] M. Yáñez, N. Fraiz, E. Cano, and F. Orallo, "(-)-Trans-ε-viniferin, a polyphenol present in wines, is an inhibitor of noradrenaline and 5-hydroxytryptamine uptake and of monoamine oxidase activity," *European Journal of Pharmacology*, vol. 542, no. 1-3, pp. 54–60, 2006.

[41] J. K. Hyo, J. C. Eun, J. B. Song et al., "Cytotoxic and antimutagenic stilbenes from seeds of Paeonia lactiflora," *Archives of Pharmacal Research*, vol. 25, no. 3, pp. 293–299, 2002.

[42] S. Rohaiza, W. A. Yaacob, L. B. Din, and I. Nazlina, "Cytotoxic oligostilbenes from shorea hopeifolia," *African Journal of Pharmacy and Pharmacology*, vol. 5, no. 10, pp. 1272–1277, 2011.

[43] S. Mishima, K. Matsumoto, Y. Futamura et al., "Antitumor effect of stilbenoids from Vateria indica against allografted sarcoma S-180 in animal model," *Journal of Experimental Therapeutics and Oncology*, vol. 3, no. 5, pp. 283–288, 2003.

[44] C. Quiney, D. Dauzonne, C. Kern et al., "Flavones and polyphenols inhibit the NO pathway during apoptosis of leukemia B-cells," *Leukemia Research*, vol. 28, no. 8, pp. 851–861, 2004.

[45] M. Ohyama, T. Tanaka, T. Ito, M. Iinuma, K. F. Bastow, and K.-H. Lee, "Antitumor agents 200. Cytotoxicity of naturally occurring resveratrol oligomers and their acetate derivatives," *Bioorganic and Medicinal Chemistry Letters*, vol. 9, no. 20, pp. 3057–3060, 1999.

[46] S. Zhi and X. Guang, "Growth inhibitory effect of stilbenoids on lung cancer lines," *Acta Academiae Medicinae Sinicae*, vol. 25, pp. 327–330, 1998.

[47] S. Atun, R. A. Nurfina, and M. Niwa, "Balanocarpol and Heimiol A, two resveratrol dimers from stem bark Hopea mengarawan (Dipterocarpaceae), Indo," *Indonesian Journal of Chemistry*, vol. 6, no. 1, pp. 75–78, 2006.

[48] S. Atun, R. A. Nurfina, and M. Niwa, "Balanocarpol and ampelopsin H, two resveratrol dimers from stem bark Hopea mengarawan (Dipterocarpaceae)," *Indonesian Journal of Chemistry*, vol. 6, no. 3, pp. 307–311, 2006.

[49] K. Ohguchi, T. Tanaka, T. Ito et al., "Inhibitory effects of resveratrol derivatives from dipterocarpaceae plants on tyrosinase activity," *Bioscience, Biotechnology and Biochemistry*, vol. 67, no. 7, pp. 1587–1589, 2003.

[50] S.-H. Lee, N.-H. Shin, S.-H. Kang et al., "α-Viniferin: a prostaglandin H2 synthase inhibitor from root of Carex humilis," *Planta Medica*, vol. 64, no. 3, pp. 204–207, 1998.

[51] S. H. Sung, S. Y. Kang, K. Y. Lee et al., "(+)-Alpha-viniferin, a stilbene trimer from Caragana chamlague, inhibits acetylcholinesterase," *Biological & pharmaceutical bulletin*, vol. 25, no. 1, pp. 125–127, 2002.

[52] M. Bobrowska-Hägerstrand, M. Lillås, L. Mrówczyñska et al., "Resveratrol oligomers are potent MRP1 transport inhibitors," *Anticancer Research*, vol. 26, no. 3 A, pp. 2081–2084, 2006.

[53] A. Wibowo, N. Ahmat, A. S. Hamzah et al., "Malaysianol A, a new trimer resveratrol oligomer from the stem bark of Dryobalanops aromatica," *Fitoterapia*, vol. 82, no. 4, pp. 676–681, 2011.

[54] S. A. Chowdhury, K. Kishino, R. Satoh et al., "Tumor-specificity and apoptosis-inducing activity of stilbenes and flavonoids," *Anticancer Research*, vol. 25, no. 3 B, pp. 2055–2063, 2005.

[55] S. Zhi, T. Chunyan, W. Yuxiong, H. Hong, and X. Guang, "Effects of miyabenol-C on protein kinase-C in two lung carcinoma cell lines," *Chinese Medical Journal*, vol. 6, p. 001, 1999.

[56] T. Ito, Y. Akao, H. Yi et al., "Antitumor effect of resveratrol oligomers against human cancer cell lines and the molecular mechanism of apoptosis induced by vaticanol C," *Carcinogenesis*, vol. 24, no. 9, pp. 1489–1497, 2003.

[57] H. A. Guebailia, K. Chira, T. Richard et al., "Hopeaphenol: the first resveratrol tetramer in wines from North Africa," *Journal of Agricultural and Food Chemistry*, vol. 54, no. 25, pp. 9559–9564, 2006.

[58] J. R. Zgoda-Pols, A. J. Freyer, L. B. Killmer, and J. R. Porter, "Antimicrobial resveratrol tetramers from the stem bark of Vatica oblongifolia ssp. oblongifolia," *Journal of Natural Products*, vol. 65, no. 11, pp. 1554–1559, 2002.

[59] A. E. A. Bala, A. Kollmann, P.-H. Ducrot et al., "Cis ε-viniferin: a new antifungal resveratrol dehydrodimer from Cyphostemma crotalarioides roots," *Journal of Phytopathology*, vol. 148, no. 1, pp. 29–32, 2000.

[60] D. Colin, A. Lancon, D. Delmas et al., "Antiproliferative activities of resveratrol and related compounds in human hepatocyte derived HepG2 cells are associated with biochemical cell disturbance revealed by fluorescence analyses," *Biochimie*, vol. 90, no. 11-12, pp. 1674–1684, 2008.

[61] H. J. Kim, E. J. Chang, S. H. Cho, S. K. Chung, H. D. Park, and S. W. Choi, "Antioxidative activity of resveratrol and its derivatives isolated from seeds of Paeonia lactiflora," *Bioscience, Biotechnology and Biochemistry*, vol. 66, no. 9, pp. 1990–1993, 2002.

[62] D. Colin, A. Gimazane, G. Lizard et al., "Effects of resveratrol analogs on cell cycle progression, cell cycle associated proteins and 5fluoro-uracil sensitivity in human derived colon cancer cells," *International Journal of Cancer*, vol. 124, no. 12, pp. 2780–2788, 2009.

[63] A.-K. Marel, G. Lizard, J.-C. Izard, N. Latruffe, and D. Delmas, "Inhibitory effects of trans-resveratrol analogs molecules on the proliferation and the cell cycle progression of human colon tumoral cells," *Molecular Nutrition and Food Research*, vol. 52, no. 5, pp. 538–548, 2008.

[64] V. Vingtdeux, U. Dreses-Werringloer, H. Zhao, P. Davies, and P. Marambaud, "Therapeutic potential of resveratrol in Alzheimer's disease," *BMC Neuroscience*, vol. 9, no. supplement 2, p. S6, 2008.

[65] M. A. Khan, S. G. Nabi, S. Prakash, and A. Zaman, "Pallidol, a resveratrol dimer from Cissus pallida," *Phytochemistry*, vol. 25, no. 8, pp. 1945–1948, 1986.

[66] H. J. Kim, M. Saleem, S. H. Seo, C. Jin, and Y. S. Lee, "Two new antioxidant stilbene dimers, parthenostilbenins A and B from Parthenocissus tricuspidata," *Planta Medica*, vol. 71, no. 10, pp. 973–976, 2005.

[67] J. L. Marx, "Oxygen free radicals linked to many diseases," *Science*, vol. 235, no. 4788, pp. 529–531, 1987.

[68] S. He, L. Jiang, B. Wu, Y. Pan, and C. Sun, "Pallidol, a resveratrol dimer from red wine, is a selective singlet oxygen quencher," *Biochemical and Biophysical Research Communications*, vol. 379, no. 2, pp. 283–287, 2009.

[69] T. Hofer, C. Badouard, E. Bajak, J.-L. Ravanat, Å. Mattsson, and I. A. Cotgreave, "Hydrogen peroxide causes greater oxidation in cellular RNA than in DNA," *Biological Chemistry*, vol. 386, no. 4, pp. 333–337, 2005.

[70] D. H. Kim, S.-H. Kim, H. J. Kim, C. Jin, K. C. Chung, and H. Rhim, "Stilbene derivatives as human 5-HT6 receptor antagonists from the root of Caragana sinica," *Biological and Pharmaceutical Bulletin*, vol. 33, no. 12, pp. 2024–2028, 2010.

[71] S. Sahidin, E. H. Hakim, L. D. Juliawaty et al., "Cytotoxic properties of oligostilbenoids from the tree barks of Hopea dryobalanoides," *Zeitschrift fur Naturforschung C Journal of Biosciences*, vol. 60, no. 9-10, pp. 723–727, 2005.

[72] K. G. Lim, A. I. Gray, S. Pyne, and N. J. Pyne, "Resveratrol dimers are novel sphingosine kinase 1 inhibitors and affect sphingosine kinase 1 expression and cancer cell growth and survival," *British Journal of Pharmacology*, vol. 166, no. 5, pp. 1605–1616, 2012.

[73] P. Kulanthaivel, W. P. Janzen, L. M. Ballas et al., "Naturally occurring protein kinase C inhibitors; II. Isolation of oligomeric stilbenes from Caragana sinica," *Planta Medica*, vol. 61, no. 1, pp. 41–44, 1995.

[74] E. Y. Chung, B. H. Kim, M. K. Lee et al., "Anti-inflammatory effect of the oligomeric stilbene α-viniferin and its mode of the action through inhibition of cyclooxygenase-2 and inducible nitric oxide synthase," *Planta Medica*, vol. 69, no. 8, pp. 710–714, 2003.

[75] E. Y. Chung, E. Roh, J.-A. Kwak et al., "α-Viniferin suppresses the signal transducer and activation of transcription-1 (stat-1)-inducible inflammatory genes in interferon-γ-stimulated macrophages," *Journal of Pharmacological Sciences*, vol. 112, no. 4, pp. 405–414, 2010.

[76] K. Ohguchi, Y. Akao, K. Matsumoto et al., "Vaticanol C-induced cell death is associated with inhibition of pro-survival signaling in HL60 human leukemia cell line," *Bioscience, Biotechnology and Biochemistry*, vol. 69, no. 2, pp. 353–356, 2005.

[77] D. A. Martin, R. M. Siegel, L. Zheng, and M. J. Lenardo, "Membrane oligomerization and cleavage activates the caspase-8 (FLICE/MACHα1) death signal," *The Journal of Biological Chemistry*, vol. 273, no. 8, pp. 4345–4349, 1998.

[78] C.-Y. Tian, C.-Q. Hu, G. Xu, and H.-Y. Song, "Assessment of estrogenic activity of natural compounds using improved E-screen assay," *Acta Pharmacologica Sinica*, vol. 23, no. 6, pp. 572–576, 2002.